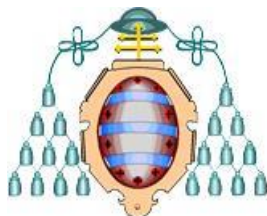


Departamento de Química Orgánica e Inorgánica
Programa de Doctorado Síntesis y Reactividad Química
UNIVERSIDAD DE OVIEDO



Avances en la Química de Coordinación de Tetrilenos Pesados

TESIS DOCTORAL

Diego Polo Coca

2015



RESUMEN DEL CONTENIDO DE TESIS DOCTORAL

1.- Título de la Tesis	
Español/Otro Idioma: AVANCES EN LA QUÍMICA DE COORDINACIÓN DE TETRILENOS PESADOS	Inglés: ADVANCES IN THE COORDINATION CHEMISTRY OF HEAVIER TETRYLENES
2.- Autor	
Nombre: DIEGO POLO COCA	DNI/Pasaporte/NIE:
Programa de Doctorado: SÍNTESIS Y REACTIVIDAD QUÍMICA	
Órgano responsable: UNIVERSIDAD DE OVIEDO	

RESUMEN (en español)

Esta tesis doctoral se enmarca en el campo de la Química Inorgánica y, más concretamente, en el de la química que asocia los metales de transición (Ms) con los parientes más pesados de los carbenos, conocidos comúnmente como ttrilenos pesados (TPs) o metalilenos. Su formato es el de "Compendio de Publicaciones" y contiene los 10 artículos científicos que hasta ahora se han publicado sobre su contenido.

En la primera parte de la memoria se describen reacciones de ttrilenos pesados acíclicos y cíclicos simples con $[Ru_3(CO)_{12}]$ (Capítulo 1) y con $[AuCl(THT)]$ (THT = tetrahidrotiofeno) (Capítulo 2). En particular, se han utilizado los TPs de Lappert $E(HMDS)_2$ [$E = Ge, Sn$; $HMDS = N(SiMe_3)_2$] como TPs acíclicos y los de tipo imidazol $E(N^tBu)_2C_2H_2$ ($E = Si, Ge$) o benzimidazol $E(NCH_2^tBu)_2C_6H_4$ ($E = Si, Ge, Sn$) como TPs cíclicos simples. Como resultado se han preparado los primeros bis(amido)germileno y -estannileno de rutenio, así como los primeros complejos de oro conteniendo un estannileno neutro. También se ha aumentado la pequeña familia de complejos de oro que contienen germileno neutros. En estas reacciones, el volumen y la naturaleza cíclica o acíclica del TP empleado, así como el tamaño del átomo E, juegan un papel determinante sobre la naturaleza de los productos obtenidos.

En la segunda parte de la memoria se describen reacciones de $[Ru_3(CO)_{12}]$, $[Co_2(CO)_8]$ y $[MnBr(CO)_5]$ con ttrilenos pesados cíclicos estabilizados por grupos amidinato, particularmente $E(RR^tBzam)X$ ($E = Si, Ge$; R, R' = grupos orgánicos; X = grupo aniónico; bzam = benzamidinato; muchos de ellos preparados por primera vez en este trabajo). El capítulo 3 recoge la reactividad del germileno $Ge(^tPr_2bzam)(HMDS)$ frente a los precursores metálicos mencionados anteriormente. En el Capítulo 4 se estudia la influencia que tiene el volumen de los grupos R y R' del benzamidinato (tPr , tBu ó Et) y la naturaleza del átomo E (Si o Ge) en la reactividad de los TPs $E(RR^tBzam)(HMDS)$. En el Capítulo 5 se analizan los cambios de reactividad observados cuando los germileno empleados tienen $X = ^tBu, Ge(RR^tBzam)^tBu$. En todas estas reacciones las diferentes características electrónicas y estéricas de los TPs han dado lugar a patrones de reactividad y a modos de coordinación muy diferentes que, en algunos casos, no habían sido observados previamente. En particular, destaca la síntesis de complejos binucleares de rutenio y cobalto en los que el TP se coordina por primera vez en modo puente y bidentado $\mu-k^2Ge,N$, o la síntesis de complejos mononucleares de manganeso que contienen TPs bidentados sin precedentes, de tipo k^2Ge,N -iminagermanato. Hemos demostrado que estos modos de coordinación bidentados sólo son posibles cuando, al menos, uno de los grupos N-R del fragmento amidinato es más pequeño que un grupo *tert*-butilo. Los complejos descritos en esta segunda parte de la memoria resultaron ser bastante estables. Algunos de ellos han sido objeto de estudios posteriores, entre los que se incluyen reacciones con agentes nucleófilos (neutros y/o aniónicos), activaciones de enlaces H-X con formación de derivados coordinativamente insaturados ($X = H, SiEt_3, SnPh_3$), adiciones reversibles de CO, estudios de termólisis e hidrólisis, y reducciones electroquímicas de CO_2 . Finalmente, en el



Capítulo 6 se incluye una revisión bibliográfica sobre el estado actual (2015) de la química de complejos de tipo amidinato-TP-M.

RESUMEN (en Inglés)

This PhD thesis can be inscribed into the area of Inorganic Chemistry, being specifically related to the transition metal (M) chemistry of the heavier carbene analogues, also known as heavier tetrylenes (HTs) or metalylenes. It is formatted as a "Compilation of Scientific Articles" (its content has hitherto given rise to 10 scientific publications).

In Part I, reactions of $[\text{Ru}_3(\text{CO})_{12}]$ (Chapter 1) and $[\text{AuCl}(\text{THT})]$ (THT = tetrahydrothiophene) (Chapter 2) with the acyclic Lappert's HTs $\text{E}(\text{HMDS})_2$ [E = Ge, Sn; HMDS = $\text{N}(\text{SiMe}_3)_2$] and the simple cyclic ones $\text{E}(\text{N}^t\text{Bu})_2\text{C}_2\text{H}_2$ (E = Si, Ge) or $\text{E}(\text{NCH}_2^t\text{Bu})_2\text{C}_6\text{H}_4$ (E = Si, Ge, Sn) are described. We have been able to prepare the first bis(amido)germylenes and -stannylenes of ruthenium, as well as the first gold complexes containing neutral stannylenes. The currently small family of germylene-gold complexes has also been enlarged. In all these reactions, the volume and the cyclic or acyclic nature of the HT play an important role in the processes that determine the nature of the final products.

Part II deals with reactions of intramolecularly stabilized cyclic HTs that contain amidinato groups, particularly $\text{E}(\text{RR}'\text{bzam})\text{X}$ (E = Si, Ge; R, R' = organic groups; X = anionic group; bzam = benzamidinate), with $[\text{Ru}_3(\text{CO})_{12}]$, $[\text{Co}_2(\text{CO})_8]$ and $[\text{MnBr}(\text{CO})_5]$. Chapter 3 describes the reactivity of the germylene $\text{Ge}(\text{Pr}_2\text{bzam})(\text{HMDS})$ with the metallic precursors mentioned above. Chapter 4 deals with the influence exerted by R and R' groups (Pr, ^tBu or Et) and the E atom (Si or Ge) on the reactivity of the HTs $\text{E}(\text{RR}'\text{bzam})(\text{HMDS})$. Chapter 5 describes the different results that were obtained when the germylene X group was changed to ^tBu (from HMDS). All these electronic and steric modifications have allowed us to find new reactivity patterns and very different coordination modes for amidinato-HTs that, in some cases, had never been observed before. For example, the synthesis of binuclear ruthenium or cobalt complexes with a novel bidentate $\mu\text{-}\kappa^2\text{Ge},\text{N}$ -amidinato-TP ligand, and the synthesis of mononuclear manganese complexes containing unprecedented $\kappa^2\text{Ge},\text{N}$ -iminegermanato ligands are remarkable. We have also demonstrated that the bidentate $\mu\text{-}\kappa^2\text{Ge},\text{N}$ -coordination mode is only possible when at least one N-R group of the amidinato-HT is smaller than a *tert*-butyl group. The complexes described in this part are quite stable and some of them have been used as precursors in subsequent studies, for example, in reactions with nucleophiles (neutral or anionic), activation of inorganic H-X bonds (X = H, SiEt₃, SnPh₃) to give coordinatively unsaturated derivatives, reversible reactions with CO, thermolysis and hydrolysis studies, and electrochemical reduction of CO₂. Finally, Chapter 6 comprehensively reviews the current state of the art (2015) of the chemistry related to amidinato-HT-M complexes.

Quiero expresar mi más sincero agradecimiento:

Al profesor Javier A. Cabeza y al Dr. Pablo García Álvarez, por confiar en mí durante estos años y por ayudarme en todo momento a lanzar mi carrera. Os doy las gracias por haberme enseñado todo lo que sé, pero, sobre todo, por transmitirme vuestra pasión por la investigación.

A José M. Fernández Colinas y a Ignacio del Río, por ayudarme en mis primeros pasos como investigador e introducirme en el mejor grupo posible.

Al Dr. Pablo García Álvarez, por la resolución de la mayoría de las estructuras de rayos-X que se recogen en este trabajo y al Dr. Enrique Pérez Carreño, por la realización de los cálculos teóricos.

Al Ministerio de Economía y Competitividad (MINECO), por la ayuda predoctoral que me ha permitido llevar a cabo esta tesis doctoral.

A Inés y a los compañeros que he tenido, tanto de mi laboratorio como de otros del departamento, por su ayuda y por los buenos momentos vividos. En especial me gustaría agradecer a Laura, Brugos y Rober, por hacerme muy ameno estos últimos meses de escritura. A Luci, por ser la mejor compañera que se puede tener y estar siempre dispuesta a ayudarme, a apoyarme y, por supuesto, a liarla parda siempre que fuera necesario. Te has convertido en una verdadera amiga dentro y, sobre todo, fuera del laboratorio, algo que es muy difícil conseguir. Esta amistad es, sin duda, lo más valioso que me llevo porque estoy convencido que va a durar siempre.

A toda mi familia, por su apoyo durante estos años. De manera especial a mis padres, que se desviven todos los días por mí y que siempre están dispuestos a ayudarme en todas las facetas de mi vida. Algún día espero poder compensar todo vuestro esfuerzo.

Por último quiero agradecer de manera muy especial a Eva, por ser mi compañera de viaje en absolutamente todo lo que hago. Me faltan palabras para poder expresar todo lo que haces por mí, lo mucho que me apoyas y lo especial que me haces sentir siempre. Los momentos más felices de mi vida han sido posibles gracias a ti, pero estoy seguro que los mejores momentos están aún por llegar y que siempre estaremos juntos para vivirlos. Gracias por ser como eres y por haber cambiado mi mundo.

Abreviaturas











Ar	arilo
bzam	benzamidinato
Bu	butilo
^t Bu	<i>tert</i> -butilo
°C	grado Celsius
cm	centímetro
CNH	carbeno <i>N</i> -heterocíclico
COD	1,5-ciclooctadieno
COE	cicloocteno
Cp	ciclopentadienilo
Cp*	pentametilciclopentadienilo
Cy	ciclohexilo
d	débil
D	grupo dador
DAB	1,4-di- <i>is</i> opropil-1,4-diaza-1,3-butadieno
Dipp	2,6-di- <i>is</i> opropilfenilo
dmpe	1,2-bis(dimetilfosfano)etano
dppm	bis(difenilfosfano)metano
dppe	1,2-bis(difenilfosfano)etano
DFT	Density Functional Theory
Et	etilo
equiv.	equivalente
f	fuerte
h	hora
HMDS	hexametildisililazanuro
I	Introducción

IP	Introducción a la Parte II
IR	infrarrojo
K	grado Kelvin
L	ligando genérico
m	intensidad media
Me	metilo
Mes	mesitilo (2,4,6-trimetilfenilo)
mf	muy fuerte
min	minuto
M	metal de transición
NBO	Natural Bond Orbital
NOE	Nuclear Overhauser Effect
Np	<i>neo</i> -pentilo
ⁱ Pr	<i>iso</i> -propilo
OP	Objetivos y Planteamiento
o-tol	<i>orto</i> -tolilo
OTf	triflato
Ph	fenilo
ppm	parte por millón
<i>p</i> -tol	<i>para</i> -tolilo
pyt	piridina-2-tionato
RMN	Resonancia Magnética Nuclear
THT	tetrahidrotiofeno
TMS	trimetilsililo
TP	tetrileno pesado
TPNH	tetrileno pesado <i>N</i> -heterocíclico
S	separador
SCE	saturated calomel electrode

Índice

Introducción:	1
I.1. Los tetrilenos pesados (TPs)	3
I.2. Aspectos generales de la química de coordinación de los tetrilenos pesados	5
I.3. Tipos de tetrilenos pesados en química de coordinación	8
I.4. Desarrollo de la química de coordinación de los tetrilenos pesados	10
I.4.1. Tetrilenos pesados acíclicos	10
I.4.2. Tetrilenos pesados cíclicos simples	11
I.4.3. Tetrilenos pesados cíclicos estabilizados intramolecularmente	14
I.5. Modos de coordinación de los tetrilenos pesados	18
Objetivos y Planteamiento de la Memoria	23
Discusión de Resultados – Parte I: Incorporación de tetrilenos pesados acíclicos y cíclicos simples a complejos de metales de transición	29
Capítulo 1. Reactividad de tetrilenos pesados acíclicos y cíclicos simples con $[\text{Ru}_3(\text{CO})_{12}]$	31
1.1. Introducción	33
1.2. Resultados	35
1.3. Conclusiones	40
Capítulo 2. Reactividad de tetrilenos pesados acíclicos y cíclicos simples con $[\text{AuCl}(\text{THT})]$	43
2.1. Introducción	45
2.2. Resultados	48
2.3. Conclusiones	51

Discusión de Resultados – Parte II: Incorporación de tetrilenos pesados cíclicos estabilizados intramolecularmente (amidinato-TPs) a complejos de metales de transición	53
Introducción a la Parte II	55
Capítulo 3. Nuevos modos de coordinación de los amidinato-TPs	63
3.1. Introducción	65
3.2. Resultados	65
3.3. Conclusiones	71
Capítulo 4. La influencia de pequeños cambios en el volumen del fragmento amidinato	73
4.1. Introducción	75
4.2. Resultados	75
4.3. Conclusiones	79
Capítulo 5. Aumentando la capacidad de coordinación de los amidinato-TPs	81
5.1. Introducción	83
5.2. Resultados	84
5.3. Conclusiones	92
Capítulo 6. Revisión de la química de coordinación de los amidinato-TPs	93
6.1. Presentación de la revisión	95
6.2. Conclusiones	95
Conclusiones Generales	97
Referencias	101

Publicaciones	115
Artículo I	
Artículo II	
Artículo III	
Artículo IV	
Artículo V	
Artículo VI	
Artículo VII	
Artículo VIII	
Artículo IX	
Artículo X	

Introducción

I.1. Los tetrirenos pesados (TPs)

La química de los parientes más pesados de los carbenos, que responden a la fórmula general EX_2 (sililenos $E = Si$, germilenos $E = Ge$, estannilenos $E = Sn$, plumbilenos $E = Pb$; $X =$ grupo aniónico) y que son conocidos comúnmente como tetrirenos pesados (TPs) o metalilenos, está cobrando mucha importancia en los últimos años.¹⁻⁴ El estado de oxidación del átomo central E de estos compuestos EX_2 es +2 y su estabilidad suele ser mayor al bajar en el grupo 14. De hecho, mientras que los dicloruroderivados $PbCl_2$ y $SnCl_2$ son compuestos totalmente estables, el $GeCl_2$ se comercializa estabilizado con dioxano y el $SiCl_2$ sólo ha podido ser aislado recientemente^{5a} formando un aducto con un carbeno N -heterocíclico (CNH).

Los TPs tienen, en general, un comportamiento químico muy diferente del de los carbenos. Las principales causas de esta diferencia son tres. En primer lugar, los elementos del grupo 14 más pesados que el carbono tienen una menor tendencia a formar orbitales híbridos porque la separación energética existente entre los orbitales s y p aumenta a medida que se baja en el grupo; por ejemplo, en base a cálculos teóricos, la diferencia de energía entre el estado triplete y el estado singlete para las especies EH_2 es de 16.7 ($E = Si$), 21.8 ($E = Ge$), 24.8 ($E = Sn$) y 34.8 ($E = Pb$) kcal mol⁻¹ (su estado fundamental es un singlete),⁶ mientras que para CH_2 es -14.0 kcal mol⁻¹ (su estado fundamental es un triplete).⁷ A nivel experimental, la dificultad que tienen las moléculas EX_2 para alcanzar su estado triplete se traduce en que los TPs tienen una mayor capacidad para actuar como ácidos de Lewis (su orbital p vacante facilita su reactividad frente a nucleófilos externos) que sus parientes los carbenos. Además, su fortaleza como bases de Lewis no es muy elevada, especialmente en comparación con la de carbenos de tipo singlete como los CNHs, debido al aumento del carácter s del par de electrones al bajar en el grupo 14.⁸ En segundo lugar, las posibles interacciones de tipo mesomérico entre el orbital vacante p del átomo E y los orbitales llenos con simetría π presentes en los sustituyentes (grupos halogenuro, alcóxido, amida, etc) son menos efectivas al bajar en el grupo porque aumenta el tamaño del orbital p . Esto tiene como consecuencia que, por ejemplo, los CNHs, donde las interacciones existentes entre los pares de electrones de los sustituyentes nitrogenados y el orbital p del átomo carbénico son muy fuertes, sean especies casi exclusivamente dadoras.⁹ Sin embargo, los TPNHs (tetrirenos pesados N -heterocíclicos) son capaces de aceptar densidad π (por ejemplo, por retrodonación en complejos metálicos) en ese orbital p , ya que no está tan estabilizado mesoméricamente.¹⁰ En último lugar, el mencionado mayor tamaño de los elementos E (y por tanto el de sus orbitales) y su menor electronegatividad hacen que los enlaces $E-X$ sean normalmente más débiles y más polares que los $C-X$, lo que se traduce

en que los grupos X de los TPs tienden a participar también en las reacciones de estas especies (ver más adelante). La Figura I.1 muestra las características generales de las moléculas EX_2 , las cuales se acentúan cuanto más se baja en el grupo 14.

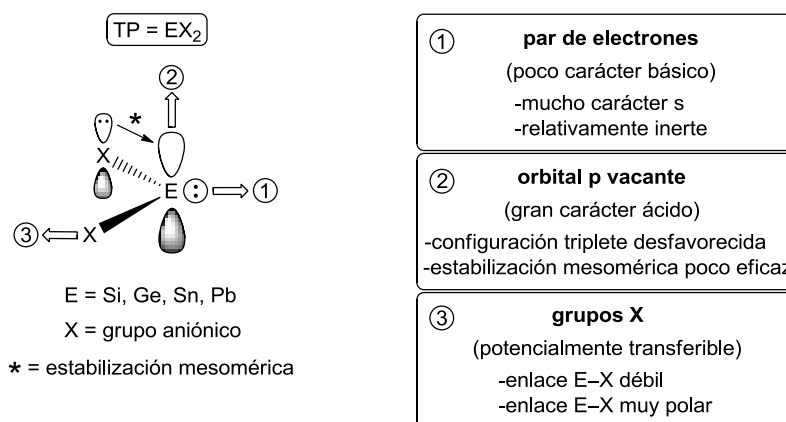


Figura I.1. Características generales de los TPs

La reactividad general de los TPs, condicionada por las características anteriormente descritas, es muy amplia y ha sido recogida en varias revisiones bibliográficas.²⁻⁴ Por ejemplo, los TPs son capaces de: (i) formar aductos actuando como ácidos o como bases de Lewis, lo que permite estabilizar sililenos tan inestables como el $SiCl_2$ ^{5a} o formar aductos con ácidos como los boranos,^{3f,3h,11} (ii) participar en procesos redox, por ejemplo, reduciendo calcógenos,¹² (iii) insertarse en enlaces σ , activando, por ejemplo, enlaces inertes como C-F,¹³ (iv) participar en procesos de adición, activando moléculas como el CO_2 ¹⁴ (v) promover procesos de cicloadición, dando lugar a metalaciclos,¹⁵ (vi) modificar sus grupos X, por ejemplo, en reacciones de transaminación,¹⁶ y, por supuesto, (vii) actuar como ligandos frente a metales de transición (Ms) (Figura I.2).³⁻⁴

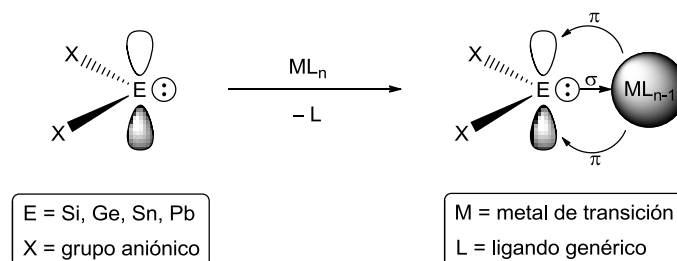
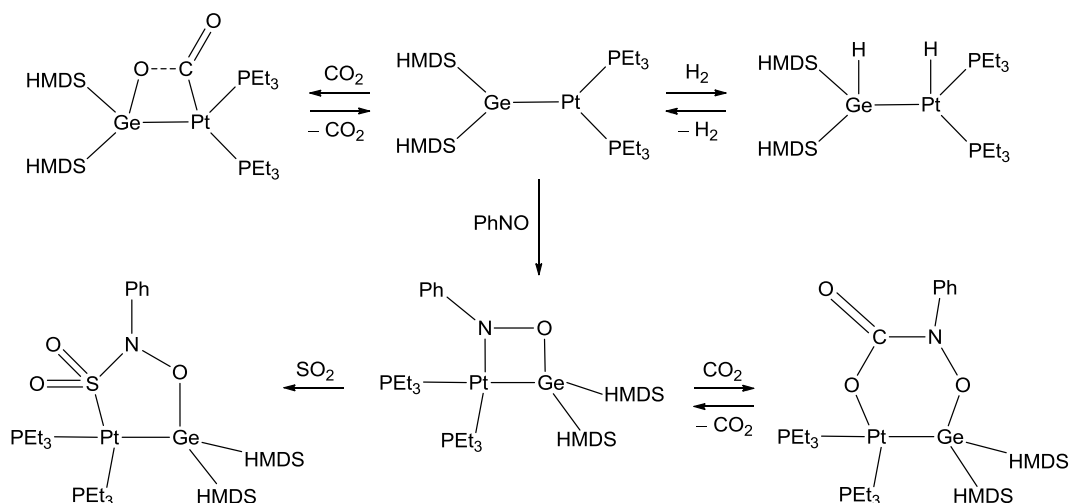


Figura I.2. Coordinación de TPs a Ms

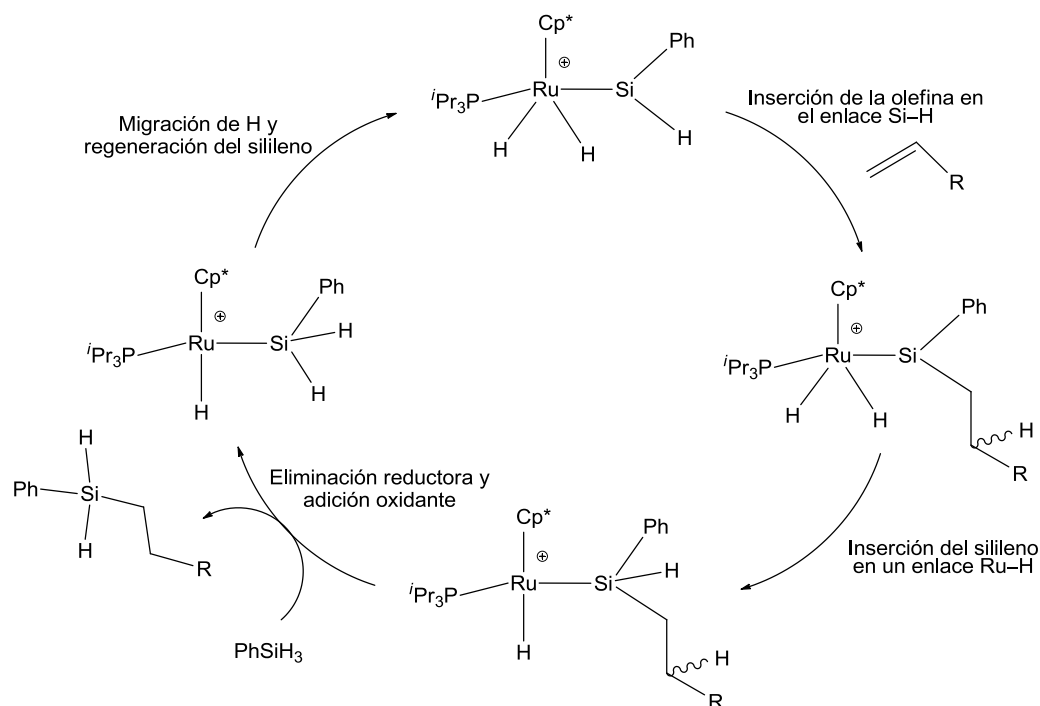
I.2. Aspectos generales de la química de coordinación de los tetrienos pesados

Se conocen complejos de los tetrienos pesados con casi todos los Ms de la tabla periódica.³⁻⁴ Es destacable que la presencia del orbital vacante p sobre el átomo E y la polaridad de los enlaces E–X hacen que los TPs puedan ser más que simples ligandos espectadores (a diferencia de sus parientes de tipo CNH). En algunas ocasiones, la naturaleza no inocente de los TPs y su cooperación con el M al que se encuentran coordinados han demostrado ser claves en procesos de interés y/o poco convencionales. Por ejemplo, Holl y colaboradores han descrito que moléculas pequeñas de alto valor sintético, como H₂ o CO₂, pueden activarse de modo reversible usando un derivado bis(amido)germilenos de platino (Esquema I.1).¹⁷ Este mismo complejo es capaz de activar sustratos de tipo arilnitroso, facilitando la posterior formación de nuevos enlaces N–C y N–S por reacción del metalacido formado con moléculas insaturadas como CO₂, SO₂, H₂CO y PhNCO (Esquema I.1).¹⁸



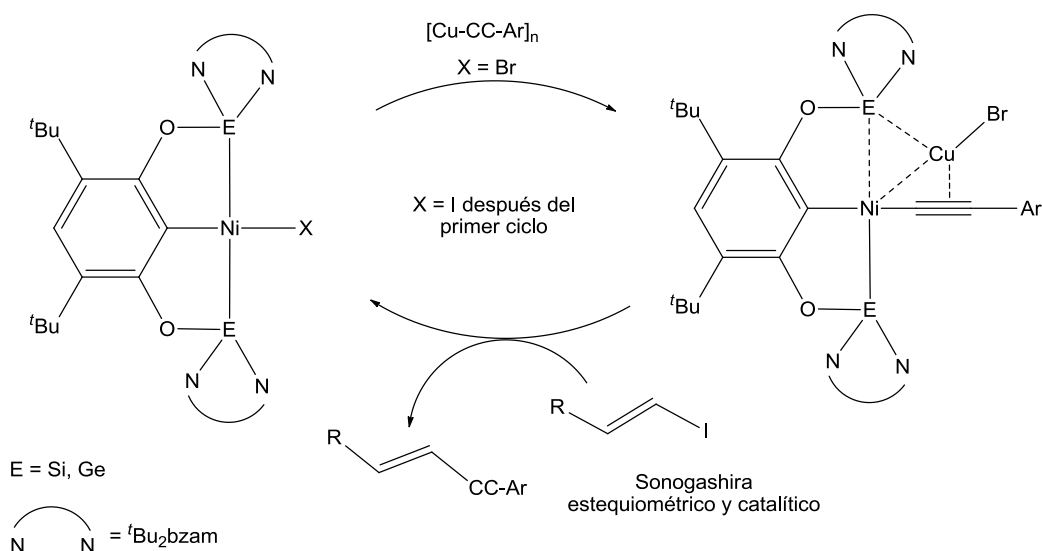
Esquema I.1. Activación de H₂, CO₂ y PhNO por un bis(amido)germilenos de platino y posteriores reacciones del metalacido PtGeON con SO₂ y CO₂

Son muy importantes las contribuciones de Tilley,^{4c,19} que ha demostrado que, por ejemplo, algunos complejos catiónicos de rutenio o iridio con aril(hidruro)sililenos catalizan la hidrosililación de olefinas a través de un mecanismo novedoso que implica una primera inserción de la olefina en el enlace Si–H y la inserción posterior del silileno generado en un enlace metal–hidruro (Esquema I.2), formándose de este modo silanos secundarios con una selectividad *anti*-Markovnikov inusualmente alta.¹⁹

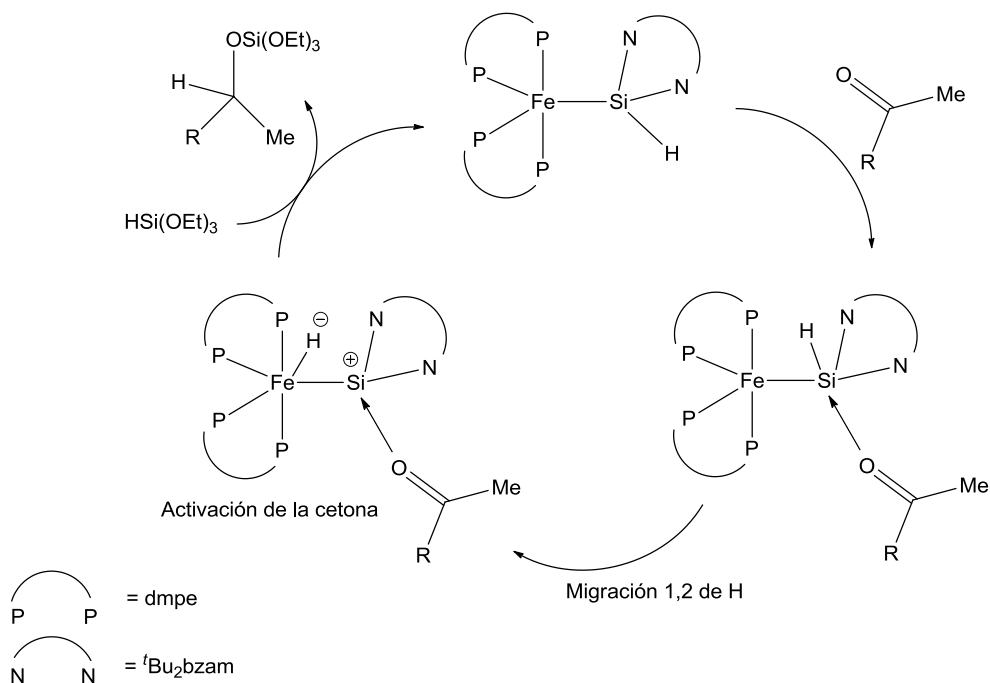


Esquema I.2. Hidrosililación de olefinas promovida por un complejo fenil(hidruro)silileno de rutenio

Recientemente, los grupos de Driess y Hartwig han publicado que los complejos con ligandos de tipo pincer [(LCL)NiBr], donde L son fragmentos amidinato(alcoxi)silileno o -germileno, son catalizadores activos en reacciones de tipo Sonogashira,²⁰ con actividades comparables a las de derivados isoelectrónicos con ligandos pincer PCP.²⁰ Resulta muy interesante que la especie catalíticamente activa es un aducto entre el níquel, uno de los átomos E del pincer y el CuBr liberado en la etapa inicial de transmetalación (Esquema I.3). El propio Driess, ha descrito la capacidad que tiene un ligando amidinato(hidruro)silileno coordinado a un complejo de hierro para activar varias cetonas y promover su hidrosililación catalítica con excelentes conversiones, estableciendo que el paso determinante de la reacción es una migración 1,2 desde el hidrógeno del silileno al átomo de hierro, la cual está promovida por la formación previa de un aducto ácido-base entre la cetona y el silileno (Esquema I.4).²¹



Esquema I.3. Acoplamiento de tipo Sonogashira donde un amidinato(alcoxi)-TP coopera con níquel y cobre para formar la especie catalíticamente activa



Esquema I.4. Hidrosililación de cetonas promovida por un amidinato(hidruro)sileno de hierro

Los antecedentes descritos demuestran que el binomio TP-M, cuya reactividad puede centrarse no sólo en el metal, posee un gran potencial a la hora de promover transformaciones inalcanzables usando ligandos espectadores convencionales como fosfanos o CNHs. Sin embargo, a pesar de estas premisas, la química de coordinación de

los TPs, fundamentalmente en lo que se refiere a estudios sistemáticos de reactividad y/o catálisis con sus complejos, está muy lejos de la madurez alcanzada por la de sus parientes los carbenos y, particularmente, los CNHs. Esto es sorprendente teniendo en cuenta que los primeros bis(amido)-TPs estables se conocen desde los años 70,^{26,22} mucho antes que el primer CNH estable descrito por Arduengo y colaboradores.²³ Este subdesarrollo se debe fundamentalmente a la baja estabilidad de los complejos TP–M, tanto frente al aire y a la humedad (hidrólisis y/u oxidación) como frente a procesos de sustitución (desplazamiento por otros ligandos), ya que los enlaces E–X son muy polares²⁴ y los enlaces E–M son generalmente débiles (tanto más cuanto más abajo esté E en el grupo 14 de la tabla de periodos).²⁵

1.3. Tipos de tetrilenos pesados en química de coordinación

Los ligandos TPs pueden clasificarse en tres grupos básicos (Figura 1.3): (i) acíclicos: equipados con grupos X terminales, (ii) cíclicos simples: equipados sólo con un fragmento dianiónico que actúa como quelato frente al átomo E, y (iii) cíclicos estabilizados intramolecularmente: equipados con uno o más fragmentos SD monoaniónicos (S = separador, D = átomo dador). En este último grupo, el átomo D del fragmento SD interacciona con el orbital p del átomo E formando un aducto ácido-base. Estos tres tipos básicos de TPs pueden acoger numerosas variaciones más complejas, como aquellas que también implican dadores externos, neutros o aniónicos (D = CNHs, PR₃, Cl). En la Figura 1.3 se recogen varios ejemplos ilustrativos^{21,26} de cada uno de los grupos descritos.

La preparación de complejos TP–M, derivados de cualquiera de los tres tipos de tetrilenos pesados que se muestran en la Figura 1.3, se lleva a cabo generalmente usando los TPs en estado puro como reactivos, con las dificultades que ello conlleva por su inestabilidad frente al aire y a la humedad. Esto supone una desventaja frente a la mayoría de CNHs, que generalmente no necesitan ser aislados para la preparación de sus complejos metálicos (p. ej., los imidazol-2-ilidenos se pueden generar *in situ* desprotonando sales de imidazolio). Esta complicación se acentúa en el caso de los sililenos, que se tienen que preparar por reducción de derivados de silicio(IV) al no haber precursores de silicio(II) de fácil acceso.^{4c} Cabe mencionar que existen otras vías menos comunes para generar complejos TP–M sin la necesidad de partir de un TP aislado y que han sido fundamentalmente desarrolladas para la síntesis de complejos con sililenos; por ejemplo: (i) la doble metátesis de especies ER₂X₂ (X = halogenuro) con precursores metálicos como K₂[Fe(CO)₄] o Na[Cr(CO)₅],²⁷ (ii) la abstracción de grupos aniónicos (Y) de especies del tipo R₂YE–M (Y = Cl, OTf) utilizando agentes electrofílicos como Na[BPh₄] o Li[B(C₆F₅)₄],²⁸ (iii) la

migración 1,2, normalmente de un ligando hidruro, en especies de tipo R_3E-M , promovida por la generación de una vacante de coordinación en el metal de transición,²⁹ (iv) la captura con un complejo metálico adecuado de especies ER_2 inestables generadas fotoquímicamente,³⁰ (v) la metátesis de fragmentos dianiónicos $[ER_2]^{2-}$ con dihalogenuros metálicos (p. ej., $[TiCp_2Cl_2]$),³¹ (vi) la adición oxidante de especies HER_3 a clusters de metales de transición seguida de una eliminación de HR ,³² etc.

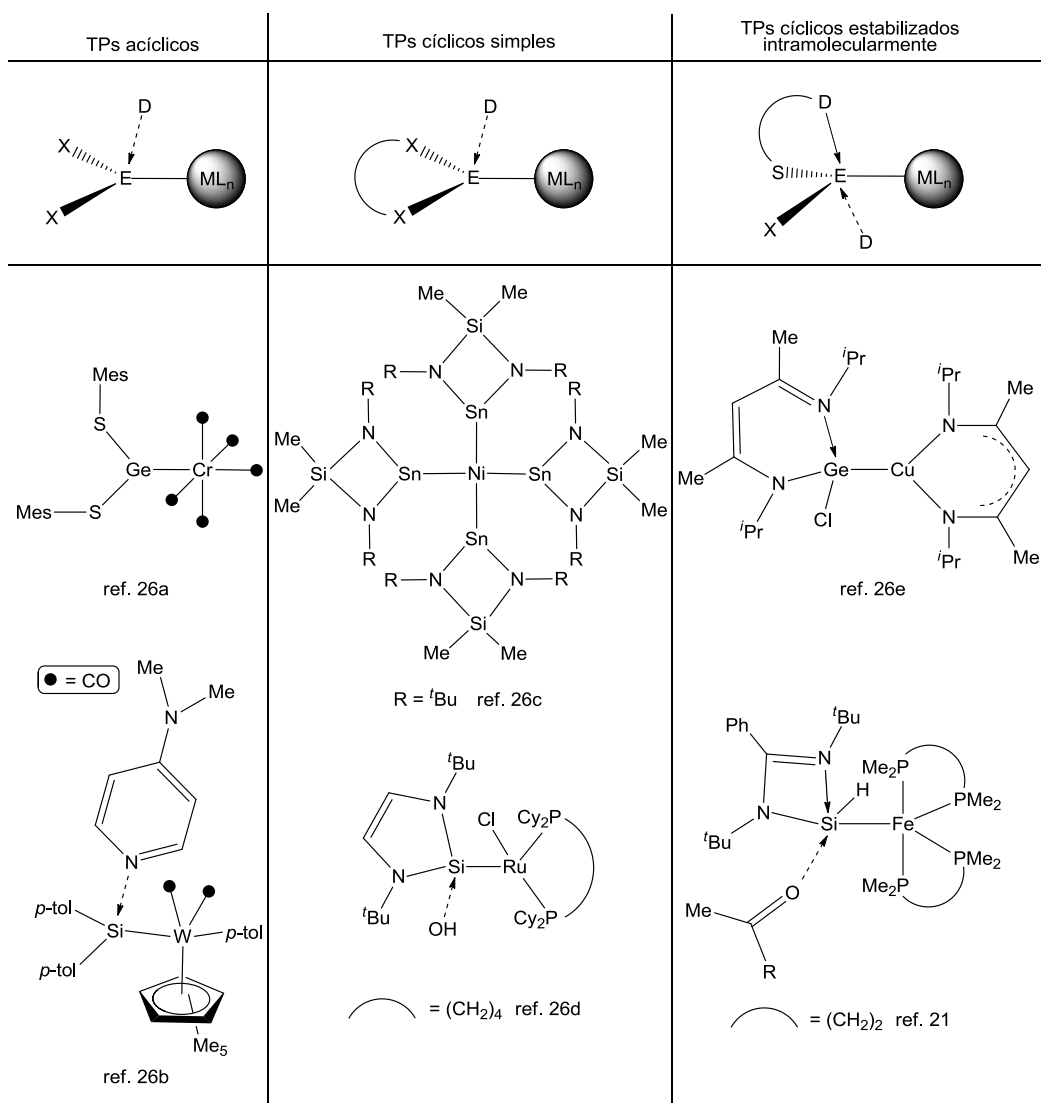


Figura 1.3. Tipos de ligandos TP básicos en química de coordinación (arriba) y ejemplos ilustrativos (abajo) de complejos con metales de transición

I.4. Desarrollo de la química de coordinación de los tetrilenos pesados

A pesar de los problemas mencionados a nivel de síntesis y estabilidad relacionados con los tetrilenos pesados, su química de coordinación a Ms no ha dejado de avanzar desde los años 70. Puesto que la vía de síntesis principal de los complejos TP–M requiere utilizar TPs puros como reactivos, la evolución de esta química de coordinación ha estado condicionada, a menudo, por la disponibilidad de nuevos TPs que sean suficientemente estables para su aislamiento y manejo. En los siguientes apartados se describen los TPs que más se han utilizado en química de coordinación. Este análisis sigue la clasificación hecha en el apartado I.3 (Figura I.3).

I.4.1. Tetrilenos pesados acíclicos

Los dihalogenuro-TPs son la versión más simple de los TPs acíclicos (p. ej., GeCl_2 -dioxano, SnCl_2 y PbCl_2 ; Figura I.4, compuestos **A**) y su uso como ligandos frente a metales de transición se conoce desde hace muchos años.^{2e,4f,33} Sin embargo, éstos se usan principalmente, tanto en su estado libre como ya coordinados a metales de transición, para la síntesis de TPs o TP–Ms más complejos, respectivamente, mediante procesos de metátesis de los grupos halogenuro. Por su parte, los dihalogenurosililenos (SiX_2) son especies que no han podido ser aisladas a temperatura ambiente, ya que se condensan para formar SiX_2 polimérico o se desproporcionan a Si metal y SiX_4 .³⁴ Sólo recientemente, los grupos de Roesky^{5a} y Filippou^{5b} han conseguido estabilizar SiCl_2 y SiBr_2 , respectivamente, mediante la formación de aductos con CNHs muy voluminosos (Figura I.4, compuestos **B**). Estos aductos, aunque todavía no se han utilizado como precursores para preparar otros sililenos en estado libre, ya han demostrado tener una excelente capacidad para actuar como ligandos frente a metales de transición.^{3a}

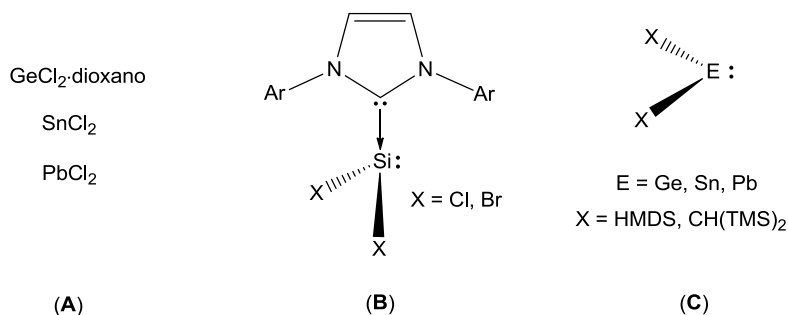


Figura I.4. Ejemplos representativos de TPs acíclicos utilizados en química de coordinación

La familia de TPs acíclicos que han dado lugar al mayor número de complejos metálicos^{4e,f} son los bis(amido)- o bis(alquil)-TPs desarrollados por Lappert y colaboradores en los años 70 (p. ej., $E(\text{HMDS})_2$ y $E[(\text{CH}(\text{TMS})_2)_2]$, donde $E = \text{Ge}, \text{Sn}, \text{Pb}$; $\text{HMDS} = \text{N}(\text{SiMe}_3)_2$; $\text{TMS} = \text{SiMe}_3$; Figura I.4, compuestos **C**).^{22a,b,e} Estos tetrilenos pesados están provistos de grupos muy voluminosos unidos al átomo E para aumentar su estabilidad. Existen estudios de reactividad muy interesantes con complejos metálicos equipados con TPs de Lappert, como, por ejemplo, los descritos en la Esquema I.1.¹⁷ La alta inestabilidad de los TPs acíclicos de silicio no estabilizados por donores adicionales ha dificultado su uso como ligandos en química de coordinación. Por ejemplo, la versión de silicio de los compuestos bis(amido) de Lappert, $\text{Si}(\text{HMDS})_2$,³⁵ fue caracterizada por West en el año 2003, encontrando que su vida media es de 12 h a $-20\text{ }^\circ\text{C}$ y de unos pocos minutos a $0\text{ }^\circ\text{C}$.

I.4.2. Tetrilenos pesados cíclicos simples

La Figura I.5 muestra algunos ejemplos representativos de TPs cíclicos simples que han sido utilizados en química de coordinación. Entre estos ejemplos destacan, en primer lugar, los tetrilenos pesados de Veith, que responden a la fórmula $E(\text{N}^t\text{Bu})_2\text{SiMe}_2$ ($E = \text{Ge}, \text{Sn}, \text{Pb}$; Figura I.5, compuestos **D**).^{2h} Estos TPs, que han sido utilizados como ligandos en numerosos complejos de metales de transición,³⁶ están estabilizados por un fragmento

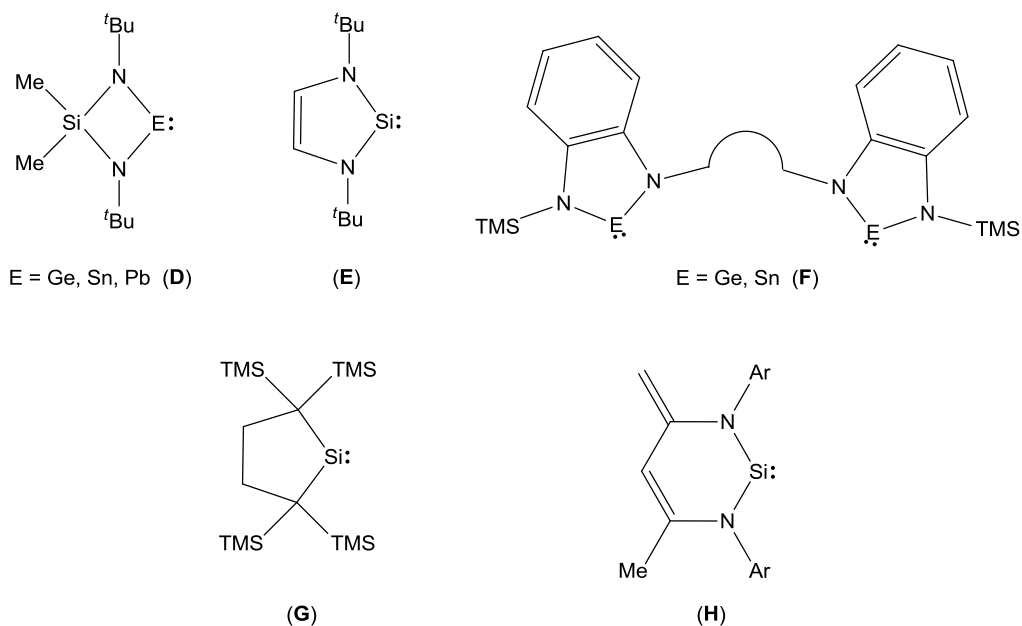
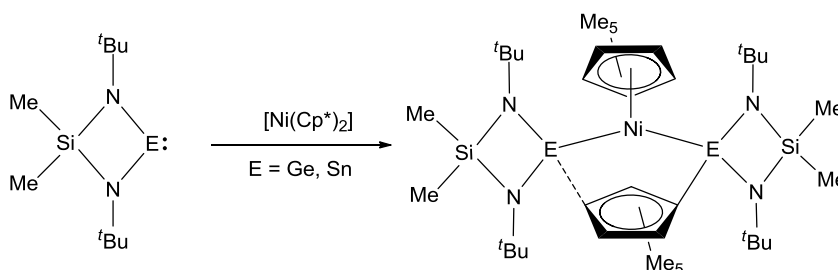


Figura I.5. Ejemplos representativos de TPs cíclicos simples utilizados en química de coordinación

dimetil-*N,N'*-bis(*tert*-butil)siladiazanuro que se une en forma quelato al átomo E, formando un anillo de cuatro miembros. Entre estos complejos destacan los formados por reacción de $E(N^tBu)_2SiMe_2$ ($E = Ge, Sn$) con $[Ni(Cp^*)_2]$, que dan lugar a la inserción de dos unidades de ligando entre el níquel y uno de los anillos Cp^* , quedando patente la capacidad del TP para actuar a la vez como base y como ácido de Lewis (Esquema I.5).^{36f} De nuevo, cabe mencionar que la versión de silicio de estos TPs, concretamente $Si(N^tBu)_2SiMe_2$, sólo es estable a temperaturas inferiores a los 77 K.³⁷



Esquema I.5. Reacciones de TPs de Veith con $[Ni(Cp^*)_2]$

La síntesis del primer silileno cíclico simple estable, llevada a cabo por el grupo de Denk en 1994,³⁸ supuso un gran avance en la química de coordinación de los TPs. Se trata, en concreto, del derivado de tipo imidazol $Si(N^tBu)_2C_2H_2$ (Figura I.5, compuesto **E**), que es análogo a los CNHs de Arduengo.²³ La química de coordinación derivada de este silileno y de sistemas similares equipados con diferentes grupos N-R, ciclos saturados, ciclos benzoanulados, etc., ha sido ampliamente desarrollada por diferentes grupos de investigación^{3j-k} e incluso ha dado lugar a algunas aplicaciones catalíticas. En la Figura I.6

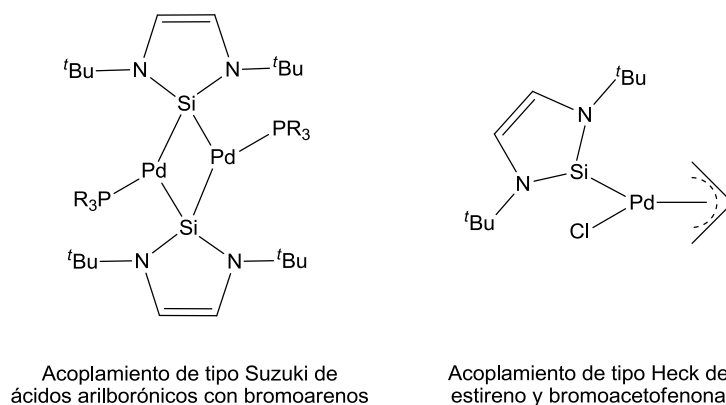


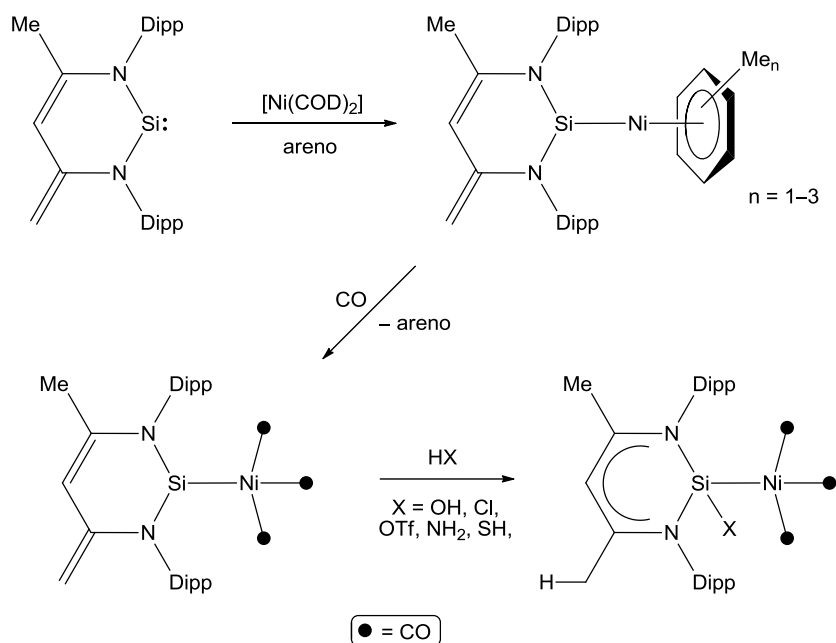
Figura I.6. Ejemplos de complejos metálicos derivados de SiNHs activos en catálisis

se muestran los dos complejos derivados del silileno tipo **E** que han demostrado ser activos en catálisis. El primero de ellos (Fürstner, 2001; Figura I.6, izquierda) es un dímero de

paladio capaz de promover acoplamientos de tipo Suzuki de ácidos arilborónicos con bromoarenos.³⁹ El segundo (Figura I.6, derecha) es un complejo de paladio sintetizado por el grupo de Roesky en 2008, que demostró ser un precatalizador muy activo en reacciones de acoplamiento de tipo Heck de estireno y acetofenona.⁴⁰ La química de coordinación de los TPs más pesados que el silicio análogos a **E** también ha sido considerablemente estudiada.^{39-i,41,42} De hecho, los estannilenos (Schuefler y Zuckerman en 1974)^{22d} y germilenos (Meller en 1989)⁴³ análogos a **E** fueron sintetizados bastante antes que el propio silileno. Con estos sistemas, destacan las aportaciones durante la primera década de los 2000 del grupo de investigación de Hahn, usando, entre otros, germilenos y estannilenos bidentados con ciclos benzoanulados (Figura I.5, compuestos **F**).⁴²

Más adelante, en 1999, Kira y colaboradores consiguieron aislar el primer silileno cíclico no estabilizado por átomos de nitrógeno, el derivado dialquílico $\text{Si}\{\text{C}(\text{TMS})_2\}_2\text{C}_2\text{H}_4$ (Figura I.5, compuesto **G**).^{44a} Su química de coordinación, dada la baja estabilidad de este silileno, se ha desarrollado muy poco, restringiéndose fundamentalmente a complejos de los grupos 10 y 11 de la tabla periódica.^{3e,45} Los análogos a **G** de germanio^{44b} y estaño^{44c} también existen, pero no se conoce ningún complejo derivado de los mismos.

Finalmente, el grupo de Driess ha descubierto recientemente el primer silileno estable de tipo heterofulveno (Figura I.5, compuesto **H**),^{46a} que ha permitido llevar a cabo estudios de reactividad muy interesantes con sus complejos,^{4b,47} principalmente con derivados de níquel (Esquema I.6). Entre otras características, los complejos que contienen sililenos de tipo heterofulveno sufren reacciones de adición 1,4 al silileno con moléculas de diferente naturaleza (H_2O , HOTf, HCl, H_2S , NH_3 , etc) que dan lugar a derivados que contienen sililenos estabilizados intramolecularmente por un fragmento β -dicetiminato (Esquema I.6).^{4b} Hay que destacar que esta es la única vía de síntesis que hasta ahora se ha utilizado para la preparación de complejos con β -dicetiminatosililenos, ya que éstos no son estables en su forma libre.^{46a} El análogo a **H** de germanio^{46b} también existe, pero no se conoce ningún complejo derivado del mismo.

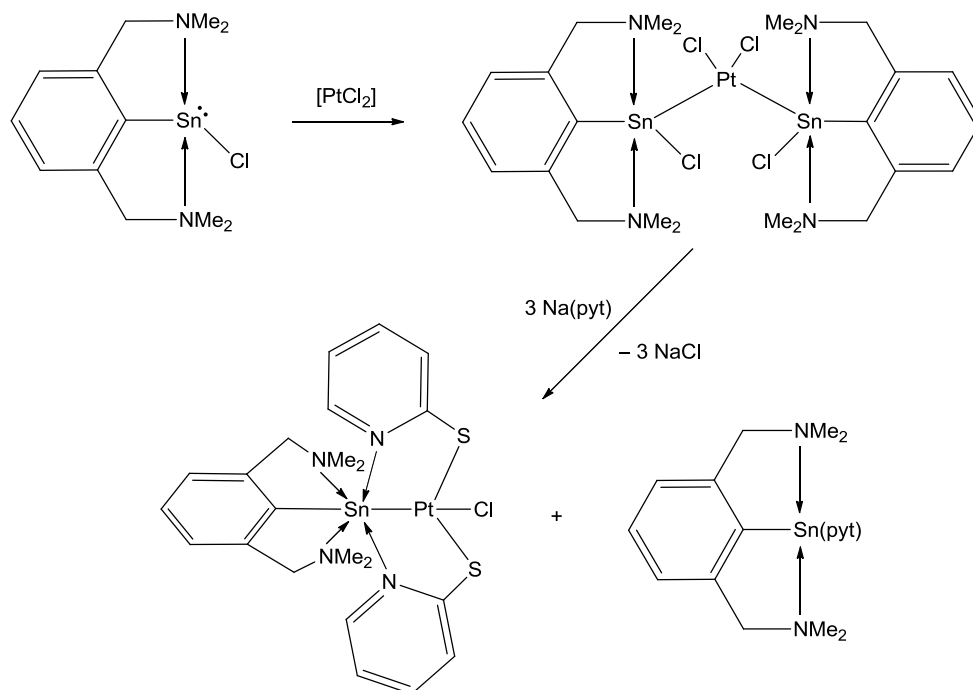


Esquema I.6. Reactividad de un silileno de tipo heterofulveno de níquel frente a moléculas H-X: Síntesis de β -dicetiminatosilenos coordinados

I.4.3. Tetrilenos pesados cíclicos estabilizados intramolecularmente

Como ya se ha mencionado anteriormente, este grupo de TPs posee un fragmento aniónico SD donde el átomo dador D interacciona con el orbital p vacío del átomo E formando un aducto ácido-base. La Figura I.7 muestra algunos ejemplos representativos de los TPs cíclicos estabilizados intramolecularmente más utilizados en química de coordinación, que poseen, como fragmentos SD, grupos β -dicetiminato (Figura I.7, compuestos **I**), β -dicetonato (Figura I.7, compuestos **J**), aminotropiminato (Figura I.7, compuestos **K**), 2,6-bis(D)fenil [D = CH₂NMe₂, P(=O)(OⁱPr)₂] (Figura I.7, compuestos **L**) y amidinato (Figura I.7, compuestos **M**). La química de coordinación de estos TPs está experimentando un notable crecimiento en los últimos años, lo que se debe fundamentalmente a que: (i) son electrónicamente y estéricamente más estables y por tanto más fáciles de manejar que los TPs acíclicos y los cíclicos simples, ya que el aducto dador-aceptor interno les hace menos electrófilos y les otorga una mayor protección estérica (el átomo E es al menos tricoordinado), y (ii) son más fáciles de modificar estéricamente y electrónicamente sin necesidad de rediseñar por completo el ligando, ya que el grupo X, inicialmente un halógeno (ver secciones posteriores), se puede reemplazar fácilmente por otro grupo aniónico.

complejo de platino con dos estannilenos de tipo **L** estabilizados intramolecularmente por grupos dimetilamino y su posterior reacción con Na(pyt). Esta reacción da lugar, gracias a la enorme capacidad del átomo de estaño para formar aductos, a un estannileno catiónico fuertemente estabilizado.^{52f}



Esquema I.7. Síntesis de un complejo bis(estannileno) de platino y posterior transmetalación con Na(pyt)

Finalmente, de los cinco grupos de TPs cíclicos estabilizados intramolecularmente que se han presentado anteriormente en la Figura I.7, aquellos estabilizados por fragmentos amidinato (**M**) se erigen como los más relevantes y se puede decir que han revolucionado la química de coordinación de los tetraenilos pesados en general. De hecho, desde el año 2006, gracias fundamentalmente a la síntesis por el grupo de Roesky⁵³ del primer amidinatosilileno, la química de este tipo de TPs ha crecido exponencialmente, manteniendo hoy una rápida expansión. Cabe destacar que en este corto periodo de tiempo se ha generado una familia de complejos de metales de transición^{20,21,54-56} que incluye metales de la mayoría de los grupos de la tabla periódica (excepto el grupo 3). Más relevante es el hecho de que muchos de estos complejos amidinato-TP-M han demostrado ser catalíticamente activos en procesos de interés, como acoplamiento Sonogashira,²⁰ hidrosililación de cetonas,^{21,56a} reacciones de acoplamiento de halogenuros de arilo con reactivos de Grignard,^{56b} cicloadiciones [2+2+2]^{56c} y reacciones de borilación de enlaces C-H de arenos^{56d} (Figura I.8). Además, es muy interesante el hecho de que, tal y como se

comentó en la sección 1.2, algunas de estas transformaciones catalíticas se llevan a cabo con la participación activa del TP (Esquemas 1.3 e 1.4).

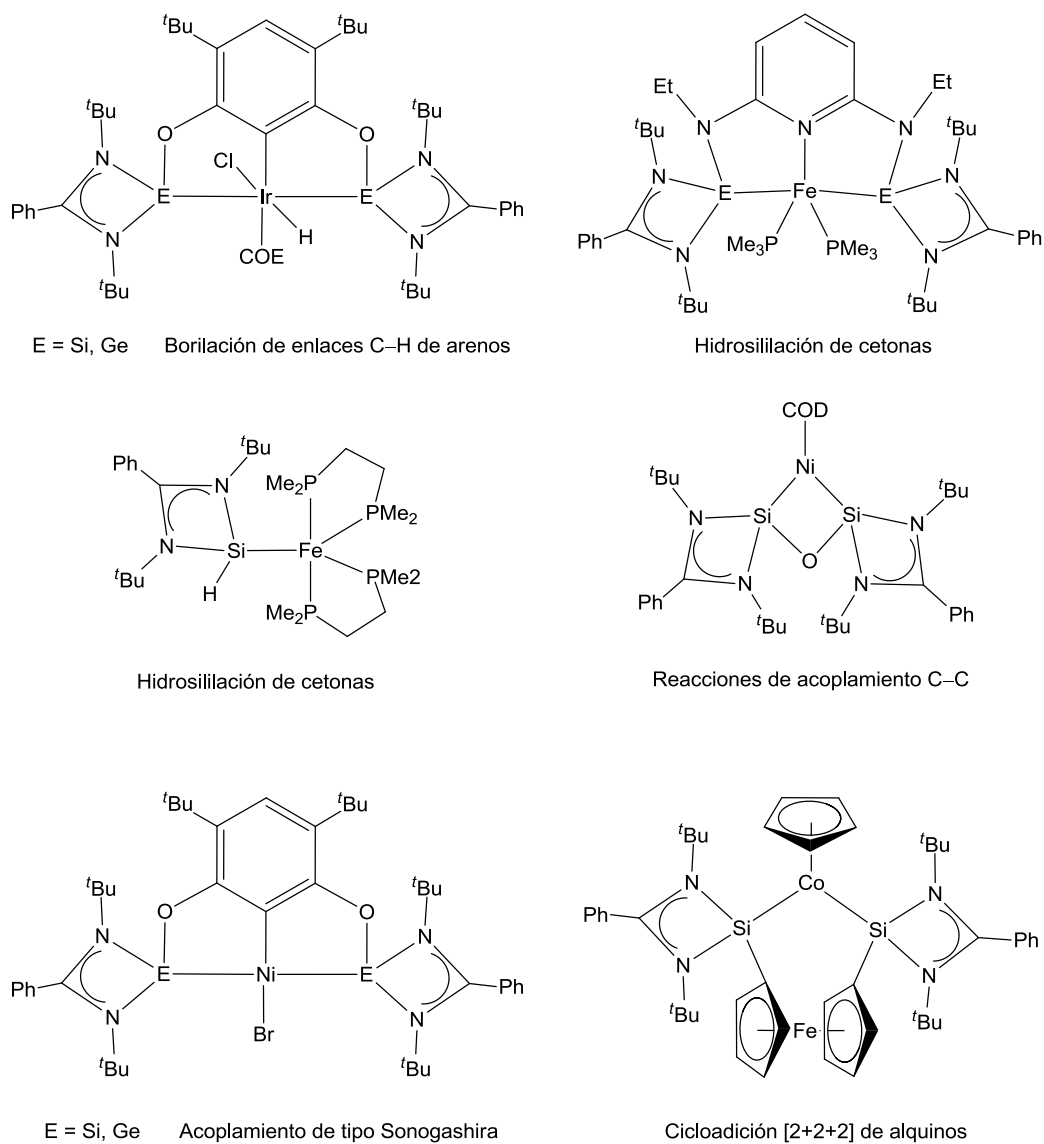


Figura 1.8. Complejos de amidinato-TPs activos en catálisis

I.5. Modos de coordinación de los tetrelenos pesados

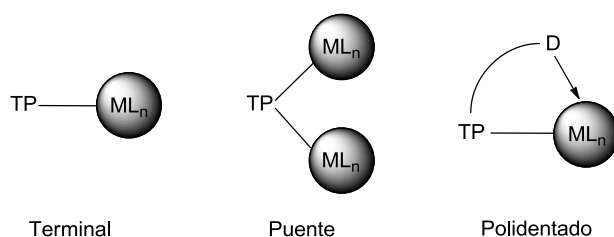


Figura I.9. Los distintos modos de coordinación de los TPs

Los tetrelenos pesados se coordinan a metales de transición siguiendo los tres modos básicos que se muestran en la Figura I.9. La gran mayoría de los complejos que se encuentran descritos contienen TPs que se coordinan de manera monodentada. Menos habitual, aunque también común, es encontrar ligandos TPs que se unen de forma puente. Un ejemplo de estos últimos es el dímero de paladio con dos SiNHs puentes que resulta de la reacción de $[\text{Pd}(\text{PPh}_3)_4]$ con $\text{Si}(\text{N}^t\text{Bu})_2\text{C}_2\text{H}_2$ (Figura I.10 arriba / izquierda).³⁹ Como se mencionó en la sección I.4.2, este complejo, descrito por el grupo de Fürstner, es capaz de catalizar reacciones de tipo Suzuki.³⁹ Otro ejemplo es el formado por reacción del TP de Veith $\text{Ge}(\text{N}^t\text{Bu})_2\text{SiMe}_2$ con $[\text{FeCp}(\text{CO})_2]_2$, en el que el germileno rompe el dímero de hierro precursor para acabar coordinándose en modo puente entre las dos unidades $\text{FeCp}(\text{CO})_2$

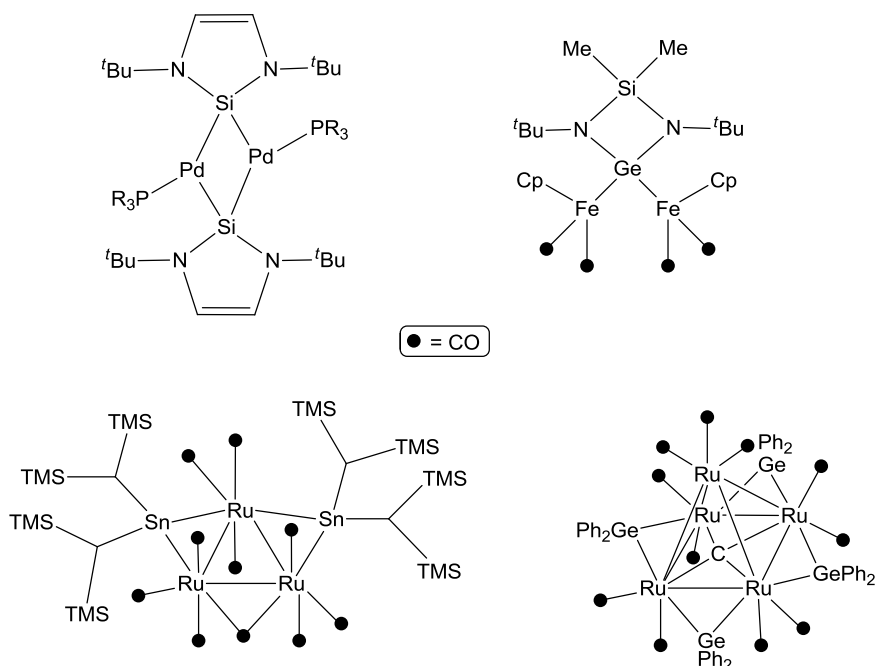


Figura I.10. Ejemplos de complejos que contienen TPs puentes

(Figura I.10, arriba / derecha).^{36e} Muy comunes son los ejemplos de μ -TPs en química de clusters de metales de transición, como los que se muestran en la Figura I.10, sintetizados por los grupos de Cardin⁵⁷ (abajo / izquierda) y Adams^{32g} (abajo / derecha). De hecho, hasta la realización de esta tesis doctoral, no se conocía ningún cluster carbonílico provisto de un ligando TP que no estuviese en modo puente.

La coordinación polidentada en sistemas TP–M a través del átomo E y de otro grupo dador adicional también cuenta con precedentes bibliográficos. Por ejemplo, el grupo de Hahn ha logrado sintetizar varios complejos metálicos que contienen TP's coordinados en modo bidentado, como los derivados de molibdeno que se muestran en la Figura I.11

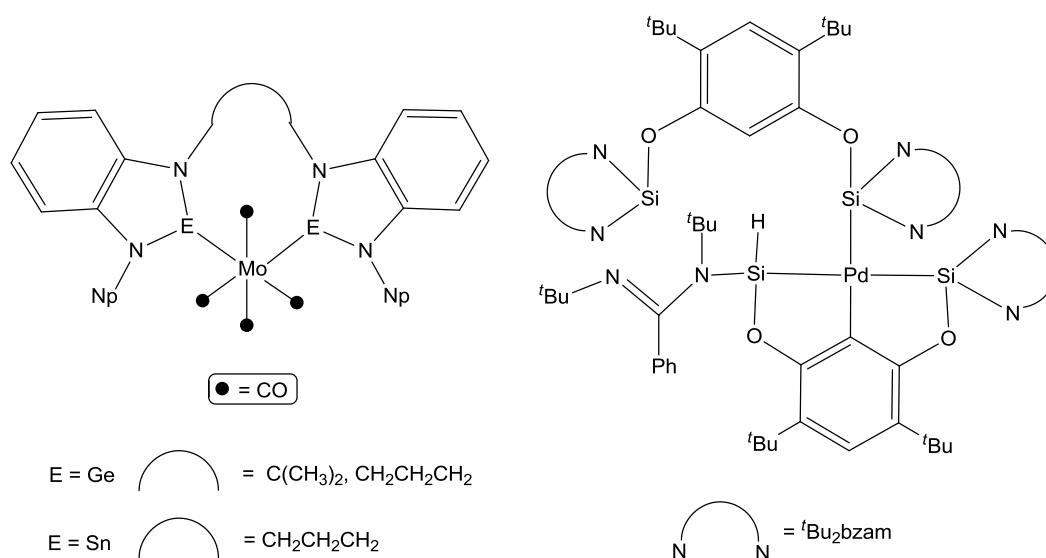
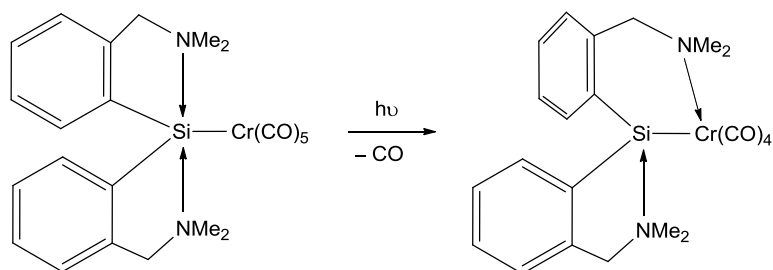


Figura I.11. Ejemplos de complejos que contienen TP's polidentados

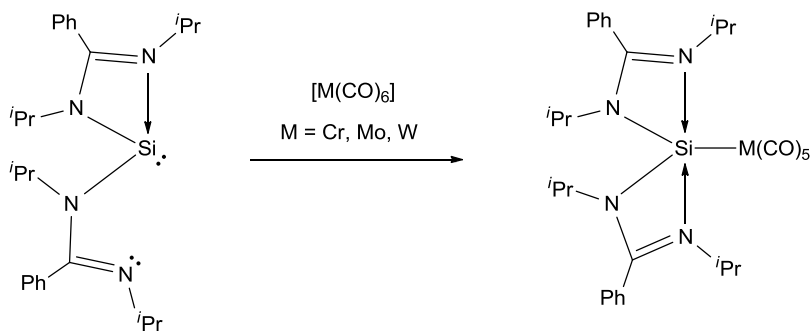
(izquierda).^{16b,42b} En la Figura I.8 también aparecen otros ejemplos de coordinación polidentada, donde destacan los complejos con ligandos tipo pincer ECE de iridio^{56d} y níquel²⁰ y ENE de hierro,^{56a} donde E = Si, Ge. La formación del ligando pincer en los complejos de iridio y níquel, al igual que en el de paladio mostrado en la Figura I.11 (derecha),^{54l} se produce por la activación C–H del anillo de resorcinol que actúa de espaciador entre las dos unidades amidinato-TP. En el caso del complejo de paladio, el hidruro generado como consecuencia de esa activación C–H migra a uno de los átomos de silicio. Los derivados de hierro se obtienen por reacción directa con un ligando tridentado ENE, donde N representa a un grupo piridina.

Cabe destacar que todos los ejemplos de coordinación polidentada de TPs a Ms que hemos comentado se preparan partiendo de TPs que ya son polidentados en su forma libre. Sin embargo, en 1993, el grupo de Auner⁵⁸ describió que un silileno coordinado a cromo es



Esquema I.8. Transformación $\kappa^1\text{Si}$ a $\kappa^2\text{Si},\text{N}$ de un silileno cíclico estabilizado intramolecularmente coordinado a cromo

capaz de cambiar su modo de coordinación de $\kappa^1\text{Si}$ a $\kappa^2\text{Si},\text{N}$. Esto ocurre a través de la migración de un grupo dador NMe_2 , que se encontraba formando un aducto con el átomo de silicio, al centro metálico de cromo (Esquema I.8). Esta transformación (transferencia al metal del grupo dador D de un TP cíclico estabilizado intramolecularmente) no se ha vuelto a observar hasta el desarrollo de esta tesis doctoral, posiblemente porque la coordinación de un TP a un metal a través del átomo E incrementa la acidez de Lewis del mismo, lo que provoca que la interacción del átomo E con el átomo dador D se refuerce. Un ejemplo que ilustra perfectamente este comportamiento ha sido descrito recientemente por el grupo de Tacke.⁵⁴⁰ En él se muestra cómo un bis(amidinato)silileno, que contiene un grupo amidinato terminal y otro quelato cuando se encuentra en su forma libre, pasa a tener los dos amidinatos unidos en modo quelato al átomo de silicio cuando éste se coordina a un fragmento $\text{M}(\text{CO})_5$ ($\text{M} = \text{Cr}, \text{Mo}, \text{W}$). De esta manera, los dos amidinatos compensan el aumento de acidez de Lewis del átomo de silicio (Esquema I.9). En esta tesis veremos que



Esquema I.9. Coordinación de un bis(amidinato)silileno que da lugar al cierre del amidinato terminal sobre el átomo de silicio

el aumento de acidez del TP al unirse al metal de transición no es el único factor que controla la coordinación de los grupos donores D en TPs estabilizados intramolecularmente.

Objetivos y Planteamiento de la Memoria

Los antecedentes expuestos en la Introducción demuestran que el binomio TP–M, cuya reactividad puede no centrarse sólo en el M, posee un gran potencial a la hora de promover transformaciones inalcanzables usando ligandos espectadores convencionales, como fosfanos o CNHs. Sin embargo, por los problemas de estabilidad descritos, la química de coordinación de los TPs, fundamentalmente en lo que se refiere a la realización de estudios sistemáticos de reactividad de sus complejos, está muy lejos de la madurez alcanzada por la de sus parientes los carbenos y, particularmente, los CNHs. Por todo ello, para la presente tesis doctoral nos planteamos, como objetivo general, **ampliar los conocimientos existentes sobre la química de coordinación de los tetrilenos pesados**.

Este objetivo general lo orientamos, en primer lugar, hacia la **síntesis de combinaciones TP–M desconocidas** hasta el comienzo de esta tesis doctoral, llevando a cabo estudios de reactividad de TPs, conocidos o no, con complejos metálicos. En segundo lugar, nos propusimos llevar a cabo **estudios de reactividad y/o catálisis con aquellos compuestos preparados que fueran suficientemente estables**. En tercer lugar, nos planteamos **estudiar el efecto de las modificaciones estéricas y/o electrónicas de los TPs preparados** en su reactividad frente a metales de transición y en la estabilidad y reactividad de los complejos generados.

El trabajo recogido en esta tesis doctoral ha dado lugar, hasta el momento, a la publicación de 10 artículos científicos, por lo que la presente memoria se presenta como compendio de los mismos, divididos en dos bloques principales:

En la **Parte I de la Discusión de Resultados** se recogen los resultados obtenidos en reacciones de tetrilenos pesados acíclicos y cíclicos simples con el cluster de rutenio $[\text{Ru}_3(\text{CO})_{12}]$ (**Capítulo 1**) y con el compuesto de oro $[\text{AuCl}(\text{THT})]$ (**Capítulo 2**). Particularmente, se utilizaron TPs clásicos, como los acíclicos de Lappert $\text{E}(\text{HMDS})_2$ ($\text{E} = \text{Ge}, \text{Sn}$), y los cíclicos simples de tipo imidazol $\text{E}(\text{N}^t\text{Bu})_2\text{C}_2\text{H}_2$ ($\text{E} = \text{Si}, \text{Ge}$) o benzimidazol $\text{E}(\text{NCH}_2^t\text{Bu})_2\text{C}_6\text{H}_4$ ($\text{E} = \text{Si}, \text{Ge}, \text{Sn}$).

En la **Parte II de la Discusión de Resultados** se recogen los resultados obtenidos en reacciones de tetrilenos pesados cíclicos estabilizados por fragmentos amidinato, particularmente $\text{E}(\text{RR}'\text{bzam})\text{X}$ ($\text{E} = \text{Si}, \text{Ge}$; $\text{R}, \text{R}' =$ grupos orgánicos; $\text{X} =$ grupo aniónico; $\text{bzam} =$ benzamidinato), con el cluster trinuclear $[\text{Ru}_3(\text{CO})_{12}]$, con el complejo binuclear $[\text{Co}_2(\text{CO})_8]$ y con el compuesto mononuclear $[\text{MnBr}(\text{CO})_5]$. El planteamiento de esta Parte II, que estuvo motivado en gran medida por los resultados obtenidos en la Parte I, así como las síntesis de los nuevos TPs utilizados (muchos de ellos no conocidos anteriormente), vienen recogidos en la **Introducción a la Parte II**. En el **Capítulo 3** se describe la reactividad del germileno $\text{Ge}(\text{Pr}_2\text{bzam})(\text{HMDS})$ frente a los precursores metálicos mencionados anteriormente. En el **Capítulo 4** se recogen los estudios realizados sobre la influencia de los

grupos R y R' (Pr, ^tBu o Et) y del átomo E (Si o Ge) de los tetrilenos pesados E(RR'^tzám)(HMDS) en la reactividad de los mismos. En el **Capítulo 5** se analizan los cambios de reactividad de los germilenos empleados cuando X = ^tBu en vez de HMDS. Finalmente, en el **Capítulo 6** se incluye una revisión bibliográfica extensa sobre la química de coordinación de los TPs estabilizados por fragmentos amidinato publicada hasta el año 2015.

Cada uno de estos capítulos incluye una breve introducción, un resumen aclaratorio de la discusión incluida en los artículos publicados y las conclusiones parciales de cada trabajo. En la Tabla OP.1 se resume la distribución de los diferentes capítulos en los que está dividida la memoria y las publicaciones asociadas a los mismos.

La exposición de los resultados se completa con una sección de Conclusiones Generales, donde se destacan las aportaciones más relevantes de esta tesis doctoral.

Tabla OP.1. Distribución por capítulos de la presente memoria y publicaciones asociadas

Parte I – Incorporación de TPs acíclicos y cíclicos simples a complejos de Ms	
Capítulos	Publicaciones
1. Reactividad de tetrilenos pesados acíclicos y cíclicos simples con [Ru₃(CO)₁₂]	I. Reactivity of Diaminogermynes with Ruthenium Carbonyl: Ru ₃ Ge ₃ and RuGe ₂ Derivatives, <i>Inorg. Chem.</i> , 2011 , 50, 6195
	II. Synthesis of Mixed Tin-Ruthenium and Tin-Germanium-Ruthenium Carbonyl Clusters from [Ru ₃ (CO) ₁₂] and Diaminometalenes (M = Sn, Ge), <i>Inorg. Chem.</i> , 2012 , 51, 2569
2. Reactividad de tetrilenos pesados acíclicos y cíclicos simples con [AuCl(THT)]	III. Diaminogermylene and Diaminostannylene Derivatives of Gold(I): Novel AuM and AuM ₂ (M = Ge, Sn) Complexes, <i>Inorg. Chem.</i> , 2012 , 51, 3896

Parte II – Incorporación de TPs cíclicos estabilizados intramolecularmente (amidinato-TPs) a complejos de Ms	
Capítulos	Publicaciones
3. Nuevos modos de coordinación de los amidinato-TPs	IV. Expanding the Coordination Chemistry of Donor-Stabilized Group-14 Metalenes, <i>Dalton Trans.</i> , 2013 , 42, 1329
	V. Reactivity Studies on a Binuclear Ruthenium(0) Complex Equipped with a Bridging $\kappa^2\text{N,Ge}$ -Amidinatogermylene Ligand, <i>Inorg. Chem.</i> , 2015 , 54, 4850
4. La influencia de pequeños cambios en el volumen del fragmento amidinato	VI. Ring Opening and Bidentate Coordination of Amidinate Germynes and Silylenes on Carbonyl Dicobalt Complexes: The Importance of a Slight Difference in Ligand Volume, <i>Chem. Eur. J.</i> , 2014 , 20, 8654
	VII. Steric Effects in the Reactions of Amidinate Germynes with Ruthenium Carbonyl: Isolation of a Coordinatively Unsaturated Diruthenium(0) Derivative, <i>RSC Adv.</i> , 2014 , 4, 31503
5. Aumentando la capacidad de coordinación de los amidinato-TPs	VIII. Amidinatogermylene Derivatives of Ruthenium Carbonyl: New Insights into the Reactivity of $[\text{Ru}_3(\text{CO})_{12}]$ with 2-Electron-Donor Reagents of High Basicity, <i>Inorg. Chem.</i> , 2015 , 54, 2983
	IX. Conversion of a Monodentate Amidinate-Germylene Ligand into Chelating Imine-Germanate Ligands (on Mononuclear Manganese Complexes), <i>Inorg. Chem.</i> , 2014 , 53, 8735
6. Revisión de la química de coordinación de los amidinato-TPs	X. The Transition-Metal Chemistry of Amidinatosilylenes, -germylenes and -stannylenes, <i>Coord. Chem. Rev.</i> , 2015 , 300, 1

Informe de las publicaciones presentadas			
Revista	Índice de Impacto (2013)	Puesto / N° revistas en el área (2013)	Área
<i>Inorganic Chemistry</i> (publicaciones I, II, III, V, VIII y IX)	4.794	4 / 45	Chemistry, Inorganic & Nuclear
<i>Dalton Transactions</i> (publicación IV)	4.097	6 / 45	Chemistry, Inorganic & Nuclear
<i>Chemistry A European Journal</i> (publicación VI)	5.696	22 / 148	Chemistry, Multidisciplinary
<i>RSC Advances</i> (publicación VII)	3.708	35 / 148	Chemistry, Multidisciplinary
<i>Coordination Chemistry Reviews</i> (publicación X)	12.098	1 / 45	Chemistry, Inorganic & Nuclear

Discusión de Resultados Parte – I

***Incorporación de tetrilenos pesados acíclicos y
cíclicos simples a complejos de metales de transición***

Capítulo 1

*Reactividad de tetrilenos pesados acíclicos
y cíclicos simples con $[Ru_3(CO)_{12}]$*

Artículo I

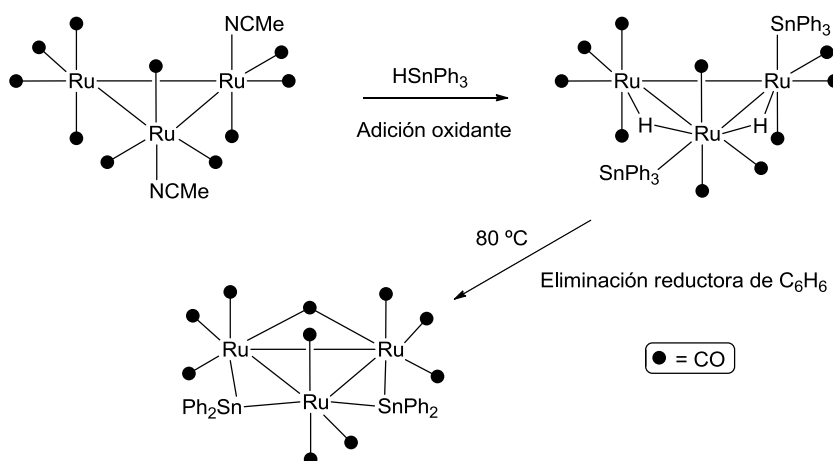
“Reactivity of Diaminogermynes with Ruthenium Carbonyl: Ru_3Ge_3 and $RuGe_2$ Derivatives”

Artículo II

“Synthesis of Mixed Tin-Ruthenium and Tin-Germanium-Ruthenium Carbonyl Clusters from $[Ru_3(CO)_{12}]$ and Diaminometalenes ($M = Sn, Ge$)”

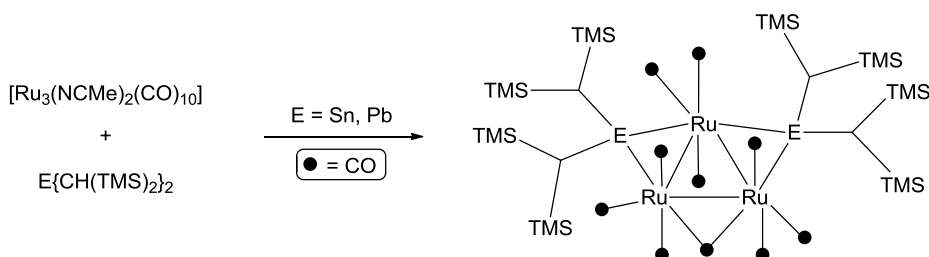
1.1. Introducción

En los últimos cincuenta años se han dedicado muchos esfuerzos al estudio de clusters carbonílicos de metales de transición.^{59,60} Sin embargo, en estos trabajos hay pocos ejemplos relativos a síntesis y reactividad de clusters que contienen TP como ligandos. La mayor parte de estos estudios han sido realizados por los grupos de Adams y Cardin, que han descrito la preparación de clusters metálicos con TP a partir de HER_3 ($R =$ alquilo o arilo)³² y distintos precursores polinucleares, como, por ejemplo, $[M_3(CO)_{12}]$ ($M = Fe, Ru, Os$), $[M_3(NCMe)_2(CO)_{10}]$ ($M = Ru, Os$), $[Ir_4(CO)_{12}]$ o $[Ru_4H_4(CO)_{12}]$. En estas reacciones, la formación de los TP es precedida de la adición oxidante del HER_3 empleado y una posterior eliminación reductora de HR (ver un ejemplo representativo en el Esquema 1.1).^{32c}

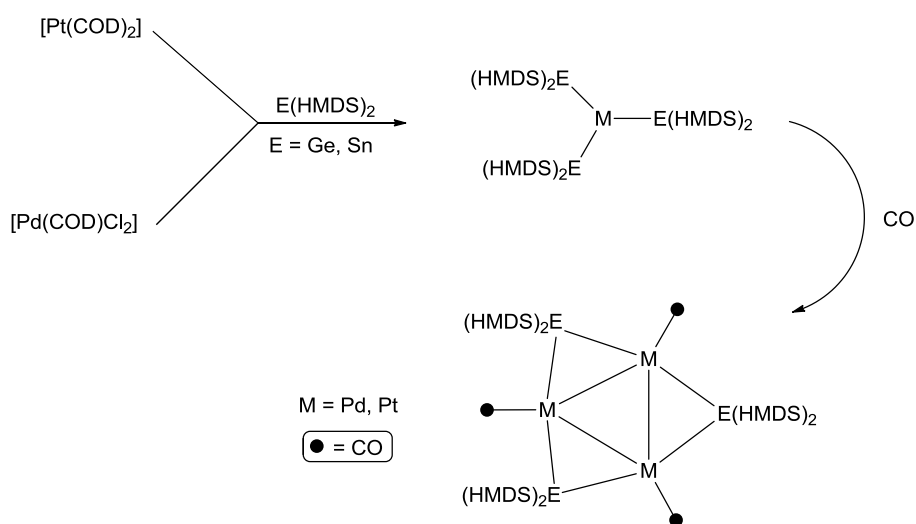


Esquema.1.1. Reacción de $[Ru_3(NCMe)_2(CO)_{10}]$ con $HSnPh_3$: vía general de síntesis de clusters de M_s que contienen diaril-TPs

Los casos en los que los clusters se preparan por reacción directa con TPs aislados son menos frecuentes, destacando los trabajos de Cardin con TPs de tipo $E\{CH(TMS)_2\}_2$ ($E = Sn, Pb$) y clusters de rutenio y osmio (Esquema 1.2),^{57,61} y los de Lappert con complejos de paladio y platino y bis(amido)germilenos y -estannilenos. Estos últimos, que se preparan por carbonilación de los derivados mononucleares trisustituídos $[M\{E(HMDS)_2\}_3]$ ($M = Pd, Pt$), eran los únicos clusters con bis(amido)-TPs descritos hasta el momento de comenzar esta tesis doctoral (Esquema 1.3).⁶²



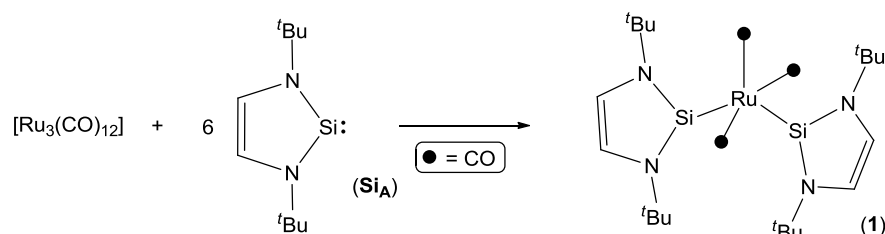
Esquema.1.2. Clusters de rutenio derivados de $E\{CH(SiMe_3)_2\}$ ($E = Sn, Pb$)



Esquema.1.3. Clusters de paladio y platino derivados de $E(HMDS)_2$ ($E = Ge, Sn$)

De la química de coordinación de clusters carbonílicos que contienen TPs previa al desarrollo de esta tesis doctoral cabe destacar que: (i) en todos los ejemplos, los TPs siempre se coordinaban puente a través del átomo E y (ii) no se conocía ningún cluster carbonílico que contuviese un ligando TPNH. Esto contrasta con el hecho de que la química de complejos polinucleares derivada de CNHs, que son los parientes más ligeros de los TPNHs, está ampliamente desarrollada (fundamentalmente por nuestro grupo de

investigación)⁶⁰ y con que los CNHs se comportan siempre como ligandos terminales. Debe tenerse en cuenta que West y col. describieron que la reacción de $[\text{Ru}_3(\text{CO})_{12}]$ con seis equivalentes del silileno *N*-heterocíclico $\text{Si}(\text{N}^t\text{Bu})_2\text{C}_2\text{H}_2$ (**Si_A**) conduce a la especie mononuclear $[\text{Ru}\{\text{Si}(\text{N}^t\text{Bu})_2\text{C}_2\text{H}_2\}_2(\text{CO})_3]$ (**1**)⁶³ (Esquema 1.4).



Esquema 1.4. Reacción de $[\text{Ru}_3(\text{CO})_{12}]$ con el silileno *N*-heterocíclico $\text{Si}(\text{N}^t\text{Bu})_2\text{C}_2\text{H}_2$ (**Si_A**)

Teniendo en cuenta los antecedentes descritos y la experiencia de nuestro grupo de investigación en la química derivada de $[\text{Ru}_3(\text{CO})_{12}]$, nos planteamos explorar la reactividad de este cluster con: (i) los TPs cíclicos simples $\text{E}(\text{N}^t\text{Bu})_2\text{C}_2\text{H}_2$ ($\text{E} = \text{Si}$ (**Si_A**),³⁸ Ge (**Ge_A**)⁶⁴) y $\text{E}(\text{NCH}_2^t\text{Bu})_2\text{C}_6\text{H}_4$ ($\text{E} = \text{Si}$ (**Si_B**), Ge (**Ge_B**), Sn (**Sn_B**),⁶⁵ Figura 1.1) y (ii) con los TPs acíclicos de Lappert $\text{E}(\text{HMDS})_2$ ($\text{E} = \text{Ge}$ (**Ge_C**), Sn (**Sn_C**);^{22b,e} Figura 1.1).

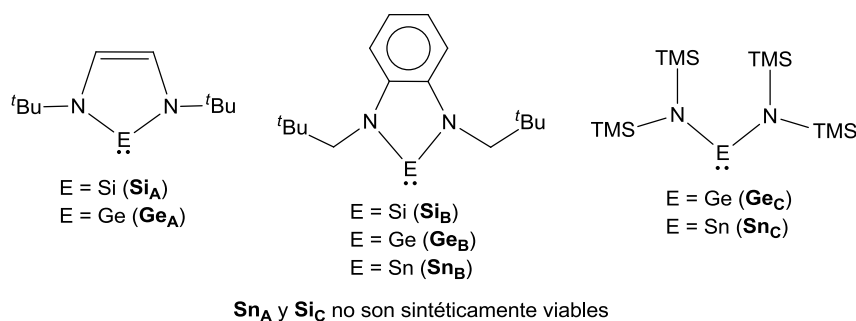


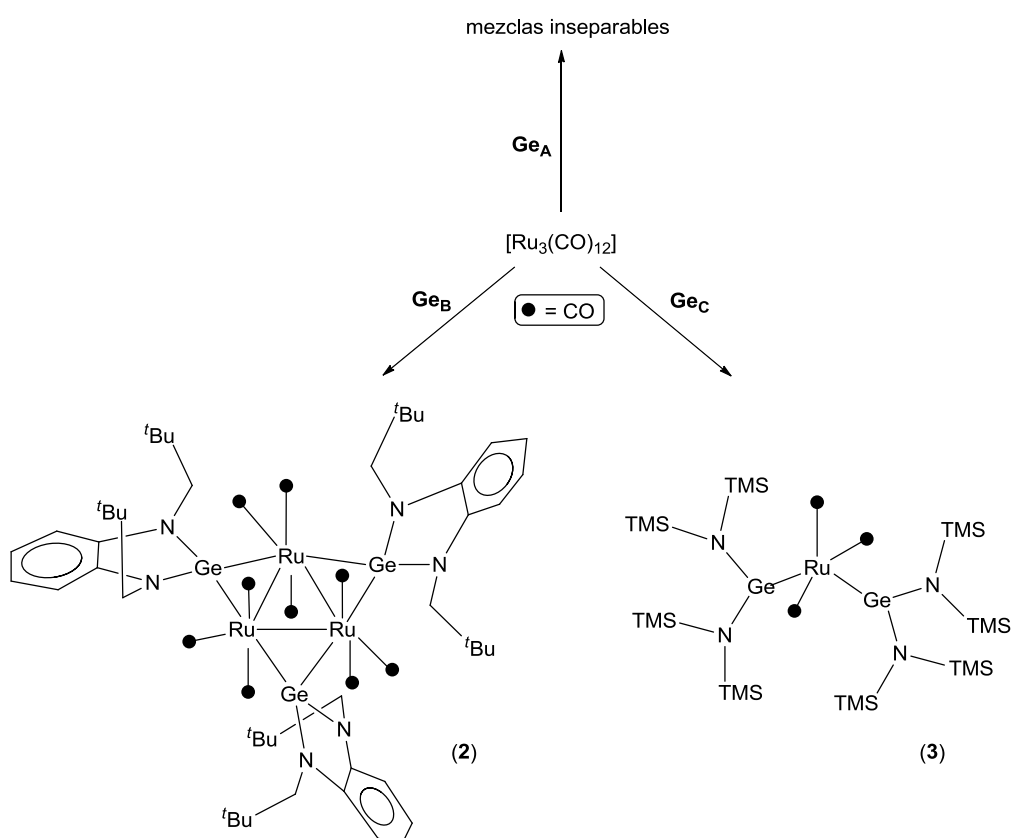
Figura 1.1. TPs acíclicos y cíclicos simples utilizados en el Capítulo 1

1.2. Resultados

La reacción de **Ge_A** con $[\text{Ru}_3(\text{CO})_{12}]$, utilizando las mismas condiciones descritas por West para la síntesis del derivado mononuclear **1** (6 equiv. del TP y temperatura ambiente en THF como disolvente), no tuvo lugar. La menor capacidad dadora que, a nivel general, tienen los germilenos en comparación con los sililenos (la fortaleza del enlace E–M decrece al bajar en el grupo 14)²⁵ parece explicar la diferencia de reactividad observada entre **Si_A** y **Ge_A** con $[\text{Ru}_3(\text{CO})_{12}]$. La misma reacción llevada a cabo a temperaturas más altas en THF o

tolueno y usando 1, 3, 6 o más equiv. de **Ge_A**, dio lugar, en todos los casos, a mezclas complejas que no se pudieron resolver.

El germileno **Ge_A** está provisto de grupos N-^tBu muy voluminosos, por lo que razonamos que una disminución del tamaño de estos grupos podría aumentar la reactividad y/o selectividad del germileno en su reacción con $[Ru_3(CO)_{12}]$. La reacción de $Ge(NCH_2^tBu)_2C_6H_4$ (**Ge_B**), que contiene grupos *neo*-pentilo, con $[Ru_3(CO)_{12}]$ ($Ge/Ru_3 \geq 3$) dio lugar al derivado trinuclear trisustituido $[Ru_3\{\mu-Ge(NCH_2^tBu)_2C_6H_4\}_3(CO)_9]$ (**2**) (Esquema 1.5). Los germilenos de **2** se coordinan en modo puente a cada arista del triángulo metálico.



Esquema 1.5. Reacciones de $[Ru_3(CO)_{12}]$ con los germilenos cíclicos simples **Ge_A** y **Ge_B**, y con el acíclico **Ge_C**: Síntesis de los compuestos **2** y **3**

No se observó reacción a temperatura ambiente y usando relaciones $Ge/Ru_3 < 3$ a mayor temperatura se obtuvieron mezclas que no se pudieron separar. Es destacable que **2** no evoluciona hacia especies mononucleares a altas temperaturas, incluso en presencia de grandes excesos de germileno libre, permaneciendo inalterado. La clave de la diferente reactividad de **Ge_A** y **Ge_B** es la posibilidad que tienen los grupos *neo*-pentilo de **Ge_B** de

minimizar su impacto estérico alejando los restos ^tBu (mediante el giro del enlace ^tBu-CH₂N) de los carbonilos próximos (esta opción no es posible en **Ge_A**).

Por último, la reacción de [Ru₃(CO)₁₂] con al menos seis equiv. del germileno acíclico Ge(HMDS)₂ (**Ge_C**) permitió aislar el derivado mononuclear disustituido [Ru{Ge(HMDS)₂}(CO)₃] (**3**) (Esquema 1.5). El complejo **3** es estructuralmente análogo al silileno derivado **1**. No se observó reacción a temperatura ambiente y, usando relaciones Ge/Ru₃ < 6, se obtuvieron mezclas irresolubles. La diferente reactividad de **Ge_B** y **Ge_C** con [Ru₃(CO)₁₂] parece estar gobernada por el mayor volumen de **Ge_C**, cuyos grupos HMDS son mucho más voluminosos que los *neo*-pentilos de **Ge_B**. Por otro lado, la diferente reactividad de **Ge_A** y **Ge_C** no se ha podido explicar porque ambos germilenos rivalizan en volumen, aunque es posible que radique en que la mayor capacidad π-aceptora de **Ge_C** de lugar a enlaces Ge-Ru más fuertes. La planaridad de los bis(amido)germilenos cíclicos favorece la donación π N→Ge desde los orbitales p llenos de los átomos de N al orbital p vacante en el germanio, lo que hace que estos germilenos sean menos π-aceptores que los acíclicos.

Teniendo en cuenta los resultados descritos, se decidió utilizar las versiones de silicio accesibles análogas a los germilenos anteriores y así extender la química iniciada por West con la síntesis del complejo mononuclear disustituido **1**.⁶³ El silileno acíclico Si(HMDS)₂ (**Si_C**) se descartó por ser demasiado inestable,³⁵ pero sí se estudió la reactividad de [Ru₃(CO)₁₂] con los SiNHs Si(N^tBu)₂C₂H₂ (**Si_A**) y Si(NCH₂^tBu)₂C₆H₄ (**Si_B**), utilizando diferentes condiciones experimentales. En el caso de **Si_A**, usando relaciones Si/Ru₃ < 6 (concretamente 1 y 3 equiv. de **Si_A** por cluster metálico) a distintas temperaturas, se obtuvieron mezclas que no se pudieron separar. En el caso del silileno **Si_B**, equipado con grupos *neo*-pentilo, se obtuvo (con Si/Ru₃ ≥ 3) el mismo resultado que con su análogo de germanio, pudiéndose aislar el derivado trinuclear trisustituido [Ru₃{μ-Si(NCH₂^tBu)₂C₆H₄}(CO)₃}] (**4**). De nuevo, como ocurría con **2**, este compuesto permanece inalterado a altas temperaturas y en presencia de grandes excesos de silileno libre. El complejo **4**, que es estructuralmente análogo a **2**, no se incluyó en ninguna de las publicaciones que figuran en este capítulo. Al igual que ocurre con los derivados de germanio, la diferente reactividad de **Si_A** y **Si_B** es consecuencia de su distinta naturaleza estérica.

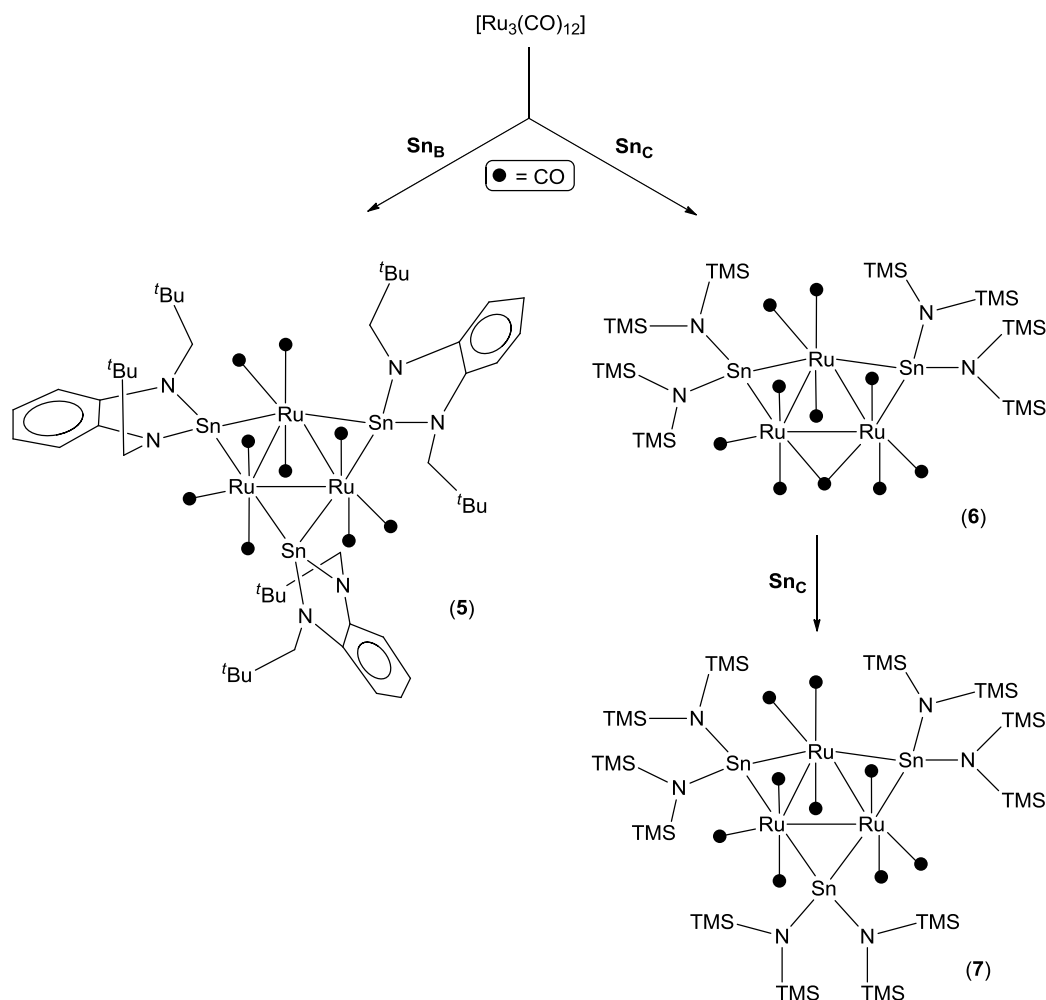
Las reacciones descritas con germanio en el artículo I se trasladan a estaño en el artículo II. La reacción de [Ru₃(CO)₁₂] con el estannileno cíclico simple Sn(N^tBu)₂C₂H₂ (**Sn_A**)⁶⁶ no se pudo llevar a cabo debido a la gran inestabilidad térmica del mismo. El tratamiento de [Ru₃(CO)₁₂] con Sn(NCH₂^tBu)₂C₆H₄ (**Sn_B**) condujo de nuevo, en condiciones similares a las utilizadas con el germileno y el silileno análogos **Ge_B** y **Si_B**, a un derivado trinuclear trisustituido, el complejo [Ru₃{μ-Sn(NCH₂^tBu)₂C₆H₄}(CO)₃}] (**5**), que es

isoestructural a **2** y **4** (Esquema 1.6). El compuesto **5** también demostró ser estable en presencia de exceso de estannileno libre. Estos tres compuestos, de fórmula $[\text{Ru}_3\{\mu\text{-E}(\text{NCH}_2^t\text{Bu})_2\text{C}_6\text{H}_4\}_3(\text{CO})_9]$, muestran, de acuerdo con su similitud estructural, el mismo patrón de bandas $\nu(\text{CO})$ en sus espectros de IR, desplazándose éstas hacia mayores números de onda al pasar del derivado de silicio al de estaño (Tabla 1.1). El aumento del carácter π -aceptor y la disminución del carácter σ -dador al bajar en el grupo 14 hace que los átomos de rutenio tengan menor densidad electrónica, lo que se traduce en una menor π -retrodonación $\text{Ru}\rightarrow\text{CO}$ y, por tanto, en una mayor fortaleza de los enlaces C–O.

Compuesto	IR (tol, cm^{-1})
$[\text{Ru}_3(\mu\text{-Si}_i)_3(\text{CO})_9]$ (4)	$\nu(\text{CO})$ 2039 (f), 2004 (mf), 1992 (m)
$[\text{Ru}_3(\mu\text{-Ge}_B)_3(\text{CO})_9]$ (2)	$\nu(\text{CO})$ 2045 (f), 2009 (mf), 1999 (m)
$[\text{Ru}_3(\mu\text{-Sn}_B)_3(\text{CO})_9]$ (5)	$\nu(\text{CO})$ 2046 (f), 2012 (mf), 2001 (m)

Tabla 1.1. Patrón de IR en la zona $\nu(\text{CO})$ característico de los compuestos **2**, **4** y **5**

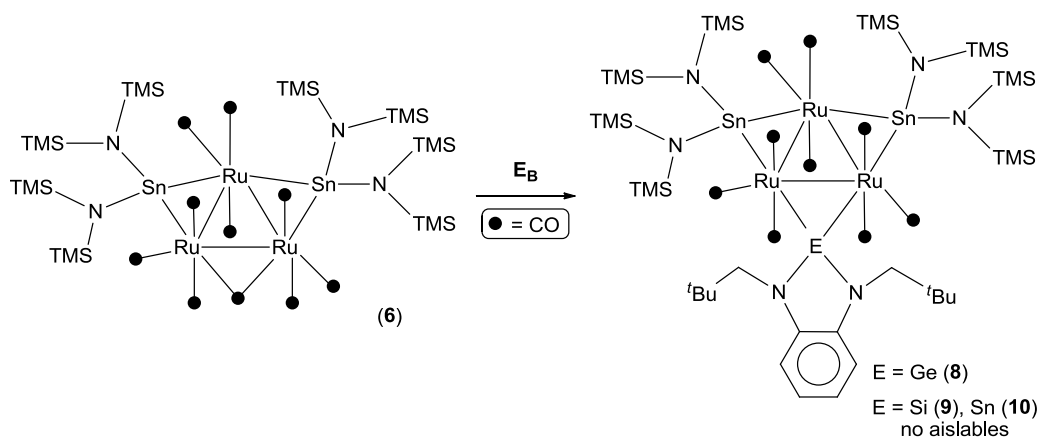
Por último, reacciones de $[\text{Ru}_3(\text{CO})_{12}]$ con el estannileno acíclico $\text{Sn}(\text{HMDS})_2$ (**Sn_C**), no dieron lugar a un derivado mononuclear análogo a **3** en ninguna de las condiciones de reacción empleadas. En ningún caso se produjo la fragmentación del cluster y se pudieron aislar, utilizando diferentes temperaturas y relaciones Ru_3/Sn , los derivados trinucleares di- y trisustituidos $[\text{Ru}_3\{\mu\text{-Sn}(\text{HMDS})_2\}_2(\mu\text{-CO})(\text{CO})_9]$ (**6**) y $[\text{Ru}_3\{\mu\text{-Sn}(\text{HMDS})_2\}_3(\text{CO})_9]$ (**7**) (Esquema 1.6). El compuesto **6** reaccionó con más cantidad de **Sn_C** para dar **7** y este último resultó estable en presencia de estannileno libre. El complejo **7** es isoestructural a **2**, **4** y **5**. El factor que determina la diferencia de nuclearidad de los productos obtenidos usando **Ge_C** y **Sn_C** ha de ser el mayor tamaño del átomo de estaño en comparación con el de germanio, que permite que los grupos HMDS estén más lejos de los átomos de rutenio y de los carbonilos cercanos, reduciendo el impacto estérico del ligando. La mayor capacidad π -aceptora de **Sn_C** en comparación con **Ge_C** no debe ser la causa de esta diferencia de reactividad, puesto que **Ge_C**, que es más π -aceptor pero más voluminoso que **Ge_B**, da lugar al derivado RuGe_2 **3**.



Esquema 1.6. Reacciones de $[Ru_3(CO)_{12}]$ con el estannileno cíclico simple Sn_B y con el acíclico Sn_C : Síntesis de los compuestos 5-7

Finalmente, como el compuesto $[Ru_3\{\mu-Sn(HMDS)_2\}_2(\mu-CO)(CO)_9]$ (**6**) demostró ser capaz de captar otro estannileno (formación de **7** a partir de **6**), también se estudiaron las reacciones de **6** con otros TPs. De esta manera se consiguieron sintetizar los derivados $[Ru_3\{\mu-Sn(HMDS)_2\}_2\{\mu-E(NCH_2^tBu)_2C_6H_4\}(CO)_9]$ (E = Ge (**8**), Si (**9**), Sn (**10**); Esquema 1.7). De estos tres compuestos, sólo **8** pudo ser aislado, ya que el resto demostraron ser muy poco estables y sólo pudieron ser caracterizados por IR (los complejos **8–10** comparten el mismo patrón $\nu(CO)$). Por ello, los complejos **9** y **10** no se incluyeron en ninguna de las publicaciones que corresponden a este capítulo. El cluster **8** representa un ejemplo poco frecuente de sustitución heteroléptica, ya que contiene dos estannilenos y un germileno en el mismo complejo. El compuesto mononuclear $[Ru(SnPh_3)(GePh_3)(CO)_2(Pr-DAB)]$,⁶⁷

descrito por Harlt y colaboradores, es el único antecedente conocido en el que coexisten en el mismo complejo de rutenio un ligando Ge-dador y otro Sn-dador.



Esquema.1.7. Reacción de **6** con los TPs cíclicos simples E_B (E = Si, Ge, Sn): Síntesis de los complejos **8–10**

1.3. Conclusiones

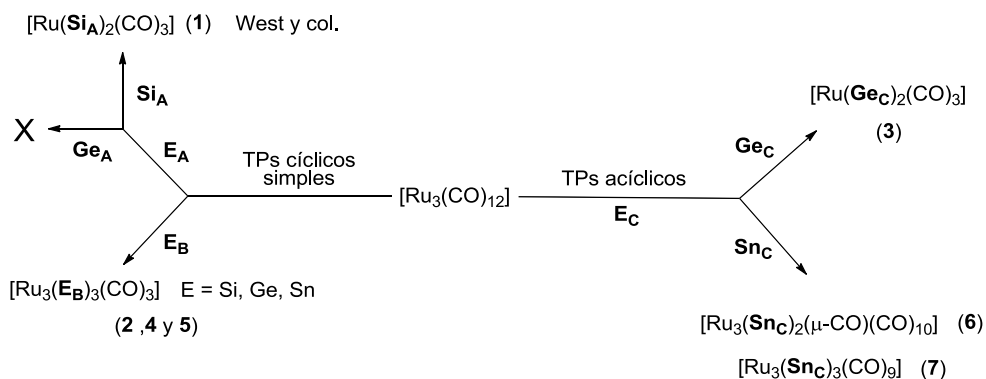


Figura 1.2. Resumen de la reactividad de $[\text{Ru}_3(\text{CO})_{12}]$ con TPs acíclicos y cíclicos simples

Los estudios descritos en este primer capítulo, junto con el trabajo publicado por West,⁶³ han demostrado que el $[\text{Ru}_3(\text{CO})_{12}]$ reacciona con tetrilenos pesados acíclicos y cíclicos simples de distinta naturaleza estérica y electrónica dando lugar a complejos trinucleares de fórmula $[\text{Ru}_3(\mu\text{-TP})_{3-x}(\mu\text{-CO})_x(\text{CO})_9]$ (**2, 4, 5, 7, 8**; $x = 0$; **6**; $x = 1$), en los que los TPs actúan siempre como ligandos puente sobre las aristas Ru–Ru (no se obtuvieron complejos monosustituidos en ninguno de los casos), y a complejos mononucleares de fórmula $[\text{Ru}(\text{TP})_2(\text{CO})_3]$ (**1** y **3**). Además, se verificó que los clusters trinucleares no son

intermedios de las especies mononucleares. En la Figura 1.2 se recoge un pequeño resumen de estos resultados.

En estas reacciones, el volumen y la naturaleza cíclica o acíclica del TP empleado, así como el tamaño del átomo E, juegan un papel determinante en la nuclearidad de los productos finales. El cluster no se fragmenta cuando el impedimento estérico provocado por los brazos N–R no es alto (bien porque el grupo R es pequeño o porque el átomo E es suficientemente grande como para alejar los grupos R voluminosos de la esfera de coordinación de los metales). La influencia de las características electrónicas de los TPs no está clara.

Esta química es muy diferente de la ya conocida para $[\text{Ru}_3(\text{CO})_{12}]$ y CNHs, dominada por la formación de productos de los tipos $\text{Ru}_3(\text{CNH})$, $\text{Ru}(\text{CNH})$ y $\text{Ru}(\text{CNH})_2$, en los que el carbeno actúa siempre como un ligando terminal y en la que nunca se han descrito clusters di- o trisustituídos.⁶⁰ Además, en muchos clusters metálicos que contienen CNHs se han observado reacciones secundarias que implican activaciones de enlaces C–H y C–N de los propios carbenos, procesos que no se han detectado con los TPs utilizados en este trabajo.

Cabe destacar que los compuestos **2–8** son los primeros bis(amido)germileno y bis(amido)estannileno de rutenio conocidos y que los compuestos **2**, **4**, **5** y **8** son los primeros clusters de Ms con un TPNH de cualquier tipo. Además, el uso de combinaciones adecuadas de TPs de germanio y estaño permitió aislar el cluster heteroléptico **8**.

Los complejos de rutenio descritos en este primer capítulo demostraron ser inestables frente a trazas de aire y humedad (en particular los derivados de TPs cíclicos), pero considerablemente inertes, particularmente, los derivados trinucleares trisustituídos, frente a otros reactivos de diferente naturaleza (alquinos, fosfanos, fuentes de hidruros, etc.). Por ello, no se llevaron a cabo estudios posteriores de reactividad y/o catálisis con estos sistemas.

Capítulo 2

***Reactividad de tetrienos pesados acíclicos
y cíclicos simples con [AuCl(THT)]***

Artículo III

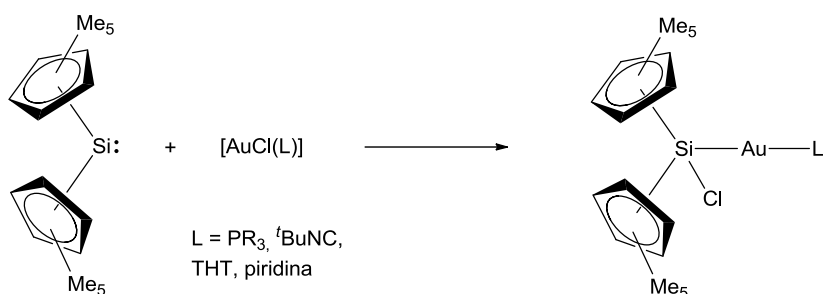
“Diaminogermylene and Diaminostannylene Derivatives of Gold(I): Novel AuM and AuM₂ (M = Ge, Sn) Complexes”

2.1. Introducción

Los compuestos de oro(I) han emergido en los últimos años como una herramienta de gran utilidad en catálisis homogénea.⁶⁸ En concreto, los que contienen carbenos (sobre todo CNHs) han ganado popularidad gracias a que estos ligandos, que combinan excelentes propiedades σ -dadoras con un perfil estérico único,⁶⁹ estabilizan el centro metálico y suelen mejorar sus propiedades catalíticas. Así, los complejos de tipo [AuX(CNH)] (X = halógeno) han demostrado ser excelentes precatalizadores en reacciones de cicloisomerización de sustratos poliinsaturados,^{68h} de adición de agua a alquinos y nitrilos,^{68b} de activación de enlaces C–H,^{68a} etc. El hecho de que algunos complejos de oro(I) con CNHs empiecen a ser comerciales demuestra el creciente interés de los mismos.

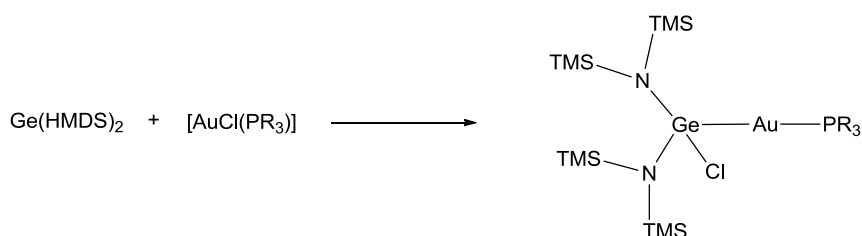
Por otro lado, entre todos los estudios de reactividad de complejos de metales de transición con TPs que se pueden encontrar en la literatura, los relacionados con metales del grupo 11 de la tabla de periodos son escasos.^{70–74} Centrándonos en la química derivada de compuestos de oro y TPs, la mayoría de los complejos descritos no contienen TPs como tal, sino ligandos aniónicos que resultan de la inserción del TP utilizado en un enlace Au–X (X = halógeno).^{71–74} De hecho, solamente se conocen complejos de oro con TPs neutros para TP = germileno.^{70a–c,e} Las inserciones de TPs en enlaces M–X son una característica habitual de este tipo de ligandos.^{4, 71–74}

En lo referente a complejos de oro y sililenos, Jutzi y colaboradores consiguieron sintetizar, trabajando con el silileno acíclico decametilsilicoceno SiCp*₂ y [AuCl(L)] (L = ligando neutro), los productos de inserción [Au(SiClCp*₂)_n] (cuando L = CO), de naturaleza polimérica, y [Au(SiClCp*₂)L] (L = PR₃, ^tBuNC, piridina, THT), todos ellos provistos de ligandos de tipo silanato (Esquema 2.1).⁷¹



Esquema 2.1. Reacciones del silileno acíclico SiCp^*_2 con $[\text{AuCl}(\text{L})]$

Pasando a la química derivada de complejos de oro y germilenos, el grupo de Sharp publicó las reacciones del germileno acíclico de Lappert $\text{Ge}(\text{HMDS})_2$ con $[\text{AuCl}(\text{PR}_3)]$ ($\text{PR}_3 = \text{PPh}_3, \text{PCy}_3, \text{PEt}_3, \text{PMe}_2\text{Ph}, \text{PMePh}_2$),⁷² que dieron lugar en todos los casos a productos de inserción análogos a los descritos por Jutzi (Esquema 2.2). Además de las reacciones de



Esquema 2.2. Reacciones del germileno acíclico $\text{Ge}(\text{HMDS})_2$ con $[\text{AuCl}(\text{PR}_3)]$

Sharp, también se han descrito las reacciones de GeCl_2 -dioxano con $[\text{AuCl}(\text{PR}_3)]$ ($\text{PR}_3 = \text{PPh}_3, \text{PPhMe}_2, \text{P}(o\text{-tol})_3$),⁷³ que dan lugar a agregados de tipo $[\text{Au}(\text{GeCl}_3)(\text{PR}_3)]_n$, en los que el germileno también se ha insertado en el enlace $\text{Au}-\text{Cl}$. Como se mencionó anteriormente, sólo existen complejos de oro que contengan TPs neutros para $\text{TP} = \text{germileno}$. Los ejemplos conocidos, que se muestran en la Figura 2.1, fueron preparados por reacciones de los germilenos cíclicos estabilizados intramolecularmente $\text{Ge}\{\text{N}(\text{SiMe}_3)\text{C}(\text{Ph})\text{C}(\text{SiMe}_3)(2\text{-C}_5\text{H}_4\text{N})\}\text{Cl}$ (Leung, 2006)^{70e} y $\text{Ge}[\text{HC}\{\text{C}(\text{Me})\text{N-Diip}\}_2](\text{CCPh})$ (Roesky, 2013),^{70a} y del acíclico estabilizado intermolecularmente $\text{Ge}(\text{CCl}=\text{PMes})_2(\text{CNH})$ (Castel, 2012)^{70b} con distintos precursores de oro. Otro ejemplo menos convencional es un cluster de osmio y oro descrito por Adams y colaboradores,^{70c} en el que un grupo GePh_2 hace de puente entre el átomo de oro y una de las aristas del triángulo de osmios. El germileno de este complejo es el resultado de la adición oxidante del enlace $\text{Ge}-\text{H}$ de una molécula de HGePh_3 a dos átomos de osmio del cluster, seguido de una eliminación reductora de benceno (Figura 2.1).^{70c}

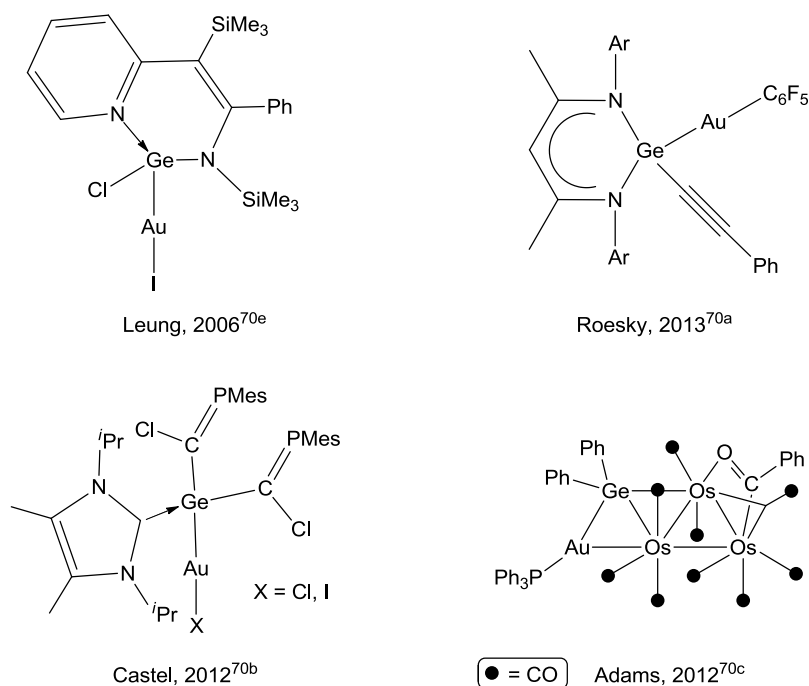


Figura 2.1. Complejos de oro que contienen germilenos

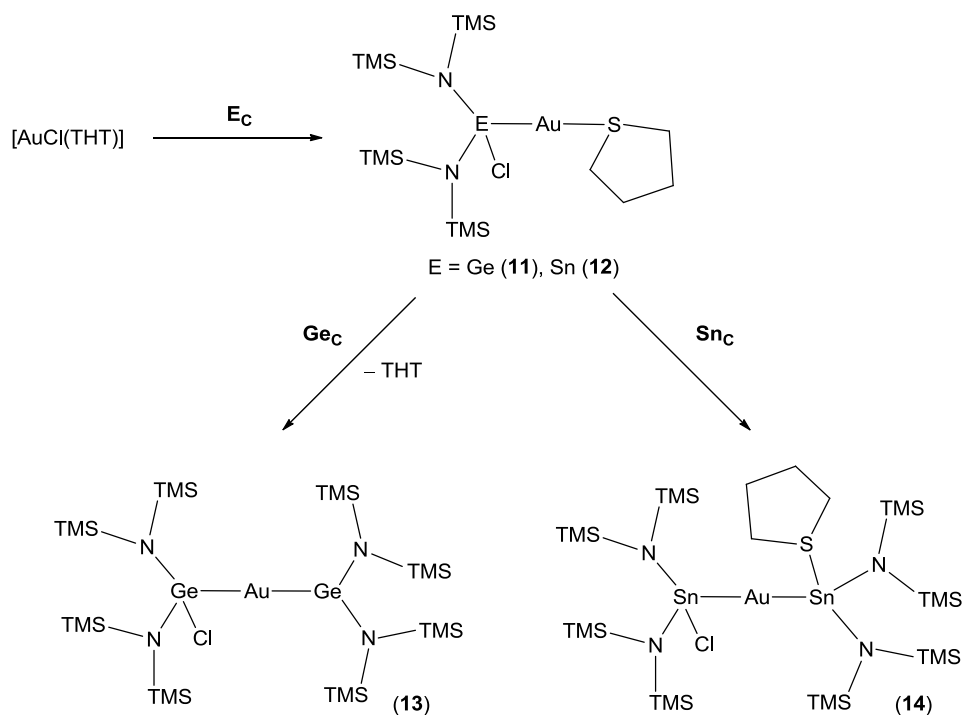
Por último, no se ha descrito ningún complejo de oro que posea estannilenos o plumbilenos neutros y, además, sólo en el caso de estaño se conocen reacciones de complejos de oro en las que intervenga un TP neutro. Se trata de las reacciones de $\text{SnCl}_2 \cdot 2\text{H}_2\text{O}$ con $[\text{AuCl}(\text{L})]$ ($\text{L} = \text{PPh}_3$ y THT),⁷⁴ que dan lugar a derivados con tricloruroestannatos. También se conocen otros derivados provistos con uno o más estannatos formados por reacción directa de precursores de oro con estannatos de litio.⁷⁵

Teniendo en cuenta la escasez de complejos de oro conteniendo TPs neutros y el poco desarrollo general de esta química, nos planteamos aumentar los conocimientos existentes en el área explorando la reactividad del derivado de oro(I) $[\text{AuCl}(\text{THT})]$ frente a los TPs acíclicos (Ge_C y Sn_C) y cíclicos simples ($\text{Si}_{A,B}$, $\text{Ge}_{A,B}$ y Sn_B) presentados en el Capítulo 1. Se escogió $[\text{AuCl}(\text{THT})]$ porque el THT (tetrahidrotiofeno) se puede desplazar fácilmente, lo que permitiría preparar derivados disustituídos con al menos un TP neutro. Además, teniendo en cuenta la actividad que los complejos $[\text{AuX}(\text{CNH})]$ han demostrado como catalizadores,⁶⁸ también nos planteamos usar los complejos preparados como precursores catalíticos.

2.2. Resultados

Las reacciones de $[\text{AuCl}(\text{THT})]$ con los TPs cíclicos simples $\text{Si}_{\text{A,B}}$, $\text{Ge}_{\text{A,B}}$ y Sn_{B} dieron lugar a productos de descomposición, con formación de oro elemental, o a mezclas de las que no se pudo aislar ningún compuesto puro. Por ello, estas reacciones no se incluyeron en los resultados descritos en el artículo III.

Las reacciones de $[\text{AuCl}(\text{THT})]$ con 1 equiv. de Ge_{C} y Sn_{C} condujeron a los complejos $[\text{Au}\{\text{ECl}(\text{HMDS})_2\}(\text{THT})]$ ($\text{E} = \text{Ge}$ (**11**), Sn (**12**); Esquema 2.3), que contienen ligandos cloruro{bis(amido)}germanato y -estannato, respectivamente, como resultado de la inserción del TP empleado en el enlace Au–Cl. Los complejos **11** y **12** son análogos a los ya descritos anteriormente por Sharp, que responden a la fórmula $[\text{Au}\{\text{GeCl}(\text{HMDS})_2\}(\text{L})]$ ($\text{L} = \text{fosfanos}$) y que se forman por reacción de $\text{Ge}(\text{HMDS})_2$ con $[\text{AuCl}(\text{PR}_3)]$.⁷² El ligando THT se pudo desplazar cuando las reacciones se llevaron a cabo con dos equiv. de Ge_{C} o Sn_{C} , formándose los derivados germanato-germileno $[\text{Au}\{\text{GeCl}(\text{HMDS})_2\}\{\text{Ge}(\text{HMDS})_2\}]$ (**13**) y estannato-estannileno $[\text{Au}\{\text{SnCl}(\text{HMDS})_2\}\{\text{Sn}(\text{HMDS})_2(\text{THT})\}]$ (**14**), respectivamente. Mientras que el compuesto **13** resulta de la sustitución del THT de **11** por Ge_{C} , en el compuesto **14**, el segundo equiv. de Sn_{C} se ha insertado en el enlace Au–S, permaneciendo



Esquema 2.3. Reacciones de $[\text{AuCl}(\text{THT})]$ con los TPs acíclicos Ge_{C} y Sn_{C} : Síntesis de los complejos **11**–

el THT unido al átomo de estaño del fragmento estannileno (Esquema 2.3). El mayor carácter metálico del estaño con respecto al germanio (mayor acidez de Lewis) y su mayor volumen parecen ser los responsables de que el THT se mantenga unido al átomo E en **14** y no en **13**.

La estructura del compuesto **14** en estado sólido no se mantiene en disolución a temperatura ambiente, ya que el complejo participa en un proceso dinámico que hace equivalentes (en la escala de tiempo de RMN) los entornos de los dos átomos de estaño. En sus espectros de ^1H y ^{13}C RMN se observan dos singletes anchos correspondientes a los grupos metilénicos del THT y un singlete ancho a 0.44 ppm que engloba a todos los grupos SiMe_3 . Experimentos de ^1H RMN a temperatura variable con **14** han demostrado que el proceso dinámico se mantiene activo incluso a 193 K, puesto que la señal a 0.44 ppm se desdobra en dos señales que se mantienen anchas a 0.61 y 0.28 ppm y las correspondientes al THT prácticamente desaparecen (Figura 2.2, arriba / derecha). Estas observaciones son, *a priori*, compatibles con dos procesos dinámicos que conllevan la participación de intermedios simétricos que contienen ligandos puente cloruro, bien de manera intramolecular a través de una especie tricoordinada de oro(I) (Figura 2.2, Mecanismo **A**), o intermolecular por pérdida de THT del compuesto **14** y formación de agregados, posiblemente especies dímeras de tipo Au_2Sn_4 (Figura 2.2, Mecanismo **B**). Se conocen algunos bis(amido)estannilenos puenteados por ligandos cloruro, por ejemplo, en complejos de rodio^{36h} y paladio.^{36d} Un estudio adicional de ^1H RMN a temperatura variable con una mezcla de **14** y un exceso de THT en la disolución permitió probar que el THT inhibe este proceso dinámico, avalando un mecanismo intermolecular (Mecanismo **B**). La ausencia de un proceso dinámico en el complejo AuGe_2 **13** se puede explicar por el menor volumen del átomo de germanio, con respecto al de estaño, y por la gran congestión estérica que provocan los grupos HMDS, que dificultan la formación de especies dímeras de tipo Au_2Ge_4 con cloruros puentes como las planteadas para **14**.

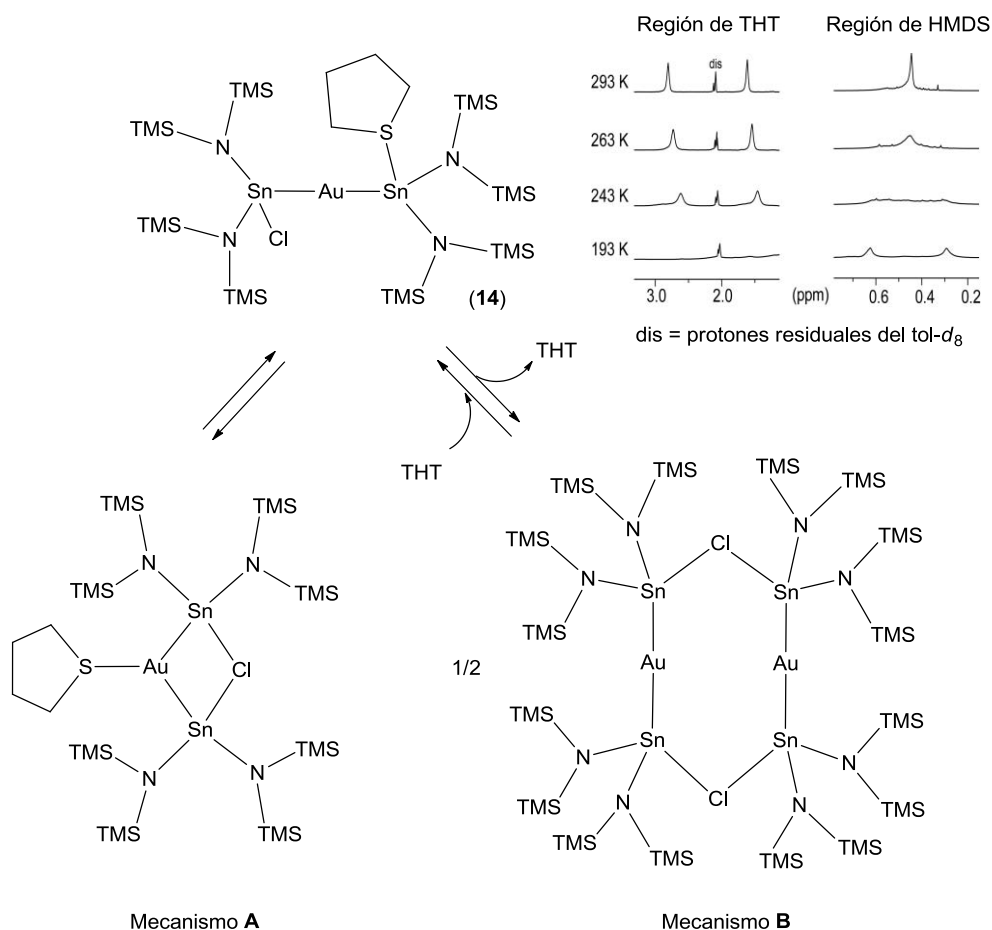
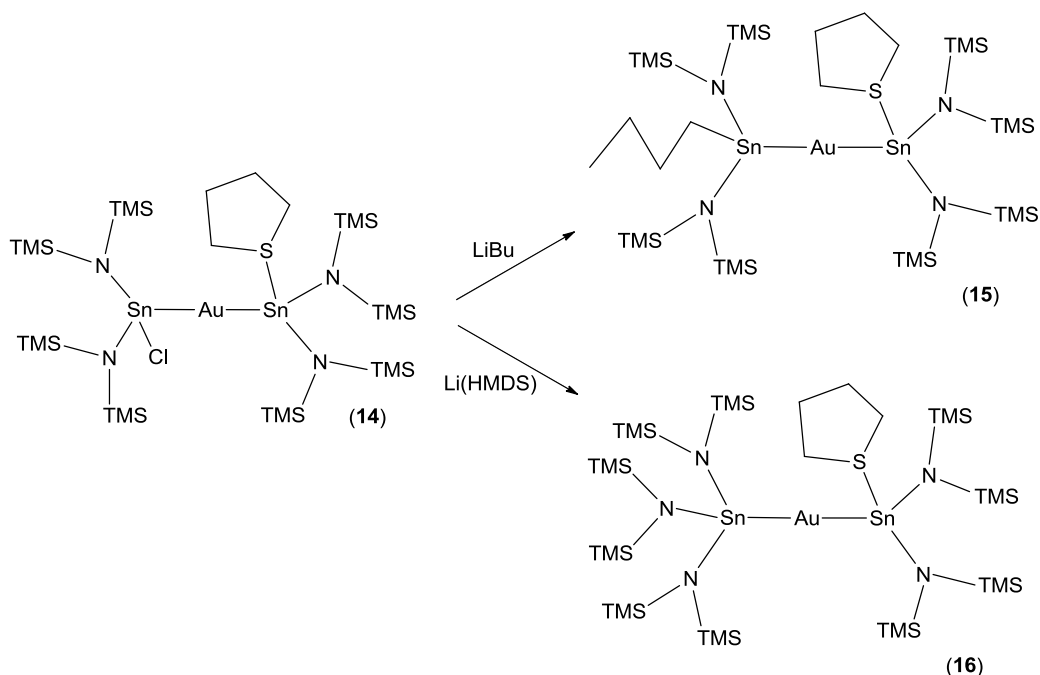


Figura 2.2. Posibles mecanismos para el proceso dinámico en el que participa el compuesto **14** en disolución y estudio de este proceso ^1H RMN a temperatura variable (arriba / derecha)

Con el propósito de corroborar que la presencia del cloruro es esencial para que exista el proceso dinámico observado en **14**, se llevó a cabo su sustitución por otros grupos aniónicos con menos tendencia a formar puentes entre metales. El tratamiento de **14** con LiBu y Li(HMDS) condujo a los derivados $[\text{Au}\{\text{SnX}(\text{HMDS})_2\}\{\text{Sn}(\text{HMDS})_2(\text{THT})\}]$ ($\text{X} = \text{Bu}$ (**15**), HMDS (**16**), respectivamente; Esquema 2.4). Ambos compuestos, cuyas estructuras son esencialmente análogas a la de **14** en estado sólido, no se encuentran involucrados en ningún proceso dinámico en disolución a temperatura ambiente y, por tanto, avalan la participación del cloruro en el proceso dinámico descrito para **14**. Cabe destacar que los estannatos $\text{SnBu}(\text{HMDS})_2$ y $\text{Sn}(\text{HMDS})_3$ de **15** y **16**, respectivamente, no tienen precedentes en la bibliografía.



Esquema 2.4. Reacciones de **14** con LiR ($R = \text{Bu}, \text{HMDS}$): Síntesis de los complejos **15** y **16**

2.3. Conclusiones

Las reacciones descritas en el Capítulo 2 permiten establecer que el precursor metálico $[\text{AuCl}(\text{THT})]$ reacciona con $\text{E}(\text{HMDS})_2$ ($\text{E} = \text{Ge}, \text{Sn}$) dando lugar: (i) en presencia de un sólo equiv. de TP libre, a derivados monosustituidos que contienen ligandos de tipo tetranato pesado formados por la inserción del TP en el enlace $\text{Au}-\text{Cl}$ (compuestos **11** y **12**), y (ii) en presencia de más de un equiv. de TP libre, a complejos disustituidos conteniendo un TP neutro y un tetranato pesado (compuestos **13** y **14**). Estos resultados difieren de la reactividad conocida para $[\text{AuCl}(\text{THT})]$ y $\text{CNHs}^{76\text{a,c}}$ o fosfanos,^{76b,d} en los que se suele producir, en primer lugar, la sustitución del ligando THT.

El tamaño y la acidez de Lewis del átomo E condicionan la estructura de los productos disustituidos. Así, el complejo AuSn_2 **14** y sus productos de transmetalación **15** y **16** contienen un enlace entre la unidad estannileno y el THT liberado en la reacción que no se observa en el derivado de AuGe_2 **13**. Además, el compuesto **14** se ve involucrado en un proceso fluxional a través de la formación de agregados, posiblemente especies dímeras de tipo Au_2Sn_4 con ligandos cloruro puente entre átomos de estaño. Este proceso no ocurre en su análogo de germanio **13**.

Los compuestos **14–16** son los primeros derivados de oro que poseen estannilenos neutros.

Desafortunadamente, todos los compuestos que se recogen en este capítulo demostraron ser muy inestables frente a trazas de aire y humedad. Por ello, más allá de las reacciones de transmetalación descritas, no se pudieron realizar estudios posteriores de reactividad y/o catálisis.

Los procesos de descomposición observados en las reacciones de $[\text{AuCl}(\text{THT})]$ con los TPs benzoanulados **Si_B**, **Ge_B** y **Sn_B** están relacionados, posiblemente, con la poca protección estérica que ofrecen los grupos NCH_2^tBu de estos TPs cíclicos. En el caso de los TPs de tipo imidazol **Si_A** y **Ge_A**, no disponemos de una explicación que ayude a comprender el resultado de sus reacciones.

Discusión de Resultados – Parte II

***Incorporación de tetrilenos pesados cíclicos
estabilizados intramolecularmente (amidinato-TPs) a
complejos de metales de transición***

Introducción a la Parte II

Planteamiento de la Parte II de la memoria

Los resultados descritos en la Parte I de esta memoria, aunque novedosos, desaconsejaron el uso de TPs acíclicos o cíclicos simples para la realización de estudios de reactividad y/o catálisis con sus complejos TP–Ms. La gran inestabilidad de la mayor parte de los compuestos de rutenio y oro sintetizados frente a trazas de aire y humedad y/o su gran inercia química frente a otros reactivos, hizo imposible que se pudieran realizar estos estudios. Además, la difícil preparación y la baja estabilidad de los TPs utilizados (sobre todo los cíclicos) ralentizaron enormemente las tareas de síntesis y caracterización de los mismos, lo que también desaconsejó el uso de estos TPs para realizar nuevos estudios.

Estos resultados (Parte I) nos llevaron a intentar utilizar un tipo de TPs que se pudieran sintetizar y manejar más fácilmente y que dieran lugar, *a priori*, a complejos metálicos más estables. Con estas premisas, escogimos TPs con fragmentos amidinato en su estructura puesto que: (i) son TPs estabilizados intramolecularmente y, por tanto, más fáciles de manejar que los TPs acíclicos y los cíclicos simples y más fáciles de modificar estérica- y electrónicamente sin necesidad de rediseñar por completo el ligando, y (ii) algunos de sus complejos ya han demostrado ser catalíticamente activos (ver algunos ejemplos en la Introducción).

La química de coordinación de amidinato-TPs, hasta el momento en que nuestro grupo de investigación empezó a trabajar con estos sistemas (2012), contaba con complejos metálicos de la mayoría de los grupos de la tabla periódica (excepto los grupos 3 y 11), aunque no de todos los metales de cada grupo (Figura IP.1). Sin embargo, hay que destacar que gran parte de los complejos descritos hasta ese momento se habían preparado usando amidinato-TPs (fundamentalmente silileno) equipados con un fragmento benzamidinato provisto de grupos N-^tBu y un halógeno como grupo X (ver Figura IP.1). Por otro lado, nos llamó la atención la ausencia de complejos polinucleares derivados de amidinato-TPs.

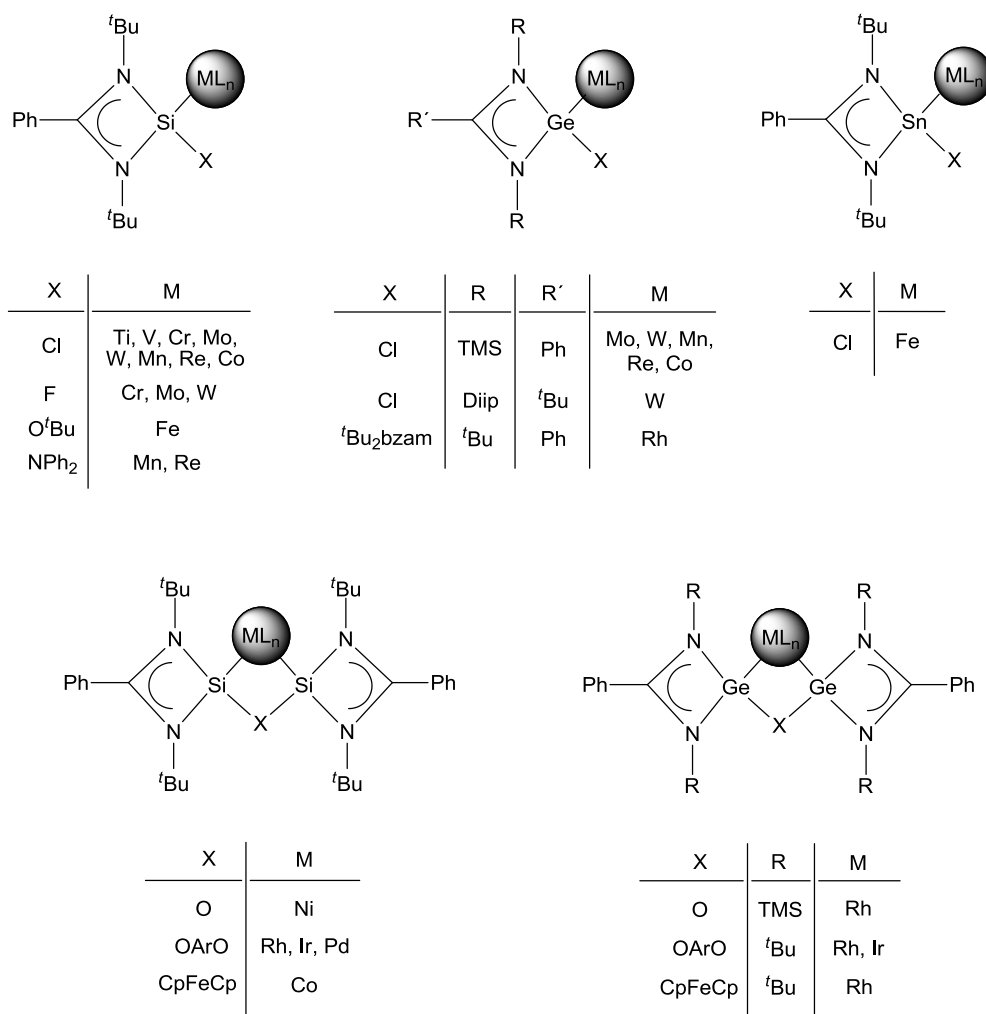


Figura IP.1. Complejos de Ms con amidinato-TPs descritos hasta finales de 2012

Teniendo en cuenta estos antecedentes, decidimos estudiar la reactividad de sistemas metálicos mono- y polinucleares con amidinato-TPs no investigados hasta el momento. En concreto, en la Parte II de esta memoria se recogen los estudios realizados con amidinato-TPs de fórmula general E(RR'bzam)X (E = Si, Ge; R, R' = ^tPr, ^tBu, Et; X = HMDS, ^tBu; bzam = benzamidinato; no se han preparado todas las combinaciones posibles) y con los precursores metálicos [Ru₃(CO)₁₂], [Co₂(CO)₈] y [MnBr(CO)₅] (Figura IP.2). Cabe destacar que, de entre los tres precursores metálicos citados, sólo se conocía en ese momento la reacción de [Co₂(CO)₈] con un amidinato-TP, el silileno Si(^tBu₂bzam)Cl.^{54q}

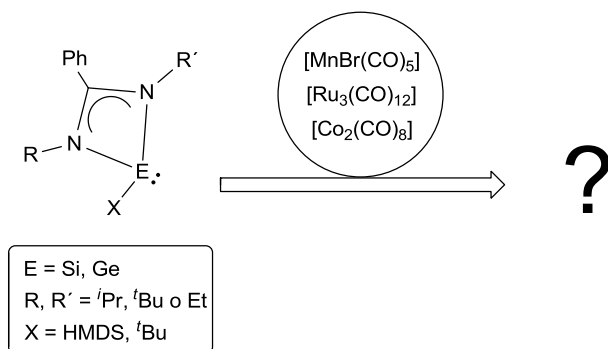
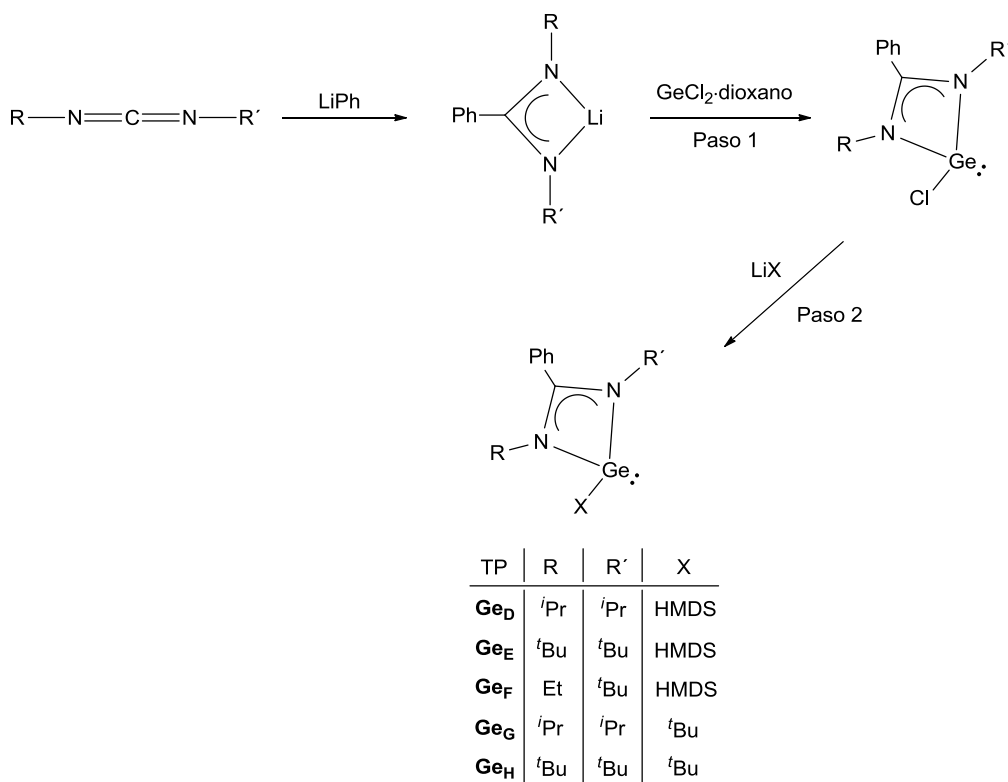


Figura IP.2. Esquema general de la reactividad que se describe en la Parte II de esta memoria

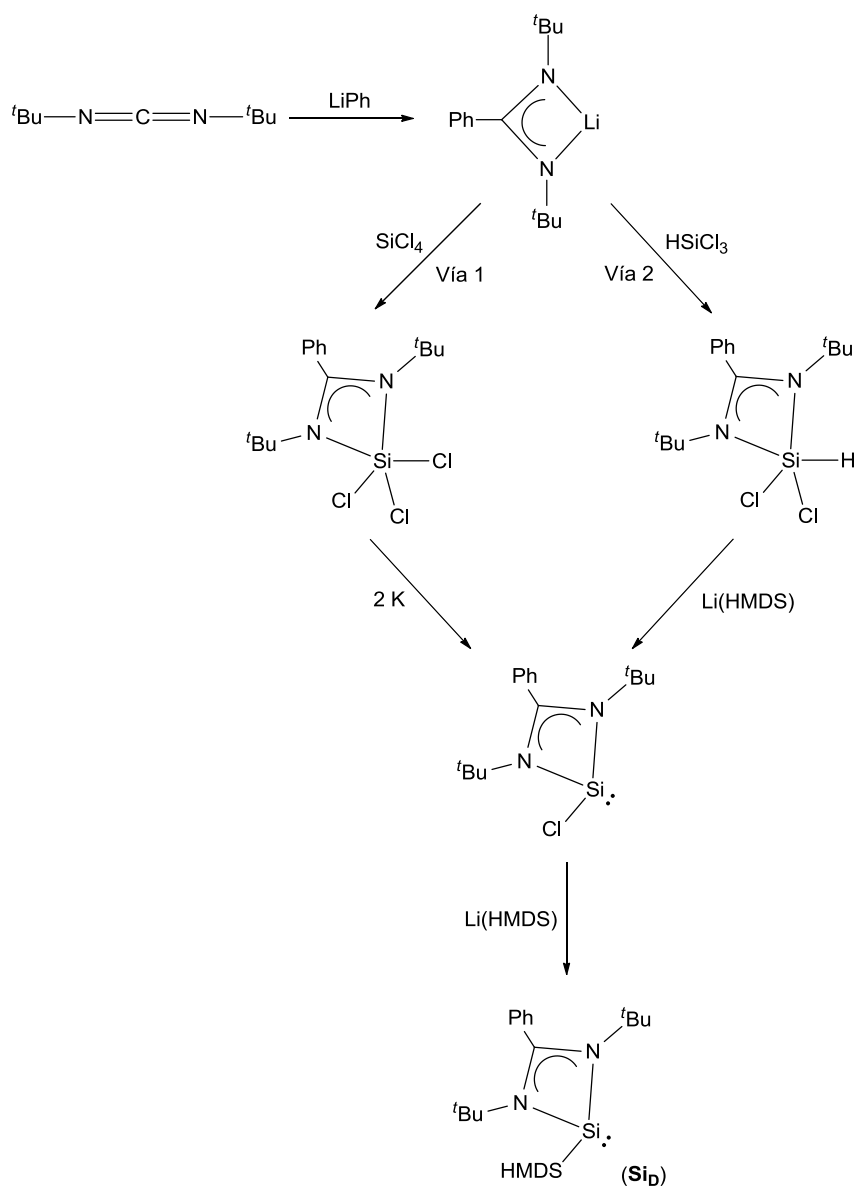
La síntesis de los amidinatogermilenos $\text{Ge}(\text{RR}'\text{bzam})\text{X}$ ($\text{Ge}_{\text{D-H}}$; Esquema IP.1) se llevó a cabo en dos pasos por reacción de GeCl_2 :dioxano con el correspondiente benzamidinato litiado $\text{Li}(\text{RR}'\text{bzam})$, lo que dio lugar a los clorogermilenos $\text{Ge}(\text{RR}'\text{bzam})\text{Cl}$, que fueron seguidamente transmetalados con el litiado LiX correspondiente (Esquema IP.1). El germileno Ge_{E} y su precursor con cloruro ya habían sido descritos por el grupo de investigación de Roesky en 2013^{77a} y 2008,^{77b} respectivamente; sin embargo, los germilenos Ge_{D} , $\text{Ge}_{\text{F-H}}$ y sus cloruros precursores se han preparado por primera vez en esta tesis



Esquema IP.1. Síntesis de los amidinatogermilenos $\text{Ge}_{\text{D-H}}$ utilizados en la Parte II de esta memoria

doctoral. Tanto los clorurogermilenos intermedios formados en el paso 1, $\text{Ge}(\text{RR}'\text{bzam})\text{Cl}$, como los productos de transmetalación finales, $\text{Ge}_{\text{D-H}}$, se obtuvieron con altos rendimientos.^{55c,e,f}

La síntesis de amidinatosililenos es mucho más compleja que la de sus análogos más pesados, puesto que, como se comentó en la Introducción, se tienen que preparar por reducción de derivados de silicio(IV). El primer amidinatosilileno que se aisló fue el derivado $\text{Si}(\text{tBu}_2\text{bzam})\text{Cl}$,⁵³ descrito por el grupo de Roesky en 2006. Su preparación original consistía



Esquema IP.2. Síntesis del amidinatosilileno Si_{D}

en una reducción con potasio metal de $\text{Si}(\text{}^t\text{Bu}_2\text{bzam})\text{Cl}_3$ (preparado a partir de SiCl_4 y del amidinato que resulta de tratar di-*tert*-butilcarbodiimida con PhLi; Esquema IP.2; vía 1).⁵³ El rendimiento conseguido a partir de este método no llegó a superar el 10 %. Sin embargo, el mismo grupo de investigación descubrió poco después una vía de síntesis mucho más eficiente. En ella, $\text{Si}(\text{}^t\text{Bu}_2\text{bzam})\text{HCl}_2$ (preparado a partir de di-*tert*-butilcarbodiimida y PhLi, seguido de un tratamiento con HSiCl_3) es sometido a una dehidrocloración con Li(HMDS), lo que conduce al clorosilileno deseado con un rendimiento del 90 % (Esquema IP.2; vía 2).⁷⁸ Posteriormente, se puede modificar el silileno por medio de una reacción con un litiado LiX para preparar los productos de transmetalación correspondientes. En nuestro caso, hemos utilizado el amidinatosilileno $\text{Si}(\text{}^t\text{Bu}_2\text{bzam})(\text{HMDS})$ (**Si_D**), cuya síntesis ya había sido descrita en la literatura.⁷⁹

En nuestro grupo de investigación, y también en otros, se han intentado preparar, siguiendo el procedimiento del Esquema IP.2, amidinatosililenos análogos a los anteriores con sustituyentes menos voluminosos que el ${}^t\text{Bu}$ (p. ej., ${}^i\text{Pr}$, Cy, SiMe_3),^{3f} pero, desafortunadamente, todos los intentos han sido infructuosos.

Los amidinatoestannilenos y -plumbilenos se descartaron para este trabajo, a pesar de la casi total ausencia de estudios con los mismos y Ms, por su baja estabilidad frente a procesos de hidrólisis (la polaridad del enlace E–N aumenta a medida que se baja en el grupo 14), por la debilidad del enlace E–M (E = Sn, Pb) y, en el caso de los plumbilenos, por su elevada toxicidad.

Capítulo 3

Nuevos modos de coordinación de los amidinato-TPs

Artículo IV

“Expanding the Coordination Chemistry of Donor-Stabilized Group-14 Metalenes”

Artículo V

“Reactivity Studies on a Binuclear Ruthenium(0) Complex Equipped with a Bridging $\kappa^2 N, Ge$ -Amidinatogermylene Ligand”

3.1. Introducción

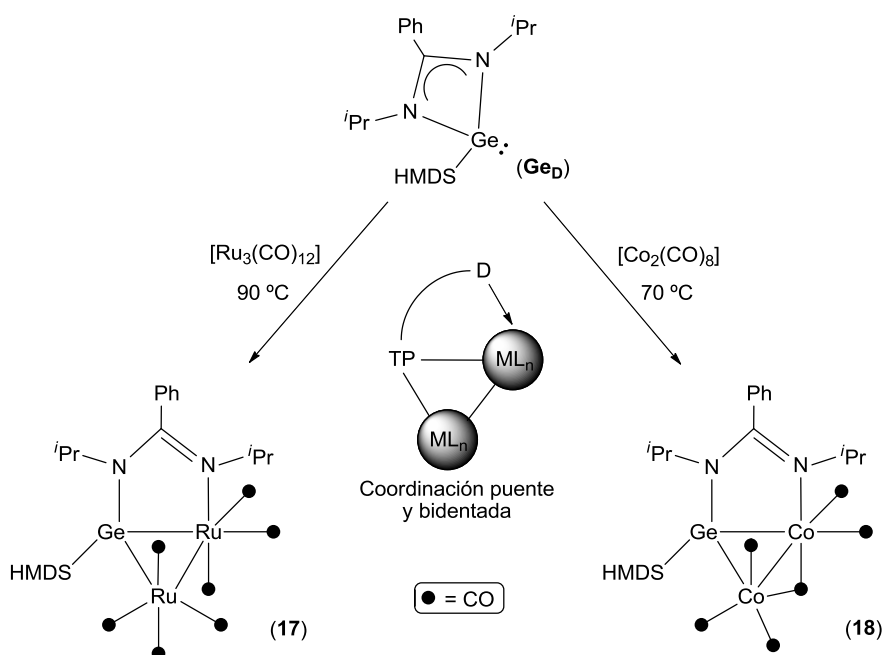
Este capítulo describe la reactividad del amidinatogermileno $Ge(iPr_2bzam)(HMDS)$ (**Ge_D**) frente a $[Ru_3(CO)_{12}]$, $[Co_2(CO)_8]$ y $[MnBr(CO)_5]$. Este germileno se escogió por: (i) poseer grupos N-*i*Pr en su fragmento amidinato (apenas estudiados antes del inicio de esta tesis doctoral), (ii) el bajo precio de la carbodiimida precursora necesaria para su síntesis (*N,N'*-di-*isopropil*carbodiimida; 3 €/g), en comparación con el de la utilizada para la preparación de los amidinato-TPs habituales con grupos N-*t*Bu (*N,N'*-di-*ter*butilcarbodiimida; 34 €/g), y (iii) estar equipado con un grupo terminal HMDS, que es mucho más voluminoso y más dador que un cloruro.

3.2. Resultados

Las reacciones de **Ge_D** con $[MnBr(CO)_5]$ dieron lugar a productos de descomposición cuya naturaleza no pudo ser establecida y, por tanto, no se incluyeron en ninguna publicación.

Las reacciones de **Ge_D** con $[Ru_3(CO)_{12}]$ y $[Co_2(CO)_8]$, a 90 y 70 °C, respectivamente, condujeron a los complejos binucleares $[Ru_2\{\mu-\kappa^2 Ge, N-Ge(iPr_2bzam)(HMDS)\}(CO)_7]$ (**17**) y $[Co_2\{\mu-\kappa^2 Ge, N-Ge(iPr_2bzam)(HMDS)\}(\mu-CO)(CO)_5]$ (**18**) (Esquema 3.1). Las estructuras moleculares de ambos son análogas y difieren únicamente en el número y en el modo de coordinación de los COs (siete COs terminales en **17** y cinco terminales y uno puente en **18**). En estos compuestos, el ligando **Ge_D** adopta una disposición puente bidentada $\mu-\kappa^2 Ge, N$ sobre la especie bimetalica, de modo que el átomo de germanio se coordina puente sobre la arista M-M (M = Ru, Co) y uno de los átomos de nitrógeno del fragmento amidinato se coordina a uno de los dos átomos metálicos. La formación de **17** y **18** implica que **Ge_D**,

que en su forma libre posee su fragmento amidinato unido en modo quelato al átomo de germanio y que dispone solamente de un par de electrones sobre el átomo de germanio para coordinarse, se convierte en un ligando dador de 4 electrones de tipo iminagermileno (rotura de un enlace Ge–N y transferencia del grupo imina al centro metálico). La participación como ligando del grupo dador D de un TP estabilizado intramolecularmente sólo había sido descrita anteriormente por Auner⁵⁸ y col. (Esquema I.8). La apertura del fragmento amidinato se confirmó también en disolución, puesto que los espectros de RMN de los compuestos **17** y **18** muestran señales diferentes para cada uno de los dos grupos N–*i*Pr, lo que indica que éstos no son equivalentes (ambos grupos N–*i*Pr son equivalentes en el germileno libre). Estos resultados se recogen en el artículo IV.



Esquema 3.1. Reacciones del amidinatogermileno Ge_D con $[\text{Ru}_3(\text{CO})_{12}]$ y $[\text{Co}_2(\text{CO})_8]$: Síntesis de los complejos binucleares **17** y **18**

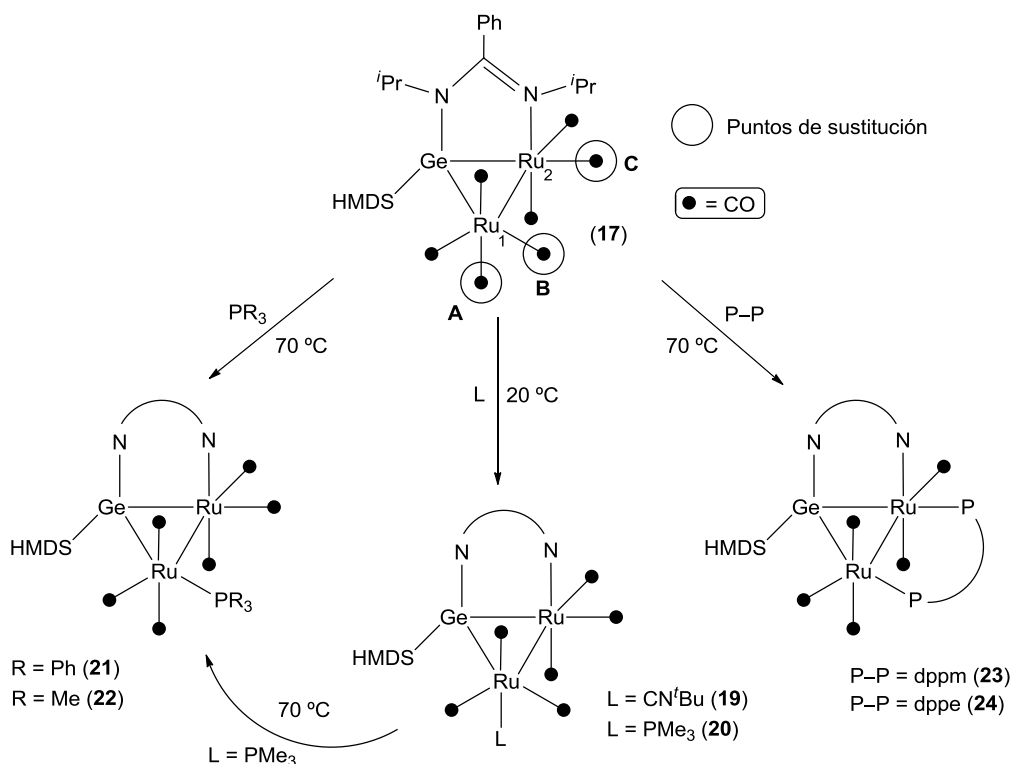
La capacidad de Ge_D de coordinarse en modo $\kappa^2\text{Ge},\text{N}$ es llamativa, puesto que la coordinación inicial a través del átomo de germanio (ver capítulo 4) aumenta la acidez del mismo y, por tanto, la fortaleza de los enlaces Ge–N. Este aumento de la acidez del átomo E con su coordinación es una tendencia general de todos los TPs y su efecto sobre la fortaleza del aducto D–E en TPs estabilizados intramolecularmente es conocido (ver un ejemplo representativo en el Esquema I.9 de la Introducción).^{54o} Es posible que la naturaleza polinuclear de los precursores metálicos utilizados sea un factor clave en el comportamiento bidentado de Ge_D , ya que ésta permite que el germileno se coordine en modo puente $\mu\text{-Ge}$, aliviando así la insaturación generada después de que se rompa el

enlace Ge–N. Otro factor clave es la presencia del grupo HMDS, cuya presión estérica al acercarse el amidinatogermileno al metal se ve aliviada con la apertura del fragmento amidinato. De hecho, en los productos derivados de otras reacciones de amidinato-TPs que no tienen grupos tan grandes como el HMDS (generalmente Cl) con precursores polinucleares como $[\text{Fe}_2(\text{CO})_9]$,^{54u} $[\text{Co}_2(\text{CO})_8]$,^{54q} $[\text{Mn}_2(\text{CO})_{10}]$ ^{54ñ,r} y $[\text{Re}_2(\text{CO})_{10}]$,^{54ñ,r} el ligando TP siempre es $\kappa^1 E$ monodentado.

El derivado de rutenio **17**, a diferencia de la mayoría de complejos metálicos que contienen TPs, es estable al aire y a la humedad durante largos periodos de tiempo. Este factor, unido a la novedad de su ligando puente, nos impulsó a realizar un estudio sistemático de su reactividad, que se encuentra recogido en el artículo V. El derivado de cobalto **18** demostró ser más inestable (tanto frente al aire y a la humedad como frente a procesos de sustitución del ligando) y no nos planteamos estudiar su reactividad.

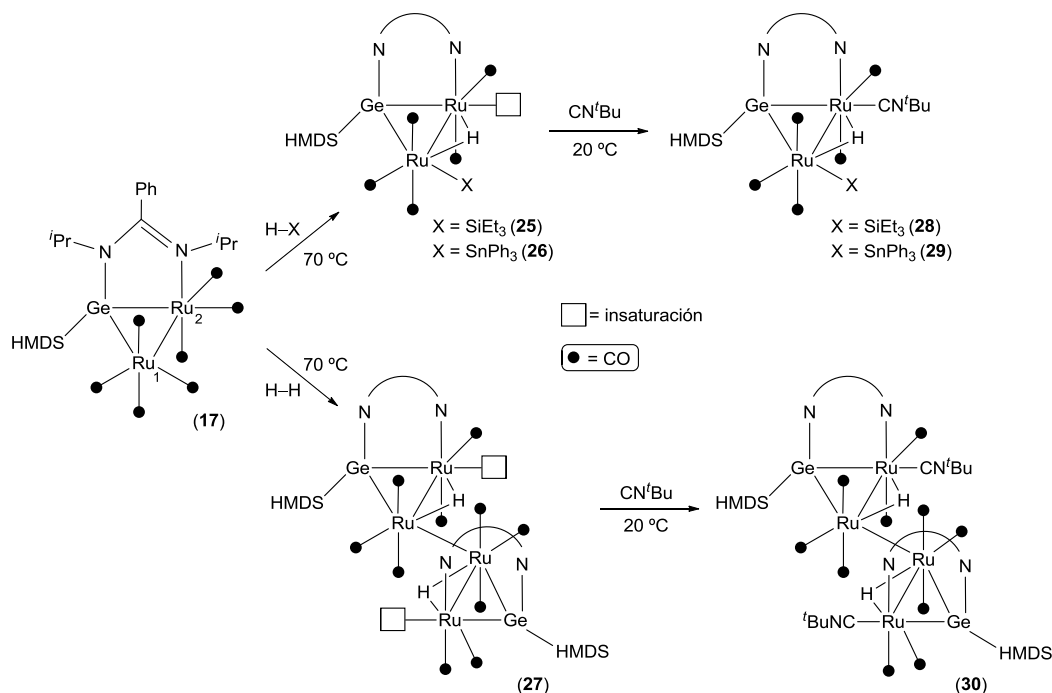
Llevamos a cabo reacciones del complejo **17** con agentes nucleofílicos simples con el propósito de evaluar la posible hemilabilidad de su ligando iminagermileno y la estabilidad del complejo, así como para determinar sus posiciones de coordinación más accesibles. Las reacciones de **17** con CN^tBu y PMe_3 a temperatura ambiente dieron lugar a los derivados $[\text{Ru}_2\{\mu\text{-}\kappa^2\text{Ge}, N\text{-Ge}(\text{Pr}_2\text{bzam})(\text{HMDS})\}\text{L}(\text{CO})_6]$ (L = CN^tBu (**19**); L = PMe_3 (**20**); Esquema 3.2). Estos compuestos resultan de la sustitución de uno de los COs axiales del átomo de rutenio que no está unido al nitrógeno del fragmento amidinato, Ru1 (posición **A**). El compuesto **17** no reaccionó con PPh_3 a temperatura ambiente, presumiblemente por la menor basicidad y el mayor volumen del PPh_3 . Sin embargo, llevando a cabo la reacción a 70 °C, se formó el compuesto $[\text{Ru}_2\{\mu\text{-}\kappa^2\text{Ge}, N\text{-Ge}(\text{Pr}_2\text{bzam})(\text{HMDS})\}(\text{PPh}_3)(\text{CO})_6]$ (**21**), en el que el PPh_3 ocupa la posición ecuatorial **B** sobre Ru1 (Esquema 3.2). Es interesante que el complejo **20** se isomeriza a 70 °C hacia un isómero $[\text{Ru}_2\{\mu\text{-}\kappa^2\text{Ge}, N\text{-Ge}(\text{Pr}_2\text{bzam})(\text{HMDS})\}(\text{PMe}_3)(\text{CO})_6]$ (**22**), en el que el ligando PMe_3 ocupa la misma posición ecuatorial que el PPh_3 en **21** (Esquema 3.2). La posición ecuatorial de los fosfanos de **21** y **22** no pudo determinarse en estado sólido; sin embargo, fue deducida mediante el análisis de los espectros de IR y de experimentos NOE, unidos al hecho de que una isomerización de este tipo es mucho más probable que ocurra sobre el mismo átomo de rutenio. Esta premisa fue posteriormente confirmada mediante la realización de cálculos DFT, que revelaron que el compuesto **20** (producto de control cinético) es 5.3 kcal mol⁻¹ menos estable que su isómero **22** (producto de control termodinámico) y que la transformación que ocurre entre ellos es un proceso muy común de tipo “trigonal twist” (entre el PMe_3 y dos COs sobre el mismo átomo de rutenio) con una barrera de activación de 29.2 kcal mol⁻¹.

Finalmente, el compuesto **17** reaccionó con fosfanos bidentados, como dppm y dppe, para formar $[\text{Ru}_2\{\mu\text{-}\kappa^2\text{Ge}, N\text{-Ge}(\text{Pr}_2\text{bzam})(\text{HMDS})\}\text{L}(\text{CO})_5]$ (L = dppm (**23**); L = dppe (**24**); Esquema 3.2). Estos compuestos son el resultado de una doble sustitución de CO (posiciones **B** y **C** en **17**), de modo que los fosfanos se disponen puentes sobre Ru1 y Ru2 ocupando dos posiciones ecuatoriales (aproximadamente *trans* al Ge).



Esquema 3.2. Reacciones de sustitución de CO sobre el compuesto **17**: Síntesis de los complejos **19–24**

El compuesto **17** también reaccionó con compuestos inorgánicos de tipo H–X (X = SiEt_3 , SnPh_3 , H) dando lugar a productos coordinativamente insaturados que resultan, entre otros procesos, de la adición oxidante del H–X. Mientras que las reacciones con HSiEt_3 y HSnPh_3 dieron lugar a los compuestos binucleares $[\text{Ru}_2\text{X}(\mu\text{-H})\{\mu\text{-}\kappa^2\text{Ge}, N\text{-Ge}(\text{Pr}_2\text{bzam})(\text{HMDS})\}(\text{CO})_5]$ (X = SiEt_3 (**25**); X = SnPh_3 (**26**)), la reacción con H_2 condujo al derivado tetranuclear $[\text{Ru}_4(\mu\text{-H})_2\{\mu\text{-}\kappa^2\text{Ge}, N\text{-Ge}(\text{Pr}_2\text{bzam})(\text{HMDS})\}_2(\text{CO})_{10}]$ (**27**) (Esquema 3.3). En los tres compuestos: (i) el ligando hidruro se coordina puente sobre la arista de rutenios, (ii) la vacante de coordinación se sitúa en la posición ecuatorial **C** de Ru2, que está unido al nitrógeno del fragmento amidinato, y (iii) el grupo X (X = SiEt_3 (**25**), SnPh_3 (**26**)) o una unidad $[\text{Ru}_2(\mu\text{-H})\{\mu\text{-}\kappa^2\text{Ge}, N\text{-Ge}(\text{Pr}_2\text{bzam})(\text{HMDS})\}(\text{CO})_5]$ (en el caso de **27**) están unidos al átomo de rutenio que no está conectado al grupo amidinato (posición ecuatorial **B** de Ru1).



Esquema 3.3. Reacciones de activación de enlaces H-X ($X = \text{SiEt}_3$, SnPh_3 , H) con el compuesto **17**: Síntesis de los complejos **25–30**

La vacante de coordinación puede ser ocupada de manera irreversible por otros ligandos, como CN^tBu , lo que permitió aislar los derivados saturados $[\text{Ru}_2(\mu\text{-H})\text{X}\{\mu\text{-}\kappa^2\text{Ge}, \text{N-Ge}(\text{Pr}_2\text{bzam})(\text{HMDS})\}(\text{CN}^t\text{Bu})(\text{CO})_5]$ ($X = \text{SiEt}_3$ (**28**); $X = \text{SnPh}_3$ (**29**)) y $[\text{Ru}_4(\mu\text{-H})_2\{\mu\text{-}\kappa^2\text{Ge}, \text{N-Ge}(\text{Pr}_2\text{bzam})(\text{HMDS})\}_2(\text{CN}^t\text{Bu})_2(\text{CO})_{10}]$ (**30**) (Esquema 3.3). Si, por el contrario, el ligando utilizado es CO, esta ocupación tiene lugar de forma reversible, pudiéndose eliminar el CO incorporado por simple evaporación del disolvente a vacío o por calentamiento del complejo correspondiente en disolución. En la Figura 3.1 se muestra, a modo de ejemplo, la reacción del compuesto insaturado **26** con CO para dar el derivado saturado $[\text{Ru}_2(\mu\text{-H})(\text{SnPh}_3)\{\mu\text{-}\kappa^2\text{Ge}, \text{N-Ge}(\text{Pr}_2\text{bzam})(\text{HMDS})\}(\text{CO})_6]$ (**31**), así como los espectros de ^{13}C RMN de ambos compuestos en la zona de ligandos CO de muestras enriquecidas en ^{13}C . Esta transformación fue la única que pudo ser caracterizada correctamente por RMN, ya que los productos de incorporación de CO a **25** y **27** se descompusieron hacia sus precursores al intentar su aislamiento. Las estructuras de **25–31** se confirmaron por métodos espectroscópicos (RMN e IR) y por difracción de rayos-X de monocristal (para **28** y **30**). La realización de cálculos DFT sobre la estructura del compuesto **28**, optimizándola eliminando el CN^tBu de **30**, reveló que la insaturación en los compuestos **25–27** está aliviada por una interacción agóstica entre el átomo de rutenio unido al fragmento amidinato y un átomo de hidrógeno de un grupo ^iPr del mismo.

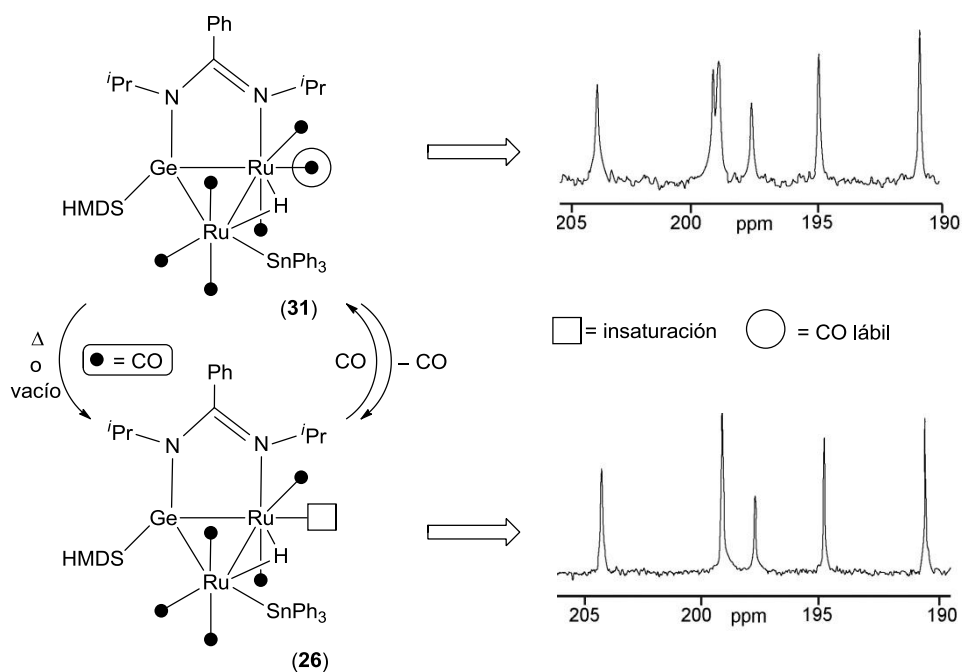
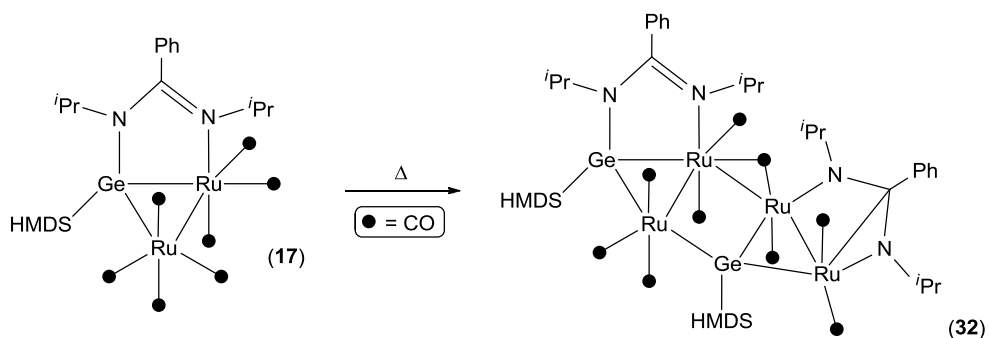


Figura 3.1. Pérdida reversible de CO en el compuesto **31** (izq.). Región de ligandos CO de los espectros de ^{13}C RMN de **31** y **26** (dcha.)

Finalmente, se evaluó la estabilidad térmica del compuesto **17**. Este demostró ser estable durante largos periodos de tiempo a 90–100 °C en tolueno. Sin embargo, a la temperatura de reflujo del mismo, evolucionó hacia el derivado tetranuclear $[\text{Ru}_4\{\mu\text{-}\kappa^2\text{Ge}, N\text{-Ge}(\text{Pr}_2\text{bzam})(\text{HMDS})\}\{\mu_3\text{-}\kappa^1\text{Ge-Ge}(\text{HMDS})\}\{\mu\text{-}\kappa^3 N, C, N\text{-}(\text{Pr}_2\text{bzam})\}(\mu\text{-CO})(\text{CO})_8]$ (**32**), cuya estructura se determinó inequívocamente por difracción de rayos-X (Esquema 3.4). Este compuesto, que resulta de la condensación de dos moléculas de **17** con pérdida formal de cinco COs (los procesos de descarbonilación son comunes en clusters carbonílicos a altas temperaturas),⁸⁰ mantiene la integridad del ligando iminogermileno en una de las unidades



Esquema 3.4. Reacción de termólisis del compuesto **17**: Síntesis del complejo tetranuclear **32**

Ru_2Ge , mientras que en la otra se ha producido la fragmentación del ligando original para dar un germilidino [$\mu_3\text{-}\kappa^1\text{Ge-Ge(HMDS)}$] y un benzamidinato [$\mu\text{-}\kappa^3\text{N,C,N-}(\text{Pr}_2\text{bzam})$]. La fragmentación de amidinato-TPs unidos a Ms ya se ha observado previamente. El grupo de Castel, por ejemplo, describió la evolución de amidinatogermilenos de rodio(I) [$\text{RhCl(COD)}\{\kappa^1\text{Ge-Ge(R}_2\text{bzam)}_2\}$] ($\text{R} = \text{tBu, SiMe}_3$) hacia complejos amidinatorodio de fórmula general [$\text{Rh(R}_2\text{bzam)(COD)}$].⁸¹

3.3. Conclusiones

En este capítulo se ha demostrado que cambios en el volumen de los amidinato-TPs, junto con su incorporación a derivados polimetálicos, permiten expandir la química de coordinación de los TPs. Así, el germileno $\text{Ge}(\text{Pr}_2\text{bzam})(\text{HMDS})$ (**Ge_D**), que cuenta únicamente con un par de electrones en el átomo de germanio para coordinarse, se transforma en un ligando puente dador de cuatro electrones de tipo $\mu\text{-}\kappa^2\text{Ge,N-}$ iminagermileno cuando se hace reaccionar con [$\text{Ru}_3(\text{CO})_{12}$] o [$\text{Co}_2(\text{CO})_8$] (compuestos **17** y **18**). Esta transformación nunca se había descrito antes para amidinato-TPs, cuyo único modo de coordinación conocido era $\kappa^1\text{E}$. Los factores clave que parecen regir este comportamiento inusual de **Ge_D** son el gran volumen del grupo HMDS (la apertura del fragmento amidinato alivia los impedimentos estéricos ejercidos por este grupo) y la presencia de más de un metal de transición, que permite la coordinación puente del átomo de germanio y que éste siga siendo tetracoordinado.

Las reacciones llevadas a cabo con el compuesto **17** han permitido conocer: (i) sus principales puntos de reactividad en sus reacciones con fosfanos e isocianuros (compuestos **19–24**), (ii) su capacidad para activar enlaces H–X ($\text{X} = \text{SiEt}_3, \text{SnPh}_3, \text{H}$) en condiciones suaves (70 °C), dando lugar a productos de adición oxidante que son coordinativamente insaturados (compuestos **25–27**). Estos derivados, cuya vacante coordinativa se ve aliviada por uno de los grupos Pr del fragmento amidinato, son capaces de alojar nuevos ligandos en esta vacante reversible- e irreversiblemente (compuestos **28–30**), y (iii) el resultado de su termólisis (compuesto **32**). Este estudio de reactividad reveló la gran estabilidad del ligando iminagermileno, ya que éste permanece inalterado en la mayoría de las reacciones descritas. Sin embargo, esta estabilidad también impidió observar un comportamiento hemilábil del mismo.

Capítulo 4

***La influencia de pequeños cambios en el volumen
del fragmento amidinato***

Artículo VI

“Ring Opening and Bidentate Coordination of Amidinate Germynes and Silylenes on Carbonyl Dicobalt Complexes: The Importance of a Slight Difference in Ligand Volume”

Artículo VII

“Steric Effects in the Reactions of Amidinate Germynes with Ruthenium Carbonyl: Isolation of a Coordinatively Unsaturated Diruthenium(0) Derivative”

4.1. Introducción

Este capítulo describe reacciones de los germilenos $\text{Ge}(\text{tBu}_2\text{bzam})(\text{HMDS})$ (Ge_E) y $\text{Ge}(\text{tBuEtbzam})(\text{HMDS})$ (Ge_F) y del silileno $\text{Si}(\text{tBu}_2\text{bzam})(\text{HMDS})$ (Si_D) frente a $[\text{Ru}_3(\text{CO})_{12}]$, $[\text{Co}_2(\text{CO})_8]$ y $[\text{MnBr}(\text{CO})_5]$. Estos amidinato-TPs se escogieron para conocer el efecto que otros grupos N–R de diferente volumen y distintos átomos E tienen sobre la reactividad de amidinato-TPs.

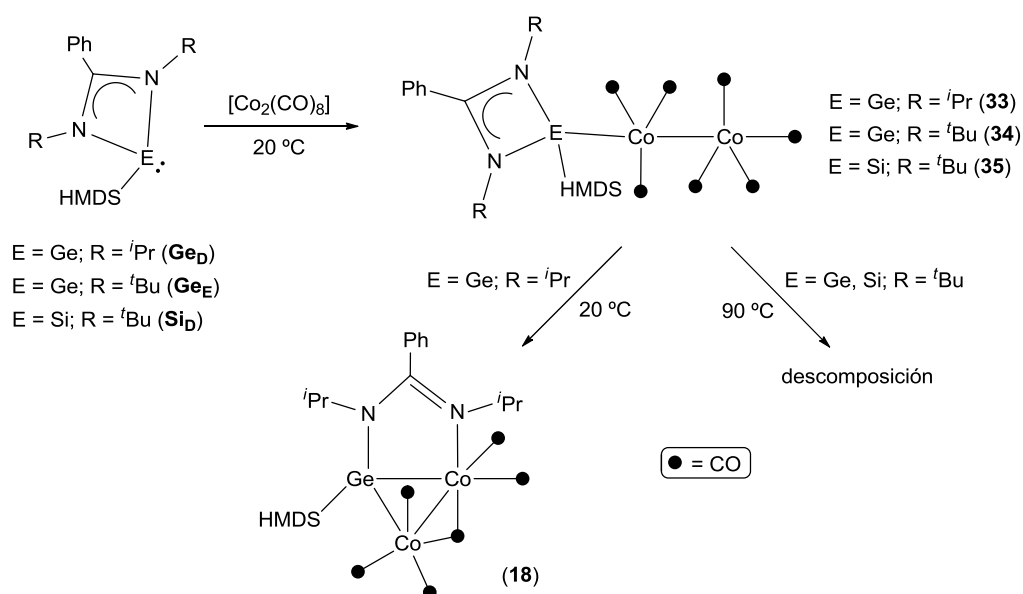
4.2. Resultados

Las reacciones de $\text{Ge}_{E,F}$ y Si_D con $[\text{MnBr}(\text{CO})_5]$ dieron lugar a productos de descomposición cuya naturaleza no pudo ser establecida y, por tanto, no se incluyeron en ninguna publicación.

El seguimiento por IR de las reacciones de $[\text{Ru}_3(\text{CO})_{12}]$ y $[\text{Co}_2(\text{CO})_8]$ con $\text{Ge}(\text{tPr}_2\text{bzam})(\text{HMDS})$ (Ge_D), descritas en el capítulo anterior (Esquema 3.1; síntesis de los derivados **17** y **18**), permitió detectar algunas especies intermedias. En la reacción de $[\text{Ru}_3(\text{CO})_{12}]$ con Ge_D , que sólo ocurre a 90 °C, se detectó el derivado trinuclear $[\text{Ru}_3\{\kappa^1\text{Ge}-\text{Ge}(\text{tPr}_2\text{bzam})(\text{HMDS})\}(\text{CO})_{11}]$ (por comparación del patrón de bandas $\nu(\text{CO})$ de su espectro de IR con los de otros complejos $[\text{Ru}_3(\kappa^1\text{L})(\text{CO})_{11}]$ descritos),⁸² aunque no pudo ser aislado. Sin embargo, en la reacción de $[\text{Co}_2(\text{CO})_8]$ con Ge_D a temperatura ambiente, sí se pudo aislar y caracterizar el derivado $[\text{Co}_2\{\kappa^1\text{Ge}-\text{Ge}(\text{tPr}_2\text{bzam})(\text{HMDS})\}(\text{CO})_7]$ (**33**), en el que el amidinatogermileno actúa como un ligando terminal. Este compuesto es térmicamente

inestable y se transforma de forma cuantitativa, incluso a temperatura ambiente, en el compuesto **18** (Esquema 4.1).

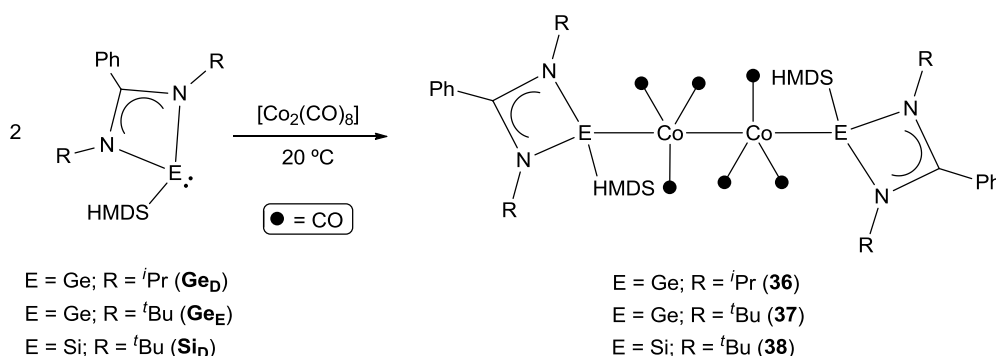
Las reacciones a temperatura ambiente de Ge_E y Si_D , que contienen grupos $\text{N-}^t\text{Bu}$ en sus fragmentos amidinato, con $[\text{Co}_2(\text{CO})_8]$ (Artículo VI) formaron los complejos $[\text{Co}_2\{\kappa^1 E\text{-E}(\text{Pr}_2\text{bzam})(\text{HMDS})\}(\text{CO})_7]$ ($E = \text{Ge}$ (**34**); $E = \text{Si}$ (**35**); Esquema 4.1), que son análogos a **33**. Sin embargo, estos derivados resultaron ser estables a temperatura ambiente y, al contrario que **33**, no evolucionaron hacia un compuesto $\kappa^2\text{Ge,N}$ estable, sino que se descompusieron al ir aumentando la temperatura, dejando claro que el volumen de los grupos N-R juega un papel importante en esta transformación.



Esquema 4.1. Reacciones de $[\text{Co}_2(\text{CO})_8]$ con los amidinato-TPs Ge_D , Ge_E y Si_D : Síntesis de los complejos **18** y **33–35**

Para conocer el mecanismo por el cual se produce la apertura y la coordinación bidentada de amidatosililenos o -germilenos en fragmentos dicobalto se llevó a cabo un estudio computacional (DFT). Este estudio demostró que el proceso apenas se ve afectado por la naturaleza del átomo E (Si o Ge), pero que sí depende en gran medida del volumen de los grupos N-R , ya que es termodinámicamente favorable para $R = ^i\text{Pr}$ pero es desfavorable para $R = ^t\text{Bu}$. Por ello, si existiese una vía de síntesis para el amidatosilileno $\text{Si}(^i\text{Pr}_2\text{bzam})(\text{HMDS})$, se podría observar un comportamiento bidentado del mismo. Los cálculos DFT también indicaron que los compuestos teóricos análogos a **18** con grupos $\text{N-}^t\text{Bu}$ en vez de $\text{N-}^i\text{Pr}$ son considerablemente menos estables, lo que avala los resultados experimentales observados.

Las reacciones de $[\text{Co}_2(\text{CO})_8]$ con 2 equiv. de Ge_D , Ge_E y Si_D condujeron a los complejos disustituidos $[\text{Co}_2\{\kappa^1 E\text{-E}(\text{R}_2\text{bzam})(\text{HMDS})\}_2(\text{CO})_6]$ ($E = \text{Ge}$, $R = i\text{Pr}$ (**36**); $E = \text{Ge}$, $R = t\text{Bu}$ (**37**); $E = \text{Si}$, $R = t\text{Bu}$ (**38**); Esquema 4.2). Estos complejos se ven afectados, de nuevo, por el volumen del grupo N–R, de tal manera que los derivados con N– $t\text{Bu}$ (**37** y **38**) resultaron ser estables, mientras que el compuesto **36** sólo se pudo detectar pero no aislar. El valor de la absorción $\nu(\text{CO})$ más intensa en los espectros de IR de estos complejos nos permitió establecer, por comparación con los espectros de IR de otros derivados $[\text{Co}_2\text{L}_2(\text{CO})_6]$, que la capacidad dadora de estos amidinato-TPs es comparable (en el caso de los germilenos Ge_D y Ge_E) e incluso superior (en el caso del silileno Si_D) a la de CNHs o fosfanos muy básicos.⁸³

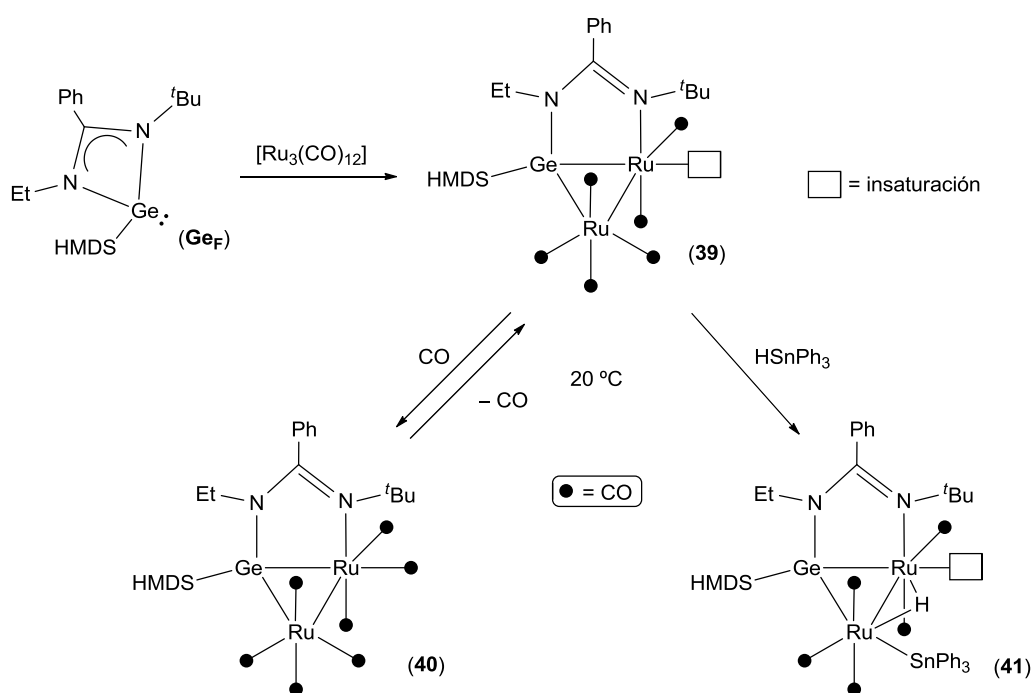


Esquema 4.2. Reacciones de $[\text{Co}_2(\text{CO})_8]$ con 2 equiv. de los amidinato-TPs Ge_D , Ge_E y Si_D : Síntesis de los complejos disustituidos **36–38**

La química descrita con cobalto en el artículo VI nos impulsó a estudiar las reacciones de $[\text{Ru}_3(\text{CO})_{12}]$ con los amidinato-TPs Ge_E y Si_D , que contienen grupos N– $t\text{Bu}$. Las reacciones, al igual que cuando usamos Ge_D , sólo ocurrían a 90 °C y de nuevo se detectó inicialmente la formación de especies intermedias de tipo $[\text{Ru}_3(\kappa^1 L)(\text{CO})_{11}]$. Sin embargo, mayores tiempos de reacción no dieron lugar a derivados análogos a **17**, sino que se formaron mezclas de productos que no pudieron ser identificados ni aislados. Estos resultados, que se mantienen en la línea observada en las reacciones de $[\text{Co}_2(\text{CO})_8]$ con los amidinato-TPs Ge_E y Si_D , nos indican que, también en derivados polimetálicos de rutenio, la presencia de los grupos N– $t\text{Bu}$ impide la formación de complejos estables con ligandos $\kappa^2 E, N$.

A la vista de estos datos decidimos comprobar si la reducción del volumen de sólo uno de los grupos N–R del fragmento amidinato sería suficiente para conseguir una coordinación $\kappa^2 E, N$ como la observada en **17** y **18**. Para ello, se hizo reaccionar el amidinatogermileno asimétrico $\text{Ge}(t\text{BuEt}\text{bzam})(\text{HMDS})$ (Ge_F), provisto de un grupo N– $t\text{Bu}$ y otro N–Et, con $[\text{Ru}_3(\text{CO})_{12}]$. De esta reacción se pudo aislar, de nuevo pasando por un

intermedio de tipo $[\text{Ru}_3(\kappa^1\text{L})(\text{CO})_{11}]$, el complejo binuclear $[\text{Ru}_2\{\mu\text{-}\kappa^2\text{Ge}, \text{N-Ge}(\text{tBuEtbzam})(\text{HMDS})\}(\text{CO})_6]$ (**39**), en el que se ha producido la apertura del fragmento amidinato (Esquema 4.3). Es destacable que esta apertura ocurre de forma selectiva, puesto que sólo se forma el complejo en el que el grupo N–Et está unido al átomo de germanio y el grupo N–^tBu a rutenio. El compuesto **39** es muy parecido a **17**, pero con una importante diferencia, que es la presencia de una vacante de coordinación en el átomo de rutenio unido al fragmento amidinato. Cabe destacar que los complejos binucleares insaturados de rutenio(0) son muy poco habituales.⁸⁴



Esquema 4.3. Reacción de $[\text{Ru}_3(\text{CO})_{12}]$ con Ge_F : Síntesis y reactividad del complejo **39**

Esta vacante, de un modo similar a lo observado en los compuestos **25–27**, está estabilizada por interacciones agósticas con átomos de hidrógeno, del grupo N–^tBu en este caso. Por RMN se pudo detectar que el grupo N–Et está muy cerca del fragmento HMDS, lo que explica por qué este tipo de complejos no se pueden preparar con los bis(*tert*-butil)amidinato-TPs Ge_E y Si_D (el grupo N–^tBu no cabe entre los grupos Ph y HMDS cuando se produce la apertura del amidinato). Por último, se llevaron a cabo las reacciones de **39** con CO y HSnPh_3 , que permitieron establecer que: (i) la vacante de coordinación puede ser ocupada de forma reversible por CO para dar **40** (Esquema 4.3), que sólo es estable bajo atmósfera de CO, evolucionando hacia **39** bajo atmósfera de argón o a vacío), y (ii) la activación del enlace H–Sn ocurre con pérdida de CO, manteniéndose la vacante

coordinativa (síntesis de **41**; Esquema 4.3). La síntesis de **39** y el estudio preliminar de su reactividad se recogen en el artículo VII.

4.3. Conclusiones

Los estudios experimentales y teóricos descritos en este capítulo arrojan luz sobre el papel que juega el volumen de los grupos N–R del fragmento amidinato en las reacciones de amidinato-TPs de tipo E(RR'bzam)(HMDS) (E = Si, Ge; R, R' = diferentes grupos; **Ge_{D,F}** y **Si_D**) con [Co₂(CO)₈] y [Ru₃(CO)₁₂]. Se puede concluir que los amidinato-TPs equipados con, al menos, un grupo N–R menos voluminoso que N–^tBu (R = ⁱPr, Et) se pueden coordinar en modo puente y bidentado (compuestos **17**, **18** y **39**). Se pudo demostrar que la formación de estos complejos se produce mediante la apertura del fragmento amidinato de precursores donde los ligandos se coordinan en modo terminal $\kappa^1 E$ (complejo **33** y derivados detectados [Ru₃($\kappa^1 L$)(CO)₁₁] (L = **Ge_{D,F}**). Si estos TP's no cuentan con un grupo N–R poco voluminoso sólo es posible su coordinación $\kappa^1 E$ (complejos **34** y **35** y derivados detectados [Ru₃($\kappa^1 L$)(CO)₁₁] (L = **Ge_E** y **Si_D**)).

Analizando los datos de IR en la región $\nu(\text{CO})$ de **36–38** se pudo establecer que la capacidad dadora de los amidinato-TPs empleados es muy alta, incluso superior a la de muchos CNHs en el caso del amidinatosilileno **Si_D**.

El compuesto **39**, que deriva del amidinatogermileno asimétrico **Ge_F**, es un complejo binuclear de rutenio(0) insaturado que es capaz de reaccionar reversiblemente con CO y de activar el enlace H–SnPh₃ a temperatura ambiente (compuestos **40** y **41**). En estos compuestos, el fragmento N–^tBu unido a rutenio es capaz de estabilizar de modo muy eficiente la vacante coordinativa situada *cis* al mismo, como demuestra la estabilidad de los compuestos **39** y **41** y la inestabilidad del derivado saturado **40**.

Capítulo 5

***Aumentando la capacidad de coordinación
de los amidinato-TPs***

Artículo VIII

“Amidinatogermylene Derivatives of Ruthenium Carbonyl: New Insights into the Reactivity of $[Ru_3(CO)_{12}]$ with 2-Electron-Donor Reagents of High Basicity”

Artículo IX

“Conversion of a Monodentate Amidinate-Germylene Ligand into Chelating Imine-Germanate Ligands (on Mononuclear Manganese Complexes)”

5.1. Introducción

Este capítulo describe la reactividad de los germilenos $Ge(R_2bzam)(^tBu)$ ($R = ^iPr$, **Ge_G**; $R = ^tBu$, **Ge_H**) frente a $[Ru_3(CO)_{12}]$, $[Co_2(CO)_8]$ y $[MnBr(CO)_5]$. Estos TPs difieren de los utilizados en los capítulos 3 y 4 en que el grupo X terminal unido al átomo de germanio es ahora tBu y antes era HMDS. Este cambio, que *a priori* no parece muy significativo, ha provocado un gran cambio en la capacidad de coordinación de estos amidinatogermilenos. De hecho, el uso de **Ge_G** y **Ge_H** ha permitido incrementar considerablemente la pequeña familia de complejos de rutenio que contienen amidinato-TPs y, además, ha dado lugar, por primera vez a lo largo de este trabajo, a resultados positivos con $[MnBr(CO)_5]$.

Por otro lado, algunos complejos carbonílicos de manganeso(I) han sido recientemente identificados como catalizadores eficientes en la reducción electroquímica de CO_2 .⁸⁵ Teniendo en cuenta que el manganeso es el tercer metal de transición más abundante en la corteza terrestre, su empleo en esta reacción catalítica supone una gran ventaja con respecto al de otros complejos de Ms menos abundantes y más caros, por ejemplo de renio (Figura 5.1).⁸⁶ En este campo, destacan estudios recientes de los grupos de investigación de Kubiak,^{85b,c} de Chardon-Noblat y Deronzier,^{85d} y de Agarwal,^{85a} empleando complejos de manganeso(I) de tipo $[MnX(N-N)(CO)_3]$ ($X = \text{halógeno}$; $N-N = \text{bipiridina con y sin sustituyentes}$; Figura 5.1). Estos complejos catalizan, de manera eficiente y selectiva, la reducción de CO_2 a CO a potenciales menos negativos que sus análogos de renio y, por ello, suponen una vía de investigación con gran potencial. En la actualidad, se están dedicando muchos esfuerzos a mejorar los grados de conversión de CO_2 hacia sus posibles productos de reducción (principalmente CO), así como en reducir los potenciales de trabajo de estos sistemas mediante la funcionalización del ligando

bipiridina o incluso su sustitución por otro tipo de ligandos. Por ejemplo, en 2014^{85a} aparecieron los primeros complejos de manganeso(I) conteniendo un CNH capaces de llevar a cabo este proceso a potenciales comparables con los de los derivados de bipiridinas (Figura 5.1).

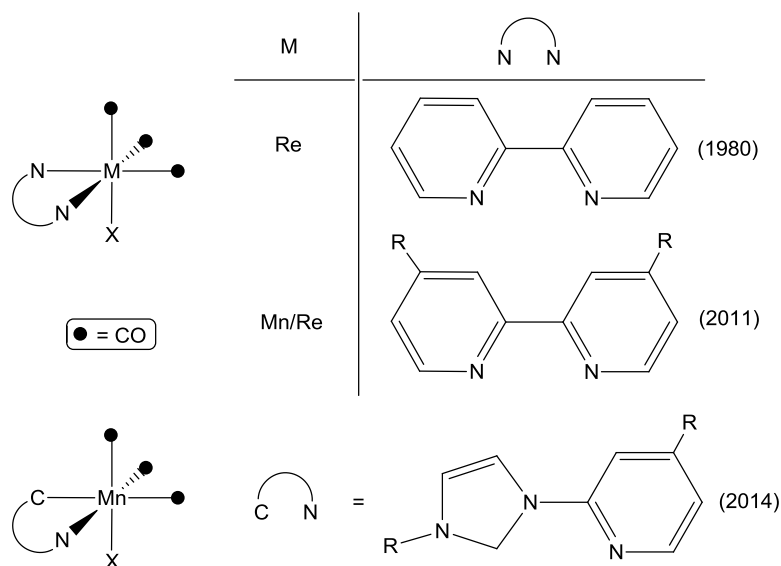


Figura 5.1. Complejos de manganeso(I) y renio(I) usados en la reducción electroquímica de CO_2

Estos datos recientes nos animaron a explorar la actividad catalítica en la reducción electroquímica de CO_2 de algunos de los compuestos de manganeso(I) derivados de amidinatogermilenos descritos en este capítulo.

5.2. Resultados

Las reacciones de Ge_G y Ge_H con $[\text{Co}_2(\text{CO})_8]$ condujeron a mezclas de reacción muy complejas de las que no se pudo aislar ningún compuesto puro y, por tanto, no se incluyeron en ninguna publicación.

Las reacciones de $[\text{Ru}_3(\text{CO})_{12}]$ con Ge_G y Ge_H (artículo VIII), utilizando diferentes temperaturas y relaciones molares de reactivos, dieron lugar a mezclas en las cuales se pudo detectar y/o aislar derivados tri-, bi- y/o mononucleares con diferentes grados de sustitución (Figura 5.2). En todos los casos salvo en el complejo binuclear **51**, en el que el germileno Ge_G se coordina en modo $\mu\text{-}\kappa^2\text{Ge}_2\text{N}$, los ligandos se coordinan en modo terminal $\kappa^1\text{Ge}$. Cabe destacar que, mientras que $[\text{Ru}_3(\text{CO})_{12}]$ sólo reacciona con Ge_{D-F} (provistos de un grupo HMDS unido a germanio) a partir de 90 °C, Ge_G y Ge_H , provistos de un grupo N- t Bu, son capaces de reaccionar a temperatura ambiente.

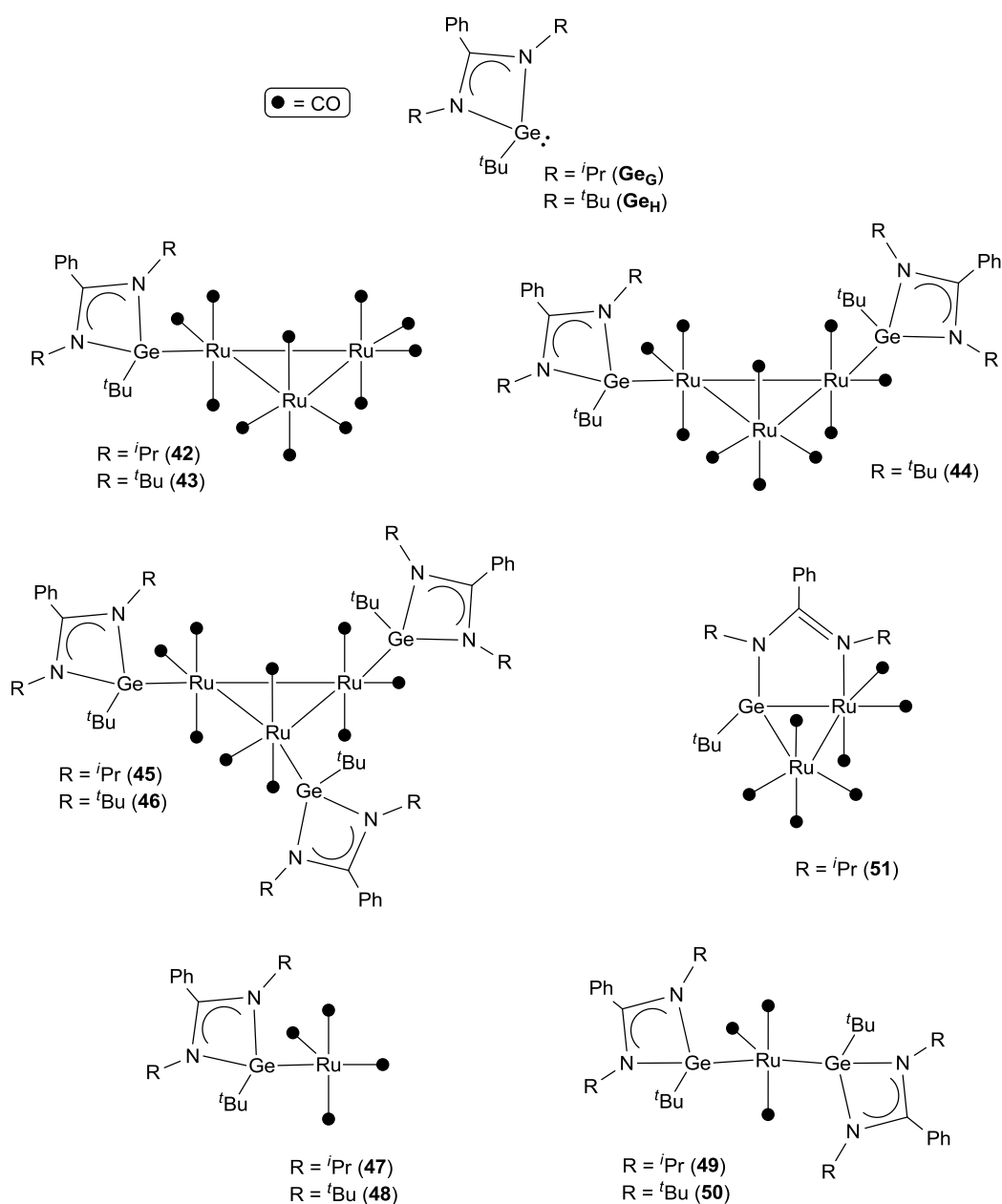
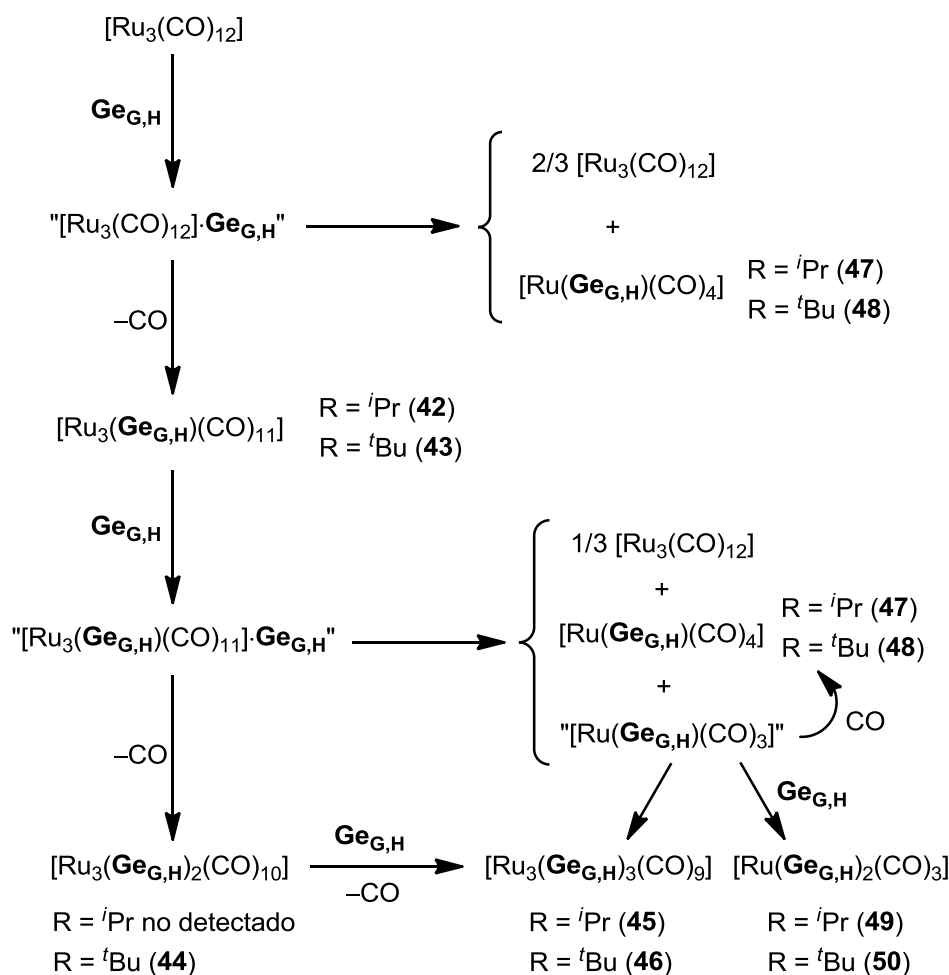


Figura 5.2. Complejos 42–51

Un análisis cuidadoso de la composición de estas mezclas y la realización de una gran cantidad de experimentos independientes permitieron proponer un esquema de reacciones que relaciona los productos obtenidos. A temperatura ambiente (Esquema 5.1), los germilenos $\text{Ge}_{G,H}$ reaccionan con $[\text{Ru}_3(\text{CO})_{12}]$ formando, posiblemente, aductos de tipo “ $[\text{Ru}_3(\text{CO})_{12}] \cdot \text{Ge}_{G,H}$ ” que no pudieron ser detectados. Éstos pueden evolucionar de dos maneras: (i) perdiendo un ligando CO, lo que conduce a los derivados trinucleares

monosustituidos $[\text{Ru}_3\{\kappa^1\text{Ge-Ge}(\text{R}_2\text{bzam})(\text{tBu})\}(\text{CO})_{11}]$ ($\text{R} = \textit{i}\text{Pr}$ (**42**); $\text{R} = \textit{t}\text{Bu}$ (**43**)), y/o (ii) fragmentándose, dando lugar a los derivados mononucleares monosustituidos $[\text{Ru}\{\kappa^1\text{Ge-Ge}(\text{R}_2\text{bzam})(\text{tBu})\}(\text{CO})_4]$ ($\text{R} = \textit{i}\text{Pr}$ (**47**); $\text{R} = \textit{t}\text{Bu}$ (**48**)) y a $[\text{Ru}_3(\text{CO})_{12}]$. Los derivados trinucleares **42** y **43** pueden reaccionar con otro equiv. de $\text{Ge}_{\text{G,H}}$ formando, presumiblemente, aductos de tipo “ $[\text{Ru}_3(\text{Ge}_{\text{G,H}})(\text{CO})_{11}] \cdot \text{Ge}_{\text{G,H}}$ ” que tampoco pudieron ser detectados. Estos aductos de nuevo pueden evolucionar de dos maneras: (i) perdiendo un

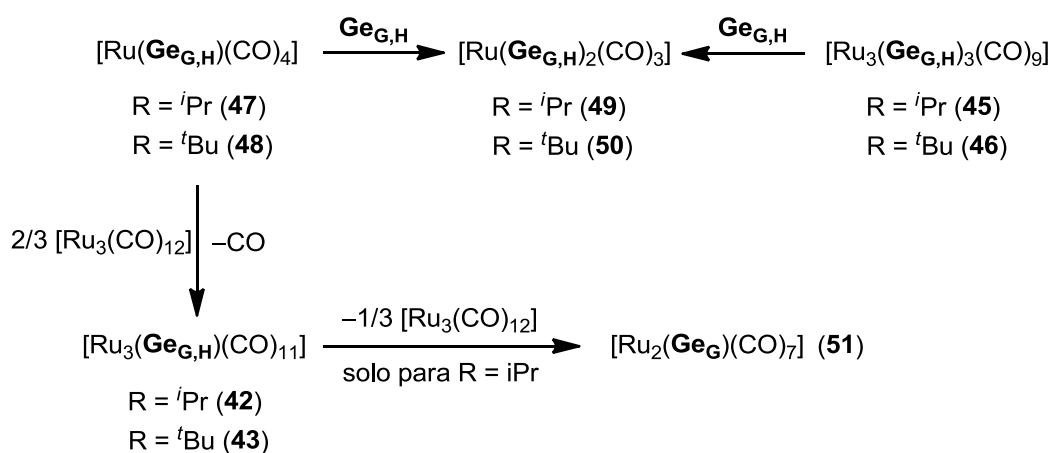


Esquema 5.1. Relación existente entre los productos obtenidos y/o detectados en las reacciones de $[\text{Ru}_3(\text{CO})_{12}]$ con $\text{Ge}_{\text{G,H}}$ a temperatura ambiente

ligando CO, lo que conduce a los derivados trinucleares disustituidos $[\text{Ru}_3\{\kappa^1\text{Ge-Ge}(\text{R}_2\text{bzam})(\text{tBu})\}_2(\text{CO})_{10}]$ ($\text{R} = \textit{i}\text{Pr}$, no pudo ser detectado; $\text{R} = \textit{t}\text{Bu}$ (**44**)) que, por reacción con otro equiv. de $\text{Ge}_{\text{G,H}}$, pierden otro CO, formando los derivados trinucleares trisustituidos $[\text{Ru}_3\{\kappa^1\text{Ge-Ge}(\text{R}_2\text{bzam})(\text{tBu})\}_3(\text{CO})_9]$ ($\text{R} = \textit{i}\text{Pr}$ (**45**); $\text{R} = \textit{t}\text{Bu}$ (**46**)), y/o (ii) fragmentándose, dando lugar a una mezcla de $[\text{Ru}_3(\text{CO})_{12}]$, de los derivados mononucleares **47** ó **48** y las especies insaturadas “ $[\text{Ru}(\text{Ge}_{\text{G,H}})(\text{CO})_3]$ ”. Estas últimas pueden evolucionar a su vez de tres

maneras diferentes: (i) trimerizándose, para formar los complejos trinucleares **45** ó **46**, (ii) reaccionando con CO, dando lugar a los derivados mononucleares **47** ó **48**, y/o (iii) reaccionando con otro equiv. de $\text{Ge}_{\text{G,H}}$, para formar los derivados mononucleares disustituidos $[\text{Ru}\{\kappa^1\text{Ge-Ge}(\text{R}_2\text{bzam})(^t\text{Bu})\}_2(\text{CO})_3]$ ($\text{R} = ^i\text{Pr}$ (**49**); $\text{R} = ^t\text{Bu}$ (**50**)).

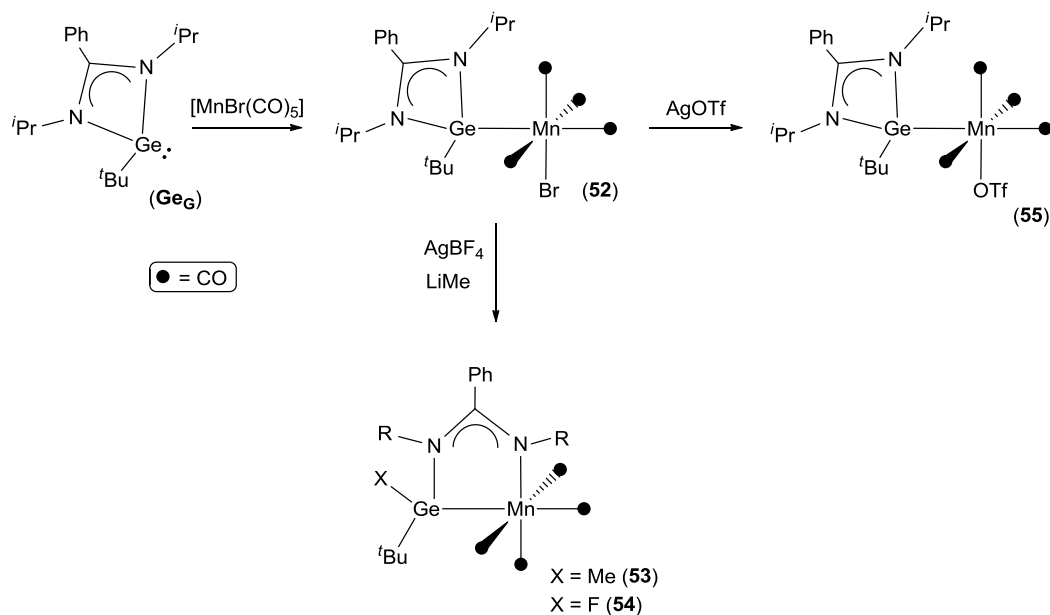
Cuando estas reacciones se llevaron a cabo a 90 °C se observaron otros procesos que no son posibles a temperatura ambiente (Esquema 5.2). Por ejemplo, los complejos mononucleares **47** y **48** y los trinucleares **45** y **46** reaccionaron con $\text{Ge}_{\text{G,H}}$ para dar los derivados mononucleares **49** y **50**, respectivamente. De gran relevancia, puesto que este tipo de reacción nunca había sido descrito en la gran cantidad de estudios existentes con $[\text{Ru}_3(\text{CO})_{12}]$ con otros ligandos dadores de dos electrones, es la reacción de los complejos mononucleares **47** y **48** con $[\text{Ru}_3(\text{CO})_{12}]$, que condujo a los derivados trinucleares **42** y **43**, respectivamente. Además, mientras que el compuesto **43** es estable a 90 °C, **42**, provisto de grupos N- ^iPr en su fragmento amidinato, evoluciona en esas condiciones hacia el complejo binuclear $[\text{Ru}_2\{\mu\text{-}\kappa^2\text{Ge}, \text{N-Ge}(^i\text{Pr}_2\text{bzam})(^t\text{Bu})\}(\text{CO})_7]$ (**51**), análogo a los derivados **17** y **40**.



Esquema 5.2. Procesos que ocurren a 90 °C

Los procesos descritos en el Esquema 5.2 y la secuencia de reacciones propuesta en el Esquema 5.1 (cuya justificación se analiza con profundidad en el artículo VIII) son claves para entender el origen y la cantidad de los productos obtenidos en las reacciones de $[\text{Ru}_3(\text{CO})_{12}]$ con $\text{Ge}_{\text{G,H}}$ a distintas temperaturas y estequiometrías. Además, estos resultados ayudan a racionalizar otras reacciones del cluster trinuclear $[\text{Ru}_3(\text{CO})_{12}]$ con reactivos muy básicos dadores de dos electrones, como trialquilfosfanos⁸⁷ y CNHs,^{60,88} que no siempre han podido ser explicadas satisfactoriamente.

En el artículo IX se describe la síntesis y la reactividad frente a distintos nucleófilos del complejo de manganeso $[\text{MnBr}\{\kappa^1\text{Ge-Ge}(\text{Pr}_2\text{bzam})(\text{tBu})\}(\text{CO})_4]$ (**52**), que se preparó por reacción de Ge_6 con $[\text{MnBr}(\text{CO})_5]$ a temperatura ambiente (Esquema 5.3). En el complejo **52**, el germileno y el ligando bromuro están dispuestos entre ellos en modo *cis*. Es conocida la tendencia que tienen los ligandos TPs a insertarse en enlaces M–X (X = grupo aniónico).^{4,71–74} Para amidinato-TPs, esa inserción formal puede provocar la apertura del fragmento amidinato, como se observó en el complejo de paladio mostrado en la Figura I.11 tras la inserción de un grupo amidinatosilileno en un enlace Pd–H.^{54l} En ese caso, el fragmento amidinato abierto permanece sin coordinarse a ningún metal. Impulsados por estos resultados y conocida la capacidad de Ge_6 de coordinarse en modo bidentado (complejo **51**), intentamos forzar la apertura del amidinato en **52** con varias fuentes de hidruro, pero en todos los casos obtuvimos mezclas de compuestos inestables que no pudieron ser aislados. El compuesto **52** se calentó a 90 °C para forzar la inserción directa del germanio en el enlace Mn–Br, pero de nuevo se formaron mezclas inseparables. Sin embargo, la reacción de **52** con LiMe condujo al complejo $[\text{Mn}\{\kappa^2\text{Ge}, N\text{-GeMe}(\text{Pr}_2\text{bzam})(\text{tBu})\}(\text{CO})_4]$ (**53**) (Esquema 5.3), que contiene un ligando aniónico de tipo $\kappa^2\text{Ge}, N$ -iminagermanato sin precedentes bibliográficos. En esta reacción, el grupo metilo, que reemplaza al ligando bromuro de **52**, se une al átomo de germanio forzando la apertura del fragmento amidinato y su coordinación al centro metálico.



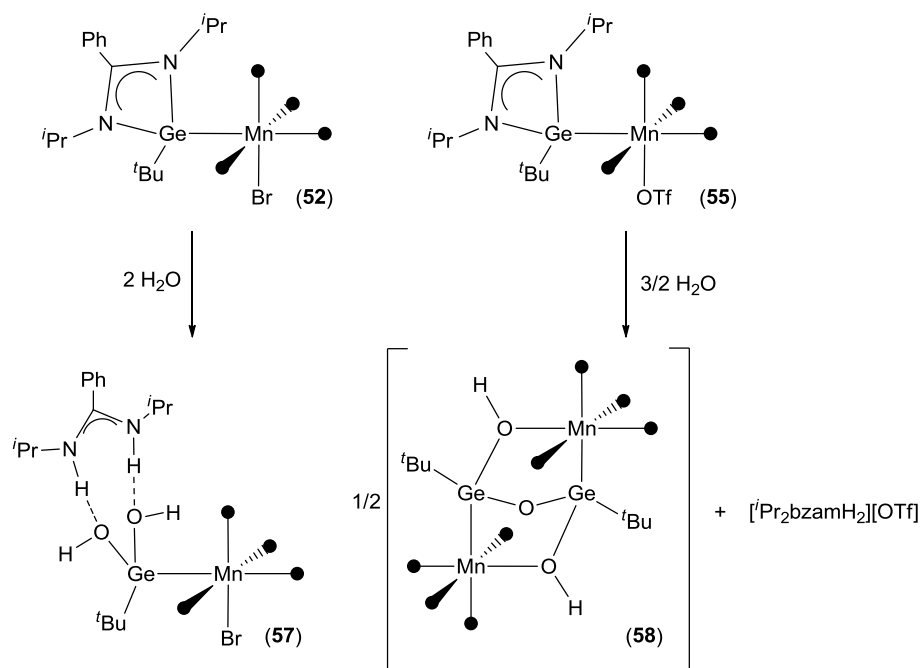
Esquema 5.3. Síntesis y reactividad del complejo **52**: Síntesis de los complejos **53–55**

También se llevaron a cabo reacciones de **52** con sales de plata AgX, con la intención de formar derivados de tipo $[\text{Mn}\{\kappa^2\text{Ge}, N\text{-Ge}(\text{Pr}_2\text{bzam})(\text{tBu})\}(\text{CO})_4][\text{X}]$. La insaturación generada al abstraer el bromuro se vería compensada por la apertura y coordinación del fragmento amidinato del ligando. Sin embargo, al hacer reaccionar **52** con AgBF_4 y AgOTf , se obtuvieron los compuestos neutros $[\text{Mn}\{\kappa^2\text{Ge}, N\text{-GeF}(\text{Pr}_2\text{bzam})(\text{tBu})\}(\text{CO})_4]$ (**54**) y $[\text{Mn}(\text{OTf})\{\kappa^1\text{Ge-Ge}(\text{Pr}_2\text{bzam})(\text{tBu})\}(\text{CO})_4]$ (**55**), respectivamente. **54** es estructuralmente análogo a **53**, pero provisto de un fluoruro unido al átomo de germanio (el fluoruro debe provenir del anión BF_4^-). **55** es análogo a **52**, donde el ligando bromuro ha sido reemplazado por un grupo OTf, sin que se haya producido la migración del anión al átomo de germanio. La termólisis de **55** a 90 °C condujo a mezclas inseparables.

El mecanismo más probable por el cual se forman **53** y **54** parece involucrar la sustitución inicial del bromuro de **52** por Me^- y F^- , respectivamente, y una posterior migración de los mismos desde el manganeso al átomo de germanio. Esto se apoya en: (i) la formación de **55**, (ii) la detección por IR de una especie de tipo $[\text{MnX}\{\kappa^1\text{Ge-Ge}(\text{Pr}_2\text{bzam})(\text{tBu})\}(\text{CO})_4]$ ($\text{X} = \text{BF}_4^-$ o F^-) cuando se lleva a cabo la reacción de **52** con AgBF_4 a $T < 0$ °C, la cual evoluciona cuantitativamente hacia **54** cuando $T > 0$ °C, y (iii) la localización del LUMO de **52** en el enlace Mn–Br.

La reacción de Ge_H con $[\text{MnBr}(\text{CO})_5]$ dio lugar al complejo $[\text{MnBr}\{\kappa^1\text{Ge-Ge}(\text{tBu}_2\text{bzam})(\text{tBu})\}(\text{CO})_4]$ (**56**), análogo a **52**, cuya reactividad frente a nucleófilos todavía no se ha estudiado. La presencia de grupos N–tBu en el fragmento amidinato de Ge_H hace prever que esta reactividad será diferente a la de **52**.

Algunos de los compuestos de manganeso descritos en este capítulo demostraron ser muy inestables frente a trazas de humedad y/o oxígeno. De hecho, los compuestos **52** y **55** reaccionaron selectivamente con agua para dar lugar a los productos de hidrólisis $[\text{Pr}_2\text{bzamH}_2][\text{MnBr}\{\kappa^1\text{Ge-Ge}(\text{OH})_2(\text{tBu})\}(\text{CO})_4]$ (**57**) y $[\text{Mn}_2\{\mu\text{-}\kappa^4\text{Ge}_2, \text{O}_2\text{-Ge}_2(\text{tBu})_2(\text{OH})_2\text{O}\}(\text{CO})_8]$ (**58**), respectivamente (Esquema 5.4). En estos compuestos se ha producido la hidrólisis del fragmento amidinato, formándose cationes amidinio $[\text{Pr}_2\text{bzamH}_2]^+$ y ligandos de tipo germanato que se mantienen unidos a los átomos de manganeso. Sin embargo, mientras que el germanato $\text{Ge}(\text{tBu})(\text{OH})_2$ de **57** está estabilizado por un catión amidinio mediante puentes de hidrógeno, el derivado **58** contiene un ligando digermanato $[\text{tBu}(\text{OH})\text{GeOGe}(\text{OH})(\text{tBu})]^{-2}$ unido a dos unidades $[\text{Mn}(\text{CO})_4]^+$ y el catión amidinio se ha liberado como $[\text{Pr}_2\text{bzamH}_2][\text{OTf}]$. Esta diferencia está debida, presumiblemente, a la mayor capacidad del OTf^- , con respecto al Br^- , para actuar como grupo saliente. De esta manera, la formación de la sal $[\text{Pr}_2\text{bzamH}_2][\text{OTf}]$ provoca que el fragmento $[\text{Mn}\{\text{Ge}(\text{tBu})(\text{OH})_2\}(\text{CO})_4]$ restante, que es coordinativamente insaturado, se condense con otra unidad análoga para formar el producto final.



Esquema 5.4. Reacciones de hidrólisis de **52** y **54**: Síntesis de los complejos **57** y **58**

Los últimos resultados experimentales incluidos en esta memoria se refieren a estudios realizados para evaluar la actividad en la reducción electroquímica de CO_2 de algunos de los complejos de manganeso descritos anteriormente. Estos estudios se encuentran en su fase preliminar y todavía no han dado lugar a ninguna publicación.

El comportamiento electroquímico de **52** se estudió por medio de voltamperometría cíclica en diclorometano. En atmósfera de argón se observó un pico a -1.4 V vs SCE correspondiente a un proceso de reducción irreversible (Figura 5.3). La intensidad de esta reducción se hizo 1.7 veces mayor cuando se repitió el experimento en atmósfera de CO_2 (Figura 5.3), lo que se asocia a un proceso catalítico de reducción del CO_2 .⁸⁵ Desafortunadamente, este compuesto demostró ser muy inestable durante los experimentos de voltamperometría cíclica, ya que perdía actividad rápidamente. Por ello, nos propusimos repetir estos experimentos utilizando el complejo de hidrólisis **57**, que es muy estable tanto en estado sólido como en disolución y que se puede preparar en gran cantidad sin apenas purificación. Este compuesto mostró un pico de reducción a -0.7 V vs SCE que aumentó su intensidad 3.8 veces cuando se realizó el experimento en atmósfera de CO_2 , indicando de nuevo que había actividad catalítica (Figura 5.4). El complejo **57** mantuvo su actividad cuando fue sometido a varios barridos de potencial consecutivos, al contrario que su precursor **52**.

De los dos complejos evaluados, **57** es sin duda el candidato más prometedor para llevar a cabo la reducción electroquímica de CO_2 a mayor escala. No sólo es más estable que **52**, sino que es mucho más activo (menor sobrepotencial requerido y mayor aumento de la intensidad de corriente en presencia de CO_2). Se ha de destacar que **57** es capaz de promover la reducción electrocatalítica de CO_2 a potenciales considerablemente menos negativos que cualquier otro complejo de Mn(I) descrito.⁸⁵

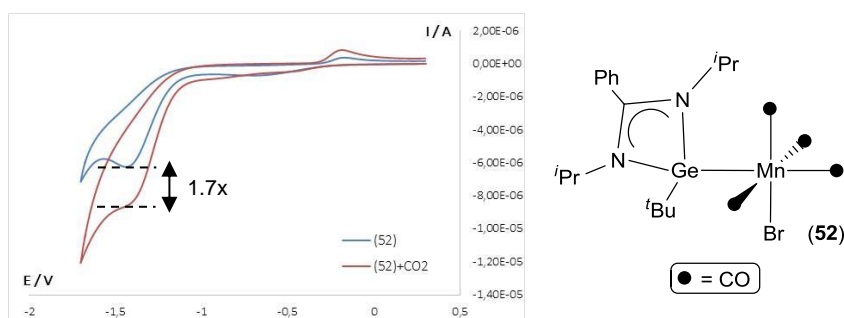


Figura 5.3. Voltamperograma cíclico de **52** vs SCE ($v = 100 \text{ mV/s}$) en atmósfera de Ar (línea azul) y de CO_2 (línea roja). Los siguientes ciclos (hasta un máximo de 10) mostraron pérdida de actividad del complejo

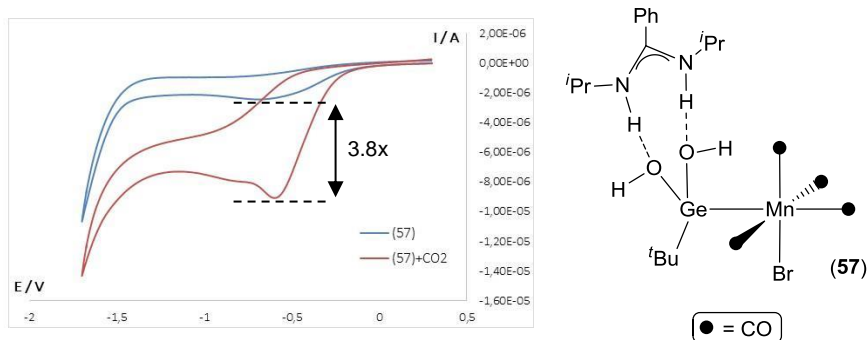


Figura 5.4. Voltamperograma cíclico de **57** vs SCE ($v = 100 \text{ mV/s}$) en atmósfera de Ar (línea azul) y de CO_2 (línea roja). Los siguientes ciclos (hasta un máximo de 10) no mostraron pérdida de actividad del complejo

En la actualidad estamos investigando estas reacciones electroquímicas en colaboración con el grupo del doctor Jay Agarwal (Universidad de Georgia, USA). En concreto, estamos analizando y cuantificando los posibles productos derivados de la reducción catalítica de CO_2 en experimentos de electrolisis a potencial controlado utilizando el complejo **57** como catalizador.

5.3. Conclusiones

Este capítulo demuestra que, cambiando adecuadamente la estructura de los amidinato-TPs, se consigue aumentar considerablemente su capacidad como ligandos y modificar sus patrones de reactividad. Los amidinatogermilenos $\text{Ge}(\text{R}_2\text{bzam})(\text{tBu})$ ($\text{R} = \text{tPr}$, Ge_G ; $\text{R} = \text{tBu}$, Ge_H), que contienen un grupo tBu unido al átomo de germanio, son capaces de reaccionar con metales de transición en condiciones muy suaves. Por ejemplo, mientras que Ge_{D-F} (provistos de un grupo HMDS) sólo reaccionaban con $[\text{Ru}_3(\text{CO})_{12}]$ a $90\text{ }^\circ\text{C}$, $\text{Ge}_{G,H}$ son capaces de reaccionar a temperatura ambiente.

Un estudio cuidadoso de la gran variedad de compuestos que se derivan de las reacciones de estos TPs con $[\text{Ru}_3(\text{CO})_{12}]$ (complejos **42–51**) ha permitido discernir cómo se relacionan entre sí estos compuestos, tanto a temperatura ambiente como a alta temperatura, y nos ha llevado a proponer un camino de reacción general que explica los resultados obtenidos en este trabajo, así como los observados previamente en reacciones de $[\text{Ru}_3(\text{CO})_{12}]$ con otros ligandos dadores de dos electrones de gran basicidad.

Los compuestos **42–46** son los primeros clusters carbonílicos que contienen TPes coordinados en modo terminal $\kappa^1 E$.

Se han preparado los primeros complejos de manganeso con amidinatogermilenos por reacción de los germilenos Ge_G y Ge_H con $[\text{MnBr}(\text{CO})_5]$. Un tratamiento del complejo **52**, que deriva de Ge_G ($\text{R} = \text{tPr}$), con agentes nucleófilos ha permitido transformar el TP monodentado en un ligando bidentado de tipo iminagermanato (complejos **53** y **54**). Este tipo de ligandos no había sido descrito previamente.

Los derivados **52** y **54** reaccionan selectivamente con agua dando lugar a los productos de hidrólisis **57** y **58**, respectivamente. Estudios preliminares han demostrado que el complejo **57**, que contiene un ligando germanato estabilizado por un catión amidinio, es capaz de reducir CO_2 electroquímicamente a un potencial menos negativo que los descritos utilizando otras especies carbonílicas de Mn(I) .

Capítulo 6

***Revisión de la química de coordinación
de los amidinato-TPs***

Artículo X

“The Transition-Metal Chemistry of Amidinatosilylenes, -germylenes and -stannylenes”

6.1. Presentación de la revisión

El último capítulo de esta memoria incluye una revisión sobre la química de coordinación de amidinato-TPs. A pesar de la importancia que estos TPs tienen en la química actual, su química de coordinación todavía no había sido recopilada de una manera específica. Por ello, en 2014, decidimos llevar a cabo esta revisión aprovechando nuestra experiencia en el tema. El artículo X recoge la síntesis, propiedades estructurales, estudios teóricos, reactividad y aplicaciones catalíticas de todos los complejos amidinato-TP–M descritos hasta finales de 2014 (ordenados de acuerdo con el grupo de la tabla periódica al que pertenecen). Ya que la información recogida en este artículo es muy extensa e incluye gran parte de los resultados que se han presentado en esta memoria, este capítulo no incluye una discusión de los resultados específica. Sin embargo, sí creemos conveniente resaltar las conclusiones más relevantes que se derivan de esta revisión.

6.2. Conclusiones

La química de coordinación de los amidinato-TPs no ha dejado de crecer desde la síntesis en 2008 (Jones y colaboradores)^{54x} de los primeros complejos amidinato-TP–M. Hoy en día se conocen más de 100 ejemplos pertenecientes a esta familia de compuestos.^{20,21,54–56}

El gran interés que hoy suscitan estos TPs se debe a que (i) su estabilización intramolecular hace que se puedan manejar más fácilmente que otros TPs, (ii) sus características estéricas y electrónicas se pueden modificar fácilmente, (iii) se ha encontrado recientemente una ruta accesible para la síntesis de amidinatosilileno que, en general, son mejores ligandos que sus congéneres más pesados, y (iv) han demostrado ser ligandos muy dadores, incluso más que los CNHs, lo que es muy importante para el diseño de complejos que sean ricos en densidad electrónica y, por tanto, potencialmente capaces de promover procesos de activación de enlaces.

La mayoría de los complejos amidinato-TP-M descritos contienen amidinatosilileno o -germileno. Sólo se conoce un complejo con un amidinatoestannileno, el compuesto de hierro $[\text{Fe}\{\kappa^1\text{Sn-Sn}(\text{tBu}_2\text{bzam})\text{Cl}\}(\text{CO})_4]$,^{54u} y no existe ninguno derivado de amidinatoplumbileno. Este menor interés en los amidinato-TPs más pesados se atribuye, fundamentalmente, a la menor estabilidad del enlace E–M al bajar en el grupo 14²⁵ y a factores de carácter medioambiental.

Los amidinato-TPs se comportan, en general, como ligandos monodentados. La coordinación bidentada de tipo $\kappa^2\text{E,N}$ de estos TPs ha sido descubierta muy recientemente, encontrándose casos en los que los amidinato-TPs actúan como ligandos neutros dadores de 4 electrones (con modos de coordinación $\mu\text{-}\kappa^2\text{Ge,N}$ o $\kappa^2\text{Si,N}$) o como ligandos aniónicos dadores de 3 electrones (exhibiendo un modo de coordinación $\kappa^2\text{Ge,N}$). Las investigaciones realizadas hasta ahora sugieren que esta coordinación bidentada, que implica la rotura de un enlace E–N del fragmento amidinato del ligando, sólo ocurre si en el producto final se mantiene el índice de coordinación cuatro en el átomo E. Otros factores, tanto estéricos como electrónicos, que pueden provenir de cualquiera de los tres puntos modificables de los amidinato-TPs (átomo E, fragmento amidinato, grupo X terminal), también han de tenerse en consideración, como ha quedado claramente demostrado en esta tesis doctoral.

A diferencia de las escasas aplicaciones catalíticas descritas para complejos metálicos derivados de otros TPs,^{4c,19,39,40} muchos amidinato-TP–Ms, a pesar de su reciente descubrimiento, ya han demostrado ser catalíticamente activos en procesos de interés, como acoplamiento Sonogashira,²⁰ hidrosililación de cetonas,^{21,56a} reacciones de acoplamiento de halogenuros de arilo con reactivos de Grignard,^{56b} cicloadiciones $[2+2+2]$ ^{56c} y reacciones de borilación de enlaces C–H de arenos.^{56d} La mayor parte de estos complejos activos en catálisis poseen sus amidinato-TPs integrados en ligandos polidentados, lo que posiblemente es de gran importancia para minimizar la descomposición de los complejos. Se ha de destacar, además, el hecho de que algunas de estas transformaciones catalíticas ocurren con la participación activa del TP.

Esta revisión, que sirve además como guía para cualquier investigador del área, pone de manifiesto que la química de coordinación derivada de los amidinato-TPs es un campo con grandes posibilidades todavía por explotar.

Conclusiones Generales

En esta tesis doctoral se han ampliado los conocimientos existentes sobre la química de coordinación de los tetrilenos pesados mediante la síntesis de nuevos complejos de metales de transición (rutenio, oro, cobalto y manganeso) equipados con TPs de distinta naturaleza química.

En primer lugar, hemos descubierto que las reacciones de TPs clásicos, como los cíclicos simples de tipo imidazol $E(N^tBu)_2C_2H_2$ ($E = Si$ (**Si_A**), Ge (**Ge_A**)) y benzimidazol $E(NCH_2^tBu)_2C_6H_4$ ($E = Si$ (**Si_B**), Ge (**Ge_B**), Sn (**Sn_B**)) o los acíclicos de Lappert $E(HMDS)_2$ ($E = Ge$ (**Ge_C**), Sn (**Sn_C**)), con $[Ru_3(CO)_{12}]$ dan lugar a productos cuya nuclearidad depende del volumen y la naturaleza cíclica o acíclica del TP empleado, así como del tamaño del átomo E. Estos factores también condicionan la estructura de los productos obtenidos en las reacciones de estos TPs con $[AuCl(THT)]$. Los complejos de estas reacciones demostraron ser muy inestables frente a trazas de aire y humedad o considerablemente inertes frente a otros reactivos. Por ello, no se pudieron abordar estudios posteriores de reactividad y/o catálisis con estos sistemas.

Tras trasladar el desarrollo de la tesis doctoral hacia el uso de tetrilenos cíclicos estabilizados intramolecularmente de tipo $E(RR'bzam)X$ ($E = Si, Ge; R, R' = ^iPr, ^tBu, Et; X = HMDS, ^tBu; Ge_{D-H}$ y **Si_D**), que contienen grupos benzamidinato (bzam), hemos podido corroborar que éstos son excelentes ligandos en química de coordinación, ya que son capaces de formar complejos muy estables. La fácil modificación de las propiedades estéricas y electrónicas de estos TPs (cambios en R, R', y/o en X) ha permitido observar patrones de reactividad y modos de coordinación muy diferentes, alguno de ellos sin precedentes. Destaca, por ejemplo, la síntesis de complejos binucleares de rutenio y cobalto en los que el amidinato-TP exhibe por primera vez un modo de coordinación a la vez puente y bidentado, o la síntesis de complejos mononucleares de manganeso que contienen TPs bidentados de tipo iminagermanato. Además, hemos demostrado que estos modos de coordinación bidentados sólo son posibles cuando al menos uno de los grupos N-R del grupo amidinato es más pequeño que un grupo *tert*-butilo.

Algunos de los complejos derivados de amidinato-TPs, en concreto los compuestos **17**, **39** y **52**, han sido sometidos a estudios de reactividad. Entre éstos se incluyen reacciones con agentes nucleófilos (neutros y/o aniónicos), activación de enlaces H-X ($X = SiEt_3, SnPh_3, H$) con formación de derivados coordinativamente insaturados, adiciones reversibles de CO y estudios de termólisis e hidrólisis. Además, se ha llevado a cabo un estudio preliminar de catálisis con el complejo **57**, que ha demostrado ser un prometedor precursor catalítico en la reducción electroquímica de CO_2 , actuando a potenciales de reducción considerablemente menos negativos que los observados con cualquier otro complejo de manganeso conocido hasta la fecha.

Referencias

1. V. Y. Lee y A. Sekiguchi, *Organometallic Compounds of Low Coordinate Si, Ge, Sn and Pb: From Phantom Species to Stable Compounds*; Wiley, Chichester, UK, **2010**.
2. Revisiones sobre la síntesis y reactividad general de TPs: (a) K. Izod, *Coord. Chem. Rev.*, **2013**, 257, 924; (b) Y. Xiong, S. Yao y M. Driess, *Angew. Chem. Int. Ed.*, **2013**, 52, 4302; (c) S. K. Mandal y H. W. Roesky, *Acc. Chem. Res.*, **2012**, 45, 298; (d) S. Yao, Y. Xiong y M. Driess, *Organometallics*, **2011**, 30, 1748; (e) Y. Mizuhata, T. Sasamori y N. Tokitoh, *Chem. Rev.*, **2009**, 109, 3479; (f) J. Barrau y G. Rima, *Coord. Chem. Rev.*, **1998**, 178, 593; (g) W. P. Neumann, *Chem. Rev.*, **1991**, 91, 311; (h) M. Veith, *Angew. Chem. Int. Ed.*, **1987**, 26, 1.
3. Revisiones sobre la síntesis y reactividad general de TPs, incluyendo algunos ejemplos de coordinación a Ms: (a) R. S. Ghadwal, R. Azhakar y H. W. Roesky, *Acc. Chem. Res.*, **2013**, 46, 444; (b) H. W. Roesky, *J. Organomet. Chem.*, **2013**, 730, 57; (c) M. Asay, C. Jones y M. Driess, *Chem. Rev.*, **2011**, 111, 354; (d) S. K. Mandal y H. W. Roesky, *Chem. Commun.*, **2010**, 46, 6016; (e) M. Kira, *Chem. Commun.*, **2010**, 46, 2893; (f) S. Nagendran y H. W. Roesky, *Organometallics*, **2008**, 27, 457; (g) A. V. Zabula y F. E. Hahn, *Eur. J. Inorg. Chem.*, **2008**, 5165; (h) W.-P. Leung, K.-W. Kan y K.-H. Chong, *Coord. Chem. Rev.*, **2007**, 251, 2253; (i) O. Kühn, *Coord. Chem. Rev.*, **2004**, 248, 411; (j) B. Gehrhus y M. F. Lappert, *J. Organomet. Chem.*, **2001**, 617-618, 209; (k) M. Haaf, T. A. Schmedake y R. West, *Acc. Chem. Res.*, **2000**, 33, 704; (l) N. Tokitoh y R. Okazaki, *Coord. Chem. Rev.*, **2000**, 210, 251.
4. Revisiones sobre la química de coordinación de los TPs: (a) B. Blom, D. Gallego y M. Driess, *Inorg. Chem. Front.*, **2014**, 1, 134; (b) B. Blom, M. Stoelzel y M. Driess, *Chem. Eur. J.*, **2013**, 19, 40; (c) R. Waterman, P. G. Hayes y T. D. Tilley, *Acc. Chem. Res.*, **2007**, 40, 712; (d) M. Okazaki, H. Tobita y H. Ogino, *Dalton Trans.*, **2003**, 493; (e) M. F. Lappert y R. S. Rowe, *Coord. Chem. Rev.*, **1990**, 100, 267; (f) W. Petz, *Chem. Rev.*, **1986**, 86, 1019; (g) M. F. Lappert y P. P. Power, *J. Chem. Soc., Dalton Trans.*, **1985**, 51.
5. (a) R. S. Ghadwal, H. Roesky, S. Merkel, J. Henn y D. Stalke, *Angew. Chem. Int. Ed.* **2009**, 48, 5683; (b) A. C. Filippou, O. Chernov y G. Schnakenburg, *Angew. Chem. Int. Ed.* **2009**, 48, 5687.
6. (a) T. Sasamori y N. Tokitoh en *Encyclopedia of Inorganic Chemistry II*; R. A. Scott, D. Atwood, C. M. Lukehart, R. H. Crabtree y R. B. King, Eds.; Wiley, Chichester, UK, **2005**,

- p. 1698; (b) S. Nagase en *The Transition State: A Theoretical Approach*; T. Fueno, Ed.; Gordon and Breach Science Publishers, Langhorne, PA, **1999**, p. 147.
7. G. Trinquier, *J. Am. Chem. Soc.*, **1990**, *112*, 2130.
 8. (a) T. Heidemann y S. Mathur, *Eur. J. Inorg. Chem.*, **2014**, 506; (b) R. C. Fischer y P. P. Power, *Chem. Rev.*, **2010**, *110*, 3877.
 9. (a) L. Carvallo, A. Correa, C. Costabile, H. Jacobsen, *J. Organomet. Chem.*, **2005**, 690, 5407; (b) T. Strassner, *Top. Organomet. Chem.*, **2004**, *13*, 1.
 10. (a) C. Heinemann, T. Müller, Y. Apeloig y H. Schwarz, *J. Am. Chem. Soc.*, **1996**, *118*, 2023; (b) P. von Ragué Schleyer y P. D. Stout, *J. Chem. Soc., Chem. Commun.*, **1986**, 1373.
 11. A. Jana, D. Leusser, I. Objartel, H. W. Roesky y D. Stalke, *Dalton Trans.*, **2011**, *40*, 5458.
 12. A. Akkari, J. J. Byrne, I. Saur, G. Rima, H. Gornitzka y J. Barrau, *J. Organomet. Chem.*, **2001**, *622*, 190.
 13. A. Jana, P. P. Samuel, G. Tavčar, H. W. Roesky y C. Schulzke, *J. Am. Chem. Soc.*, **2010**, *132*, 10164.
 14. A. Jana, H. W. Roesky, C. Schulzke y A. Döring, *Angew. Chem. Int. Ed.*, **2009**, *48*, 1106.
 15. S. Yao, C. van Wuelen, X. Y. Sun y M. Driess, *Angew. Chem. Int. Ed.*, **2008**, *47*, 3250.
 16. (a) F. E. Hahn, L. Wittenbecher, D. Le Van y A. V. Zabula, *Inorg. Chem.*, **2007**, *46*, 7662; (b) A. V. Zabula, F. E. Hahn, T. Pape y A. Hepp, *Organometallics*, **2007**, *26*, 1972.
 17. K. E. Litz, K. Henderson, R. W. Gourley y M. M. B. Holl, *Organometallics*, **1995**, *14*, 5008.
 18. K. E. Litz, J. W. Kampf y M. M. B. Holl, *J. Am. Chem. Soc.*, **1998**, *120*, 7484.
 19. P. B. Glaser y T. D. Tilley, *J. Am. Chem. Soc.*, **2003**, *125*, 13640.
 20. D. Gallego, A. Brück, E. Irran, F. Meier, M. Kraupp, M. Driess y J. F. Hartwig, *J. Am. Chem. Soc.*, **2013**, *135*, 15617.
 21. B. Blom, S. Enthaler, S. Inoue, E. Irran y M. Driess, *J. Am. Chem. Soc.*, **2013**, *135*, 6703.
 22. (a) M. F. Lappert, P. P. Power y J. Slade, *J. Chem. Soc., Chem. Commun.*, **1979**, 369; (b) M. J. S. Gynane, D. H. Harris, M. F. Lappert, P. P. Power, P. Rivière y M. Rivière-

- Baudet, *J. Chem. Soc., Dalton Trans.*, **1977**, 2004; (c) M. Veith, *Angew. Chem. Int. Ed.* **1975**, *14*, 263; (d) C. D. Schuefler y C. D. Zuckerman, *J. Am. Chem. Soc.*, **1974**, *96*, 7160; (e) D. H. Harris y M. F. Lappert, *J. Chem. Soc., Chem. Commun.*, **1974**, 895.
23. (a) A. J. Arduengo III, R. L. Harlow y M. Kline, *J. Am. Chem. Soc.*, **1991**, *113*, 361.
24. (a) M. F. Lappert, P. P. Power, A. Potchenko y A. Seeber, *Metal Amide Chemistry*; J. Wiley & Sons, Chichester, UK, **2009**; (b) M. F. Lappert, P. P. Power, A. R. Sanger y R. C. Srivastava, *Metal and Metalloid Amides: Syntheses, Structures and Physical and Chemical Properties*; J. Wiley & Sons, Chichester, UK, **1979**.
25. (a) T. A. N. Nguyen y G. Frenking, *Chem. Eur. J.*, **2012**, *18*, 12733; (b) H. Arp, J. Baumgartner, C. Marschner, P. Zark y T. Müller, *J. Am. Chem. Soc.*, **2012**, *134*, 10864; (c) J. T. York, V. G. Young Jr. y W. B. Tolman, *Inorg. Chem.*, **2006**, *45*, 4191; (d) H. Yoo, P. J. Carroll y D. H. Berry, *J. Am. Chem. Soc.*, **2006**, *128*, 6038; (e) W. J. Evans, J. M. Perotti, J. W. Ziller, D. F. Moser y R. West, *Organometallics*, **2003**, *22*, 1160; (f) W. A. Herrmann, P. Harter, C. W. K. Gstottmayr, F. Bieleert, N. Seeboth y P. Sirsch, *J. Organomet. Chem.*, **2002**, *649*, 141; (g) C. Boehme y G. Frenking, *Organometallics*, **1998**, *17*, 5801.
26. (a) M. F. Lappert, S. J. Miles y P. P. Power, *J. Chem. Soc., Chem. Commun.*, **1977**, 458; (b) E. Suzuki, T. Komuro, Y. Kanno y H. Tobita, *Organometallics*, **2013**, *32*, 748; (c) M. Veith, L. Stahl y V. Huch, *Chem. Commun.*, **1990**, 359. (d) D. Amoroso, M. Haaf, G. P. A. Yap, R. West y D. E. Fogg, *Organometallics*, **2002**, *21*, 534; (e) H. Arai, F. Nakadate y K. Mochida, *Organometallics*, **2009**, *28*, 4909.
27. (a) B. Blom, M. Pohl, G. Tan, D. Gallego y M. Driess, *Organometallics*, **2014**, *33*, 5272; (b) H. Handwerker, C. Leis, R. Probst, P. Bissinger, A. Grohmann, P. Kiprof, E. Herdtweck, J. Blumel, N. Auner y C. Zybill, *Organometallics*, **1993**, *12*, 2162; (c) C. Zybill y G. Müller, *Angew. Chem. Int. Ed.*, **1987**, *26*, 669; (d) T. J. Marks, *J. Am. Chem. Soc.*, **1971**, *93*, 7090.
28. (a) M. E. Fasulo, P. B. Glaser y T. D. Tilley, *Organometallics*, **2013**, *30*, 5524; (b) P. B. Glaser, P. W. Wanandi y T. D. Tilley, *Organometallics*, **2004**, *23*, 693; (c) S. K. Grumbine, G. P. Mitchell, D. A. Straus, T. D. Tilley y A. L. Rheingold, *Organometallics*, **1998**, *17*, 5607; (d) S. K. Grumbine, T. D. Tilley, F. P. Arnold y A. L. Rheingold, *J. Am. Chem. Soc.*, **1994**, *116*, 5495; (e) S. D. Grumbine, T. D. Tilley, F. P. Arnold y A. L. Rheingold, *J. Am. Chem. Soc.*, **1993**, *115*, 7884; (f) D. A. Straus, S. D. Grumbine y T. D. Tilley, *J. Am. Chem. Soc.*, **1990**, *112*, 7801; (g) D. A. Straus, T. D. Tilley, A. L. Rheingold y S. J. Geib, *J. Am. Chem. Soc.*, **1987**, *109*, 5872; (h) M. E. Fasulo y T. D. Tilley, *Chem. Commun.*, **2012**, *48*, 7690.

29. (a) H.-J. Liu, C. Raynaud, O. Eisenstein y T. D. Tilley, *J. Am. Chem. Soc.*, **2014**, *136*, 11473; (b) H.-J. Liu, J. Guihaumé, T. Davin, C. Raynaud, O. Eisenstein y T. D. Tilley, *J. Am. Chem. Soc.*, **2014**, *136*, 13991; (c) E. Suzuki, T. Komuro, M. Okazaki y H. Tobita, *Organometallics*, **2009**, *28*, 1791; (d) P. G. Hayes, C. Beddie, M. B. Hall, R. Waterman y T. D. Tilley, *J. Am. Chem. Soc.*, **2006**, *128*, 428; (e) B. V. Mork y T. D. Tilley, *J. Am. Chem. Soc.*, **2004**, *126*, 4375; (f) B. V. Mork, T. D. Tilley, A. J. Schultz y J. A. Cowan, *J. Am. Chem. Soc.*, **2004**, *126*, 10428; (g) B. V. Mork y T. D. Tilley, *Angew. Chem. Int. Ed.*, **2003**, *42*, 357; (h) J. D. Feldman, J. C. Peters y T. D. Tilley, *Organometallics*, **2002**, *21*, 4065; (i) J. C. Peters, J. D. Feldman y T. D. Tilley, *J. Am. Chem. Soc.*, **1999**, *121*, 9871; (j) G. P. Mitchell y T. D. Tilley, *Angew. Chem. Int. Ed.*, **1998**, *37*, 2524.
30. (a) J. D. Feldman, G. P. Mitchell, J.-O. Nolte y T. D. Tilley, *Can. J. Chem.*, **2003**, *81*, 1127; (b) J. D. Feldman, G. P. Mitchell, J.-O. Nolte y T. D. Tilley, *J. Am. Chem. Soc.*, **1998**, *120*, 11184.
31. (a) V. Y. Lee, S. Aoki, T. Yokoyama, S. Horiguchi, A. Sekiguchi, H. Gornitzka, J.-D. Guo y S. Nagase, *J. Am. Chem. Soc.*, **2013**, *135*, 2987; (b) N. Nakata, T. Fujita y A. Sekiguchi, *J. Am. Chem. Soc.*, **2006**, *128*, 16024.
32. (a) R. D. Adams, Y. Kan y Q. Zhang, *Organometallics*, **2011**, *30*, 328; (b) R. D. Adams, M. Chem, E. Trufan y Q. Zhang, *Organometallics*, **2011**, *30*, 661; (c) R. D. Adams, B. Captain y E. Trufan, *J. Organomet. Chem.*, **2008**, *3*, 593; (d) R. D. Adams, B. Captain y E. Trufan, *J. Cluster Sci.*, **2007**, *18*, 642; (e) R. D. Adams, B. Captain, M. Hall, E. Trufan y X. Yang, *J. Am. Chem. Soc.*, **2007**, *129*, 12328; (f) R. D. Adams, B. Captain, y J. L. Smith Jr., *Inorg. Chem.*, **2005**, *44*, 1413; (g) R. D. Adams, B. Captain y W. Fu, *Inorg. Chem.*, **2003**, *42*, 1328; (h) C. J. Cardin, D. J. Cardin, M. A. Convery y M. M. Devereux, *J. Chem. Soc., Chem. Commun.*, **1991**, 687.
33. (a) P. Jutzi, W. Steiner y K. Stroppel, *Chem. Ber.*, **1980**, *113*, 3357; (b) W.-W. duMont y H. J. Kroth, *Z. Naturforsch.* **1980**, *35B*, 700; (c) F. R. Kreissl y W. Held, *Chem. Ber.* **1977**, *110*, 799; (d) A. H. Cohen y B. M. Hoffman, *Inorg. Chem.* **1974**, *13*, 1484; (e) F. R. Kreissl, C. G. Kreiter y E. O. Fischer, *Angew. Chem.* **1972**, *84*, 679.
34. J. R. Koe, D. R. Powell, J. J. Buffy, S. Hayase y R. West, *Angew. Chem. Int. Ed.*, **1998**, *37*, 1441.
35. G. H. Lee, R. West y T. Müller, *J. Am. Chem. Soc.*, **2003**, *125*, 8114.
36. (a) J. K. West, G. L. Fondong, B. C. Noll y L. Stahl, *Dalton Trans.*, **2013**, *42*, 3835; (b) P. Braunstein, M. Veith, J. Blin y V. Huch, *Organometallics*, **2011**, *20*, 627; (c) M. Knorr, E. Hallauer, V. Huch, M. Veith y P. Braunstein, *Organometallics*, **1996**, *15*, 3868; (d) M. Veith, A. Mueller, L. Stahl, M. Noetzel, M. Jarczyk y V. Huch, *Inorg. Chem.*, **1996**, *35*,

- 3848; (e) M. Veith, L. Stahl y V. Huch, *Organometallics*, **1993**, *12*, 1914; (f) M. Veith y L. Stahl, *Angew. Chem. Int. Ed.*, **1993**, *32*, 106; (g) M. Veith, L. Stahl y V. Huch, *Inorg. Chem.*, **1989**, *28*, 3278; (h) M. Veith, H. Lange, K. Braeuer y R. Bachmann, *R. J. Organomet. Chem.*, **1981**, *216*, 377.
37. M. Veith, E. Werle, R. Lisowsky, R. Löppe y H. Schnöckel, *Chem. Ber.*, **1992**, *125*, 1375.
38. M. Denk, R. Lennon, R. Hayashi, R. West., A. V. Belyakov, H. P. Verne, A. Haaland, M. Wagner y N. Metzler, *J. Am. Chem. Soc.*, **1994**, *116*, 2691.
39. A. Fürstner, H. Krause y C. W. Lehmann, *Chem. Commun.*, **2001**, 2372.
40. M. Zhang, X. Liu, C. Shi, C. Ren, Y. Ding y H. W. Roesky, *Z. Anorg. Allg. Chem.*, **2008**, *634*, 1755.
41. (a) D. Heitmann, T. Pape, A. Hepp, C. Mück-Lichtenfeld, S. Grimme y F. E. Hahn, *J. Am. Chem. Soc.*, **2011**, *133*, 11118; (b) S. M. Mansell, R. H. Herber, I. Nowik, D. H. Ross, C. A. Russell y D. F. Wass, *Inorg. Chem.*, **2011**, *50*, 2252; (c) F. Ullah, O. Kühl, G. Bajor, T. Veszpremi, P. G. Jones y J. Heinicke, *Eur. J. Inorg. Chem.*, **2009**, 221; (d) O. Kühl, P. Lönnecke y J. Heinicke, *Inorg. Chem.*, **2003**, *42*, 2836; (e) W. A. Herrmann, M. Denk, J. Behm, W. Scherer, F.-R. Klingan, H. Bock, B. Solouki y M. Wagner, *Angew. Chem. Int. Ed.*, **1992**, *31*, 1485.
42. (a) A. V. Zabula, T. Pape, A. Hepp y F. E. Hahn, *Dalton Trans.*, **2008**, 5886; (b) F. E. Hahn, A. V. Zabula, T. Pape, A. Hepp, R. Tonner, R. Haunschild y G. Frenking, *Chem. Eur. J.*, **2008**, *14*, 10716; (c) F. E. Hahn, A. V. Zabula, T. Pape y A. Hepp, *Z. Anorg. Allg. Chem.*, **2008**, *634*, 2397; (d) A. V. Zabula, T. Pape, A. Hepp y F. E. Hahn, *Organometallics*, **2008**, *27*, 2756.
43. J. Pfeiffer, W. Maringgele, M. Noltemeyer y A. Meller, *Chem. Ber.*, **1989**, *122*, 245.
44. (a) M. Kira, S. Ishida, T. Iwamoto y C. Kabuto, *J. Am. Chem. Soc.*, **1999**, *121*, 9722; (b) M. Kira, S. Ishida, T. Iwamoto, M. Ichinohe, C. Kabuto, L. Ignatovich y H. Sakurai, *Chem. Lett.*, **1999**, *3*, 263. (c) M. Kira, R. Yauchibara, R. Hirano, C. Kabuto y H. Sakurai, *J. Am. Chem. Soc.*, **1991**, *113*, 7785.
45. (a) Y. Inagawa, S. Ishida y T. Iwamoto; *Chem. Lett.*, **2014**, *43*, 1665; (b) C. Watanabe, Y. Inagawa, T. Iwamoto y M. Kira, *Dalton Trans.*, **2010**, *39*, 9414; (c) C. Watanabe, T. Iwamoto, C. Kabuto y M. Kira, *Angew. Chem. Int. Ed.*, **2008**, *47*, 5386; (d) C. Watanabe, T. Iwamoto, C. Kabuto y M. Kira, *Chem. Lett.*, **2007**, *36*, 284.

46. (a) M. Driess, S. Yao, M. Brym, C. van Wüllen y D. Lentz, *J. Am. Chem. Soc.*, **2006**, *128*, 9628; (b) M. Driess, S. Yao, M. Brym, C. van Wüllen, *Angew. Chem. Int. Ed.*, **2006**, *45*, 4349.
47. (a) M. Stoelzel, C. Präsang, S. Inoue, S. Enthaler y M. Driess, *Angew. Chem. Int. Ed.*, **2012**, *51*, 399; (b) Y. Xiong, S. Yao y M. Driess, *Chem. Eur. J.*, **2012**, *18*, 3316; (c) A. Meltzer, S. Inoue, C. Präsang y M. Driess, *J. Am. Chem. Soc.*, **2010**, *132*, 3038; (d) A.-K. Jungton, A. Meltzer, C. Praesang, T. Braun, M. Driess y A. Penner, *Dalton Trans.*, **2010**, *39*, 5436; (e) A. Meltzer, C. Prasang, C. Milsmann y M. Driess, *Angew. Chem. Int. Ed.*, **2009**, *48*, 3170; (f) A. Meltzer, C. Präsang y M. Driess, *J. Am. Chem. Soc.*, **2009**, *131*, 7232.
48. (a) N. Zhao, J. Zhang, Y. Yang, G. Chen, H. Zhu y H. W. Roesky, *Organometallics*, **2013**, *32*, 762; (b) A. Jana, P. P. Samuel, H. W. Roesky y C. Schulzke, *J. Fluorine Chem.*, **2010**, *131*, 1096; (c) A. Jana, R. Azhakar, H. W. Roesky, I. Objartel y D. Stalke, *Z. Anorg. Allg. Chem.*, **2011**, *637*, 1795; (d) A. Jana, H. W. Roesky, C. Schulzke y P. P. Samuel, *Inorg. Chem.*, **2010**, *49*, 3461; (e) A. Jana, S. P. Sarish, H. W. Roesky, C. Schulzke y P. P. Samuel, *Chem. Commun.*, **2010**, *46*, 707; (f) L. W. Pineda, V. Jancik, J. F. Colunga-Valladares, H. W. Roesky, A. Hofmeister y J. Magull, *Organometallics*, **2006**, *25*, 2381.
49. (a) N. Zhao, J. Zhang, Y. Yang, H. Zhu, Y. Li y G. Fu, *Inorg. Chem.*, **2012**, *51*, 8710; (b) L. Ferro, P. B. Hitchcock, M. P. Coles y J. R. Fulton, *Inorg. Chem.*, **2012**, *51*, 1544; (c) H. Aii, F. Nakadate y K. Mochida, *Organometallics*, **2009**, *28*, 4909; (d) I. Saur, S. Garcia Alonso, H. Gornitzka, V. Lemierre, A. Chrostowska y J. Barrau, *Organometallics*, **2005**, *24*, 2988; (e) I. Saur, G. Rima, K. Miqueu, H. Gornitzka y J. Barrau, *J. Organomet. Chem.*, **2003**, *672*, 77; (f) A. Akkari, J. J. Byrne, I. Saur, G. Rima, H. Gornitzka y J. Barrau, *J. Organomet. Chem.*, **2001**, *622*, 190.
50. (a) V. V. Bashilov, V. I. Sokolov, Y. L. Slovokhotov y Y. T. Struchkov, *J. Organomet. Chem.*, **1987**, *327*, 285; (b) G. W. Bushnell, D. T. Eadie, A. Pidcock, A. R. Sam, R. D. Holmes-Smith, S. R. Stobart, E. T. Brennan y T. S. Cameron, *J. Am. Chem. Soc.*, **1982**, *104*, 5837; (c) P. F. R. Ewings y P. G. Harrison, *Inorg. Chim. Acta.*, **1978**, *28*, L167; (d) A. B. Cornwell y P. G. Harrison, *J. Chem. Soc., Dalton Trans.*, **1976**, *12*, 1054; (e) B. Anthony P. G. Cornwell y J. Harrison, *J. Chem. Soc., Dalton Trans.*, **1976**, 1608; (f) A. B. Cornwell y P. G. Harrison, *J. Chem. Soc., Dalton Trans.*, **1975**, 1486; (g) A. B. Cornwell, P. G. Harrison y J. A. Richards, *J. Organomet. Chem.*, **1974**, *76*, C26.
51. (a) H. V. Rasika Dias, X. Wang y H. V. K. Diyabalanage, *Inorg. Chem.*, **2005**, *44*, 7322; (b) A. E. Ayers y H. V. Rasika Dias, *Inorg. Chem.*, **2002**, *41*, 3259; (c) H. V. Rasika Dias

- y Z. Wang, *Inorg. Chem.*, **2000**, 39, 3890; (d) H. V. R. Dias y Z. Wang, *J. Am. Chem. Soc.*, **1997**, 119, 4650.
52. (a) S. Krabbe, M. Wagner, C. Löw, C. Dietz, M. Schürmann, A. Hoffmann, S. Herres-Pawlis, M. Lutter y K. Jurkschat, *Organometallics*, **2014**, 33, 4433; (b) M. Wagner, V. Deáky, C. Dietz, J. Martincová, B. Mahieu, R. Jambor, S. Herres-Pawlis y K. Jurkschat, *Chem. Eur. J.*, **2013**, 19, 6695; (c) M. Wagner, M. Henn, C. Dietz, M. Schürmann, M. H. Prosenc y K. Jurkschat, *Organometallics*, **2013**, 32, 2406; (d) R. Jambor, S. Herres-Pawlis, M. Schürmann y K. Jurkschat, *Eur. J. Inorg. Chem.*, **2012**, 344; (e) M. Henn, V. Deáky, S. Krabbe, M. Schürmann, M. Prosenc, S. Herres-Pawlis, B. Mahieu y K. Jurkschat, *Z. Anorg. Allg. Chem.*, **2011**, 637, 211; (f) J. Martincová, L. Dostál, S. Herres-Pawlis, A. Růžička y R. Jambor, *Chem. Eur. J.*, **2011**, 17, 7423; (g) J. Martincová, R. Dostálová, L. Dostál, A. Růžička y R. Jambor, *Organometallics*, **2009**, 28, 4823; (h) J. Martincová, R. Jambor, M. Schürmann, K. Jurkschat, J. Honzíček y F. A. Almeida Paz, *Organometallics*, **2009**, 28, 4778; (i) J. Martincová, L. Dostál, A. Růžička, J. Taraba y R. Jambor, *Organometallics*, **2007**, 26, 4102; (j) M. Henn, M. Schürmann, B. Mahieu, P. Zanello, A. Cinquantini y K. Jurkschat, *J. Organomet. Chem.*, **2006**, 691, 1560; (k) M. Mehring, C. Löw, M. Schürmann, F. Uhlig, K. Jurkschat y M. Mahieu, *Organometallics*, **2000**, 19, 4613.
53. C.-W. So, H. W. Roesky, J. Magull y R. B. Oswald, *Angew. Chem. Int. Ed.*, **2006**, 45, 3948.
54. (a) S. Schäfer, R. Köppe, M. T. Gamer y P. W. Roesky, *Chem. Commun.*, **2014**, 50, 11401; (b) G. Tan, B. Blom, D. Gallego y M. Driess, *Organometallics*, **2014**, 33, 363; (c) D. Gallego, S. Inoue, B. Blom y M. Driess, *Organometallics*, **2014**, 33, 6685; (d) H.-X. Yeong, Y. Li y C.-W. So, *Organometallics*, **2014**, 33, 3646; (e) F. M. Mück, D. Kloß, J. A. Baus, C. Burschka y R. Tacke, *Chem. Eur. J.*, **2014**, 20, 9620; (f) K. Junold, J. A. Baus, C. Burschka, T. Vent-Schmidt, S. Riedel y R. Tacke, *Inorg. Chem.*, **2013**, 52, 11593; (g) B. Blom, S. Enthaler, S. Inoue, E. Irran y M. Driess, *J. Am. Chem. Soc.*, **2013**, 135, 6703; (h) R. Azhakar, R. S. Ghadwal, H. W. Roesky, J. Hey, L. Krause y D. Stalke, *Dalton Trans.*, **2013**, 42, 10277; (i) C. I. Someya, M. Haberberger, W. Wang, S. Enthaler y S. Inoue, *Chem. Lett.*, **2013**, 42, 286; (j) D. Gallego, A. Brück, E. Irran, F. Meier, M. Kaupp y M. Driess, *J. Am. Chem. Soc.*, **2013**, 135, 15617; (k) N. C. Breit, T. Szilvási, T. Suzuki, D. Gallego, S. Inoue y M. Driess, *J. Am. Chem. Soc.*, **2013**, 135, 17958; (l) W. Wang, S. Inoue, E. Irran y M. Driess, *Angew. Chem. Int. Ed.*, **2012**, 51, 3691; (m) A. Brück, D. Gallego, W. Wang, E. Irran, M. Driess y J. F. Hartwig, *Angew. Chem. Int. Ed.*, **2012**, 51, 11478; (n) W. Wang, S. Inoue, S. Enthaler y M. Driess, *Angew. Chem. Int. Ed.*, **2012**, 51, 6167; (ñ) R. Azhakar, H. W. Roesky, J. J. Holstein y

- B. Dittrich, *Dalton. Trans.*, **2012**, *41*, 12096; (o) K. Junold, J. A. Baus, C. Burschka y R. Tacke, *Angew. Chem. Int. Ed.*, **2012**, *51*, 7020; (p) R. Azhakar, R. S. Ghadwal, H. W. Roesky, H. Wolf y D. Stalke, *J. Am. Chem. Soc.*, **2012**, *134*, 2423; (q) R. Azhakar, R. S. Ghadwal, H. W. Roesky, J. Hey y D. Stalke, *Chem. Asian. J.*, **2012**, *7*, 528; (r) R. Azhakar, S. P. Sarish, H. W. Roesky, J. Hey y D. Stalke, *Inorg. Chem.*, **2011**, *50*, 5039; (s) W. Wang, S. Inoue, S. Yao y M. Driess, *J. Am. Chem. Soc.*, **2010**, *132*, 15890; (t) G. Tavčar, S. S. Sen, R. Azhakar, A. Thorn y H. W. Roesky, *Inorg. Chem.*, **2010**, *49*, 10199; (u) S. S. Sen, M. P. Kritzler-Kosch, S. Nagendran, H. W. Roesky, T. Beck, A. Pal y R. Herbst-Irmer, *Eur. J. Inorg. Chem.*, **2010**, 5304; (v) D. Matioszek, N. Katir, N. Saffon y A. Castel, *Organometallics*, **2010**, *29*, 3039; (w) W. Yang, H. Fu, H. Wang, M. Chen, Y. Ding, H. W. Roesky y A. Jana, *Inorg. Chem.*, **2009**, *48*, 5058; (x) C. Jones, R. P. Rose y A. Stasch, *Dalton. Trans.*, **2008**, 2871
55. Complejos con amidinato-TPs que han resultado del trabajo realizado durante esta tesis doctoral: (a) L. Álvarez-Rodríguez, J. A. Cabeza, P. García-Álvarez y D. Polo, *Coord. Chem. Rev.*, **2015**, *300*, 1; (b) J. A. Cabeza, J. M. Fernández-Colinas, P. García-Álvarez, E. Pérez-Carreño y D. Polo, *Inorg. Chem.*, **2015**, *54*, 4850; (c) L. Álvarez-Rodríguez, J. A. Cabeza, P. García-Álvarez, E. Pérez-Carreño y D. Polo, *Inorg. Chem.*, **2015**, *54*, 2983; (d) J. A. Cabeza, P. García-Álvarez, E. Pérez-Carreño y D. Polo, *Inorg. Chem.*, **2014**, *53*, 8735; (e) J. A. Cabeza, P. García-Álvarez, E. Pérez-Carreño y D. Polo, *Chem. Eur. J.*, **2014**, *20*, 8654; (f) J. A. Cabeza, J. M. Fernández-Colinas, P. García-Álvarez y D. Polo, *RSC Adv.*, **2014**, *4*, 31503; (g) J. A. Cabeza, P. García-Álvarez y D. Polo, *Dalton. Trans.*, **2013**, *42*, 1329.
56. (a) D. Gallego, S. Inoue, B. Blom y M. Driess, *Organometallics*, **2014**, *33*, 6685; (b) C. I. Someya, M. Haberberger, W. Wang, S. Enthaler y S. Inoue, *Chem. Lett.*, **2013**, *42*, 286; (c) W. Wang, S. Inoue, S. Enthaler y M. Driess, *Angew. Chem. Int. Ed.*, **2012**, *51*, 6167; (d) A. Brück, D. Gallego, W. Wang, E. Irran, M. Driess y J. F. Hartwig, *Angew. Chem. Int. Ed.*, **2012**, *51*, 11478.
57. C. J. Cardin, D. J. Cardin, G. A. Lawless, J. M. Power y M. B. Power, *J. Organomet. Chem.*, **1987**, *325*, 203.
58. H. Handwerker, C. Leis, R. Probst, P. Bissinger, A. Grohmann, P. Kiprof, E. Herdtweck, J. Blümel, N. Auner y C. Zybilla, *Organometallics*, **1993**, *12*, 2162.
59. (a) Y. Li y W. T. Wong, *Coord. Chem. Rev.*, **2003**, *243*, 191; (b) J. A. Cabeza, *Eur. J. Inorg. Chem.*, **2002**, 1559; (c) P. J. Dyson y J. S. McIndoe, *Transition Metal Carbonyl Cluster Chemistry*; Gordon & Breach, Amsterdam, The Netherlands, **2000**, p. 73; (d) *Metal Clusters in Chemistry*; P. Braunstein, L. A. Oro y P. R. Raithby, Eds.; Wiley-VCH,

- Weinheim, Germany, **1999**; (e) *Comprehensive Organometallic Chemistry II*; E. W. Abel, F. G. A. Stone y G. Wilkinson, Eds; vol. 7, D. F. Shriver y M. I. Bruce, Eds.; Pergamon, Oxford, UK, **1995**; (f) R. D. Adams en *The Chemistry of Metal Cluster Complexes*; D. F. Shriver, H. D. Kaesz y R. D. Adams, Eds.; Wiley-VCH, New York, USA, **1990**, p. 121; (g) M. I. Bruce, *Coord. Chem. Rev.*, **1987**, 76, 1; (h) M. Moskovits, *Metal Clusters*; J. Wiley & Sons, New York, USA, **1986**.
60. J. A. Cabeza y P. García-Álvarez, *Chem. Soc. Rev.*, **2011**, 40, 5389.
61. N. C. Burton, C. J. Cardin, D. J. Cardin, B. Twanley y Y. Zubavichus, *Organometallics*, **1995**, 14, 5708.
62. G. K. Campbell, P. B. Hitchcock, M. F. Lappert y M. C. Misra, *J. Organomet. Chem.*, **1985**, 289, C1.
63. T. A. Schmedake, M. Haaf, B. J. Paradise, A. J. Millevolte, D. R. Powell y R. West, *J. Organomet. Chem.*, **2001**, 636, 17.
64. W. A. Herrmann, M. Denk, J. Behm, W. Scherer, F.-R. Klingan, H. Bock, B. Solouki y M. Wagner, *Angew. Chem. Int. Ed.*, **1992**, 31, 1485.
65. (a) O. Kühn, P. Lönnecke y J. Heinicke, *Polyhedron*, **2001**, 20, 2215; (b) H. Braunschweig, B. Gehrhus, P. B. Hitchcock y M. F. Lappert, *Z. Anorg. Allg. Chem.*, **1995**, 621, 1922; (c) B. Gehrhus, M. F. Lappert, J. Heinicke, R. Boese y D. Bläser, *J. Chem. Soc., Chem. Commun.*, **1995**, 1931.
66. I. A. Guzei, V. I. Timokhin y R. West, *Acta Cryst.*, **2006**, C62, m90.
67. M. P. Aarnts, F. Hartl, K. Peelen, D. J. Stufkens, C. Amatore y J.-N. Verpeaux, *Organometallics*, **1997**, 16, 4686.
68. (a) S. Gaillard, C. S. J. Cazin y S. P. Nolan, *Acc. Chem. Res.*, **2012**, 45, 778; (b) S. P. Nolan, *Acc. Chem. Res.*, **2011**, 44, 91; (c) S. Díez-González, N. Marion y S. P. Nolan, *Chem. Rev.*, **2009**, 109, 3612; (d) N. Marion y S. P. Nolan, *Chem. Soc. Rev.*, **2008**, 37, 1776; (e) D. J. Gorin, B. D. Sherry y F. D. Toste, *Chem. Rev.*, **2008**, 108, 3351; (f) Z. Li, C. Brouwer y C. He, *Chem. Rev.*, **2008**, 108, 3239; (g) A. Arcadi, *Chem. Rev.*, **2008**, 108, 3266; (h) E. Jiménez-Núñez y A. M. Echavarren, *Chem. Rev.*, **2008**, 108, 3326.
69. S. Díez-González y S. P. Nolan, *Coord. Chem. Rev.*, **2007**, 251, 874.
70. (a) N. Zhao, J. Zhang, Y. Yang, G. Chen, H. Zhu y H. W. Roesky, *Organometallics*, **2013**, 32, 762; (b) D. Matioszek, T.-G. Kocsor, A. Castel, G. Nemes, J. Escudé y N. Saffon, *Chem. Commun.*, **2012**, 48, 3629; (c) R. D. Adams, Y. Kan y Q. Zhang, *Organometallics*, **2012**, 31, 8639; (d) H. Arai, F. Nakadate y K. Mochida,

- Organometallics*, **2009**, *28*, 4909; (e) W.-P. Leung, C.-W. So, K.-H. Kan, H.-S. Chan y T. Mak, *Organometallics*, **2006**, *25*, 2851; (f) J. T. York, V. G. Young y W. B. Tolman, *Inorg. Chem.*, **2006**, *45*, 4191; (g) H. V. R. Dias, X. Wang y H. Diyabalange, *Inorg. Chem.*, **2005**, *44*, 7322; (h) A. G. Avent, B. Gehrhus, P. B. Hitchcock, M. F. Lappert y H. Maciejewsky, *J. Organomet. Chem.*, **2003**, *686*, 321; (i) H. V. R. Dias y A. E. Ayers, *Polyhedron*, **2002**, *21*, 611; (j) A. E. Ayers y H. V. R. Dias, *Inorg. Chem.*, **2002**, *41*, 3259; (k) H. V. R. Dias y Z. Wang, *Inorg. Chem.*, **2000**, *39*, 3890.
71. M. Theil, P. Jutzi, B. Neumann, A. Stammli y H.-G. Stammli, *J. Organomet. Chem.*, **2002**, *662*, 34.
72. U. Anandhi y P. Sharp, *Inorg. Chim. Acta*, **2006**, *359*, 3521.
73. (a) A. Bauer y H. Schmidbaur, *J. Am. Chem. Soc.*, **1996**, *118*, 5324; (b) A. Bauer, A. Schier y H. Schmidbaur, *J. Chem. Soc., Dalton Trans: Inorg. Chem.*, **1995**, *17*, 2919.
74. (a) J. A. Dilts y M. P. Johnson, *Inorg. Chem.*, **1966**, *5*, 2079; (b) B. Vilma, J. M. López-de-Luzuriaga, M. Monge, M. E. Olmos, R. Echevarría, O. Lehtonen y D. Sundholm, *ChemPlusChem*, **2014**, *79*, 67.
75. (a) M. Lutz, B. Findeis, M. Haukka, T. A. Pakkanen y L. H. Gade, *Eur. J. Inorg. Chem.*, **2001**, 3155; (b) B. Findeis, L. H. Gade, I. J. Scowen y M. McPartlin, *Inorg. Chem.*, **1997**, *36*, 960; (c) B. Findeis, M. Contel, L. H. Gade, M. Laguna, M. C. Gimeno, I. J. Scowen y M. McPartlin, *Inorg. Chem.*, **1997**, *36*, 2386; (d) M. Contel, K. W. Hellmann, L. H. Gade, M. Laguna, I. J. Scowen y M. McPartlin, *Inorg. Chem.*, **1996**, *35*, 3713.
76. (a) L.-I. Rodríguez, T. Roth, J. L. Fillol y H. Wadepohl, H. G. Lutz, *Chem. Eur. J.*, **2012**, *18*, 3721. (b) B. Sean, T. J. Clark, J. Coyle y J. J. M. Hastie, *PCT Int. Appl.*, **2012**, WO2012155264A1. (c) I. O. Kosheroy, M. Haukka, S. I. Selivanov, S. P. Tunik y T. A. Pakkanen, *Chem. Commun.*, **2010**, *46*, 8926. (d) A. Arnanz, C. González-Arellano, A. Juan, G. Villaverde, A. Corma, M. Iglesias y F. Sánchez, *Chem. Commun.*, **2010**, *46*, 3001. (e) J. Vicente, M. T. Chicote, I. Saura-Llamas, J. Turpin y J. Fernández-Baeza, *J. Organomet. Chem.*, **1987**, *333*, 129.
77. (a) P. P. Samuel, A. P. Singh, S. P. Sarish, J. Matussek, I. Objartel, H. W. Roesky y D. Stalke, *Inorg. Chem.*, **2013**, *52*, 1544; (b) S. Nagendran, S. S. Sen, H. W. Roesky, D. Koley, H. Grubmüller, A. Pal y R. Herbst-Irmer, *Organometallics*, **2008**, *27*, 5459.
78. S. S. Sen, H. W. Roesky, D. Stern, J. Henn y D. Stalke, *J. Am. Chem. Soc.*, **2010**, *132*, 1123.
79. S. S. Sen, J. Hey, R. Herbst-Irmer, H. W. Roesky y D. Stalke, *J. Am. Chem. Soc.*, **2011**, *133*, 12311.

80. (a) E. N. M. Ho y W. T. Wong, *J. Chem. Soc., Dalton Trans.*, **1998**, 4215; (b) A. J. Deeming, K. I. Hardcastle y M. Karim, *Inorg. Chem.*, **1992**, *31*, 4792; (c) U. Bodensieck, H. Stoeckli-Evans y G. Süss-Fink, *Chem. Ber.*, **1990**, *123*, 1603. (d) G. Lavigne, N. Lugañ y J. J. Bonnet, *Chem. Commun.*, **1987**, 957.
81. D. Matisozek, N. Saffon, J.-M. Sotiropoulos, K. Miqueu, A. Castel y J. Escudié, *Inorg. Chem.*, **2012**, *51*, 11716.
82. (a) G. Lavigne y H. D. Kaesz, *J. Am. Chem. Soc.*, **1984**, *106*, 4647. (b) A. Mayr, Y. C. Lin, N. M. Boag y H. D. Kaesz, *Inorg. Chem.*, **1982**, *21*, 1704. (c) C. M. Jensen, T. J. Lynch, C. B. Knobler y H. D. Kaesz, *J. Am. Chem. Soc.*, **1982**, *104*, 4679.
83. (a) H. van Rensburg, R. P. Tooze, D. F. Foster y A. M. Z. Slawin, *Inorg. Chem.*, **2004**, *43*, 2468. (b) C. D. Wood y P. E. Garrou, *Organometallics*, **1984**, *3*, 170.
84. (a) J. S. Field, R. J. Haines, J. Sundermeyer y S. F. Woollam, *J. Chem. Soc., Chem. Commun.*, **1991**, 1382. (b) J. S. Field, R. J. Haines, M. W. Stewart, J. Sundermeyer y S. F. Woollam, *J. Chem. Soc., Dalton Trans.*, **1991**, 947.
85. (a) J. Agarwal, T. W. Shaw, C. J. Stanton III, G. F. Majetich, A. B. Bocarsly y H. F. Schaefer III, *Angew. Chem. Int. Ed.*, **2014**, *53*, 5152. (b) C. Riplinger, M. D. Sampson, A. M. Ritzmann, C. P. Kubiak y E. A. Carter, *J. Am. Chem. Soc.*, **2014**, *136*, 16285. (c) J. M. Smieja, M. D. Sampson, K. A. Grice, E. E. Benson, J. D. Froehlich y C. P. Kubiak, *Inorg. Chem.*, **2013**, *52*, 2484. (d) M. Bourrez, F. Molton, S. Chardon-Noblat y A. Deronzier, *Angew. Chem. Int. Ed.*, **2011**, *50*, 9903.
86. E. E. Benson, C. P. Kubiak, A. J. Sathrum y J. M. Smieja, *Chem. Soc. Rev.*, **2009**, *38*, 89.
87. (a) M. I. Bruce en *Comprehensive Organometallic Chemistry*; vol. 4, G. Wilkinson, F. G. A. Stone y E. W. Abel, Eds.; Pergamon, Oxford, UK, **1982**, p.843; (b) N. M. J. Brodie y A. J. Poë, *Inorg. Chem.* **1988**, *27*, 3156. (c) A. J. Poë y M. V. Twigg, *Inorg. Chem.*, **1974**, *13*, 2982. (d) A. J. Poë y M. V. Twigg, *J. Chem. Soc., Dalton Trans.*, **1974**, 1860. (e) M. I. Bruce, G. Shaw y F. G. A. Stone, *J. Chem. Soc., Dalton Trans.*, **1972**, 2094. (f) R. L. Bennett, M. I. Bruce y F. G. A. Stone, *J. Organomet. Chem.*, **1972**, *38*, 325. (g) J. P. Candlin y A. C. Shortland, *J. Organomet. Chem.*, **1969**, *16*, 289. (h) F. Piacenti, M. Bianchi, E. Benedetti y G. Sbrana, *J. Inorg. Nucl. Chem.*, **1967**, *29*, 1389.
88. (a) C. Zhang, B. Li, H. Song, S. Xu y B. Wang, *Organometallics*, **2011**, *30*, 3029. (b) J. A. Cabeza, I. del Río, D. Miguel, E. Pérez-Carreño y M. G. Sánchez-Vega, *Organometallics*, **2008**, *27*, 211. (c) M. I. Bruce, M. L. Cole, R. S. C. Fung, C. M. Forsyth, M. Hilder, P. C. Junk y K. Konstas, *Dalton Trans.*, **2008**, 4118. (d) C. E. Ellul,

O. Saker, M. F. Mahon, D. C. Apperley y M. K. Whittlesey, *Organometallics*, **2008**, *27*, 100. (e) M. R. Crittall, C. E. Ellul, M. F. Mahon, O. Saker y M. K. Whittlesey, *Dalton Trans.*, **2008**, 4209. (f) C. E. Ellul, M. F. Mahon, O. Saker y M. K. Whittlesey, *Angew. Chem. Int. Ed.*, **2007**, *46*, 6343.

Publicaciones

Artículo I

***“Reactivity of Diaminogermynes with Ruthenium
Carbonyl: Ru₃Ge₃ and RuGe₂ Derivatives”***

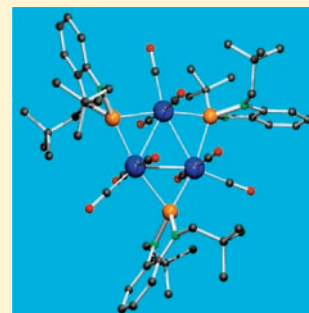
Reactivity of Diaminogermynes with Ruthenium Carbonyl: Ru_3Ge_3 and RuGe_2 Derivatives

Javier A. Cabeza,* Pablo García-Álvarez,* and Diego Polo

Departamento de Química Orgánica e Inorgánica-IUQOEM, Universidad de Oviedo-CSIC, E-33071-Oviedo, Spain

Supporting Information

ABSTRACT: The nature of the products of the reactions of $[\text{Ru}_3(\text{CO})_{12}]$ with diaminogermynes depends upon the volume and the cyclic or acyclic structure of the latter. Thus, the triruthenium cluster $[\text{Ru}_3\{\mu\text{-Ge}(\text{NCH}_2\text{CMe}_3)_2\text{C}_6\text{H}_4\}_3(\text{CO})_9]$, which has a planar Ru_3Ge_3 core and an overall C_{3h} symmetry, has been prepared in quantitative yield by treating $[\text{Ru}_3(\text{CO})_{12}]$ with an excess of the cyclic 1,3-bis(*neo*-pentyl)-2-germabenzimidazol-2-ylidene in toluene at 100 °C, but under analogous reaction conditions, the acyclic and bulkier $\text{Ge}(\text{HMDS})_2$ ($\text{HMDS} = \text{N}(\text{SiMe}_3)_2$) quantitatively leads to the mononuclear ruthenium(0) derivative $[\text{Ru}\{\text{Ge}(\text{HMDS})_2\}_2(\text{CO})_3]$. Mixtures of products have been obtained from the reactions of $[\text{Ru}_3(\text{CO})_{12}]$ with the cyclic and very bulky 1,3-bis(*tert*-butyl)-2-germimidazol-2-ylidene under various reaction conditions. The Ru_3Ge_3 and RuGe_2 products reported in this paper are the first ruthenium complexes containing diaminogermylene ligands.



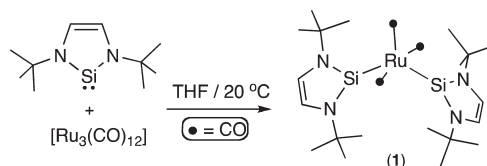
INTRODUCTION

Quite a few stable N-heterocyclic group-14 metal ylidenes (NHMs, where M can be Si, Ge, Sn, or Pb) were prepared and characterized^{1,2} before the isolation of the first stable N-heterocyclic carbene (NHC), which was reported in 1991.³ However, in contrast with the coordination chemistry of NHMs, which has been developed gradually but slowly since their discovery,^{4,5} that of NHCs blossomed very rapidly⁶ because some NHC complexes were soon demonstrated excellent homogeneous catalysts for processes that are very useful in organic synthesis.⁷ This intense NHC research activity has also included transition metal clusters,^{8–10} on which NHCs are prone to undergo multiple C–H and C–N bond activation processes that cannot occur in mononuclear complexes.^{8g–j,10}

To date, the transition metal chemistry of NHMs has been developed to a considerable extent,^{4,5,11–13} but in general, reactivity^{5f,11} and catalytic¹² studies on their complexes are scarce. Regarding transition metal clusters and NHMs, as far as we are aware, only one work has been hitherto reported.¹³ It describes that the reaction of $[\text{Ru}_3(\text{CO})_{12}]$ with a 6-fold excess of 1,3-bis(*tert*-butyl)-2-silaimidazol-2-ylidene results in the formation of the mononuclear species $[\text{Ru}\{\text{Si}(\text{N}^t\text{Bu})_2\text{C}_2\text{H}_2\}_2(\text{CO})_3]$ (**1**, Scheme 1).¹³

In this paper, we report the reactivity of $[\text{Ru}_3(\text{CO})_{12}]$ with two cyclic and one acyclic diaminogermynes. In addition to unveiling the synthesis of the first diaminogermylene derivatives of ruthenium, including a Ru_3Ge_3 cluster that is the first transition metal cluster containing an NHM ligand of any kind, we also show that the nuclearity of the products of the reactions of $[\text{Ru}_3(\text{CO})_{12}]$ with diaminogermynes strongly depends upon the volume and the cyclic or acyclic structure of the latter. This chemistry is very different from that known for $[\text{Ru}_3(\text{CO})_{12}]$ and NHCs.

Scheme 1. Reported Synthesis of Compound 1



RESULTS AND DISCUSSION

The treatment of $[\text{Ru}_3(\text{CO})_{12}]$ with the very bulky $\text{Ge}(\text{N}^t\text{Bu})_2\text{C}_2\text{H}_2$,^{2c} mimicking the reaction conditions under which the NHSi derivative **1** was prepared by West et al. (Scheme 1),¹³ i.e., using a 6-fold excess of the NHM in THF at room temperature, resulted in no reaction at all. The large volume of this NHGe ligand and the previous observation that, for complexes with NHM ligands, the strength of the metal–M bond decreases on going down in group 14^{5c,f,14} seem to account for this result. Working at higher temperatures in THF or toluene solvents and using 1, 3, 6, or more equivalents of $\text{Ge}(\text{N}^t\text{Bu})_2\text{C}_2\text{H}_2$ resulted in the formation of mixtures of compounds that could not be separated and identified. We then reasoned that a reduction of the volume of the NR arms would enhance the reactivity (and/or selectivity) of the NHGe ligands toward $[\text{Ru}_3(\text{CO})_{12}]$ and also the stability of the reaction products.

The sterically less demanding cyclic germylene $\text{Ge}(\text{NCH}_2\text{CMe}_3)_2\text{C}_6\text{H}_4$,¹⁵ which contains *N*-*neo*-pentyl groups, also failed to react with $[\text{Ru}_3(\text{CO})_{12}]$ at room temperature. In toluene at 100 °C, using Ge/Ru₃ ratios < 3, mixtures (which decomposed

Received: March 7, 2011

Published: June 09, 2011

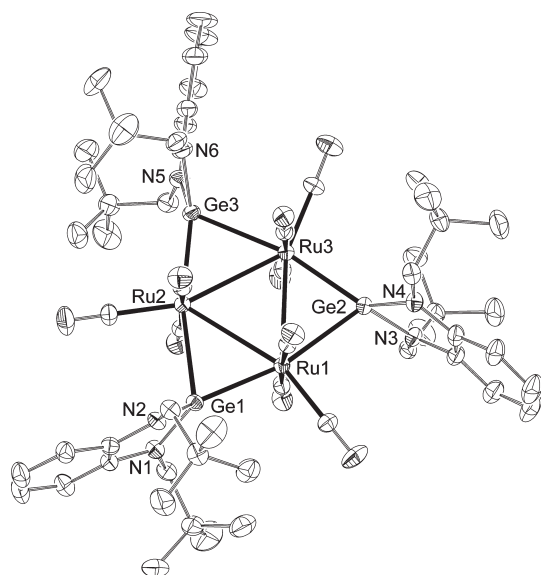
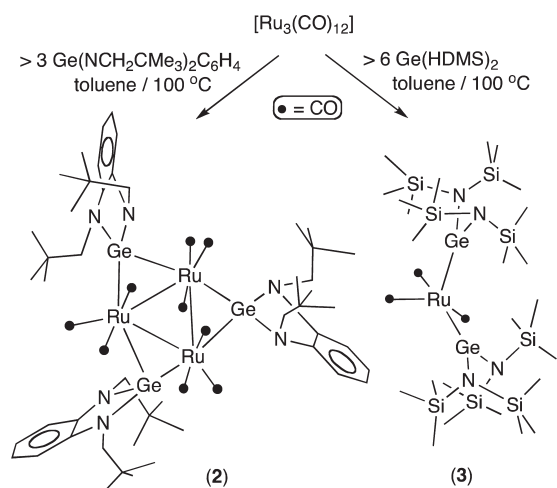
Scheme 2. Contrasting Reactivity of $[\text{Ru}_3(\text{CO})_{12}]$ with $\text{Ge}(\text{NCH}_2\text{CMe}_3)_2\text{C}_6\text{H}_4$ and $\text{Ge}(\text{HMDS})_2$


Figure 1. Molecular structure of **2**. Hydrogen atoms have been omitted for clarity. Selected bond distances (Å) and angles (deg): Ge1–Ru1 2.4335(6), Ge1–Ru2 2.6145(6), Ru1–Ru2 3.0001(4), Ge1–N1 1.843(4), Ge1–N2 1.834(4), N1–Ge1–N2 88.1(2); (Ru1Ru2Ru3)–(N1Ge1N2) 91.4(1); (Ru1Ru2)–(N1Ge1N2) 73.8(1), (Ge1Ru1)–(N1Ge1N2) 162.5(1), (Ge1Ru2)–(N1Ge1N2) 124.6(1).

on chromatographic supports) containing $[\text{Ru}_3(\text{CO})_{12}]$, the trisubstituted derivative $[\text{Ru}_3\{\mu\text{-Ge}(\text{NCH}_2\text{CMe}_3)_2\text{C}_6\text{H}_4\}_3(\text{CO})_9]$ (**2**), and other unidentified species were formed (IR and NMR analyses of the reaction mixtures). Fortunately, the use of a Ge/Ru₃ ratio of 3 or greater led to compound **2** in quantitative yield (Scheme 2). Interestingly, this complex remained unchanged when it was treated with 6 equivalents of $\text{Ge}(\text{NCH}_2\text{CMe}_3)_2\text{C}_6\text{H}_4$ in toluene at reflux temperature.

The X-ray molecular structure of **2** (Figure 1) shows that the complex has an approximate (noncrystallographic) C_{3h} symmetry, comprising a regular triangle of Ru atoms, nine carbonyl ligands (three attached to each Ru atom), and three $\text{Ge}(\text{NCH}_2\text{CMe}_3)_2\text{C}_6\text{H}_4$ ligands. Each germylene ligand asymmetrically spans an edge

of the Ru₃ triangle in such a way that (a) the two Ge–Ru distances differ by 0.18 Å, (b) the angle between the GeN₂ plane and the shorter Ge–Ru bond (Ge1–Ru1) is wider (162.5°) than that involving the longer Ge–Ru bond (124.6°), (c) the plane defined by the benzo group is perpendicular to the Ru₃ plane, (d) the ligand N atoms are in the plane of the benzo group but the Ge atom is 0.117(3) Å away from that plane (the free ligand is planar¹⁵), and (e) the *neo*-pentyl groups are disposed *syn* to each other, with both CMe₃ groups on the same side of the ligand plane. Such a *syn* disposition of the *neo*-pentyl groups has also been found in the free ligand¹⁵ and in other structurally characterized metal– $\text{Ge}(\text{NCH}_2\text{CMe}_3)_2\text{C}_6\text{H}_4$ complexes.^{5c} The peculiar arrangement of the NHGe ligands of **2** has not been observed in any of the few crystallographically characterized complexes containing bridging NHM ligands, all of them binuclear with ^tBu or Dipp (2,6-ⁱPr₂C₆H₃) N–R arms.^{5a,11a,11d,12b,16} The possibility that the *neo*-pentyl groups of **2** have to minimize their steric hindrance with the nearby carbonyl ligands bending away their bulky CMe₃ group through their CH₂ hinge seems to favor the ligand arrangement found in this cluster (such a bending is not possible for ^tBu or Dipp). The fact that both CMe₃ groups of each germylene ligand are placed on the same side of the GeN₂ plane accounts for the asymmetric coordination of this ligand with respect to the bridged metal atoms.

The NMR spectra of compound **2** confirm that the approximate C_{3h} symmetry found for this complex in the solid state is maintained in solution. Thus, the ¹³C{¹H} NMR spectrum contains two singlets (at 202.2 and 196.1 ppm, with a 2:1 integral ratio) assignable to the carbonyl groups and six singlets assignable to the C atoms of the germylene ligand. The ¹H NMR spectrum shows that the protons of each *neo*-pentyl CH₂ group are magnetically inequivalent (AB pattern at 3.93 and 3.38 ppm, *J* = 14.6 Hz), indicating the absence of free rotation around the N–CH₂ bond.

There are only two crystallographically characterized complexes with Ru₃Ge₃ frameworks related to that of compound **2**, namely, $[\text{Ru}_3(\mu\text{-GeR}_2)_3(\text{CO})_9]$ (R = Ph,¹⁷ Me¹⁸). They were prepared in low yields from $[\text{Ru}_3(\text{CO})_{12}]$ and aryl- or alkylhydrogermanes (not germylenes), and in contrast to compound **2**, their Ru atoms are symmetrically bridged by the GeR₂ groups, Ru–Ge = 2.50(1) Å for R = Ph and 2.49(1) Å for R = Me, the molecules having D_{3h} symmetry. The IR ν_{CO} bands of **2** (2045, 2009, 1999 cm^{−1}) are observed at lower wavenumbers than those of $[\text{Ru}_3(\mu\text{-GePh}_2)_3(\text{CO})_9]$ (2059, 2028, 1997 cm^{−1}),¹⁷ indicating the presence of a greater electron density in the Ru atoms of **2**. The planarity of cyclic NHGe ligands allows a non-negligible N→Ge π donation from the filled p orbitals of the N atoms to the empty p orbital of the Ge atom that lowers the π -accepting capacity of these ligands.^{5f,14}

The above-described NHGe chemistry is completely different from that involving $[\text{Ru}_3(\text{CO})_{12}]$ and NHCs, which is dominated by Ru₃(NHC),^{8g,h} Ru(NHC),^{9a} and Ru(NHC)₂ products^{9b} in which the NHCs act as terminal ligands.

For comparison purposes, we also studied the reactivity of $[\text{Ru}_3(\text{CO})_{12}]$ with an acyclic diaminogermylene, namely, $\text{Ge}(\text{HMDS})_2$ (HMDS = N(SiMe₃)₂).¹⁹ This germylene has been previously used as ligand in several transition metal complexes (not ruthenium),^{5f,20} undergoing, after coordination, interesting insertion and activation processes.^{20c–i} Heavier acyclic diamino group-14 metal ylidenes^{19,21} have been known of since the 1970s.²² In acyclic diaminogermylenes, the N→Ge π donation from the filled p orbitals of the N atoms to the empty p orbital of the Ge atom is geometrically disfavored, and therefore, they are more π -acidic than their cyclic NHGe relatives.

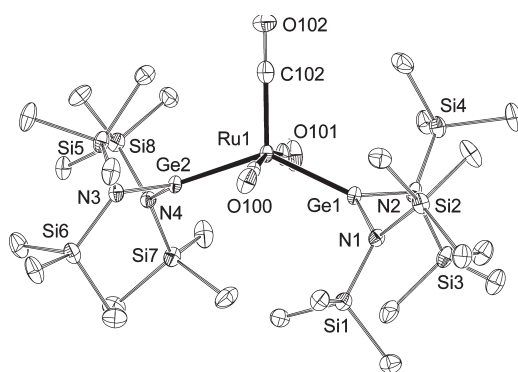


Figure 2. Molecular structure of **3** (only one of the two analogous but independent molecules found in the asymmetric unit is shown). Hydrogen atoms have been omitted for clarity. Selected bond distances (Å) and angles (deg): Ge1–Ru1 2.37(1), Ru1–C100 1.928(9), Ru1–C102 1.96(1), Ge1–N1 1.894(6), Ge1–N2 1.865(6); N1–Ge1–N2 107.3(3); Ge1–Ru1–Ge2 136.42(4), C100–Ru1–C101 167.2(4), C100–Ru1–C102 98.9(3), Ge1–Ru1–C100 86.9(2), Ge1–Ru1–C102 115.6(2), N1–Ge1–N2 107.3(3).

The mononuclear complex $[\text{Ru}\{\text{Ge}(\text{HDMS})_2\}_2(\text{CO})_3]$ (**3**) was quantitatively formed when $[\text{Ru}_3(\text{CO})_{12}]$ was treated with at least six equivalents of $\text{Ge}(\text{HMDS})_2$ in toluene at 100 °C (Scheme 2). The use of smaller amounts of the germylene led to intractable mixtures that could not be separated. IR monitoring of these reactions indicated that in no case was a Ru_3Ge_3 complex analogous to compound **2** formed as an intermediate species.

Figure 2 shows that the molecular structure of compound **3** is closely related to that of the $\text{Ru}(\text{NHSi})_2$ derivative **1** (Scheme 1).¹³ The ligand arrangement around the Ru atom is distorted trigonal bipyramidal, with the $\text{Ge}(\text{HMDS})_2$ ligands in equatorial positions. In solution, the carbonyl ligands of **3** exchange rapidly, as they are observed as a singlet in the $^{13}\text{C}\{^1\text{H}\}$ NMR spectrum. Complex **3** forms part of a small family of ruthenium species containing three-coordinate germanium-based ligands.²³

The fact that the acyclic $\text{Ge}(\text{HMDS})_2$ is bulkier than $\text{Ge}(\text{NCH}_2\text{CMe}_3)_2\text{C}_6\text{H}_4$ cannot account on its own for the different reactivity of these diaminogermylenes with $[\text{Ru}_3(\text{CO})_{12}]$ because the reactivity of the cyclic $\text{Ge}(\text{N}^t\text{Bu})_2\text{C}_2\text{H}_2$, which is also bulkier than $\text{Ge}(\text{NCH}_2\text{CMe}_3)_2\text{C}_6\text{H}_4$, is not comparable with that of $\text{Ge}(\text{HMDS})_2$. Therefore, the acyclic nature of $\text{Ge}(\text{HMDS})_2$ and, consequently, its stronger π -accepting capacity (compared with those of the two NHGe ligands used in this work) also have to be claimed as responsible for its different reactivity.

CONCLUDING REMARKS

This paper reports the syntheses of the first ruthenium complexes containing diaminogermylene ligands (**2**, **3**), one of them (**2**) also being the first transition metal cluster complex containing an NHM ligand of any kind. The results described also demonstrate that the derivative chemistry of $[\text{Ru}_3(\text{CO})_{12}]$ and diaminogermylenes depends upon the volume and the cyclic or acyclic nature of the latter. This chemistry is very different from that known for $[\text{Ru}_3(\text{CO})_{12}]$ and NHCs.

EXPERIMENTAL SECTION

General Procedures. Solvents were dried over sodium diphenyl ketyl and distilled under nitrogen before use. The reactions were carried out under nitrogen, using Schlenk-vacuum line techniques, and were

Table 1. Crystal, Measurement, and Refinement Data for $2 \cdot (\text{C}_7\text{H}_8)_2$ and **3**

	$2 \cdot (\text{C}_7\text{H}_8)_2$	3
formula	$\text{C}_{57}\text{H}_{78}\text{Ge}_3\text{N}_6\text{O}_9 \cdot \text{Ru}_3 \cdot (\text{C}_7\text{H}_8)_2$	$\text{C}_{27}\text{H}_{72}\text{Ge}_2\text{N}_4\text{O}_3\text{RuSi}_8$
fw	1696.50	971.86
cryst syst	triclinic	orthorhombic
space group	$P\bar{1}$	$\text{Pbc}2_1$
<i>a</i> , Å	13.7916(3)	14.7846(1)
<i>b</i> , Å	13.8993(5)	21.2709(2)
<i>c</i> , Å	21.8561(5)	31.7140(3)
α, β, γ (deg)	74.702(2), 83.320(2), 76.698(2)	90, 90, 90
<i>V</i> , Å ³	3925.9(2)	9973.47(1)
<i>Z</i>	2	8
<i>F</i> (000)	1724	4048
<i>D</i> _{calcd} g cm ⁻³	1.435	1.29
μ (Cu K α), mm ⁻¹	6.281	5.913
cryst size, mm	0.22 × 0.18 × 0.06	0.64 × 0.49 × 0.38
<i>T</i> , K	293(2)	100(2)
θ range, deg	3.3 to 70.00	2.8 to 60.00
min./max. <i>h, k, l</i>	−16/16, −16/16, 0/26	0/16, 0/23, 31/35
no. collected reflns	14694	12284
no. unique reflns	14694	12284
no. reflns with <i>I</i> > 2 σ (<i>I</i>)	11882	12004
no. params/restraints	825/9	859/1
GOF on <i>F</i> ²	1.016	1.067
<i>R</i> ₁ (on <i>F</i> , <i>I</i> > 2 σ (<i>I</i>))	0.0450	0.061
<i>wR</i> ₂ (on <i>F</i> ² , all data)	0.1291	0.154
min./max. $\Delta\rho$, e Å ⁻³	−1.092/1.398	−1.394/1.307

routinely monitored by solution IR spectroscopy (carbonyl stretching region). The germylenes $\text{Ge}(\text{N}^t\text{Bu})_2\text{C}_2\text{H}_2$,^{2e} $\text{Ge}(\text{NCH}_2\text{CMe}_3)_2\text{C}_6\text{H}_4$,¹⁵ and $\text{Ge}(\text{HMDS})_2$ ¹⁹ were prepared following published procedures. All remaining reagents were purchased from commercial sources. All reaction products were vacuum-dried for several hours prior to being weighed and analyzed. IR spectra were recorded in solution on a Perkin-Elmer Paragon 1000 FT spectrophotometer. NMR spectra were run on a Bruker DPX-300 instrument, using as internal standards the residual protic solvent resonances [$\delta(\text{C}_6\text{D}_5\text{CHD}_2) = 2.08$; $\delta(\text{CHCl}_3) = 7.26$] for ^1H and the solvent $\text{C}_6\text{D}_5\text{CD}_3$ ($\delta = 20.43$) or CDCl_3 ($\delta = 77.16$) resonances for ^{13}C . Microanalyses were obtained from the University of Oviedo Microanalytical Service. FAB mass spectra were obtained from the University of A Coruña Mass Spectrometric Service; data given refer to the most abundant molecular ion isotopomer.

$[\text{Ru}_3\{\mu\text{-Ge}(\text{NCH}_2\text{CMe}_3)_2\text{C}_6\text{H}_4\}_3(\text{CO})_9]$ (**2**). $\text{Ge}(\text{NCH}_2\text{CMe}_3)_2\text{C}_6\text{H}_4$ (90 mg, 0.28 mmol) was added to a suspension of $[\text{Ru}_3(\text{CO})_{12}]$ (50 mg, 0.08 mmol) in 10 mL of toluene, and the mixture was heated at 100 °C for 2 h. IR and ^1H NMR analyses of aliquots of the crude reaction solution showed the quantitative formation of complex **2**. The solvent was removed under reduced pressure, and the solid residue was washed with hexane (2 × 5 mL) and vacuum-dried to give compound **2** as a dark blue solid (85 mg, 70%). Slow evaporation of a concentrated toluene/hexane solution deposited X-ray-quality crystals of $2 \cdot (\text{C}_7\text{H}_8)_2$. Anal. Calcd for $\text{C}_{57}\text{H}_{78}\text{Ge}_3\text{N}_6\text{O}_9\text{Ru}_3$ (1512.32): C, 45.27; H, 5.20; N, 5.56. Found: C, 45.32; H, 5.37; N, 5.40. (+)-FAB MS: *m/z* 1512 [M^+]. IR (toluene, cm⁻¹): ν_{CO} 2045 (s), 2009 (vs), 1999 (m). ^1H NMR (300.1 MHz, 293 K, toluene-*d*₈, ppm): δ 6.93–6.87 (m, 1 H, CH), 6.83–6.77 (m, 1 H, CH), 3.93 (d, *J* = 14.6 Hz, 1 H, CHH), 3.38 (d, *J* = 14.6 Hz, 1 H,

(CHH), 0.96 (s, br, 9 H, CMe₃). ¹³C{¹H} NMR (75.5 MHz, 293 K, toluene-*d*₈, ppm): δ 202.2 (2 CO), 196.1 (1 CO), 144.8 (2 C, C of C₆H₄), 116.4 (2 CH of C₆H₄), 108.9 (2 CH of C₆H₄), 54.8 (2 CH₂), 36.1 (2 CMe₃), 29.1 (3 Me).

[Ru{Ge(HMDS)₂}(CO)₃] (**3**). Ge(HMDS)₂ (189 mg, 0.48 mmol) was added to a suspension of [Ru₃(CO)₁₂] (50 mg, 0.08 mmol) in 20 mL of dry toluene, and the mixture was heated at 100 °C for 1 h. The solvent was removed under reduced pressure to give compound **3** as an orange solid (230 g, 99%). X-ray-quality crystals were obtained by cooling down to -20 °C a concentrated toluene solution. IR (CH₂-Cl₂, cm⁻¹): ν_{CO} 2085 (w, br), 2031 (m, br), 1974 (s, br). ¹H NMR (300.1 MHz, 293 K, CDCl₃, ppm): 0.36 (s, 24 Me). ¹³C{¹H} NMR (75.5 MHz, 293 K, CDCl₃, ppm): 208.2 (3 CO), 6.2 (24 Me). All attempts to obtain accurate analytical data on complex **3** were unsuccessful, possibly due to its highly air-sensitive nature.

X-Ray Diffraction Analyses. Crystals of 2·(C₇H₈)₂ and **3** were analyzed by X-ray diffraction methods. A selection of crystal, measurement, and refinement data is given in Table 1. Diffraction data were collected on an Oxford Diffraction Xcalibur Nova single crystal diffractometer, using Cu Kα radiation. An empirical absorption correction was applied using XABS2.²⁴ The structures were solved by direct methods using the program SIR-97.²⁵ Isotropic and full matrix anisotropic least-squares refinements were carried out using SHELXL.²⁶ All non-H atoms were refined anisotropically. Some C atoms of the toluene solvent molecules of 2·(C₇H₈)₂, which presented high anisotropic displacement parameters due to some local disorder, were refined applying restraints on their positional and thermal parameters. All hydrogen atoms were set in calculated positions and refined riding on their parent atoms. The molecular plots were made with the PLATON program package.²⁷ The WINGX program system²⁸ was used throughout the structure determinations. CCDC deposition numbers: 824261 (2·(C₇H₈)₂) and 824262 (**3**).

■ ASSOCIATED CONTENT

S Supporting Information. Crystallographic data in CIF format and figures showing the ¹H and ¹³C{¹H} NMR, IR, and FAB MS spectra of compounds **2** and **3**. This material is available free of charge via the Internet at <http://pubs.acs.org>.

■ AUTHOR INFORMATION

Corresponding Author

*E-mail: jac@uniovi.es, pga@uniovi.es.

■ ACKNOWLEDGMENT

This work has been supported by the Spanish MICINN (projects CTQ2010-14933 and DELACIERVA-09-05) and the European Union Marie Curie actions (project FP7-2010-RG-268329) and FEDER grants.

■ REFERENCES

- (1) For recent reviews on stable NHMs, see: (a) Asay, M.; Jones, C.; Driess, M. *Chem. Rev.* **2011**, *111*, 354. (b) Mizuhata, Y.; Sasamori, T.; Tokitoh, N. *Chem. Rev.* **2009**, *109*, 3479. (c) Nagendran, S.; Roesky, H. W. *Organometallics* **2008**, *27*, 457. (d) Zabula, A. V.; Hahn, F. E. *Eur. J. Inorg. Chem.* **2008**, 5165. (e) Haaf, M.; Schmedake, T. A.; West, R. *Acc. Chem. Res.* **2000**, *33*, 704.
- (2) For representative syntheses of stable NHMs, see: (a) Schuefler, C. D.; Zuckerman, C. D. *J. Am. Chem. Soc.* **1974**, *96*, 7160. (b) Veith, M. *Angew. Chem., Int. Ed.* **1975**, *14*, 263. (c) Pfeiffer, J.; Maringgele, W.; Noltemeyer, M.; Meller, A. *Chem. Ber.* **1989**, *122*, 245. (d) Pfeiffer, J.; Noltemeyer, M.; Meller, A. *Z. Anorg. Allg. Chem.* **1989**, *572*, 145. (e)

Herrmann, W. A.; Denk, M.; Behm, J.; Scherer, W.; Klingan, F.-R.; Bock, H.; Solouki, B.; Wagner, M. *Angew. Chem., Int. Ed.* **1992**, *31*, 1485. (f) Denk, M.; Lennon, R.; Hayashi, R.; West, R.; Belyakov, A. V.; Verne, H. P.; Haaland, A.; Wagner, M.; Metzler, N. *J. Am. Chem. Soc.* **1994**, *116*, 2691. (g) Gerhrus, B.; Hitchcock, P. B.; Lappert, M. F. *J. Chem. Soc., Dalton Trans.* **2000**, 3094. (h) Gans-Eichler, T.; Gudat, D.; Nieger, M. *Angew. Chem., Int. Ed.* **2002**, *41*, 1888. (i) Hahn, F. E.; Heitmann, D.; Pape, T. *Eur. J. Inorg. Chem.* **2008**, 1039.

(3) Arduengo, A. J., III; Harlow, R. L.; Kline, M. *J. Am. Chem. Soc.* **1991**, *113*, 361.

(4) For reviews on NHMs as ligands in transition metal complexes, see: (a) Kühn, O. *Coord. Chem. Rev.* **2004**, *248*, 411. (b) Saur, I.; Rima, G.; Miqueu, K.; Gornitzka, H.; Barrau, J. *J. Organomet. Chem.* **2003**, *672*, 77. (c) Veith, M. *Angew. Chem., Int. Ed.* **1987**, *26*, 1. (d) Refs 1d and 1e.

(5) For recent examples of NHMs as ligands in transition metal complexes, see: (a) Mansell, S. M.; Herber, R. H.; Nowik, I.; Ross, D. H.; Russell, C. A.; Wass, D. F. *Inorg. Chem.* **2011**, *50*, 2252. (b) Cade, I. A.; Hill, A. F.; Kämpfe, A.; Wagler, J. *Organometallics* **2010**, *29*, 4012. (c) Ullah, F.; Kühn, O.; Bajor, G.; Veszpremi, T.; Jones, P. G.; Heinicke, J. *Eur. J. Inorg. Chem.* **2009**, 221. (d) Zabula, A. V.; Pape, T.; Hepp, A.; Hahn, F. E. *Organometallics* **2008**, *27*, 2756. (e) Zabula, A. V.; Hahn, F. E.; Pape, T.; Hepp, A. *Organometallics* **2007**, *26*, 1972. (f) York, J. T.; Young, V. G., Jr.; Tolman, W. B. *Inorg. Chem.* **2006**, *45*, 4191. (g) Neumann, E.; Pfaltz, A. *Organometallics* **2005**, *24*, 2008. (h) Kühn, O.; Lönnecke, P.; Heinicke, J. *Inorg. Chem.* **2003**, *42*, 2836.

(6) For an excellent review on the chemistry of cyclic carbenes and related species that cites all review articles and books on NHCs published since 2007 and some earlier ones, see: Melaimi, M.; Solei-havouip, M.; Bertrand, G. *Angew. Chem., Int. Ed.* **2010**, *49*, 8810.

(7) For catalytic applications of transition metal NHC complexes, see: (a) Díez-González, S.; Marion, N.; Nolan, S. P. *Chem. Rev.* **2009**, *109*, 3612. (b) Samojłowicz, C.; Bieniek, M.; Grela, K. *Chem. Rev.* **2009**, *109*, 3708. (c) Glorius, F. A. *Top. Organomet. Chem.* **2007**, *21*, 1. (d) Nolan, S. P. *N-Heterocyclic Carbenes in Synthesis*; Wiley-VCH: Weinheim, Germany, 2006.

(8) (a) Cabeza, J. A.; del Río, I.; Pérez-Carreño, E.; Pruneda, V. *Organometallics* **2011**, *30*, 1148. (b) Cabeza, J. A.; del Río, I.; Fernández-Colinas, J. M.; Pérez-Carreño, E.; Sánchez-Vega, M. G.; Vázquez-García, D. *Organometallics* **2010**, *29*, 3828. (c) Cabeza, J. A.; del Río, I.; Fernández-Colinas, J. M.; Pérez-Carreño, E.; Sánchez-Vega, M. G.; Vázquez-García, D. *Organometallics* **2010**, *29*, 3828. (d) Cabeza, J. A.; del Río, I.; Pérez-Carreño, E.; Sánchez-Vega, M. G.; Vázquez-García, D. *Organometallics* **2010**, *29*, 4464. (e) Cabeza, J. A.; del Río, I.; Fernández-Colinas, J. M.; Pérez-Carreño, E.; Sánchez-Vega, M. G.; Vázquez-García, D. *Organometallics* **2009**, *28*, 1832. (f) Cabeza, J. A.; del Río, I.; Pérez-Carreño, E.; Sánchez-Vega, M. G.; Vázquez-García, D. *Angew. Chem., Int. Ed.* **2009**, *48*, 555. (g) Cabeza, J. A.; del Río, I.; Miguel, D.; Pérez-Carreño, E.; Sánchez-Vega, M. G. *Organometallics* **2008**, *27*, 211. (h) Critall, M. R.; Ellul, C. E.; Mahon, M. F.; Saker, O.; Whittlesey, M. K. *Dalton Trans.* **2008**, 4209. (i) Cooke, C. E.; Jennings, M. C.; Katz, M. J.; Pomeroy, R. K.; Clyburne, J. A. C. *Organometallics* **2008**, *27*, 5777. (j) Ellul, C. E.; Mahon, M. F.; Saker, O.; Whittlesey, M. K. *Angew. Chem., Int. Ed.* **2007**, *46*, 6343. (k) Cabeza, J. A.; da Silva, I.; del Río, I.; Sánchez-Vega, M. G. *Dalton Trans.* **2006**, 3966.

(9) (a) Bruce, M. I.; Cole, M. L.; Fung, R. S. C.; Forsyth, C. M.; Hilder, M.; Junk, P. C.; Konstas, K. *Dalton Trans.* **2008**, 4118. (b) Ellul, C. E.; Saker, O.; Mahon, M. F.; Apperley, D. C.; Whittlesey, M. K. *Organometallics* **2008**, *27*, 100.

(10) (a) Cabeza, J. A.; del Río, I.; Miguel, D.; Sánchez-Vega, M. G. *Chem. Commun.* **2005**, 3956. (b) Cabeza, J. A.; del Río, I.; Miguel, D.; Pérez-Carreño, E.; Sánchez-Vega, M. G. *Dalton Trans.* **2008**, 1937. (c) Cabeza, J. A.; del Río, I.; Miguel, D.; Sánchez-Vega, M. G. *Angew. Chem., Int. Ed.* **2008**, *47*, 1920. (d) Cabeza, J. A.; Pérez-Carreño, E. *Organometallics* **2008**, *27*, 4697.

(11) (a) Herrmann, W. A.; Harter, P.; Gstottmayr, C. W. K.; Bielert, F.; Seeboth, N.; Sirsch, P. *J. Organomet. Chem.* **2002**, *649*, 141. (b) Amoroso, D.; Haaf, M.; Yap, G. P. A.; West, R.; Fogg, D. E. *Organometallics* **2002**, *21*, 534. (c) Petri, S. H. A.; Eikenberg, D.; Neumann, B.; Stammeler, H.-G.;

- Jutzi, P. *Organometallics* **1999**, *18*, 2615. (d) Veith, M.; Muller, A.; Stahl, L.; Notzel, M.; Jarczyk, M.; Huch, V. *Inorg. Chem.* **1996**, *35*, 3848.
- (12) (a) Zhang, M.; Liu, X.; Shi, C.; Ren, C.; Ding, Y.; Roesky, H. W. *Z. Anorg. Allg. Chem.* **2008**, *634*, 1755. (b) Furstner, A.; Krause, H.; Lehmann, C. W. *Chem. Commun.* **2001**, 2372.
- (13) Schmedake, T. A.; Haaf, M.; Paradise, B. J.; Millevolte, A. J.; Powell, D. R.; West, R. J. *Organomet. Chem.* **2001**, *636*, 17.
- (14) Boehme, C.; Frenking, G. *Organometallics* **1998**, *17*, 5801.
- (15) Kühn, O.; Lönnecke, P.; Heinicke, J. *Polyhedron* **2001**, *20*, 2215.
- (16) (a) Veith, M.; Stahl, L.; Huch, V. *Organometallics* **1993**, *12*, 1914. (b) Veith, M.; Olbrich, M.; Notzel, M.; Klein, C.; Stahl, L.; Huch, V. Private communications to CCDC, codes KODNOH, KODNIB, and KODNEX, 1999. (c) Veith, M.; Olbrich, M.; Klein, C. Private communications to CCDC, codes KODPAV, and KODNUN, 1999.
- (17) Adams, R. D.; Captain, B.; Trufan, E. J. *Cluster Sci.* **2007**, *18*, 642.
- (18) Howard, J.; Knox, S. A. R.; Stone, F. G. A.; Woodward, P. *J. Chem. Soc., Chem. Commun.* **1970**, 1477.
- (19) (a) Harris, D. H.; Lappert, M. F. *J. Chem. Soc., Chem. Commun.* **1974**, 895. (b) Gynane, M. J. S.; Harris, D. H.; Lappert, M. F.; Power, P. P.; Rivière, P.; Rivière-Baudet, M. *J. Chem. Soc., Dalton. Trans.* **1977**, 2004.
- (20) (a) Cygan, Z. T.; Bender, J. E., IV; Litz, K. E.; Kampf, J. W.; Holl, M. M. B. *Organometallics* **2002**, *21*, 5373. (b) Litz, K. E.; Bender, J. E., IV; Kampf, J. W.; Holl, M. M. B. *Angew. Chem., Int. Ed.* **1997**, *36*, 496. (c) Litz, K. E.; Henderson, K.; Gourley, R. W.; Holl, M. M. B. *Organometallics* **1995**, *14*, 5008. (d) Litz, K. E.; Holl, M. M. B.; Kampf, J. W.; Carpenter, G. B. *Inorg. Chem.* **1998**, *37*, 6461. (e) Anandhi, U.; Sharp, P. R. *Inorg. Chim. Acta* **2006**, *359*, 3521. (f) Cygan, Z. T.; Kampf, J. W.; Holl, M. M. B. *Inorg. Chem.* **2003**, *42*, 7219. (g) Litz, K. E.; Kampf, J. W.; Holl, M. M. B. *J. Am. Chem. Soc.* **1998**, *120*, 7484. (h) Hawkins, S. M.; Hitchcock, P. B.; Lappert, M. F.; Rai, A. K. *Chem. Commun.* **1986**, 1689. (i) Litz, K. E.; Bender, J. E.; Sweeder, R. D.; Holl, M. M. B.; Kampf, J. W. *Organometallics* **2000**, *19*, 1186.
- (21) For representative examples on stable heavier acyclic group-14 metal diamino ylidenes, see: (a) Chorley, R. W.; Hitchcock, P. B.; Lappert, M. F.; Leung, W. P.; Power, P. P.; Olmstead, M. M. *Inorg. Chim. Acta* **1992**, *200*, 203. (b) Schnepf, A. *Z. Anorg. Allg. Chem.* **2006**, *632*, 935. (c) Veith, M.; Rammo, A. *Z. Anorg. Allg. Chem.* **2001**, *627*, 662. (d) Meller, A.; Ossig, G.; Maringgele, W.; Noltemeyer, M.; Stalke, D.; Herbstirmer, R.; Freitag, S.; Sheldrick, G. M. *Z. Naturforsch., B: Chem. Sci.* **1992**, *47*, 162. (e) Lappert, M. F.; Slade, M. J.; Atwood, J. L.; Zaworotko, M. J. *J. Chem. Soc., Chem. Commun.* **1980**, 621. (f) Riviere-Baudet, M.; Dahrouch, M.; Gornitzka, H. J. *Organomet. Chem.* **2000**, *595*, 153. (g) Hitchcock, P. B.; Lappert, M. F.; Thorne, A. J. *J. Chem. Soc., Chem. Commun.* **1990**, 1587. (h) Fjeldberg, T.; Hope, H.; Lappert, M. F.; Power, P. P.; Thorne, A. J. *J. Chem. Soc., Chem. Commun.* **1983**, 639. (i) Babcock, J. R.; Liable-Sands, L.; Rheingold, A. L.; Sita, L. R. *Organometallics* **1999**, *18*, 4437. (j) Westerhausen, M.; Gruel, J.; Hausen, H. D.; Schwarz, W. Z. *Anorg. Allg. Chem.* **1996**, *622*, 1295. (k) Tang, Y. J.; Felix, A. M.; Zakharov, L. N.; Rheingold, A. L.; Kemp, R. A. *Inorg. Chem.* **2004**, *43*, 7239. (l) Tsutsui, S.; Sakamoto, K.; Kira, M. *J. Am. Chem. Soc.* **1998**, *120*, 9955. (m) Lee, G. H.; West, R.; Muller, T. J. *J. Am. Chem. Soc.* **2003**, *125*, 8114.
- (22) (a) Lappert, M.; Protchenko, A.; Power, P.; Seeber, A. *Metal Amide Chemistry*; Wiley-VCH: Weinheim, Germany, 2008; Chapter 9. (b) Lappert, M. F.; Rowe, R. S. *Coord. Chem. Rev.* **1990**, *100*, 267.
- (23) Only two other crystallographically characterized ruthenium complexes containing three-coordinate germanium-based ligands appear in the CCDC CSD (version 5.32; updated Nov 2010): (a) Hayes, P. G.; Waterman, R.; Glaser, P. B.; Tilley, T. D. *Organometallics* **2009**, *28*, 5082. (b) Takaoka, A.; Mendiratta, A.; Peters, J. C. *Organometallics* **2009**, *28*, 3744.
- (24) Parkin, S.; Moezzi, B.; Hope, H. *J. Appl. Crystallogr.* **1995**, *28*, 53.
- (25) Giacobozzo, C. *J. Appl. Crystallogr.* **1999**, *32*, 115.
- (26) Sheldrick, G. M. *Acta Crystallogr.* **2008**, *A64*, 112.
- (27) Spek, A. L. *PLATON: A Multipurpose Crystallographic Tool*, version 1.15; University of Utrecht: Utrecht, The Netherlands, 2008.
- (28) Farrugia, L. J. *J. Appl. Crystallogr.* **1999**, *32*, 837.

SUPPORTING INFORMATION

Reactivity of Diaminogermynes with Ruthenium Carbonyl: Ru₃Ge₃ and RuGe₂ Derivatives

Javier A. Cabeza,* Pablo García-Álvarez,* and Diego Polo

Departamento de Química Orgánica e Inorgánica-IUQOEM, Universidad de Oviedo-CSIC, E-33071-Oviedo, Spain

Contents

Figure S1. ¹ H NMR spectrum of 2	2
Figure S2. ¹³ C{ ¹ H} NMR spectrum of 2	3
Figures S3-S4. IR spectra of 2	4
Figure S5. (+)-FAB MS spectrum of 2	5
Figure S6. ¹ H NMR spectrum of 3	6
Figure S7. ¹³ C{ ¹ H} NMR spectrum of 3	7
Figures S8-S9. IR spectra of 3	8

Figure S1. ^1H NMR spectrum of $[\text{Ru}_3\{\mu\text{-Ge}(\text{NCH}_2\text{CMe}_3)_2\text{C}_6\text{H}_4\}_3(\text{CO})_9]$ (**2**) at 20 °C in toluene- d_8 .

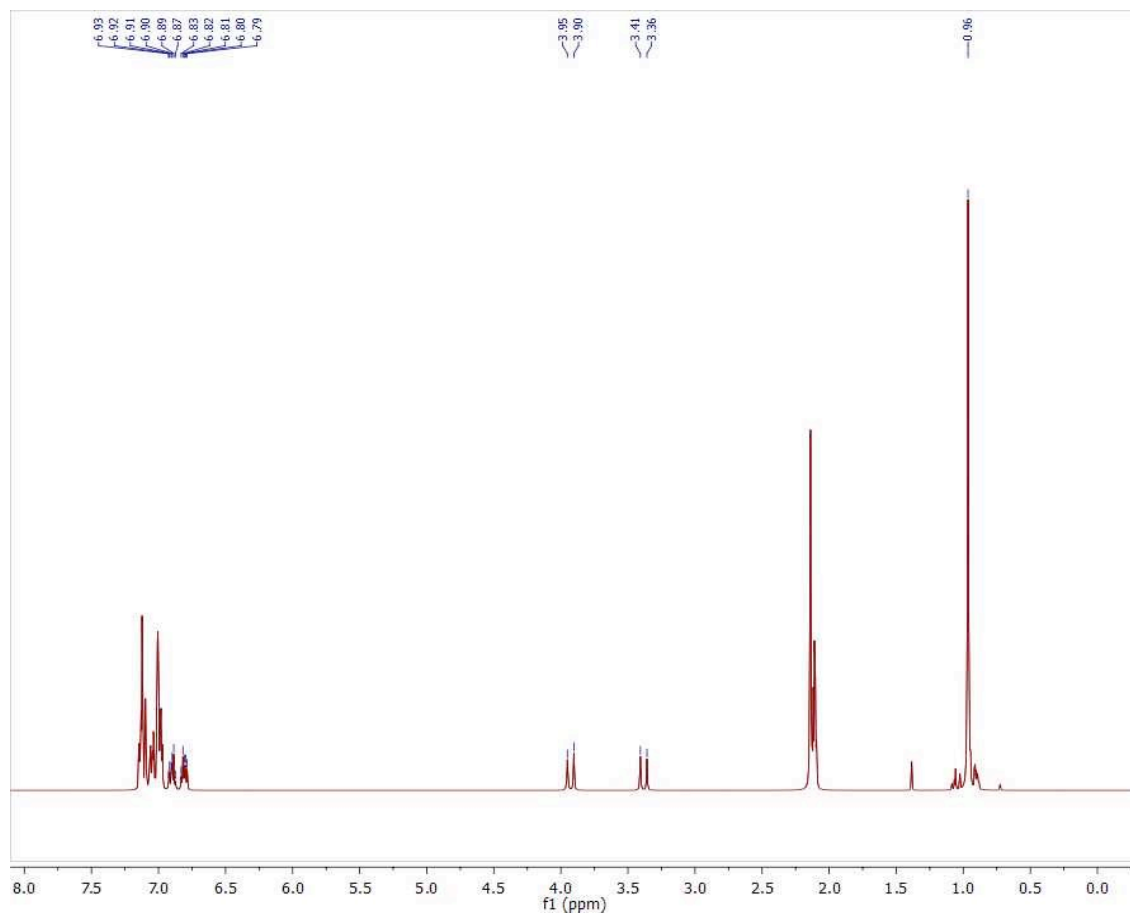


Figure S2. $^{13}\text{C}\{^1\text{H}\}$ NMR spectrum of $[\text{Ru}_3\{\mu\text{-Ge}(\text{NCH}_2\text{CMe}_3)_2\text{C}_6\text{H}_4\}_3(\text{CO})_9]$ (**2**) at 20 °C in toluene- d_8 .

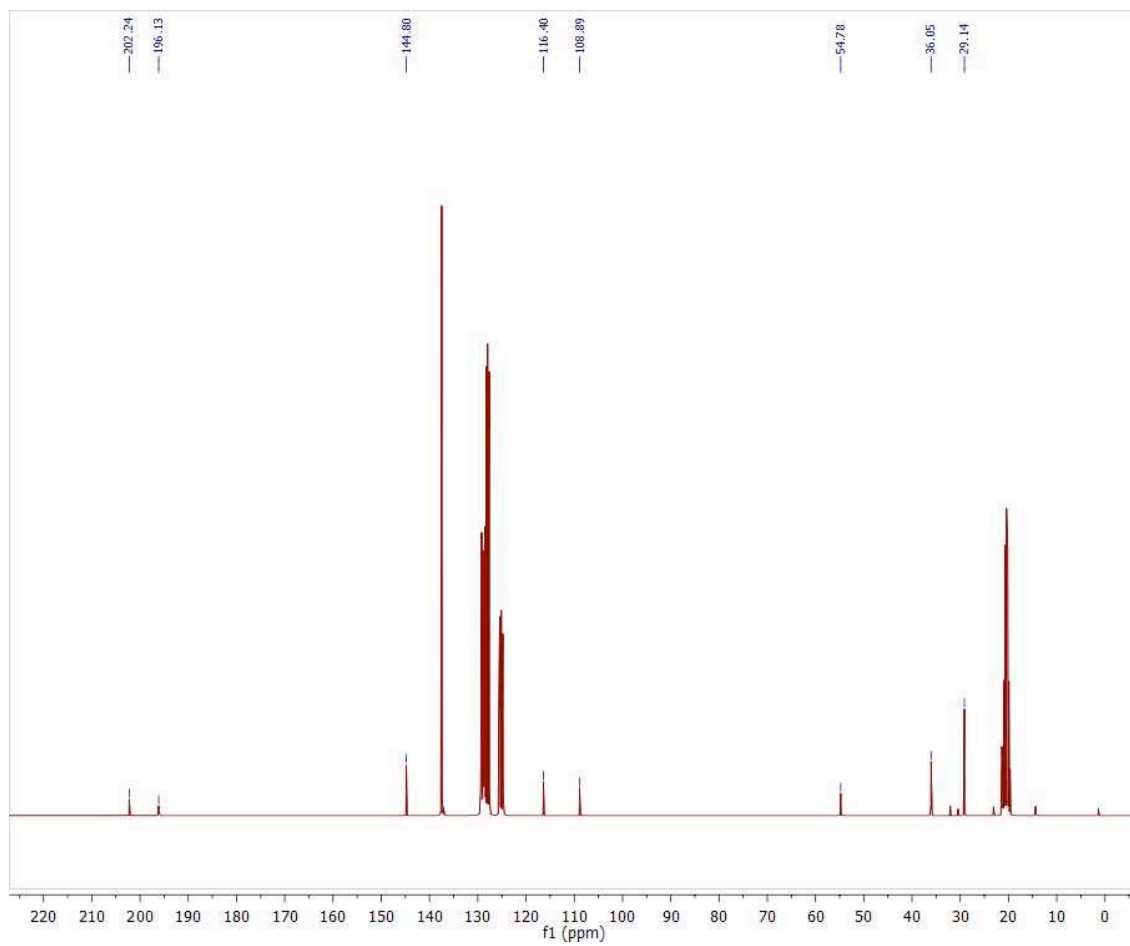


Figure S3. IR spectrum of the crude solution obtained from the reaction of $[\text{Ru}_3(\text{CO})_{12}]$ with 3.5 equivalents of $\text{Ge}(\text{NCH}_2\text{CMe}_3)_2\text{C}_6\text{H}_4$ after 2 h at 100 °C in toluene.

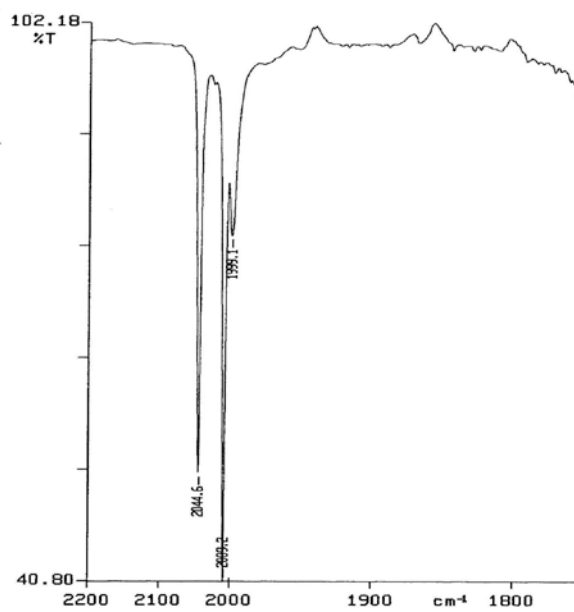


Figure S4. IR spectrum of isolated $[\text{Ru}_3\{\mu\text{-Ge}(\text{NCH}_2\text{CMe}_3)_2\text{C}_6\text{H}_4\}_3(\text{CO})_9]$ (**2**) in toluene.

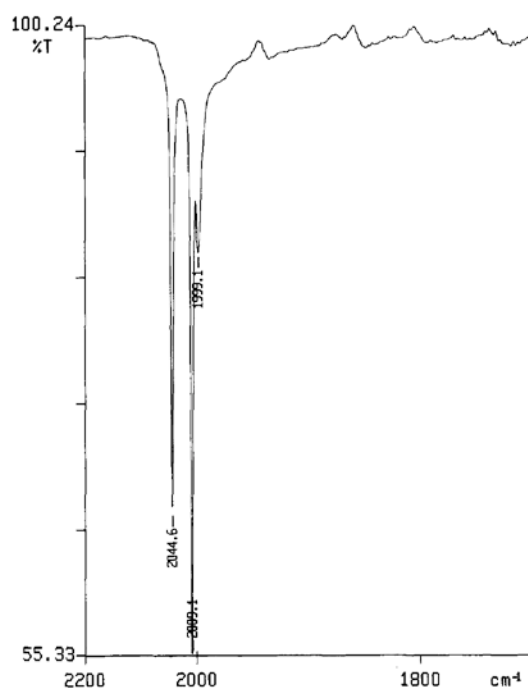


Figure S5. (+)-FAB MS spectrum of isolated $[\text{Ru}_3\{\mu\text{-Ge}(\text{NCH}_2\text{CMe}_3)_2\text{C}_6\text{H}_4\}_3(\text{CO})_9]$ (**2**) (top) and an amplification of the molecular ion region (bottom).

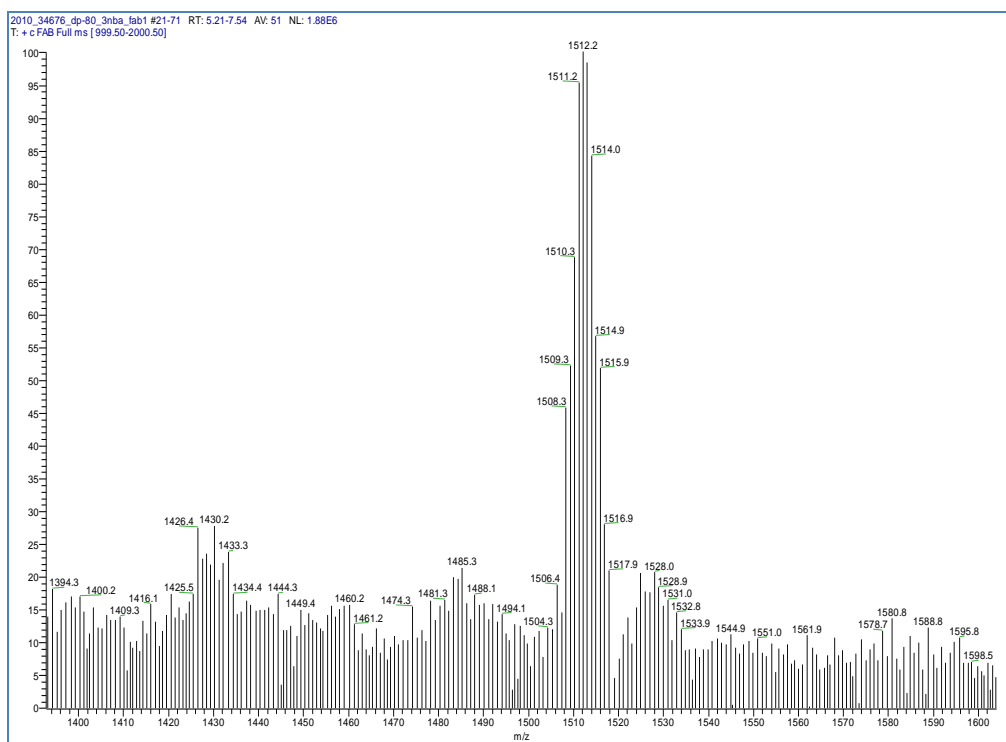
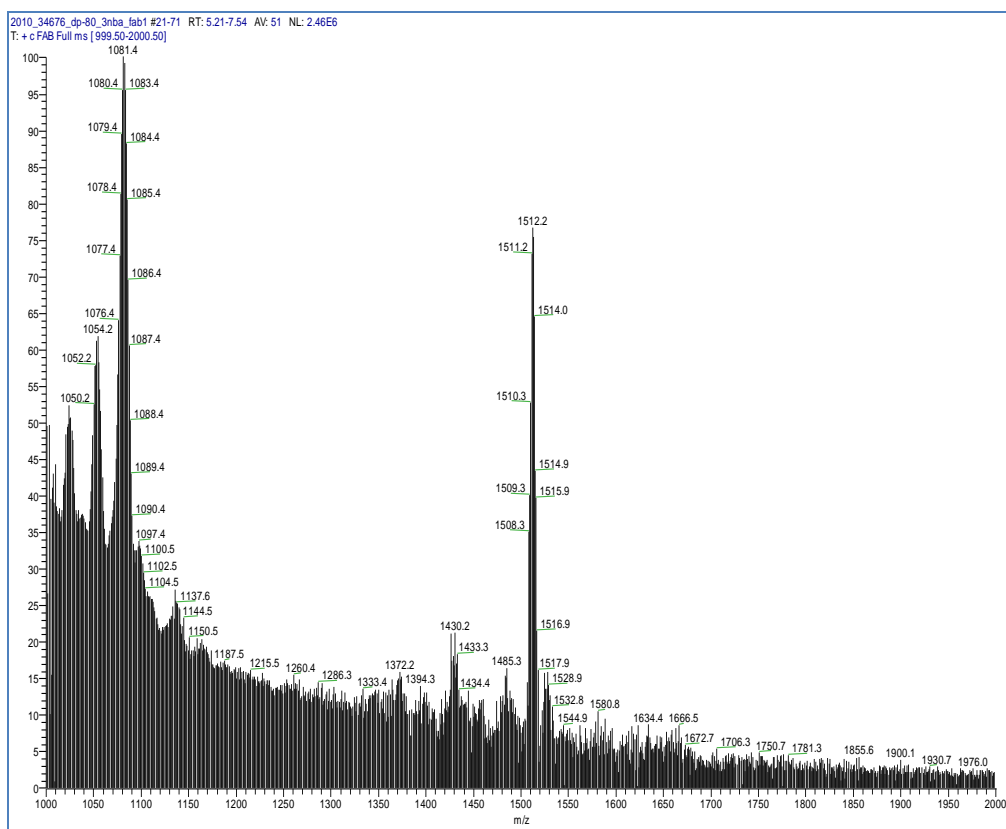


Figure S6. ^1H NMR spectrum of $[\text{Ru}\{\text{Ge}(\text{HMDS})_2\}_2(\text{CO})_3]$ (**3**) at 20 °C in CDCl_3 .

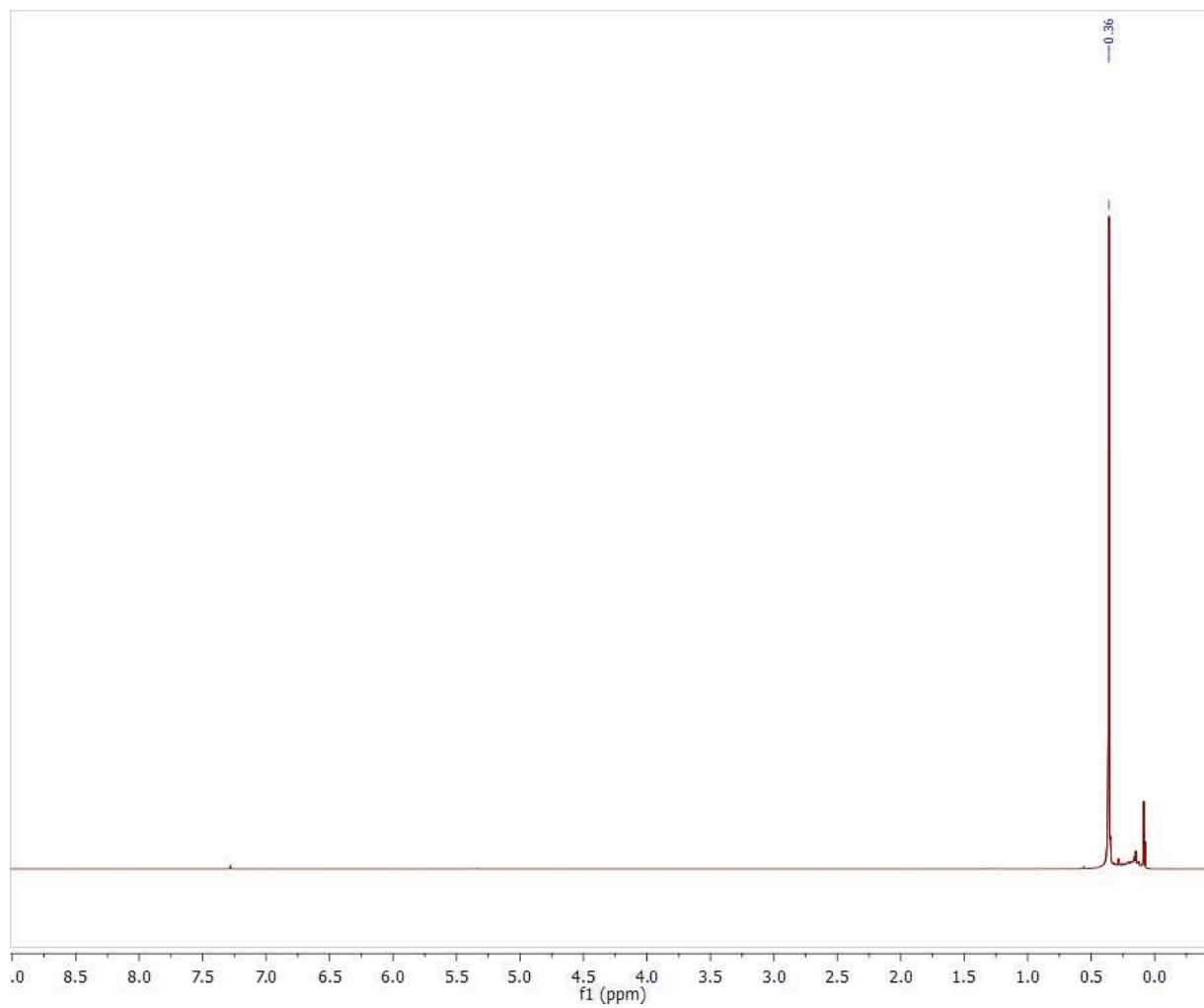


Figure S7. $^{13}\text{C}\{^1\text{H}\}$ NMR spectrum of $[\text{Ru}\{\text{Ge}(\text{HMDS})_2\}_2(\text{CO})_3]$ (**3**) at 20 °C in CDCl_3

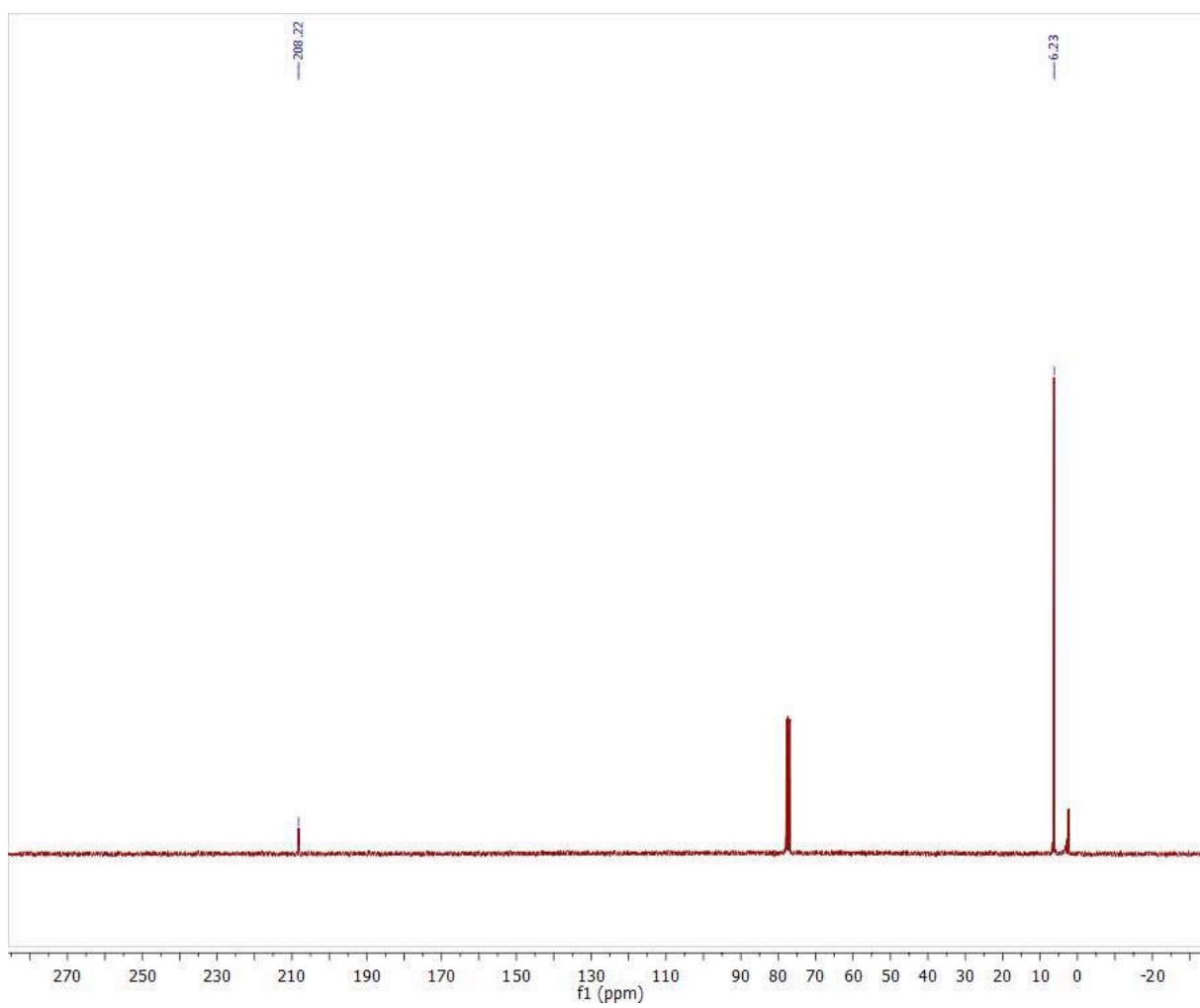


Figure S8. IR spectrum of the crude solution obtained from the reaction of $[\text{Ru}_3(\text{CO})_{12}]$ with 6 equivalents of $\text{Ge}(\text{HMDS})_2$ after 1 h at 100 °C in toluene.

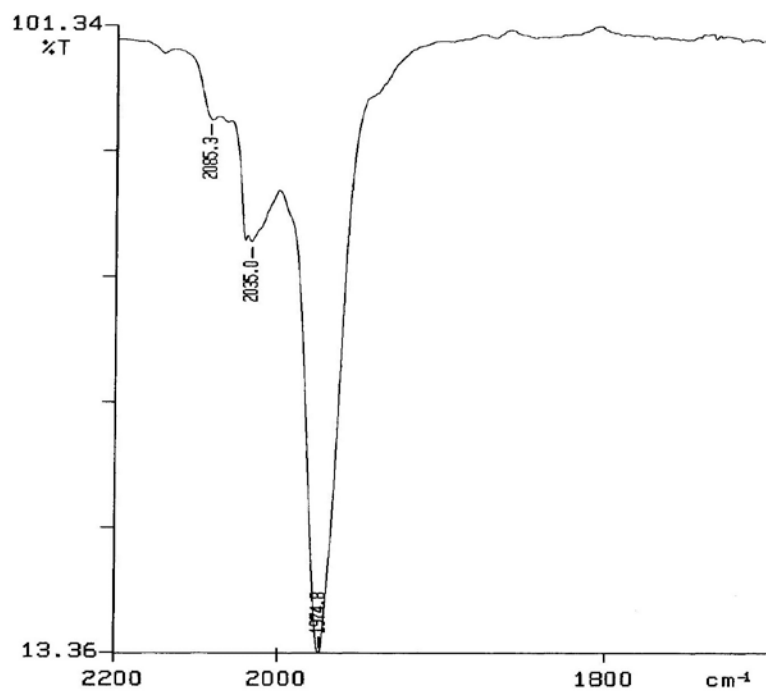
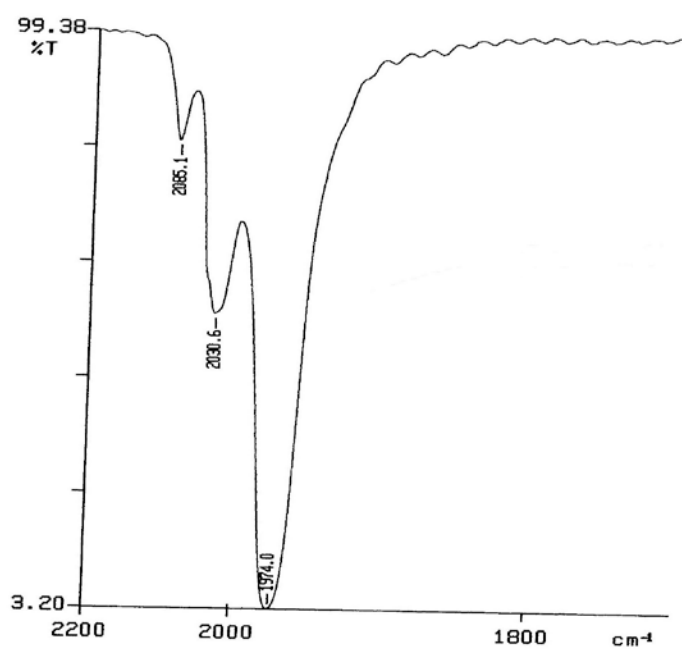


Figure S9. IR spectrum of isolated $[\text{Ru}\{\text{Ge}(\text{HMDS})_2\}_2(\text{CO})_3]$ (**3**) in CH_2Cl_2 .



Artículo II

“Synthesis of Mixed Tin-Ruthenium and Tin-Germanium-Ruthenium Carbonyl Clusters from $[Ru_3(CO)_12]$ and Diaminometalenes ($M = Sn, Ge$)”

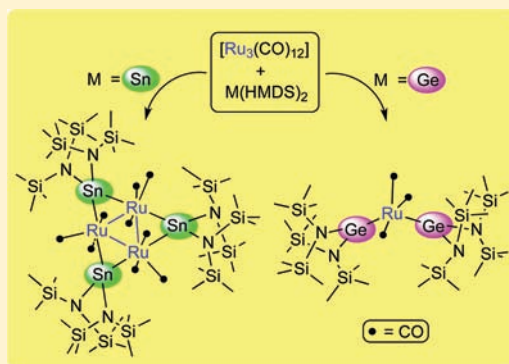
Synthesis of Mixed Tin–Ruthenium and Tin–Germanium–Ruthenium Carbonyl Clusters from $[\text{Ru}_3(\text{CO})_{12}]$ and Diaminometalenes ($\text{M} = \text{Sn}, \text{Ge}$)

Javier A. Cabeza,* Pablo García-Álvarez,* and Diego Polo

Departamento de Química Orgánica e Inorgánica-IUQOEM, Universidad de Oviedo-CSIC, E-33071 Oviedo, Spain

Supporting Information

ABSTRACT: Diaminostannylenes react with $[\text{Ru}_3(\text{CO})_{12}]$ without cluster fragmentation to give carbonyl substitution products regardless of the steric demand of the diaminostannylene reagent. Thus, the Sn_2Ru_3 clusters $[\text{Ru}_3\{\mu\text{-Sn}(\text{NCH}_2^t\text{Bu})_2\text{C}_6\text{H}_4\}_3(\text{CO})_9]$ (**4**) and $[\text{Ru}_3\{\mu\text{-Sn}(\text{HMDS})_2\}_3(\text{CO})_9]$ (**6**) [$\text{HMDS} = \text{N}(\text{SiMe}_3)_2$] have been prepared in good yields by treating $[\text{Ru}_3(\text{CO})_{12}]$ with an excess of the cyclic 1,3-bis(*neo*-pentyl)-2-stannabenzimidazol-2-ylidene and the acyclic and bulkier $\text{Sn}(\text{HMDS})_2$, respectively, in toluene at 110 °C. The use of smaller amounts of $\text{Sn}(\text{HMDS})_2$ (Sn/Ru_3 ratio = 2.5) in toluene at 80 °C afforded the Sn_2Ru_3 derivative $[\text{Ru}_3\{\mu\text{-Sn}(\text{HMDS})_2\}_2(\mu\text{-CO})(\text{CO})_9]$ (**5**). Compounds **5** and **6** represent the first structurally characterized diaminostannylene-ruthenium complexes. While a further treatment of **5** with $\text{Ge}(\text{HMDS})_2$ led to a mixture of uncharacterized compounds, a similar treatment with the sterically alleviated diaminogermylene $\text{Ge}(\text{NCH}_2^t\text{Bu})_2\text{C}_6\text{H}_4$ provided $[\text{Ru}_3\{\mu\text{-Sn}(\text{HMDS})_2\}_2\{\mu\text{-Ge}(\text{NCH}_2^t\text{Bu})_2\text{C}_6\text{H}_4\}(\text{CO})_9]$ (**7**), which is a unique example of Sn_2GeRu_3 cluster. All these reactions, coupled to a previous observation that $[\text{Ru}_3(\text{CO})_{12}]$ reacts with excess of $\text{Ge}(\text{HMDS})_2$ to give the mononuclear complex $[\text{Ru}\{\text{Ge}(\text{HMDS})_2\}_2(\text{CO})_3]$ but triruthenium products with less bulky diaminogermynes, indicate that, for reactions of $[\text{Ru}_3(\text{CO})_{12}]$ with diaminometalenes, both the volume of the diaminometalene and the size of its donor atom (Ge or Sn) are of key importance in determining the nuclearity of the final products.



INTRODUCTION

The transition-metal chemistry of heavier analogues of cyclic and acyclic diaminocarbene, that is, group-14 diaminometalenes $[\text{M}(\text{NR}_2)_2]$; $\text{M} = \text{Si}, \text{Ge}, \text{Sn},$ or Pb], has been slowly but increasingly developed^{1–4} since the seminal discovery by Lappert in 1974 of the first specimens of this family, $\text{M}(\text{HMDS})_2$ [$\text{M} = \text{Ge}, \text{Sn}, \text{Pb}$; $\text{HMDS} = \text{N}(\text{SiMe}_3)_2$].⁵ Quite a few cyclic diaminometalenes (or N-heterocyclic metalenes, NHM),⁶ which are the heavier analogues of N-heterocyclic carbene (NHC), were subsequently synthesized,⁶ even before the isolation of the first NHC in 1991.⁷ For example, stable N-heterocyclic stannylenes (NHSn) and germynes (NHGe) were described in 1974 by Schuefler and Zuckerman^{6a} and in 1989 by Meller et al.,^{6c} respectively. To date, the transition metal chemistry of group-14 diaminometalenes covers a wide range of metals,^{2–4} many reactivity studies,⁴ and a few catalytic applications.^{4d,k}

However, despite the early discovery of group-14 diaminometalenes, the current development of their coordination chemistry is far from the maturity achieved by the coordination chemistry of diaminocarbene.⁸ This can be attributed to three main factors: (a) although most diaminocarbene are very air- and temperature-sensitive, in many instances they do not need to be previously isolated to achieve the syntheses of their metal complexes (e.g., imidazol-2-ylidenes can be generated in situ

simple deprotonation of readily accessible imidazolium salts), while pure $\text{M}(\text{NR}_2)_2$ reagents are generally required to prepare their transition metal derivatives; (b) most diaminocarbene complexes⁸ are more robust and less air-sensitive than their heavier group-14 relatives;^{2–4} and (c) many NHC-metal complexes soon demonstrated to be excellent homogeneous catalysts for important organic chemistry reactions.⁹

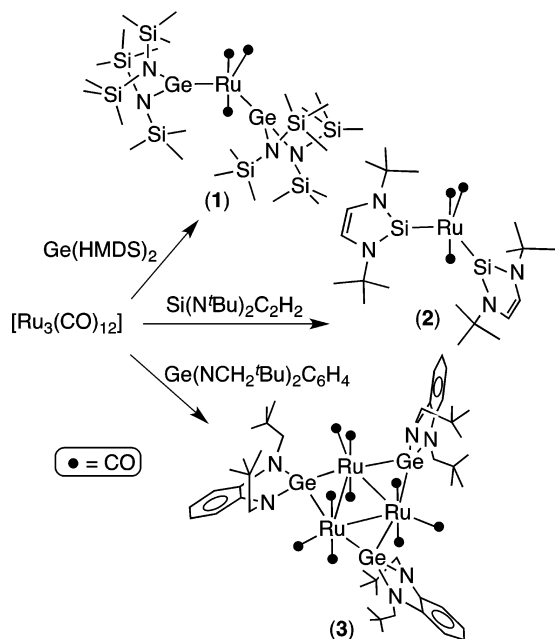
The different current state of the art of the coordination chemistry of NHC and $\text{M}(\text{NR}_2)_2$ ligands is even more noticeable in the field of transition metal carbonyl clusters. While a significant number of studies on the synthesis and reactivity of NHC derivatives of transition metal carbonyl clusters have been recently reported,^{10–12} analogous studies using $\text{M}(\text{NR}_2)_2$ ligands are, as far as we are aware, restricted to only two publications, one by West et al. in 2003^{3r} and the other by our group in 2011.^{2a} They describe that the reactions of ruthenium carbonyl with an excess of $\text{Ge}(\text{HMDS})_2$ or 1,3-bis(*tert*-butyl)-2-silaimidazol-2-ylidene give mononuclear ruthenium(0) derivatives of the type $[\text{RuL}_2(\text{CO})_3]$ (**1**: $\text{L} = \text{Ge}(\text{HMDS})_2$;^{2a} **2**: $\text{L} = \text{Si}(\text{N}^t\text{Bu})_2\text{C}_2\text{H}_2$ ^{3r}), whereas an analogous treatment with the sterically less demanding 1,3-bis(*neo*-pentyl)-2-germabenzimidazol-2-ylidene leads to the

Received: November 23, 2011

Published: January 11, 2012

trinuclear cluster complex $[\text{Ru}_3\{\mu\text{-Ge}(\text{NCH}_2\text{tBu})_2\text{C}_6\text{H}_4\}_3(\text{CO})_9]$ (**3**)^{2a} (Scheme 1). These results

Scheme 1. Previously Reported Reactions of $[\text{Ru}_3(\text{CO})_{12}]$ with $\text{Ge}(\text{HMDS})_2$, $\text{Si}(\text{N}^t\text{Bu})_2\text{C}_2\text{H}_2$, and $\text{Ge}(\text{NCH}_2\text{tBu})_2\text{C}_6\text{H}_4$



suggested that the volume of the diaminometalene reagent, (or, more precisely, the steric hindrance exerted by its N–R groups) is to be claimed as an important factor controlling the nuclearity the reaction products.

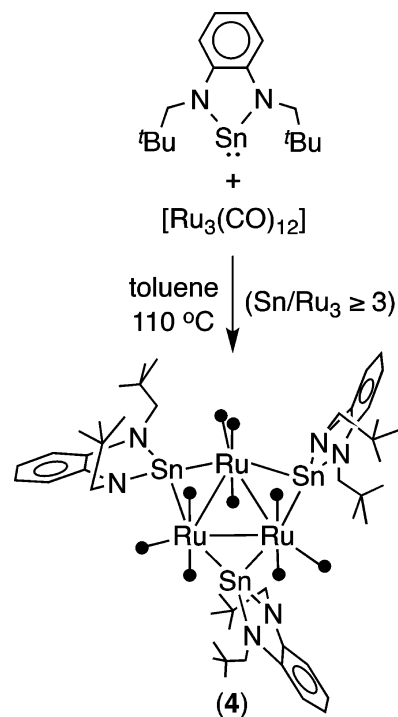
On the other hand, bimetallic tin–ruthenium cluster complexes have recently attracted great interest because of their use as precursors to bimetallic nanoparticles (by gentle thermolysis on high surface area mesoporous supports) that have been shown to be superior catalysts for hydrogenation reactions.^{13,14} There is also evidence that tin can assist in the binding of metallic nanoparticles to oxide supports when used in heterogeneous catalysis.¹⁵ Most of these bimetallic Sn–Ru complexes (and their Ge–Ru relatives) have been prepared by treating ruthenium carbonyl compounds with RSMPh_3 ,¹⁶ H_2MPh_2 ($\text{M} = \text{Sn}, \text{Ge}$).¹⁷

We now report the synthesis of novel tin–ruthenium carbonyl clusters using $[\text{Ru}_3(\text{CO})_{12}]$ and two diaminostannylenes of different steric demand as tin precursors. The herein described results, coupled to those of a previous work carried out using analogous diaminogermynes,^{2a} demonstrate that the nuclearity of the reaction products depends not only on the steric demand of the diaminometalene N–R arms but also on the nature of its donor atom (Sn or Ge). We also describe that the use of an appropriate combination of tin and germanium diaminometalenes has led to the synthesis of a unique Sn_2GeRu_3 carbonyl cluster.

RESULTS AND DISCUSSION

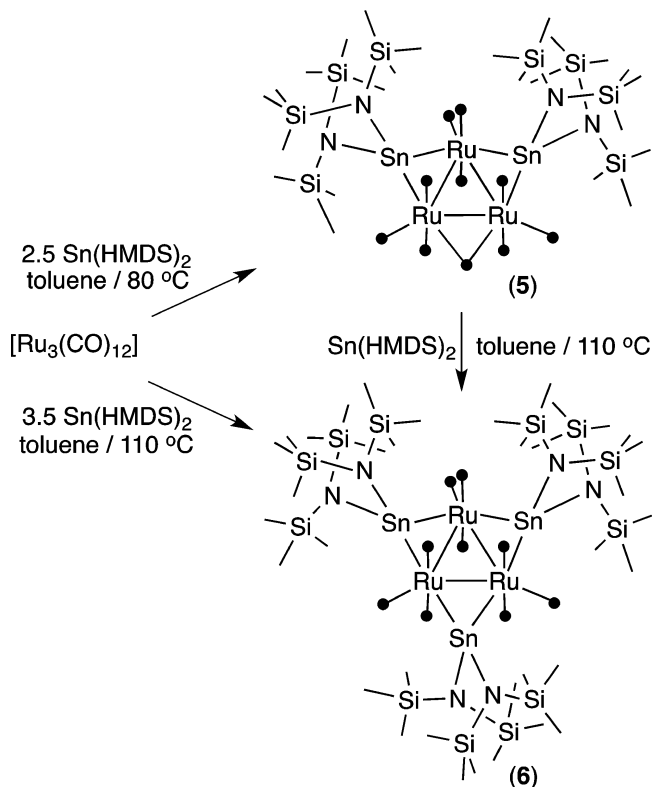
The treatment of $[\text{Ru}_3(\text{CO})_{12}]$ with the cyclic stannylene 1,3-bis(*neo*-pentyl)-2-stannabenzimidazol-2-ylidene, using Sn/Ru_3 ratios ≥ 3 in toluene at 110 °C, led to the trisubstituted derivative $[\text{Ru}_3\{\mu\text{-Sn}(\text{NCH}_2\text{CMe}_3)_2\text{C}_6\text{H}_4\}_3(\text{CO})_9]$ (**4**) in quantitative spectroscopic yield (Scheme 2). Sn/Ru_3 ratios < 3 afforded mixtures of complexes that contained compound **4**

Scheme 2. Synthesis of Compound 4



(IR and NMR analyses) but they could not be separated because they decomposed on chromatographic supports. Compound **4** itself is very air-sensitive and decomposes quickly when it is dissolved in wet solvents. Although no crystals of **4** suitable for an X-ray diffraction analysis were obtained, its NMR and IR spectra (ν_{CO} region) are analogous to those of the germylene derivative **3** (Scheme 1), whose structure has been crystallographically determined,^{2a} suggesting that both compounds have a common molecular structure. Therefore, when the steric demand of the N–R arms of germanium and tin diaminometalenes is not high, as is the case for the *neo*-pentyl groups of 1,3-bis(*neo*-pentyl)-2-metalabenzimidazol-2-ylidenes ($\text{M} = \text{Ge}, \text{Sn}$), both reagents exhibit an analogous reactivity with $[\text{Ru}_3(\text{CO})_{12}]$, leading to closely related substitution products without cluster fragmentation. The instability of **4** (in comparison to that of its germanium analogue **3**) is attributed to the higher tendency of Sn–N bonds to undergo hydrolysis, in accordance with the fact that Sn–N bonds are more polarized than Ge–N bonds.¹⁸

In the case of the bulky stannylene $\text{Sn}(\text{HMDS})_2$, its reactions with $[\text{Ru}_3(\text{CO})_{12}]$ sequentially afforded the di- and trisubstituted cluster derivatives $[\text{Ru}_3\{\mu\text{-Sn}(\text{HMDS})_2\}_2(\mu\text{-CO})(\text{CO})_9]$ (**5**) and $[\text{Ru}_3\{\mu\text{-Sn}(\text{HMDS})_2\}_3(\text{CO})_9]$ (**6**) (Scheme 3). In toluene at 110 °C and using Sn/Ru_3 ratios ≥ 3 , all reactions gave the trisubstituted cluster **6** in quantitative spectroscopic yields (NMR and IR analyses of the crude reaction solutions). A transitory intermediate species was detected when the reacting solutions were monitored by IR spectroscopy. No evolution to any other product was observed when **6** was treated with a large excess of $\text{Sn}(\text{HMDS})_2$ in toluene at reflux temperature. This observation contrasts with the fact that the related germylene $\text{Ge}(\text{HMDS})_2$ leads to a monoruthenium(0) complex when it reacts with $[\text{Ru}_3(\text{CO})_{12}]$ under analogous reaction conditions (Scheme 1).^{2a} In an attempt to trap intermediate species, $[\text{Ru}_3(\text{CO})_{12}]$ was treated with 2.5 equiv of $\text{Sn}(\text{HMDS})_2$ in toluene at 80 °C. This

Scheme 3. Reactivity of $[\text{Ru}_3(\text{CO})_{12}]$ with $\text{Sn}(\text{HMDS})_2$ 

reaction allowed the isolation of the Sn_2Ru_3 cluster **5** in good yield. As expected, **5** led to **6** when it was heated with $\text{Sn}(\text{HMDS})_2$ in refluxing toluene.

The molecular structure of compound **5** has been determined by X-ray diffraction crystallography (Figure 1,

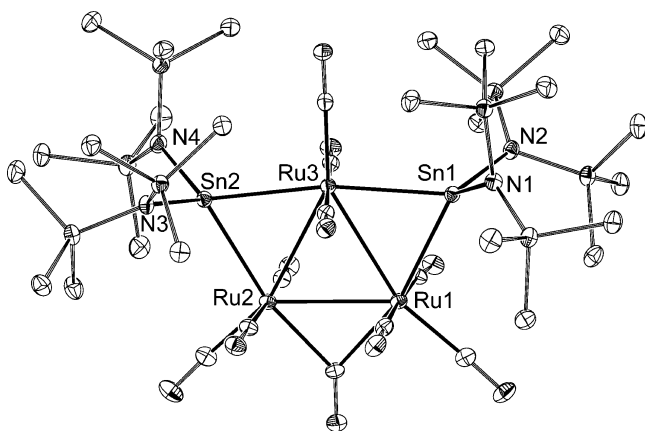


Figure 1. Molecular structure of compound **5** (thermal ellipsoids set at 20% probability). Hydrogen atoms have been omitted for clarity.

Table 1). The cluster comprises an isosceles triangle of ruthenium atoms with three terminal carbonyl ligands attached to each Ru atom, one bridging carbonyl symmetrically spanning a Ru–Ru edge, and two $\text{Sn}(\text{HMDS})_2$ ligands that symmetrically bridge the remaining Ru–Ru edges of the cluster. The tin and ruthenium atoms are essentially coplanar and the SnN_2 plane of each stannylene ligand is roughly perpendicular to the Ru_3Sn_2 plane. The stannylene-bridged Ru–Ru edges, Ru1–Ru3 = 2.9839(5) Å, Ru2–Ru3 = 2.9782(5) Å, are approximately 0.1

Table 1. Selected Interatomic Distances (Å) in Compounds **5–7**

bond	5	6	7
Ru1–Ru2	2.8721(5)	2.982(1) ^a	3.0059(5)
Ru1–Ru3	2.9839(5)	2.982(1) ^a	2.9547(5)
Ru2–Ru3	2.9782(5)	2.982(1) ^a	3.0285(5)
Ru1–Sn1	2.6967(5)	2.720(1) ^b	2.6634(4)
Ru1–Sn3		2.713(1) ^c	
Ru1–Ge1			2.5488(6)
Ru1–CO _{bridge}	2.117(5)		
Ru2–Sn2	2.6991(5)	2.713(1) ^c	2.7035(4)
Ru2–Sn3		2.720(1) ^b	
Ru2–Ge1			2.4576(6)
Ru2–CO _{bridge}	2.094(5)		
Ru3–Sn1	2.7124(4)	2.713(1) ^c	2.7341(4)
Ru3–Sn2	2.7220(5)	2.720(1) ^b	2.7008(4)
Ru–CO _{ax} (av.)	1.948(4)	1.88(1)	1.936(5)
Ru–CO _{eq} (av.)	1.898(6)	1.89(1)	1.89(1)
Sn–N(av.)	2.083(8)	2.093(6)	2.087(4)
Ge–N(av.)			1.839(2)
C–O(av.)	1.15(3)		
	1.13(1)	1.14(1)	1.143(8)

^aRu1–Ru1'. ^bRu1–Sn1. ^cRu1'–Sn1.

Å longer than that bridged by the CO ligand, Ru1–Ru2 = 2.8721(5) Å. A similar Ru–Ru distance pattern has been found for the analogous Sn_2Ru_3 cluster compounds $[\text{Ru}_3(\mu\text{-SnR}_2)_2(\mu\text{-CO})(\text{CO})_9]$ (R = CH(SiMe₃)₂,¹⁹ Ph²⁰). The approximate (non crystallographic) C_{2v} molecular symmetry found for **5** in the solid state is maintained in solution, where the N(SiMe₃)₂ groups of the stannylene ligand do not rotate about the Sn–N axis, since two singlet resonances of equal integral are observed for the methyl groups in the ¹H (0.49 and 0.52 ppm) and ¹³C{¹H} (7.42 and 7.27 ppm) NMR spectra. The IR spectrum of **5** in toluene solution shows the bridging CO ligand as a weak absorption at 1849 cm⁻¹.

The X-ray structure of compound **6** is shown in Figure 2. A selection of bond distances is given in Table 1. The molecule comprises a regular triangle of ruthenium atoms with an $\text{Sn}(\text{HMDS})_2$ ligand spanning each Ru–Ru edge. The tin atoms are in the same plane as the Ru_3 triangle and have a distorted tetrahedral environment, the SnN_2 planes being perpendicular to the Ru_3 triangle. The cluster shell is completed by nine terminal carbonyl ligands (three to each metal atom). The crystals of complex **6** belong to the hexagonal $P63/m$ space group, and their asymmetric unit contains only a part of the molecule, which has a strict C_{3h} symmetry. In solution, the symmetry is even higher (D_{3h}), since its ¹H and ¹³C{¹H} NMR spectra exhibit just one singlet resonance (at 0.56 ppm and 7.57 ppm, respectively) for all the 36 methyl groups of the molecule. The Ru–Ru bond distance, 2.982(1) Å, is similar to those observed for some related Sn_3Ru_3 cluster complexes that have been structurally characterized, namely, $[\text{Ru}_3\{\mu\text{-Sn}(\text{C}_6\text{H}_2\text{Pr}_3)_2\}_3\text{-x}\{\mu\text{-Sn}(\text{CH}(\text{SiMe}_3)_2)_2\}_x(\text{CO})_9]$ ($x = 0\text{--}2$)²¹ and $[\text{Ru}_3(\mu\text{-SnPh}_2)_3(\text{CO})_9]$,²² which are in the range 2.887(2) to 3.018(1) Å. Those Sn_3Ru_3 clusters have been prepared in low yields either by treating $[\text{Ru}_3(\text{CO})_{12}]$ with bulky diorganostannylenes²¹ or by thermally inducing the elimination of benzene from the trihydride $[\text{Ru}_3(\mu\text{-H})_3(\text{SnPh}_3)_3(\text{CO})_9]$.^{20,22} The long Ru–Sn bond distances of **6**, 2.713(1) Å and 2.720(1) Å, seem to be imposed by the large volume of the HMDS groups, since they are comparable to

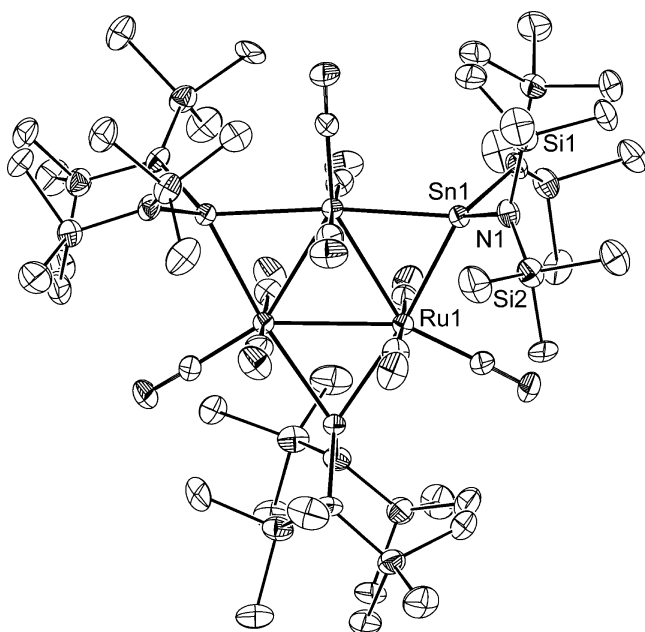


Figure 2. Molecular structure of compound **6** (thermal ellipsoids set at 20% probability). Only one of the two positions in which the SiMe₃ groups bound to N are disordered is shown. Hydrogen atoms have been omitted for clarity.

those of the aforementioned Ru₃Sn₃ complexes with bulky SnR₂ groups, R = CH(SiMe₃)₂ or C₆H₂Pr₃,²¹ but are notably longer (ca. 0.1 Å) than those of [Ru₃(μ-SnPh₂)₃(CO)₉].²² When the Cambridge Crystallographic Database was searched,²³ only seven transition metal complexes having Sn(HMDS)₂ as a ligand were found and no-one contains ruthenium.^{2c,f-i}

Both Sn(HMDS)₂ derivatives, **5** and **6**, are more stable toward hydrolysis than compound **4**. This greater kinetic stability should be due to the rigidity and larger volume of the HMDS SiMe₃ groups, which are more efficient at protecting the Ru–Sn and Sn–N bonds from external attacks than the more flexible *neo*-pentyl groups of compound **4**.

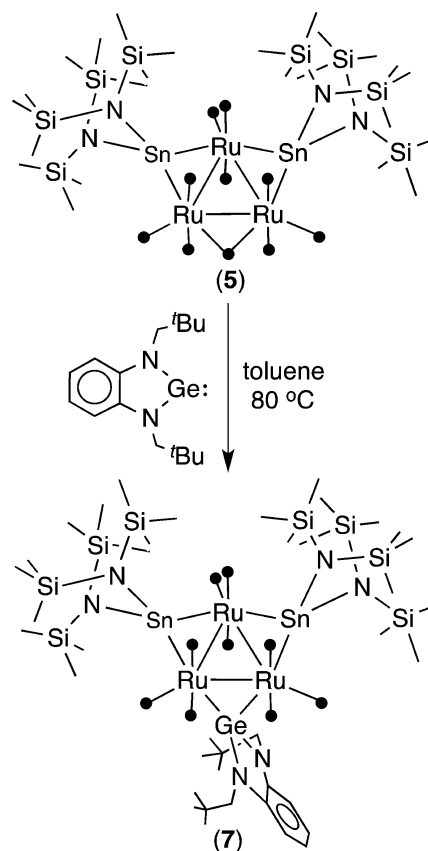
Several attempts aimed at obtaining a monosubstituted SnRu₃ cluster using a 1/1 Sn(HMDS)₂ to [Ru₃(CO)₁₂] mole ratio were carried out under various thermal conditions. However, complex **5** was always the first new species that could be observed by IR analysis of the reaction solutions. Therefore, although acting as a bridging ligand, the behavior of Sn(HMDS)₂ parallels that of phosphine ligands, which readily lead to di- or trisubstituted derivatives when they react with [Ru₃(CO)₁₂] upon thermal activation, the monosubstituted product being an ephemeral unobserved species.²⁴ This situation clearly differs from that reported for NHCs, which lead to monosubstituted [Ru₃(NHC)(CO)₁₁] derivatives through direct CO-substitution reactions.¹⁰

The cluster nature of compounds **5** and **6** markedly contrasts with the monoruthenium complex obtained from [Ru₃(CO)₁₂] and Ge(HMDS)₂ under analogous reaction conditions (Scheme 1).^{2a} We believe that the different atomic size of tin and germanium is responsible for the different reactivity of Sn(HMDS)₂ and Ge(HMDS)₂ with [Ru₃(CO)₁₂]. It seems that Ge(HMDS)₂ is not able to fit into an Ru–Ru edge without provoking the break up of the cluster, whereas the larger tin atom of Sn(HMDS)₂ places farther away the N–SiMe₃ arms, thus reducing their steric hindrance with the neighboring

carbonyl ligands. Regarding di- or polynuclear complexes containing Sn(HMDS)₂ bridges, the trimetallic clusters [M'₂(μ-M(HMDS)₂)₃(CO)₃] (M' = Pd, Pt; M = Ge, Sn), obtained by carbonylation of mononuclear [M'₂(M(HMDS)₂)₃] complexes, have already demonstrated that these metalenes are able to bridge metal–metal bonds.²¹ However, the CO ligands of these clusters are in the plane of the metal atoms and do not interact with the diaminometalene N–R arms.

As trimetallic tin–germanium–ruthenium nanoparticles might be interesting in catalysis,^{13,14} we decided to try the incorporation of a diaminogermylene to the disubstituted Sn₂Ru₃ cluster **5**, which, as shown above, is able to react with an additional mole of Sn(HMDS)₂ to give the trisubstituted Sn₃Ru₃ cluster **6**. The reaction of **5** with one equivalent of Ge(HMDS)₂ led to mixtures of complexes that could not be separated. This result supports the above-commented proposal that diaminogermynes demand more space in the cluster coordination shell than their stannylene analogues. However, the reaction of cluster **5** with the sterically more alleviated germylene Ge(NCH₂^tBu)₂C₆H₄ in toluene at 80 °C allowed the isolation of the Sn₂GeRu₃ cluster [Ru₃{μ-Sn(HMDS)₂}₂{μ-Ge(NCH₂^tBu)₂C₆H₄}(CO)₉] (**7**) in good yield (Scheme 4).

Scheme 4. Synthesis of Compound **7**



The molecular structure of **7** is shown in Figure 3 and a selection of bond distances is given in Table 1. The molecule can be described as resulting from the formal substitution of the germylene reagent for the bridging carbonyl ligand of **5**. The bridging coordination of the germylene ligand is associated with various structural features that merit to be noted: (a) the two Ge–Ru distances differ by about 0.1 Å, (b) the angle between the germylene GeN₂ plane and the shorter Ge–Ru bond

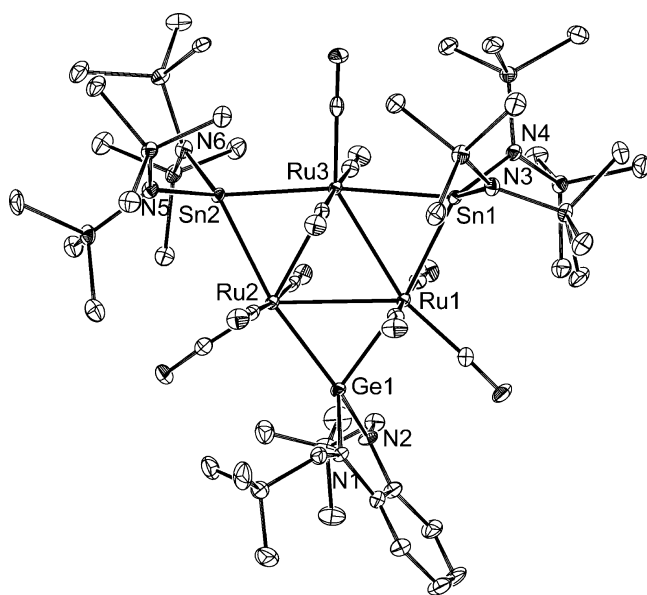


Figure 3. Molecular structure of compound **7** (ellipsoids set at 40% probability). Hydrogen atoms omitted for clarity.

(Ge1–Ru2) is wider ($158.3(1)^\circ$) than that involving the longer Ge–Ru bond ($127.5(1)^\circ$), (c) the plane defined by the benzo group is essentially perpendicular to the Ru_3 plane, (d) the ligand N atoms are in the plane of the benzo group but the Ge atom is $0.116(2)$ Å away from that plane (the free ligand is planar²⁵), and (e) the *neo*-pentyl groups are disposed *syn* to each other, with both ^tBu groups placed at the same side of the ligand plane. Such a *syn* disposition of the *neo*-pentyl groups has also been found in the free ligand²⁵ and in other structurally characterized metal–Ge(NCH₂^tBu)₂C₆H₄ complexes.^{2a,3f} This peculiar coordination of the NHGe ligand of **7**, which has only been observed before in compound **3**,^{2a} is a consequence of the possibility that the *neo*-pentyl groups of **3** or **7** have to minimize their steric hindrance with the nearby carbonyl ligands of the cluster by bending away their bulky ^tBu groups through the CH₂ hinges (such a bending is not possible for ^tBu or 2,6-ⁱPr₂C₆H₃ N–R groups). All the remaining complexes containing cyclic M(NR₂)₂ bridging ligands that have been crystallographically characterized (all are binuclear with ^tBu or 2,6-ⁱPr₂C₆H₃ N–R arms) exhibit a symmetric ligand arrangement.^{3b,4i,k,s,26} The asymmetric coordination of the germylene ligand of **7** seems to force one of the Sn(HMDS)₂ ligands to form an asymmetric bridge because the Sn–Ru distances of the bridged Ru1–Ru3 edge differ by about 0.07 Å. The NMR spectra of **7** also confirm a 2:1 ratio between stannylene and germylene ligands.

The Sn₂GeRu₃ cluster **7** represents an unusual example of heteroleptic carbonyl substitution involving stannylene and germylene ligands in the same ruthenium carbonyl cluster. In fact, to date, **7** and the mononuclear compounds [Ru(SnR₃)(GeR₃)(CO)_{4x}(ⁱPr-DAB)_x] ($x = 2$, R = Ph;²⁷ $x = 0$, R = Me;²⁸ ⁱPr-DAB = 1,4-di-isopropyl-1,4-diaza-1,3-butadiene) are the only complexes known to contain ruthenium, germanium, and tin atoms.

CONCLUDING REMARKS

In this article, we have demonstrated that [Ru₃(CO)₁₂] reacts with diaminostannylenes of different steric demand to stepwise give Sn₂Ru₃ and Sn₃Ru₃ cluster derivatives (compounds **4–6**)

in which the diaminostannylenes act as bridging ligands. All these reactions, coupled to a previous observation that [Ru₃(CO)₁₂] reacts with excess of Ge(HMDS)₂ to give the mononuclear complex [Ru{Ge(HMDS)₂}(CO)₃] but triruthenium products with less bulky diaminogermynes, indicate that, for reactions of [Ru₃(CO)₁₂] with diaminometalenes, both the volume of the diaminometalene and the size of its donor atom (Ge or Sn) are of key importance in determining the nuclearity of the final products. Taking into account these considerations and using an appropriate combination of tin and germanium diaminometalenes, we have been able to prepare a unique Sn₂GeRu₃ cluster.

EXPERIMENTAL SECTION

General Procedures. Solvents were dried over sodium diphenyl ketyl and distilled under nitrogen before use. The reactions were carried out under nitrogen, using Schlenk-vacuum line techniques, and were routinely monitored by solution IR spectroscopy (carbonyl stretching region). The diaminometalenes Ge(HMDS)₂,⁵ Sn(HMDS)₂,⁵ Ge(NCH₂^tBu)₂C₆H₄,²⁵ and Sn(NCH₂^tBu)₂C₆H₄²⁹ were prepared following published procedures. All remaining reagents were purchased from commercial sources. All reaction products were vacuum-dried for several hours prior to being weighed and analyzed. IR spectra were recorded in solution on a Perkin-Elmer Paragon 1000 FT spectrophotometer. NMR spectra were run on Bruker DPX-300 or Bruker AV-400 instruments, using as internal standards a residual protic solvent resonance for ¹H [$\delta(\text{C}_6\text{D}_5\text{CHD}_2) = 2.08$; $\delta(\text{CHCl}_3) = 7.26$; $\delta(\text{C}_6\text{HD}_5) = 7.16$] and a solvent resonance for ¹³C [$\delta(\text{C}_6\text{D}_5\text{CD}_3) = 20.4$; $\delta(\text{CDCl}_3) = 77.2$; $\delta(\text{C}_6\text{D}_6) = 128.1$]. Microanalyses were obtained from the University of Oviedo Microanalytical Service. FAB mass spectra were obtained from the University of A Coruña Mass Spectrometric Service; data given refer to the most abundant molecular ion isotopomer.

[Ru₃{ μ -Sn(NCH₂^tBu)₂C₆H₄}(CO)₉] (4**).** Sn(NCH₂^tBu)₂C₆H₄ (51 mg, 0.14 mmol) was added to a suspension of [Ru₃(CO)₁₂] (25 mg, 0.04 mmol) in 10 mL of toluene and the mixture was heated at 110 °C for 1.5 h. IR and ¹H NMR analyses of aliquots of the crude reaction solution showed the quantitative formation of complex **4**. The solvent was removed under reduced pressure, and the solid residue was washed with hexane (2 × 5 mL) and vacuum-dried to give compound **4** as a dark green solid (37 mg, 56%). IR (toluene, cm⁻¹): ν_{CO} 2046 (s), 2012 (vs), 2001 (m). ¹H NMR (300.1 MHz, 293 K, C₆D₆, ppm): δ 6.85 (m, 1 H, CH), 6.75 (m, 1 H, CH), 3.84 (s, br, 2 H, CH₂), 0.94 (s, br, 9 H, CMe₃). ¹³C{¹H} NMR (100.7 MHz, 298 K, C₆D₆, ppm): δ 199.2 (2 CO), 196.3 (1 CO), 148.2 (2 C of C₆H₄), 115.6 (2 CH of C₆H₄), 109.2 (2 CH of C₆H₄), 58.0 (2 CH₂), 35.3 (2 CMe₃), 28.9 (2 CMe₃). Satisfactory microanalysis and mass spectrum could not be obtained because of the high air- and moisture-sensitive nature of this compound.

[Ru₃{ μ -Sn(HMDS)₂}(CO)₉] (5**).** Sn(HMDS)₂ (3.3 mL of a 0.24 M solution in toluene, 0.78 mmol) was added to a suspension of [Ru₃(CO)₁₂] (200 mg, 0.31 mmol) in 20 mL of toluene, and the mixture was heated at 80 °C for 1 h. The solvent was removed under reduced pressure, and the solid residue was washed with hexane (2 × 10 mL) and vacuum-dried to give compound **5** as a yellow-orange solid (270 mg, 60%). Anal. Calcd. for C₃₄H₇₂N₄O₁₀Ru₃Si₈Sn₂ (1462.27): C, 27.93; H, 4.96; N, 3.83. Found: C, 27.96; H, 4.98; N, 3.79. (+)-FAB MS: m/z 1434 [(M–CO)⁺]. IR (toluene, cm⁻¹): ν_{CO} 2107 (w), 2071 (m), 2054 (s), 2037 (vs), 2023 (m), 2012 (m), 1997 (m), 1849 (w, br). ¹H NMR (400.1 MHz, 298 K, C₆D₆, ppm): δ 0.52 (s, Me), 0.49 (s, Me). ¹³C{¹H} NMR (100.7 MHz, 298 K, C₆D₆, ppm): δ 7.42 (Me), 7.27 (Me) (the ¹³C resonances of the CO ligands could not be observed because of the low solubility of this complex).

[Ru₃{ μ -Sn(HMDS)₂}(CO)₉] (6**).** Sn(HMDS)₂ (4.6 mL of a 0.24 M solution in toluene, 1.09 mmol) was added to a suspension of [Ru₃(CO)₁₂] (200 mg, 0.31 mmol) in 20 mL of toluene and the mixture was heated at 110 °C for 1.5 h. IR and ¹H NMR analyses of aliquots of the crude reaction solution showed the quantitative

Table 2. Crystal, Measurement, and Refinement Data for the Compounds Studied by X-ray Diffraction

	5·C ₇ H ₈	6	7·(C ₆ H ₁₄) _{0.5}
formula	C ₃₄ H ₇₂ N ₄ O ₁₀ Ru ₃ Si ₈ Sn ₂ ·C ₇ H ₈	C ₄₅ H ₁₀₈ N ₆ O ₉ Ru ₃ Si ₁₂ Sn ₃	C ₄₉ H ₉₈ GeN ₆ O ₉ Ru ₃ Si ₈ Sn ₂ ·0.5(C ₆ H ₁₄)
<i>f</i> w	1554.40	1873.73	1796.32
cryst syst	monoclinic	hexagonal	triclinic
space group	<i>P</i> 2 ₁ / <i>n</i>	<i>P</i> 63/ <i>m</i>	<i>P</i> $\bar{1}$
<i>a</i> , Å	15.4510(2),	14.9240(2)	11.7533(3)
<i>b</i> , Å	22.2487(2)	14.9240(2)	14.3899(4)
<i>c</i> , Å	19.9370(2)	20.7550(4)	23.7850(6)
α , deg	90	90	104.017(2)
β , deg	111.842(1)	90	93.241(2)
γ , deg	90	120	94.865(2)
<i>V</i> , Å ³	6361.6(3)	4003.4(1)	3876.5(2)
<i>Z</i>	4	2	2
<i>F</i> (000)	3112	1884	1814
<i>D</i> _{calcd} , g cm ⁻³	1.623	1.554	1.539
μ (Cu <i>K</i> α), mm ⁻¹	13.640	13.880	11.669
cryst size, mm	0.22 × 0.18 × 0.11	0.34 × 0.16 × 0.10	0.11 × 0.07 × 0.05
<i>T</i> , K	100(2)	297(2)	100(2)
θ range, deg	3.11 to 70.00	3.42 to 66.96	3.18 to 67.49
min./max. <i>h</i> , <i>k</i> , <i>l</i>	−18/17, 0/27, 0/24	−14/0, 0/17, 0/24	−13/14, −17/17, −28/20
no. collected reflns	11914	2455	26287
no. unique reflns	11914	2455	13691
no. reflns with <i>I</i> > 2 σ (<i>I</i>)	10611	2284	11767
no. params/restraints	638/0	210/2	761/0
GOF (on <i>F</i> ²)	1.043	1.084	1.005
<i>R</i> ₁ (on <i>F</i> , <i>I</i> > 2 σ (<i>I</i>))	0.054	0.046	0.040
<i>wR</i> ₂ (on <i>F</i> ² , all data)	0.147	0.132	0.101
min./max. $\Delta\rho$, e Å ⁻³	−1.511/1.741	−0.818/0.805	−1.542/1.240

formation of complex **6**. The solvent was removed under reduced pressure, and the solid residue was washed with hexane (2 × 10 mL) and vacuum-dried to give compound **6** as an orange solid (410 mg, 71%). Anal. Calcd. for C₄₅H₁₀₈N₆O₉Ru₃Si₁₂Sn₃ (1873.74): C, 28.85; H, 5.81; N, 4.49. Found: C, 28.77; H, 5.87; N, 4.51. (+)-FAB MS: *m/z* 1874 [M⁺]. IR (toluene, cm⁻¹): ν_{CO} 2054 (s), 2028 (vs), 1999 (m). ¹H NMR (300.1 MHz, 293 K, CDCl₃, ppm): 0.56 (s, Me). ¹³C{¹H} NMR (100.7 MHz, 298 K, C₆D₆, ppm): δ 7.57 (s, Me) (the ¹³C resonances of the CO ligands could not be observed because of the low solubility of this complex).

[Ru₃{ μ -Sn(HMDS)}₂]₂{ μ -Ge(NCH₂^tBu)₂C₆H₄}(CO)₉ (**7**). Sn-(NCH₂^tBu)₂C₆H₄ (15 mg, 0.045 mmol) was added to a suspension of compound **5** (50 mg, 0.035 mmol) in 10 mL of toluene, and the mixture was heated at 80 °C for 2 h. The solvent was removed under reduced pressure, and the solid residue was washed with hexane (2 × 5 mL) and vacuum-dried to give compound **7** as a dark-green solid (41 mg, 67%). Anal. Calcd. for C₄₉H₉₈GeN₆O₉Ru₃Si₈Sn₂ (1753.26): C, 33.57; H, 5.63; N, 4.79. Found: C, 33.60; H, 5.65; N, 4.76. (+)-FAB MS: *m/z* 1753 [M⁺]. IR (toluene, cm⁻¹): ν_{CO} 2049 (s), 2022 (vs), 1996 (m). ¹H NMR (300.1 MHz, 293 K, toluene-*d*₈, ppm): ¹H NMR (300.1 MHz, 293 K, C₆D₆, ppm): δ 6.95 (m, 1 H, CH), 6.85 (m, 1 H, CH), 3.61 (s, br, 1 H, CHH), 3.45 (s, br, 1 H, CHH), 0.09 (s, 9 H, CMe₃), 0.57 (s, br, 36 H, Me).

X-ray Diffraction Analyses. Crystals of 5·C₇H₈, **6**, and 7·(C₆H₁₄)_{0.5} were analyzed by X-ray diffraction. A selection of crystal, measurement, and refinement data is given in Table 2. Diffraction data were collected on an Oxford Diffraction Xcalibur Onyx Nova single crystal diffractometer. An empirical absorption correction for 7·(C₆H₁₄)_{0.5} was applied using the SCALE3 ABSPACK algorithm as implemented in CrysAlisPro RED.³⁰ The XABS2³¹ empirical absorption correction was applied for 5·C₇H₈ and **6**. The structures were solved using the program SIR-97.³² Isotropic and full matrix anisotropic least-squares refinements were carried out using SHELXL.³³ All non-H atoms were refined anisotropically. The hydrogen atoms were set in calculated positions and refined riding on their parent atoms. The crystal of **6** was twinned and the TWIN

law (0 1 0; 1 0 0; 0 0 1) was used for the structure refinement. Each SiMe₃ group bound to N of **6** was found disordered over two positions with a 51:49 occupancy ratio. The molecular plots were made with the PLATON program package.³⁴ The WINGX program system³⁵ was used throughout the structure determinations. CCDC deposition numbers: 859443 (5·C₇H₈), 859444 (**6**) and 859442 (7·(C₆H₁₄)_{0.5}).

■ ASSOCIATED CONTENT

📄 Supporting Information

Crystallographic data in CIF format for 5·C₇H₈, **6**, and 7·(C₆H₁₄)_{0.5}. This material is available free of charge via the Internet at <http://pubs.acs.org>.

■ AUTHOR INFORMATION

Corresponding Author

*E-mail: jac@uniovi.es (J.A.C.), pga@uniovi.es (P.G.-A.).

■ ACKNOWLEDGMENTS

This work has been supported by the Spanish MICINN (projects CTQ2010-14933 and DELACIERVA-09-05) and the European Union (FEDER grants and Marie Curie action FP7-2010-RG-268329).

■ REFERENCES

- (1) For reviews on acyclic or cyclic group-14 diaminometalenes as ligands in transition metal complexes, see: (a) Zabula, A. V.; Hahn, F. E. *Eur. J. Inorg. Chem.* **2008**, 5165. (b) Kühl, O. *Coord. Chem. Rev.* **2004**, 248, 411. (c) Gehrhus, B.; Lappert, M. F. *J. Organomet. Chem.* **2001**, 617, 209. (d) Haaf, M.; Schmedake, T. A.; West, R. *Acc. Chem. Res.* **2000**, 33, 704. (e) Lappert, M. F.; Rowe, R. S. *Coord. Chem. Rev.* **1990**, 100, 267. (f) Petz, W. *Chem. Rev.* **1986**, 86, 1019. (g) Lappert, M. F.; Power, P. P. *J. Chem. Soc., Dalton Trans.* **1985**, 51. (h) Asay, M.; Jones, C.; Driess, M. *Chem. Rev.* **2011**, 111, 354.

(2) For representative examples of acyclic group-14 diaminometalene ligands in transition metal complexes see: (a) Cabeza, J. A.; García-Álvarez, P.; Polo, D. *Inorg. Chem.* **2011**, *50*, 6195. (b) Anandhi, U.; Sharp, P. R. *Inorg. Chim. Acta* **2006**, *359*, 3521. (c) Ellis, S. L.; Hitchcock, P. B.; Holmes, S. A.; Lappert, M. F.; Slade, M. J. *J. Organomet. Chem.* **1993**, *444*, 95. (d) Hampden-Smith, M. J.; Lei, D.; Duesler, E. N. *J. Chem. Soc., Dalton Trans.* **1990**, 2953. (e) Hawkins, S. M.; Hitchcock, P. B.; Lappert, M. F.; Rai, A. K. *Chem. Commun.* **1986**, 1689. (f) Hawkins, S. M.; Hitchcock, P. B.; Lappert, M. F. *J. Chem. Soc., Chem. Commun.* **1985**, 1592. (g) Hitchcock, P. B.; Lappert, M. F.; Misra, M. C. *J. Chem. Soc., Chem. Commun.* **1985**, 863. (h) Al-Allaf, T. A. K.; Eaborn, C.; Hitchcock, P. B.; Lappert, M. F.; Pidcock, A. *J. Chem. Soc., Chem. Commun.* **1985**, 548. (i) Campbell, G. K.; Hitchcock, P. B.; Lappert, M. F.; Misra, M. C. *J. Organomet. Chem.* **1985**, *289*, C1. (j) Schnepf, A. Z. *Anorg. Allg. Chem.* **2006**, *632*, 935.

(3) For representative examples of cyclic group-14 diaminometalene ligands in transition metal complexes see: (a) Ref 2a. (b) Mansell, S. M.; Herber, R. H.; Nowik, I.; Ross, D. H.; Russell, C. A.; Wass, D. F. *Inorg. Chem.* **2011**, *50*, 2252. (c) Zark, P.; Schafer, A.; Mitra, A.; Haase, D.; Saak, W.; West, R.; Muller, T. *J. Organomet. Chem.* **2010**, *695*, 398. (d) Cade, I. A.; Hill, A. F.; Kämpfe, A.; Wagler, J. *Organometallics* **2010**, *29*, 4012. (e) Kong, L.; Zhang, J.; Song, H.; Cui, C. *Dalton Trans.* **2009**, 5444. (f) Ullah, F.; Köhl, O.; Bajor, G.; Veszpremi, T.; Jones, P. G.; Heinicke, J. *Eur. J. Inorg. Chem.* **2009**, 221. (g) Zabula, A. V.; Pape, T.; Hepp, A.; Hahn, F. E. *Organometallics* **2008**, *27*, 2756. (h) Hahn, F. E.; Zabula, A. V.; Pape, T.; Hepp, A. *Z. Anorg. Allg. Chem.* **2008**, *634*, 2397. (i) Zabula, A. V.; Pape, T.; Hepp, A.; Hahn, F. E. *Dalton Trans.* **2008**, 5886. (j) Hahn, F. E.; Zabula, A. V.; Pape, T.; Hepp, A.; Tonner, R.; Haunschild, R.; Frenking, G. *Chem.—Eur. J.* **2008**, *14*, 10716. (k) Zabula, A. V.; Hahn, F. E.; Pape, T.; Hepp, A. *Organometallics* **2007**, *26*, 1972. (l) Saur, I.; Alonso, S. G.; Gornitzka, H.; Lemierre, V.; Chrostowska, A.; Barrau, J. *Organometallics* **2005**, *24*, 2988. (m) Neumann, E.; Pfaltz, A. *Organometallics* **2005**, *24*, 2008. (n) Zeller, A.; Bielert, F.; Haerter, P.; Herrmann, W. A.; Strassner, T. *J. Organomet. Chem.* **2005**, *690*, 3292. (o) Köhl, O.; Lönnecke, P.; Heinicke, J. *Inorg. Chem.* **2003**, *42*, 2836. (p) Avent, A. G.; Gehrhuis, B.; Hitchcock, P. B.; Lappert, M. F.; Maciejewski, H. *J. Organomet. Chem.* **2003**, *686*, 321. (q) Clendenning, S. B.; Gehrhuis, B.; Hitchcock, P. B.; Moser, D. F.; Nixon, J. F.; West, R. *J. Chem. Soc., Dalton Trans.* **2002**, 484. (r) Schmedake, T. A.; Haaf, M.; Paradise, B. J.; Millevolte, A. J.; Powell, D. R.; West, R. *J. Organomet. Chem.* **2001**, *636*, 17. (s) Bazinet, P.; Yap, G. P. A.; Richeson, D. S. *J. Am. Chem. Soc.* **2001**, *123*, 11162. (t) Schmedake, T. A.; Haaf, M.; Paradise, B. J.; Powell, D.; West, R. *Organometallics* **2000**, *19*, 3263. (u) Gehrhuis, B.; Hitchcock, P. B.; Lappert, M. F.; Maciejewski, H. *Organometallics* **1998**, *17*, 5599. (v) Denk, M.; Hayashi, R. K.; West, R. *Chem. Commun.* **1994**, 33. (w) Veith, M.; Stahl, L. *Angew. Chem., Int. Ed.* **1993**, *32*, 106. (x) Veith, M.; Stahl, L.; Huch, V. *Chem. Commun.* **1990**, 359. (y) Veith, M.; Stahl, L.; Huch, V. *Inorg. Chem.* **1989**, *28*, 3278.

(4) For examples of reactivity studies on transition metal complexes having group-14 diaminometalene ligands, see: (a) Meltzer, A.; Inoue, S.; Präsang, C.; Driess, M. *J. Am. Chem. Soc.* **2010**, *132*, 3038. (b) Meltzer, A.; Präsang, C.; Driess, M. *J. Am. Chem. Soc.* **2009**, *131*, 7232. (c) Meltzer, A.; Präsang, C.; Milsmann, C.; Driess, M. *Angew. Chem., Int. Ed.* **2009**, *48*, 3170. (d) Zhang, M.; Liu, X.; Shi, C.; Ren, C.; Ding, Y.; Roesky, H. W. *Z. Anorg. Allg. Chem.* **2008**, *634*, 1755. (e) York, J. T.; Young, V. G. Jr.; Tolman, W. B. *Inorg. Chem.* **2006**, *45*, 4191. (f) Cygan, Z. T.; Kampf, J. W.; Holl, M. M. B. *Inorg. Chem.* **2003**, *42*, 7219. (g) Evans, W. J.; Perotti, J. M.; Ziller, J. W.; Moser, D. F.; West, R. *Organometallics* **2003**, *22*, 1160. (h) Cygan, Z. T.; Bender, J. E. IV; Litz, K. E.; Kampf, J. W.; Holl, M. M. B. *Organometallics* **2002**, *21*, 5373. (i) Herrmann, W. A.; Harter, P.; Gstottmayr, C. W. K.; Bielert, F.; Seeboth, N.; Sirsch, P. *J. Organomet. Chem.* **2002**, *649*, 141. (j) Amoroso, D.; Haaf, M.; Yap, G. P. A.; West, R.; Fogg, D. E. *Organometallics* **2002**, *21*, 534. (k) Fürstner, A.; Krause, H.; Lehmann, C. W. *Chem. Commun.* **2001**, 2372. (l) Braunstein, P.; Veith, M.; Blin, J.; Huch, V. *Organometallics* **2001**, *20*, 627. (m) Litz, K. E.; Bender, J. E.; Sweeder, R. D.; Holl, M. M. B.; Kampf, J. W. *Organometallics* **2000**, *19*, 1186. (n) Dysard, J. M.; Tilley, T. D. *Organometallics* **2000**, *19*,

4726. (o) Petri, S. H. A.; Eikenberg, D.; Neumann, B.; Stammeler, H.-G.; Jutzi, P. *Organometallics* **1999**, *18*, 2615. (p) Litz, K. E.; Holl, M. M. B.; Kampf, J. W.; Carpenter, G. B. *Inorg. Chem.* **1998**, *37*, 6461. (q) Litz, K. E.; Kampf, J. W.; Holl, M. M. B. *J. Am. Chem. Soc.* **1998**, *120*, 7484. (r) Litz, K. E.; Bender, J. E. IV; Kampf, J. W.; Holl, M. M. B. *Angew. Chem., Int. Ed.* **1997**, *36*, 496. (s) Veith, M.; Müller, A.; Stahl, L.; Notzel, M.; Jarczyk, M.; Huch, V. *Inorg. Chem.* **1996**, *35*, 3848. (t) Knorr, M.; Hallauer, E.; Huch, V.; Veith, M.; Braunstein, P. *Organometallics* **1996**, *15*, 3868. (u) Litz, K. E.; Henderson, K.; Gourley, R. W.; Holl, M. M. B. *Organometallics* **1995**, *14*, 5008. (v) Zabula, A. V.; Pape, T.; Hepp, A.; Schappacher, F. M.; Rodewald, U. C.; Pöttgen, R.; Hahn, F. E. *J. Am. Chem. Soc.* **2008**, *130*, 5648.

(5) (a) Harris, D. H.; Lappert, M. F. *J. Chem. Soc., Chem. Commun.* **1974**, 895. (b) Gynane, M. J. S.; Harris, D. H.; Lappert, M. F.; Power, P. P.; Rivière, P.; Rivière-Baudet, M. *J. Chem. Soc., Dalton Trans.* **1977**, 2004.

(6) For representative syntheses of stable cyclic group-14 diaminometalenes, see: (a) Schueffler, C. D.; Zuckerman, C. D. *J. Am. Chem. Soc.* **1974**, *96*, 7160. (b) Veith, M. *Angew. Chem., Int. Ed.* **1975**, *14*, 263. (c) Pfeiffer, J.; Maringgele, W.; Noltemeyer, M.; Meller, A. *Chem. Ber.* **1989**, *122*, 245. (d) Herrmann, W. A.; Denk, M.; Behm, J.; Scherer, W.; Klingan, F.-R.; Bock, H.; Solouki, B.; Wagner, M. *Angew. Chem., Int. Ed.* **1992**, *31*, 1485. (e) Denk, M.; Lennon, R.; Hayashi, R.; West, R.; Belyakov, A. V.; Verne, H. P.; Haaland, A.; Wagner, M.; Metzler, N. *J. Am. Chem. Soc.* **1994**, *116*, 2691. (f) Gans-Eichler, T.; Gudat, D.; Nieger, M. *Angew. Chem., Int. Ed.* **2002**, *41*, 1888. (g) Hahn, F. E.; Heitmann, D.; Pape, T. *Eur. J. Inorg. Chem.* **2008**, 1039. (h) Charmant, J. P. H.; Haddow, M. F.; Hahn, F. E.; Heitmann, D.; Fröhlich, R.; Mansell, S. M.; Russell, C. A.; Wass, D. F. *Dalton Trans.* **2008**, 6055. (i) Hahn, F. E.; Wittenbecher, L.; Le Van, D.; Zabula, A. V. *Inorg. Chem.* **2007**, *46*, 7662. (j) Heitmann, D.; Pape, T.; Hepp, A.; Mück-Lichtenfeld, C.; Grimme, S.; Hahn, F. E. *J. Am. Chem. Soc.* **2011**, *133*, 11118. (k) Dickschat, J. V.; Urban, S.; Pape, T.; Glorius, F.; Hahn, F. E. *Dalton Trans.* **2010**, *39*, 11519.

(7) Arduengo, A. J. III; Harlow, R. L.; Kline, M. *J. Am. Chem. Soc.* **1991**, *113*, 361.

(8) For excellent reviews on the chemistry of cyclic carbenes and related species, see: (a) Melaimi, M.; Soleihavoup, M.; Bertrand, G. *Angew. Chem., Int. Ed.* **2010**, *49*, 8810. (b) Hahn, F. E.; Jahnke, M. C. *Angew. Chem., Int. Ed.* **2008**, *47*, 3122.

(9) For catalytic applications of transition metal NHC complexes, see: (a) Díez-González, S.; Marion, N.; Nolan, S. P. *Chem. Rev.* **2009**, *109*, 3612. (b) Samojłowicz, C.; Bieniek, M.; Grela, K. *Chem. Rev.* **2009**, *109*, 3708. (c) Glorius, F. *Top. Organomet. Chem.* **2007**, *21*, 1. (d) Nolan, S. P. *N-Heterocyclic Carbenes in Synthesis*; Wiley-VCH: Weinheim, Germany, 2006.

(10) For a recent review on the N-heterocyclic carbene chemistry of transition-metal carbonyl clusters, see: Cabeza, J. A.; García-Álvarez, P. *Chem. Soc. Rev.* **2011**, *40*, 5389.

(11) (a) Cabeza, J. A.; Damonte, M.; García-Álvarez, P.; Kennedy, A. R.; Pérez-Carreño, E. *Organometallics* **2011**, *30*, 826. (b) Cabeza, J. A.; Damonte, M.; García-Álvarez, P. *Organometallics* **2011**, *30*, 2371. (c) Cabeza, J. A.; del Río, I.; Pérez-Carreño, E.; Pruneda, V. *Organometallics* **2011**, *30*, 1148. (d) Cabeza, J. A.; del Río, I.; Fernández-Colinas, J. M.; Pérez-Carreño, E.; Sánchez-Vega, M. G.; Vázquez-García, D. *Organometallics* **2010**, *29*, 3828. (e) Cabeza, J. A.; del Río, I.; Pérez-Carreño, E.; Sánchez-Vega, M. G.; Vázquez-García, D. *Organometallics* **2010**, *29*, 4464. (f) Cabeza, J. A.; del Río, I.; Fernández-Colinas, J. M.; Pérez-Carreño, E.; Sánchez-Vega, M. G.; Vázquez-García, D. *Organometallics* **2009**, *28*, 1832. (g) Cabeza, J. A.; del Río, I.; Pérez-Carreño, E.; Sánchez-Vega, M. G.; Vázquez-García, D. *Angew. Chem., Int. Ed.* **2009**, *48*, 555. (h) Cabeza, J. A.; del Río, I.; Miguel, D.; Pérez-Carreño, E.; Sánchez-Vega, M. G. *Organometallics* **2008**, *27*, 211. (i) Bruce, M. I.; Cole, M. L.; Fung, R. S. C.; Forsyth, C. M.; Hilder, M.; Junk, P. C.; Konstas, K. *Dalton Trans.* **2008**, 4118. (j) Ellul, C. E.; Saker, O.; Mahon, M. F.; Apperley, D. C.; Whittlesey, M. K. *Organometallics* **2008**, *27*, 100. (k) Critall, M. R.; Ellul, C. E.; Mahon, M. F.; Saker, O.; Whittlesey, M. K. *Dalton Trans.* **2008**, 4209. (l) Cooke, C. E.; Jennings, M. C.; Katz, M. J.; Pomeroy, R. K.;

- Clyburne, J. A. C. *Organometallics* **2008**, *27*, 5777. (m) Bruce, M. I.; Cole, M. L.; Fung, R. S. C.; Forsyth, C. M.; Hilder, M.; Junk, P. C.; Konstas, K. *Dalton Trans.* **2008**, 4118. (n) Ellul, C. E.; Saker, O.; Mahon, M. F.; Apperley, D. C.; Whittlesey, M. K. *Organometallics* **2008**, *27*, 100. (o) Ellul, C. E.; Mahon, M. F.; Saker, O.; Whittlesey, M. K. *Angew. Chem., Int. Ed.* **2007**, *46*, 6343. (p) Cabeza, J. A.; da Silva, I.; del Río, I.; Sánchez-Vega, M. G. *Dalton Trans.* **2006**, 3966.
- (12) (a) Cabeza, J. A.; del Río, I.; Miguel, D.; Sánchez-Vega, M. G. *Chem. Commun.* **2005**, 3956. (b) Cabeza, J. A.; del Río, I.; Miguel, D.; Pérez-Carreño, E.; Sánchez-Vega, M. G. *Dalton Trans.* **2008**, 1937. (c) Cabeza, J. A.; del Río, I.; Miguel, D.; Sánchez-Vega, M. G. *Angew. Chem., Int. Ed.* **2008**, *47*, 1920. (d) Cabeza, J. A.; Pérez-Carreño, E. *Organometallics* **2008**, *27*, 4697.
- (13) For a recent review on ruthenium–tin cluster complexes and their applications as bimetallic nanoscale heterogeneous hydrogenation catalysts, see: Adams, R. D.; Trufan, E. *Philos. Trans. R. Soc., A* **2010**, *368*, 1473.
- (14) (a) Hungria, A. B.; Raja, R.; Adams, R. D.; Captain, B.; Thomas, J. M.; Midgley, P. A.; Golovko, V.; Johnson, B. F. G. *Angew. Chem., Int. Ed.* **2006**, *45*, 4782. (b) Adams, R. D.; Blom, D. A.; Captain, B.; Raja, R.; Thomas, J. M.; Trufan, E. *Langmuir* **2008**, *24*, 9223. (c) Adams, R. D.; Boswell, E. M.; Captain, B.; Hungria, A. B.; Midgley, P. A.; Raja, R.; Thomas, J. M. *Angew. Chem., Int. Ed.* **2007**, *46*, 8182. (d) Yang, F.; Trufan, E.; Adams, R. D.; Goodman, D. W. *J. Phys. Chem. C* **2008**, *112*, 14233.
- (15) (a) Burch, R. J. *Catal.* **1981**, *71*, 348. (b) Burch, R.; Garla, L. C. *J. Catal.* **1981**, *71*, 360. (c) Srinivasan, R.; Davis, B. H. *Platinum Met. Rev.* **1992**, *36*, 151. (d) Fujikawa, T.; Ribeiro, F. H.; Somorjai, G. A. *J. Catal.* **1998**, *178*, 58. (e) Huber, G. W.; Shabaker, J. W.; Dumesic, J. A. *Science* **2003**, *300*, 2075. (f) Holt, M. S.; Wilson, W. L.; Nelson, J. H. *Chem. Rev.* **1989**, *89*, 11. (g) Johnson, B. F. G.; Raynor, S. A.; Brown, D. B.; Shephard, D. S.; Mashmeyer, T.; Thomas, J. M.; Hermans, S.; Raja, R.; Sankar, G. *J. Mol. Catal. A: Chem.* **2002**, *182–183*, 89.
- (16) Kabir, S. E.; Raha, A. K.; Hassan, M. R.; Nicholson, B. K.; Rosenberg, E.; Sharmin, A.; Salassa, L. *Dalton Trans.* **2008**, 4212.
- (17) See, for example: (a) Adams, R. D.; Captain, B.; Fu, W.; Smith, M. D. *Inorg. Chem.* **2002**, *41*, 5593. (b) Adams, R. D.; Captain, B.; Fu, W.; Smith, M. D. *Inorg. Chem.* **2002**, *41*, 2302. (c) Adams, R. D.; Captain, B.; Smith, J. L.; Hall, M. B.; Beddie, C. L.; Wedster, C. E.; Fu, W.; Smith, M. D. *Inorg. Chem.* **2004**, *43*, 7576. (d) Adams, R. D.; Trufan, E. *Organometallics* **2008**, *27*, 4108.
- (18) (a) Lappert, M. F.; Power, P. P.; Sanger, A. R.; Srivastava, R. C. *Metal and Metalloid Amides: Syntheses, Structures and Physical and Chemical Properties*; Ellis Horwood-John Wiley & Sons: Chichester, U.K., 1979. (b) Lappert, M. F.; Power, P. P.; Potchenko, A.; Seeber, A. *Metal Amide Chemistry*; John Wiley & Sons, Chichester, U.K., 2009.
- (19) Cardin, C. J.; Cardin, D. J.; Convery, M. A.; Dauter, Z.; Fenske, D.; Devereux, M. M.; Power, M. B. *J. Chem. Soc., Dalton Trans.* **1996**, 1133.
- (20) Adams, R. D.; Captain, B.; Trufan, E. *J. Organomet. Chem.* **2008**, *693*, 3593.
- (21) Cardin, C. J.; Cardin, D. J.; Convery, M. A.; Dauter, Z.; Fenske, D.; Devereux, M. M.; Power, M. B. *J. Chem. Soc., Dalton Trans.* **1996**, 1133.
- (22) Adams, R. D.; Captain, B.; Hall, M. B.; Trufan, E.; Yang, X. *J. Am. Chem. Soc.* **2007**, *129*, 12328.
- (23) CSD, version 5.32 (updated February 2011). See also, Allen, F. H., *Acta Crystallogr.* **2002**, *B58*, 380.
- (24) See, for example: (a) Bruce, M. I.; Shaw, G.; Stone, B. F. A. *J. Chem. Soc., Dalton Trans.* **1972**, 2094. (b) Malik, S. K.; Poë, A. *Inorg. Chem.* **1978**, *17*, 1484.
- (25) Köhl, O.; Lönnecke, P.; Heinicke, J. *Polyhedron* **2001**, *20*, 2215.
- (26) (a) Veith, M.; Stahl, L.; Huch, V. *Organometallics* **1993**, *12*, 1914. (b) Veith, M.; Olbrich, M.; Notzel, M.; Klein, C.; Stahl, L.; Huch, V. private communications to CCDC, codes KODNOH, KODNIB, and KODNEX, 1999. (c) Veith, M.; Olbrich, M.; Klein, C. private communications to CCDC, codes KODPAV and KODNUN, 1999.
- (27) Aarnts, M. P.; Hartl, F.; Peelen, K.; Stufkens, D. J.; Amatore, C.; Verpeaux, J.-N. *Organometallics* **1997**, *16*, 4686.
- (28) Knox, S. A. R.; Stone, F. G. A. *J. Chem. Soc. A.* **1971**, *18*, 2874.
- (29) Braunschweig, H.; Gehrhus, B.; Hitchcock, P. B.; Lappert, M. F. *Z. Anorg. Allg. Chem.* **1995**, *621*, 1922.
- (30) *CrysAlisPro RED*, version 1.171.34.36; Oxford Diffraction Ltd.: Oxford, UK, 2010.
- (31) Parkin, S.; Moezzi, B.; Hope, H. J. *Appl. Crystallogr.* **1995**, *28*, 53.
- (32) Altomare, A.; Burla, M. C.; Camalli, M.; Cascarano, G. L.; Giacovazzo, S.; Guagliardi, A.; Moliterni, A. G. C.; Polidori, G.; Spagna, R. *J. Appl. Crystallogr.* **1999**, *32*, 115.
- (33) *SHELXL*, version 2008; Sheldrick, G. M. *Acta Crystallogr.* **2008**, *A64*, 112.
- (34) Spek, A. L. *PLATON: A Multipurpose Crystallographic Tool*, version 1.15; University of Utrecht: Utrecht, The Netherlands, 2008.
- (35) Farrugia, L. J. *WinGX*, version 1.80.05 (2009); *J. Appl. Crystallogr.* **1999**, *32*, 837.

Artículo III

***“Diaminogermylene and Diaminostannylene
Derivatives of Gold(I): Novel AuM and AuM₂
(M = Ge, Sn) Complexes”***

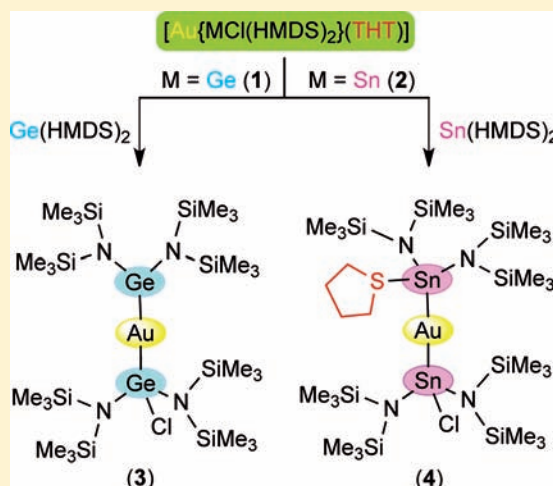
Diaminogermylene and Diaminostannylene Derivatives of Gold(I): Novel AuM and AuM₂ (M = Ge, Sn) Complexes

Javier A. Cabeza,* José M. Fernández-Colinas, Pablo García-Álvarez,* and Diego Polo

Departamento de Química Orgánica e Inorgánica-IUQOEM, Universidad de Oviedo-CSIC, E-33071 Oviedo, Spain

Supporting Information

ABSTRACT: The reactions of [AuCl(THT)] (THT = tetrahydrothiophene) with 1 equiv of the group 14 diaminometalenes M(HMDS)₂ [M = Ge, Sn; HMDS = N(SiMe₃)₂] lead to [Au{MCl(HMDS)₂}(THT)] [M = Ge (1), Sn (2)], which contain a metalate(II) ligand that arises from insertion of the corresponding M(HMDS)₂ reagent into the Au–Cl bond of the gold(I) reagent. While compound 1 reacts with more Ge(HMDS)₂ to give the germanate–germylene derivative [Au{GeCl(HMDS)₂}{Ge(HMDS)₂}] (3), which results from substitution of Ge(HMDS)₂ for the THT ligand of 1, an analogous treatment of compound 2 with Sn(HMDS)₂ gives the stannate–stannylene derivative [Au{SnCl(HMDS)₂}{Sn(HMDS)₂(THT)}] (4), which has a THT ligand attached to the stannylene tin atom and which, in solution at room temperature, participates in a dynamic process that makes its two Sn(HMDS)₂ fragments equivalent (on the NMR time scale). A similar dynamic process has not been observed for the AuGe₂ compound 3 or for the AuSn₂ derivatives [Au{SnR(HMDS)₂}{Sn(HMDS)₂(THT)}] [R = Bu (5), HMDS (6)], which have been prepared by treating complex 4 with LiR. The structures of compounds 1 and 3–6 have been determined by X-ray diffraction.



INTRODUCTION

The investigation of the transition-metal chemistry of the heavier analogues of diaminocarbenes, that is, group 14 diaminometalenes [M = Si, Ge, Sn, Pb],^{1,2} started some decades ago following the seminal discovery by Lappert in 1974 of the first specimens of this family, M(HMDS)₂ [M = Ge, Sn, Pb; HMDS = N(SiMe₃)₂].³ These acyclic compounds were soon complemented with some cyclic relatives (N-heterocyclic metalenes), with the first stable N-heterocyclic silylenes,⁴ germynes,⁵ stannylens,⁶ and plumbylenes⁷ being reported in 1994, 1989, 1974, and 1982, respectively. However, despite their early discovery, the transition-metal chemistry of group 14 diaminometalenes^{1,2} is currently underdeveloped in comparison with that of diaminocarbenes,⁸ whose first stable specimen was isolated much later (1991)⁹ than the first diaminometalenes.

Among the synthetic and reactivity studies on group 14 diaminometalene derivatives of transition metals that can be found in the chemical literature, the works regarding group 11 metals are very scarce. Those dealing with diaminoplumbylens are nonexistent, and only one involves a diaminosilylene (compound A in Figure 1).¹⁰ Disubstituted diaminogermynes are only represented in copper chemistry (compounds B and C in Figure 1),¹¹ but trisubstituted diaminogermynes have been attached to the three group 11 metals (compounds D,¹² E,¹³ and F¹⁴ in Figure 1). No copper, silver, or gold derivatives of disubstituted diaminostannylens have ever been reported,

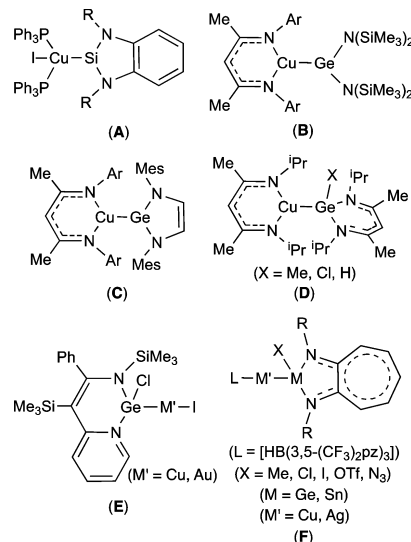


Figure 1. Examples of silicon, germanium, and tin diaminometalene derivatives of group 11 metals.

although some examples of trisubstituted diaminostannylene derivatives of copper and silver are known (compound F in Figure 1).¹⁴

Received: January 20, 2012

Published: February 29, 2012

It should be noted that all complexes shown in Figure 1 have been prepared using the corresponding diaminometalenes as reagents.

Concerning anionic group 14 di- or triaminometalate ligands in group 11 metal complexes, a few examples are known for the three transition metals. They all have been prepared by either inserting a diaminometalene into an Au–Cl bond (compound **G** in Figure 2)¹⁵ or displacing one (compound **H**

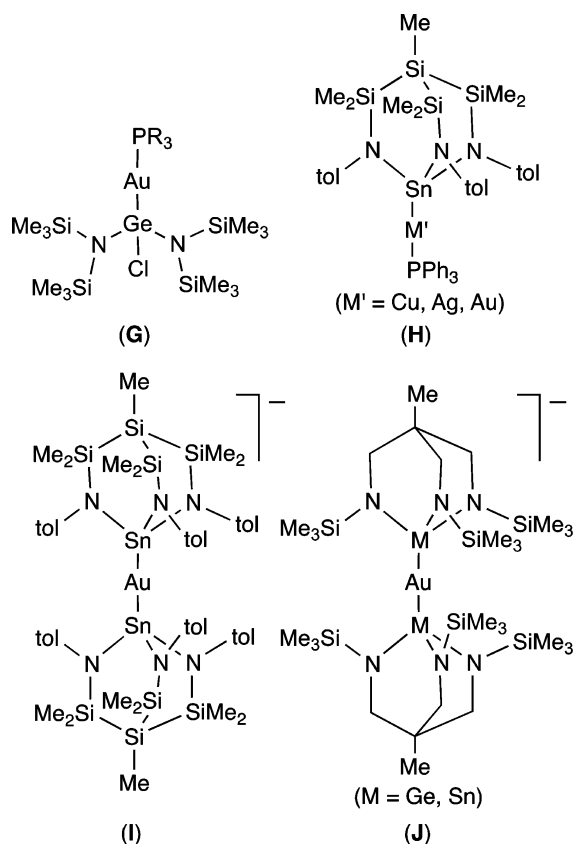


Figure 2. Examples of germanium and tin di- and triaminometalate derivatives of group 11 metals.

in Figure 2)^{16–18} or two (compounds **I**¹⁸ and **J**¹⁹ in Figure 2) anionic ligands from the appropriate transition-metal precursor with a group 14 triaminometalate reagent. Similar substitution reactions have also allowed the preparation of some gold(II) and gold(III) complexes, not depicted in Figure 2, that contain the triaminostannate ligand of **H** and **I**.¹⁸

All of the above-mentioned data prompted us to attempt the synthesis of simple germanium and tin diaminometalene derivatives of gold(I), of which no examples had been previously reported. We also had in mind that diaminocarbene complexes of gold(I) had recently been identified as very efficient catalyst precursors for many catalytic reactions that are important in organic chemistry,²⁰ and we wondered whether group 14 diaminometalene derivatives of gold(I) would also be useful in catalysis. We chose $[\text{AuCl}(\text{THT})]$ (THT = tetrahydrothiophene) as a gold(I) precursor because its THT ligand can be readily displaced by other ligands.²¹ Lappert's compounds $\text{M}(\text{HMDS})_2$ ($\text{M} = \text{Ge}, \text{Sn}$) were chosen as diaminometalene reagents because their syntheses can easily be accomplished.³

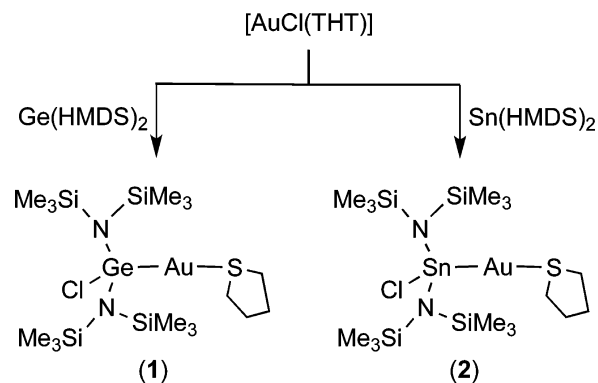
We now report that appropriate combinations of these reagents have led to novel complexes containing Au–M and M–Au–M ($\text{M} = \text{Ge}, \text{Sn}$) metallic cores in which the germanium or tin atoms belong to neutral metalene and/or anionic

metalate ligands. Unfortunately, the high sensitivity of these complexes to oxygen and moisture discourages their use in homogeneous catalysis.

RESULTS AND DISCUSSION

The treatment of $[\text{AuCl}(\text{THT})]$ with equimolar amounts of $\text{M}(\text{HMDS})_2$ ($\text{M} = \text{Ge}$ or Sn) in toluene at room temperature led to the quantitative formation of the air- and moisture-sensitive products $[\text{Au}\{\text{MCl}(\text{HMDS})_2\}(\text{THT})]$ [$\text{M} = \text{Ge}$ (**1**), Sn (**2**); Scheme 1].

Scheme 1



The ^1H and $^{13}\text{C}\{^1\text{H}\}$ NMR spectra of both compounds indicated that they contain THT and HMDS in a 1:2 ratio, denoting that these reactions do not lead to substitution of the THT ligand but to the addition of the corresponding $\text{M}(\text{HMDS})_2$ reagent to $[\text{AuCl}(\text{THT})]$. Therefore, these reactions differ from those reported for $[\text{AuCl}(\text{THT})]$ and diaminocarbenes, in which substitution of the carbene for the THT ligand occurs.²²

An X-ray diffraction analysis showed that compound **1** formally results from the insertion of $\text{Ge}(\text{HMDS})_2$ into the Au–Cl bond of $[\text{AuCl}(\text{THT})]$ because the gold atom is linearly attached to the germanium atom of a chloro(diamino)germanate(II) ligand and to the sulfur atom of a THT ligand (Figure 3 and Table 1). Related reaction processes that afford $[\text{Au}\{\text{GeCl}(\text{HMDS})_2\}(\text{PR}_3)]$ ($\text{R} = \text{Et}, \text{Cy}, \text{Ph}$) derivatives (**G** in Figure 2) have been reported to occur between $[\text{AuCl}(\text{PR}_3)]$ and $\text{Ge}(\text{HMDS})_2$.¹⁵

The treatment of $[\text{AuCl}(\text{THT})]$ with 2 equiv of $\text{M}(\text{HMDS})_2$ ($\text{M} = \text{Ge}, \text{Sn}$) quantitatively afforded the air- and moisture-sensitive AuGe_2 and AuSn_2 derivatives $[\text{Au}\{\text{GeCl}(\text{HMDS})_2\}_2\{\text{Ge}(\text{HMDS})_2\}]$ (**3**) and $[\text{Au}\{\text{SnCl}(\text{HMDS})_2\}_2\{\text{Sn}(\text{HMDS})_2\}(\text{THT})]$ (**4**), respectively (Scheme 2). These reactions demonstrate that the THT ligand of compounds **1** and **2** can be displaced from the gold atom by a group 14 diaminometalene reagent. However, while the germylene derivative **3** arises from the simple substitution of $\text{Ge}(\text{HMDS})_2$ for the THT ligand of **1**, the stannylene derivative **4** contains a THT ligand attached to the stannylene tin atom; thus, it can be considered as resulting from the formal insertion of $\text{Sn}(\text{HMDS})_2$ into the Au–S bond of compound **2**.

The molecular structures of compounds **3** (Figure 4 and Table 2) and **4** (Figure 5 and Table 3) have been determined by X-ray diffraction. Both complexes contain an almost linear M–Au–M arrangement in which the Au–M distances reflect the atomic volume and the steric congestion of the metal atoms. Thus, while both Au–Ge distances of compound **3** are very similar [2.4120(5) and 2.4038(5) Å], the Au–Sn distances

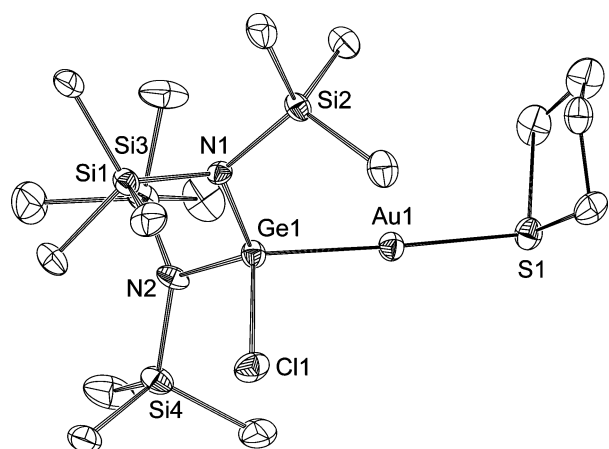


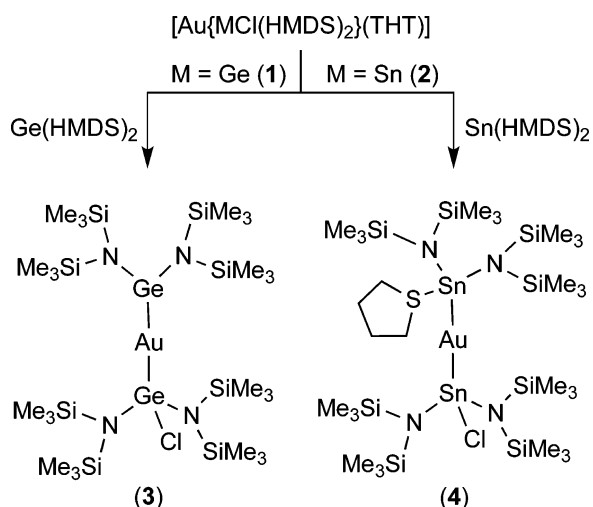
Figure 3. Molecular structure of compound **1** (thermal ellipsoids set at 30% probability). Hydrogen atoms have been omitted for clarity. The Au(THT) fragment is disordered over two positions in a 83:17 ratio. Only the fragment with 83% occupancy is represented.

Table 1. Selected Interatomic Distances (Å) and Angles (deg) in Compound **1**^a

Au1–Ge1	2.362(2)
Au1–S1	2.362(4)
Ge1–N1	1.86(1)
Ge1–N2	1.87(1)
Ge1–Cl1	2.252(4)
Ge1–Au1–S1	177.9(1)
Cl1–Ge1–N1	100.9(3)
Cl1–Ge1–N2	103.5(3)
N1–Ge1–N2	112.5(5)
Cl1–Ge1–Au1	104.62(1)
N1–Ge1–Au1	117.3(3)
N2–Ge1–Au1	104.62(1)

^aOnly data corresponding to the Au(THT) fragment with 83% occupancy are given.

Scheme 2



of compound **4** [2.5711(5) and 2.5845(5) Å] differ by 0.013 Å, with the longest one being associated with the most crowded tin atom, Sn2, which is the one attached to the THT ligand. The presence of the THT ligand in complex **4** results in

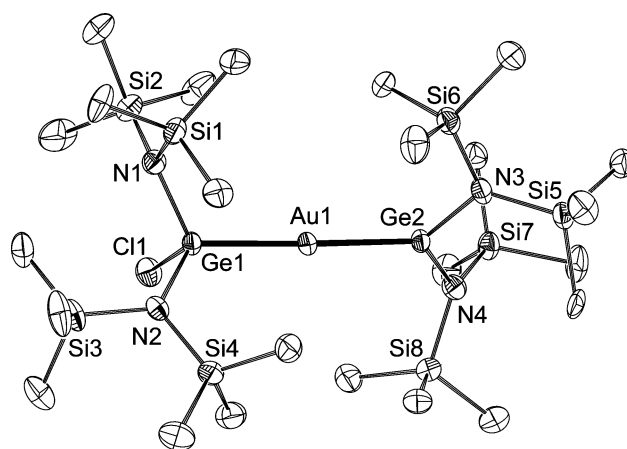


Figure 4. Molecular structure of compound **3** (thermal ellipsoids set at 40% probability). Hydrogen atoms have been omitted for clarity.

Table 2. Selected Interatomic Distances (Å) and Angles (deg) in Compound **3**

Au1–Ge1	2.4120(5)
Au1–Ge2	2.4038(5)
Ge1–Cl1	2.244(1)
Ge1–N1	1.882(4)
Ge1–N2	1.877(3)
Ge2–N3	1.819(4)
Ge2–N4	1.829(4)
Ge1–Au1–Ge2	175.64(2)
Cl1–Ge1–N1	105.6(1)
Cl1–Ge1–N2	101.5(1)
N1–Ge1–N2	109.6(2)
Cl1–Ge1–Au1	102.48(3)
N1–Ge1–Au1	116.5(1)
N2–Ge1–Au1	118.8(1)
N3–Ge2–N4	112.6(2)
N3–Ge2–Au1	123.8(1)
N4–Ge2–Au1	123.5(1)

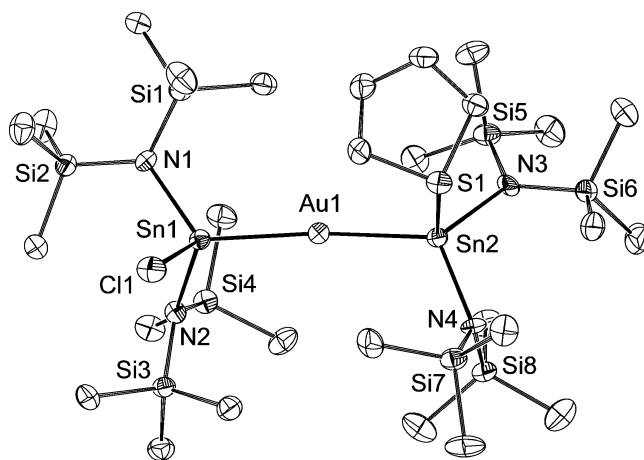


Figure 5. Molecular structure of compound **4** (thermal ellipsoids set at 40% probability). Hydrogen atoms have been omitted for clarity.

pyramidalization of the coordination sphere of the Sn2 atom and reduces the metalene N3–M2–N4 angle, which is 112.6(2)° in compound **3** (M = Ge) but only 107.7(3)° in

Table 3. Selected Interatomic Distances (Å) and Angles (deg) in Compounds 4–6

	4	5	6
Au1–Sn1	2.5711(5)	2.5767(4)	2.6087(2)
Au1–Sn2	2.5845(5)	2.5937(4)	2.6141(2)
Sn1–C25		2.183(5)	
Sn1–Cl1	2.412(2)		
Sn1–N1	2.081(6)	2.098(4)	2.101(2)
Sn1–N2	2.080(6)	2.106(5)	2.097(2)
Sn1–N5			2.115(2)
Sn2–N3	2.070(5)	2.080(5)	2.070(2)
Sn2–N4	2.092(6)	2.078(5)	2.080(2)
Sn2–S1	2.682(2)	2.718(2)	2.7154(7)
Sn1–Au1–Sn2	174.25(2)	172.59(2)	171.869(7)
Cl1–Sn1–N1	98.8(2)		
Cl1–Sn1–N2	103.3(2)		
Au1–Sn1–N1	122.2(2)	112.5(1)	110.13(7)
Au1–Sn1–N2	112.2(2)	113.3(1)	114.36(7)
C25–Sn1–N1		109.4(2)	
C25–Sn1–N2		100.9(2)	
Au1–Sn1–Cl1	107.80(6)		
Au1–Sn1–C25		111.3(2)	
N1–Sn1–N2	109.8(2)	108.8(2)	107.85(9)
N1–Sn1–N5			109.6(1)
N2–Sn1–N5			104.98(9)
Au1–Sn1–N5			109.73(6)
N3–Sn2–N4	107.7(3)	110.8(2)	108.72(9)
N3–Sn2–S1	97.5(2)	99.2(1)	97.99(7)
N4–Sn2–S1	101.2(2)	95.1(2)	93.48(7)
Au1–Sn2–N3	128.2(2)	116.9(1)	113.94(7)
Au1–Sn2–N4	115.8(2)	125.5(1)	127.56(7)
Au1–Sn2–S1	100.3(5)	101.65(3)	108.90(2)

compound **4** ($M = \text{Sn}$). In contrast, the coordination environment of the germylene Ge_2 atom in complex **3** is perfectly planar.

The higher tendency of $\text{Sn}(\text{HMDS})_2$ ligands, in comparison with that of $\text{Ge}(\text{HMDS})_2$ ligands, to retain THT (Scheme 2) may initially be intriguing. However, it has to be related to the greater metallic character (stronger Lewis acidity) and larger atomic volume (higher capacity to accommodate larger ligands) of tin. In fact, transition-metal stannylene complexes that have the tin atoms additionally attached to neutral ligands^{2e,23} are more represented in the chemical literature than their analogous germylene derivatives.²⁴ We are not aware of any transition-metal diaminometalene complex having the group 14 metal atom attached to a sulfur-donor ligand.

The room-temperature ^1H and $^{13}\text{C}\{^1\text{H}\}$ NMR spectra of the AuGe_2 compound **3** are in complete agreement with the solid-state molecular structure of this compound because they contain two singlet resonances assignable to the chemically inequivalent methyl groups of its germanate and germylene ligands. However, the room-temperature ^1H and $^{13}\text{C}\{^1\text{H}\}$ NMR spectra of the AuSn_2 compound **4** contain two broad singlets for the THT methylene groups and only a broad singlet for all of the SiMe_3 groups, indicating the occurrence of a dynamic process that makes the environments of the two tin atoms equivalent (on the NMR time scale). A variable-temperature ^1H NMR study in toluene- d_8 (Figure 6) showed that the SiMe_3 resonance of the room-temperature spectrum (0.44 ppm) is split into two very broad resonances at 193 K (0.61 and 0.28 ppm), while at this temperature, the resonances

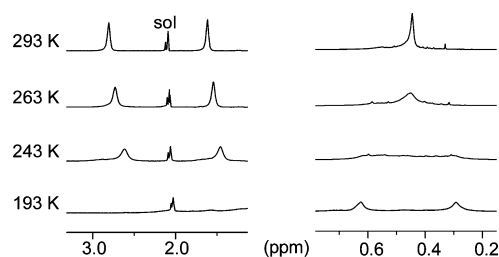
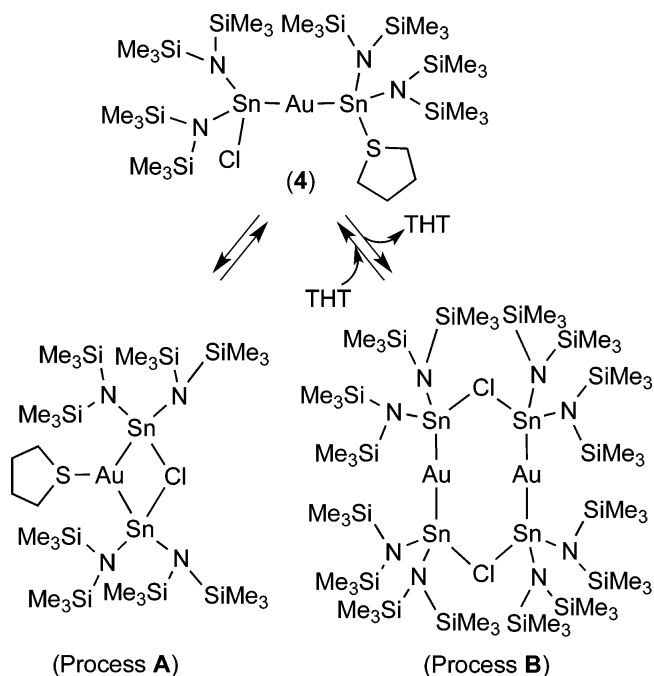


Figure 6. THT (left) and HMDS (right) regions of ^1H NMR spectra of compound **4** in toluene- d_8 at different temperatures (sol = toluene + residual protons of toluene- d_8 ; small sharp peaks are due to impurities).

of the THT ligand are almost unobserved. Therefore, the dynamic process is still active at 193 K.

The spectra shown in Figure 6 are a priori compatible with the two dynamic equilibria proposed in Scheme 3, which average the

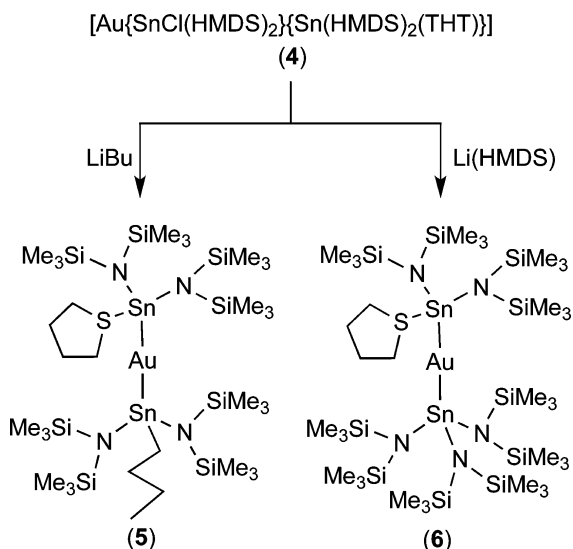
Scheme 3

ligand environment of the two tin atoms of **4** by forming symmetric chloride-bridged intermediates. Chloride-bridged diaminostannylene ligands have been previously observed in, for example, rhodium(I)²⁵ and palladium(II)²⁶ complexes. While process **A** is intramolecular and involves a symmetric AuSn_2 intermediate having an unusual²⁷ tricoordinated gold atom, process **B** involves the release of THT from **4** and dimerization of the resulting unsaturated species to form a symmetric Au_2Sn_4 intermediate. Interestingly, a variable-temperature ^1H NMR study using a 1:3 mixture of compound **4** and THT in toluene- d_8 indicated that the rate of the dynamic process is negatively affected by the presence of free THT in the solution. For example, the SiMe_3 region of the 193 K spectrum of Figure 3 is comparable to that of a spectrum of the **4**/THT mixture run at 233 K. Therefore, these data support the involvement of process **B** and rule out the participation of process **A**, which should not depend on the concentration of free THT.

The smaller atomic volume of germanium in comparison with that of tin and the great steric hindrance exerted by the large HMDS groups should make the formation of chloride-bridged Au_2Ge_4 dimeric species less favorable, similar to that depicted in Scheme 3 for $M = \text{Sn}$. In other words, we propose that the smaller volume of germanium is the differential factor that accounts for the fact that the AuGe_2 complex **3** is not involved in a dynamic process analogous to that observed in solution for the AuSn_2 complex **4**.

With the aim of confirming that the ability of the chloride ligand to bridge two metal atoms is an important factor in the dynamic process occurring in solutions of compound **4** and, thus, giving further support to our mechanistic proposal for the dynamic process, we decided to substitute the chloride ligand of compound **4** by other anionic groups with less tendency to bridge metal atoms. That was accomplished by treating compound **4** with LiBu and $\text{Li}(\text{HMDS})$. These reactions led to $[\text{Au}\{\text{SnBu}(\text{HMDS})_2\}\{\text{Sn}(\text{HMDS})_2(\text{THT})\}]$ (**5**) and $[\text{Au}\{\text{Sn}(\text{HMDS})_3\}\{\text{Sn}(\text{HMDS})_2(\text{THT})\}]$ (**6**) (Scheme 4). No pre-

Scheme 4



vious examples of transition-metal complexes containing $\text{SnBu}(\text{HMDS})_2$ or $\text{Sn}(\text{HMDS})_3$ stannate ligands have been hitherto reported.

The X-ray diffraction molecular structures of compounds **5** and **6** are shown in Figures 7 and 8, respectively. Selected interatomic distances and angles are provided in Table 3. In both structures, the atom connectivity is comparable to that of compound **4**, with the exception that the chloride ligand of the latter has been replaced by an *n*-butyl ligand in **5** or an HMDS ligand in **6**. The larger volume of the *n*-butyl and HMDS ligands, especially the latter, increases the crowding of the ligand shell of the tin atom to which they are attached, Sn1. This effect is clearly manifested by a lengthening of the Au1–Sn bond distances and a decrease of the Sn1–Au1–Sn2 and N1–Sn1–N2 bond angles on going from **4** to **5** and **6**.

The room-temperature ^1H and $^{13}\text{C}\{^1\text{H}\}$ NMR spectra of **5** and **6** contain the resonances of two types of HMDS ligands, indicating that those attached to a tin atom are not equivalent to those attached to the other tin atom. Therefore, in solution at room temperature, these complexes are not involved in a dynamic process similar to that observed for compound **4**.

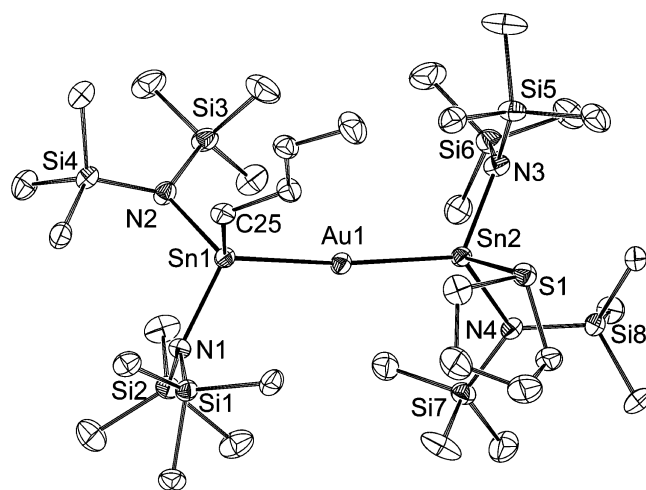


Figure 7. Molecular structure of compound **5** (thermal ellipsoids set at 40% probability). Hydrogen atoms have been omitted for clarity.

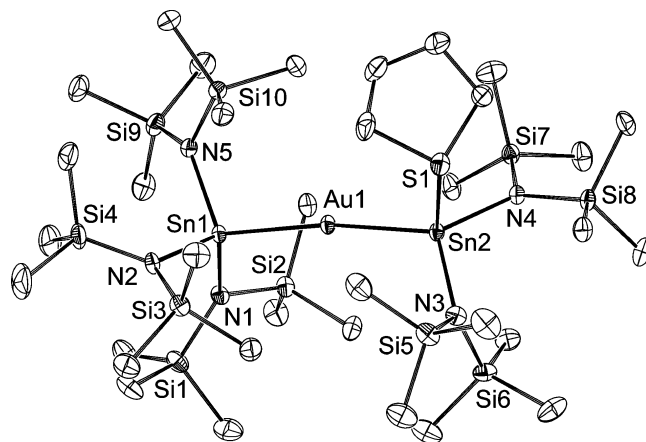


Figure 8. Molecular structure of compound **6** (thermal ellipsoids set at 40% probability). Hydrogen atoms have been omitted for clarity.

This result supports the proposal that the chloride ligand of compound **4** actively participates in the dynamic process observed in solutions of this complex.

CONCLUDING REMARKS

While the reactions of $M(\text{HMDS})_2$ ($M = \text{Ge}, \text{Sn}$) with $[\text{AuCl}(\text{THT})]$ do not result in displacement of the THT ligand but in insertion of the diaminometalene reagent into the Au–Cl bond to give the germanate and stannate derivatives $[\text{Au}\{M\text{Cl}(\text{HMDS})_2\}(\text{THT})]$ [$M = \text{Ge}$ (**1**), Sn (**2**)], the addition of a supplementary equivalent of $M(\text{HMDS})_2$ results in the subsequent displacement of THT from the gold coordination shell to give **3** and **4**. The greater metallic character and the larger atomic volume of tin with respect to those of germanium seem to be responsible for the presence of THT in compound **4** and its absence in compound **3**. Compounds **3** and **4** are the first examples of gold(I) complexes containing group 14 diaminometalenes as ligands.

In solution, compound **4** participates in a dynamic process that makes the environments of its two tin atoms equivalent on the NMR time scale. Data are provided that support that a reversible dissociation of THT and the bridging ability of the chloride ligand are essential features of this process.

Table 4. Crystal, Measurement, and Refinement Data for the Compounds Studied by X-ray Diffraction

	1	3·0.5C ₇ H ₈	4·C ₇ H ₈	5	6
formula	C ₁₆ H ₁₄ AuClGeN ₂ Si ₄	C ₂₄ H ₇₂ AuClGe ₂ N ₄ Si ₈ ·0.5C ₇ H ₈	C ₂₈ H ₈₀ AuClN ₄ SSi ₈ Sn ₂ ·C ₇ H ₈	C ₃₂ H ₈₉ AuN ₄ SSi ₈ Sn ₂	C ₃₄ H ₉₈ AuN ₅ SSi ₁₀ Sn ₂
fw	713.96	1065.24	1291.67	1221.20	1324.48
cryst syst	monoclinic	monoclinic	monoclinic	monoclinic	monoclinic
space group	<i>P</i> 2 ₁ / <i>n</i>	<i>C</i> 2/ <i>c</i>	<i>P</i> 2 ₁ / <i>n</i>	<i>P</i> 2 ₁ / <i>n</i>	<i>P</i> 2 ₁ / <i>c</i>
<i>a</i> , Å	8.8810(4)	20.4748(4)	19.8189(3)	11.3691(2)	22.3141(4)
<i>b</i> , Å	30.358(1)	14.6467(2)	11.8064(2)	31.7882(5)	13.6340(2)
<i>c</i> , Å	11.5384(4)	33.0448(6)	24.3764(3)	15.1248(3)	22.3095(4)
α , β , γ , deg	90, 112.595(5), 90	90, 97.558(2), 90	90, 90.667(1), 90	90, 90.029(1), 90	90, 118.386(2), 90
<i>V</i> , Å ³	2872.1(7)	9823.7(3)	5703.4(2)	5466.2(1)	5971.2(2)
<i>Z</i>	4	8	4	4	4
<i>F</i> (000)	1416	4326	2600	2464	2688
<i>D</i> _{calc} , g cm ⁻³	1.651	1.441	1.504	1.484	1.473
μ (Cu <i>K</i> α), mm ⁻¹	13.926	9.487	14.235	14.376	13.582
cryst size, mm	0.04 × 0.03 × 0.02	0.08 × 0.06 × 0.03	0.15 × 0.11 × 0.09	0.08 × 0.05 × 0.04	0.15 × 0.11 × 0.04
<i>T</i> , K	123(2)	123(2)	123(2)	123(2)	123(2)
θ range, deg	2.91–62.50	3.72–72.49	2.86–74.29	3.24–72.49	3.95–72.50
min/max <i>h</i> , <i>k</i> , <i>l</i>	–10/9, 0/34, 0/13	–19/24, –17/16, –40/40	–24/24, –14/12, –30/29	–13/13, –39/33, –13/18	–20/27, –16/10, –27/24
no. of colld reflns	4569	18831	27663	20904	22846
no. of unique reflns	4569	9565	11302	10629	11586
no. of reflns with <i>I</i> > 2 σ (<i>I</i>)	3541	8209	8644	9034	10797
no. of param/restraints	276/7	445/6	494/0	458/0	508/0
GOF (on <i>F</i> ²)	1.053	1.053	1.022	1.117	1.048
R1 [on <i>F</i> , <i>I</i> > 2 σ (<i>I</i>)]	0.075	0.031	0.050	0.038	0.026
wR2 (on <i>F</i> ² , all data)	0.208	0.088	0.143	0.118	0.068
min/max of $\Delta\rho$, e Å ⁻³	–3.931/3.314	–1.309/0.744	–1.716/2.371	–1.965/1.156	–1.283/1.233

The transformation of compound 4 into [Au{SnR(HMDS)₂}-{Sn(HMDS)₂(THT)}] [R = Bu (5), HMDS (6)] not only supports the proposal that the chloride ligand of compound 4 actively participates in the dynamic process observed in solutions of this complex but also demonstrates that the chloride of transition-metal SnCl(HMDS)₂ stannate complexes can be successfully replaced by other anionic groups. It is also noteworthy that no previous examples of transition-metal complexes containing SnBu(HMDS)₂ or Sn(HMDS)₃ stannate ligands have been hitherto reported.

EXPERIMENTAL SECTION

General Procedures. All reactions were carried out under nitrogen, using drybox and/or Schlenk vacuum-line techniques because of the high sensitivity of all reaction products to air and moisture. Toluene and hexane were dried over sodium diphenyl ketyl and distilled under nitrogen before use. [AuCl(THT)],^{21b} Ge(HMDS)₂,³ and Sn(HMDS)₂³ were prepared following published procedures. All remaining reagents were purchased from commercial sources. NMR spectra were run on a Bruker DPX-300 or Bruker AV-400 instrument, using as internal standards a residual protic solvent resonance for ¹H [δ (C₆D₅CHD₂) = 2.08; δ (C₆HD₅) = 7.16] and a solvent resonance for ¹³C [δ (C₆D₅CD₃) = 20.4; δ (C₆D₆) = 128.1]. Microanalyses were obtained from the University of Oviedo Microanalytical Service.

[Au{GeCl(HMDS)₂}(THT)] (1). Ge(HMDS)₂ (0.5 mL of a 0.35 M solution in toluene, 0.175 mmol) was added to a suspension of [AuCl(THT)] (50.9 mg, 0.159 mmol) in toluene (10 mL), and the mixture was stirred at room temperature for 2 h. The solvent was removed under reduced pressure to give a yellow oil that contained compound 1 and some toluene (NMR identification). A few X-ray-quality crystals of 1 were obtained by the slow evaporation of a concentrated toluene solution at room temperature. However, all attempts to isolate this compound as a pure solid (by precipitating it from various solvents at room temperature or below) were unsuccessful because they led to partial decomposition. ¹H NMR (C₆D₆, 300.1

MHz, 293 K): δ 2.36 (s, 4 H, CH₂), 1.23 (s, br, 4 H, CH₂), 0.60 (s, br, 36 H, Me). ¹³C{¹H} NMR (C₆D₆, 75.5 MHz, 293 K): δ 38.1 (s, CH₂), 30.6 (s, CH₂), 6.8 (s, Me).

[Au{SnCl(HMDS)₂}(THT)] (2). Sn(HMDS)₂ (0.5 mL of a 0.37 M solution in toluene, 0.185 mmol) was added to a suspension of [AuCl(THT)] (53.9 mg, 0.168 mmol) in toluene (10 mL), and the mixture was stirred at room temperature for 2 h. The solvent was removed under reduced pressure to give a dark-green oil that contained compound 2 and some toluene (NMR identification). All attempts to isolate this compound as a pure solid (by precipitating it from various solvents at room temperature or below) were unsuccessful because they led to partial decomposition. ¹H NMR (C₆D₆, 300.1 MHz, 293 K): δ 2.52 (s, br, 4 H, CH₂), 1.36 (s, br, 4 H, CH₂), 0.53 (s, 36 H, Me). ¹³C{¹H} NMR (C₆D₆, 75.5 MHz, 293 K): δ 37.9 (s, CH₂), 30.7 (s, CH₂), 6.9 (s, Me).

[Au{GeCl(HMDS)₂}(Ge(HMDS)₂)] (3). Ge(HMDS)₂ (1 mL of a 0.35 M solution in toluene, 0.350 mmol) was added to a suspension of [AuCl(THT)] (53.4 mg, 0.167 mmol) in toluene (10 mL), and the mixture was stirred at room temperature for 2 h. The solvent was removed under reduced pressure to give an orange oil. Slow evaporation at room temperature of a concentrated toluene solution deposited X-ray-quality crystals of 3·0.5C₇H₈ (123 mg, 69%). Anal. Calcd for C₂₄H₇₂AuClGe₂N₄Si₈·0.5C₇H₈ (1065.25): C, 31.01; H, 7.19; N, 5.26. Found: C, 31.13; H, 7.17; N, 5.32. ¹H NMR (C₆D₆, 300.1 MHz, 293 K): δ 0.63 (s, 36 H, Me), 0.31 (s, 36 H, Me). ¹³C{¹H} NMR (C₆D₆, 75.5 MHz, 293 K): δ 6.9 (s, Me), 5.5 (s, Me).

[Au{SnCl(HMDS)₂}(Sn(HMDS)₂(THT))] (4). Sn(HMDS)₂ (1 mL of a 0.37 M solution in toluene, 0.370 mmol) was added to a suspension of [AuCl(THT)] (56.4 mg, 0.176 mmol) in toluene (10 mL), and the mixture was stirred at room temperature for 2 h. The solvent was removed under reduced pressure to give an orange oil. X-ray-quality crystals of 4·C₇H₈ were obtained by maintaining at –20 °C a concentrated toluene solution (186 mg, 76%). Anal. Calcd for C₂₈H₈₀AuClN₄SSi₈Sn₂·C₇H₈ (1291.69): C, 32.55; H, 6.87; N, 4.34. Found: C, 32.59; H, 6.90; N, 4.31. ¹H NMR (C₆D₆, 300.1 MHz, 293 K): δ 2.74 (s, br, 4 H, CH₂), 1.52 (s, br, 4 H, CH₂), 0.49 (s, 72 H, Me).

$^{13}\text{C}\{^1\text{H}\}$ NMR (C_6D_6 , 75.5 MHz, 293 K): δ 37.2 (s, CH_2), 31.1 (s, CH_2), 6.9 (s, Me).

$[\text{Au}\{\text{SnBu}(\text{HMDS})_2\}_2\{\text{Sn}(\text{HMDS})_2(\text{THT})\}]$ (**5**). LiBu (110 μL of a 1.6 M solution in hexane, 0.176 mmol) was dropwise added to a solution of compound **4** (0.176 mmol) in toluene (10 mL) kept at -78°C . The mixture was stirred for 1 h while it was allowed to reach room temperature. The solvent was removed under reduced pressure to give a dark-brown oil, which contained compound **5** as the major hydrogen-containing reaction product (NMR identification). X-ray-quality crystals of this compound were obtained by maintaining at -4°C a concentrated toluene solution (110 mg, 51%). Anal. Calcd for $\text{C}_{32}\text{H}_{89}\text{AuN}_3\text{Si}_8\text{Sn}_2$ (1221.21): C, 31.47; H, 7.35; N, 4.59. Found: C, 31.49; H, 7.38; N, 4.56. ^1H NMR (C_6D_6 , 300.1 MHz, 293 K): δ 2.92 (s, br, 4 H, CH_2 of THT), 1.85 (m, 2 H, CH_2 of Bu), 1.50–1.48 (m, 8 H, 2 CH_2 of THT and 2 CH_2 of Bu), 1.02 (t, $J = 7$ Hz, 3 H, Me of Bu), 0.48 (s, 36 H, Me of HMDS), 0.32 (s, 36 H, Me of HMDS). $^{13}\text{C}\{^1\text{H}\}$ NMR (C_6D_6 , 75.5 MHz, 298 K): δ 37.0 (s, CH_2 of THT), 31.0 (s, CH_2 of THT), 30.9 (s, CH_2 of Bu), 30.8 (s, CH_2 of Bu), 28.2 (s, CH_2 of Bu), 14.4 (s, Me of Bu), 7.1 (s, Me of HMDS), 6.3 (s, Me of HMDS).

$[\text{Au}\{\text{Sn}(\text{HMDS})_3\}_2\{\text{Sn}(\text{HMDS})_2(\text{THT})\}]$ (**6**). Li(HMDS) $_2$ (68 μL of a 1.0 M solution in hexane, 0.068 mmol) was dropwise added to a solution of compound **4** (0.067 mmol) in toluene (2 mL) kept at -78°C . The mixture was stirred for 1 h while it was allowed to reach room temperature. The solvent was removed under reduced pressure to give a dark-brown oil, which contained compound **6** as the major hydrogen-containing reaction product (NMR identification). X-ray-quality crystals of this compound were obtained by maintaining at -4°C a concentrated toluene solution (39 mg, 44%). Anal. Calcd for $\text{C}_{34}\text{H}_{98}\text{AuN}_3\text{Si}_{10}\text{Sn}_2$ (1324.48): C, 30.83; H, 7.46; N, 5.29. Found: C, 30.86; H, 7.50; N, 5.25. ^1H NMR (C_6D_6 , 300.1 MHz, 293 K): δ 2.67 (s, br, 4 H, CH_2), 1.41 (s, br, 4 H, CH_2), 0.61 (s, 36 H, Me), 0.30 (s, 54 H, Me). $^{13}\text{C}\{^1\text{H}\}$ NMR (C_6D_6 , 75.5 MHz, 293 K): δ 35.7 (s, CH_2), 30.5 (s, CH_2), 8.1 (s, Me), 5.7 (s, Me).

X-ray Diffraction Analyses. Crystals of **1**, $3\text{-}0.5\text{C}_7\text{H}_8$, $4\text{-C}_7\text{H}_8$, **5**, and **6** were analyzed by X-ray diffraction. A selection of crystal, measurement, and refinement data are given in Table 4. Diffraction data were collected on an Oxford Diffraction Xcalibur Onyx Nova single-crystal diffractometer. Empirical absorption corrections for $3\text{-}0.5\text{C}_7\text{H}_8$, $4\text{-C}_7\text{H}_8$, **5**, and **6** were applied using the SCALE3 ABSPACK algorithm as implemented in *CrysAlisPro RED*.²⁸ The XABS2²⁹ empirical absorption correction was applied for **1**. The structures were solved using the program *SIR-97*.³⁰ Isotropic and full-matrix anisotropic least-squares refinements were carried out using *SHELXL*.³¹ The Au(THT) fragment of compound **1** was found disordered over two positions in a 83:17 ratio, with restraints on the geometrical parameters of the THT molecules being required. The solvent molecule of $3\text{-}0.5\text{C}_7\text{H}_8$ was disordered about a center of symmetry and required restraints on its geometrical parameters. All non-hydrogen atoms were refined anisotropically, except the carbon atoms of the 17% occupancy THT molecule of **1**, which were kept isotropic because of their tendency to give nonpositive definite ellipsoids. The molecular plots were made with the *PLATON* program package.³² The *WINGX* program system³³ was used throughout the structure determinations. CCDC deposition numbers: 866820 (**1**), 866819 ($3\text{-}0.5\text{C}_7\text{H}_8$), 866816 ($4\text{-C}_7\text{H}_8$), 866817 (**5**), and 866818 (**6**).

■ ASSOCIATED CONTENT

■ Supporting Information

Crystallographic data in CIF format. This material is available free of charge via the Internet at <http://pubs.acs.org>.

■ AUTHOR INFORMATION

Corresponding Author

*E-mail: jac@uniovi.es (J.A.C.), pga@uniovi.es (P.G.-A.).

Notes

The authors declare no competing financial interest.

■ ACKNOWLEDGMENTS

This work has been supported by the Spanish MICINN-FEDER Projects CTQ2010-14933 and DELACIERVA-09-05 and the European Union Marie Curie Action FP7-2010-RG-268329.

■ REFERENCES

- (1) For reviews on acyclic and/or cyclic group 14 diaminometalenes as ligands in transition-metal complexes, see: (a) Asay, M.; Jones, C.; Driess, M. *Chem. Rev.* **2011**, *111*, 354. (b) Nagendran, S.; Roesky, H. W. *Organometallics* **2008**, *27*, 457. (c) Zabala, A. V.; Hahn, F. E. *Eur. J. Inorg. Chem.* **2008**, 5165. (d) Kühn, O. *Coord. Chem. Rev.* **2004**, *248*, 411. (e) Gehrhus, B.; Lappert, M. F. *J. Organomet. Chem.* **2001**, *617*, 209. (f) Haaf, M.; Schmedake, T. A.; West, R. *Acc. Chem. Res.* **2000**, *33*, 704. (g) Lappert, M. F.; Rowe, R. S. *Coord. Chem. Rev.* **1990**, *100*, 267. (h) Petz, W. *Chem. Rev.* **1986**, *86*, 1019. (i) Lappert, M. F.; Power, P. P. *J. Chem. Soc., Dalton Trans.* **1985**, 51.
- (2) For representative articles that contain an extensive literature coverage on group 14 diaminometalenes as ligands in transition-metal complexes, see: (a) Cabeza, J. A.; García-Álvarez, P.; Polo, D. *Inorg. Chem.* **2012**, *51*, 2569. (b) Cabeza, J. A.; García-Álvarez, P.; Polo, D. *Inorg. Chem.* **2011**, *50*, 5165. (c) Mansell, S. M.; Herber, R. H.; Nowik, I.; Ross, D. H.; Russell, C. A.; Wass, D. F. *Inorg. Chem.* **2011**, *50*, 2252. (d) Ullah, F.; Kühn, O.; Bajor, G.; Veszpremi, T.; Jones, P. G.; Heinicke, J. *Eur. J. Inorg. Chem.* **2009**, 221. (e) Hahn, F. E.; Zabala, A. V.; Pape, T.; Hepp, A.; Tonner, R.; Haunschild, R.; Frenking, G. *Chem.—Eur. J.* **2008**, *14*, 10716. (f) Saur, I.; Rima, G.; Miqueu, K.; Gornitzka, H.; Barrau, J. *J. Organomet. Chem.* **2003**, *672*, 77. (g) Bazinet, P.; Yap, G. P. A.; Richeson, D. S. *J. Am. Chem. Soc.* **2001**, *123*, 11162.
- (3) (a) Harris, D. H.; Lappert, M. F. *J. Chem. Soc., Chem. Commun.* **1974**, 895. (b) Gynane, M. J. S.; Harris, D. H.; Lappert, M. F.; Power, P. P.; Rivière, P.; Rivière-Baudet, M. *J. Chem. Soc., Dalton Trans.* **1977**, 2004.
- (4) Denk, M.; Lennon, R.; Hayashi, R.; West, R.; Belyakov, A. V.; Verne, H. P.; Haaland, A.; Wagner, M.; Metzler, N. *J. Am. Chem. Soc.* **1994**, *116*, 2691.
- (5) Pfeiffer, J.; Maringgele, W.; Noltmeyer, M.; Meller, A. *Chem. Ber.* **1989**, *122*, 245.
- (6) Schuefler, C. D.; Zuckerman, C. D. *J. Am. Chem. Soc.* **1974**, *96*, 7160.
- (7) Veith, M.; Grosser, M. *Z. Naturforsch.* **1982**, *B37*, 1375.
- (8) For excellent reviews on the chemistry of cyclic carbenes and related species, see: (a) Melaimi, M.; Soleihavoup, M.; Bertrand, G. *Angew. Chem., Int. Ed.* **2010**, *49*, 8810. (b) Hahn, F. E.; Jahnke, M. C. *Angew. Chem., Int. Ed.* **2008**, *47*, 3122.
- (9) Arduengo, A. J. III; Harlow, R. L.; Kline, M. *J. Am. Chem. Soc.* **1991**, *113*, 361.
- (10) Avent, A. G.; Gehrhus, B.; Hitchcock, P. B.; Lappert, M. F.; Maciejewsky, H. *J. Organomet. Chem.* **2003**, *686*, 321.
- (11) York, J. T.; Young, V. G.; Tolman, W. B. *Inorg. Chem.* **2006**, *45*, 4191.
- (12) Arai, H.; Nakadate, F.; Mochida, K. *Organometallics* **2009**, *28*, 4909.
- (13) Leung, W.-P.; So, C.-W.; Chong, K.-H.; Kan, K.-W.; Chan, H.-S.; Mak, T. *Organometallics* **2006**, *25*, 2851.
- (14) (a) Dias, H. V. R.; Wang, X.; Diyabalange, H. *Inorg. Chem.* **2005**, *44*, 7322. (b) Dias, H. V. R.; Ayers, A. E. *Polyhedron* **2002**, *21*, 611. (c) Ayers, A. E.; Dias, H. V. R. *Inorg. Chem.* **2002**, *41*, 3259. (d) Dias, H. V. R.; Wang, Z. *Inorg. Chem.* **2000**, *39*, 3890.
- (15) Anandhi, U.; Sharp, P. R. *Inorg. Chim. Acta* **2006**, *359*, 3521.
- (16) Lutz, M.; Findeis, B.; Haukka, M.; Pakkanen, T. A.; Gade, L. H. *Eur. J. Inorg. Chem.* **2001**, 3155.
- (17) Findeis, B.; Gade, L. H.; Scowen, I. J.; McPartlin, M. *Inorg. Chem.* **1997**, *36*, 960.
- (18) Findeis, B.; Contel, M.; Gade, L. H.; Laguna, M.; Gimeno, M. C.; Scowen, I. J.; McPartlin, M. *Inorg. Chem.* **1997**, *36*, 2386.

(19) Contel, M.; Hellmann, K. W.; Gade, L. H.; Laguna, M.; Scowen, I. J.; McPartlin, M. *Inorg. Chem.* **1996**, *35*, 3713.

(20) For reviews on the catalytic uses of carbene (mostly diaminocarbene) gold complexes, see: (a) Gaillard, S.; Cazin, C. S. J.; Nolan, S. P. *Acc. Chem. Res.* **2012**, *45*, DOI: 10.1021/ar200188f. (b) Nolan, S. P. *Acc. Chem. Res.* **2011**, *44*, 91. (c) Díez-González, S.; Marion, N.; Nolan, S. P. *Chem. Rev.* **2009**, *109*, 3612. (d) Marion, N.; Nolan, S. P. *Chem. Soc. Rev.* **2008**, *37*, 1776.

(21) [AuCl(THT)] was first mentioned in a 1972 paper, but a detailed and easy synthetic procedure was not reported until 1989: (a) Allen, E. A.; Wilkinson, W. *Spectrochim. Acta* **1972**, *A28*, 2257. (b) Usón, R.; Laguna, A.; Laguna, M. *Inorg. Synth.* **1989**, *26*, 85.

(22) (a) Chow, A. L.-F.; So, M.-H.; Lu, W.; Zhu, N.-Y.; Che, C.-M. *Chem.—Asian J.* **2011**, *6*, 544. (b) Jahnke, M. C.; Paley, J.; Hupka, F.; Weigand, J. J.; Hahn, F. E. *Z. Naturforsch.* **2009**, *B64*, 1458. (c) Deetlefs, M.; Raubenheimer, H. G.; Esterhuysen, M. W. *Catal. Today* **2002**, *72*, 259.

(23) For example, see: (a) Jambor, R.; Kasna, B.; Koller, S. G.; Strohmann, C.; Schurmann, M.; Jurkschat, K. *Eur. J. Inorg. Chem.* **2010**, 902. (b) Zabula, A. V.; Pape, T.; Hepp, A.; Hahn, E. F. *Dalton Trans.* **2008**, 5886. (c) Martincova, J.; Dostal, L.; Ruzicka, A.; Taraba, J.; Jambor, R. *Organometallics* **2007**, *26*, 4102. (d) Khrustalev, V. N.; Portnyagin, I. A.; Nechaev, M. S.; Bukalov, S. S.; Leites, L. A. *Dalton Trans.* **2007**, 3489. (e) Jurkschat, K.; Tzschach, A.; Meunier-Piret, J.; van Meerssche, M. J. *Organomet. Chem.* **1998**, *349*, 143. (f) Brice, M. D.; Cotton, F. A. *J. Am. Chem. Soc.* **1973**, *95*, 4529.

(24) For example, see: (a) Okazaki, M.; Kimura, H.; Komuro, T.; Okada, H.; Tobita, H. *Chem. Lett.* **2007**, *36*, 990. (b) Tobita, H.; Ishiyama, K.; Kawano, Y.; Inomata, S.; Ogino, H. *Organometallics* **1998**, *17*, 789. (c) Knorr, M.; Hallauer, E.; Huch, V.; Veith, M.; Braunstein, P. *Organometallics* **1996**, *15*, 3868.

(25) Veith, M.; Stahl, L.; Huch, V. *Inorg. Chem.* **1989**, *28*, 3278.

(26) Veith, M.; Müller, A.; Stahl, L.; Nötzel, M.; Jarczyk, M.; Huch, V. *Inorg. Chem.* **1996**, *35*, 3848.

(27) Gimeno, M. C.; Laguna, A. *Chem. Rev.* **1997**, *97*, 511.

(28) *CrysAlisPro RED*, version 1.171.34.36; Oxford Diffraction Ltd.: Oxford, U.K., 2010.

(29) Parkin, S.; Moezzi, B.; Hope, H. *J. Appl. Crystallogr.* **1995**, *28*, 53.

(30) Altomare, A.; Burla, M. C.; Camalli, M.; Cascarano, G.; Giacovazzo, C.; Guagliardi, A.; Moliterni, A. G. C.; Polidori, G.; Spagna, R. *J. Appl. Crystallogr.* **1999**, *32*, 115.

(31) *SHELXL*: Sheldrick, G. M.; *Acta Crystallogr.* **2008**, *A64*, 112.

(32) Spek, A. L. *PLATON: A Multipurpose Crystallographic Tool*, version 1.15; University of Utrecht: Utrecht, The Netherlands, 2008.

(33) *WinGX*, version 1.80.05: Farrugia, L. J. *J. Appl. Crystallogr.* **1999**, *32*, 837.

Artículo IV

“Expanding the Coordination Chemistry of Donor-Stabilized Group-14 Metalenes”

COMMUNICATION

Expanding the coordination chemistry of donor-stabilized group-14 metalenest

Cite this: *Dalton Trans.*, 2013, **42**, 1329Received 2nd October 2012,
Accepted 6th November 2012

DOI: 10.1039/c2dt32654j

www.rsc.org/dalton

Javier A. Cabeza,* Pablo García-Álvarez* and Diego Polo

The transformation of an amidinate germylene, equipped with just one accessible lone pair of electrons on the Ge atom, into a bidentate 4-electron donor $\kappa^2\text{Ge},\text{N}$ -ligand, has been achieved for the first time, opening new doors to the non-carbene-like coordination chemistry of heavier carbene analogues.

Heavier carbene analogues, also known as group-14 metalenes (MR_2 ; M = Si, Ge, Sn, or Pb; R = anionic group), are species of fundamental interest in main-group chemistry.^{1–3} They are very reactive molecules that, as a result of their dual Lewis acid–base character,⁴ display a unique and rich reactivity (able to coordinate to transition-metal (TM) complexes, activate small molecules, insert into organic and inorganic σ -bonds, add to unsaturated substrates, form donor–acceptor adducts, *etc.*) that has been the subject of several recent reviews.^{2,3} However, the current development of their coordination chemistry, although covering a wide range of TMs,^{3,5} is far from the maturity achieved by that of their carbene relatives and, particularly, that of *N*-heterocyclic carbenes (NHCs).⁶ This comparative underdevelopment can be attributed to some synthetic problems⁷ and to the weaker M–TM bond of MR_2 –TM complexes (whose strength decreases on going down along the group-14 column of the Periodic Table⁸), which have discouraged the investigation of their potential catalytic applications (only a few MR_2 –TM complexes have already been recognized as active homogeneous catalysts⁹), while many NHC–TM complexes were soon demonstrated to be excellent catalysts for important organic transformations.¹⁰ Having all this in mind, it is clear that further development of the coordination chemistry of group-14 metalenes is necessary because their unique properties may lead to metal complexes having outstanding structural, reactivity and/or catalytic features.

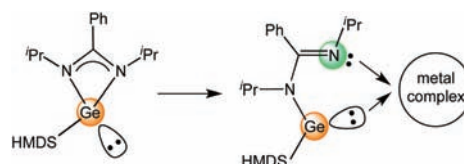
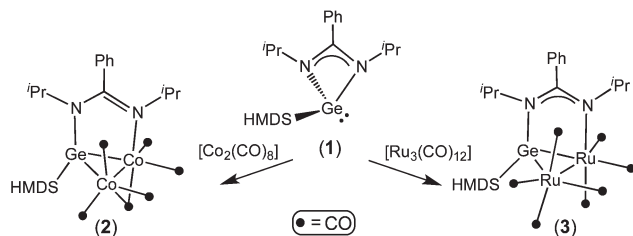


Fig. 1 Schematic transformation of an intramolecularly donor-stabilized group-14 metalene into a bidentate ligand.

It has been shown that interaction of an MR_2 molecule with a strong Lewis base provides additional stabilization of the metalene moiety.^{11,12} For example, the elusive and poorly sterically-shielded SiX_2 molecules (X = Cl^{11d} and Br^{11e}) have been recently isolated and characterized as NHC– SiX_2 adducts and have also been used as SiX_2 -transfer reagents.^{11a} In this field, continuing our efforts to synthesize new, more robust and versatile transition metal complexes derived from group 14-metalenes¹³ and inspired by several reports revealing the lability of such donor–acceptor adducts,^{14,15} we have now focused our attention on donor-stabilized group-14 metalenes in which the MR_2 fragment is intramolecularly stabilized by additional interaction of the M atom with a donor group (Fig. 1, left).¹² We reasoned that these donor-stabilized metalenes can potentially behave as bidentate ligands through intermediate release of the donor group from the M atom (Fig. 1, right), thus providing a synthetically attractive way to obtain more robust MR_2 –TM complexes. However, to achieve such bidentate behaviour is a challenging task because the coordination of a donor-stabilized metalene to a TM through the metalene M atom increases the Lewis acidity of this atom, thus strengthening its interaction with the donor group. An example that well illustrates this behaviour has been recently reported by Tacke *et al.*, who have shown that the bis(amidinato)silylene $\text{Si}\{\text{PhC}(\text{N}^i\text{Pr})_2\}_2$, which contains one chelating and one terminal amidinate group, closes its pendant imino arm towards the silicon atom upon its coordination of a tungsten centre.^{14a} In fact, although the coordination chemistry of intramolecularly donor-stabilized MR_2 molecules is well represented in the

Departamento de Química Orgánica e Inorgánica-IUQOEM, Universidad de Oviedo-CSIC, E-33071 Oviedo, Spain. E-mail: jac@uniovi.es, pga@uniovi.es

† Electronic supplementary information (ESI) available: Synthesis and characterization details. CCDC 901726 (2) and 901725 (3). For ESI and crystallographic data in CIF or other electronic format see DOI: 10.1039/c2dt32654j



Scheme 1 Reactivity of $\text{Ge}(\text{HMDS})\{\text{PhC}(\text{N}^i\text{Pr})_2\}$ (**1**) with $[\text{Co}_2(\text{CO})_8]$ and $[\text{Ru}_3(\text{CO})_{12}]$.

chemical literature,^{15–17} they generally behave as terminal 2-electron donor ligands.

We now report that a readily accessible donor-stabilized germylene, namely $\text{Ge}(\text{HMDS})\{\text{PhC}(\text{N}^i\text{Pr})_2\}$ (**1**; HMDS = $\text{N}(\text{SiMe}_3)_2$; $\text{PhC}(\text{N}^i\text{Pr})_2 = N,N'$ -bis(iso-propyl)benzamidinate), which contains a very bulky HMDS group and a strained four-membered GeNCN ring, is likely to open that ring by breaking a Ge-N bond and forming a TM-N bond when treated with TM complexes, such as $[\text{Co}_2(\text{CO})_8]$ or $[\text{Ru}_3(\text{CO})_{12}]$, leading to stable products that contain a bidentate 4-electron donor $\kappa^2\text{Ge}, N$ -ligand. These results show for the first time that the hemilabile character of widely-used and easy-to-synthesise amidinate group-14 metalenes can be used to prepare robust easy-to-handle TM derivatives, opening new doors to the coordination chemistry of heavier carbene analogues.

The bulky donor-stabilized germylene $\text{Ge}(\text{HMDS})\{\text{PhC}(\text{N}^i\text{Pr})_2\}$ (**1**; Scheme 1) was easily synthesised in two steps from GeCl_2 -dioxane, $\text{Li}\{\text{PhC}(\text{N}^i\text{Pr})_2\}$ and $\text{Li}(\text{HMDS})$.¹⁸ The chelating arrangement of the amidinate fragment on the germanium atom of **1** was established by NMR spectroscopy, which confirmed that its two iso-propyl groups are symmetry-related (C_s).

Compound **1** reacted with $[\text{Co}_2(\text{CO})_8]$ (1 : 1 mole ratio, 1 h, 60 °C, toluene solution) to give the bimetallic trinuclear derivative $[\text{Co}_2\{\mu\text{-}\kappa^2\text{Ge}, N\text{-Ge}(\text{HMDS})\{\text{PhC}(\text{N}^i\text{Pr})_2\}\}(\mu\text{-CO})(\text{CO})_5]$ (**2**), which was isolated in 71% yield (Scheme 1). The molecular structure of **2**, determined by an X-ray diffraction analysis, is shown in Fig. 2. The complex contains a Co_2Ge triangle that has a Co-Ge edge bridged by the amidinate ligand in such a way that the mean plane of the Ge1-N2-C4-N1-Co1 five-membered ring forms a dihedral angle of $112.59(3)^\circ$ with the Co_2Ge plane. The C–N bond distances within the amidinate group indicate the presence of a localized C=N double bond involving the N atom attached to Co (C4-N1 1.311(3) Å, C4-N2 1.364(3) Å), which indicates that the Co1 atom is attached to an imine-type ligand. Similar C–N bond length distributions have been reported for bimetallic cobalt complexes containing $\kappa^1 N$ -amidinate ligands.¹⁸ The germanium atom adopts a very distorted tetrahedral arrangement, being bonded to the two Co atoms (with an acute Co1-Ge1-Co2 angle of $66.67(2)^\circ$) and to two N atoms (one belonging to the amidinate backbone, N2, and the other corresponding to the HMDS group, N3). The coordination sphere of **2** is completed by six CO ligands, five of which are terminal while one is bridging the Co–Co edge.

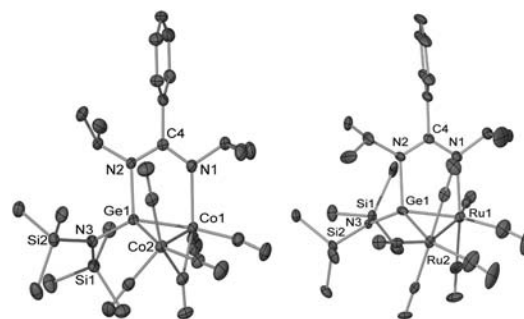


Fig. 2 Molecular structures of $[\text{Co}_2\{\mu\text{-}\kappa^2\text{Ge}, N\text{-Ge}(\text{HMDS})\{\text{PhC}(\text{N}^i\text{Pr})_2\}\}(\mu\text{-CO})(\text{CO})_5]$ (**2**, left) and $[\text{Ru}_2\{\mu\text{-}\kappa^2\text{Ge}, N\text{-Ge}(\text{HMDS})\{\text{PhC}(\text{N}^i\text{Pr})_2\}\}(\text{CO})_7]$ (**3**, right). Selected bond lengths (Å) for **2**: Co1-Co2 2.5624(5), Co1-N1 2.067(2), Co1-Ge1 2.2983(4), Co2-Ge1 2.3633(4), Ge1-N2 1.885(2), Ge1-N3 1.845(2), N1-C4 1.311(3), N2-C4 1.364(3), N3-Si1 1.766(2), N3-Si2 1.754(2). Selected bond lengths (Å) involving non-disordered atoms for **3**: Ru1-N1 2.202(4), Ru1-Ge1 2.3957(7), Ge1-N2 1.925(4), N1-C4 1.325(6), N2-C4 1.337(6).

The reaction of **1** with $[\text{Ru}_3(\text{CO})_{12}]$ (3 h, 90 °C, toluene solution) took place with cluster fragmentation and led to the bimetallic trinuclear derivative $[\text{Ru}_2\{\mu\text{-}\kappa^2\text{Ge}, N\text{-Ge}(\text{HMDS})\{\text{PhC}(\text{N}^i\text{Pr})_2\}\}(\text{CO})_7]$ (**3**) (Scheme 1), which was isolated in 63% yield using a 1 to 2/3 mole ratio of the reagents. The molecular structure of **3**, determined by X-ray diffraction (Fig. 2), is essentially analogous to that of **2**, except for the number and coordination mode of the carbonyl ligands, exhibiting also the same $\mu\text{-}\kappa^2\text{Ge}, N$ -coordination for the germylene ligand. In this case, the amidinate C–N bond distances show a higher degree of delocalization of the N=C double bond than in **2**, as the C4-N1 and C4-N2 distances of **3** differ by only 0.01 Å. In the crystal, the fragments $\text{Ru}(\text{CO})_4$, HMDS and the amidinate iso-propyl groups were found to be disordered over two positions and, although their connectivity is unequivocal, this disorder prevents a discussion of their associated metrical parameters.

The solution ^1H and $^{13}\text{C}\{^1\text{H}\}$ NMR spectra of **2** and **3** are in agreement with a $\kappa^2\text{Ge}, N$ -coordination mode of their germylene ligand, as two different sets of signals are observed for each N^iPr arm. The observed inequivalence of the HMDS SiMe_3 groups reflects that rotation of the HMDS group around the corresponding N-Ge bond is not allowed and confirms the existence of steric hindrance between the HMDS and the nearby groups.

Notably, in contrast with the vast majority of TM complexes containing group-14 metalenes as ligands, which are moisture and/or air-sensitive regardless of their TM,^{3,5} compound **3** is stable in air for several weeks and compound **2** can be handled in air for a few minutes (being therefore as stable as all cobalt(0) complexes, which are air-sensitive).

Therefore, the bulky donor-stabilized germylene **1**, initially equipped with just one accessible lone pair of electrons, has been proven capable of acting as a bidentate 4-electron donor ligand. This behaviour clearly contrasts with the general tendency that coordination of a metalene to a TM increases the Lewis acidity of the M atom³ and, thus, the strength of its interaction with a donor group.^{14a}

In our case, a key factor accounting for the $\kappa^2\text{Ge},N$ -coordination mode observed for the germylene ligand in **2** and **3** is the bulkiness of the HMDS group, that, in order to release the steric hindrance generated by the coordination of the Ge atom to the corresponding TM, forces the transfer of one arm of the amidinate group to the TM. In fact, it has been previously shown that related amidinate group-14 metalenes, all of them equipped with less bulky substituents at the M centre, behave as monodentate M-donor ligands.¹⁶ An additional factor that may also help release the donor group from the Ge atom is the presence of more than one metal atom in the TM reagent, since this allows the formation of a bridging germylene, a common coordination mode for germylenes.^{13,19} However, it seems that the presence of the HMDS group in **1** is also crucial to get germylene-bridged products because it has been reported that the reactions of related but less bulky amidinate group-14 metalenes with $[\text{Fe}_2(\text{CO})_9]$,^{12f,16h} $[\text{Co}_2(\text{CO})_8]$,^{16a} $[\text{Mn}_2(\text{CO})_{10}]$ ^{16c,e} and $[\text{Re}_2(\text{CO})_{10}]$ ^{16c,e} afford mononuclear derivatives containing a monodentate metalene ligand.

The results we have herein reported open new doors to the non-carbene-like coordination chemistry of heavier carbene analogues. We are currently performing experimental and theoretical work aimed at shedding more light on the herein reported ligand behaviour of intramolecularly stabilized group-14 metalenes.

This work has been supported by the Spanish MEC-FEDER grants CTQ2010-14933 and DELACIERVA-09-05, and the European Union Marie Curie action FP7-2010-RG-268329.

Notes and references

- 1 V. Y. Lee and A. Sekiguchi, *Organometallic Compounds of Low Coordinate Si, Ge, Sn and Pb: From Phantom Species to Stable Compounds*, Wiley, Chichester, UK, 2010.
- 2 For recent reviews on the chemistry of MR_2 species, see, for example: (a) S. K. Mandal and H. W. Roesky, *Acc. Chem. Res.*, 2012, **45**, 298; (b) S. Yao, Y. Xiong and M. Driess, *Organometallics*, 2011, **30**, 1748; (c) M. Kira, *Chem. Commun.*, 2010, **46**, 2893; (d) Y. Mizuhata, T. Sasamori and N. Tokitoh, *Chem. Rev.*, 2009, **109**, 3479.
- 3 For recent reviews on the chemistry of MR_2 species (including TM derivatives), see, for example: (a) M. Asay, C. Jones and M. Driess, *Chem. Rev.*, 2011, **111**, 354; (b) A. V. Zabula and F. E. Hahn, *Eur. J. Inorg. Chem.*, 2008, 5165; (c) W.-P. Leung, K.-W. Kan and K.-H. Chong, *Coord. Chem. Rev.*, 2007, **251**, 2253; (d) O. Kühn, *Coord. Chem. Rev.*, 2004, **248**, 411; (e) B. Gehrhus and M. F. Lappert, *J. Organomet. Chem.*, 2001, **617–618**, 209.
- 4 MR_2 molecules have an ambiphilic character as they are equipped with nucleophilic (lone pair of electrons) and electrophilic (vacant p orbital) reactive sites at the metalene atom.
- 5 For reviews on the TM chemistry of MR_2 species, see, for example: (a) M. F. Lappert and R. S. Rowe, *Coord. Chem. Rev.*, 1990, **100**, 267; (b) W. Petz, *Chem. Rev.*, 1986, **86**, 1019.
- 6 See, for example: (a) M. Melaimi, M. Soleihavoup and G. Bertrand, *Angew. Chem., Int. Ed.*, 2010, **49**, 8810; (b) F. E. Hahn and M. C. Jahnke, *Angew. Chem., Int. Ed.*, 2008, **47**, 3122.
- 7 The synthesis of MR_2 -TM complexes commonly requires air-sensitive MR_2 reagents, while the use of pure NHCs is often unnecessary for the preparation of NHC-TM complexes (for example, imidazol-2-ylidenes can be generated *in situ* from readily available imidazolium salts).
- 8 See, for example: (a) T. A. N. Nguyen and G. Frenking, *Chem.-Eur. J.*, 2012, **18**, 12733; (b) H. Arp, J. Baumgartner, C. Marschner, P. Zark and T. Müller, *J. Am. Chem. Soc.*, 2012, **134**, 10864; (c) C. Boehme and G. Frenking, *Organometallics*, 1998, **17**, 5801.
- 9 (a) W. Wang, S. Inoue, S. Enthaler and M. Driess, *Angew. Chem., Int. Ed.*, 2012, **51**, 6167; (b) B. M. Day, P. W. Dyer and M. P. Coles, *Dalton Trans.*, 2012, **41**, 7457; (c) M. Zhang, X. Liu, C. Shi, C. Ren, Y. Ding and H. W. Roesky, *Z. Anorg. Allg. Chem.*, 2008, **634**, 1755; (d) A. Fürstner, H. Krause and W. C. Lehmann, *Chem. Commun.*, 2001, 2372.
- 10 See, for example: (a) S. Díez-González, N. Marion and S. P. Nolan, *Chem. Rev.*, 2009, **109**, 3612; (b) F. A. Glorius, *Top. Organomet. Chem.*, 2007, **21**, 1; (c) *N-Heterocyclic Carbenes in Synthesis*, ed. S. P. Nolan, Wiley-VCH, Weinheim, Germany, 2006.
- 11 For intermolecularly donor-stabilized MR_2 molecules, see: (a) Y. Xiong, S. Yao, S. Inoue, E. Irran and M. Driess, *Angew. Chem., Int. Ed.*, 2012, **51**, 10074; (b) H. Arp, J. Baumgartner and C. Marschner, *J. Am. Chem. Soc.*, 2012, **134**, 6409; (c) S. Yao, Y. Xiong, W. Wang and M. Driess, *Chem.-Eur. J.*, 2011, **17**, 4890; (d) R. S. Ghadwal, H. W. Roesky, S. Merkel, J. Henn and D. Stalke, *Angew. Chem., Int. Ed.*, 2009, **48**, 5683; (e) A. C. Filippou, O. Chernov and G. Schnakenburg, *Angew. Chem., Int. Ed.*, 2009, **48**, 5687; (f) B. Gehrhus, P. B. Hitchcock and M. F. Lappert, *J. Chem. Soc., Dalton Trans.*, 2000, 3094.
- 12 For intramolecularly donor-stabilized MR_2 molecules, see: (a) Y. Yang, N. Zhao, H. Zhu and H. W. Roesky, *Organometallics*, 2012, **31**, 1958; (b) J. Berthe, J. M. Garcia, E. Ocando, T. Kato, N. Saffon-Merceron, A. De Cózar, F. P. Cossío and A. Baceiredo, *J. Am. Chem. Soc.*, 2011, **133**, 15930; (c) M. Henn, V. Deáky, S. Krabbe, M. Schürmann, M. H. Prosenc, S. Herres-Pawlis, B. Mahieu and K. Jurkschat, *Z. Anorg. Allg. Chem.*, 2011, **637**, 211; (d) H. Aarii, F. Nakadate, K. Mochida and T. Kawashima, *Organometallics*, 2011, **30**, 4471; (e) S. S. Sen, H. W. Roesky, D. Stern, J. Henn and D. Stalke, *J. Am. Chem. Soc.*, 2010, **132**, 1123; (f) S. S. Sen, M. P. Kritzler-Kosch, S. Nagendran, H. W. Roesky, T. Beck, A. Pal and R. Herbst-Irmer, *Eur. J. Inorg. Chem.*, 2010, 5304; (g) K. Izod, J. Stewart, E. R. Clark, W. McFarlane, B. Allen, W. Clegg and R. W. Harrington, *Organometallics*, 2009, **28**, 3327; (h) S. Nagendran, S. S. Sen, H. W. Roesky, D. Koley, H. Grubmüller, A. Pal and R. Herbst-Irmer, *Organometallics*, 2008, **27**, 5459; (i) W. C. Jones, R. P. Rose and

- A. Stasch, *Dalton Trans.*, 2008, 2871; (j) W.-P. Leung, C.-W. So, Y.-S. Wu, H.-W. Li and T. C. W. Mak, *Eur. J. Inorg. Chem.*, 2005, 3, 513.
- 13 (a) J. A. Cabeza, P. García-álvarez and D. Polo, *Inorg. Chem.*, 2012, 51, 2569; (b) J. A. Cabeza, P. García-álvarez and D. Polo, *Inorg. Chem.*, 2011, 50, 6195; (c) J. A. Cabeza, J. M. Fernández-Colinas, P. García-álvarez and D. Polo, *Inorg. Chem.*, 2012, 51, 3896.
- 14 For adduct dissociation on donor-stabilized MR₂ molecules, see: (a) K. Junold, J. A. Baus, C. Burschka and R. Tacke, *Angew. Chem., Int. Ed.*, 2012, 51, 7020; (b) H. Vaňkátová, L. Broeckert, F. De Proft, R. Olejník, J. Turek, Z. Padělková and A. Ružička, *Inorg. Chem.*, 2011, 50, 9454; (c) S. Khan, S. S. Sen, D. Kratzert, G. Tavčar, H. W. Roesky and D. Stalke, *Eur. J. Inorg. Chem.*, 2011, 1370; (d) D. Matioszek, N. Katir, N. Saffon and A. Castel, *Organometallics*, 2010, 29, 3039; (e) N. N. Zemlyansky, I. V. Borisova, M. G. Kuznetsova, V. N. Khrustalev, Y. A. Ustynyuk, M. S. Nechaev, V. V. Lunin, J. Barrau and G. Rima, *Organometallics*, 2003, 22, 1675; (f) S. R. Foley, C. Bensimon and D. S. Richeson, *J. Am. Chem. Soc.*, 1997, 119, 10359; (g) Ref. 12g; (h) H.-X. Yeong, S.-H. Zhang, H.-W. Xi, J.-D. Guo, K. H. Lim, S. Nagase and C.-W. So, *Chem.-Eur. J.*, 2012, 18, 2685.
- 15 For adduct dissociation on donor-stabilized MR₂ ligands coordinated to TMs, see: (a) J. M. García, E. Ocando-Mavárez, T. Kato, D. Santiago Coll, A. Briceño, N. Saffon-Merceron and A. Baceiredo, *Inorg. Chem.*, 2012, 51, 8187; (b) N. Seidel, K. Jacob and A. K. Fischer, *Organometallics*, 2001, 20, 578; (c) H. Handwerker, C. Leis, R. Probst, P. Bissinger, A. Grohmann, P. Kiprof, E. Herdtweck, J. Blumel, N. Auner and C. Zybilla, *Organometallics*, 1993, 12, 2162.
- 16 For examples of transition metal complexes containing amidinate type group-14 metalenes, see: (a) R. Azhakar, R. S. Ghadwal, H. W. Roesky, J. Hey and D. Stalke, *Chem.-Asian J.*, 2012, 7, 528; (b) R. Azhakar, R. S. Ghadwal, H. W. Roesky, H. Wolf and D. Stalke, *J. Am. Chem. Soc.*, 2012, 134, 2423; (c) R. Azhakar, S. P. Sarish, H. W. Roesky, J. Hey and D. Stalke, *Inorg. Chem.*, 2011, 50, 5039; (d) G. Tavčar, S. S. Sen, R. Azhakar, A. Thorn and H. W. Roesky, *Inorg. Chem.*, 2010, 49, 10199; (e) R. Azhakar, H. W. Roesky, J. J. Holstein and B. Dittrich, *Dalton Trans.*, 2012, 41, 12096; (f) W. Wang, S. Inoue, E. Irra and M. Driess, *Angew. Chem., Int. Ed.*, 2012, 51, 3691; (g) W. Wang, S. Inoue, S. Yao and M. Driess, *J. Am. Chem. Soc.*, 2010, 132, 15890; (h) W. Yang, H. Fu, H. Wang, M. Chen, Y. Ding, H. W. Roesky and A. Jana, *Inorg. Chem.*, 2009, 48, 5058; (i) Ref. 9a, 12f,i and 14a,d.
- 17 For recent examples, see: (a) L. Iovkova-Berends, T. Berends, T. Zöllner, D. Schollmeyer, G. Bradtmöller and K. Jurkschat, *Eur. J. Inorg. Chem.*, 2012, 3463; (b) A. Jana, S. P. Sarish, H. W. Roesky, C. Schulzke and P. P. Samuel, *Chem. Commun.*, 2010, 46, 707; (c) A. Meltzer, S. Inoue, C. Präsang and M. Driess, *J. Am. Chem. Soc.*, 2010, 132, 3038; (d) J. Martincová, R. Jambor, M. Schürmann, K. Jurkschat, J. Honzíček and F. A. A. Paz, *Organometallics*, 2009, 28, 4778; (e) W.-P. Leung, C.-W. So, K.-H. Chong, K.-W. Kan, H.-S. Chan and T. C. W. Mak, *Organometallics*, 2006, 25, 2851; (f) I. Saur, S. Garcia-Alonso, H. Gornitzka, V. Lemierre, A. Chrostowska and J. Barrau, *Organometallics*, 2005, 24, 2988; (g) H. V. R. Dias, X. Wang and H. V. K. Diyabalanage, *Inorg. Chem.*, 2005, 44, 7322.
- 18 (a) S.-T. Liu, H. Yan, X. Hu and Q.-W. Liu, *Huaxue Xuebao (Chin.)*, *Acta Chim. Sin.*, 1992, 50, 1173; (b) R. D. Adams, D. F. Chodosh, N. M. Golembeski and E. C. Weissman, *J. Organomet. Chem.*, 1979, 172, 251.
- 19 See, for example: R. D. Adams and E. Trufan, *Organometallics*, 2010, 29, 4346.

ELECTRONIC SUPPLEMENTARY INFORMATION

for

Expanding the coordination chemistry of donor-stabilized group-14 Metalenes

Javier A. Cabeza,* Pablo García-Álvarez,* and Diego Polo

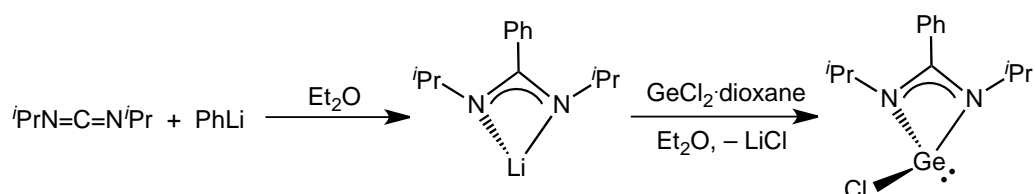
General methods	2
Synthesis and characterization of $\text{GeCl}\{\text{PhC}(\text{N}^i\text{Pr})_2\}$	3
Synthesis and characterization of 1	5
Synthesis and characterization of 2	7
Synthesis and characterization of 3	9

General methods

All manipulations were performed under nitrogen gas using standard glove-box and Schlenk-vacuum line techniques. Solvents were dried over sodium diphenyl ketyl (hexane, diethyl ether, toluene) and distilled under nitrogen before use. PhLi (1.8 M solution in dibutyl ether), Li(HMDS) (1.0 M solution in hexanes), *N,N'*-bis(*iso*-propyl)carbodiimide, GeCl₂·dioxane and [Co₂(CO)₈] were purchased from Aldrich Chemicals. [Ru₃(CO)₁₂] was prepared following a published method.¹ The reactions were routinely monitored by solution IR spectroscopy (carbonyl stretching region; Perkin-Elmer Paragon 1000) and spot TLC (silica gel). All reaction products were vacuum-dried for several hours prior to being weighed and analysed. NMR spectra were run on 300 MHz Bruker DPX-300 and Bruker AV-300, using as standards a protic residual solvent resonance for ¹H [$\delta(\text{C}_6\text{HD}_5) = 7.16$] and a solvent resonance for ¹³C [$\delta(\text{C}_6\text{D}_6) = 128.1$]. Microanalyses were obtained from the University of Oviedo Microanalytical Service (Perkin-Elmer 2400 instrument). FAB mass spectra of pure samples of **2** and **3** were obtained from the University of A Coruña Mass Spectrometric Service (VG Autospec double-focusing mass spectrometer operating in the FAB+ mode; positive ions were produced with a standard Cs⁺ gun at *ca.* 30 kV; 3-nitrobenzyl alcohol (NBA) was used as matrix). In all cases, the given MS data refer to the most abundant molecular ion isotopomer.

Synthesis and characterization of $\text{GeCl}\{\text{PhC}(\text{N}^i\text{Pr})_2\}$

PhLi (10.8 mL, 19.4 mmol, 1.8 M in dibutyl ether) was added to a solution of *N,N'*-bis(*iso*-propyl)carbodiimide (3.0 mL, 19.4 mmol) in diethyl ether (100 mL) at -78°C . The solution was allowed to warm up to room temperature and then stirred for 4 h. The resulting pale yellow solution was cooled down again to -78°C and then added dropwise to a stirred suspension of $\text{GeCl}_2\cdot\text{dioxane}$ (4.49 g, 19.4 mmol) in diethyl ether (20 mL) at -78°C . The reaction mixture was allowed to warm up to room temperature and then stirred for 3 days. The precipitated LiCl was filtered off, the solvent was removed, and the resulting residue was extracted into hexane (2 x 30 mL). Solvent removal allowed the isolation of $\text{GeCl}\{\text{PhC}(\text{N}^i\text{Pr})_2\}$ as a white powder (5.35 g, 89 %).



Anal. Calcd. for $\text{C}_{13}\text{H}_{19}\text{ClGeN}_2$ (311.37): C, 50.15; H, 6.15; N, 9.00. Found: C, 50.21; H, 6.26; N, 8.87. ^1H NMR (C_6D_6 , 300.1 MHz, 293 K): $\delta = 7.00\text{--}6.87$ (m, 5 H, 5 CH of Ph), 3.32 (sept, $J = 6.3$ Hz, 2 H, 2 CH of ^iPr), 1.11 (d, $J = 6.3$ Hz, 6 H, 2 CH_3 of ^iPr), 0.90 (d, $J = 6.3$ Hz, 6 H, 2 CH_3 of ^iPr). $^{13}\text{C}\{^1\text{H}\}$ NMR (C_6D_6 , 75.5 MHz, 293 K): $\delta = 172.7$ (NCN), 140.3 (C_{ipso} of Ph), 130.2 (CH of Ph), 129.0 (2 CH of Ph), 127.2 (2 CH of Ph), 47.2 (2 CH of ^iPr), 25.4 (2 CH_3 of ^iPr), 24.2 (2 CH_3 of ^iPr).

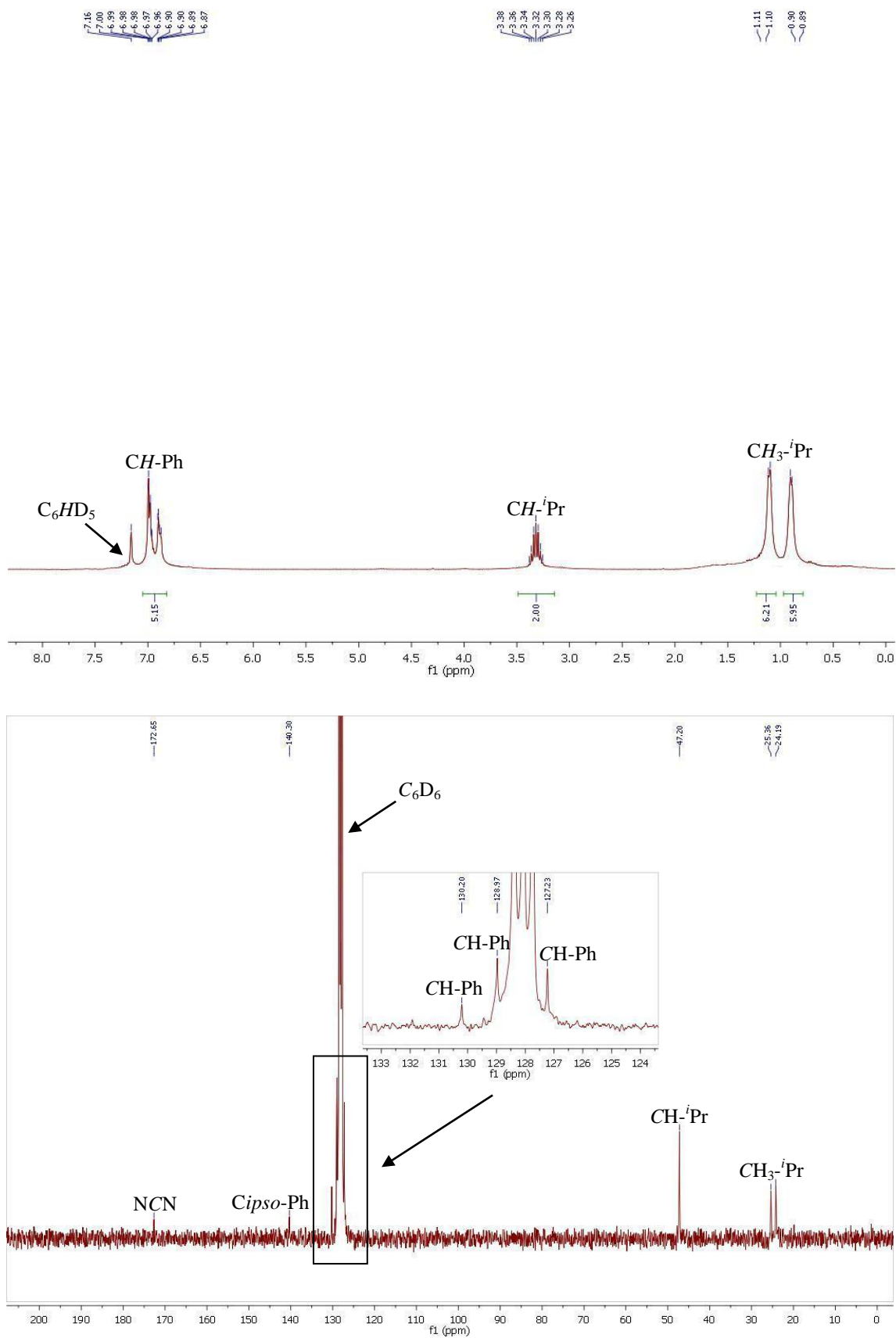
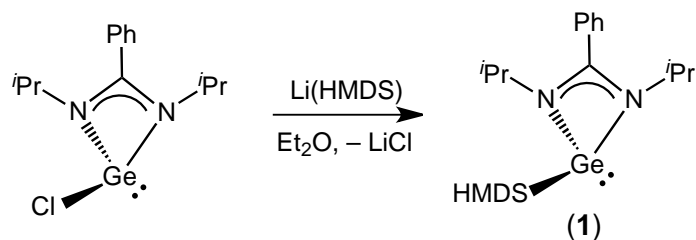


Figure S1. ^1H (top) and $^{13}\text{C}\{^1\text{H}\}$ (bottom) NMR spectra of $\text{GeCl}\{\text{PhC}(\text{N}^i\text{Pr})_2\}$ in C_6D_6 (20°C).

Synthesis and characterization of Ge(HMDS){PhC(N^{*i*}Pr)₂} (1)

Li(HMDS) (12.8 mL, 1.0 M in hexanes, 12.80 mmol) was added to a solution of GeCl{PhC(N^{*i*}Pr)₂} (4.00 g, 12.80 mmol) in diethyl ether (30 mL) at -78 °C. The resulting suspension was allowed to warm up to room temperature and then stirred for 12 h. The solvents were removed under reduced pressure and the residue was extracted into hexane (2 x 30 mL). The solvent of the filtrate was removed to give **1** as a yellowish oily material (4.75 g, 85 %).



Anal. Calcd. for C₁₉H₃₇GeN₃Si₂ (436.30): C, 52.30; H, 8.55; N, 9.63. Found: C, 52.52; H, 8.70; N, 9.59. ¹H NMR (C₆D₆, 300.1 MHz, 293 K): δ = 7.05 (s, br, 5 H, 5 CH of Ph), 3.41 (sept, *J* = 6.4 Hz, 2 H, 2 CH of ^{*i*}Pr), 1.12 (d, *J* = 6.4 Hz, 6 H, 2 CH₃ of ^{*i*}Pr), 1.11 (d, *J* = 6.4 Hz, 6 H, 2 CH₃ of ^{*i*}Pr), 0.51 (s, 18 H, 6 CH₃ of HMDS). ¹³C{¹H} NMR (C₆D₆, 75.5 MHz, 293 K): δ = 164.6 (NCN), 134.9 (*C*_{ipso} of Ph), 129.5 (CH of Ph), 129.0 (2 CH of Ph), 127.2 (2 CH of Ph), 47.5 (2 CH of ^{*i*}Pr), 27.2 (2 CH₃ of ^{*i*}Pr), 24.5 (2 CH₃ of ^{*i*}Pr), 5.9 (6 CH₃ of HMDS).

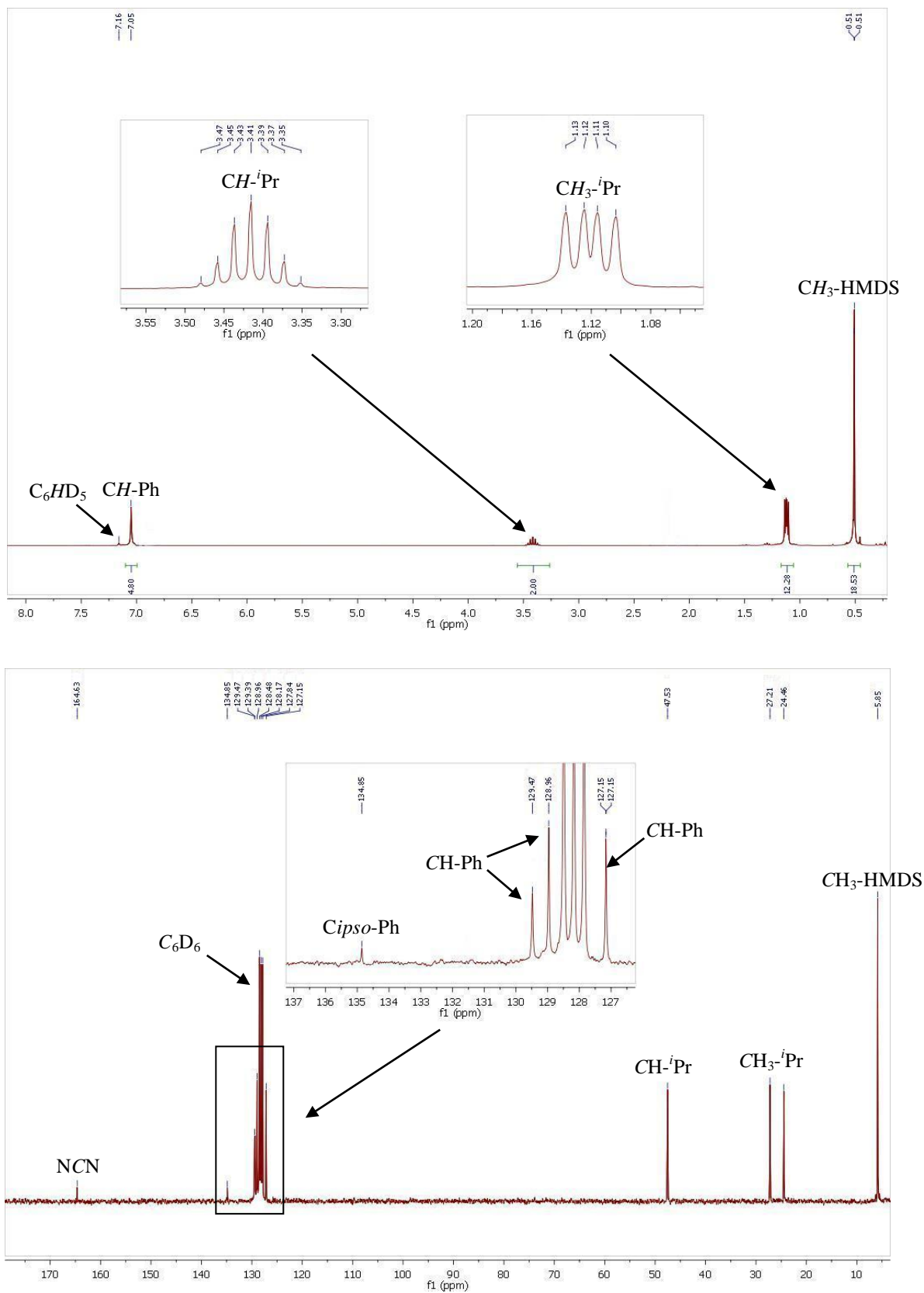
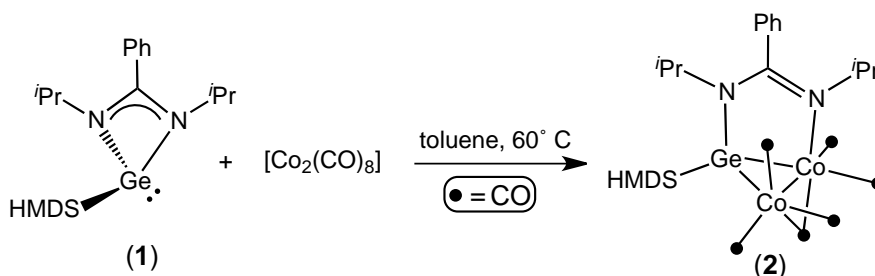


Figure S2. ^1H (top) and $^{13}\text{C}\{^1\text{H}\}$ (bottom) NMR spectra of **1** in C_6D_6 ($20\text{ }^\circ\text{C}$).

Synthesis and characterization of $[\text{Co}_2\{\mu\text{-}\kappa^2\text{Ge},\text{N-Ge}(\text{HMDS})(\text{PhC}(\text{N}^i\text{Pr})_2)\}(\mu\text{-CO})(\text{CO})_5]$ (**2**)

1 (0.8 mL of a 0.27 M solution in toluene, 0.216 mmol) was added to a solution of $[\text{Co}_2(\text{CO})_8]$ (73 mg, 0.214 mmol) in 20 mL of toluene and the mixture was stirred at 60 °C for 1 h. The initial dark red color changed to dark orange. Purification by flash chromatography eluting with hexane (2 x 5 cm silica gel column packed in hexane) furnished **2** as a light orange solid (110 mg, 71 %). Slow evaporation of a concentrated solution of **2** in hexane deposited crystals suitable for X-ray crystallographic analysis.



Anal. Calcd. for $\text{C}_{25}\text{H}_{37}\text{Co}_2\text{GeN}_3\text{O}_6\text{Si}_2$ (722.23): C, 41.58; H, 5.16; N, 5.82. Found: C, 41.69; H, 5.19; N, 5.70. (+)-FAB MS: $m/z = 722$ $[\text{M}]^+$. IR (toluene, cm^{-1}): $\nu_{\text{CO}} = 2058$ (m), 2017 (vs), 1996 (m), 1974 (m, br), 1814 (w, br). ^1H NMR (C_6D_6 , 300.1 MHz, 293 K): $\delta = 7.03\text{--}6.97$ (m, 5 H, 5 CH of Ph), 4.23 (m, 1 H, CH of ^iPr), 3.45 (m, 1 H, CH of ^iPr), 1.41 (d, $J = 6.4$ Hz, 3 H, CH_3 of ^iPr), 1.15 (d, $J = 6.5$ Hz, 3 H, CH_3 of ^iPr), 0.92 (d, $J = 6.5$ Hz, 3 H, CH_3 of ^iPr), 0.86 (d, $J = 6.6$ Hz, 3 H, CH_3 of ^iPr), 0.45 (s, 9 H, 3 CH_3 of HMDS), 0.36 (s, 9 H, 3 CH_3 of HMDS). $^{13}\text{C}\{^1\text{H}\}$ NMR (C_6D_6 , 75.5 MHz, 293 K): $\delta = 205.4$ (COs), 205.1 (COs), 167.3 (NCN), 135.9 (C_{ipso} of Ph), 129.0 (2 CH of Ph), 128.4 (CH of Ph), 128.2 (CH of Ph), 127.7 (CH of Ph), 54.7 (CH of ^iPr), 48.0 (CH of ^iPr), 24.8 (CH_3 of ^iPr), 23.9 (CH_3 of ^iPr), 23.7 (CH_3 of ^iPr), 23.5 (CH_3 of ^iPr), 5.5 (3 CH_3 of HMDS), 4.9 (3 CH_3 of HMDS).

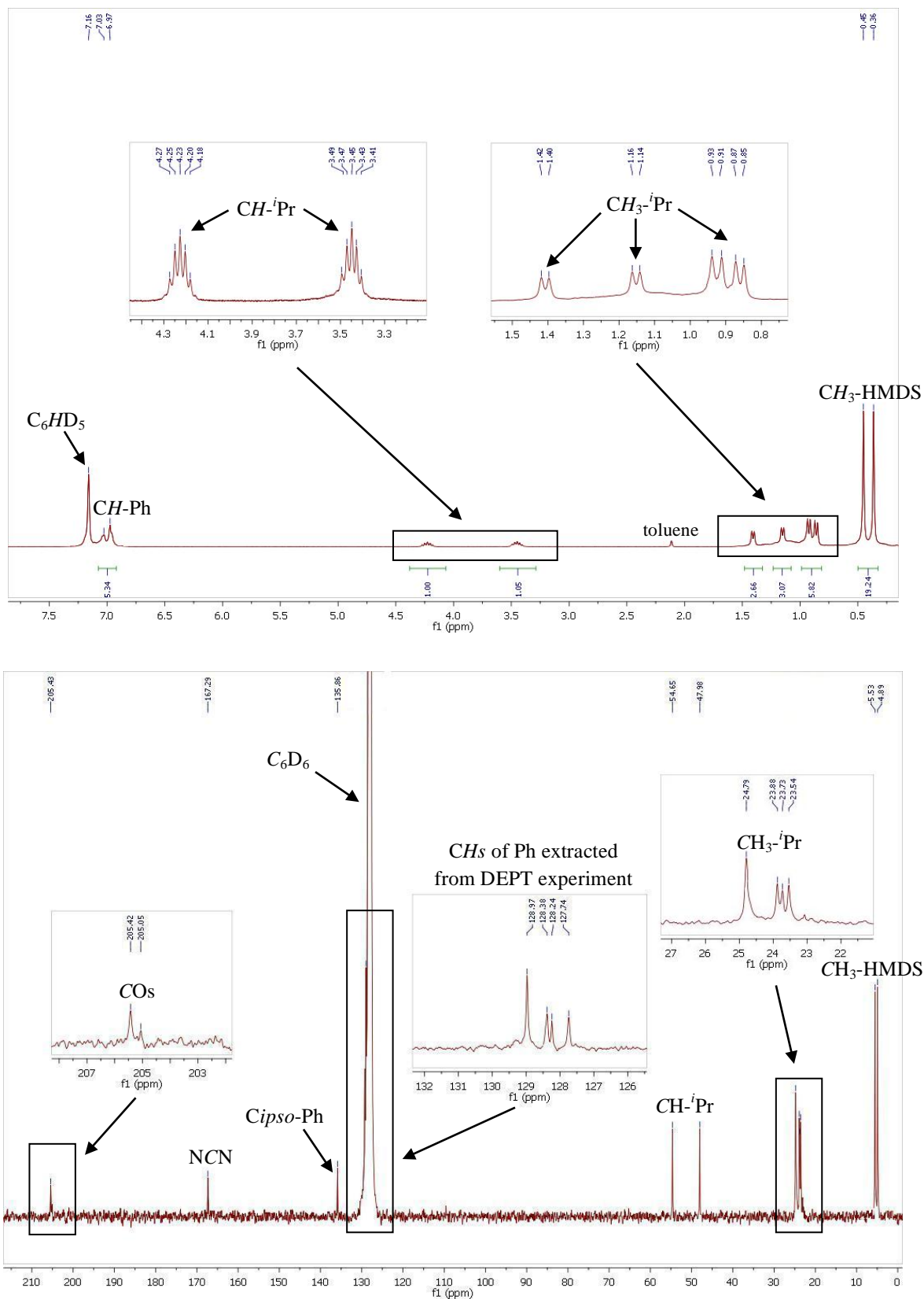
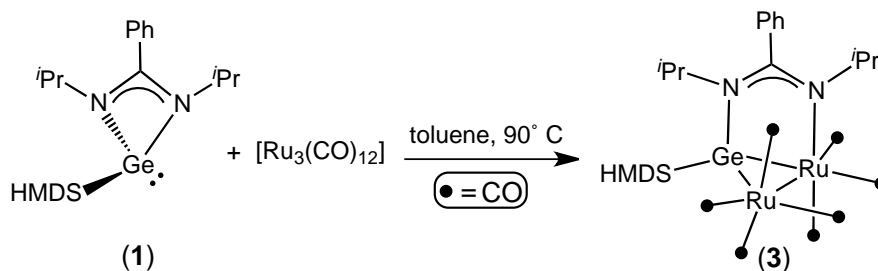


Figure S3. ^1H (top) and $^{13}\text{C}\{^1\text{H}\}$ (bottom) NMR spectra of **2** in C_6D_6 ($20\text{ }^\circ\text{C}$).

Synthesis and characterization of $[\text{Ru}_2\{\mu\text{-}\kappa^2\text{Ge}, N\text{-Ge(HMDS)(PhC(N}^i\text{Pr)}_2)\}(\text{CO})_7]$ (**3**)

1 (3.0 mL of a 0.35 M solution in toluene, 1.05 mmol) was added to a suspension of $[\text{Ru}_3(\text{CO})_{12}]$ (0.5 g, 0.8 mmol) in 20 mL of toluene and the mixture was stirred at 90 °C for 3 h. The initial orange color changed to dark red. Purification by flash chromatography eluting with hexane (2 x 5 cm silica gel column packed in hexane) furnished **3** as a light orange solid (620 mg, 62 %). Keeping a concentrated hexane solution of **3** at -20 °C afforded crystals suitable for X-ray crystallographic analysis.



Anal. Calcd. for $\text{C}_{26}\text{H}_{37}\text{GeN}_3\text{O}_7\text{Ru}_2\text{Si}_2$ (834.51): C, 37.42; H, 4.47; N, 5.04. Found: C, 37.53; H, 4.50; N, 4.89. (+)-FAB MS: $m/z = 751$ $[\text{M} - 3 \text{ CO}]^+$. IR (toluene, cm^{-1}): $\nu_{\text{CO}} = 2085$ (m), 2034 (vs), 2013 (m), 2002 (s), 1992 (m), 1973 (w), 1959 (w). ^1H NMR (C_6D_6 , 300.1 MHz, 293 K): $\delta = 6.97\text{--}6.83$ (m, 5 H, 5 CH of Ph), 3.88 (m, 1 H, CH of ^iPr), 3.41 (m, 1 H, CH of ^iPr), 1.15 (d, $J = 6.6$ Hz, 3 H, CH_3 of ^iPr), 1.06–1.03 (m, 6 H, 2 CH_3 of ^iPr), 0.80 (d, $J = 6.5$ Hz, 3 H, CH_3 of ^iPr), 0.52 (s, 18 H, 6 CH_3 of HMDS). $^{13}\text{C}\{^1\text{H}\}$ NMR (C_6D_6 , 75.5 MHz, 293 K): $\delta = 201.7$ (COs), 201.5 (COs), 200.2 (COs), 166.8 (NCN), 137.3 (C_{ipso} of Ph), 128.9 (CH of Ph), 128.5 (CH of Ph), 128.4 (CH of Ph), 127.7 (CH of Ph), 126.6 (CH of Ph), 55.7 (CH of ^iPr), 50.4 (CH of ^iPr), 26.5 (CH_3 of ^iPr), 24.6 (CH_3 of ^iPr), 24.4 (CH_3 of ^iPr), 22.8 (CH_3 of ^iPr), 6.5 (3 CH_3 of HMDS), 5.6 (3 CH_3 of HMDS).

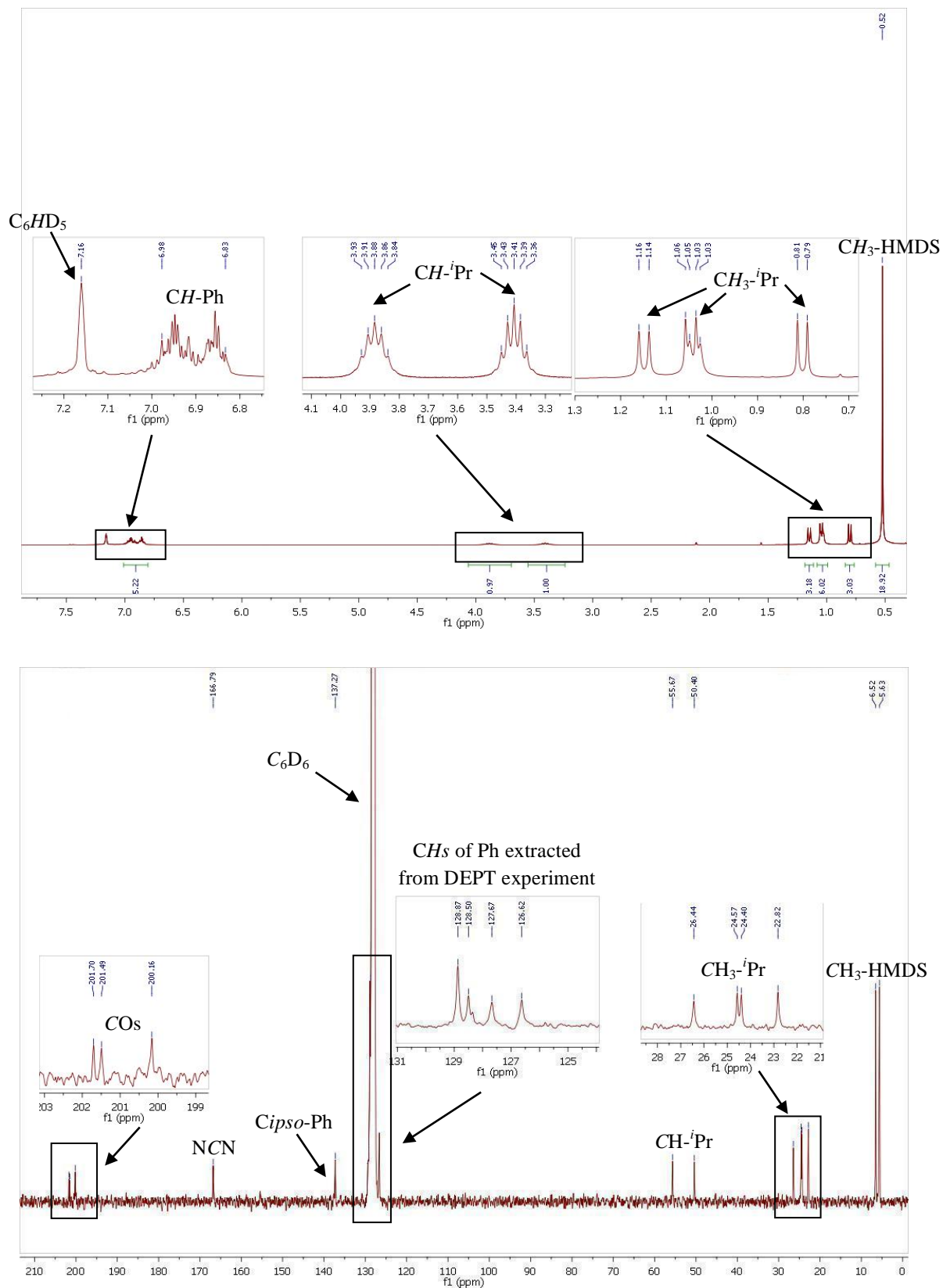


Figure S4. 1H (top) and $^{13}C\{^1H\}$ (bottom) NMR spectra of **3** in C_6D_6 ($20^\circ C$).

Artículo V

***“Reactivity Studies on a Binuclear Ruthenium(0)
Complex Equipped with a Bridging κ^2 N,Ge-
Amidinatogermylene Ligand”***

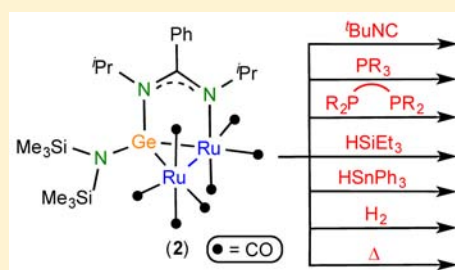
Reactivity Studies on a Binuclear Ruthenium(0) Complex Equipped with a Bridging κ^2N,Ge -Amidinogermylene Ligand

Javier A. Cabeza,^{*,†} José M. Fernández-Colinas,[†] Pablo García-Álvarez,^{*,†} Enrique Pérez-Carreño,[‡] and Diego Polo[†]

[†]Departamento de Química Orgánica e Inorgánica-IUQOEM, and [‡]Departamento de Química Física y Analítica, Universidad de Oviedo-CSIC, E-33071 Oviedo, Spain

Supporting Information

ABSTRACT: The amidinatogermylene-bridged diruthenium(0) complex $[\text{Ru}_2\{\mu-\kappa^2\text{Ge},N\text{-Ge}(\text{Pr}_2\text{bzam})(\text{HMDS})\}(\text{CO})_7]$ (**2**; $\text{Pr}_2\text{bzam} = N,N'$ -bis(*iso*-propyl)benzaminate; $\text{HMDS} = \text{N}(\text{SiMe}_3)_2$) reacted at room temperature with ${}^t\text{BuNC}$ and PMe_3 to give $[\text{Ru}_2\{\mu-\kappa^2\text{Ge},N\text{-Ge}(\text{Pr}_2\text{bzam})(\text{HMDS})\}(\text{L})(\text{CO})_6]$ ($\text{L} = {}^t\text{BuNC}$, **3**; PMe_3 , **4**), which contain the new ligand in an axial position on the Ru atom that is not attached to the amidinato fragment. At 70 °C, **2** reacted with PPh_3 , PMe_3 , dppm , and dppe to give the equatorially substituted derivatives $[\text{Ru}_2\{\mu-\kappa^2\text{Ge},N\text{-Ge}(\text{Pr}_2\text{bzam})(\text{HMDS})\}(\text{L})(\text{CO})_6]$ ($\text{L} = \text{PPh}_3$, **5**; PMe_3 , **6**) and $[\text{Ru}_2\{\mu-\kappa^2\text{Ge},N\text{-Ge}(\text{Pr}_2\text{bzam})(\text{HMDS})\}(\mu-\kappa^2\text{P},\text{P}'\text{-L}_2)(\text{CO})_5]$ ($\text{L}_2 = \text{dppm}$, **7**; dppe , **8**). HSiEt_3 and HSnPh_3 were oxidatively added to complex **2** at 70 °C, leading to the coordinatively unsaturated products $[\text{Ru}_2(\text{ER}_3)(\mu\text{-H})\{\mu-\kappa^2\text{Ge},N\text{-Ge}(\text{Pr}_2\text{bzam})(\text{HMDS})\}(\text{CO})_5]$ ($\text{ER}_3 = \text{SiEt}_3$, **9**; SnPh_3 , **10**), which easily reacted with ${}^t\text{BuNC}$ and CO to give the saturated derivatives $[\text{Ru}_2(\text{ER}_3)(\mu\text{-H})\{\mu-\kappa^2\text{Ge},N\text{-Ge}(\text{Pr}_2\text{bzam})(\text{HMDS})\}(\text{BuNC})(\text{CO})_5]$ ($\text{ER}_3 = \text{SiEt}_3$, **11**; SnPh_3 , **12**) and $[\text{Ru}_2(\text{ER}_3)(\mu\text{-H})\{\mu-\kappa^2\text{Ge},N\text{-Ge}(\text{Pr}_2\text{bzam})(\text{HMDS})\}(\text{CO})_6]$ ($\text{ER}_3 = \text{SiEt}_3$, **13**; SnPh_3 , **14**), respectively. Compounds **9–14** have their ER_3 group on the Ru atom that is not attached to the amidinato fragment. In contrast, the reaction of **2** with H_2 at 70 °C led to the unsaturated tetranuclear complex $[\text{Ru}_4(\mu\text{-H})_2\{\mu-\kappa^2\text{Ge},N\text{-Ge}(\text{Pr}_2\text{bzam})(\text{HMDS})\}_2(\text{CO})_{10}]$ (**15**), which also reacted with ${}^t\text{BuNC}$ and CO to give the saturated derivatives $[\text{Ru}_4(\mu\text{-H})_2\{\mu-\kappa^2\text{Ge},N\text{-Ge}(\text{Pr}_2\text{bzam})(\text{HMDS})\}_2(\text{L})_2(\text{CO})_{10}]$ ($\text{L} = {}^t\text{BuNC}$, **16**; CO , **17**). All tetraruthenium complexes contain an unbridged metal–metal connecting two germylene-bridged diruthenium units. Under CO atmosphere, complex **17** reverted to compound **2**. All of the coordinatively unsaturated products (**9**, **10**, and **15**) have their unsaturation(s) located on the Ru atom(s) that is(are) attached to the amidinato fragment(s). In the absence of added reagents, the thermolysis of **2** in refluxing toluene led to $[\text{Ru}_4\{\mu-\kappa^2\text{Ge},N\text{-Ge}(\text{Pr}_2\text{bzam})(\text{HMDS})\}\{\mu_3-\kappa\text{Ge-Ge}(\text{HMDS})\}(\mu-\kappa^2\text{N},\text{C},\text{N}'\text{-Pr}_2\text{bzam})(\mu\text{-CO})(\text{CO})_8]$ (**18**), which contains two new ligands, a triply bridging germlylidyne and a bridging benzaminate, and that results from the condensation of two molecules of **2** and the activation of the Ge–N bond of the benzamidinogermylene ligand of **2**.



INTRODUCTION

Divalent compounds of silicon, germanium, tin, and lead, also known as heavier carbene analogues, group 14 metalylenes, or heavier tetrylenes (HTs), are species of fundamental interest in main-group chemistry.^{1–3} They are very reactive molecules capable of coordinating to transition-metals (TM), activating small molecules, inserting into organic and inorganic σ -bonds, forming donor–acceptor adducts, adding to unsaturated substrates, promoting cycloadditions, participating in redox processes, etc.^{2,3} However, studies on the derivative chemistry and possible catalytic applications of their TM complexes are still scarce,^{3,4} probably because HTs and their TM complexes are, in general, very sensitive toward air and moisture,⁵ and in addition, the M–TM ($\text{M} = \text{Si}, \text{Ge}, \text{Sn}, \text{Pb}$) bonds of HT–TM complexes are generally weaker than the C–TM bonds of carbene–TM complexes (this effect is more and more evident on going down along group 14 of the periodic table).⁶ Fortunately, overcoming some of these stability issues, new generations of HTs, particularly silylenes and germlylenes stabilized by amidinato, β -diketiminato, and other chelating

fragments, have recently emerged, uncovering new avenues for HT–TM chemistry.^{4a,b} Among them, the current extent of the coordination chemistry of amidinato-HTs is quite noteworthy since they are known to form stable complexes with almost all of the TMs,^{5a,7–13} and some of these complexes have already proven to be active (pre)catalysts for useful reactions,^{4a} such as ketone hydrosilylations,^{7b,e} $[2 + 2+2]$ cycloadditions,^{7f} arene C–H borylations,^{7g} and Sonogashira,^{7d} Kumada,^{12b} and Negishi^{12b} cross-couplings.

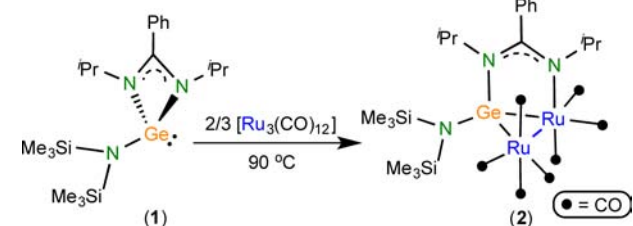
Among our recent contributions to HT–TM chemistry,^{11,14} we have reported that the amidinatogermylene $\text{Ge}(\text{Pr}_2\text{bzam})(\text{HMDS})$ (**1**; $\text{Pr}_2\text{bzam} = N,N'$ -bis(*iso*-propyl)benzaminate; $\text{HMDS} = \text{N}(\text{SiMe}_3)_2$), which is armed with just one lone pair of electrons on the Ge atom, can be transformed into a 4-electron-donor $\kappa^2\text{Ge},N$ -ligand upon treatment with cobalt^{11b,e} and ruthenium^{11e} carbonyls. For example, the reaction of **1** with $[\text{Ru}_3(\text{CO})_{12}]$ leads to the diruthenium(0) derivative

Received: February 19, 2015

Published: May 6, 2015

$[\text{Ru}_2\{\mu-\kappa^2\text{Ge}_e\text{N-Ge}(\text{iPr}_2\text{bzam})(\text{HMDS})\}(\text{CO})_7]$ (**2**), which contains a bridging bidentate germylene-imine ligand (Scheme 1).^{11e} It is noteworthy that, despite the great number of

Scheme 1. Reported Synthesis of Compound 2



amidinato-HT-TM complexes that are already known,^{5a,7–13} additional bidentate κ^2M,N -tetraylene-imine ligands have only been recently identified in a diruthenium complex^{11a,c} and in a few mononuclear group-6 (TM = Cr, Mo, W) complexes.^{9a}

Considering the current importance of amidinato-HTs in coordination chemistry,^{4a,b,7–13} we thought it of interest to explore the yet little investigated reactivity and stability of TM complexes containing a ring-opened amidinato-HT ligand.^{9a,11} Herein, we report an experimental study on the reactivity of the amidinatogermylene diruthenium complex **2**. This investigation has unveiled the reactive coordination sites of this complex in CO substitution reactions (with ^tBuNC and mono- and diphosphines) and its capacity to activate inorganic H–E bonds (E = Si, Sn, H) under mild conditions, and has also revealed that most products of these reactions are stable enough toward air and moisture to resist preparative chromatographic separations. Remarkably, the steric protection exerted by the imine *iso*-propyl fragment of the amidinato group has allowed the isolation of coordinatively unsaturated complexes.

RESULTS AND DISCUSSION

Reactions with Simple Nucleophilic Reagents.

The reactivity of compound **2** with various 2- and 4-electron-donor reagents was investigated looking for a possible hemilabile behavior of the amidinatogermylene ligand of complex **2**, which, presumably, might be susceptible to undergo a bidentate $\kappa^2\text{Ge}_e\text{N}$ - to monodentate κGe -coordination change upon the addition of a nucleophilic reagent. Besides, these reactions could alternatively or concomitantly lead to CO-substitution products. In any case, the results of these reactions would help locate the reactive coordination sites of complex **2**.

Complex **2** reacted readily with *tert*-butylisocyanide and trimethylphosphine in toluene at room temperature to give the CO-substitution derivatives $[\text{Ru}_2\{\mu-\kappa^2\text{Ge}_e\text{N-Ge}(\text{iPr}_2\text{bzam})(\text{HMDS})\}(\text{L})(\text{CO})_6]$ (L = ^tBuNC, **3**; PMe_3 , **4**), as the only reaction products (Scheme 2). No reaction intermediates were detected when the reactions were monitored by IR spectroscopy.

The X-ray diffraction (XRD) structure of the isocyanide derivative **3** (Figure 1 and Table 1) showed that the molecule maintains the Ru1–Ge1–Ru2 triangular array and the bidentate coordination found for the germylene ligand in **2**^{11e} and that the substituted carbonyl ligand has been the *exo*-axial CO of the $\text{Ru}(\text{CO})_4$ fragment of **2** (CO_A in Scheme 2). In this arrangement, the isocyanide ligand minimizes any steric interaction between its ^tBu group and the SiMe_3 and *i*Pr groups of the germylene ligand. The slight increase in the IR ν_{CN} absorption of the isocyanide ligand of **3** (2144 cm^{-1}),

Scheme 2. Reactivity of Compound 2 with Simple Nucleophilic Reagents

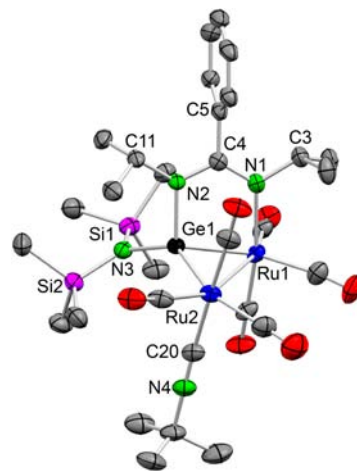
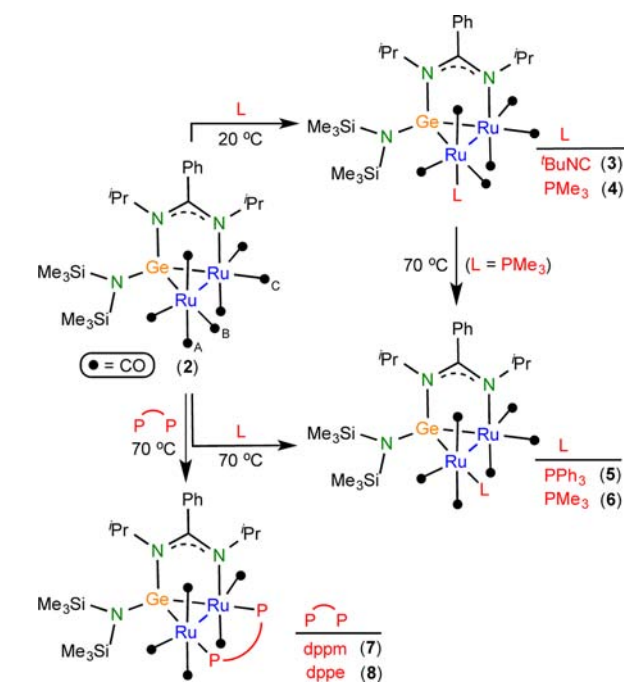


Figure 1. XRD Molecular Structure of Compound **3**. Thermal ellipsoids are drawn at 40% probability. All H atoms have been omitted for clarity.

compared to that of free ^tBuNC (2135 cm^{-1}), indicates that the isocyanide C–N multiple bond is more electron-rich when the isocyanide is uncoordinated.

The molecular structure of the trimethylphosphine derivative **4** could not be determined by XRD. However, the similarity of the ν_{CO} region of its IR spectrum with that of complex **3** strongly suggests that both compounds possess a similar ligand arrangement. In both cases (compounds **3** and **4**), the replacement of a CO group of **2** by the corresponding ligand (^tBuNC or PMe_3) was also confirmed by other analytical data (CHN microanalysis, mass spectrum, and ¹H, ³¹P, and ¹³C NMR spectra were routinely obtained for all isolated complexes).

Triphenylphosphine did not react with complex **2** in toluene at room temperature, probably because it is much less basic than PMe_3 , but a color change from orange to yellow was

Table 1. Selected XRD Interatomic Distances (Å) and Angles (deg) for Compounds 3, 7, and 11

atoms	3	7	11
Ru1–Ru2	2.9608(4)	2.9515(3)	3.0755(4)
Ru1–Ge1	2.4194(4)	2.3866(4)	2.4324(5)
Ru1–N1	2.199(3)	2.202(2)	2.205(3)
Ru1–C26			2.071(4)
Ru1–H100			1.95(5)
Ru1–P1		2.3996(8)	
Ru2–Ge1	2.4829(4)	2.5026(4)	2.5094(5)
Ru2–C20	2.026(4)		
Ru2–Si3			2.482(1)
Ru2–H100			1.66(5)
Ru2–P2		2.3892(9)	
Ge1–N2	1.945(2)	1.946(2)	1.951(3)
Ge1–N3	1.878(3)	1.876(3)	1.880(3)
C3–N1	1.497(4)	1.502(4)	1.486(5)
C4–N1	1.325(4)	1.311(4)	1.321(5)
C4–C5	1.510(4)	1.527(4)	1.512(5)
C4–N2	1.349(4)	1.346(4)	1.347(5)
C11–N2	1.494(4)	1.494(4)	1.493(4)
N3–Si1	1.761(3)	1.764(3)	1.760(3)
N3–Si2	1.744(3)	1.742(3)	1.750(3)
C20–N4	1.149(4)		
C26–N4			1.157(5)
C32–P1		1.845(3)	
C32–P2		1.846(3)	
Ru1–Ge1–N2	98.64(8)	99.32(8)	98.45(9)
Ru1–Ge1–N3	130.23(9)	129.94(8)	125.88(9)
Ru2–Ge1–N2	109.18(8)	113.45(8)	108.13(9)
Ru2–Ge1–N3	134.92(9)	129.80(8)	136.40(9)
N2–Ge1–N3	103.6(1)	105.2(1)	104.3(1)
Ru1–Ge1–Ru2	74.30(1)	74.23(1)	76.96(2)
Ru2–Ru1–Ge1	53.83(1)	54.68(1)	52.64(1)
Ru1–Ru2–Ge1	51.87(1)	51.09(1)	50.40(1)

observed when the temperature was raised to 70 °C. After 1 h, all of complex 2 had reacted (the reaction was monitored by IR) and the CO-substitution product $[\text{Ru}_2\{\mu\text{-}\kappa^2\text{Ge}_2\text{N-Ge}(\text{Pr}_2\text{bzam})(\text{HMDS})\}(\text{PPh}_3)(\text{CO})_6]$ (5) was quantitatively formed (Scheme 2). As the IR ν_{CO} pattern of this complex is very different from those of 3 or 4, we decided to maintain 3 and 4 in toluene at 70 °C for 1 h. While only extensive decomposition was observed from the BuNC complex 3, such a thermal treatment triggered the transformation of the PMe_3 complex 4 into an isomeric product, compound 6, whose IR ν_{CO} pattern is very similar to that of the PPh_3 derivative 5, indicating that 5 and 6 have the same ligand arrangement. Although the molecular structures of 5 and 6 could not be determined by XRD, the structural assignment depicted in Scheme 2 for these complexes was deduced from the following observations: (a) their structure should be different from that of complex 4; (b) complex 6 should have its PMe_3 ligand on the same Ru atom as in complex 4 because the exchange of PMe_3 and a CO group between two metal atoms is expected to be energetically more demanding than an axial-to-equatorial rearrangement of the PMe_3 ligand on the same metal atom (through a trigonal twist rotation of two COs and the PMe_3 ligand);¹⁵ and (c) the absence of ^1H NMR NOE interaction between any group of the germylene ligand and the Ph or Me groups of PPh_3 and PMe_3 , respectively, discards the *endo*-axial coordination site and the equatorial coordination site that is

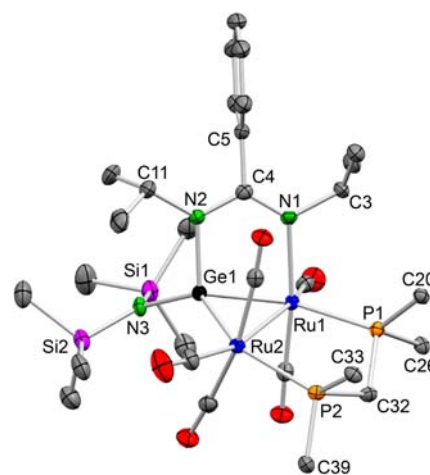
adjacent to the HMDS group as possible positions for the P-donor ligand of 5 and 6. In other words, the phosphine ligand of these complexes is located on the less hindered equatorial site of the Ru atom that is not attached to the benzamidinato group (*trans* to the Ge atom).

A DFT calculation, at the wB97XD/LanL2DZ/6-31G(d,p) level of theory (ΔG° , 298.15 K, toluene solvent) indicated that isomer 4 is 5.3 kcal mol⁻¹ less stable than isomer 6 and that the transformation of 4 into 6 is an elemental process (trigonal twist of PMe_3 and two CO ligands over their Ru atom) with an energy barrier (TS_{4-6}) of 29.2 kcal mol⁻¹. Therefore, complex 4 is the kinetically controlled product, whereas 6 is the thermodynamically controlled product of the reaction of compound 2 with PMe_3 . Images of the DFT-optimized structures of 4, 6, and TS_{4-6} are provided in the Supporting Information (Figure S16).

The outcomes of the above reactions of compound 2 with simple 2-electron-donor ligands, which led to CO-substituted derivatives having the new ligand on the Ru atom that is not attached to the amidinato imine fragment, discarded a hemilabile behavior for the bridging amidinatogermylene ligand of complex 2, which would have placed the new ligand in the other Ru atom.

The bidentate diphosphines bis(diphenylphosphino)methane (dppm) and 1,2-bis(diphenylphosphino)ethane (dppe) also failed to react with complex 2 in toluene at room temperature but led to the disubstituted derivatives $[\text{Ru}_2\{\mu\text{-}\kappa^2\text{Ge}_2\text{N-Ge}(\text{Pr}_2\text{bzam})(\text{HMDS})\}(\mu\text{-}\kappa^2\text{P,P}'\text{-L}_2)(\text{CO})_5]$ ($\text{L}_2 = \text{dppm}$, 7; dppe , 8), when the reactions were performed at 70 °C (Scheme 2).

The XRD structure of complex 7 (Figure 2 and Table 1) confirmed that the germylene ligand maintains its original

**Figure 2.** XRD molecular structure of compound 7. Thermal ellipsoids are drawn at 40% probability. All H atoms and the dppm phenyl rings (except the C_{ipso} atoms) have been omitted for clarity.

coordination and that the diphosphine ligand bridges the two Ru atoms through its P atoms, which occupy the two equatorial coordination sites that are approximately *trans* to the Ge atom (those occupied by CO_B and CO_C in complex 2; Scheme 2). An interesting feature of this structure is that, in order to minimize the steric interaction between the bulky diphosphine ligand and the methyl groups of the *iso*-propyl fragment attached to N1, the latter are much closer to the benzamidinato phenyl group in 7 than in 3 (Figure 1) or 2.^{11e} As the IR ν_{CO}

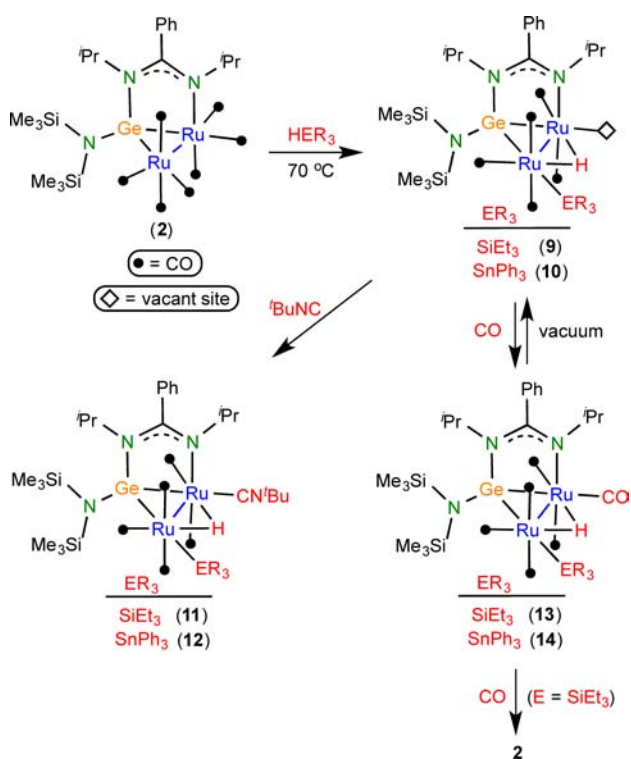
pattern and the $^{31}\text{P}\{^1\text{H}\}$ NMR spectra of **7** are closely related to those of the dpppe derivative **8**, we conclude that both compounds have an analogous ligand arrangement.

Activation of Inorganic H–E Bonds (E = Si, Sn, and H).

Having in mind a potential implication of complex **2** in homogeneous catalysis, we decided to investigate the reactivity of this complex with inorganic reagents that are useful to transform organic substrates. The following paragraphs describe the results we have obtained using triethylsilane, triphenylstannane, and dihydrogen as inorganic reagents.

Triethylsilane failed to react with complex **2** in toluene at room temperature, but it reacted at 70 °C to give $[\text{Ru}_2(\text{SiEt}_3)(\mu\text{-H})\{\mu\text{-}\kappa^2\text{Ge},\text{N-Ge}(\textit{iPr}_2\text{bzam})(\text{HMDS})\}(\text{CO})_5]$ (**9**) (Scheme 3). In contrast, triphenylstannane reacted with **2** at

Scheme 3. Compounds Derived from **2** and HSiEt_3 or HSnPh_3



room temperature to give a transient species (IR monitoring of the solution) that, under vacuum or upon heating, evolved to $[\text{Ru}_2(\text{SnPh}_3)(\mu\text{-H})\{\mu\text{-}\kappa^2\text{Ge},\text{N-Ge}(\textit{iPr}_2\text{bzam})(\text{HMDS})\}(\text{CO})_5]$ (**10**) (Scheme 3). The ^1H NMR spectra of **9** and **10** confirmed the oxidative addition of the corresponding reagent since, in addition to the resonances of the SiEt₃ or SnPh₃ group, a hydride resonance was observed at -10.30 ppm for **9** and -10.40 ppm for **10**. The addition of HSiEt_3 and HSnPh_3 to ruthenium carbonyl complexes containing N-donor ligands has been previously observed.¹⁶ Interestingly, the mass spectra and $^{13}\text{C}\{^1\text{H}\}$ NMR spectra of **9** and **10** clearly indicated that they contain only 5 CO ligands, suggesting that they are coordinatively unsaturated species. As we could not get crystals of **9** and **10** to unambiguously determine their molecular structures by XRD, we set up some reactions that could confirm their unsaturation, the results of which are described below.

Complexes **9** and **10** reacted immediately with tBuNC at room temperature to give the pentacarbonyl isonitrile

derivatives $[\text{Ru}_2(\text{ER}_3)(\mu\text{-H})\{\mu\text{-}\kappa^2\text{Ge},\text{N-Ge}(\textit{iPr}_2\text{bzam})(\text{HMDS})\}(\text{tBuNC})(\text{CO})_5]$ ($\text{ER}_3 = \text{SiEt}_3$, **11**; SnPh_3 , **12**), in quantitative yields (Scheme 3). The XRD molecular structure of compound **11** (Figure 3 and Table 1) confirmed the

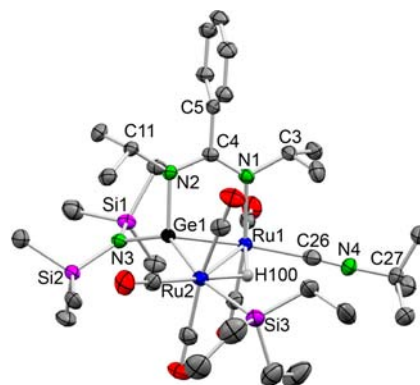


Figure 3. XRD molecular structure of compound **11**. Thermal ellipsoids are drawn at 40% probability. All H atoms have been omitted for clarity.

incorporation of tBuNC to the Ru atom that is attached to the amidinato N atom, on the equatorial coordination site that is *trans* to the Ge atom. The presence of the hydride and SiMe₃ or SnPh₃ ligands was also confirmed by the ^1H and $^{13}\text{C}\{^1\text{H}\}$ NMR spectra of **11** and **12**, whose IR spectra also displayed a similar ν_{CO} absorption pattern.

Toluene solutions of complexes **9** and **10** were also treated with CO gas (1 atm) at room temperature. An immediate reaction was observed in both cases by IR spectroscopy, which also confirmed that the tin derivative was the species that was transiently observed in the room temperature reaction of **2** with HSnPh_3 . These new products, labeled as **13** (Si) and **14** (Sn) in Scheme 3, underwent decarbonylation when their solutions were heated or placed under vacuum, reverting to their respective precursors (**9** and **10**). While the IR and ^1H and $^{13}\text{C}\{^1\text{H}\}$ NMR spectra of **14** could be satisfactorily acquired (Figure 4), complex **13** was characterized only by its IR spectrum because (a) it released CO when its solutions were left to stand under argon at room temperature, and (b) it reacted further with CO at room temperature to give back complex **2** and HSiEt_3 . The reversible reductive substitution of HSiEt_3 by a 2-electron-donor ligand is not new in carbonyl ruthenium chemistry.^{16a} As expected, the IR ν_{CO} pattern of **9** is similar to that of **10**, and those of **13** and **14** are also similar to each other, indicating that the complexes of each pair have an analogous structure. These data support the hypothesis that **13** and **14** are the hexacarbonyl derivatives $[\text{Ru}_2(\text{SiEt}_3)(\mu\text{-H})\{\mu\text{-}\kappa^2\text{Ge},\text{N-Ge}(\textit{iPr}_2\text{bzam})(\text{HMDS})\}(\text{CO})_6]$ (**13**) and $[\text{Ru}_2(\text{SnPh}_3)(\mu\text{-H})\{\mu\text{-}\kappa^2\text{Ge},\text{N-Ge}(\textit{iPr}_2\text{bzam})(\text{HMDS})\}(\text{CO})_6]$ (**14**) (Scheme 3).

Therefore, the above-described reactions strongly support the hypothesis that compounds **9** and **10** are coordinatively unsaturated species that have their unsaturation at the coordination site occupied by the tBuNC ligand in complex **11** (Scheme 3). A DFT calculation of the structure of complex **9** (the molecule resulting from removing the isonitrile ligand of compound **11** was optimized by DFT methods at the $\text{wB97XD/LanL2DZ}/6\text{-}31\text{G}(\text{d,p})$ level of theory) confirmed that the unsaturation of this molecule is alleviated by an agostic $\text{Ru}\cdots\text{H}-\text{CH}_2$ interaction ($\text{Ru}\cdots\text{H}$ 2.573 Å) that involves the

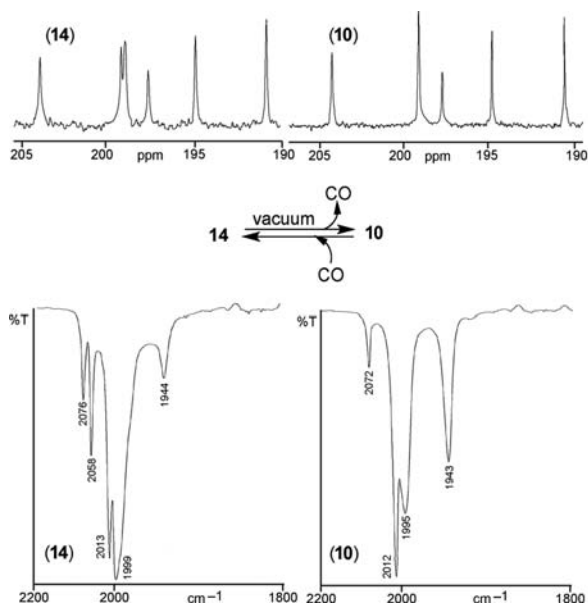


Figure 4. Carbonyl regions of the $^{13}\text{C}\{^1\text{H}\}$ NMR (acquired in $\text{C}_6\text{D}_5\text{CD}_3$ using ^{13}C -enriched samples) (top) and IR (acquired in toluene) (bottom) spectra of the SnPh_3 derivatives **14** and **10**.

unsaturated Ru atom and a methyl group of the closest $\text{N}-i\text{Pr}$ fragment (Supporting Information; Figures S17 and S18). We have previously shown that the presence of a *tert*-butyl group on an amidinato N atom of the germylene $\text{Ge}(\text{Et}^i\text{bzam}^i\text{Bu})$ (HMDS) provokes its diruthenium derivatives to be coordinatively unsaturated and that their “vacant” site contains an agostic $\text{Ru}\cdots\text{H}-\text{CH}_2$ interaction in the solid state that involves a methyl group of the *tert*-butyl fragment.^{11c}

Complex **2** also reacted with dihydrogen (1 atm) in THF at 70 °C to give a product, subsequently formulated as $[\text{Ru}_4(\mu\text{-H})_2\{\mu\text{-}\kappa^2\text{Ge},\text{N-Ge}(^i\text{Pr}_2\text{bzam})(\text{HMDS})\}_2(\text{CO})_{10}]$ (**15**) (Scheme 4), whose spectroscopic data were very surprising. The absorption pattern of the ν_{CO} region of its IR spectrum (very similar to those of the unsaturated complexes **9** and **10**) and its $^{13}\text{C}\{^1\text{H}\}$ NMR spectrum (it contained, in addition to the expected resonances of the germylene ligand, only five resonances assignable to carbonyl ligands) suggested a structure related to that of **9** or **10**, but, unexpectedly, its ^1H NMR spectrum only contained one hydride resonance (at -10.90 ppm), and the hydride/germylene integral ratio was clearly 1:1 (instead of the expected 2:1). The same ^1H NMR spectrum was obtained at -80 °C, ruling out the existence of a dynamic process at room temperature that could average two hydride resonances. These data puzzled us because a GeRu_2 monohydride derivative of complex **2** should be paramagnetic. Since, unfortunately, we could not get a mass spectrum of this product and we had no success in obtaining single crystals of it, we set up a couple of additional reactions aimed at providing more information on the structure of this complex.

A THF solution of complex **15** reacted immediately with $^i\text{BuNC}$ at room temperature to give $[\text{Ru}_4(\mu\text{-H})_2\{\mu\text{-}\kappa^2\text{Ge},\text{N-Ge}(^i\text{Pr}_2\text{bzam})(\text{HMDS})\}_2(^i\text{BuNC})_2(\text{CO})_{10}]$ (**16**). The crystal structure of this product was established by XRD (Figure 5 and Table 2). The molecule is a dimer comprising two $[\text{Ru}_2(\mu\text{-H})\{\mu\text{-}\kappa^2\text{Ge},\text{N-Ge}(^i\text{Pr}_2\text{bzam})(\text{HMDS})\}(^i\text{BuNC})(\text{CO})_5]$ units interconnected by an unbridged Ru–Ru bond. Each unit is essentially identical to that resulting from detaching the SiEt_3 group from compound **11** (Figure 3), and therefore, it contains

Scheme 4. Compounds Derived from **2** and H_2

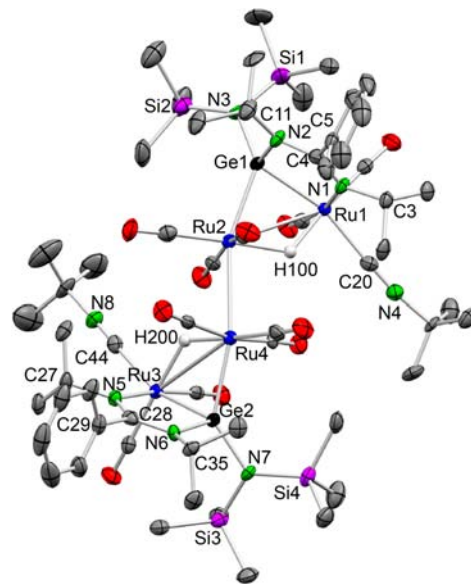
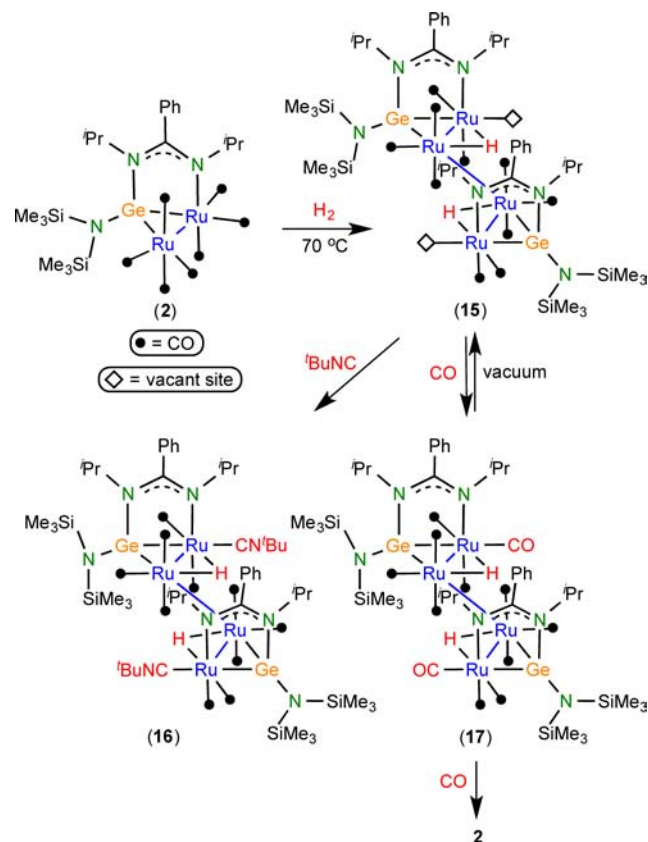


Figure 5. XRD molecular structure of compound **16**. Thermal ellipsoids are drawn at 60% probability. All H atoms have been omitted for clarity.

only one hydride and one isonitrile ligand. Overall, the dimer has no symmetry in the solid state, and this asymmetry is also maintained in solution since its IR spectrum in toluene contained seven ν_{CO} absorptions, and its NMR spectra displayed the resonances of two very similar but not quite equivalent $[\text{Ru}_2(\mu\text{-H})\{\mu\text{-}\kappa^2\text{Ge},\text{N-Ge}(^i\text{Pr}_2\text{bzam})(\text{HMDS})\}(^i\text{BuNC})(\text{CO})_5]$ units.

Table 2. Selected XRD Interatomic Distances (Å) and Angles (deg) for Compound 16

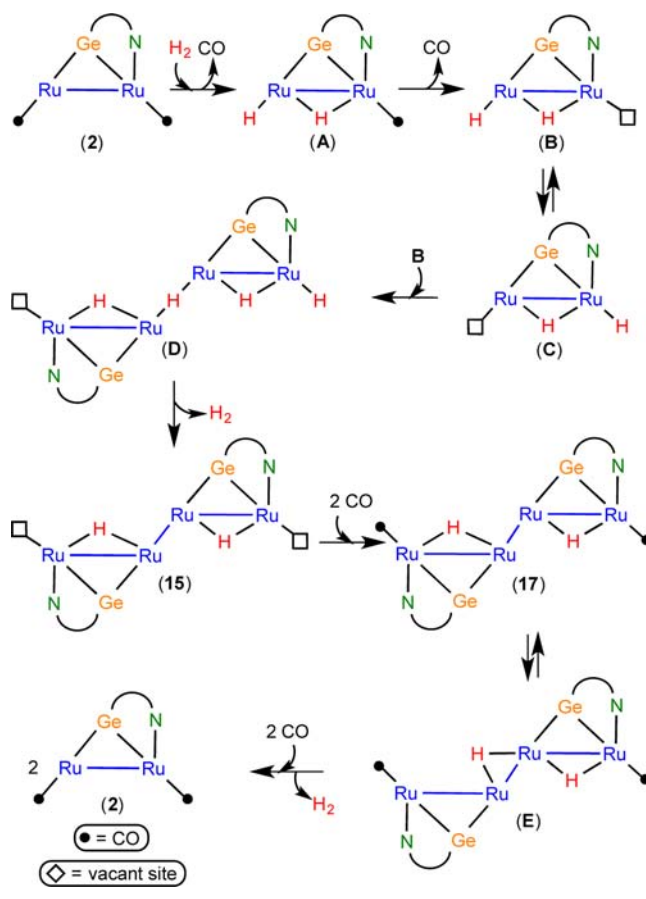
atoms		atoms	
Ru1–Ru2	3.1017(5)	Ru3–Ru4	3.0788(5)
Ru1–Ge1	2.4251(6)	Ru3–Ge2	2.4374(6)
Ru1–N1	2.186(3)	Ru3–N5	2.206(3)
Ru1–C20	2.071(6)	Ru3–C44	2.078(5)
Ru1–H100	1.77(4)	Ru3–H200	1.80(4)
Ru2–Ge1	2.4721(7)	Ru4–Ge2	2.4485(7)
Ru2–H100	1.83(4)	Ru4–H200	1.65(5)
Ge1–N2	1.954(3)	Ge2–N6	1.949(3)
Ge1–N3	1.885(4)	Ge2–N7	1.879(4)
C3–N1	1.490(6)	C27–N5	1.501(6)
C4–N1	1.329(6)	C28–N5	1.332(6)
C4–C5	1.520(6)	C28–C29	1.521(6)
C4–N2	1.347(6)	C28–N6	1.343(6)
C11–N2	1.487(6)	C35–N6	1.489(5)
N3–Si1	1.763(4)	N7–Si3	1.770(4)
N3–Si2	1.748(4)	N7–Si4	1.749(4)
C20–N4	1.156(6)	C44–N8	1.151(6)
Ru2–Ru4	2.9183(6)		
Ru1–Ge1–N2	97.9(1)	Ru3–Ge2–N6	98.7(1)
Ru1–Ge1–N3	125.6(1)	Ru3–Ge2–N7	126.7(1)
Ru2–Ge1–N2	105.5(1)	Ru4–Ge2–N6	108.6(1)
Ru2–Ge1–N3	137.3(1)	Ru4–Ge2–N7	134.6(1)
N2–Ge1–N3	104.9(2)	N6–Ge2–N7	104.1(2)
Ru1–Ge1–Ru2	78.59(2)	Ru3–Ge2–Ru4	78.12(2)
Ru2–Ru1–Ge1	51.38(2)	Ru4–Ru3–Ge2	51.10(2)
Ru1–Ru2–Ge1	50.03(2)	Ru3–Ru4–Ge2	50.78(2)

Complex 15 also reacted within seconds with carbon monoxide (1 atm) in THF solution at room temperature to give a product, for which we propose the formulation $[\text{Ru}_4(\mu\text{-H})_2\{\mu\text{-}\kappa^2\text{Ge}_2\text{N-Ge}(\text{Pr}_2\text{bzam})(\text{HMDS})\}_2(\text{CO})_{12}]$ (17) (Scheme 4), that could not be isolated as a pure solid because it was gradually converted into complex 2 upon a longer exposure to CO gas, and it reverted to compound 15 when the solvent was removed under reduced pressure. Its IR spectrum, which was taken from the reacting solution, and its ^1H NMR spectrum, which was acquired from a solution prepared by treating a C_6D_6 solution of 15 with CO in an NMR tube (it also contained a small amount of 2), were consistent with the presence of two very similar but not quite equivalent $[\text{Ru}_2(\mu\text{-H})\{\mu\text{-}\kappa^2\text{Ge}_2\text{N-Ge}(\text{Pr}_2\text{bzam})(\text{HMDS})\}(\text{CO})_6]$ units. Hence, the reaction of 15 with CO seems to follow the same pathway as that with $^t\text{BuNC}$, both leading to an asymmetrical dimer.

Therefore, the analytical and spectroscopic data of compound 15 and the results obtained from its reactions with $^t\text{BuNC}$ and CO strongly support the symmetric and coordinatively unsaturated dimeric structure proposed for this complex in Scheme 4. The asymmetry of its coordinatively saturated derivatives 16 and 17 has to be associated with the steric repulsion exerted by the new ligand ($^t\text{BuNC}$ or CO) of each half of 16 or 17 over the ligands of the remaining half of the molecule, making it more difficult to rotate about the Ru–Ru bond that joins them. It should be noted that the formation of unbridged metal–metal bonds between two nonmononuclear transition metal complexes has rarely been observed.¹⁷

Although the elimination/addition of CO or H_2 from/to a transition metal complex may lead to the formation/cleavage of a metal–metal bond, the synthesis of the unsaturated dimeric complex 15 from 2 and H_2 and the recovery of complex 2 when

the saturated dihydride dimer 17 was exposed to a CO atmosphere were very unexpected results. A tentative reaction pathway that provides some mechanistic clues about the outcomes of these experiments is proposed in Scheme 5.

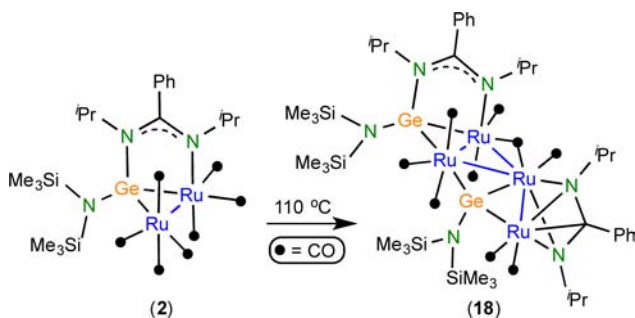
Scheme 5. Proposed Reaction Pathway That Goes from 2 to 2 through 15 and 17

Taking into account that the 70 °C reactions of 2 with HSiEt_3 and HSnPh_3 led to the unsaturated derivatives 9 and 10, respectively (Scheme 3), we propose (Scheme 5) that the 70 °C reaction of 2 with H_2 should initially follow a similar reaction pathway, leading first to intermediate A through an oxidative substitution of CO by H_2 and then to intermediate B (which is similar to 9 and 10) through the elimination of a CO ligand from A. As a terminal-to-bridging migration of a hydride ligand is generally an easy process,¹⁵ B could be easily converted into intermediate C and, as a hydride can easily bridge two metal atoms (in contrast with the SiEt_3 and SnPh_3 groups), C can alleviate its unsaturation by interacting with the terminal hydride ligand of B. As the resulting intermediate D contains two hydride ligands attached to the same metal atom, it can undergo a reductive elimination of H_2 , leading to compound 15, which contains a new Ru–Ru bond and two vacant coordination sites. The participation of intermediate C in this process is necessary because, due to the steric protection exerted by the *iso*-propyl group, the new Ru–Ru bond should not involve Ru atoms that are attached to the amidinato N– ^iPr fragment. However, as compound 2 has no hydrides, its formation from 17 and CO should start with a hydride migration step because a reductive elimination of H_2 requires an intermediate having two hydride ligands attached to a

common metal atom, such as E in Scheme 5. Under a CO atmosphere, intermediate E should rapidly undergo both the reductive substitution of H₂ by CO and the cleavage of the unbridged Ru–Ru bond, ending in two molecules of 2.

Thermolysis of Complex 2. With the aim of investigating the robustness of compound 2 at higher temperatures, a toluene solution of this complex was stirred at reflux temperature under argon. IR monitoring indicated the complete consumption of the starting complex after 20 min. A chromatographic separation of the crude reaction mixture allowed the isolation of [Ru₄{μ-κ²Ge,N-Ge(Pr₂bzam)-(HMDS)}]{μ₃-κGe-Ge(HMDS)}{μ-κ³N,C,N'-Pr₂bzam}(μ-CO)(CO)₈ (18) in 59% yield (Scheme 6).

Scheme 6. Thermolysis of Complex 2



An XRD study (Figure 6 and Table 3) established that 18 is a tetranuclear complex that arises from a decarbonylative

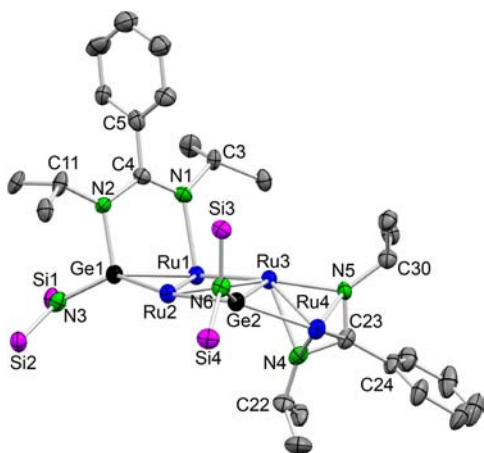


Figure 6. XRD molecular structure of compound 18. Thermal ellipsoids are drawn at 35% probability. The HMDS methyl groups, all CO ligands, and all H atoms have been omitted for clarity.

condensation of two molecules of 2 (5 CO ligands are released). While one diruthenium unit (Ru1–Ru2) maintains the original amidinatogermylene ligand coordinated to the metal atoms in the same way as in 2, the other diruthenium unit (Ru3–Ru4) has inserted into the Ge–N bond of the original amidinatogermylene ligand, transforming it into two independent ligands, a germylydine, Ge(HMDS), and a benzamidinato, Pr₂bzam. In 18, the germylydine has the Ge atom attached to three Ru atoms (Ru2, Ru3, and Ru4), and the benzamidinato ligand spans two metal atoms (Ru3 and Ru4) through the three atoms of its functional group (N4, C23, and N5). Regarding germylydine ligands,¹⁸ Ge(HMDS) is unprecedented. In 18,

Table 3. Selected XRD Interatomic Distances (Å) for Compound 18

atoms		atoms	
Ru1–Ru2	2.982(1)	Ge1–N3	1.87(1)
Ru1–Ru3	2.836(1)	Ge2–N6	1.87(1)
Ru1–Ge1	2.411(2)	C3–N1	1.50(2)
Ru1–N1	2.25(1)	C4–N1	1.32(2)
Ru2–Ru3	2.935(1)	C4–C5	1.54(2)
Ru2–Ge1	2.533(2)	C4–N2	1.39(2)
Ru2–Ge2	2.478(2)	C11–N2	1.45(2)
Ru3–Ru4	2.716(1)	N3–Si1	1.77(1)
Ru3–Ge2	2.649(2)	N3–Si2	1.75(1)
Ru3–N4	2.25(1)	C22–N4	1.45(2)
Ru3–N5	2.12(1)	C23–N4	1.40(2)
Ru4–Ge2	2.388(2)	C23–C24	1.51(2)
Ru4–N4	2.19(1)	C23–N5	1.35(2)
Ru4–C23	2.25(1)	C30–N5	1.47(2)
Ru4–N5	2.25(1)	N6–Si3	1.72(1)
Ge1–N2	1.93(1)	N6–Si4	1.75(1)

the benzamidinato C23–N4 distance, 1.40(2) Å, is longer than the C23–N5 distance, 1.35(1) Å, and the Ru4–C23 and Ru4–N5 distances, both 2.25(1) Å, are longer than the Ru4–N4 distance, 2.19(1) Å, confirming the presence of a localized double bond between C25 and N5 that is π-coordinated to Ru4. The coordination mode found for the benzamidinato ligand in 18, in which it acts as a 5-electron-donor bridging ligand, has been previously observed only in binuclear Ru₂(η²-C₅Me₅)₂ complexes.¹⁹

Therefore, the thermolysis provoked a decarbonylation of compound 2, and in the absence of added reagents, the resulting intermediates relieved their unsaturation by undergoing aggregation and intramolecular Ge–N bond activation processes. A similar Ge–N bond breakage has also been observed on the monomeric bis(amidinato)germylene rhodium complexes [RhCl(cod){κ¹-Ge-Ge(R₂bzam)₂}] (R = tBu, SiMe₃; cod = 1,5-cyclooctadiene), which evolved to the amidinatorhodium derivatives [Rh(R₂bzam)(cod)] and other products.^{5a} Interestingly, in our case, the two fragments resulting from the ligand breakage, Ge(HMDS) and Pr₂bzam, were maintained in the final molecule 18.

CONCLUSIONS

This work has established that the germylene-bridged complex 2 is prone to react with simple 2-electron-donor nucleophiles (to give the carbonyl substitution products 3–8) and to activate the H–E bond (E = Si, Sn, H) of HSiEt₃, HSnPh₃, and H₂ (to give compounds 9, 10, and 15 by decarbonylative oxidative addition) under mild conditions (20–70 °C).

Given the bridging nature of the κ²Ge,N-amidinatogermylene ligand of complex 2, it was expected that it could behave as a hemilabile ligand. However, the reactions reported in this work have confirmed that this ligand is strongly attached to the metal atoms. The breakage of the Ge–N bond of the amidinatogermylene ligand of complex 2 has been observed at high temperatures (>110 °C), but this ligand degradation is probably provoked by previous thermally induced decarbonylation processes rather than by an intrinsic thermal instability of the ligand.

The unexpected coordinative unsaturation of compounds 9, 10, and 15 has been confirmed by the outcomes of their reactions with tBuNC and CO, which afforded ligand-addition

products (compounds 11–14, 16, and 17). The volume of the amidinato *iso*-propyl group has to be claimed as responsible (at least in part) for the unsaturation of these complexes and for their relative stability.

The unsaturated tetraruthenium compound 15 was prepared from complex 2 and dihydrogen. This unusual and unexpected complex and its saturated derivatives 16 and 17 contain two Ru₂Ge units interconnected by an Ru–Ru bond that is not supported by bridging ligands.

EXPERIMENTAL SECTION

General Procedures. Toluene, hexane, and THF were dried over sodium diphenyl ketyl and were distilled under argon before use. All reactions were carried out under argon, using drybox and/or Schlenk-vacuum line techniques and were routinely monitored by solution IR spectroscopy. All reaction products were vacuum-dried for several hours prior to being weighted and analyzed. The compound [Ru₂{μ-κ²Ge,N-Ge(*Pr*₂bzam)}(HMDS)}(CO)₇] (2) was prepared following a published procedure.^{11e} A ¹³C-enriched sample of 2 was prepared from ¹³C-enriched [Ru₃(CO)₁₂].²⁰ All remaining reagents were purchased from commercial sources. NMR spectra were run on Bruker DPX-300 or Bruker AV-400 instruments, using as standards a residual protic solvent resonance for ¹H [δ(C₆D₅CHD₂) = 2.08; δ(C₆HD₅) = 7.16; δ(CD₂HCl₂) = 5.32], a solvent resonance for ¹³C [δ(C₆D₅CD₃) = 20.4; δ(C₆D₆) = 128.1; δ(CD₂Cl₂) = 53.84], and external aqueous 85% H₃PO₄ for ³¹P [δ(H₃PO₄) = 0.00]. Elemental analyses were obtained from a PerkinElmer 2400B microanalyzer. Mass spectra (MS) were run on a VG Autospec double-focusing mass spectrometer operating in the FAB+ mode; ions were produced with a standard Cs⁺ gun at about 30 kV; 3-nitrobenzyl alcohol was used as the matrix; the data given correspond to the most abundant isotopomer of the molecular ion or of the greatest mass fragment.

[Ru₂{μ-κ²Ge,N-Ge(*Pr*₂bzam)}(HMDS)}(*t*BuNC)(CO)₆] (3). *t*BuNC (3.5 μL, 0.03 mmol) was added to a solution of complex 2 (25 mg, 0.03 mmol) in toluene (10 mL) at –78 °C. The solution was then allowed to reach room temperature. The color changed from orange to yellow. The solvent was removed under reduced pressure to give compound 3 as an orange solid (25 mg, 94%). Anal. Calcd for C₃₀H₄₆GeN₄O₆Ru₂Si₂ (889.63): C, 40.50; H, 5.21; N, 6.30; found, C, 40.71; H, 5.26; N, 6.28. (+)-FAB MS: *m/z* 806 [M – 3 CO]⁺. IR (toluene, cm⁻¹): ν_{CN} 2144 (m), ν_{CO} 2063 (m), 1998 (vs), 1982 (m), 1971 (m), 1933 (m). ¹H NMR (C₆D₆, 300.1 MHz, 293 K): δ 7.06–6.98 (m, 5 H, 5 CH of Ph), 4.06 (spt, *J* = 6.9 Hz, 1 H, CH of ¹Pr), 3.62 (spt, *J* = 6.7 Hz, 1 H, CH of ¹Pr), 1.41 (d, *J* = 6.7 Hz, 3 H, Me of ¹Pr), 1.17 (d, *J* = 6.9 Hz, 3 H, Me of ¹Pr), 1.13 (d, *J* = 6.9 Hz, 3 H, Me of ¹Pr), 1.02 (s, 9 H, 3 Me of ¹Bu), 0.97 (d, *J* = 6.7 Hz, 3 H, Me of ¹Pr), 0.64 (s, 9 H, 3 Me of HMDS), 0.62 (s, 9 H, 3 Me of HMDS). ¹³C{¹H} NMR (C₆D₆, 100.6 MHz, 293 K): δ 204.3 (s, CO), 203.0 (s, br, COs), 202.5 (s, CO), 166.4 (s, NCN), 150.3 (s, CN^{*t*}Bu), 138.2 (s, C_{ipso} of Ph), 128.7 (s, CH of Ph), 128.6 (s, CH of Ph), 128.3 (s, CH of Ph), 127.8 (s, CH of Ph), 127.0 (s, CH of Ph), 57.1 (s, C of ¹Bu), 55.5 (s, CH of ¹Pr), 50.1 (s, CH of ¹Pr), 29.9 (s, 3 Me of ¹Bu), 26.6 (s, Me of ¹Pr), 24.7 (s, Me of ¹Pr), 24.5 (s, Me of ¹Pr), 23.0 (s, Me of ¹Pr), 6.8 (s, 3 Me of HMDS), 5.8 (s, 3 Me of HMDS).

[Ru₂{μ-κ²Ge,N-Ge(*Pr*₂bzam)}(HMDS)}(PMe₃)(CO)₆] (Isomer 4). PMe₃ (3 μL, 0.03 mmol) was added to a solution of complex 2 (25 mg, 0.03 mmol) in toluene (10 mL), and the mixture was stirred at room temperature for 10 min. The color changed from orange to yellow. The solvent was removed under reduced pressure, and the crude reaction mixture was separated by column chromatography on silica-gel (2 × 5 cm). Hexane–dichloromethane (1:1) eluted compound 4, which was isolated as a pale orange solid (20 mg, 75%). Anal. Calcd for C₂₈H₄₆GeN₃O₆PRu₂Si₂ (882.58): C, 38.10; H, 5.25; N, 4.76; found, C, 38.16; H, 5.28; N, 4.71. (+)-FAB MS: *m/z* 799 [M – 3 CO]⁺. IR (toluene, cm⁻¹): ν_{CO} 2061 (m), 1994 (vs), 1978 (m), 1969 (m), 1918 (m). ¹H NMR (C₆D₆, 300.1 MHz, 293 K): δ 7.02–6.90 (m, 5 H, 5 CH of Ph), 4.06 (m, br, 1 H, CH of ¹Pr), 3.67 (m, br, 1 H, CH of ¹Pr), 1.25 (d, *J* = 6.6 Hz, 9 H, PMe₃), 1.17–1.12

(m, 12 H, 4 Me of ¹Pr), 0.68 (s, 9 H, 3 Me of HMDS), 0.58 (s, 9 H, 3 Me of HMDS). ³¹P{¹H} NMR (C₆D₆, 121.5 MHz, 293 K): δ –30.8 (s). ¹³C{¹H} NMR (C₆D₆, 75.5 MHz, 293 K): δ 205.5 (s, CO), 204.3 (s, br, COs), 203.1 (s, CO), 202.3 (s, br, COs), 167.3 (s, NCN), 137.8 (s, C_{ipso} of Ph), 128.9 (s, CH of Ph), 128.4 (s, CH of Ph), 127.7 (s, CH of Ph), 127.2 (s, CH of Ph), 126.8 (s, CH of Ph), 50.6 (s, 2 CH of ¹Pr), 25.7 (s, Me of ¹Pr), 25.0 (s, Me of ¹Pr), 24.8 (s, Me of ¹Pr), 24.2 (s, Me of ¹Pr), 19.2 (s, br, PMe₃), 6.5 (s, 3 Me of HMDS), 5.7 (s, 3 Me of HMDS).

[Ru₂{μ-κ²Ge,N-Ge(*Pr*₂bzam)}(HMDS)}(PPh₃)(CO)₆] (5). PPh₃ (8 mg, 0.03 mmol) was added to a solution of complex 2 (25 mg, 0.03 mmol) in toluene (10 mL). As no reaction was observed at room temperature, the mixture was heated at 70 °C for 1 h. The color changed from orange to yellow. The solvent was removed under reduced pressure, and the crude reaction mixture was separated by column chromatography on silica-gel (2 × 5 cm). Hexane–dichloromethane (1:1) eluted compound 5, which was isolated as a yellow solid (26 mg, 81%). Anal. Calcd for C₄₃H₅₂GeN₃O₆PRu₂Si₂ (1068.78): C, 48.32; H, 4.90; N, 3.93; found, C, 48.36; H, 4.94; N, 3.89. (+)-FAB MS: *m/z* 985 [M – 3 CO]⁺. IR (toluene, cm⁻¹): ν_{CO} 2046 (w), 2011 (vs), 1972 (vs), 1959 (m), 1940 (m). ¹H NMR (CD₂Cl₂, 300.1 MHz, 293 K): δ 7.81–7.75 (m, 6 H, 6 CH of Ph), 7.14–6.87 (m, 14 H, 14 CH of Ph), 3.62 (m, 1 H, CH of ¹Pr), 3.42 (m, 1 H, CH of ¹Pr), 1.25 (d, *J* = 6.1 Hz, 3 H, Me of ¹Pr), 1.18 (d, *J* = 6.4 Hz, 3 H, Me of ¹Pr), 1.13 (d, *J* = 6.6 Hz, 3 H, Me of ¹Pr), 0.80 (d, *J* = 6.3 Hz, 3 H, Me of ¹Pr), 0.48 (s, 9 H, 3 Me of HMDS), 0.42 (s, 9 H, 3 Me of HMDS). ³¹P{¹H} NMR (C₆D₆, 121.5 MHz): δ 35.8 (s). ¹³C{¹H} NMR (CD₂Cl₂, 75.5 MHz, 293 K): δ 204.7 (s, br, COs), 204.6 (s, CO), 204.5 (s, CO), 203.5 (s, CO), 201.7 (s, CO), 166.5 (s, NCN), 137.0–126.6 (Ph groups of the germylene and PPh₃ ligands), 55.9 (s, CH of ¹Pr), 51.4 (s, CH of ¹Pr), 26.9 (s, Me of ¹Pr), 25.0 (s, Me of ¹Pr), 24.5 (s, Me of ¹Pr), 23.2 (s, Me of ¹Pr), 6.5 (s, 3 Me of HMDS), 5.8 (s, 3 Me of HMDS).

[Ru₂{μ-κ²Ge,N-Ge(*Pr*₂bzam)}(HMDS)}(PMe₃)(CO)₆] (Isomer 6). PMe₃ (3 μL, 0.03 mmol) was added to a solution of complex 2 (25 mg, 0.03 mmol) in toluene (10 mL) at 70 °C, and the mixture was heated at this temperature for 1 h. The color remained orange. The solvent was removed under reduced pressure, and the crude reaction mixture was separated by column chromatography on silica-gel (2 × 5 cm). Hexane–dichloromethane (1:1) eluted compound 6, which was isolated as a pale orange solid (22 mg, 83%). Anal. Calcd for C₂₈H₄₆GeN₃O₆PRu₂Si₂ (882.58): C, 38.10; H, 5.25; N, 4.76; found, 38.20; H, 5.31; N, 4.65. (+)-FAB MS: *m/z* 855 [M – CO]⁺. IR (toluene, cm⁻¹): ν_{CO} 2043 (w), 2004 (vs), 1966 (vs), 1960 (m), 1944 (m). ¹H NMR (C₆D₆, 400.1 MHz, 293 K): δ 7.04–6.96 (m, 5 H, 5 CH of Ph), 3.80 (spt, *J* = 6.7 Hz, 1 H, CH of ¹Pr), 3.54 (m, 1 H, CH of ¹Pr), 1.31 (d, *J* = 6.7 Hz, 3 H, Me of ¹Pr), 1.27 (d, *J* = 7.3 Hz, 3 H, Me of ¹Pr), 1.21 (d, *J* = 8.7 Hz, 9 H, PMe₃), 1.19 (d, *J* = 6.7 Hz, 3 H, Me of ¹Pr), 0.99 (d, *J* = 6.5 Hz, 3 H, Me of ¹Pr), 0.66 (s, 9 H, 3 Me of HMDS), 0.65 (s, 9 H, 3 Me of HMDS). ³¹P{¹H} NMR (C₆D₆, 121.5 MHz, 293 K): δ –18.3 (s). ¹³C{¹H} NMR (C₆D₆, 100.6 MHz, 293 K): δ 208.0 (s, br, COs), 204.5 (s, br, COs), 202.8 (s, CO), 202.7 (s, CO), 166.4 (s, NCN), 138.3 (s, C_{ipso} of Ph), 128.8 (s, CH of Ph), 128.5 (s, CH of Ph), 127.8 (s, CH of Ph), 127.5 (s, CH of Ph), 126.8 (s, CH of Ph), 55.9 (s, CH of ¹Pr), 51.1 (s, CH of ¹Pr), 27.0 (s, Me of ¹Pr), 25.0 (s, Me of ¹Pr), 24.4 (s, Me of ¹Pr), 23.2 (s, Me of ¹Pr), 21.4 (d, *J* = 27.0 Hz, PMe₃), 6.7 (s, 3 Me of HMDS), 5.9 (s, 3 Me of HMDS).

[Ru₂{μ-κ²Ge,N-Ge(*Pr*₂bzam)}(HMDS)}(μ-κ²P,P'-dppm)(CO)₅] (7). dppm (11.5 mg, 0.03 mmol) was added to a solution of complex 2 (25 mg, 0.03 mmol) in toluene (10 mL), and the mixture was heated at 70 °C for 2 h. The color changed from orange to yellow. The solvent was removed under reduced pressure, and the crude reaction mixture was separated by column chromatography on silica-gel (2 × 5 cm). Hexane–dichloromethane (1:1) eluted compound 7, which was isolated as a yellow solid (32 mg, 92%). Anal. Calcd for C₄₉H₅₉GeN₃O₅P₂Ru₂Si₂ (1162.88): C, 50.60; H, 5.11; N, 3.61; found, 50.68; H, 5.17; N, 3.55. (+)-FAB MS: *m/z* 1163 [M]⁺. IR (toluene, cm⁻¹): ν_{CO} 2030 (m), 1965 (vs), 1948 (m), 1902 (m, br). ¹H NMR (C₆D₆, 300.1 MHz, 293 K): δ 8.02–7.99 (m, 2 H, 2 CH of

Ph), 7.72–7.69 (m, 2 H, 2 CH of Ph), 7.38–7.33 (m, 2 H, 2 CH of Ph), 7.25–6.58 (m, 19 H, 19 CH of Ph), 4.37–4.29 (m, 2 H, CH of ¹Pr and CHH of dppe), 3.78–3.68 (m, 2 H, CH of ¹Pr and CHH of dppe), 1.41–1.23 (m, 12 H, 4 Me of ¹Pr), 0.77 (s, 9 H, 3 Me of HMDS), 0.66 (s, 9 H, Me₃ of HMDS). ³¹P{¹H} NMR (C₆D₆, 162.0 MHz, 293 K): δ 34.7 (d, J = 132 Hz), 23.8 (d, J = 131 Hz). ¹³C{¹H} NMR (C₆D₆, 100.6 MHz, 293 K): δ 209.5 (d, J = 10 Hz, CO), 208.6 (s, CO), 207.2 (m, COs), 205.0 (s, CO), 167.2 (s, NCN), 139.2–128.1 (Ph groups of the germylene and dppe ligands), 50.8 (s, 2 CH of ¹Pr), 48.2 (t, J = 21.7 Hz, CH₂ of dppe), 26.5 (s, Me of ¹Pr), 25.0 (s, Me of ¹Pr), 24.7 (s, Me of ¹Pr), 24.5 (s, Me of ¹Pr), 6.6 (s, 3 Me of HMDS), 5.8 (s, 3 Me of HMDS).

[Ru₂{μ-κ²Ge,N-Ge(¹Pr₂bzam)(HMDS)}{μ-κ²P,P'-dppe}(CO)₅] (8). dppe (12 mg, 0.03 mmol) was added to a solution of complex 2 (25 mg, 0.03 mmol) in toluene (10 mL), and the mixture was heated at 70 °C for 2 h. The color changed from orange to yellow. The solvent was removed under reduced pressure, and the crude reaction mixture was separated by column chromatography on silica-gel (2 × 5 cm). Hexane–dichloromethane (1:1) eluted compound 8, which was isolated as a yellow solid (33 mg, 94%). Anal. Calcd for C₅₀H₆₁GeN₃O₃P₂Ru₂Si₂ (1176.91): C, 51.03; H, 5.22; N, 3.57; found, C, 51.12; H, 5.32; N, 3.52. (+)-FAB MS: m/z 1177 [M]⁺. IR (toluene, cm⁻¹): ν_{CO} 2019 (m), 1958 (vs), 1916 (m, br), 1901 (m). ¹H NMR (C₆D₆, 300.1 MHz, 293 K): δ 8.02–7.96 (m, 4 H, 4 CH of Ph), 7.26–6.65 (m, 21 H, 21 CH of Ph), 4.20 (spt, J = 6.8 Hz, 1 H, CH of ¹Pr), 3.91 (m, 1 H, CH of ¹Pr), 2.71–2.28 (m, 4 H, 2 CH₂ of dppe), 1.32 (d, J = 6.8 Hz, 6 H, 2 Me of ¹Pr), 1.23 (d, J = 6.8 Hz, 6 H, 2 Me of ¹Pr), 0.83 (s, 9 H, 3 Me of HMDS), 0.59 (s, 9 H, Me₃ of HMDS). ³¹P{¹H} NMR (C₆D₆, 121.5 MHz, 293 K): δ 37.5 (d, J = 13 Hz), 18.5 (d, J = 13 Hz). ¹³C{¹H} NMR (C₆D₆, 75.5 MHz, 293 K): δ 212.3 (d, J = 12 Hz, CO), 208.1 (s, CO), 207.0 (d, J = 8 Hz, CO), 206.5 (s, CO), 204.3 (d, J = 12 Hz, CO), 167.9 (s, NCN), 141.4–126.6 (Ph groups of the germylene and dppe ligands), 50.2 (s, 2 CH of ¹Pr), 25.8 (d, J = 23.9 Hz, CH₂ of dppe), 25.14 (s, Me of ¹Pr), 24.8–24.7 (m, 2 Me of ¹Pr and CH₂ of dppe), 24.1 (s, Me of ¹Pr), 6.7 (s, 3 Me of HMDS), 5.9 (s, 3 Me of HMDS).

[Ru₂(SiEt₃)(μ-H){μ-κ²Ge,N-Ge(¹Pr₂bzam)(HMDS)}(CO)₅] (9). HSiEt₃ (7 μL, 0.042 mmol) was added to a solution of complex 2 (25 mg, 0.03 mmol) in toluene (10 mL), and the mixture was heated at 80 °C for 3 h. The color changed from orange to dark orange. The solvent was removed under reduced pressure, and the crude reaction mixture was separated by column chromatography on silica-gel (2 × 5 cm). Compound 9 was eluted with hexane, and it was isolated as an orange solid (20 mg, 75%). Anal. Calcd for C₃₀H₃₃GeN₃O₃Ru₂Si₃ (894.77): C, 40.27; H, 5.97; N, 4.70; found, C, 40.33; H, 6.03; N, 4.47. (+)-FAB MS: m/z 895 [M]⁺. IR (toluene, cm⁻¹): ν_{CO} 2067 (w), 2006 (vs), 1986 (m), 1937 (m, br). ¹H NMR (C₆D₆, 300.1 MHz, 293 K): δ 7.12–7.00 (m, 5 H, 5 CH of Ph), 3.7–3.53 (m, 2 H, 2 CH of ¹Pr), 1.29–1.04 (m, 21 H, 3 CH₂ and 3 Me of Et; and 2 Me of ¹Pr), 0.97 (d, J = 5.8 Hz, 3 H, Me of ¹Pr), 0.84 (d, J = 6.1 Hz, 3 H, Me of ¹Pr), 0.54 (s, 9 H, 3 Me of HMDS), 0.53 (s, 9 H, 3 Me of HMDS), -10.40 (s, 1 H, μ-H). ¹³C{¹H} NMR (C₆D₆, 75.5 MHz, 293 K): δ 203.1 (s, CO), 201.8 (s, CO), 199.4 (s, CO), 197.6 (s, CO), 195.8 (s, CO), 165.0 (s, NCN), 135.0 (s, C_{ipso} of Ph), 129.0 (s, CH of Ph), 128.7 (s, CH of Ph), 128.6 (s, CH of Ph), 128.5 (s, CH of Ph), 127.6 (s, CH of Ph), 54.7 (s, CH of ¹Pr), 51.9 (s, CH of ¹Pr), 25.7 (s, Me of ¹Pr), 25.4 (s, Me of ¹Pr), 25.1 (s, Me of ¹Pr), 20.5 (s, Me of ¹Pr), 12.2 (s, 3 CH₂ of Et), 9.2 (s, 3 Me of Et), 6.2 (s, 3 Me of HMDS), 6.1 (s, 3 Me of HMDS).

[Ru₂(SnPh₃)(μ-H){μ-κ²Ge,N-Ge(¹Pr₂bzam)(HMDS)}(CO)₅] (10). HSnPh₃ (11 mg, 0.03 mmol) was added to a solution of complex 2 (25 mg, 0.03 mmol) in toluene (10 mL), and the mixture was stirred at room temperature for 4 h. The color changed from orange to dark orange. The solvent was removed under reduced pressure, and the crude reaction mixture was separated by column chromatography on silica-gel (2 × 5 cm). Compound 10 was eluted with hexane, and it was isolated as an orange solid (30 mg, 89%). Anal. Calcd for C₄₂H₅₃GeN₃O₃Ru₂Si₂Sn (1129.53): C, 44.66; H, 4.73; N, 3.72; found, C, 44.72; H, 4.91; N, 3.69. (+)-FAB MS: m/z 1129 [M]⁺. IR (toluene, cm⁻¹): ν_{CO} 2072 (w), 2012 (vs), 1995 (m), 1943 (m). ¹H NMR

(C₆D₆, 300.1 MHz, 293 K): δ 8.06–7.90 (m, sat, 6 H, 6 CH_{ortho} of Ph), 7.29 (t, J = 7.2 Hz, 6 H, 6 CH_{meta} of Ph), 7.18–6.85 (m, 8 H, 8 CH of Ph), 3.66 (m, 1 H, CH of ¹Pr), 3.38 (m, 1 H, CH of ¹Pr), 1.18 (d, J = 6.8 Hz, 3 H, Me of ¹Pr), 1.08 (d, J = 6.7 Hz, 3 H, Me of ¹Pr), 0.86 (d, J = 6.3 Hz, 3 H, Me of ¹Pr), 0.52 (d, J = 6.7 Hz, 3 H, Me of ¹Pr), 0.50 (s, 9 H, 3 Me of HMDS), 0.47 (s, 9 H, 3 Me of HMDS), -10.30 (s, sat, 1 H, μ-H). ¹³C{¹H} NMR (C₆D₆, 75.5 MHz, 293 K): δ 165.3 (s, NCN), 144.4 (s, 3 C_{ipso} of Ph), 137.8–127.5 (Ph groups of the germylene and SnPh₃ ligands), 54.9 (s, CH of ¹Pr), 51.7 (s, CH of ¹Pr), 25.4 (s, Me of ¹Pr), 25.3 (s, Me of ¹Pr), 25.0 (s, Me of ¹Pr), 19.9 (s, Me of ¹Pr), 6.3 (s, 3 Me of HMDS), 6.2 (s, 3 Me of HMDS). ¹³C{¹H} NMR of a ¹³CO-enriched sample (C₆D₅CD₃, 75.5 MHz, 293 K): δ 204.2 (s, CO), 199.1 (s, CO), 197.7 (s, CO), 194.8 (s, CO), 190.6 (s, CO).

[Ru₂(SiEt₃)(μ-H){μ-κ²Ge,N-Ge(¹Pr₂bzam)(HMDS)}(¹BuNC)(CO)₅] (11). ¹BuNC (2 μL, 0.018 mmol) was added to a solution of 9 (15 mg, 0.017 mmol) in toluene (10 mL), and the mixture was stirred at room temperature for 5 min. The color changed from dark orange to yellow. The solvent was removed under reduced pressure to give compound 11 as a pure yellow solid (16 mg, 96%). Anal. Calcd for C₃₅H₆₂GeN₄O₃Ru₂Si₃ (977.91): C, 42.99; H, 6.39; N, 5.73; found, C, 43.04; H, 6.44; N, 5.69. (+)-FAB MS: m/z 978 [M]⁺. IR (toluene, cm⁻¹): ν_{CN} 2156 (w); ν_{CO} 2053 (w), 2014 (vs), 1974 (s), 1955 (m). ¹H NMR (C₆D₆, 300.1 MHz, 293 K): δ 7.08–6.97 (m, 5 H, 5 CH of Ph), 3.87 (spt, J = 6.7 Hz, 1 H, 1 CH of ¹Pr), 3.49 (spt, J = 6.7 Hz, 1 H, 1 CH of ¹Pr), 1.39–0.90 (m, 36 H, 3 CH₂ and 3 Me of Et; 4 Me of ¹Pr and 3 Me of ¹Bu), 0.67 (s, 18 H, 6 Me of HMDS), -11.4 (s, 1 H, μ-H). ¹³C{¹H} NMR (C₆D₆, 75.5 MHz, 293 K): δ 208.5 (s, CO), 202.4 (s, COs), 197.8 (s, CO), 166.3 (s, NCN), 139.4 (s, NC), 135.4 (s, C_{ipso} of Ph), 129.1 (s, CH of Ph), 128.8 (s, CH of Ph), 128.7 (s, CH of Ph), 127.3 (s, CH of Ph), 127.1 (s, CH of Ph), 57.4 (s, C of ¹Bu), 54.9 (s, CH of ¹Pr), 51.7 (s, CH of ¹Pr), 30.0 (s, 3 Me of ¹Bu), 25.5 (s, Me of ¹Pr), 25.2 (s, 2 Me of ¹Pr), 23.5 (s, Me of ¹Pr), 12.3 (s, 3 CH₂ of Et), 9.7 (s, 3 Me of Et), 6.7 (s, 3 Me of HMDS), 6.6 (s, 3 Me of HMDS).

[Ru₂(SnPh₃)(μ-H){μ-κ²Ge,N-Ge(¹Pr₂bzam)(HMDS)}(¹BuNC)(CO)₅] (12). ¹BuNC (2 μL, 0.018 mmol) was added to a solution of 11 (20 mg, 0.018 mmol) in toluene (10 mL), and the mixture was stirred at room temperature for 5 min. The color changed from dark orange to yellow. The solvent was removed under reduced pressure to give compound 12 as a pure pale orange solid (18 mg, 84%). Anal. Calcd for C₄₇H₆₂GeN₄O₃Ru₂Si₂Sn (1212.65): C, 46.55; H, 5.15; N, 4.62; found, C, 46.61; H, 5.22; N, 4.51. (+)-FAB MS: m/z 1212 [M]⁺. IR (toluene, cm⁻¹): ν_{CN} 2163 (w); ν_{CO} 2060 (w), 2019 (vs), 1986 (s), 1960 (m). ¹H NMR (C₆D₆, 300.1 MHz, 293 K): δ 8.10–7.94 (m, sat, 6 H, 6 CH_{ortho} of Ph), 7.60–7.58 (m, 3 H, 3 CH_{para} of Ph), 7.28 (t, J = 7.3 Hz, 6 H, 6 CH_{meta} of Ph), 6.94–6.84 (m, 5 H, 5 CH of Ph), 3.82 (spt, J = 6.5 Hz, 1 H, CH of ¹Pr), 3.42 (spt, J = 6.5 Hz, 1 H, CH of ¹Pr), 1.37 (d, J = 6.5 Hz, 3 H, Me of ¹Pr), 1.21 (d, J = 6.5 Hz, 3 H, Me of ¹Pr), 1.16 (d, J = 6.5 Hz, 3 H, Me of ¹Pr), 0.83 (s, 9 H, 3 Me of ¹Bu), 0.75 (d, 3 H, Me of ¹Pr), 0.66 (s, 9 H, 3 Me of HMDS), 0.61 (s, 9 H, 3 Me of HMDS), -11.2 (s, 1 H, μ-H). ¹³C{¹H} NMR (C₆D₆, 75.5 MHz, 293 K): δ 204.6 (s, CO), 201.6 (s, CO), 200.2 (s, CO), 198.8 (s, CO), 197.6 (s, CO), 166.9 (s, NCN), 146.3 (s, CN), 138.1–125.7 (m, Ph groups of the germylene and SnPh₃ ligands), 57.7 (s, C of ¹Bu), 55.1 (s, CH of ¹Pr), 51.8 (s, CH of ¹Pr), 29.6 (s, 3 Me of ¹Bu), 25.3 (s, Me of ¹Pr), 25.2 (s, Me of ¹Pr), 25.0 (s, Me of ¹Pr), 23.3 (s, Me of ¹Pr), 6.6 (s, 3 Me of HMDS), 6.5 (s, 3 Me of HMDS).

[Ru₂(SiEt₃)(μ-H){μ-κ²Ge,N-Ge(¹Pr₂bzam)(HMDS)}(CO)₆] (13). Carbon monoxide was bubbled for 10 s through a solution of complex 9 (10 mg, 0.011 mmol) in toluene (5 mL). The color changed from dark orange to pale orange, and the IR spectrum of the resulting solution indicated the complete transformation of 9 into 13. IR (toluene, cm⁻¹): ν_{CO} 2072 (w), 2050s (m), 2005 (m), 1993 (vs), 1936 (w, br). This product could not be isolated in pure form because it reverted to compound 9 upon heating or when the solvent was removed under reduced pressure, and it was converted into complex 2 upon a longer exposure to CO gas (10 min).

[Ru₂(SnPh₃)(μ-H){μ-κ²Ge,N-Ge(¹Pr₂bzam)(HMDS)}(CO)₆] (14). CO gas was bubbled for 20 s through a solution of complex 10 (10 mg, 0.009 mmol) in toluene (5 mL). The color changed from dark orange

to pale orange, and the IR spectrum of the resulting solution indicated the complete transformation of **10** into **14**. IR (toluene, cm^{-1}): ν_{CO} 2076 (w), 2058 (m), 2013 (m), 1999 (vs), 1944 (w, br). This product could not be isolated in pure form because it reverted to compound **10** upon heating or under reduced pressure. The following NMR data of **14** were obtained from a sample maintained under CO in a J. Young NMR tube. ^1H NMR (CD_2Cl_2 , 300.1 MHz, 293 K): δ 7.66–7.47 (m, sat, 6 H, 6 CH_{ortho} of Ph), 7.43–7.17 (m, 12 H, 12 CH of Ph), 7.02 (d, $J = 7.1$ Hz, 1 H, CH of Ph), 6.80 (d, $J = 7.1$ Hz, 1 H, CH of Ph), 3.89 (m, 1 H, CH of ^iPr), 3.27 (m, 1 H, CH of ^iPr), 1.31 (d, $J = 6.6$ Hz, 3 H, CH_3 of ^iPr), 1.20 (d, $J = 6.6$ Hz, 3 H, Me of ^iPr), 1.01 (d, $J = 6.6$ Hz, 3 H, Me of ^iPr), 0.50–0.45 (m, 21 H, Me of ^iPr and Me₆ of HMDS), –11.6 (s, sat, 1 H, $\mu\text{-H}$). $^{13}\text{C}\{^1\text{H}\}$ NMR (CD_2Cl_2 , 75.5 MHz, 293 K): 203.9 (s, CO), 198.7 (s, 2 CO), 197.6 (s, CO), 194.8 (s, CO), 190.6 (s, CO), 167.6 (s, NCN), 144.9–125.6 (Ph groups of the germylene and SnPh₃ ligands), 55.0 (s, CH of ^iPr), 51.8 (s, CH of ^iPr), 25.2 (s, Me of ^iPr), 25.3 (s, Me of ^iPr), 25.0 (s, Me of ^iPr), 19.9 (s, Me of ^iPr), 6.3 (s, 3 Me of HMDS), 6.2 (s, 3 Me of HMDS). $^{13}\text{C}\{^1\text{H}\}$ NMR of a ^{13}C -enriched sample ($\text{C}_6\text{D}_5\text{CD}_3$, 75.5 MHz, 293 K): δ 204.0 (s, CO), 199.2 (s, CO), 199.0 (s, CO), 197.7 (s, CO), 194.9 (s, CO), 190.8 (s, CO).

$[\text{Ru}_4(\mu\text{-H})_2(\mu\text{-}\kappa^2\text{Ge}_2\text{N-Ge}^i\text{Pr}_2\text{bzam})(\text{HMDS})_2(\text{CO})_{10}]$ (**15**). Hydrogen gas was bubbled for 1 h through a solution of complex **2** (25 mg, 0.03 mmol) in THF (10 mL) at 70 °C. The color changed from orange to dark red. The solvent was removed under reduced pressure, and the crude reaction mixture was separated by column chromatography on neutral alumina (activity IV, 2 × 3 cm). Compound **15** was eluted with hexane, and it was isolated as a dark red solid (12 mg, 51%). Anal. Calcd for $\text{C}_{48}\text{H}_{76}\text{Ge}_2\text{N}_6\text{O}_{10}\text{Ru}_4\text{Si}_4$ (1559.01): C, 36.98; H, 4.91; N, 5.39; found, C, 37.03; H, 5.12; N, 5.26. IR (toluene, cm^{-1}): ν_{CO} 2070 (w), 2008 (vs), 1986 (m), 1937 (m). ^1H NMR (C_6D_6 , 300.1 MHz, 293 K): δ 7.24–7.00 (m, 5 H, 5 CH of Ph), 3.69 (m, 2 H, 2 CH of ^iPr), 1.39 (d, $J = 6.2$ Hz, 3 H, Me of ^iPr), 1.19 (d, $J = 6.5$ Hz, 3 H, Me of ^iPr), 1.04 (d, $J = 6.3$ Hz, 3 H, Me of ^iPr), 1.03 (d, $J = 6.5$ Hz, 3 H, Me of ^iPr), 0.61 (s, 9 H, 3 Me of HMDS), 0.60 (s, 9 H, 3 Me of HMDS), –10.90 (s, 1 H, $\mu\text{-H}$). $^{13}\text{C}\{^1\text{H}\}$ NMR (C_6D_6 , 75.5 MHz, 293 K): δ 208.4 (s, CO), 207.1 (s, CO), 205.7 (s, CO), 197.7 (s, CO), 195.4 (s, CO), 165.2 (s, NCN), 135.0 (s, C_{ipso} of Ph), 129.2 (s, CH of Ph), 129.0 (s, CH of Ph), 128.6 (s, CH of Ph), 128.0 (s, CH of Ph), 127.2 (s, CH of Ph), 55.1 (s, CH of ^iPr), 51.9 (s, CH of ^iPr), 25.4 (s, 2 Me of ^iPr), 25.1 (s, 2 Me of ^iPr), 6.5 (s, 3 Me of HMDS), 6.3 (s, 3 Me of HMDS).

$[\text{Ru}_4(\mu\text{-H})_2(\mu\text{-}\kappa^2\text{Ge}_2\text{N-Ge}^i\text{Pr}_2\text{bzam})(\text{HMDS})_2(^i\text{BuNC})_2(\text{CO})_{10}]$ (**16**). Hydrogen gas was gently bubbled (1 h) from a needle through a solution of complex **2** (40 mg, 0.048 mmol) in THF (10 mL) at 70 °C. The resulting red solution was cooled to room temperature, the hydrogen supply was stopped, and $^i\text{BuNC}$ (7 μL , 0.06 mmol) was added. The color changed from dark red to orange. The solvent was removed under reduced pressure, and the crude reaction mixture was separated by column chromatography on neutral alumina (activity IV, 2 × 3 cm). Compound **16** was eluted with hexane/ CH_2Cl_2 (2:1), and it was isolated as an orange solid (17 mg, 41%). Anal. Calcd for $\text{C}_{58}\text{H}_{94}\text{Ge}_2\text{N}_8\text{O}_{10}\text{Ru}_4\text{Si}_4$ (1725.27): C, 40.38; H, 5.49; N, 6.50; found, C, 40.42; H, 5.51; N, 6.42. IR (toluene, cm^{-1}): ν_{CN} 2161 (m); ν_{CO} 2053 (w), 2018 (vs), 1995 (m), 1975 (s), 1968 (s), 1956 (m), 1950 (m). ^1H NMR (C_6D_6 , 300.1 MHz, 293 K): δ 7.26–6.98 (m, 10 H, 10 CH of 2 Ph), 3.91 (m, 2 H, 2 CH of 2 ^iPr), 3.56 (m, 2 H, 2 CH of 2 ^iPr), 1.64 (d, $J = 6.9$ Hz, 3 H, Me of ^iPr), 1.60 (d, $J = 6.9$ Hz, 3 H, Me of ^iPr), 1.44–1.30 (m, 12 H, 4 Me of 2 ^iPr), 1.16–1.08 (m, 24 H, 2 Me of ^iPr and 6 Me of 2 ^iBu), 0.80–0.77 (m, 36 H, 12 Me of 2 HMDS), –12.00 (s, 1 H, $\mu\text{-H}$), –12.11 (s, 1 H, $\mu\text{-H}$). $^{13}\text{C}\{^1\text{H}\}$ NMR (C_6D_6 , 75.5 MHz, 293 K): δ 210.6 (CO), 210.3 (CO), 210.0 (CO), 209.2 (CO), 208.1 (CO), 207.3 (CO), 197.6 (CO), 197.4 (CO), 166.4 (2 NCN), 143.9 (2 CN^iBu), 138.9 (2 C_{ipso} of 2 Ph), 129.3–127.0 (CHs of 2 Ph), 57.2 (2 C of 2 ^iBu), 55.3 (CH of ^iPr), 55.1 (CH of ^iPr), 52.0 (CH of ^iPr), 51.9 (CH of ^iPr), 30.0 (6 Me of 2 ^iBu), 25.5 (2 Me of ^iPr), 25.3 (2 Me of ^iPr), 23.8 (2 Me of ^iPr), 23.8 (2 Me of ^iPr), 7.0 (6 Me of HMDS), 6.8 (6 Me of HMDS).

$[\text{Ru}_4(\mu\text{-H})_2(\mu\text{-}\kappa^2\text{Ge}_2\text{N-Ge}^i\text{Pr}_2\text{bzam})(\text{HMDS})_2(\text{CO})_{12}]$ (**17**). Carbon monoxide was bubbled for 5 min through a solution of complex **15** (18 mg, 0.012 mmol) in THF (5 mL). The color changed from dark red to orange, and the IR spectrum of the resulting solution indicated the complete transformation of **15** into complex **17**. IR (THF, cm^{-1}): ν_{CO} 2078 (m), 2065 (s), 2048 (m), 2017 (vs), 1999 (s), 1994 (s), 1971 (m), 1951 (w). This product could not be isolated in pure form because it was gradually converted into complex **2** upon longer exposure to CO gas, and it reverted to compound **15** when the solvent was removed under reduced pressure. The ^1H NMR data (300.1 MHz, 293 K) of this complex were obtained from a solution prepared by treating a C_6D_6 solution of **15** with CO in an NMR tube (it was contaminated with some **2**, see the Supporting Information): δ 7.08–6.85 (m, 10 H, 10 CH of 2 Ph), 3.78 (m, 2 H, 2 CH of 2 ^iPr), 3.36 (m, 2 H, 2 CH of 2 ^iPr), 1.52–1.22 (m, 12 H, 4 Me of 2 ^iPr), 0.98–0.91 (m, 12 H, 4 Me of 2 ^iPr), 0.71 (s, 18 H, 6 Me of HMDS), 0.62 (s, 18 H, 6 Me of HMDS), –11.89 (s, 1 H, $\mu\text{-H}$), –11.90 (s, 1 H, $\mu\text{-H}$).

$[\text{Ru}_4(\mu\text{-}\kappa^2\text{Ge}_2\text{N-Ge}^i\text{Pr}_2\text{bzam})(\text{HMDS})_2(\mu\text{-}\kappa\text{Ge-Ge}(\text{HMDS}))(\mu\text{-}\kappa^2\text{N}_2\text{C}_i\text{N}^i\text{Pr}_2\text{bzam})(\mu\text{-CO})(\text{CO})_6]$ (**18**). A solution of complex **2** (50 mg, 0.06 mmol) in toluene (10 mL) was heated at reflux temperature for 20 min. The color changed from orange to dark red. The solvent was removed under reduced pressure, and the crude reaction mixture was separated by column chromatography on silica-gel (2 × 5 cm). Hexane–dichloromethane (1:1) eluted compound **18**, which was isolated as a dark red solid (27 mg, 59%). Anal. Calcd for $\text{C}_{47}\text{H}_{74}\text{Ge}_2\text{N}_6\text{O}_9\text{Ru}_4\text{Si}_4$ (1528.97): C, 36.92; H, 4.88; N, 5.50; found, C, 37.03; H, 4.96; N, 5.35. IR (hexane, cm^{-1}): ν_{CO} 2053 (w), 2000 (m), 1994 (vs), 1984 (s), 1935 (m), 1927 (w), 1811 (m, br). ^1H NMR (CD_2Cl_2 , 300.1 MHz, 293 K): δ 8.10 (m, 1 H, CH of Ph), 7.82 (d, $J = 7.7$ Hz, 1 H, CH of Ph), 7.60–7.13 (m, 7 H, 7 CH of Ph), 6.90 (d, $J = 7.7$ Hz, 1 H, CH of Ph), 3.89 (m, 1 H, CH of ^iPr), 3.54 (m, 1 H, CH of ^iPr), 3.11 (spt, $J = 6.4$ Hz, 1 H, CH of ^iPr), 2.49 (spt, $J = 6.8$ Hz, 1 H, CH of ^iPr), 1.43 (d, $J = 6.6$ Hz, 3 H, Me of ^iPr), 1.42 (d, $J = 6.8$ Hz, 3 H, Me of ^iPr), 1.35 (d, $J = 6.4$ Hz, 3 H, Me of ^iPr), 1.13 (d, $J = 6.8$ Hz, 3 H, Me of ^iPr), 0.90–0.84 (m, 9 H, 3 Me of ^iPr), 0.66 (d, $J = 6.8$ Hz, 3 H, Me of ^iPr), 0.54 (s, 9 H, 3 Me of HMDS), 0.49 (s, 9 H, 3 Me of HMDS), 0.46 (s, 9 H, 3 Me of HMDS), 0.42 (s, 9 H, 3 Me of HMDS). $^{13}\text{C}\{^1\text{H}\}$ NMR (CD_2Cl_2 , 100.6 MHz, 293 K): δ 170.8 (s, NCN), 167.5 (s, NCN), 136.9 (s, C_{ipso} of Ph), 136.6 (s, C_{ipso} of Ph), 130.7 (s, CH of Ph), 128.9 (s, CH of Ph), 128.7 (s, CH of Ph), 128.5 (s, CH of Ph), 128.1 (s, CH of Ph), 128.0 (s, CH of Ph), 127.3 (s, CH of Ph), 125.2 (s, CH of Ph), 125.0 (s, CH of Ph), 54.4 (CH of ^iPr), 53.3 (CH of ^iPr), 52.7 (CH of ^iPr), 51.6 (CH of ^iPr), 28.6 (s, 3 Me of ^iPr), 27.1 (s, Me of ^iPr), 26.8 (s, Me of ^iPr), 25.6 (s, Me of ^iPr), 25.1 (s, Me of ^iPr), 24.9 (s, Me of ^iPr), 24.7 (s, Me of ^iPr), 24.4 (s, Me of ^iPr), 5.7 (s, 3 Me of HMDS), 5.5 (s, 3 Me of HMDS), 3.3 (s, 3 Me of HMDS), 3.1 (s, 3 Me of HMDS).

Computational Details. DFT calculations were carried out using the wB97XD functional,²¹ which includes the second generation of Grimme's dispersion interaction correction²² as well as long-range interactions effects. This functional was chosen because it has shown to provide the best overall performance in a study^{11a} that compared its efficiency in reproducing X-ray diffraction molecular structures of various transition metal complexes with those of the two popular density functionals B3LYP²³ and M06.²⁴ It also corrects the systematic overestimation of nonbonded distances seen for all the density functionals that do not include estimates of dispersion.²⁵ The LanL2DZ basis set,²⁶ with relativistic effective core potentials, was used for the Ru and Ge atoms. The basis set used for the remaining atoms was the 6-31G(d,p).²⁷ The molecular structures of **4**, **6**, and **9** were fully optimized in gas phase and confirmed as energy minima by the analytical calculation of frequencies (all positive eigenvalues). The connection of the transition state $\text{TS}_{4,6}$ (one imaginary eigenvalue) to **4** and **6** was confirmed by IRC calculations. The electronic energies of the optimized structures were used to calculate the zero-point corrected energies and the enthalpic and entropic contributions via vibrational frequency calculations. Solvation free energies were obtained from the gas phase calculations using the self-consistent reaction field SCRf approximation to the standard continuum solvation model (CPCM).^{28,29} All calculations were carried out with

the Gaussian 09 package.³⁰ The atomic coordinates of all DFT-optimized structures are given in the Supporting Information.

X-ray Diffraction Analyses. Diffraction data were collected on Oxford Diffraction Xcalibur Onyx Nova (3, 7·(C₇H₈)_{0.5}, **11**, and **18**; CuK α radiation) and Scalibur Ruby Gemini (16·(C₆H₁₄)_{0.5}; MoK α radiation) single crystal diffractometers. Empirical absorption corrections were applied using the SCALE3 ABSPACK algorithm as implemented in CrysAlisPro RED.³¹ The structures were solved using SIR-97.³² Isotropic and full matrix anisotropic least-squares refinements were carried out using SHELXL.³³ One of the ethyl groups (C20 and C21) of the SiEt₃ fragment of **11** was found to be disordered over two positions with a 3:1 occupancy ratio. All non-H atoms were refined anisotropically. All H atoms were set in calculated positions and refined riding on their parent atoms, except for the hydride ligands of **11**- and **16**·(C₆H₁₄)_{0.5} that were found in the corresponding Fourier difference maps and were freely refined. The WINGX program system³⁴ was used throughout the structure determinations. A selection of crystal, measurement, and refinement data is given in Table S3 of the Supporting Information. CCDC deposition numbers: **3**, 1049250; 7·(C₇H₈)_{0.5}, 1049251; **11**, 1049252; 16·(C₆H₁₄)_{0.5}, 1049253; and **18**, 1049254.

■ ASSOCIATED CONTENT

● Supporting Information

¹H and ¹³C NMR spectra of all reaction products, atomic coordinates of all the DFT-optimized structures, and crystallographic data (including CIF files). The Supporting Information is available free of charge on the ACS Publications website at DOI: 10.1021/acs.inorgchem.5b00412.

■ AUTHOR INFORMATION

Corresponding Authors

*(J.A.C.) E-mail: jac@uniovi.es.

*(P.G.-A.) E-mail: pga@uniovi.es.

Notes

The authors declare no competing financial interest.

■ ACKNOWLEDGMENTS

This work has been supported by a European Union Marie Curie reintegration grant (No. FP7-2010-RG-268329), by Spanish MINECO-FEDER research projects (Nos. CTQ2010-14933, RYC2012-10491, CTQ2013-40619-P, and MAT2013-40950-R), and by a research grant from the Government of Asturias (No. GRUPIN14-009).

■ REFERENCES

- (1) Lee, V. Y.; Sekiguchi, A. *Organometallic Compounds of Low Coordinate Si, Ge, Sn and Pb: From Phantom Species to Stable Compounds*; Wiley-VCH: Chichester, UK, 2010.
- (2) For reviews on the chemistry of HTs, see: (a) Baumgartner, J.; Marschner, C. *Rev. Inorg. Chem.* **2014**, *34*, 119–152. (b) Izod, K. *Coord. Chem. Rev.* **2013**, *257*, 924–945. (c) Xiong, Y.; Yao, S.; Driess, M. *Angew. Chem., Int. Ed.* **2013**, *52*, 4302–4311. (d) Mandal, S. K.; Roesky, H. W. *Acc. Chem. Res.* **2012**, *45*, 298–307. (e) Yao, S.; Xiong, Y.; Driess, M. *Organometallics* **2011**, *30*, 1748–1767. (f) Panday, K. K.; Power, P. P. *Organometallics* **2011**, *30*, 3353–3361. (g) Mizuhata, Y.; Sasamori, T.; Tokitoh, N. *Chem. Rev.* **2009**, *109*, 3479–3511. (h) Barrau, J.; Rima, G. *Coord. Chem. Rev.* **1998**, *178–180*, 593–622. (i) Neumann, W. P. *Chem. Rev.* **1991**, *91*, 311–334. (j) Veith, M. *Angew. Chem., Int. Ed.* **1987**, *26*, 1–14.
- (3) For reviews on the chemistry of HTs, including some coordination chemistry, see: (a) Prabhusankar, G.; Sathyanarayana, A.; Suresh, P.; Babu, C. N.; Srinivas, K.; Metla, B. P. R. *Coord. Chem. Rev.* **2014**, *229*, 96–133. (b) Rivard, E. *Dalton Trans.* **2014**, *43*, 8577–8586. (c) Ghadwal, R. S.; Azhakar, R.; Roesky, H. W. *Acc. Chem. Res.* **2013**, *46*, 444–456. (d) Roesky, H. W. *J. Organomet. Chem.* **2013**, *730*,

- 57–62. (e) Asay, M.; Jones, C.; Driess, M. *Chem. Rev.* **2011**, *111*, 354–396. (f) Mandal, S. K.; Roesky, H. W. *Chem. Commun.* **2010**, *46*, 6016–6041. (g) Kira, M. *Chem. Commun.* **2010**, *46*, 2893–2903. (h) Nagendran, S.; Roesky, H. W. *Organometallics* **2008**, *27*, 457–492. (i) Zabula, A. V.; Hahn, F. E. *Eur. J. Inorg. Chem.* **2008**, 5165–5179. (j) Leung, W.-P.; Kan, K.-W.; Chong, K.-H. *Coord. Chem. Rev.* **2007**, *251*, 2253–2265. (k) Kühl, O. *Coord. Chem. Rev.* **2004**, *248*, 411–427. (l) Gehrhus, B.; Lappert, M. F. *J. Organomet. Chem.* **2001**, *617–618*, 209–223. (m) Haaf, M.; Schmedake, T. A.; West, R. *Acc. Chem. Res.* **2000**, *33*, 704–714. (n) Tokitoh, N.; Okazaki, R. *Coord. Chem. Rev.* **2000**, *210*, 251–277.

(4) For reviews on HTs as ligands in TM complexes, see: (a) Blom, B.; Gallego, D.; Driess, M. *Inorg. Chem. Front.* **2014**, *1*, 134–148. (b) Blom, B.; Stoelzel, M.; Driess, M. *Chem.—Eur. J.* **2013**, *19*, 40–62. (c) Waterman, R.; Hayes, P. G.; Tilley, T. D. *Acc. Chem. Res.* **2007**, *40*, 712–719. (d) Okazaki, M.; Tobita, H.; Ogino, H. *Dalton Trans.* **2003**, 493–506. (e) Lappert, M. F.; Rowe, R. S. *Coord. Chem. Rev.* **1990**, *100*, 267–292. (f) Petz, W. *Chem. Rev.* **1986**, *86*, 1019–1047.

(5) For examples of oxidation and/or hydrolysis processes on coordinated HTs, see: (a) Matioszek, D.; Saffon, N.; Sotiropoulos, J.-M.; Miqueu, K.; Castel, A.; Escudé, J. *Inorg. Chem.* **2012**, *51*, 11716–11721. (b) Zhanga, M.; Liua, X.; Shia, C.; Rena, C.; Dinga, Y.; Roesky, H. W. *Z. Anorg. Allg. Chem.* **2008**, *634*, 1755–1758. (c) Amoroso, D.; Haaf, M.; Yap, G. P. A.; West, R.; Fogg, D. E. *Organometallics* **2002**, *21*, 534–540. (d) Petri, S. H. A.; Eikenberg, D.; Neumann, B.; Stammler, H.-G.; Jutzi, P. *Organometallics* **1999**, *18*, 2615–2618.

(6) See, for example: (a) Nguyen, T. A. N.; Frenking, G. *Chem.—Eur. J.* **2012**, *18*, 12733–12749. (b) Arp, H.; Baumgartner, J.; Marschner, C.; Zark, P.; Müller, T. J. *Am. Chem. Soc.* **2012**, *134*, 10864–10875. (c) Boehme, C.; Frenking, G. *Organometallics* **1998**, *17*, 5801–5809. (d) Evans, W. J.; Perotti, J. M.; Ziller, J. W.; Moser, D. F.; West, R. *Organometallics* **2003**, *22*, 1160–1163. (e) Herrmann, W. A.; Härter, P.; Gstöttmayr, C. W. K.; Bielert, F.; Seeboth, N.; Sirsch, P. *J. Organomet. Chem.* **2002**, *649*, 141–146. (f) York, J. T.; Young, V. G., Jr.; Tolman, W. B. *Inorg. Chem.* **2006**, *45*, 4191–4198. (g) Yoo, H.; Carroll, P. J.; Berry, D. H. *J. Am. Chem. Soc.* **2006**, *128*, 6038–6039.

(7) (a) Blom, B.; Pohl, M.; Tan, G.; Gallego, D.; Driess, M. *Organometallics* **2014**, *33*, 5272–5282. (b) Gallego, D.; Inoue, S.; Blom, B.; Driess, M. *Organometallics* **2014**, *33*, 6885–6897. (c) Tan, G.; Blom, B.; Gallego, G.; Driess, M. *Organometallics* **2014**, *33*, 363–369. (d) Gallego, D.; Brück, A.; Irran, E.; Meier, F.; Kaupp, M.; Driess, M.; Hartwig, J. F. *J. Am. Chem. Soc.* **2013**, *135*, 15617–15626. (e) Blom, B.; Enthaler, S.; Inoue, S.; Irran, E.; Driess, M. *J. Am. Chem. Soc.* **2013**, *135*, 6703–6713. (f) Wang, W.; Inoue, S.; Enthaler, S.; Driess, M. *Angew. Chem., Int. Ed.* **2012**, *51*, 6167–6171. (g) Brück, A.; Gallego, D.; Wang, W.; Irran, E.; Driess, M.; Hartwig, J. F. *Angew. Chem., Int. Ed.* **2012**, *51*, 11478–11482. (h) Blom, B.; Driess, M.; Gallego, D.; Inoue, S. *Chem.—Eur. J.* **2012**, *18*, 13355–13360. (i) Wang, W.; Inoue, S.; Irran, E.; Driess, M. *Angew. Chem., Int. Ed.* **2012**, *51*, 3691–3694. (j) Wang, W.; Inoue, S.; Yao, S.; Driess, M. *J. Am. Chem. Soc.* **2010**, *132*, 15890–15892.

(8) (a) Schäfer, S.; Köppe, R.; Gamer, M. T.; Roesky, P. W. *Chem. Commun.* **2014**, *50*, 11401–11403. (b) Azhakar, R.; Ghadwal, R. S.; Roesky, H. W.; Hey, J.; Krause, L.; Stalke, D. *Dalton Trans.* **2013**, *42*, 10277–10281. (c) Azhakar, R.; Ghadwal, R. S.; Roesky, H. W.; Hey, J.; Stalke, D. *Chem. Asian J.* **2012**, *7*, 528–533. (d) Azhakar, R.; Roesky, H. W.; Holstein, J. J.; Dittrich, B. *Dalton Trans.* **2012**, *41*, 12096–12100. (e) Azhakar, R.; Ghadwal, R. S.; Roesky, H. W.; Wolf, H.; Stalke, D. *J. Am. Chem. Soc.* **2012**, *134*, 2423–2428. (f) Azhakar, R.; Sarish, S. P.; Roesky, H. W.; Hey, J.; Stalke, D. *Inorg. Chem.* **2011**, *50*, 5039–5043. (g) Sen, S. S.; Kratzer, D.; Stern, D.; Roesky, H. W.; Stalke, D. *Inorg. Chem.* **2010**, *49*, 5786–5788. (h) Tavčar, G.; Sen, S. S.; Azhakar, R.; Thorn, A.; Roesky, H. W. *Inorg. Chem.* **2010**, *49*, 10199–10202. (i) Sen, S. S.; Kritzler-Kosch, M. P.; Nagendran, S.; Roesky, H. W.; Beck, T.; Pal, A.; Herbst-Irmer, R. *Eur. J. Inorg. Chem.* **2010**, *5304–5311*. (j) Yang, W.; Fu, H.; Wang, H.; Chen, M.; Ding, Y.; Roesky, H. W.; Jana, A. *Inorg. Chem.* **2009**, *48*, 5058–5060.

(9) (a) Müick, F. M.; Kloß, D.; Baus, J. A.; Burschka, C.; Tacke, R. *Chem.—Eur. J.* **2014**, *20*, 9620–9626. (b) Junold, K.; Baus, J. A.;

- Burschka, C.; Vent-Schmidt, T.; Riedel, S.; Tacke, R. *Inorg. Chem.* **2013**, *52*, 11593–11599. (c) Junold, K.; Baus, J. A.; Burschka, C.; Tacke, R. *Angew. Chem., Int. Ed.* **2012**, *51*, 7020–7023.
- (10) (a) El Ezzi, M.; Kocsor, T. B.; D'Accrisio, F.; Madec, D.; Mallet-Ladeira, S.; Castel, A. *Organometallics* **2015**, *34*, 571–576. (b) Matioszek, D.; Katir, N.; Saffon, N.; Castel, A. *Organometallics* **2010**, *29*, 3039–3046.
- (11) (a) Álvarez-Rodríguez, L.; Cabeza, J. A.; García-Álvarez, P.; Pérez-Carreño, E.; Polo, D. *Inorg. Chem.* **2015**, *54*, 2983–2994. (b) Cabeza, J. A.; García-Álvarez, P.; Pérez-Carreño, E.; Polo, D. *Chem.—Eur. J.* **2014**, *20*, 8654–8663. (c) Cabeza, J. A.; Fernández-Colinas, J. M.; García-Álvarez, P.; Polo, D. *RSC Adv.* **2014**, *4*, 31503–31506. (d) Cabeza, J. A.; García-Álvarez, P.; Pérez-Carreño, E.; Polo, D. *Inorg. Chem.* **2014**, *53*, 8735–8741. (e) Cabeza, J. A.; García-Álvarez, P.; Polo, D. *Dalton Trans.* **2013**, *42*, 1329–1332.
- (12) (a) Breit, N. C.; Szilvási, T.; Suzuki, T.; Gallego, D.; Inoue, S. *J. Am. Chem. Soc.* **2013**, *135*, 17958–17968. (b) Someya, C. I.; Haberberger, M.; Wang, W.; Enthaler, S.; Inoue, S. *Chem. Lett.* **2013**, *42*, 286–288.
- (13) (a) Yeong, H.-X.; Li, Y.; So, C.-W. *Organometallics* **2014**, *33*, 3646–3648. (b) Jones, C.; Rose, R. P.; Stasch, A. *Dalton Trans.* **2008**, 2871–2878.
- (14) (a) Álvarez-Rodríguez, L.; Cabeza, J. A.; García-Álvarez, P.; Polo, D. *Organometallics* **2013**, *32*, 3557–3561. (b) Cabeza, J. A.; Fernández-Colinas, J. M.; García-Álvarez, P.; Polo, D. *Inorg. Chem.* **2012**, *51*, 3896–3903. (c) Cabeza, J. A.; García-Álvarez, P.; Polo, D. *Inorg. Chem.* **2012**, *51*, 2569–2576. (d) Cabeza, J. A.; García-Álvarez, P.; Polo, D. *Inorg. Chem.* **2011**, *50*, 6195–6199.
- (15) Cabeza, J. A.; Pérez-Carreño, E. *Organometallics* **2008**, *27*, 4697–4702.
- (16) For examples of addition of HSiEt₃ and HSnPh₃ to ruthenium carbonyl complexes containing N-donor ligands, see: (a) Cabeza, J. A.; Llamazares, A.; Riera, V.; Triki, S.; Ouahab, L. *Organometallics* **1992**, *11*, 3334–3339. (b) Cabeza, J. A.; García-Granda, S.; Llamazares, A.; Riera, V.; Van der Maelen, J. F. *Organometallics* **1993**, *12*, 157–163. (c) Cabeza, J. A.; Franco, R. J.; Llamazares, A.; Riera, V.; Bois, C.; Jeannin, Y. *Inorg. Chem.* **1993**, *32*, 4640–4642. (d) Cabeza, J. A.; García-Granda, S.; Llamazares, A.; Riera, V.; Van der Maelen, J. F. *Organometallics* **1993**, *12*, 2973–2979. (e) Cabeza, J. A.; Franco, R. J.; Riera, V. *Inorg. Chem.* **1994**, *33*, 5952–5954. (f) Cabeza, J. A.; Franco, R. J.; Riera, V.; García-Granda, S.; Van der Maelen, J. F. *Organometallics* **1995**, *14*, 3342–3348.
- (17) See, for example: (a) Tejel, C.; Ciriano, M. A.; Villarroya, B. E.; Gelpi, R.; López, J. A.; Lahoz, F.; Oro, L. A. *Angew. Chem., Int. Ed.* **2001**, *40*, 4084–4086. (b) Tejel, C.; Ciriano, M. A.; López, J. A.; Lahoz, F.; Oro, L. A. *Angew. Chem., Int. Ed.* **1998**, *37*, 1542–1545. (c) Cabeza, J. A.; del Río, I.; Riera, V.; Grepioni, F. *Organometallics* **1995**, *14*, 3124–3126. (d) Ciriano, M. A.; Sebastián, S.; Oro, L. A.; Tiripicchio, A.; Tiripicchio-Camellini, M. T.; Lahoz, F. *J. Angew. Chem., Int. Ed.* **1988**, *27*, 402–403. (e) Demartin, F.; Manassero, M.; Sansoni, M.; Garlaschelli, L.; Raimondi, C.; Martinengo, S.; Canziani, F. *Chem. Commun.* **1981**, 528–529.
- (18) For examples of terminal,^{18a-c} bridging,^{18d} and triply bridging^{18e-h} germylidyne ligands, see: (a) Filippou, A. C.; Barandov, A.; Schnakenburg, G.; Lewall, B.; van Gastel, M.; Marchanka, A. *Angew. Chem., Int. Ed.* **2012**, *51*, 789–793. (b) Filippou, A. C.; Chakraaborty, U.; Schnakenburg, G. *Chem.—Eur. J.* **2013**, *19*, 5676–5686. (d) Figge, L. K.; Carroll, P. J.; Berry, D. H. *Angew. Chem., Int. Ed.* **1996**, *35*, 435–437. (e) Saha, S.; Isrow, D.; Captain, B. *J. Organomet. Chem.* **2014**, *751*, 815–820. (f) Adams, R. D.; Captain, B.; Fu, W. *Inorg. Chem.* **2003**, *42*, 1328–1333. (g) Zhang, V.; Wang, B.; Xu, S.; Zhou, X. *Organometallics* **2001**, *20*, 3829–3832. (h) Boese, R.; Schmid, G. *J. Chem. Soc., Chem. Commun.* **1979**, 349–350. (c) Filippou, A. C.; Schnakenburg, G.; Philippopoulos, A. I.; Weidenmann, N. *Angew. Chem., Int. Ed.* **2005**, *44*, 5979–5985.
- (19) (a) Kondo, H.; Yamaguchi, Y.; Nagashima, H. *J. Am. Chem. Soc.* **2001**, *123*, 500–501. (b) Kondo, H.; Matsubara, K.; Nagashima, H. *J. Am. Chem. Soc.* **2002**, *124*, 534–535. (c) Terasawa, J.; Kondo, H.; Matsumoto, T.; Kirchner, J.; Motoyama, Y.; Nagashima, H. *J. Organometallics* **2005**, *24*, 2713–2721. (d) Hayashida, T.; Kondo, H.; Terasawa, J.; Kirchner, J.; Sunada, Y.; Nagashima, H. *J. Organomet. Chem.* **2007**, *692*, 382–394.
- (20) Cabeza, J. A.; Riera, V.; Villa-García, M. A.; Ouahab, L.; Triki, S. *J. Organomet. Chem.* **1992**, *441*, 323–331.
- (21) Chai, J.-D.; Head-Gordon, M. *Phys. Chem. Chem. Phys.* **2008**, *10*, 6615–6620.
- (22) (a) Ehrlich, S.; Moellmann, J.; Grimme, S. *Acc. Chem. Res.* **2013**, *46*, 916–926. (b) Grimme, S. *Comp. Mol. Sci.* **2011**, *1*, 211–228. (c) Schwabe, T.; Grimme, S. *Acc. Chem. Res.* **2008**, *41*, 569–579.
- (23) (a) Becke, A. D. *J. Chem. Phys.* **1993**, *98*, 5648–5652. (b) Lee, C.; Yang, W.; Parr, R. G. *Phys. Rev. B* **1988**, *37*, 785–789.
- (24) Zhao, Y.; Truhlar, D. G. *Theor. Chem. Acc.* **2008**, *120*, 215–241.
- (25) Minenkov, Y.; Singstad, A.; Occhipinti, G.; Jensen, V. R. *Dalton Trans.* **2012**, *41*, 5526–5541.
- (26) Hay, P. J.; Wadt, W. R. *J. Chem. Phys.* **1985**, *82*, 299–310.
- (27) Hariharan, P. C.; Pople, J. A. *Theor. Chim. Acta* **1973**, *28*, 213–222.
- (28) Barone, V.; Cossi, M. *J. Phys. Chem. A* **1998**, *102*, 1995–2001.
- (29) Cossi, M.; Rega, N.; Scalmani, G.; Barone, V. *J. Comput. Chem.* **2003**, *24*, 669–681.
- (30) Frisch, M. J.; Trucks, G. W.; Schlegel, H. B.; Scuseria, G. E.; Robb, M. A.; Cheeseman, J. R.; Scalmani, G.; Barone, V.; Mennucci, B.; Petersson, G. A.; Nakatsuji, H.; Caricato, M.; Li, X.; Hratchian, H. P.; Izmaylov, A. F.; Bloino, J.; Zheng, G.; Sonnenberg, J. L.; Hada, M.; Ehara, M.; Toyota, K.; Fukuda, R.; Hasegawa, J.; Ishida, M.; Nakajima, T.; Honda, Y.; Kitao, O.; Nakai, H.; Vreven, T.; Montgomery, J. A., Jr.; Peralta, J. E.; Ogliaro, F.; Bearpark, M.; Heyd, J. J.; Brothers, E.; Kudin, K. N.; Staroverov, V. N.; Keith, T.; Kobayashi, R.; Normand, J.; Raghavachari, K.; Rendell, A.; Burant, J. C.; Iyengar, S. S.; Tomasi, J.; Cossi, M.; Rega, N.; Millam, N. J.; Klene, M.; Knox, J. E.; Cross, J. B.; Bakken, V.; Adamo, C.; Jaramillo, J.; Gomperts, R.; Stratmann, R. E.; Yazyev, O.; Austin, A. J.; Cammi, R.; Pomelli, C.; Ochterski, J. W.; Martin, R. L.; Morokuma, K.; Zakrzewski, V. G.; Voth, G. A.; Salvador, P.; Dannenberg, J. J.; Dapprich, S.; Daniels, A. D.; Farkas, Ö.; Foresman, J. B.; Ortiz, J. V.; Cioslowski, J.; Fox, D. J. *Gaussian 09*, revision B.01; Gaussian, Inc.: Wallingford, CT, 2010.
- (31) *CrysAlisPro RED*, version 1.171.34.36; Oxford Diffraction Ltd.: Oxford, UK, 2010.
- (32) Altomare, A.; Burla, M. C.; Camalli, M.; Cascarano, G. L.; Giacovazzo, Guagliardi, A.; Moliterni, A. G. C.; Polidori, G.; Spagna, R. *J. Appl. Crystallogr.* **1999**, *32*, 115–119.
- (33) SHELXL; Sheldrick, G. M. *Acta Crystallogr., Sect. A* **2008**, *64*, 112–122.
- (34) WINGX, version 1.80.05 (2009); Farrugia, L. J. *J. Appl. Crystallogr.* **1999**, *32*, 837–838.

Reactivity Studies on a Binuclear Ruthenium(0) Complex Equipped with a Bridging κ^2N,Ge -Amidinatogermylene Ligand

Javier A. Cabeza,^{†*} José M. Fernández-Colinas,[†] Pablo García-Álvarez,^{†*}
Enrique Pérez-Carreño,[‡] and Diego Polo[†]

[†]*Departamento de Química Orgánica e Inorgánica-IUQOEM, Universidad de Oviedo-CSIC, E-33071 Oviedo, Spain*

[‡]*Departamento de Química Física y Analítica, Universidad de Oviedo, E-33071 Oviedo, Spain*

<u>CONTENTS</u>	<u>Pages</u>
^1H and $^{13}\text{C}\{^1\text{H}\}$ NMR Spectra	S3–S17
DFT-Optimized Molecular Structures	S18–S19

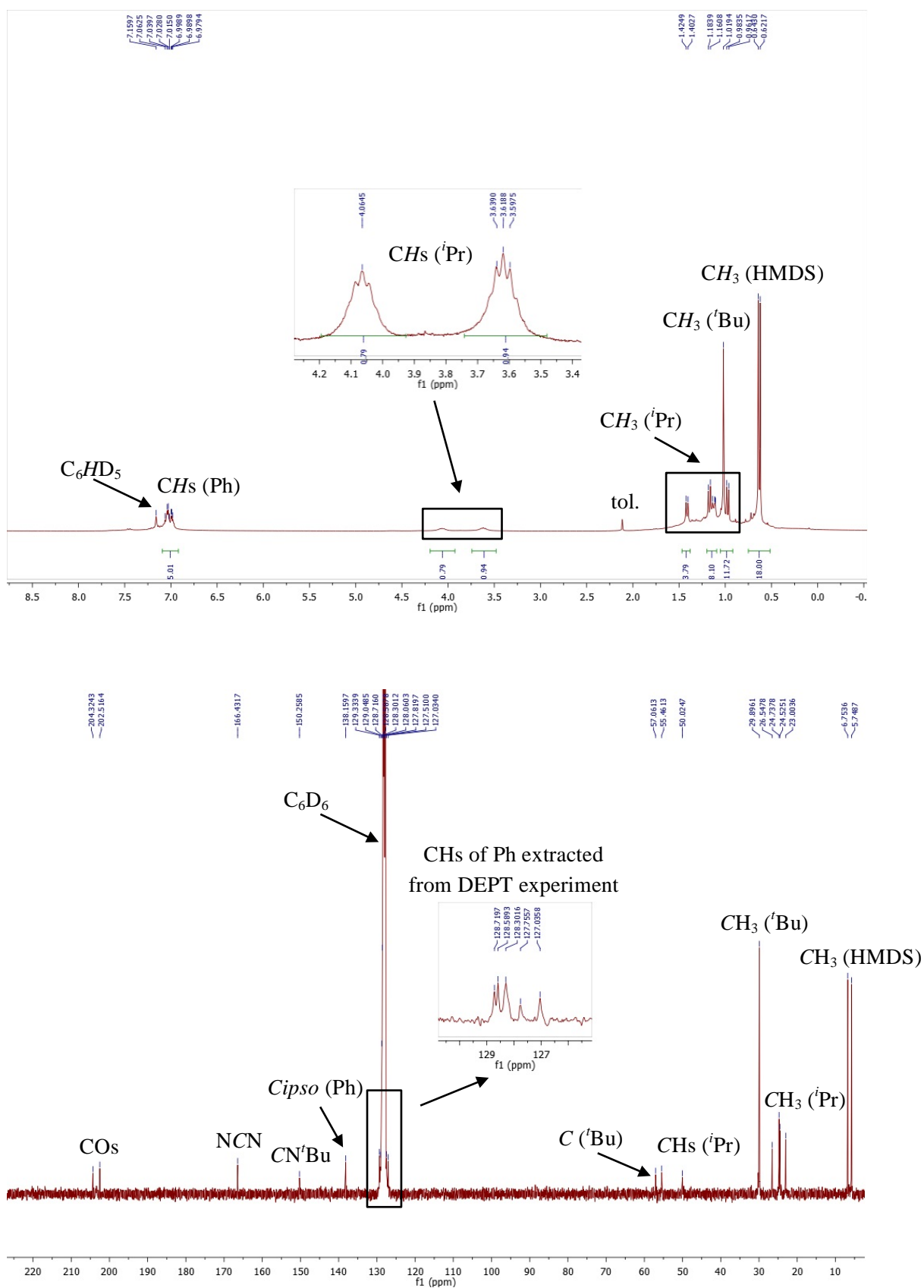


Figure S1. 1H (top) and $^{13}C\{^1H\}$ (bottom) NMR spectra of $[Ru_2\{\mu-\kappa^2Ge,N\{-Ge(iPr_2bzam)(HMDS)\}(CN^tBu)(CO)_6\}]$ (**3**) in C_6D_6 (20 °C).

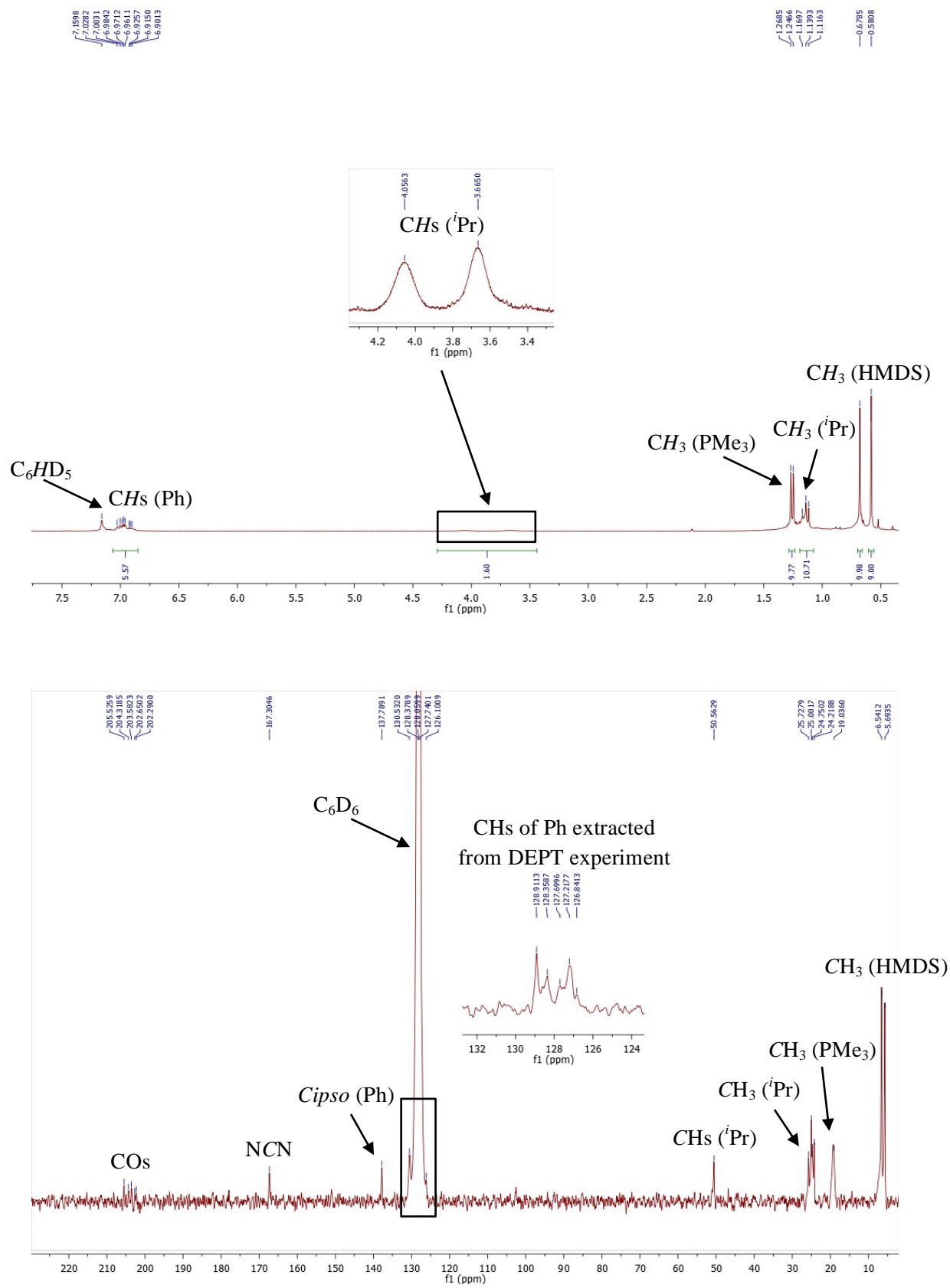


Figure S2. 1H (top) and $^{13}C\{^1H\}$ (bottom) NMR spectra of $[Ru_2\{\mu-\kappa^2Ge,N-Ge(iPr)_2bzam\}(HMDS)\}(PMe_3)(CO)_6]$ (**4**) in C_6D_6 (20 °C).

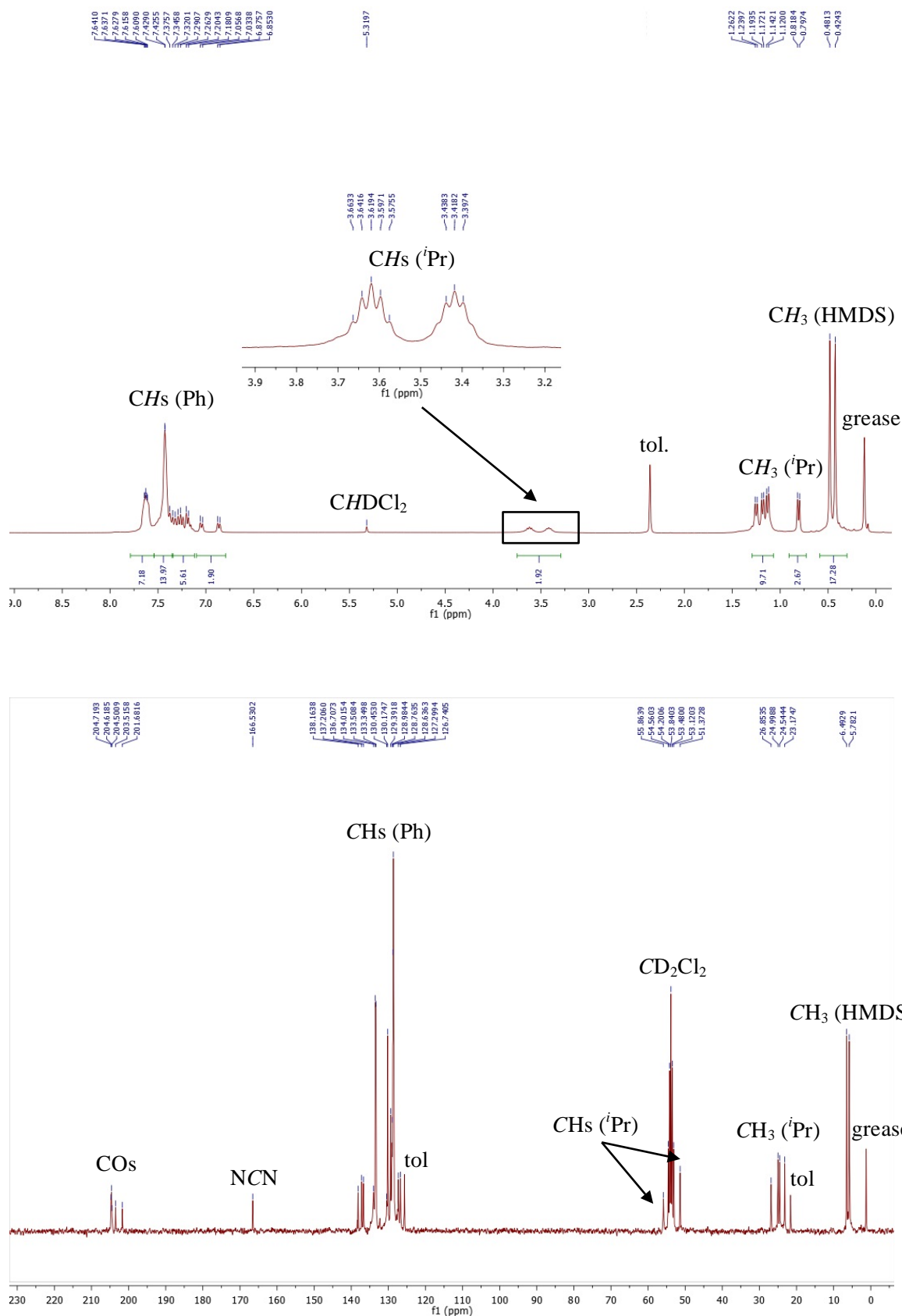
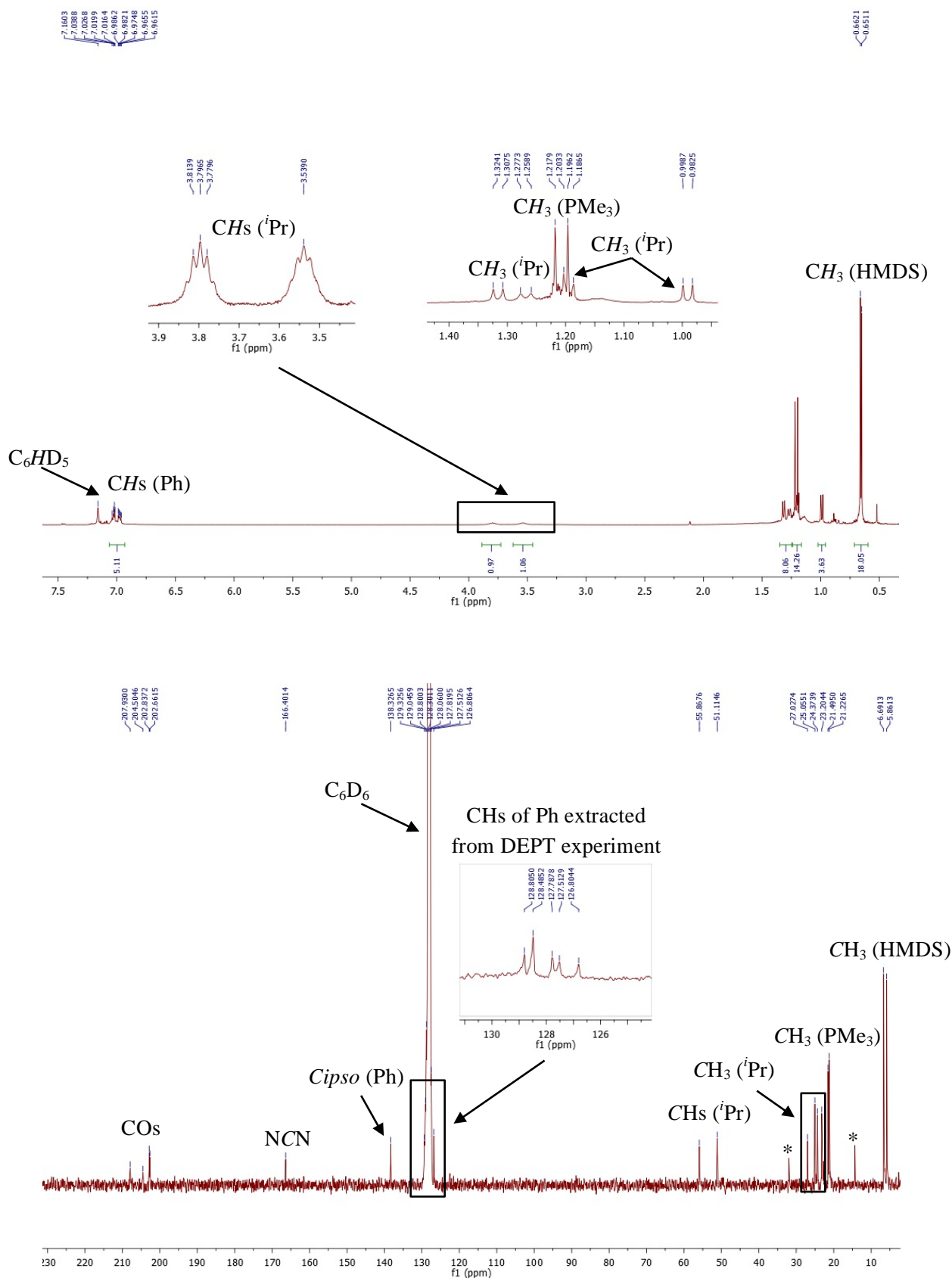


Figure S3. ¹H (top) and ¹³C{¹H} (bottom) NMR spectra of [Ru₂{μ-κ²Ge,N-Ge(*i*Pr₂bzam)(HMDS)}PPh₃(CO)₆] (**5**) in CD₂Cl₂ (20 °C).



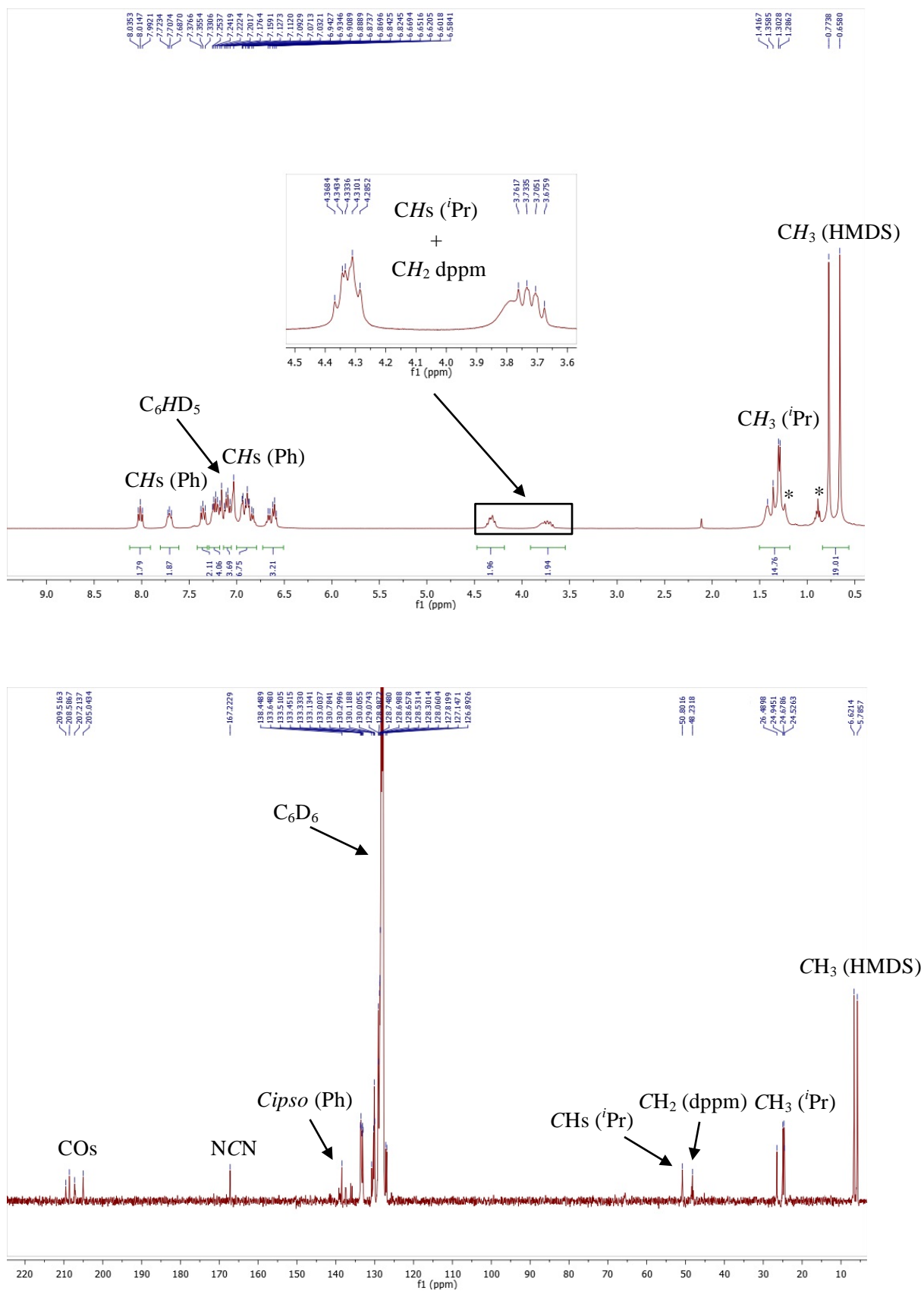


Figure S5. 1H (top) and $^{13}C\{^1H\}$ (bottom) NMR spectra of $[Ru_2\{\mu-\kappa^2Ge,N-Ge(iPr)_2bzam\}(HMDS)\}(dppm)(CO)_5]$ (**7**) in C_6D_6 ($20\text{ }^\circ C$). The peaks marked with an asterisk (*) are due to hexane.

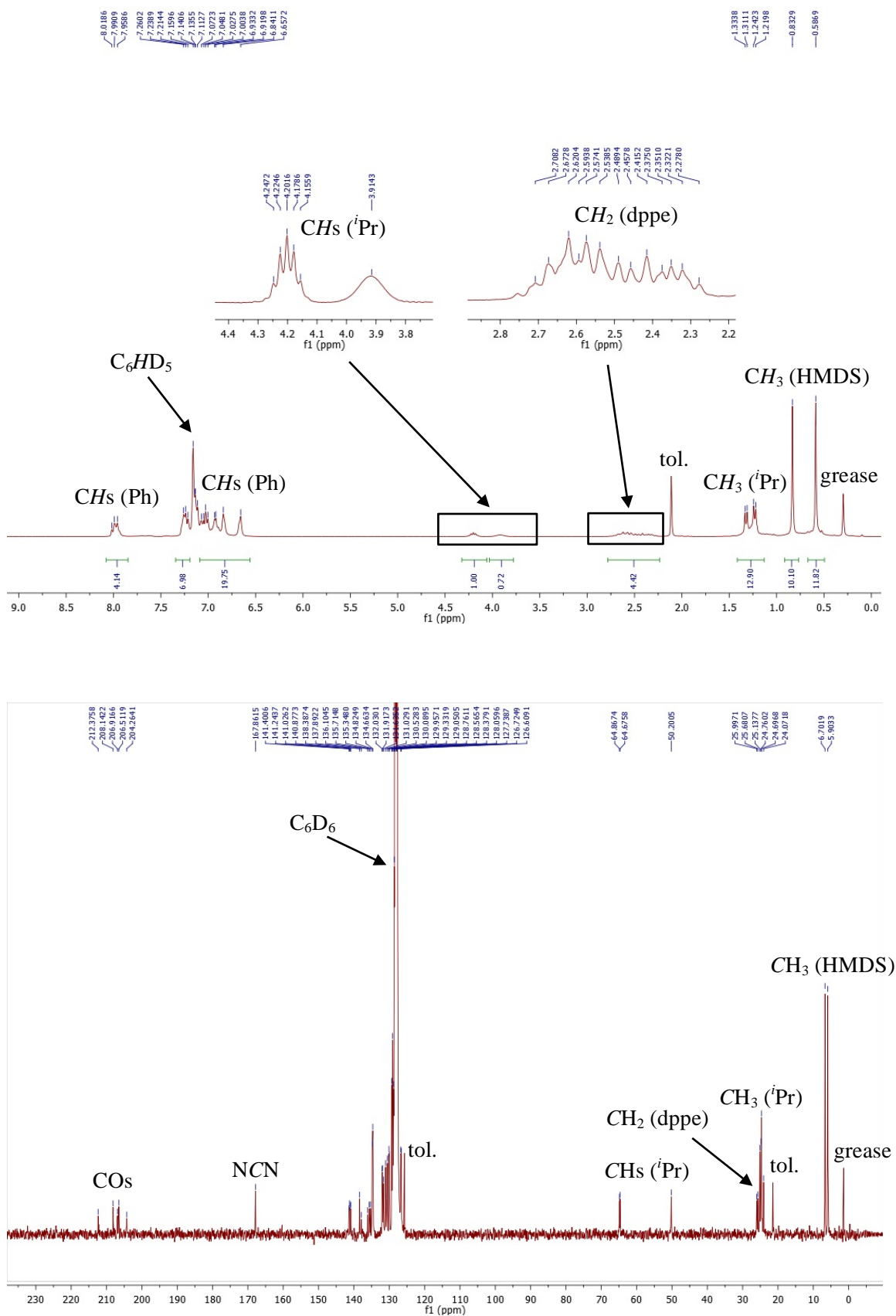


Figure S6. 1H (top) and $^{13}C\{^1H\}$ (bottom) NMR spectra of $[Ru_2\{\mu-\kappa^2Ge,N\{-Ge(iPr_2bzam)(HMDS)\}(dppe)(CO)_5\}]$ (**8**) in C_6D_6 (20 °C).

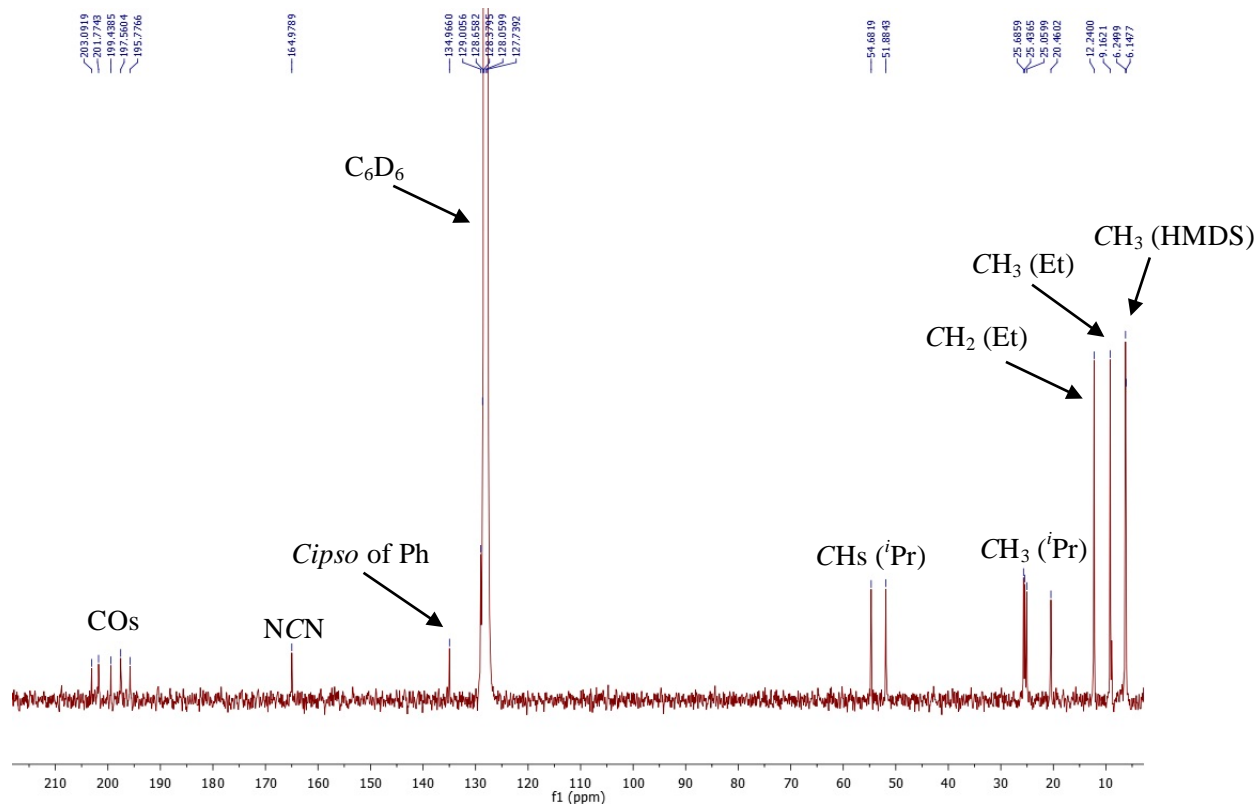
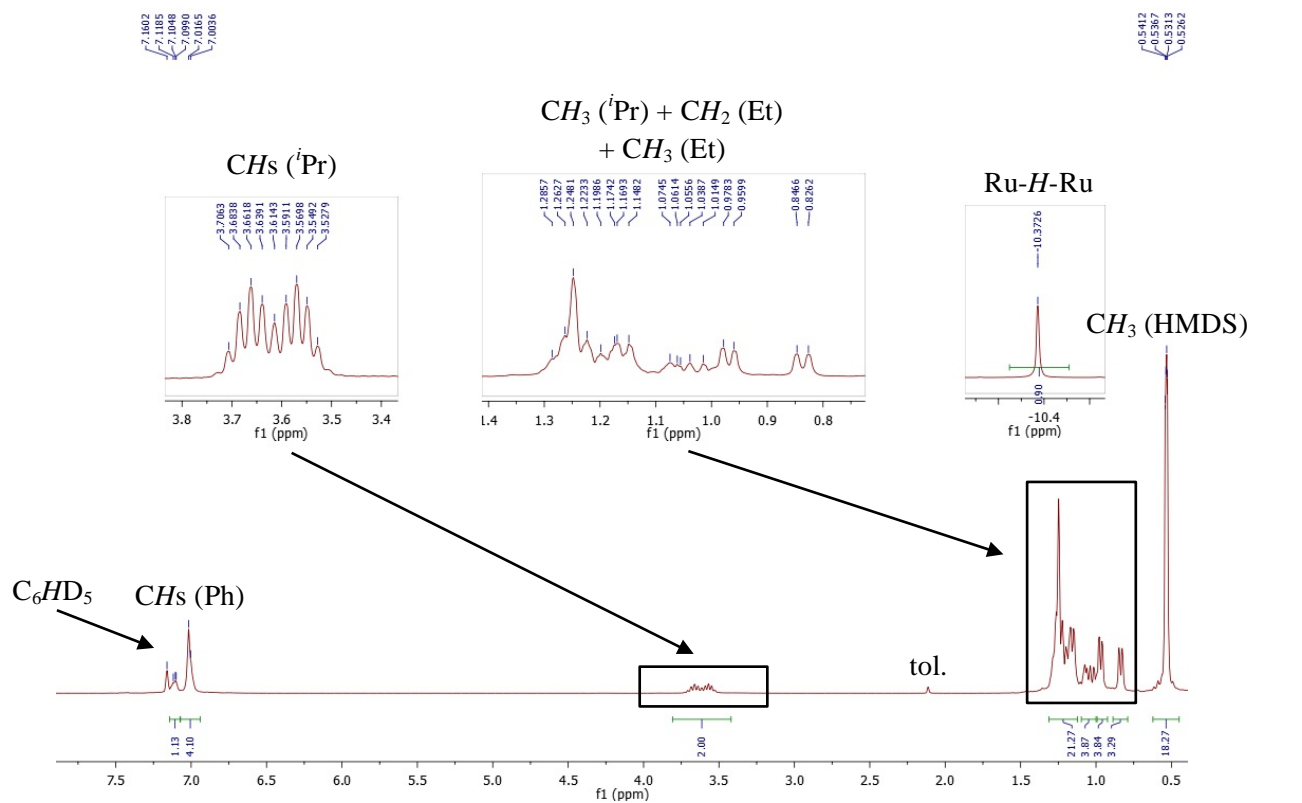


Figure S7. ^1H (top) and $^{13}\text{C}\{^1\text{H}\}$ (bottom) NMR spectra of $[\text{Ru}_2(\text{SiEt}_3)(\mu\text{-H})\{\mu\text{-}\kappa^2\text{Ge},\text{N}\text{-Ge}(\text{iPr}_2\text{bzam})(\text{HMDS})\}(\text{CO})_5]$ (**9**) in C_6D_6 (20 °C).

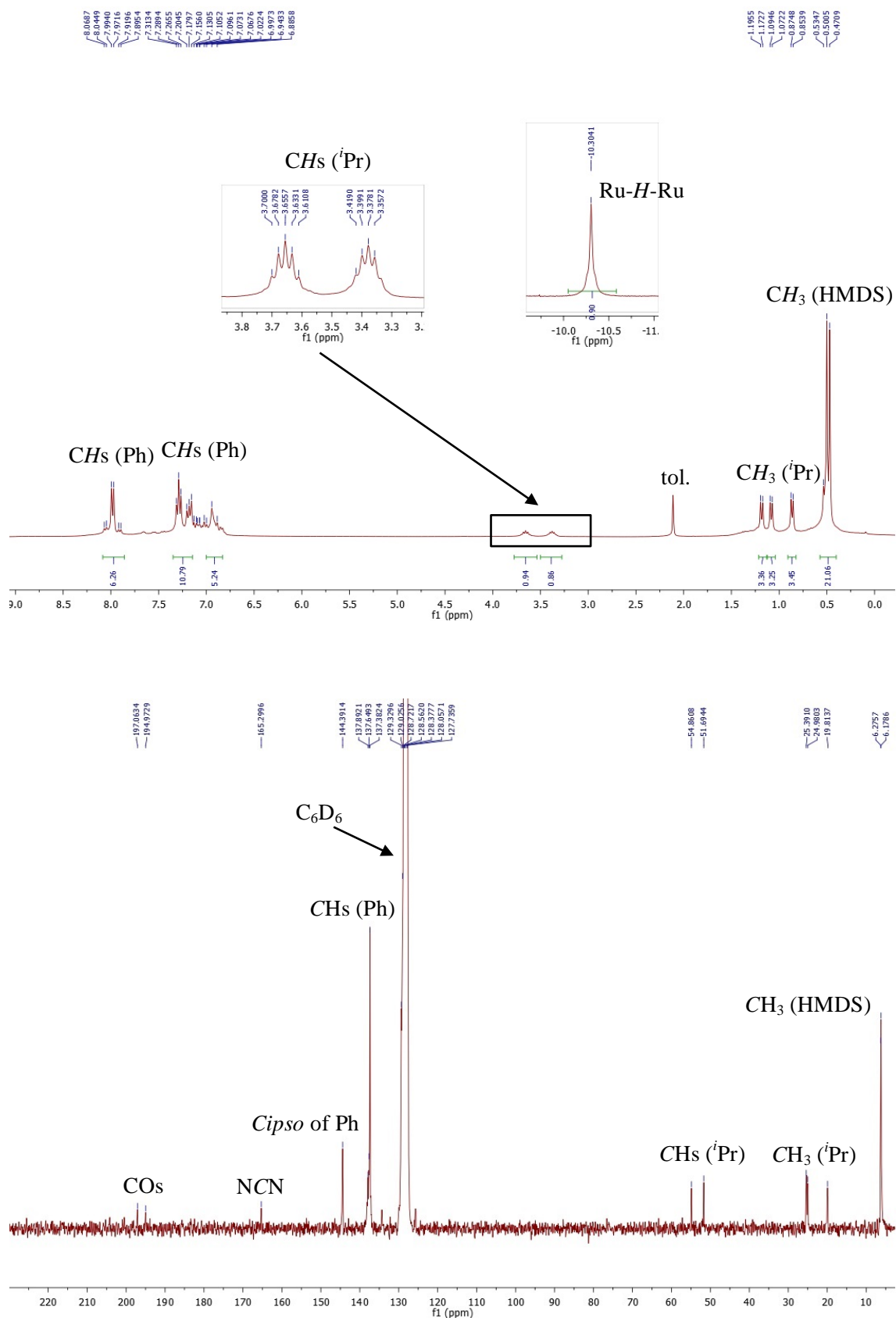
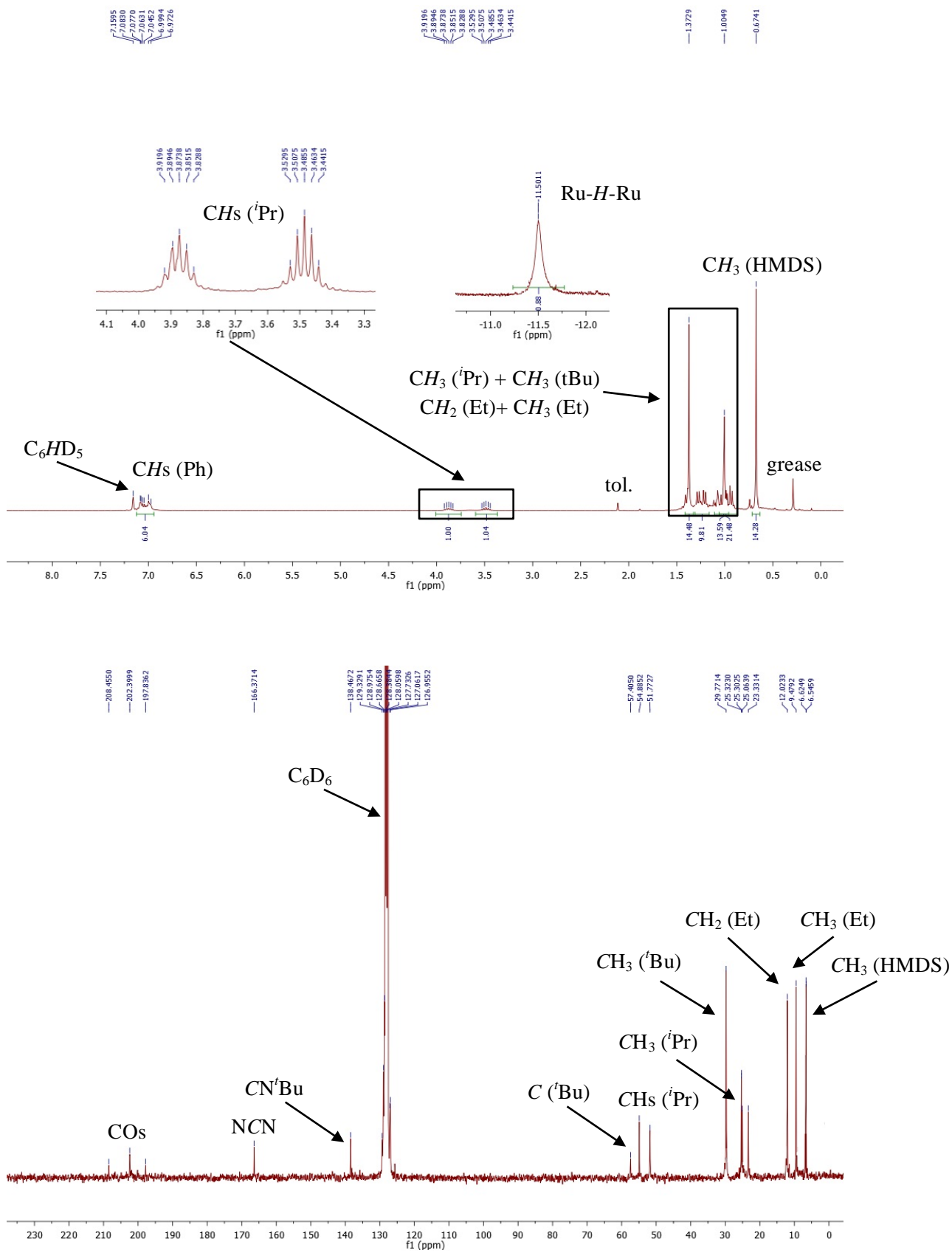


Figure S8. ^1H NMR spectra of $[\text{Ru}_2(\text{SnPh}_3)(\mu\text{-H})\{\mu\text{-}\kappa^2\text{Ge,N-Ge}(\text{iPr})_2\text{bzam}\}(\text{HMDS})\}(\text{CO})_5]$ (**10**) in C_6D_6 (20 °C).



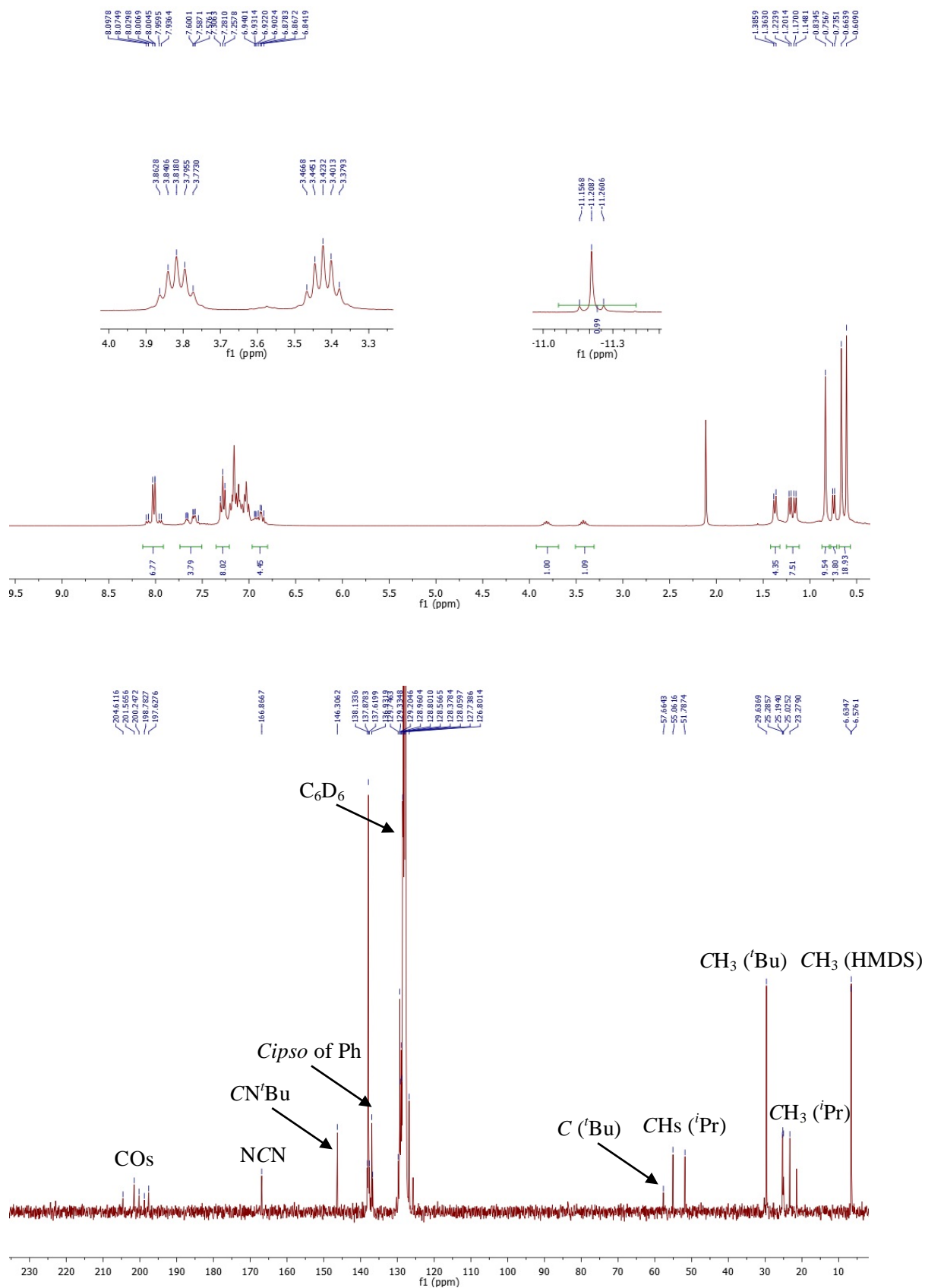


Figure S10. 1H (top) and $^{13}C\{^1H\}$ (bottom) NMR spectra of $[Ru_2(SnPh_3)(\mu-H)\{\mu-\kappa^2Ge,N-Ge(iPr_2bzam)(HMDS)\}(^tBuNC)(CO)_5]$ (**12**) in C_6D_6 (20 °C).

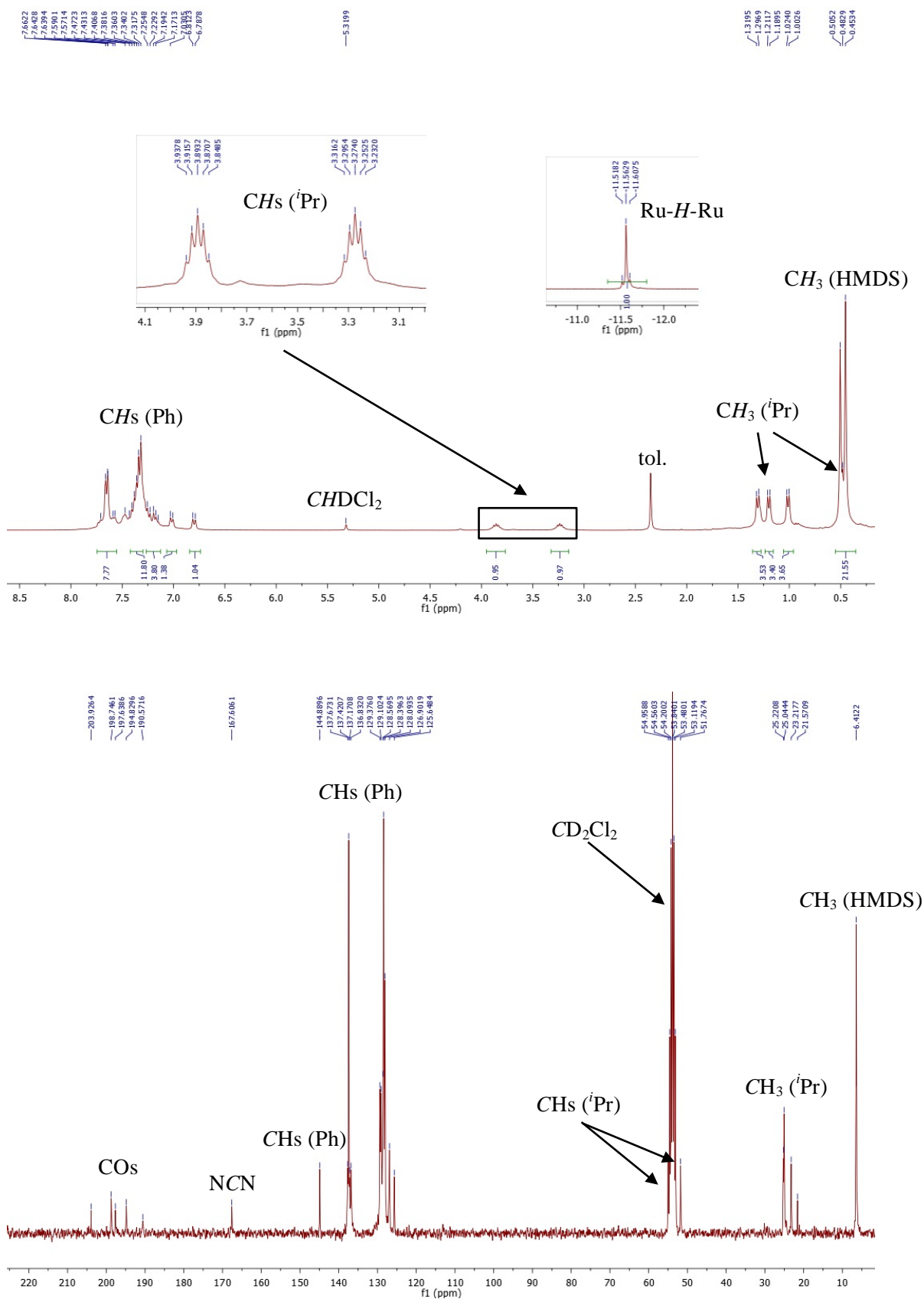


Figure S11. ^1H (top) and $^{13}\text{C}\{^1\text{H}\}$ (bottom) NMR spectra of $[\text{Ru}_2(\text{SnPh}_3)(\mu\text{-H})\{\mu\text{-}\kappa^2\text{Ge,N-Ge}(i\text{Pr}_2\text{bzam})(\text{HMDS})\}(\text{CO})_6]$ (**14**) in CD_2Cl_2 (20 °C).

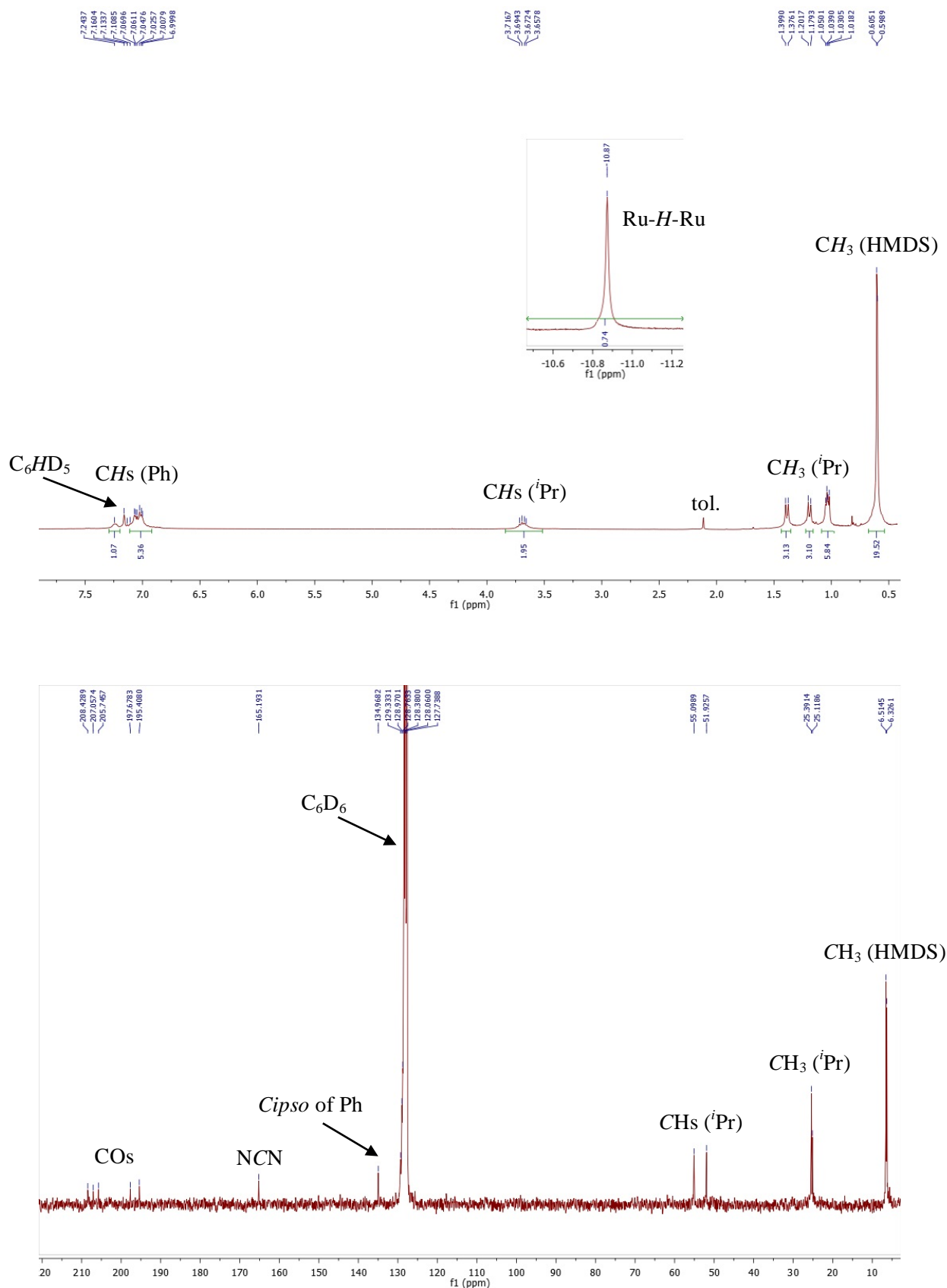


Figure S12. 1H (top) and $^{13}C\{^1H\}$ (bottom) NMR spectra of $[Ru_4(\mu-H)_2\{\mu-\kappa^2Ge,N-Ge(iPr)_2bzam\}(HMDS)\}_2(CO)_{10}$ (**15**) in C_6D_6 (20 °C).

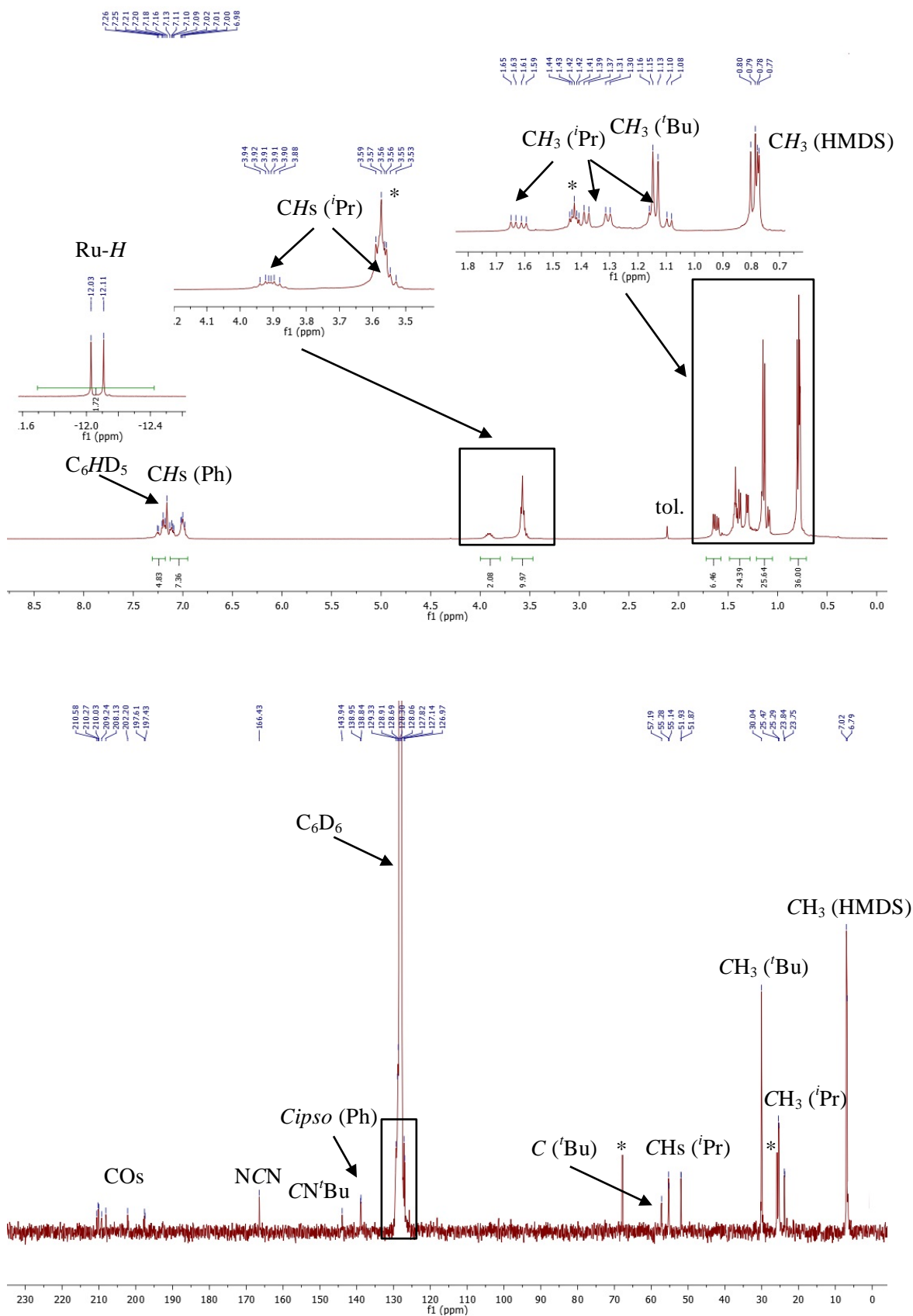


Figure S13. 1H (top) and $^{13}C\{^1H\}$ (bottom) NMR spectra of $[Ru_4(\mu-H)_2\{\mu-\kappa^2Ge,N-Ge(iPr_2bzam)(HMDS)\}_2(tBuNC)_2(CO)_{10}]$ (**16**) in C_6D_6 (20 °C). The peaks marked with an asterisk (*) are due to THF.

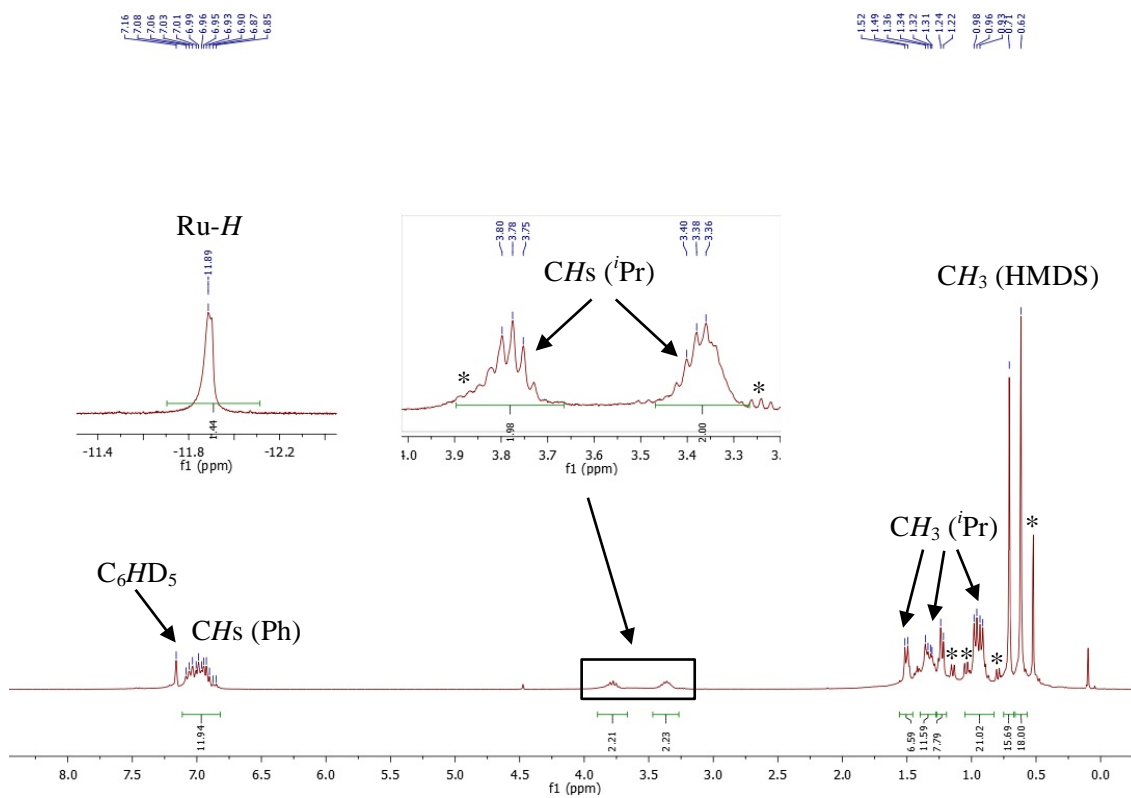


Figure S14. ^1H NMR spectrum of $[\text{Ru}_4(\mu\text{-H})_2\{\mu\text{-}\kappa^2\text{Ge}, N\text{-Ge}(i\text{Pr}_2\text{bzam})(\text{HMDS})\}_2(\text{CO})_{12}]$ (**17**) in C_6D_6 ($20\text{ }^\circ\text{C}$). The peaks marked with an asterisk (*) are due to complex **2**.

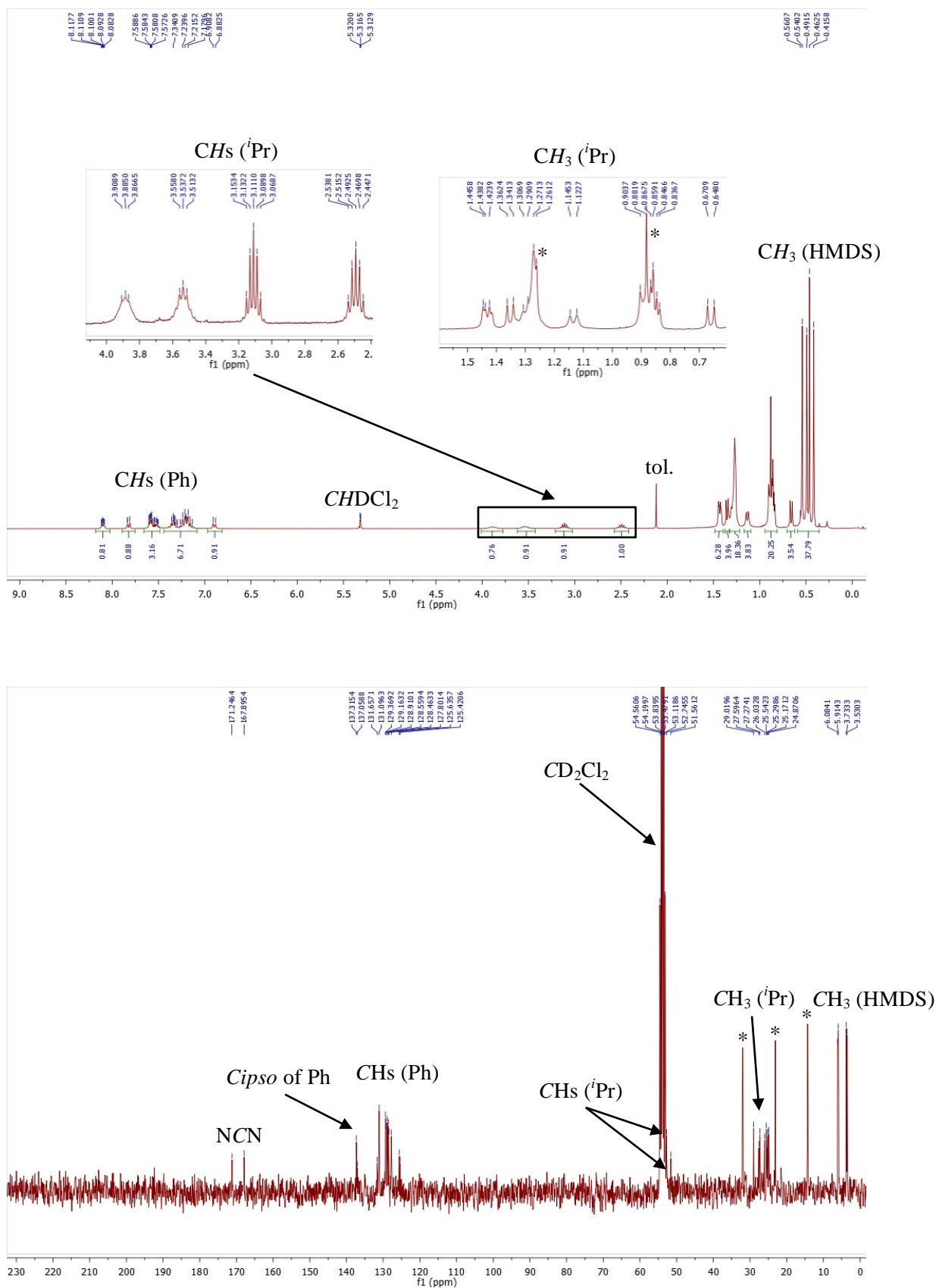


Figure S15. ^1H (top) and $^{13}\text{C}\{^1\text{H}\}$ (bottom) NMR spectra of $[\text{Ru}_4\{\mu\text{-}\kappa^2\text{Ge}, N\text{-Ge}(i\text{Pr}_2\text{bzam})(\text{HMDS})\}\{\mu_3\text{-}\kappa\text{Ge-Ge}(\text{HMDS})\}(\mu\text{-}\kappa^2 N, C, N'\text{-}i\text{Pr}_2\text{bzam})(\mu\text{-CO})(\text{CO})_8]$ (**18**) in CD_2Cl_2 (20 °C). The peaks marked with an asterisk (*) are due to hexane.

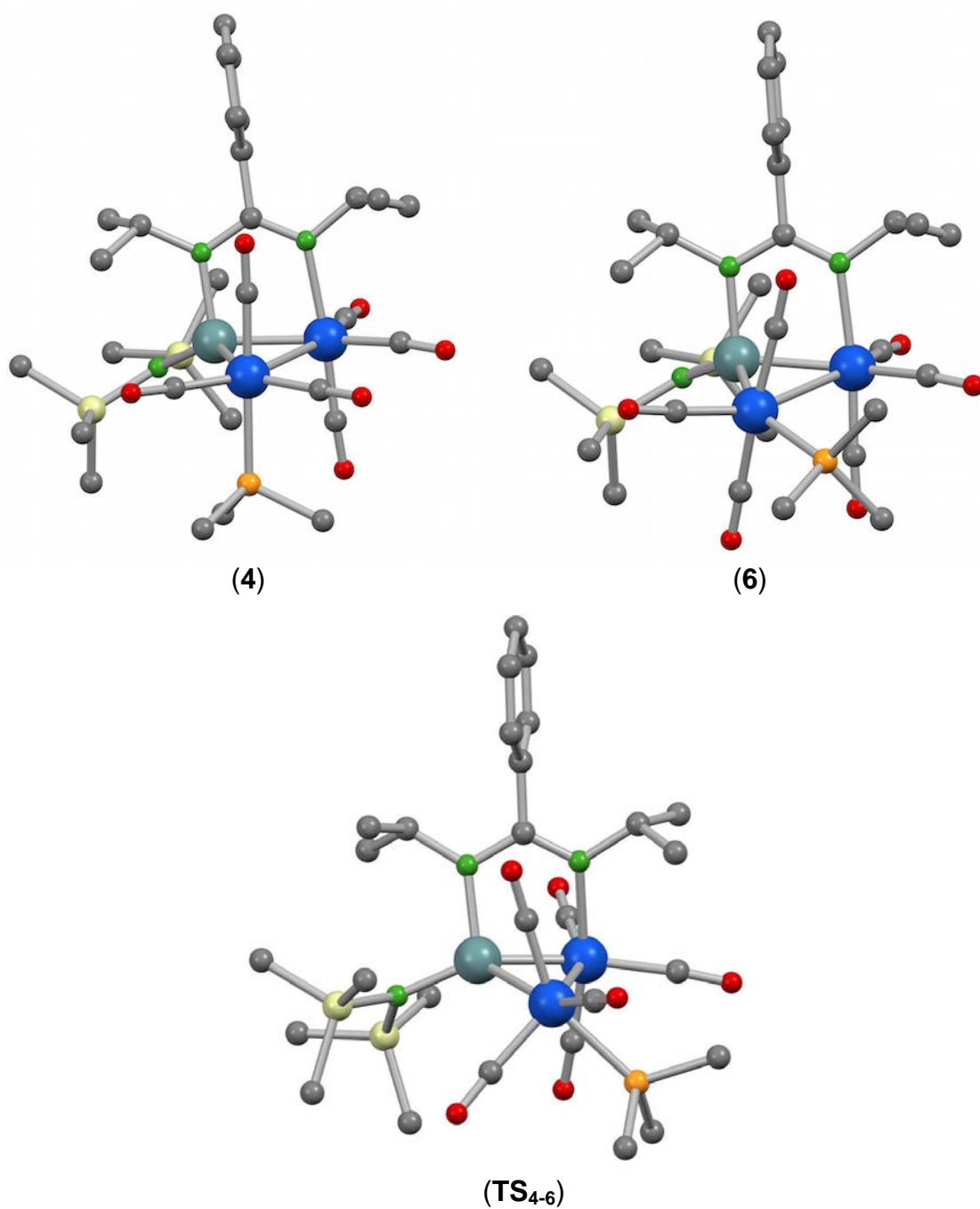


Figure S16. DFT-optimized structures of **4**, **6** and TS_{4-6} (H atoms have been omitted for clarity).

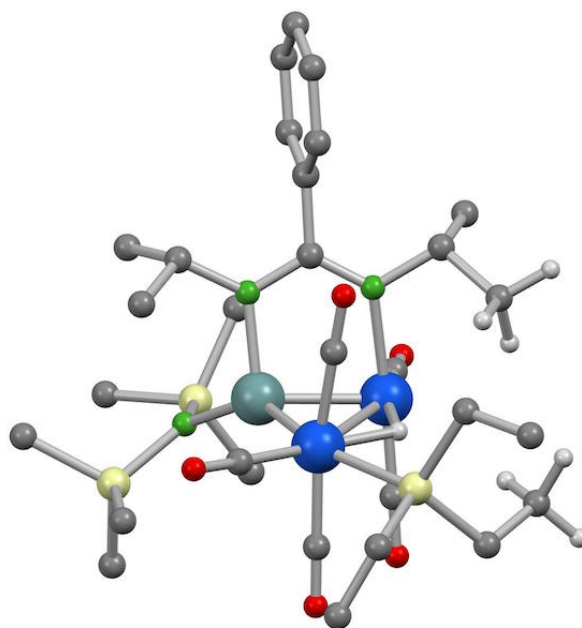


Figure S17. DFT-optimized structure of complex **9** (H atoms, except the hydride and those of the methyl groups that are close to the unsaturated Ru atom, have been omitted for clarity).

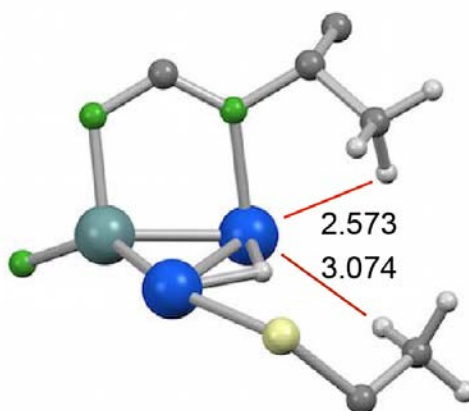


Figure S18. A fragment of the DFT-optimized structure of complex **9**, showing the Ru \cdots H distances (\AA) between the unsaturated Ru atom and the two nearest methyl H atoms.

Artículo VI

***“Ring Opening and Bidentate Coordination of
Amidinate Germylenes and Silylenes on Carbonyl
Dicobalt Complexes: The Importance of a Slight
Difference in Ligand Volume”***

Ligand Effects

Ring Opening and Bidentate Coordination of Amidinate Germylenes and Silylenes on Carbonyl Dicobalt Complexes: The Importance of a Slight Difference in Ligand Volume

Javier A. Cabeza,^{*[a]} Pablo García-Álvarez,^{*[a]} Enrique Pérez-Carreño,^[b] and Diego Polo^[a]

Abstract: The reactions of $[\text{Co}_2(\text{CO})_8]$ with one equiv of the benzamidinate (R_2bzam) group-14 tetrylenes $[\text{M}(\text{R}_2\text{bzam})\text{-(HMDS)}]$ ($\text{HMDS} = \text{N}(\text{SiMe}_3)_2$; **1**: $\text{M} = \text{Ge}$, $\text{R} = i\text{Pr}$; **2**: $\text{M} = \text{Si}$, $\text{R} = t\text{Bu}$; **3**: $\text{M} = \text{Ge}$, $\text{R} = t\text{Bu}$) at 20°C led to the monosubstituted complexes $[\text{Co}_2\{\kappa^1\text{M}-\text{M}(\text{R}_2\text{bzam})(\text{HMDS})\}(\text{CO})_7]$ (**4**: $\text{M} = \text{Ge}$, $\text{R} = i\text{Pr}$; **5**: $\text{M} = \text{Si}$, $\text{R} = t\text{Bu}$; **6**: $\text{M} = \text{Ge}$, $\text{R} = t\text{Bu}$), which contain a terminal $\kappa^1\text{M}$ -tetrylene ligand. Whereas the Co_2Si and Co_2Ge *tert*-butyl derivatives **5** and **6** are stable at 20°C , the Co_2Ge isopropyl derivative **4** evolved to the ligand-bridged derivative $[\text{Co}_2\{\mu-\kappa^2\text{Ge}, \text{N-Ge}(i\text{Pr}_2\text{bzam})(\text{HMDS})\}(\mu\text{-CO})(\text{CO})_5]$ (**7**), in which the Ge atom spans the Co–Co bond and one arm of the amidinate fragment is attached to a Co atom. The mechanism of this reaction has been modeled with the

help of DFT calculations, which have also demonstrated that the transformation of amidinate-tetrylene ligands on the dicobalt framework is negligibly influenced by the nature of the group-14 metal atom (Si or Ge) but is strongly dependent upon the volume of the amidinate N–R groups. The disubstituted derivatives $[\text{Co}_2\{\kappa^1\text{M}-\text{M}(\text{R}_2\text{bzam})(\text{HMDS})\}_2(\text{CO})_6]$ (**8**: $\text{M} = \text{Ge}$, $\text{R} = i\text{Pr}$; **9**: $\text{M} = \text{Si}$, $\text{R} = t\text{Bu}$; **10**: $\text{M} = \text{Ge}$, $\text{R} = t\text{Bu}$), which contain two terminal $\kappa^1\text{M}$ -tetrylene ligands, have been prepared by treating $[\text{Co}_2(\text{CO})_8]$ with two equiv of **1–3** at 20°C . The IR spectra of **8–10** have shown that the basicity of germylenes **1** and **3** is very high (comparable to that of trialkylphosphanes and 1,3-diarylimidazol-2-ylidenes), whereas that of silylene **2** is even higher.

Introduction

Heavier carbene analogues,^[1] also known as heavier tetrylenes (or group-14 metalylenes or metalenes), are very reactive molecules that, as a result of their dual Lewis acid/base character,^[2] display a very rich reactivity. They are able to activate small molecules, insert into organic and inorganic σ -bonds, form donor–acceptor adducts, add to unsaturated substrates, promote cycloadditions, participate in redox processes, coordinate to transition-metal (TM) complexes, and so on.^[3,4] However, their coordination chemistry, although currently covering a wide range of TMs,^[4] is far from the extent achieved by that of their carbene siblings and, particularly, that of N-heterocyclic carbenes (NHCs)^[5] because heavier tetrylene–TM complexes are usually less stable towards air, moisture, and substitution processes,^[6,7] and their syntheses generally require the use of pure tetrylenes as reagents.^[8]

In the last few years, new generations of cyclic heavier tetrylene molecules, particularly silylenes and germylenes stabilized by amidinate, β -diketiminato, and other chelating fragments,^[4a] have allowed a significant advance of the tetrylene–TM chemistry. Among them, the most studied ones have been those derived from amidinates, which form isolatable tetrylene–TM complexes with almost all of the groups of the TM series,^[9] some of which have already been successfully tested as catalyst precursors for useful reactions,^[10] such as Sonogashira cross-couplings,^[9a] ketone hydrosilylations,^[9b] [2+2+2] cycloadditions,^[9c] arene C–H borylations,^[9d] and cross-coupling reactions of aryl halides with organometallic zinc and Grignard reagents.^[9w]

As part of our work on tetrylene–TM chemistry,^[11] we have preliminary communicated that the amidinate-germylene $[\text{Ge}(i\text{Pr}_2\text{bzam})(\text{HMDS})]$ (**1**; $i\text{Pr}_2\text{bzam} = N,N'$ -bis(isopropyl)benzamidinate), which is equipped with a very bulky hexamethyldisilazane group (HMDS) and armed with just one accessible lone pair of electrons on the Ge atom, can be transformed into a bridging 4-electron-donor $\kappa^2\text{Ge}, \text{N}$ -ligand when treated with $[\text{Co}_2(\text{CO})_8]$.^[12] The accomplishment of such a bidentate coordination mode, which was unprecedented for amidinate-tetrylene ligands, implies the breaking of a Ge–N bond and the subsequent formation of a TM–N bond. In this contribution, in addition to extending the cobalt chemistry described in our preliminary communication to very bulky *tert*-butyl-substituted amidinate-germylene and -silylene reagents, we provide experimental and DFT theoretical data that shed light on 1) the crucial importance that the volume of the amidinate N–R groups

[a] Prof. J. A. Cabeza, Dr. P. García-Álvarez, D. Polo
Departamento de Química Orgánica e Inorgánica-IUQOEM
Universidad de Oviedo-CSIC, E-33071 Oviedo (Spain)
Fax: (+34) 985103446
E-mail: jac@uniovi.es
pga@uniovi.es

[b] Dr. E. Pérez-Carreño
Departamento de Química Física y Analítica
Universidad de Oviedo, E-33071 Oviedo (Spain)

Supporting information for this article is available on the WWW under <http://dx.doi.org/10.1002/chem.201402295>.

has on the monodentate to bidentate transformation of $[\text{Ge}(\text{R}_2\text{bzam})(\text{HMDS})]$ carbonyl dicobalt complexes, 2) the mechanism of that transformation, and 3) the effect that the use of a different group-14 metal atom (Si or Ge) has on the final outcome of the reactions of $[\text{Co}_2(\text{CO})_8]$ with amidinate-tetrylenes of the type $[\text{M}(\text{R}_2\text{bzam})(\text{HMDS})]$.

Results and Discussion

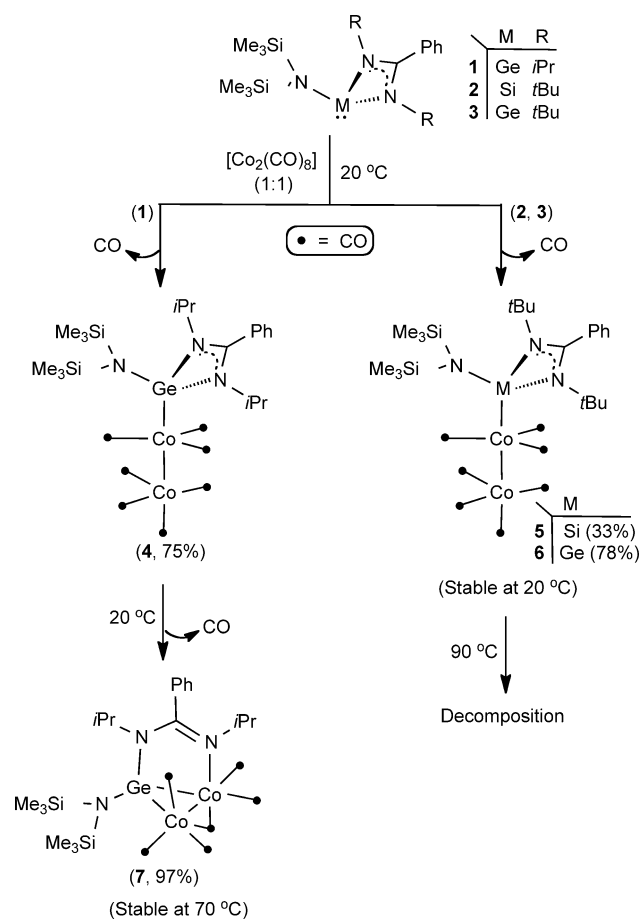
Synthesis and characterization of dicobalt mono- and ditetrylene complexes

The room temperature reactions of $[\text{Co}_2(\text{CO})_8]$ with one equivalent of the amidinate-tetrylenes $[\text{Ge}(\text{iPr}_2\text{bzam})(\text{HMDS})]$ (**1**) ($\text{iPr}_2\text{bzam} = N,N'$ -bis(isopropyl)benzaminate; $\text{HMDS} = \text{N}(\text{SiMe}_3)_2$) and $[\text{M}(\text{tBu}_2\text{bzam})(\text{HMDS})]$ ($\text{M} = \text{Si}$ (**2**), Ge (**3**); $\text{tBu}_2\text{bzam} = N,N'$ -bis(*tert*-butyl)benzaminate) led to mixtures of products from which the analogous monosubstituted complexes $[\text{Co}_2\{\kappa^1\text{M}-\text{M}(\text{R}_2\text{bzam})(\text{HMDS})\}(\text{CO})_7]$ (**4**: $\text{M} = \text{Ge}$, $\text{R} = \text{iPr}$; **5**: $\text{M} = \text{Si}$, $\text{R} = \text{tBu}$; **6**: $\text{M} = \text{Ge}$, $\text{R} = \text{tBu}$) were isolated in 75, 33, and 78% yield, respectively (Scheme 1). IR spectroscopic analyses of the reaction solutions revealed that small amounts of the corresponding disubstituted derivative (**8**, **9**, or **10**; see below) and the salt $[\text{CoL}_2(\text{CO})_3]^+[\text{Co}(\text{CO})_4]^-$ ($\text{L} = \text{1-3}$; ^[13]) a strong

peak around 1890 cm^{-1} is indicative of the $[\text{Co}(\text{CO})_4]^-$ anion^[14,15] were also formed. The salt was more abundant in the reaction solution of silylene **2** than in those of germynes **1** and **3**, resulting in a lower yield of the silylene dicobalt complex **5**.

It has been reported that mixtures of monosubstituted products and disproportionation salts are also formed when $[\text{Co}_2(\text{CO})_8]$ is treated with tertiary phosphanes^[14] and that the higher the basicity of the phosphane, the greater the amount of the ionic product.^[14a] In the same context, the salt $[\text{Co}(\text{CO})_3-\text{IMes}]_2^+[\text{Co}(\text{CO})_4]^-$ ($\text{IMes} = 1,3$ -dimesitylimidazol-2-ylidene) was the only observed product of the reaction of $[\text{Co}_2(\text{CO})_8]$ with one equivalent of the very basic NHC IMes.^[15b] Consequently, the higher basicity of silylenes (in comparison with that of germynes) accounts for the lower yield of complex **5** (in comparison with those of **4** and **6**).

Complexes **4-6** contain their tetrylene ligand in an axial coordination site and have a staggered arrangement of the equatorial CO ligands (at least in the solid state). These structural features were inferred from their IR spectra, whose $\tilde{\nu}_{\text{CO}}$ pattern is very similar to those of other previously reported axially monosubstituted heptacarbonyl dicobalt derivatives,^[14a,c,16] and were unambiguously determined by X-ray diffraction (XRD) in the case of the Co_2Ge *tert*-butyl derivative **6** (Figure 1, Table S1 of the Supporting Information).



Scheme 1. Synthesis of compounds **4-7** (yields of the isolated products are given in parenthesis).

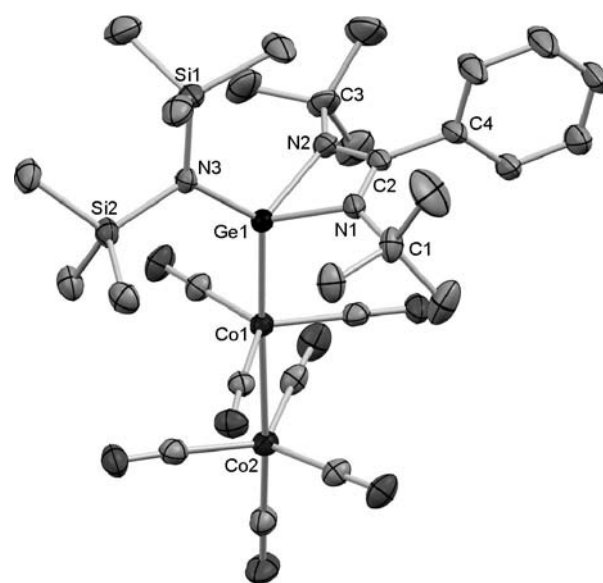
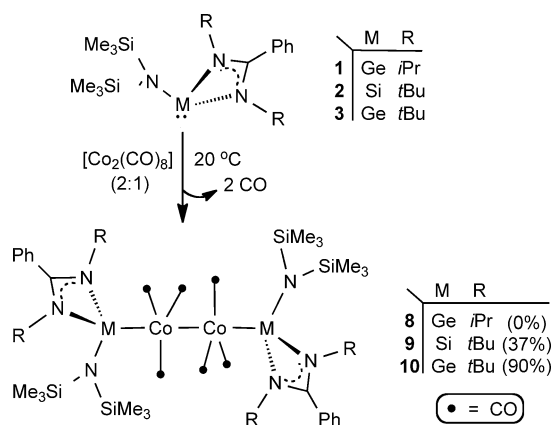


Figure 1. XRD molecular structure of compound **6** (thermal ellipsoids set at 30% probability). H atoms have been omitted for clarity.

The Co_2Ge isopropyl derivative **4** proved to be thermally unstable at room temperature, leading quantitatively in 90 min (toluene, $20\text{ }^\circ\text{C}$) to the hexacarbonyl derivative $[\text{Co}_2\{\mu-\kappa^2\text{Ge}, N\text{-Ge}(\text{iPr}_2\text{bzam})(\text{HMDS})\}(\mu\text{-CO})(\text{CO})_5]$ (**7**) (Scheme 1). Interestingly, an analogous transformation was not observed for the Co_2Si and Co_2Ge *tert*-butyl derivatives **5** and **6**, which were stable for several hours in solution room temperature but they decom-



Scheme 2. Synthesis of compounds **8–10** (yields of the isolated products are given in parenthesis; compound **8** was detected in the reaction solution by IR spectroscopy).

posed to unidentified solids when their solutions were heated to higher temperatures.

The XRD molecular structure of **7** is shown in Figure 2. A selection of bond lengths and angles are given in Table S1 (Supporting Information). The complex contains a Co₂Ge triangle

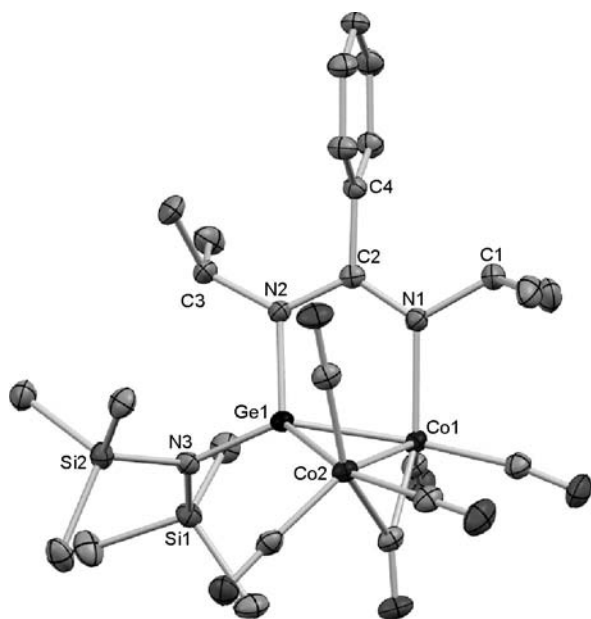


Figure 2. XRD molecular structure of compound **7** (thermal ellipsoids set at 30% probability). H atoms have been omitted for clarity.

with a Co–Ge edge bridged by the amidinate fragment in such a way that the mean plane of the Ge1–N2–C2–N1–Co1 five-membered ring forms a dihedral angle of 112.59(3)° with the Co₂Ge plane. The C–N bond lengths within the amidinate group indicate the presence of a localized C=N double bond involving the N atom attached to Co (C2–N1 1.311(3) Å, C2–N2 1.364(3) Å), denoting that the Co1 atom is attached to an imine-type ligand. Similar C–N bond length distributions have been reported for cobalt complexes containing κ¹N-amidinate

ligands.^[17] The Ge atom adopts a distorted tetrahedral arrangement, being bonded to the two Co atoms with an acute Co1–Ge1–Co2 angle, 66.68(1)°, to the N2 atom of the amidinate fragment and to the N3 atom of the HMDS group. The ligand shell of **7** is completed by six CO ligands, five of which are terminally attached to the Co atoms whereas one is bridging the Co–Co edge.

Remarkably, the behavior displayed by ligand **1** (a donor-stabilized tetrylene) in the transformation **4**→**7**+CO clearly contrasts with the general belief that the coordination of a tetrylene molecule to a TM increases the Lewis acidity of the M atom and, thus, the strength of its interaction with a donor group (in our case, the imine group of the amidinate). An example that well illustrates this behavior has been recently reported by Tacke et al., who have shown that the bis(amidinate)silylene [Si(*i*Pr₂bzam)₂], in which one amidinate is chelating and the other is terminal, closes the pendant imino arm of the terminal amidinate towards the Si atom when the latter coordinates to a tungsten complex.^[9h] In our case, a factor that may facilitate the terminal to bridging rearrangement of the amidinate-germylene in the reaction that transforms **4** into **7** is the binuclear character of the TM reagent, since the release of an amidinate arm from the Ge atom may then be compensated by the formation of a germanium bridge between the two metal atoms, a situation that is common in the coordination chemistry of disubstituted tetrylene ligands (M=Si, Ge, Sn).^[11c,d,9w,18] In addition, the presence of the very bulky HMDS group in **1** also seems to favor the formation of complex **7** because the transfer of one arm of the amidinate group to the TM relaxes the steric crowding exerted by the HMDS group over the nearby CO ligands, as indicated by a widening of the Co1–Ge1–N3 angle from 128.1(1)° in **6** (structurally analogous to **4**) to 138.81(6)° in **7**. The importance of the HMDS group in this transformation is also supported by the fact that reactions of [Fe₂(CO)₉], [Co₂(CO)₈], [Mn₂(CO)₁₀], and [Re₂(CO)₁₀] with related amidinate-tetrylenes having anionic groups smaller than HMDS do not afford derivatives containing bridging ligands, but products having monodentate M-donor tetrylene ligands, such as [Fe{κ¹Sn–Sn(*t*Bu₂bzam)Cl}(CO)₄]^[9p] [Fe{κ¹Si–Si(*t*Bu₂bzam)OtBu}(CO)₄]^[9q] [Co{κ¹Si–Si(*t*Bu₂bzam)Cl}(CO)₃][Co(CO)₄]^[9f] [TM{κ¹Si–Si(*t*Bu₂bzam)Cl}(CO)_{6–x}][TM(CO)₅] (TM = Mn, Re)^[9l] and [TM{κ¹Si–Si(*t*Bu₂bzam)NPh₂}(CO)₄][TM(CO)₅] (TM = Mn, Re).^[9l]

The above data indicate that the volume of the HMDS and amidinate N–R groups of tetrylenes of the type [M(R₂bzam)-(HMDS)] (M=Si, Ge) plays an important role in the terminal to bridging transformation of these tetrylene ligands carbonyl dicobalt complexes. However, we have been unable to experimentally shed light on the role played by the M atoms (Si vs. Ge) in this transformation because we^[19] and others^[20] have been unable to prepare silylenes of the type [Si(R₂bzam)Cl] with N–R groups different from N–*t*Bu (to be used as precursors to the final HMDS derivatives).

For completeness, the disubstituted derivatives [Co₂{κ¹M–M–(R₂bzam)(HMDS)}₂(CO)₆] (**8**: M=Ge, R=*i*Pr; **9**: M=Si, R=*t*Bu; **10**: M=Ge, R=*t*Bu), which contain two κ¹M-tetrylene ligands in the two axial positions and a staggered arrangement of

equatorial CO ligands, were synthesized by treating $[\text{Co}_2(\text{CO})_8]$ with two equivalents of **1–3** at room temperature (Scheme 2). The salts $[\text{CoL}_2(\text{CO})_3]^+[\text{Co}(\text{CO})_4]^-$ ($L = \mathbf{1–3}$) were also formed (IR analysis of the reaction solutions). In accordance with the results described above for the monosubstituted derivatives **4–6**, the volume of the amidinate N–R group also affected the thermal stability of **8–10**. Thus, **9** and **10** ($R = t\text{Bu}$) were stable at room temperature and were isolated in 37 and 90% yield, respectively. However, the Co_2Ge_2 isopropyl derivative **8** decomposed during the purification process. The structural features of **8–10** were inferred from their IR spectra, whose $\tilde{\nu}_{\text{CO}}$ pattern is very similar to those of other reported axially disubstituted hexacarbonyl dicobalt derivatives,^[14b,c,21] and were unambiguously established in the case of **10** by XRD (Figure 3, Table S1 of the Supporting Information).

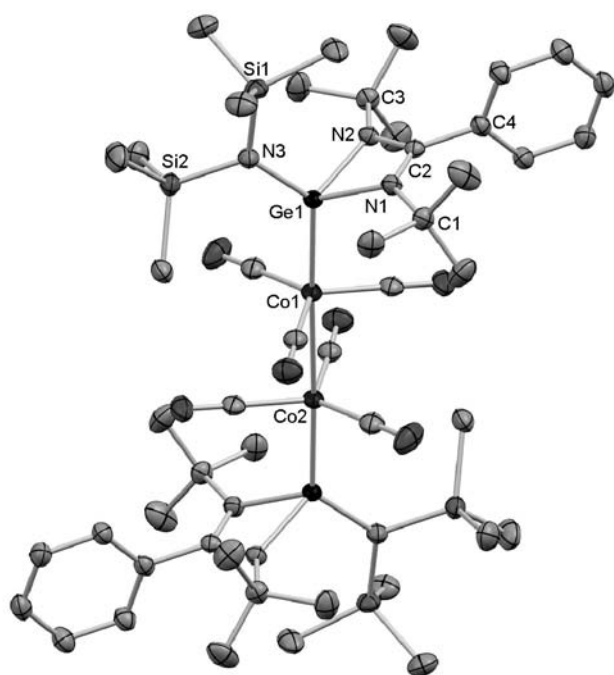


Figure 3. XRD molecular structure of compound **10**. The two equivalent parts of the molecule are related by a crystallographic inversion center (thermal ellipsoids set at 30% probability). H atoms have been omitted for clarity.

Compounds **4–6**, **9**, and **10** represent, with the unique exception of the bis(germylene) derivative $[\text{Co}_2\{\kappa^1\text{Ge}[\text{N}(\text{SiMe}_2/\text{Pr})_2]_2\}_2(\text{CO})_6]$,^[22] the first examples of dicobalt compounds containing terminal heavier tetrylene ligands. In this group, the geometrical parameters of the complexes characterized by XRD (**6** and **10**) are scarcely affected by the grade of substitution of the dicobalt fragment (Table S1 of the Supporting Information). The Co–Co bond lengths, 2.664(1) Å in **6** and 2.657(1) Å in **10**, are in the range of those reported for unsupported Co–Co mono-^[16a,23] or disubstituted^[21,22,24] carbonyl complexes. However, they are considerable longer than that of **7** (2.5625(5) Å), which has a doubly bridged Co–Co bond. The Co–Co and Ge–Co bonds of **6** and **10** are almost co-linear, al-

locating their germylene ligands in axial positions. Their Ge–Co bond lengths, 2.2938(8) Å in **6** and 2.2959(6) Å in **10**, are approximately 0.07 Å longer than those of the related compound $[\text{Co}_2\{\kappa^1\text{Ge}[\text{N}(\text{SiMe}_2/\text{Pr})_2]_2\}_2(\text{CO})_6]$,^[22] which has a smaller germylene ligand. Within the amidinate fragments, the C–N bond lengths indicate, as expected, a higher degree of delocalization of the C=N double bonds than that observed in **7**. The germanium atoms adopt a distorted tetrahedral arrangement, with acute N1–Ge1–N2 angles of 66.41(2)° for **6** and 66.1(1)° for **10**, each one being bonded to a Co atom and three N atoms, two belonging to the amidinate backbone, N1 and N2, and the other corresponding to the HMDS group, N3. Regarding the Ge–N3 (HMDS) bond lengths, 1.8473(3) Å in **6** and 1.859(3) Å in **10**, they are very similar to that of **7**, 1.845(2) Å, and other HMDS-equipped germylene ligands.^[8f,11b,d]

The relative electron-donating capabilities of a wide range of ligands *L* can be conveniently estimated by comparing the $\tilde{\nu}_{\text{CO}}$ frequencies of a selected group of carbonyl TM complexes, $[\text{TML}(\text{CO})_n]$,^[25] but studies of this type with heavier tetrylene ligands are hitherto scarce. The IR spectra of complexes of the type $[\text{NiL}(\text{CO})_3]$,^[10] $[\text{CrL}(\text{CO})_3]$,^[26] and $[\text{FeL}(\text{CO})_4]$ ^[26] have been used to evaluate the donor properties of a family of amidinate-silylene ligands *L*.^[10] NMR spectroscopy has also been used to appraise the basicity of bis(silylene) and bis(germylene) pincer complexes in iridium and rhodium complexes.^[9d] In our case, a comparison of the $\tilde{\nu}_{\text{CO}}$ absorptions of compounds **8–10** with those of previously known $[\text{Co}_2\text{L}_2(\text{CO})_6]$ complexes allows a comparative appraisal of the basicity of tetrylenes **1–3**. Toluene solutions of complexes **8–10** show their strongest $\tilde{\nu}_{\text{CO}}$ absorption at 1937, 1920, and 1937 cm^{-1} , respectively (their IR spectra contain various $\tilde{\nu}_{\text{CO}}$ absorptions but only one is very strong). A comparison of these values with those corresponding to the strongest $\tilde{\nu}_{\text{CO}}$ absorption of related $[\text{Co}_2\text{L}_2(\text{CO})_6]$ complexes, in which *L* = PPh₃ (1960 cm^{-1}),^[14c] PCy₃ (1943 cm^{-1}),^[14c] *Pn*-Bu₃ (1943 cm^{-1}),^[14c] PEt₃ (1945 cm^{-1}),^[14c] and IMes (1941 cm^{-1}),^[21b] indicates that germylenes **1** and **3** are as strong electron donors as very basic phosphanes or NHCs and that the donor character of silylene **2** is even stronger.

The ¹H and ¹³C NMR spectra of **4–7**, **9**, and **10** show the resonances expected for the amidinate, HMDS, and carbonyl groups. In all compounds, the HMDS SiMe₃ fragments are non-equivalent, indicating that the rotation of the HMDS group around the corresponding N–Ge bond is not allowed and confirms the existence of steric hindrance between the HMDS and the nearby amidinate N–R groups and CO ligands. Regarding the amidinate moieties, the *tert*-butyl derivatives **5**, **6**, **9**, and **10** show only one set of signals for both N–*t*Bu arms, reflecting, as observed in the X-ray structures of **6** and **10**, the symmetric attachment of their amidinate fragments. This fact contrasts with the two different sets of signals observed for each N–*i*Pr arm of **7**, which is in agreement with a $\kappa^2\text{Ge},N$ -coordination of its germylene ligand.

Computational studies

We resorted to DFT calculations to shed light on 1) the mechanism operating in the monodentate to bidentate transforma-

tion of $[\text{Ge}(\text{R}_2\text{bzam})(\text{HMDS})]$ in carbonyl dicobalt complexes, 2) the crucial importance that the volume of the amidinate N–R groups has on the final outcome of the reactions of $[\text{Co}_2(\text{CO})_8]$ with amidinate-tetrylenes of the type $[\text{M}(\text{R}_2\text{bzam})(\text{HMDS})]$, and 3) the role played by the different group-14 metal atom (Si vs. Ge) in these reactions. The DFT calculations were carried at the B3LYP/LanL2DZ(Co)/6-31+G** level. The given energies, ΔG_{tol} , are Gibbs energies that include zero-point energy correction and solvent effect (toluene).

As the large number of atoms of this system and the high level of theory of the calculations resulted in an unacceptably slow progress, we decided to use a simplified model having *N,N'*-dimethylacetamidinate (Me_2acam) and dimethylamide (NMe_2) instead of *iPr*₂bzam and HMDS, respectively, for the mechanistic studies. Figure 4 displays a calculated mechanism that accounts for the transformation of the model compound $[\text{Co}_2\{\kappa^1\text{Ge}-\text{Ge}(\text{Me}_2\text{acam})(\text{NMe}_2)\}(\text{CO})_7]$ ($\text{A}_{\text{Ge-Me}}$) into $[\text{Co}_2\{\mu-\kappa^2\text{Ge},\text{N}-\text{Ge}(\text{Me}_2\text{acam})(\text{NMe}_2)\}(\mu\text{-CO})(\text{CO})_5]$ ($\text{B}_{\text{Ge-Me}}$) + CO. The first two steps ($\text{A}_{\text{Ge-Me}} \rightarrow \text{i1} \rightarrow \text{i2}$), which have very low barriers (3.3 and 11.0 kcal mol⁻¹ from $\text{A}_{\text{Ge-Me}}$), move the tetrylene ligand towards the unsubstituted metal atom Co1 in such a way that, in **i2**, the methyl group attached to the amidinate N1 atom is very close to one of the CO ligands attached to Co1. The next

step (**i2** → **i3**) has the highest activation barrier of the whole reaction (21.1 kcal mol⁻¹) and involves the release of that CO ligand to give a coordinatively unsaturated intermediate (**i3**) that has its vacant site protected by the methyl group. In the following step (**i3** → **i4**), an insertion of the Co1 atom into the Ge–N1 bond of **i3** is accompanied by a shift to a bridging position of one of the CO ligands attached to Co1. Lastly, an easy rearrangement of the bridging CO ligand of **i4** leads to the final product $\text{B}_{\text{Ge-Me}}$. It should be noticed that the energy barrier of the rate-determining step (21.1 kcal mol⁻¹, **ts3**) is low enough to allow the reaction to proceed at room temperature and that, although the overall process has a positive ΔG_{tol} (4.7 kcal mol⁻¹), the experimental irreversibility of the CO-elimination step (CO gas is released out of the reacting solution), and the fact that the energies of **i3** (8.1 kcal mol⁻¹) and **i4** (8.9 kcal mol⁻¹) are higher than that of the final product (4.7 kcal mol⁻¹), should drive the reaction equilibrium toward the right.

The key geometric parameters of compound **7** (labeled $\text{B}_{\text{Ge-}i\text{Pr}}$ in the calculations) are comparable to those computed for the model compound $\text{B}_{\text{Ge-Me}}$ (Table 1) and the computed ΔG_{tol} of the reaction $\text{A}_{\text{Ge-}i\text{Pr}} \rightarrow \text{B}_{\text{Ge-}i\text{Pr}} + \text{CO}$, 2.7 kcal mol⁻¹ (Table 2), is similar to that of the model reaction $\text{A}_{\text{Ge-Me}} \rightarrow$

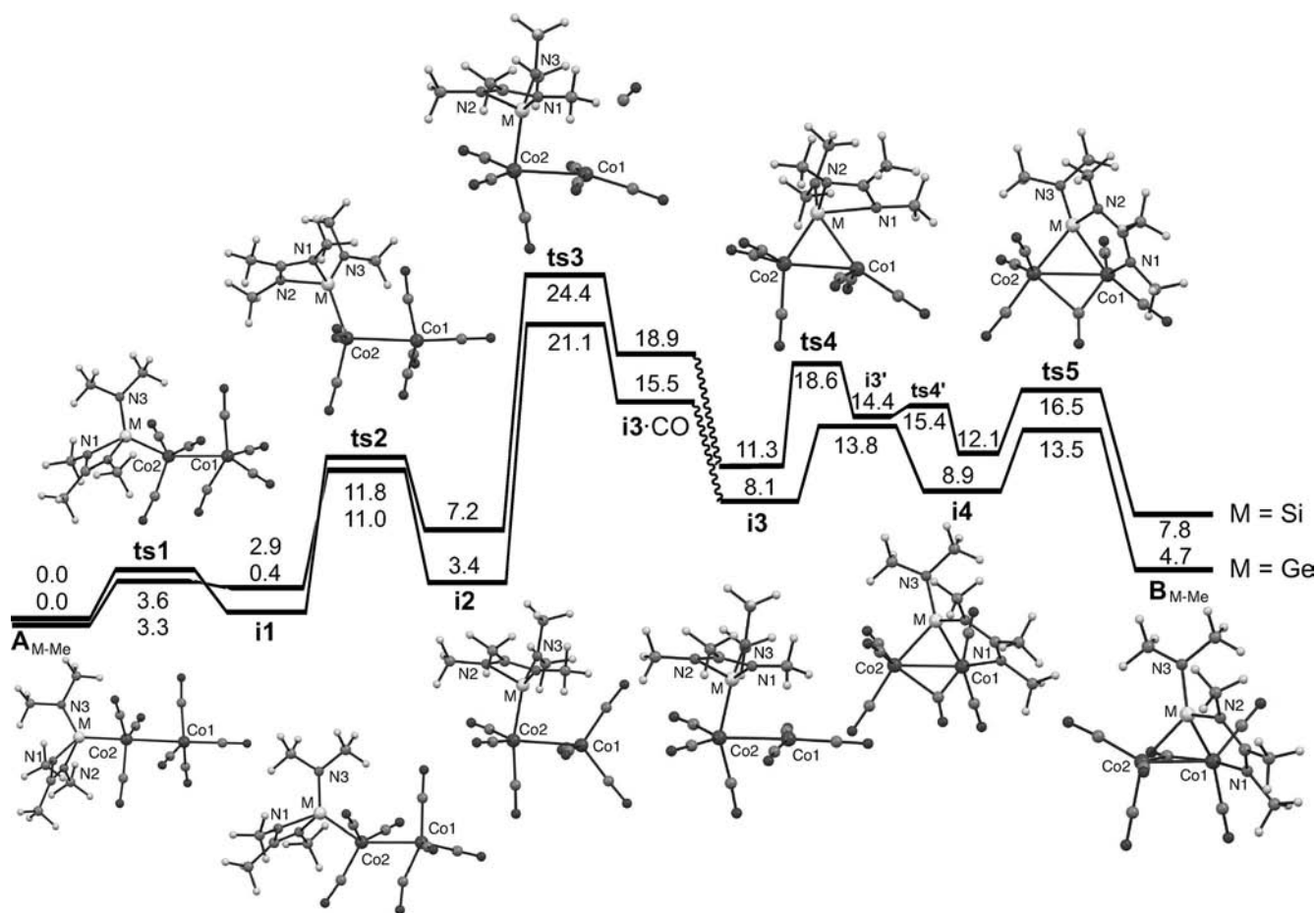
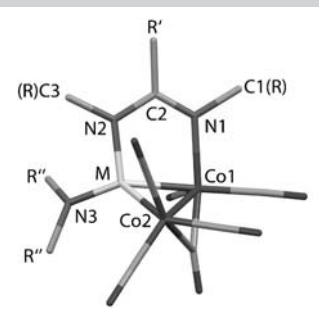


Figure 4. DFT-optimized structures and relative energy profiles (ΔG_{tol} [kcal mol⁻¹]) of the stationary points involved in the transformations of $\text{A}_{\text{M-Me}}$ into $\text{B}_{\text{M-Me}} + \text{CO}$, for $\text{M} = \text{Si}$ or Ge . The given energies are relative to that of $\text{A}_{\text{M-Me}}$; for comparative purposes, those of the species to the right of **i3** (inclusive) also contain the energy of a CO molecule.

Table 1. Selected interatomic distances [Å] in compounds of the type B_{M-R} (DFT data).


Bond	B_{Ge-Me}	B_{Ge-iPr}	B_{Ge-tBu}	B_{Si-Me}	B_{Si-iPr}	B_{Si-tBu}
Co1–Co2	2.647	2.588	2.600	2.622	2.565	2.565
Co1–M	2.320	2.320	2.293	2.266	2.272	2.242
Co1–N1	2.089	2.133	2.212	2.074	2.110	2.180
Co2–M	2.319	2.386	2.416	2.264	2.338	2.377
M–N2	1.913	1.930	1.963	1.799	1.815	1.843
M–N3	1.848	1.881	1.894	1.730	1.758	1.770
N1–C1	1.465	1.489	1.532	1.464	1.490	1.533
N1–C2	1.313	1.319	1.328	1.308	1.314	1.322
N2–C2	1.363	1.368	1.376	1.373	1.377	1.388
N2–C3	1.465	1.492	1.535	1.469	1.499	1.545

Table 2. DFT-calculated ΔG_{tot} [kcal mol⁻¹] for the reactions $A_{M-R} \rightarrow B_{M-R} + CO$.

M	Me	<i>i</i> Pr	<i>t</i> Bu
Ge	4.7	2.7	26.3
Si	7.8	7.6	29.7

$B_{Ge-Me} + CO$ (4.7 kcal mol⁻¹). These data, in addition to the fact that the reaction that transforms compound **4** into **7** + CO should also have a low activation barrier (it occurs at room temperature), indicate that the replacement of the amidinate N–Me and amide N–Me groups for N–*i*Pr and N–SiMe₃ groups, respectively, does not strongly affect the kinetics and thermodynamics of these reactions. Therefore, it is reasonable to propose that the reactions $A_{Ge-Me} \rightarrow B_{Ge-Me} + CO$ and $A_{Ge-iPr} \rightarrow B_{Ge-iPr} + CO$ follow similar mechanisms.

With the aim of shedding some light on the answer to why the reactivity of the isopropyl complex **4** is so different from that of the *tert*-butyl complex **6** (the latter is stable at room temperature and undergoes a general decomposition upon heating), we optimized the molecular structure of the hypothetical *tert*-butyl equivalent of compound **7**, [Co₂{μ-κ²Ge(*N*-Ge(*t*Bu₂bzam)(HMDS))}(μ-CO)(CO)₅] (hereafter named B_{Ge-tBu}), which was never synthesized from complex **6**. Although the overall shape of this complex is reminiscent of that of its isopropyl analogue, a careful analysis of its computed geometrical parameters revealed that some of its bond lengths are considerably different from the equivalent ones of B_{Ge-iPr} (Table 1). In fact, the steric hindrance exerted by the amidinate N–*t*Bu groups of B_{Ge-tBu} over their neighboring CO and SiMe₃ groups, with respect to the geometrical parameters of B_{Ge-iPr} , results in a 0.03 Å shortening of the Co1–Ge distance and a noticeable

lengthening (0.03–0.08 Å) of the Co2–Ge, Co1–N1, Ge–N2, N1–C1, and N2–C3 distances. These “anomalous” bond lengths reduce the stability of B_{Ge-tBu} to the point that the computed ΔG_{tot} value for the reaction $A_{Ge-tBu} \rightarrow B_{Ge-tBu} + CO$ is strongly positive, 26.3 kcal mol⁻¹ (Table 2). These data explain why the thermally mediated elimination of CO from the *tert*-butyl complex **6** (A_{Ge-tBu}) does not lead to the *tert*-butyl analogue of **7** (B_{Ge-tBu}) (in fact, it leads to general decomposition).

Finally, to investigate the effect that changing the group-14 metal atom would have in these reactions, we performed all the DFT calculations described in the above paragraphs using Si instead of Ge. The results of these calculations clearly indicate that the structures of the final products (Table 1) and the kinetics and thermodynamics of the studied reactions (Figure 4, Table 2) depend very little upon the nature of the M atom. Therefore, the different reactivity experimentally observed for [Ge(*i*Pr₂bzam)(HMDS)] (**1**) and [Si(*t*Bu₂bzam)(HMDS)] (**2**) in their reactions with [Co₂(CO)₈] is essentially due to the different volume of their amidinate N–R groups.

Conclusion

This contribution describes the synthesis, characterization, and thermal stability of the first dicobalt carbonyl complexes containing amidinate-germylenes and -silylenes as ligands. In contrast to the vast majority of studies hitherto carried out with ligands of this kind, this work uses amidinate-tetrylenes equipped with a very bulky HMDS group. Remarkably, an unprecedented ring opening concomitant with a terminal to bridging transformation of the amidinate-tetrylene ligand has been observed for M=Ge and amidinate N–R=N–*i*Pr. A combined experimental and computational DFT study has shown that such a transformation is negligibly influenced by the nature of the group-14 donor atom (Si or Ge) but is strongly dependent upon the steric hindrance exerted by the amidinate N–R groups, since the process is thermodynamically favorable for R=*i*Pr but not for R=*t*Bu. Thus, if amidinate-silylenes equipped with a bulky HMDS fragment on the Si atom and isopropyl (or smaller) groups on the amidinate N atoms were synthetically viable, their transformation into bidentate ligands could also be possible.

Considering the fundamental role that amidinate-tetrylene ligands (specially silylenes) are playing in modern coordination chemistry, we hope that the information provided in this paper will help researchers to design and prepare new heavier tetrylene–TM complexes for use in coordination chemistry and catalysis.

Experimental Section

General

All manipulations were performed under argon using standard glovebox and Schlenk-vacuum line techniques. Solvents were dried over sodium diphenyl ketyl and were distilled under argon before use. The reactions were routinely monitored by solution IR spectroscopy (carbonyl stretching region). PhLi (1.8 M solution in dibu-

tyl ether), *N,N'*-bis(isopropyl)carbodiimide, *N,N'*-bis(*tert*-butyl)carbodiimide, Li(HMDS) (1.0 M solution in hexanes), HSiCl₃, and [Co₂(CO)₈] were purchased from Sigma–Aldrich Chemicals. [GeCl₂]-dioxane was purchased from Gelest. [Ge(*i*Pr₂bzam)(HMDS)] (1),^[12] [Si(*t*Bu₂bzam)(HMDS)] (2),^[19] and [Ge(*t*Bu₂bzam)(HMDS)] (3)^[27] were synthesized following previously reported procedures. All reaction products were vacuum-dried for several hours prior to being weighed and analyzed. NMR spectra were run in C₆D₆ on Bruker DPX-300 or Bruker AV-400 instruments; the residual protic solvent resonance $\delta(\text{C}_6\text{HD}_5) = 7.16$ ppm; $\delta(\text{C}_6\text{D}_5\text{CD}_2\text{H}) = 2.08$ ppm was used as reference for ¹H, whereas the solvent resonance $\delta(\text{C}_6\text{D}_6) = 128.1$ ppm; $\delta(\text{C}_6\text{D}_5\text{CD}_3) = 137.5$ ppm was used as reference for ¹³C. Microanalyses were obtained from the University of Oviedo Microanalytical Service. FAB+ mass spectra were obtained from the University of A Coruña Mass Spectrometric Service (30 kV Cs⁺ gun, 3-nitrobenzyl alcohol as matrix); in all cases, the given MS data refer to the most abundant molecular ion isotopomer.

Syntheses

[Co₂{κ¹Ge–Ge(*i*Pr₂bzam)(HMDS)}(CO)₇] (4): [Ge(*i*Pr₂bzam)(HMDS)] (1) (0.25 mL of a 0.27 M solution in toluene, 0.068 mmol) was added to a solution of [Co₂(CO)₈] (23 mg, 0.068 mmol) in toluene (10 mL) and the mixture was stirred at room temperature for 5 min. The initial dark-red color changed to dark orange. A flash chromatography purification (2×3 cm silica gel column packed in hexane, hexane as eluent) separated compound **4**, which was isolated as a light-orange solid after solvent removal (38 mg, 75%). As compound **4** evolves in solution at room temperature to complex **7** (see below), the IR and NMR spectra of freshly prepared samples of **4** always showed the presence of some **7**. The spectral data given below for **4** were obtained by comparing the obtained spectra with those of pure **7**. Satisfactory microanalysis and mass spectra of **4** could not be obtained. ¹H NMR (C₆D₆, 300.1 MHz, 293 K): $\delta = 7.05$ – 6.98 (m, 5H; 5 CH of Ph), 3.51 (sp, *J* = 6.5 Hz, 2H; 2 CH of *i*Pr), 1.20 (d, *J* = 6.5 Hz, 3H; *Me* of *i*Pr), 1.03 (d, *J* = 6.5 Hz, 3H; *Me* of *i*Pr), 0.96–0.91 (m, 6H; 2 *Me* of *i*Pr), 0.58 (s, 9H; 3 *Me* of HMDS), 0.46 ppm (s, 9H; 3 *Me* of HMDS); ¹³C{¹H} NMR (C₆D₆, 75.5 MHz, 293 K): $\delta = 202.4$ (COs), 166.2 (NCN), 130.0–127.7 (m; Ph), 48.3 (CH of *i*Pr), 48.2 (CH of *i*Pr), 24.5, (2 *Me* of *i*Pr), 23.5 (2 *Me* of *i*Pr), 6.7 (3 *Me* of HMDS), 6.5 ppm (3 *Me* of HMDS); IR (toluene): $\tilde{\nu}_{\text{CO}} = 2073$ (m), 2016 (m), 1989 (vs), 1944 (m) cm⁻¹.

[Co₂{κ¹Si–Si(*t*Bu₂bzam)(HMDS)}(CO)₇] (5): [Si(*t*Bu₂bzam)(HMDS)] (2) (0.30 mL of a 0.25 M solution in toluene, 0.075 mmol) was added to a solution of [Co₂(CO)₈] (25 mg, 0.074 mmol) in toluene (10 mL) and the mixture was stirred at room temperature for 20 min. The initial dark-red color changed to dark orange. A flash chromatography purification (2×3 cm silica gel column packed in hexane, hexane/dichloromethane 1:1 as eluent) separated compound **5**, which was isolated as an orange solid after solvent removal (18 mg, 33%). ¹H NMR (C₆D₆, 300.1 MHz, 293 K): $\delta = 7.06$ – 6.84 (m, 5H; 5 CH of Ph), 1.20 (s, 18H; 6 *Me* of *t*Bu), 0.66 (s, 9H; 3 *Me* of HMDS), 0.42 ppm (s, 9H; 3 *Me* of HMDS); ¹³C{¹H} NMR (C₆D₆, 75.5 MHz, 293 K): $\delta = 204.2$ (COs), 166.8 (NCN), 132.6 (C_{ipso} of Ph), 129.9 (CH of Ph), 129.5 (CH of Ph), 128.6 (2 CH of Ph), 127.5 (CH of Ph), 56.2 (2 C of *t*Bu), 31.5 (6 *Me* of *t*Bu), 7.5 (3 *Me* of HMDS), 7.3 ppm (3 *Me* of HMDS); (+)-FAB MS: *m/z*: 733.1 [*M*⁺]; IR (toluene, cm⁻¹): $\tilde{\nu}_{\text{CO}} = 2066$ (m), 2005 (m), 1973 (vs), 1932 (m); elemental analysis calcd (%) for C₂₈H₄₁Co₂N₃O₇Si₃ (*M*_w = 733.76 amu): C 45.83, H 5.63, N 5.73; found: C 45.86, H 5.65, N, 5.71.

Thermal evolution of 5: Complex **5** (15 mg, 0.020 mmol) was dissolved in toluene (5 mL) and the solution was stirred at room temperature for 60 min. As no reaction occurred (IR analysis), the tem-

perature was raised to 90 °C. After 15 min, an untreatable solid precipitated and the IR spectrum of the solution showed the almost complete disappearance of the $\tilde{\nu}_{\text{CO}}$ absorptions.

[Co₂{κ¹Ge–Ge(*t*Bu₂bzam)(HMDS)}(CO)₇] (6): [Ge(*t*Bu₂bzam)(HMDS)] (3) (0.20 mL of a 0.34 M solution in toluene, 0.068 mmol) was added to a solution of [Co₂(CO)₈] (23 mg, 0.068 mmol) in toluene (10 mL) and the mixture was stirred at room temperature for 5 min. The initial dark-red color changed to dark orange. A flash chromatography purification (2×3 cm silica gel column packed in hexane, hexane as eluent) separated compound **6**, which was isolated as a light-orange solid after solvent removal (41 mg, 78%). ¹H NMR (C₆D₆, 300.1 MHz, 293 K): $\delta = 6.95$ – 6.85 (m, 5H; 5 CH of Ph), 1.13 (s, 18H; 6 *Me* of *t*Bu), 0.63 (s, 9H; 3 *Me* of HMDS), 0.42 ppm (s, 9H; 3 *Me* of HMDS); ¹³C{¹H} NMR (C₆D₅CD₃, 75.5 MHz, 293 K): $\delta = 202.5$ (COs), 167.0 (NCN), 131.9 (C_{ipso} of Ph), 130.4 (CH of Ph), 128.7 (2 CH of Ph), 128.2 (CH of Ph), 127.7 (CH of Ph), 56.2 (2 C of *t*Bu), 31.6 (6 *Me* of *t*Bu), 6.8 (3 *Me* of HMDS), 6.5 ppm (3 *Me* of HMDS); (+)-FAB MS: *m/z*: 667 [*M*⁺–4CO]; IR (toluene): $\tilde{\nu}_{\text{CO}} = 2072$ (m), 2013 (m), 1983 (vs), 1940 cm⁻¹ (m); elemental analysis calcd (%) for C₂₈H₄₁Co₂GeN₃O₇Si₂ (*M*_w = 778.29 amu): C 43.21, H 5.31, N 5.40; found: C 43.23, H 5.33, N 5.35.

Thermal evolution of 6: Complex **6** (40 mg, 0.051 mmol) was dissolved in toluene (10 mL) and the solution was stirred at room temperature for 60 min. As no reaction occurred (IR analysis), the temperature was raised to 90 °C. After 15 min, an untreatable solid precipitated and the IR spectrum of the solution showed the almost complete disappearance of the $\tilde{\nu}_{\text{CO}}$ absorptions.

[Co₂{μ–κ²Ge,*N*–(Ge(*i*Pr₂bzam)(HMDS))}(μ–CO)(CO)₅] (7): *Method 1:* Complex **4** (32 mg, 0.043 mmol) was dissolved in toluene (10 mL) and the solution was stirred at room temperature. After 90 min, compound **7** was quantitatively formed (IR analysis). It was isolated as a light-orange solid after solvent removal (30 mg, 97%).

Method 2: [Ge(*i*Pr₂bzam)(HMDS)] (1) (0.80 mL of a 0.27 M solution in toluene, 0.216 mmol) was added to a solution of [Co₂(CO)₈] (73 mg, 0.214 mmol) in toluene (20 mL) and the mixture was heated at 60 °C for 1 h. The initial dark-red color changed to dark orange. A flash chromatographic purification (2×3 cm silica gel column packed in hexane, hexane as eluent) separated complex **7**, which was isolated as a light-orange solid after solvent removal (110 mg, 71%). ¹H NMR (C₆D₆, 300.1 MHz, 293 K): $\delta = 7.03$ – 6.97 (m, 5H; 5 CH of Ph), 4.23 (sp, *J* = 6.5 Hz, 1H; CH of *i*Pr), 3.45 (sp, *J* = 6.5 Hz, 1H; CH of *i*Pr), 1.41 (d, *J* = 6.5 Hz, 3H; *Me* of *i*Pr), 1.15 (d, *J* = 6.5 Hz, 3H; *Me* of *i*Pr), 0.92 (d, *J* = 6.5 Hz, 3H; *Me* of *i*Pr), 0.86 (d, *J* = 6.5 Hz, 3H; *Me* of *i*Pr), 0.45 (s, 9H; 3 *Me* of HMDS), 0.36 ppm (s, 9H; 3 *Me* of HMDS); ¹³C{¹H} NMR (C₆D₆, 75.5 MHz, 293 K): $\delta = 205.4$ (COs), 205.1 (COs), 167.3 (NCN), 135.9 (C_{ipso} of Ph), 129.0 (2 CH of Ph), 128.4 (CH of Ph), 128.2 (CH of Ph), 127.7 (CH of Ph), 54.7 (CH of *i*Pr), 48.0 (CH of *i*Pr), 24.8, 23.9, 23.7, 23.5 (4 *Me* of *i*Pr), 5.5 (3 *Me* of HMDS), 4.9 ppm (3 *Me* of HMDS); (+)-FAB MS: *m/z*: 722 [*M*⁺]; IR (toluene): $\tilde{\nu}_{\text{CO}} = 2058$ (m), 2017 (vs), 1996 (m), 1974 (m, br), 1814 cm⁻¹ (w, br); elemental analysis calcd (%) for C₂₅H₃₇Co₂GeN₃O₆Si₂ (*M*_w = 722.23 amu): C 41.58, H 5.16, N 5.82; found: C 41.69, H 5.19, N 5.70.

[Co₂{κ¹Ge–Ge(*i*Pr₂bzam)(HMDS)}₂(CO)₆] (8): [Ge(*i*Pr₂bzam)(HMDS)] (1) (0.50 mL of a 0.27 M solution in toluene, 0.135 mmol) was added to a solution of [Co₂(CO)₈] (22 mg, 0.065 mmol) in toluene (10 mL) and the mixture was stirred at room temperature for 1 h. Complex **8** was clearly detected by IR spectroscopy in the reacting solution ($\tilde{\nu}_{\text{CO}} = 1960$ (m), 1937 cm⁻¹ (vs)) along with other unidentified products, but it could not be isolated because it decomposed during the purification process.

[Co₂{κ¹Si–Si(tBu₂bzam)(HMDS)}₂(CO)₆] (9): [Si(tBu₂bzam)(HMDS)] (2) (0.60 mL of a 0.25 M solution in toluene, 0.150 mmol) was added to a solution of [Co₂(CO)₈] (25 mg, 0.074 mmol) in toluene (10 mL) and the mixture was stirred at room temperature for 1 h. The initial dark-red color changed to dark orange. A flash chromatography purification (2×3 cm silica gel column packed in hexane, hexane/CH₂Cl₂ 1:1 as eluent) separated compound **9**, which was isolated as a dark-orange solid after solvent removal (31 mg, 37%). ¹H NMR (C₆D₅CD₃, 300.1 MHz, 293 K): δ = 7.49 (s, br, 1H; CH of Ph), 7.09–6.95 (m, 4H; 4 CH of Ph), 1.36 (s, 18H; 6 Me of tBu), 0.76 (s, 9H; 3 Me of HMDS), 0.51 ppm (s, 9H; 3 Me of HMDS); ¹³C{¹H} NMR (C₆D₅CD₃, 75.5 MHz, 293 K): δ = 208.6 (COs), 167.3 (NCN), 134.3 (C_{ipso} of Ph), 130.3 (CH of Ph), 129.9 (CH of Ph), 128.6 (2 CH of Ph), 127.4 (CH of Ph), 55.7 (2 C of tBu), 31.6 (6 Me of tBu), 7.7 (3 Me of HMDS), 7.3 ppm (3 Me of HMDS); (+)-FAB MS: *m/z*: 1124.4 [*M*⁺]; IR (toluene): $\tilde{\nu}_{\text{CO}}$ = 1936 (m), 1920 (vs), 1900 cm⁻¹ (w); elemental analysis calcd (%) for C₄₈H₈₂Co₂N₆O₆Si₆ (*M_w* = 1125.58 amu): C 51.22, H 7.34, N 7.47; found: C 51.25, H 7.37, N 7.44.

[Co₂{κ¹Ge–Ge(tBu₂bzam)(HMDS)}₂(CO)₆] (10): [Ge(tBu₂bzam)(HMDS)] (3) (0.40 mL of a 0.34 M solution in toluene, 0.136 mmol) was added to a solution of [Co₂(CO)₈] (23 mg, 0.068 mmol) in toluene (10 mL) and the mixture was stirred at room temperature for 1 h. The initial dark-red color changed to dark orange. A flash chromatography purification (2×3 cm silica gel column packed in hexane, hexane/CH₂Cl₂ 1:1 as eluent) separated compound **10**, which was isolated as a dark-orange solid after solvent removal (74 mg, 90%). ¹H NMR (C₆D₆, 300.1 MHz, 293 K): δ = 7.41 (m, 1H; CH of Ph), 7.03–6.79 (m, 4H; 4 CH of Ph), 1.30 (s, 18H; tBu), 0.77 (s, 9H; 3 Me of HMDS), 0.52 ppm (s, 9H; 3 Me of HMDS); ¹³C{¹H} NMR (C₆D₅CD₃, 75.5 MHz, 293 K): δ = 206.0 (COs), 166.3 (NCN), 133.3 (C_{ipso} of Ph), 130.8 (CH of Ph), 130.5 (CH of Ph), 129.4 (2 CH of Ph), 128.4 (CH of Ph), 55.9 (2 C of tBu), 31.9 (6 Me of tBu), 7.1 (3 Me of HMDS), 6.7 ppm (3 Me of HMDS); (+)-FAB MS: *m/z*: 1214.3 [*M*⁺]; IR (toluene): $\tilde{\nu}_{\text{CO}}$ = 1958 (m), 1937 (vs), 1912 cm⁻¹ (vw); elemental analysis calcd (%) for C₄₈H₈₂Co₂Ge₂N₆O₆Si₄ (*M_w* = 1214.63 amu): C 47.46, H 6.80, N 6.92; found: C 47.51, H 6.89, N 6.87.

X-ray diffraction analyses

Crystals of **6**, **7**, and **10**·2THF were analyzed by using X-ray diffraction. Diffraction data were collected on an Oxford Diffraction Xcalibur Onyx Nova single-crystal diffractometer. An empirical absorption correction was applied using the SCALE3 ABSPACK algorithm as implemented in CrysAlisPro RED.^[28] The structures were solved using the program SIR-97.^[29] Isotropic and full matrix anisotropic least square refinements were carried out using SHELXL.^[30] All non-H atoms were refined anisotropically. The hydrogen atoms were set in calculated positions and refined riding on their parent atoms. The WINGX program system^[31] was used throughout the structure determinations. A selection of interatomic distances and angles in the compounds studied by XRD is given in Table S1 (Supporting Information). A selection of crystal, measurement, and refinement data is given in Table S2 (Supporting Information). CCDC-985354 (**6**), CCDC-901726 (**7**), and CCDC-985355 (**10**·2THF) contain the supplementary crystallographic data for this paper. These data can be obtained free of charge from The Cambridge Crystallographic Data Centre via www.ccdc.cam.ac.uk/data_request/cif.

Computational details

DFT calculations were carried out using the Becke's 3-parameter hybrid exchange-correlation functional^[32] and the hybrid B3LYP nonlocal gradient correction.^[33] The LanL2DZ basis set,^[34] with relativistic effective core potentials, was used for the Co atom. The

basis set used for the remaining atoms was the diffuse and polarized 6–31+G(d,p).^[35] All stationary points of the mechanistic studies were fully optimized in gas phase and confirmed as energy minima (reactants, products, and intermediates; all positive eigenvalues) or transition states (one imaginary eigenvalue) by analytical calculation of frequencies. These calculations were also used to determine the zero-point-corrected gas phase Gibbs energies (*G*). IRC calculations were used to verify that the transition states found were correct saddle points connecting the proposed minima. For each stationary point, the effect of the solvent was estimated by computing the polarizable continuum model (CPCM) energy,^[36] *E*_{CPCM}, in a single-point calculation ($\epsilon_{\text{toluene}} = 2.3741$). Solvent effect-corrected Gibbs energies, *G*_{sol}, were calculated by using the equation *G*_{sol} = *E*_{CPCM} + (*G* – *E*), in which *E* is the potential (electronic) energy.^[37] All calculations were carried out without symmetry constraints employing the Gaussian 09 package.^[38] Cartesian coordinates for all optimized structures are given in the Supporting Information.

Acknowledgements

This work has been supported by the Spanish MICINN/FEDER grants CTQ2010–14933, MAT2010–15094, DELACIERVA-09–05, and RYC-2012–10491 and the European Union Marie Curie action FP7–2010-RG-268329.

Keywords: cobalt · germanium · ligand effects · main group elements · silicon

- [1] V. Y. Lee, A. Sekiguchi, *Organometallic Compounds of Low Coordinate Si, Ge, Sn and Pb: From Phantom Species to Stable Compounds*, John Wiley & Sons, Chichester, 2010.
- [2] Heavier tetrylenes have an ambiphilic character because its tetrylene atom possesses a vacant p orbital (Lewis acid character) and a lone pair of electrons (Lewis base character). This dual Lewis acid/base character is in most cases markedly higher than that of their carbene relatives. See, for example: a) A. V. Zabula, F. E. Hahn, T. Pape, A. Hepp, *Organometallics* 2007, 26, 1972–1980; b) A. V. Zabula, T. Pape, A. Hepp, F. M. Schappacher, U. C. Rodewald, R. Pöttgen, F. E. Hahn, *J. Am. Chem. Soc.* 2008, 130, 5648–5647; c) A. V. Zabula, T. Pape, A. Hepp, F. E. Hahn, *Organometallics* 2008, 27, 2756–2760.
- [3] For recent reviews on the chemistry of heavier tetrylenes, see: a) S. K. Mandal, H. W. Roesky, *Acc. Chem. Res.* 2012, 45, 298–307; b) M. Asay, C. Jones, M. Driess, *Chem. Rev.* 2011, 111, 354–396; c) S. Yao, Y. Xiong, M. Driess, *Organometallics* 2011, 30, 1748–1767; d) S. K. Mandal, H. W. Roesky, *Chem. Commun.* 2010, 46, 6016–6041; e) M. Kira, *Chem. Commun.* 2010, 46, 2893–2903; f) Y. Mizuhata, T. Sasamori, N. Tokitoh, *Chem. Rev.* 2009, 109, 3479–3511; g) S. Nagendran, H. W. Roesky, *Organometallics* 2008, 27, 457–492.
- [4] For reviews on the coordination chemistry of heavier tetrylene compounds, see: a) B. Blom, M. Stoelzel, M. Driess, *Chem. Eur. J.* 2013, 19, 40–62; b) A. V. Zabula, F. E. Hahn, *Eur. J. Inorg. Chem.* 2008, 5165–5179; c) W.-P. Leung, K.-W. Kan, K.-H. Chong, *Coord. Chem. Rev.* 2007, 251, 2253–2265; d) R. Waterman, P. G. Hayes, T. D. Tilley, *Acc. Chem. Res.* 2007, 40, 712–719; e) O. Kühn, *Coord. Chem. Rev.* 2004, 248, 411–427; f) M. Okazaki, H. Tobita, H. Ogino, *Dalton Trans.* 2003, 493–506; g) B. Gehrhus, M. F. Lappert, *J. Organomet. Chem.* 2001, 617–618, 209–223; h) M. F. Lappert, R. S. Rowe, *Coord. Chem. Rev.* 1990, 100, 267–292; i) W. Petz, *Chem. Rev.* 1986, 86, 1019–1047.
- [5] See, for example: a) D. Martin, M. Melaimi, M. Soleilhavoup, G. Bertrand, *Organometallics* 2011, 30, 5304–5313; b) M. Melaimi, M. Soleilhavoup, G. Bertrand, *Angew. Chem.* 2010, 122, 8992–9032; *Angew. Chem. Int. Ed.* 2010, 49, 8810–8849; c) S. Díez-González, N. Marion, S. P. Nolan, *Chem. Rev.* 2009, 109, 3612–3676; d) O. Schuster, L. Yang, H. G. Raubenheimer, M. Albrecht, *Chem. Rev.* 2009, 109, 3445–3478; e) M. Poyatos, J. A.

- Mata, E. Peris, *Chem. Rev.* **2009**, *109*, 3677–3707; f) F. E. Hahn, M. C. Jahnke, *Angew. Chem.* **2008**, *120*, 3166–3216; *Angew. Chem. Int. Ed.* **2008**, *47*, 3122–3172.
- [6] Coordinated heavier tetrylenes are prone to suffer oxidation and/or hydrolysis, processes. See, for example: a) D. Matioszek, N. Saffon, J.-M. Sotiropoulos, K. Miqueu, A. Castel, J. Escudie, *Inorg. Chem.* **2012**, *51*, 11716–11721; b) D. Amoroso, M. Haaf, G. P. A. Yap, R. West, D. E. Fogg, *Organometallics* **2002**, *21*, 534–540.
- [7] The M–TM bonds of heavier tetrylene–TM complexes are generally weaker than the C–TM bonds of NHC–TM complexes. This trend increases on going down along group-14 of the periodic table. See, for example: a) T. A. N. Nguyen, G. Frenking, *Chem. Eur. J.* **2012**, *18*, 12733–12748; b) H. Arp, J. Baumgartner, C. Marschner, P. Zark, T. Müller, *J. Am. Chem. Soc.* **2012**, *134*, 10864–10875; c) C. Boehme, G. Frenking, *Organometallics* **1998**, *17*, 5801–5805; d) W. J. Evans, J. M. Perotti, J. W. Ziller, D. F. Moser, R. West, *Organometallics* **2003**, *22*, 1160–1163; e) W. A. Herrmann, P. Härter, C. W. K. Gstöttmayr, F. Bielert, N. Seeboth, P. Sirsch, *J. Organomet. Chem.* **2002**, *649*, 141–146; f) J. T. York, V. G. Young Jr., W. B. Tolman, *Inorg. Chem.* **2006**, *45*, 4191–4198.
- [8] The synthesis of heavier tetrylene–TM complexes commonly requires the use of air-sensitive tetrylene reagents, whereas the use of pure NHCs is often unnecessary for the preparation of NHC–TM complexes (for example, imidazol-2-ylidenes can be generated in situ from readily available imidazolium salts).
- [9] For TM complexes containing amidinate-tetrylene ligands, see: a) D. Gallego, A. Brück, E. Irran, F. Meier, M. Kaupp, M. Driess, J. F. Hartwig, *J. Am. Chem. Soc.* **2013**, *135*, 15617–15626; b) B. Blom, S. Enthaler, S. Inoue, E. Irran, M. Driess, *J. Am. Chem. Soc.* **2013**, *135*, 6703–6713; c) W. Wang, S. Inoue, S. Enthaler, M. Driess, *Angew. Chem.* **2012**, *124*, 6271–6275; *Angew. Chem. Int. Ed.* **2012**, *51*, 6167–6171; d) A. Brück, D. Gallego, W. Wang, E. Irran, M. Driess, J. F. Hartwig, *Angew. Chem.* **2012**, *124*, 11645–11649; *Angew. Chem. Int. Ed.* **2012**, *51*, 11478–11482; e) B. Blom, M. Driess, D. Gallego, S. Inoue, *Chem. Eur. J.* **2012**, *18*, 13355–13360; f) R. Azhakar, R. S. Ghadwal, H. W. Roesky, J. Hey, D. Stalke, *Chem. Asian J.* **2012**, *7*, 528–533; g) R. Azhakar, R. S. Ghadwal, H. W. Roesky, H. Wolf, D. Stalke, *J. Am. Chem. Soc.* **2012**, *134*, 2423–2428; h) K. Junold, J. A. Baus, C. Burschka, R. Take, *Angew. Chem.* **2012**, *124*, 7126–7129; *Angew. Chem. Int. Ed.* **2012**, *51*, 7020–7023; i) R. Azhakar, H. W. Roesky, J. J. Holstein, B. Dittich, *Dalton Trans.* **2012**, *41*, 12096–12100; j) W. Wang, S. Inoue, E. Irran, M. Driess, *Angew. Chem.* **2012**, *124*, 3751–3754; *Angew. Chem. Int. Ed.* **2012**, *51*, 3691–3694; k) reference 7a; l) R. Azhakar, S. P. Sarish, H. W. Roesky, J. Hey, D. Stalke, *Inorg. Chem.* **2011**, *50*, 5039–5043; m) G. Tavčar, S. S. Sen, R. Azhakar, A. Thorn, H. W. Roesky, *Inorg. Chem.* **2010**, *49*, 10199–10202; n) W. Wang, S. Inoue, S. Yao, M. Driess, *J. Am. Chem. Soc.* **2010**, *132*, 15890–15892; o) D. Matioszek, N. Katir, N. Saffon, A. Castel, *Organometallics* **2010**, *29*, 3039–3046; p) S. S. Sen, M. P. Kritzer-Kosch, S. Nagendran, H. W. Roesky, T. Beck, A. Pal, R. Herbst-Irmer, *Eur. J. Inorg. Chem.* **2010**, 5304–5311; q) W. Yang, H. Fu, H. Wang, M. Chen, Y. Ding, H. W. Roesky, A. Jana, *Inorg. Chem.* **2009**, *48*, 5058–5060; r) C. Jones, R. P. Rose, A. Stasch, *Dalton Trans.* **2008**, 2871–2878; s) K. Junold, J. A. Baus, C. Burschka, T. Vent-Schmidt, S. Riedel, R. Take, *Inorg. Chem.* **2013**, *52*, 11593–11599; t) R. Azhakar, R. S. Ghadwal, H. W. Roesky, J. Hey, L. Krause, D. Stalke, *Dalton Trans.* **2013**, *42*, 10277–10281; u) G. Tan, B. Blom, G. Gallego, M. Driess, *Organometallics* **2014**, *33*, 363–369; v) S. S. Sen, D. Kratzer, D. Stern, H. W. Roesky, D. Stalke, *Inorg. Chem.* **2010**, *49*, 5786–5788; w) N. C. Breit, T. Szilvási, T. Suzuki, D. Gallego, S. Inoue, *J. Am. Chem. Soc.* **2013**, *135*, 17958–17968; x) C. I. Someya, M. Haberberger, W. Wang, S. Enthaler, S. Inoue, *Chem. Lett.* **2013**, *42*, 286–288.
- [10] For a recent review on N-heterocyclic silylene complexes in catalysis, see: B. Blom, D. Gallego, M. Driess, *Inorg. Chem. Front.* **2014**, *1*, 134–148.
- [11] a) L. Álvarez-Rodríguez, J. A. Cabeza, P. García-Álvarez, D. Polo, *Organometallics* **2013**, *32*, 3557–3561; b) J. A. Cabeza, J. M. Fernández-Colinas, P. García-Álvarez, D. Polo, *Inorg. Chem.* **2012**, *51*, 3896–3903; c) J. A. Cabeza, P. García-Álvarez, D. Polo, *Inorg. Chem.* **2012**, *51*, 2569–2576; d) J. A. Cabeza, P. García-Álvarez, D. Polo, *Inorg. Chem.* **2011**, *50*, 6195–6199.
- [12] Preliminary communication of this work: J. A. Cabeza, P. García-Álvarez, D. Polo, *Dalton Trans.* **2013**, *42*, 1329–1332.
- [13] No attempts were made to isolate these ionic byproducts in pure form.
- [14] For reactions of $[\text{Co}_2(\text{CO})_8]$ with phosphanes, see, for example (and references therein): a) P. Szabo, L. Fekete, G. Bor, Z. Nagy-Magos, L. Markó, *J. Organomet. Chem.* **1968**, *12*, 245–248; b) A. R. Manning, *J. Chem. Soc. A* **1968**, 1135–1137; c) C. D. Wood, P. E. Garrou, *Organometallics* **1984**, *3*, 170–174; d) M. Absi-Halabi, J. D. Atwood, N. P. Forbus, T. L. Brown, *J. Am. Chem. Soc.* **1980**, *102*, 6248–6254; e) W. Hieber, W. Freyer, *Chem. Ber.* **1958**, *91*, 1230–1233.
- [15] For examples regarding $[\text{CoL}_2(\text{CO})_3]^+[\text{Co}(\text{CO})_4]^-$ derivatives ($\text{L} \neq \text{PR}_3$), see: a) reference [9f]; b) H. van Rensburg, R. P. Tooze, D. F. Foster, S. Otto, *Inorg. Chem.* **2007**, *46*, 1963–1965.
- [16] See, for example: a) N. Ungvari, E. Fordos, T. Kegl, L. Parkanyi, F. Ungvary, *Organometallics* **2010**, *29*, 3837–3851; b) S. E. Gibson, C. Johnstone, J. A. Loch, J. W. Steed, A. Stevenazzi, *Organometallics* **2003**, *22*, 5374–5377.
- [17] See, for example: a) S.-T. Liu, H. Yan, X. Hu, Q.-W. Liu, *Huaxue Xuebao* (Chin.), *Acta Chim. Sin.* **1992**, *50*, 1173–1178; b) R. D. Adams, D. F. Chodosh, N. M. Golembeski, E. C. Weissman, *J. Organomet. Chem.* **1979**, *172*, 251–267.
- [18] For examples of bi- and trinuclear TM complexes containing bridging heavier tetrylene ligands, see: a) R. D. Adams, E. Trufan, *Organometallics* **2010**, *29*, 4346–4353; b) R. D. Adams, B. Captain, E. Trufan, *J. Organomet. Chem.* **2008**, *693*, 3593–3602; c) A. Fürstner, H. Krause, C. W. Lehmann, *Chem. Commun.* **2001**, 2372–2373; d) C. J. Cardin, D. J. Cardin, M. A. Convery, Z. Dauter, D. Fenske, M. M. Devereux, M. B. Power, *J. Chem. Soc. Dalton Trans.* **1996**, 1133–1144; e) M. Veith, A. Müller, L. Stahl, M. Notzel, M. Jarczyk, V. Huch, *Inorg. Chem.* **1996**, *35*, 3848–3855; f) M. Knorr, E. Hallauer, V. Huch, M. Veith, P. Braunstein, *Organometallics* **1996**, *15*, 3868–3875.
- [19] R. Azhakar, R. S. Ghadwal, H. W. Roesky, H. Wolf, D. Stalke, *Organometallics* **2012**, *31*, 4588–4592. In our hands, the procedure used in this reference to prepare $[\text{Si}(\text{tBu}_2\text{bzam})\text{Cl}]$ from $[\text{Si}(\text{tBu}_2\text{bzam})\text{Cl}_2]\text{H}$ failed to render a silylene when $i\text{Pr}_2\text{bzam}$ is used instead of tBu_2bzam .
- [20] Reference [3g] contains the following sentence: “Amidinatotrichlorosilanes $[\text{Si}(\text{R}_2\text{bzam})\text{Cl}_3]$ ($\text{R} = i\text{Pr}$, Cy , $2,6\text{-}i\text{Pr}_2\text{C}_6\text{H}_3$) were prepared and reduced with two equivalents of potassium at room temperature, but none of these precursors produced a chlorosilylene. This study underlines the importance of the substituents on the nitrogen atoms to obtain a stable chlorosilylene”.
- [21] See, for example: a) N. Casati, P. Macchi, A. Sironi, *Angew. Chem.* **2005**, *117*, 7914–7917; *Angew. Chem. Int. Ed.* **2005**, *44*, 7736–7739; b) H. van Rensburg, R. P. Tooze, D. F. Foster, A. M. Z. Slawin, *Inorg. Chem.* **2004**, *43*, 2468–2470.
- [22] A. Schnepf, *Z. Anorg. Allg. Chem.* **2006**, *632*, 935–938.
- [23] D.-Z. Wang, B.-F. Wu, Q.-T. Hu, N. M. Dax, *Xue. Zir. Kex.* (Chin.), *Acta Sci. Nat. Univ. Nei Mongol.* **2003**, *34*, 284–287.
- [24] a) P. N. Bungu, S. Otto, *Dalton Trans.* **2011**, *40*, 9238–9249; b) M. Haumann, R. Meijboom, J. R. Moss, A. Roodt, *Dalton Trans.* **2004**, 1679–1686; c) R. A. Jones, M. H. Seeberger, A. L. Stuart, B. R. Whittlesey, T. C. Wright, *Acta Cryst.* **1986**, *C42*, 399–402; d) J. A. Ibers, *J. Organomet. Chem.* **1968**, *14*, 423–428.
- [25] See, for example: a) D. J. Nelson, S. P. Nolan, *Chem. Soc. Rev.* **2013**, *42*, 6723–6753; b) A. R. Chianese, X. Li, M. C. Janzen, J. W. Faller, R. H. Crabtree, *Organometallics* **2003**, *22*, 1663–1667; c) O. Kühn, *Coord. Chem. Rev.* **2005**, *249*, 693–704; d) R. A. Kelly III, H. Clavier, S. Giudice, N. M. Scott, E. D. Stevens, J. Bordner, I. Samardjiev, C. D. Hoff, L. Cavallo, S. P. Nolan, *Organometallics* **2008**, *27*, 202–210.
- [26] I. A. Portnyagin, M. S. Nechaev, *J. Organomet. Chem.* **2009**, *694*, 3149–3153.
- [27] P. P. Samuel, A. P. Singh, S. P. Sarish, J. Matussek, I. Objartel, H. W. Roesky, D. Stalke, *Inorg. Chem.* **2013**, *52*, 1544–1554.
- [28] CrysAlisPro RED, version 1.171.34.36, Oxford Diffraction Ltd., Oxford, UK, **2010**.
- [29] A. Altomare, M. C. Burla, M. Camalli, G. Cascarano, C. Giacovazzo, A. Guagliardi, A. G. C. Moliterni, G. Polidori, R. Spagna, *J. Appl. Crystallogr.* **1999**, *32*, 115–119.
- [30] SHELXL: G. M. Sheldrick, *Acta Crystallogr.* **2008**, *A64*, 112–122.
- [31] WINGX, version 1.80.05 (2009): L. J. Farrugia, *J. Appl. Crystallogr.* **1999**, *32*, 837–838.
- [32] A. D. Becke, *J. Chem. Phys.* **1993**, *98*, 5648–5652.
- [33] C. Lee, W. Yang, R. G. Parr, *Phys. Rev. B* **1988**, *37*, 785–789.
- [34] P. J. Hay, W. R. Wadt, *J. Chem. Phys.* **1985**, *82*, 299–310.

- [35] P. C. Hariharan, J. A. Pople, *Theor. Chim. Acta* **1973**, *28*, 213–222.
- [36] V. Barone, M. Cossi, *J. Phys. Chem. A* **1998**, *102*, 1995–2001.
- [37] a) D. Balcells, G. Ujaque, I. Fernández, N. Khiar, F. Maseras, *J. Org. Chem.* **2006**, *71*, 6388–6396; b) A. A. C. Braga, G. Ujaque, F. Maseras, *Organometallics* **2006**, *25*, 3647–3658.
- [38] Gaussian 09, Revision B.01, M. J. Frisch, G. W. Trucks, H. B. Schlegel, G. E. Scuseria, M. A. Robb, J. R. Cheeseman, G. Scalmani, V. Barone, B. Men-
nucci, G. A. Petersson, H. Nakatsuji, M. Caricato, X. Li, H. P. Hratchian,
A. F. Izmaylov, J. Bloino, G. Zheng, J. L. Sonnenberg, M. Hada, M. Ehara,
K. Toyota, R. Fukuda, J. Hasegawa, M. Ishida, T. Nakajima, Y. Honda, O.
Kitao, H. Nakai, T. Vreven, J. A. Montgomery, Jr., J. E. Peralta, F. Ogliaro,
M. Bearpark, J. J. Heyd, E. Brothers, K. N. Kudin, V. N. Staroverov, T. Keith,
R. Kobayashi, J. Normand, K. Raghavachari, A. Rendell, J. C. Burant, S. S.
Iyengar, J. Tomasi, M. Cossi, N. Rega, J. M. Millam, M. Klene, J. E. Knox,
J. B. Cross, V. Bakken, C. Adamo, J. Jaramillo, R. Gomperts, R. E. Strat-
mann, O. Yazyev, A. J. Austin, R. Cammi, C. Pomelli, J. W. Ochterski, R. L.
Martin, K. Morokuma, V. G. Zakrzewski, G. A. Voth, P. Salvador, J. J. Dan-
nenberg, S. Dapprich, A. D. Daniels, O. Farkas, J. B. Foresman, J. V. Ortiz,
J. Cioslowski, D. J. Fox; Gaussian, Inc., Wallingford, Connecticut, **2010**.

Received: February 21, 2014

Published online on June 11, 2014

CHEMISTRY

A **European** Journal

Supporting Information

© Copyright Wiley-VCH Verlag GmbH & Co. KGaA, 69451 Weinheim, 2014

Ring Opening and Bidentate Coordination of Amidinate Germylenes and Silylenes on Carbonyl Dicobalt Complexes: The Importance of a Slight Difference in Ligand Volume

Javier A. Cabeza,^{*[a]} Pablo García-Álvarez,^{*[a]} Enrique Pérez-Carreño,^[b] and Diego Polo^[a]

chem_201402295_sm_miscellaneous_information.pdf

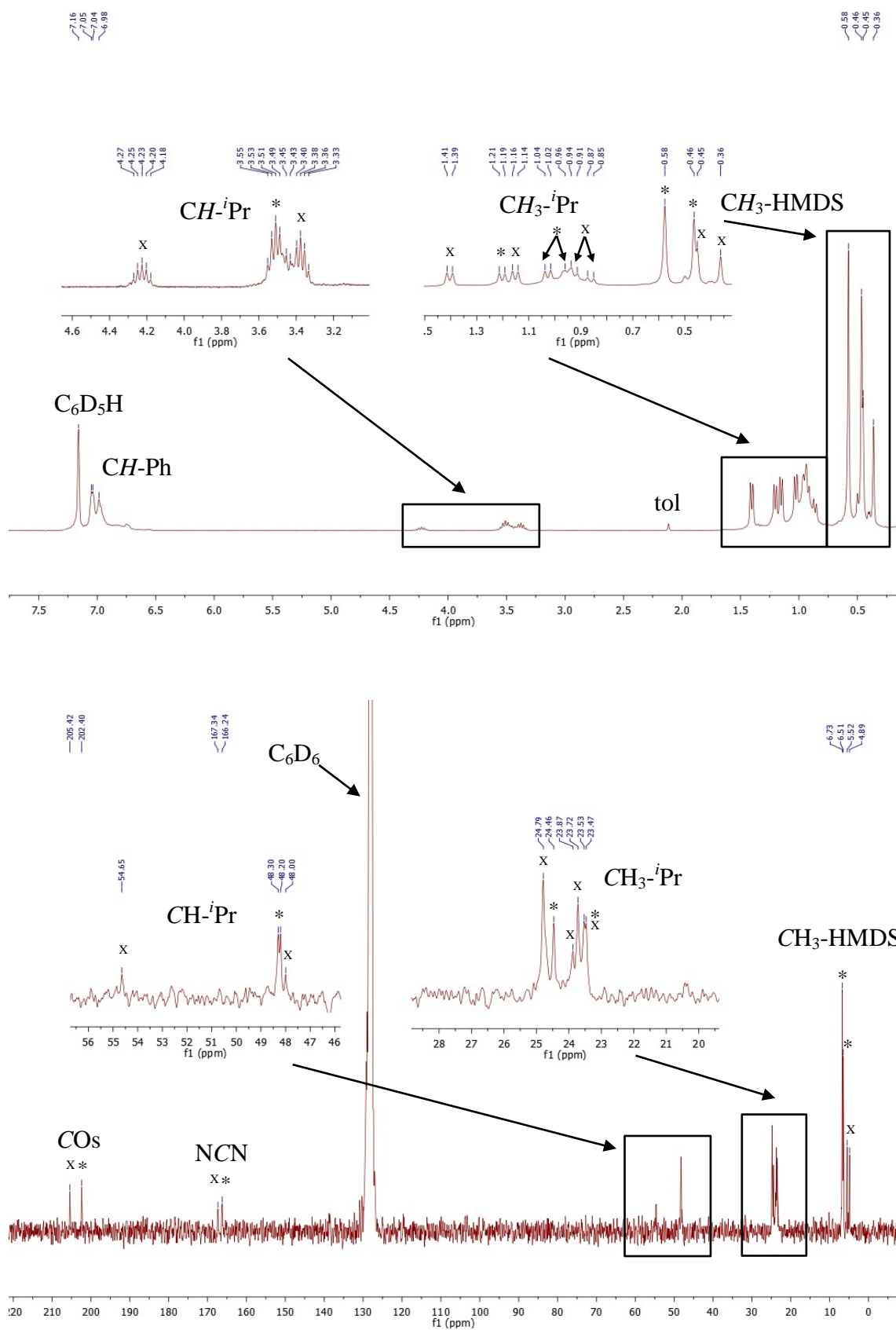


Figure S1 1H (top) and $^{13}C\{^1H\}$ (bottom) NMR spectra of a mixture of 4 (*) and 7 (x) in C_6D_6 (20 °C).

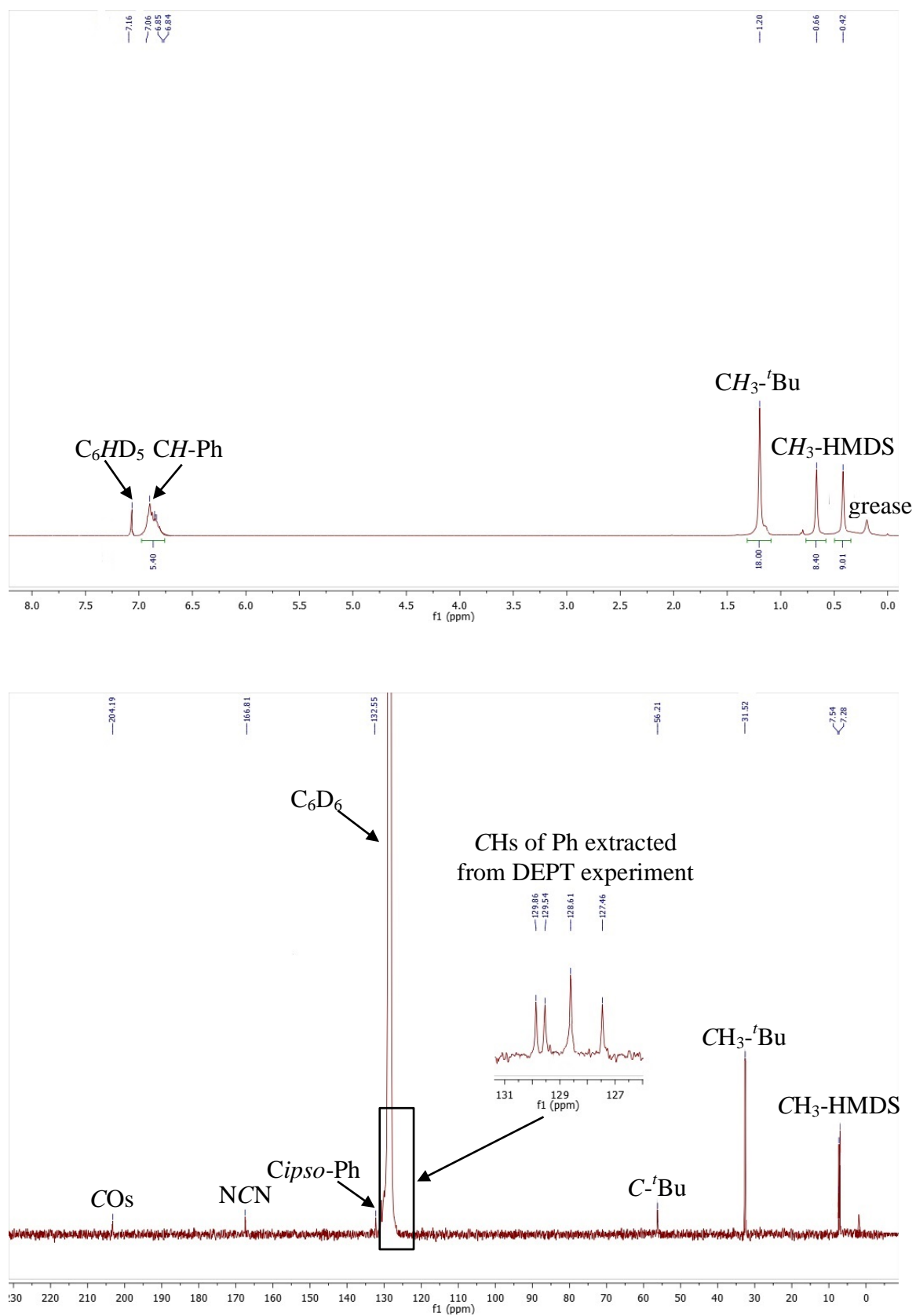


Figure S2 1H (top) and $^{13}C\{^1H\}$ (bottom) NMR spectra of **5** in C_6D_6 (20 °C).

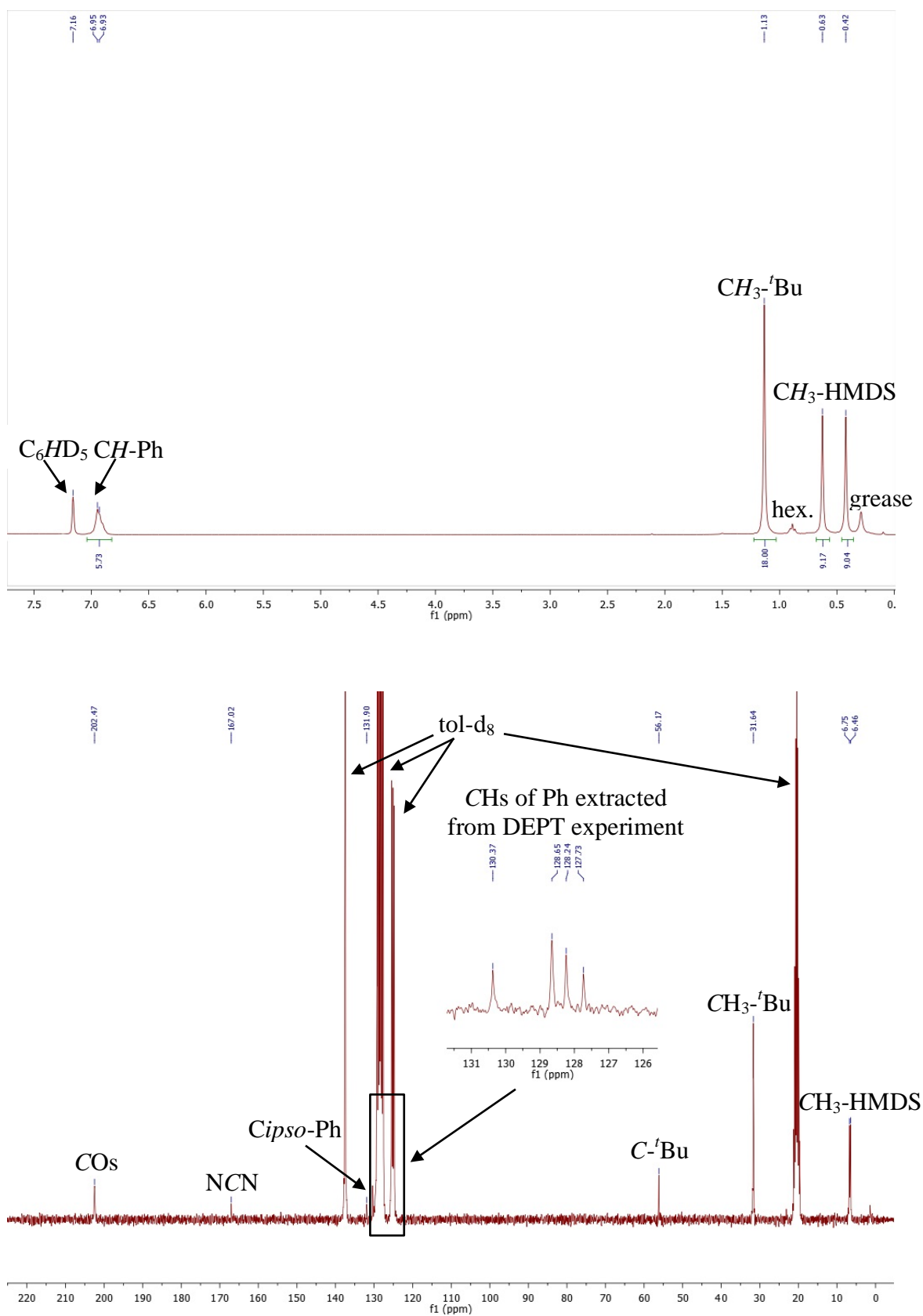


Figure S3 ^1H (top, C_6D_6) and $^{13}\text{C}\{^1\text{H}\}$ (bottom, tol-d_8) NMR spectra of **6** (20 °C).

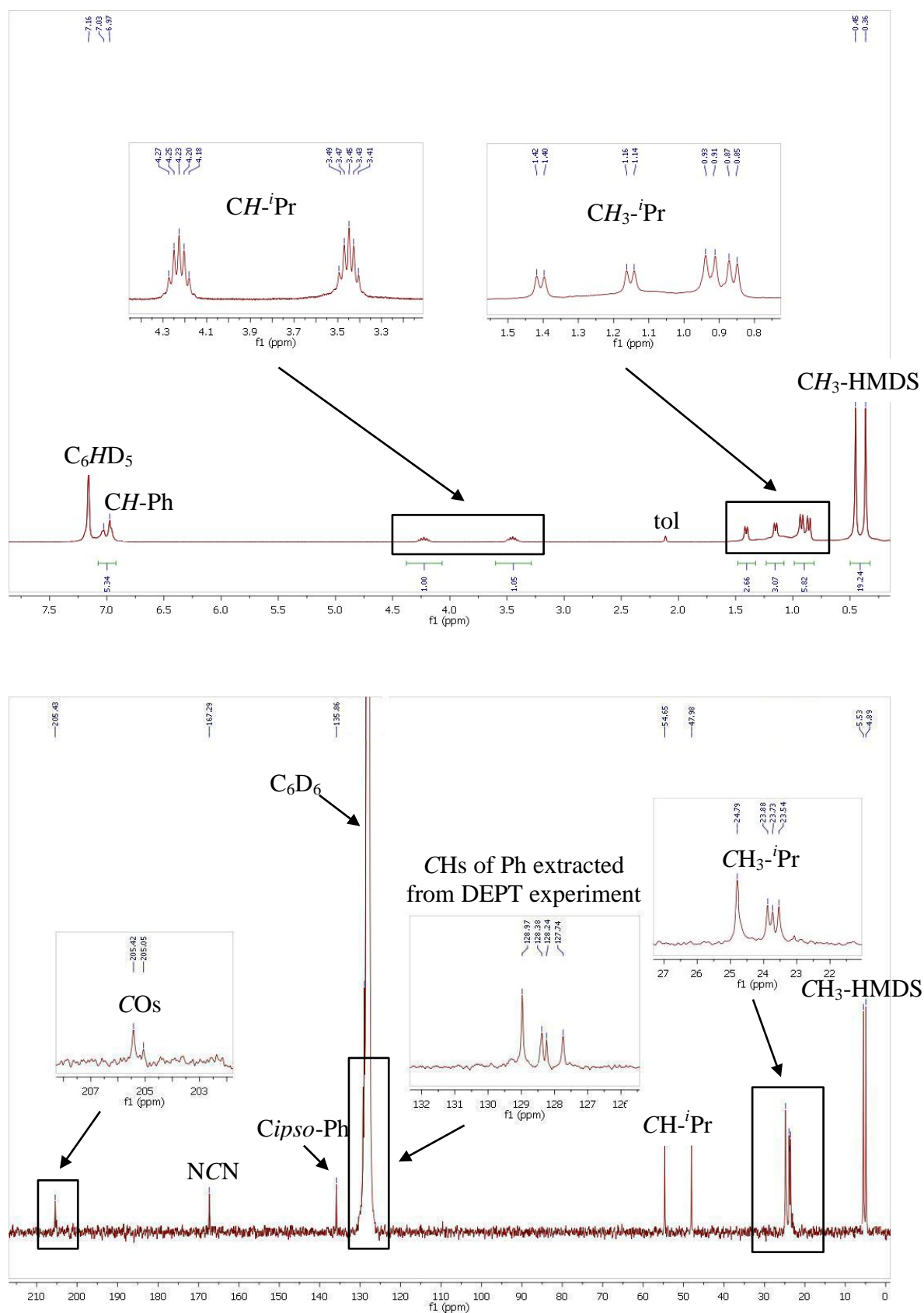


Figure S4 ^1H (top) and $^{13}\text{C}\{^1\text{H}\}$ (bottom) NMR spectra of **7** in C_6D_6 ($20\text{ }^\circ\text{C}$).

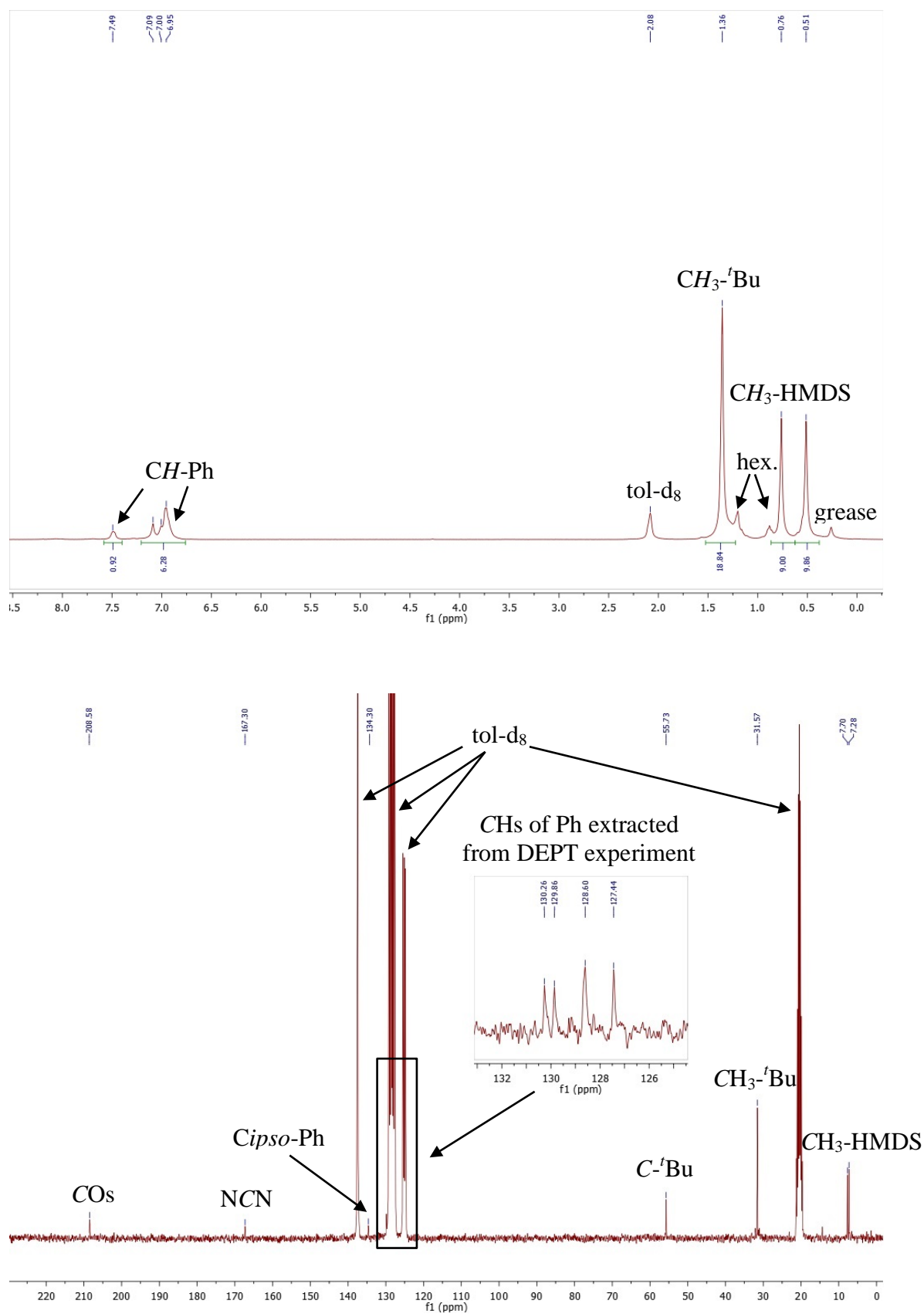


Figure S5 ^1H (top) and $^{13}\text{C}\{^1\text{H}\}$ (bottom) NMR spectra of **9** in $\text{tol-}d_8$ (20 °C).

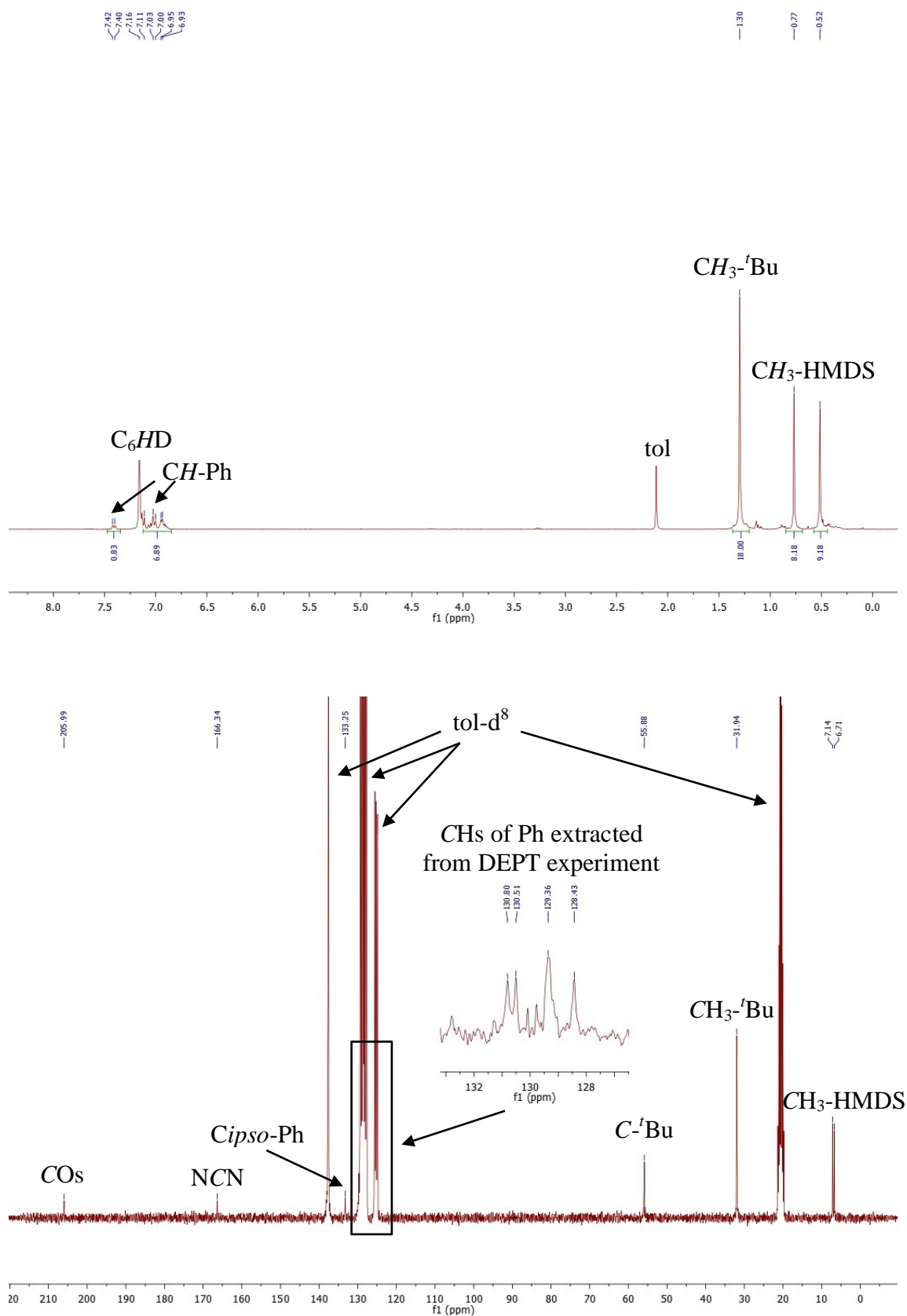


Figure S6 ^1H (top, C_6D_6) and $^{13}\text{C}\{^1\text{H}\}$ (bottom, $\text{tol-}d_8$) NMR spectra of **10** (20 °C).

Artículo VII

***“Steric Effects in the Reactions of Amidinate
Germynes with Ruthenium Carbonyl: Isolation of a
Coordinatively Unsaturated Diruthenium(0)
Derivative”***

COMMUNICATION

Cite this: *RSC Adv.*, 2014, 4, 31503Received 6th May 2014
Accepted 8th July 2014

DOI: 10.1039/c4ra05972g

www.rsc.org/advances

Steric effects in the reactions of amidinate germynes with ruthenium carbonyl: isolation of a coordinatively unsaturated diruthenium(0) derivative†

Javier A. Cabeza,* José M. Fernández-Colinas, Pablo García-Álvarez* and Diego Polo

Coordinatively unsaturated germylene-bridged diruthenium(0) complexes can be prepared by treating $[\text{Ru}_3(\text{CO})_{12}]$ with amidinate germynes of the type $\text{Ge}(\text{R}^1\text{bzamR}^2)(\text{HMDS})$ [$\text{R}^1\text{bzamR}^2 = 1\text{-R}^1\text{-3-R}^2\text{-benzamidinate}$, $\text{HMDS} = \text{N}(\text{SiMe}_3)_2$], but only when the amidinate contains just one very bulky R group (^tBu) (not two).

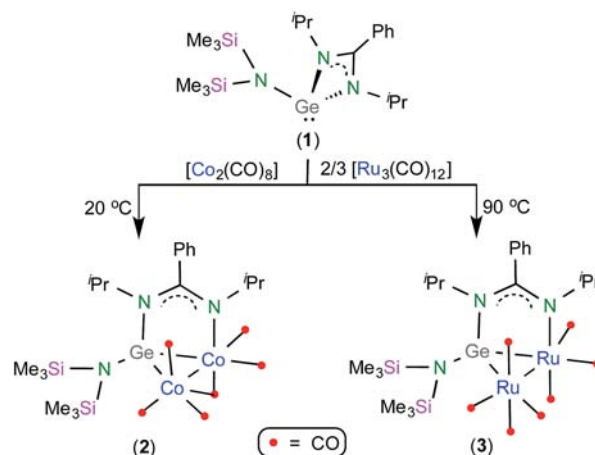
Although heavier carbene analogues,¹ also known as heavier tetrylenes or group-14 metalylenes or metalenes, are very reactive molecules,² the current extent of their coordination chemistry is still far from that of their carbene relatives.³ Nevertheless and interestingly, some heavier tetrylene-transition-metal complexes have already been successfully tested as catalyst precursors for useful reactions,⁴ such as Sonogashira cross-couplings,⁵ ketone hydrosilylations,⁶ [2 + 2 + 2] cycloadditions,⁷ arene C-H borylations,⁸ and couplings of aryl halides with organometallic zinc and Grignard reagents.⁹

As part of our work on heavier tetrylene-transition-metal chemistry,¹⁰ we have recently reported that the amidinate germylene $\text{Ge}(\text{Pr}_2\text{bzam})(\text{HMDS})$ (**1**; $\text{Pr}_2\text{bzam} = 1,3\text{-bis}(\text{iso-propyl})\text{-benzamidinate}$), which is equipped with just one accessible lone pair of electrons on the Ge atom and contains a very bulky hexamethyldisilazane group (HMDS), can be transformed into a bridging 4-electron-donor $\kappa^2\text{Ge},\text{N}$ -ligand when treated with $[\text{Co}_2(\text{CO})_8]$ and $[\text{Ru}_3(\text{CO})_{12}]$ (Scheme 1).¹¹ Until that work, such a bidentate coordination mode was unknown for amidinate tetrylene ligands. A subsequent in-depth study of the $[\text{Co}_2(\text{CO})_8]$ system¹² has provided additional insights into (a) the influence that the volume of the amidinate N-R groups has on the monodentate to bidentate transformation of $\text{Ge}(\text{R}_2\text{bzam})(\text{HMDS})$ in dicobalt complexes, (b) the mechanism of that transformation and (c) the effect that the group-14 atom has on the final

outcome of the reactions of amidinate tetrylenes of the type $\text{M}(\text{R}_2\text{bzam})(\text{HMDS})$ ($\text{M} = \text{Si}, \text{Ge}$) with $[\text{Co}_2(\text{CO})_8]$.

The above precedents led us to investigate whether the reactions of $[\text{Ru}_3(\text{CO})_{12}]$ with amidinate germynes of the type $\text{Ge}(\text{R}_2\text{bzam})(\text{HMDS})$ are affected by the volume of the amidinate N-R groups. We now report that this study has led to the isolation of a germylene-bridged diruthenium(0) complex that is coordinatively unsaturated, demonstrating that the synthesis of such interesting unsaturated complexes can only be achieved when the germylene contains just one very bulky R group (^tBu) in the amidinate fragment.

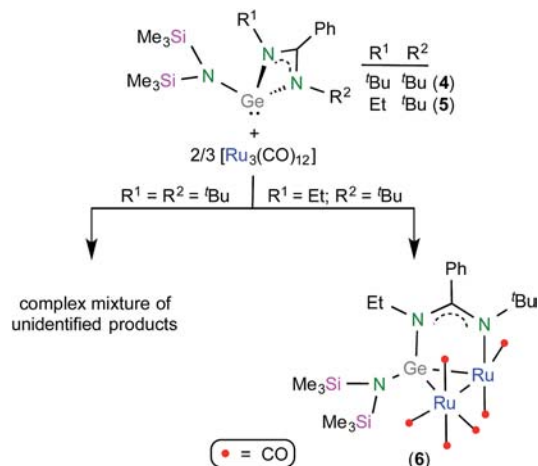
The germylene-bridged diruthenium(0) complex $[\text{Ru}_2\{\mu\text{-}\kappa^2\text{Ge},\text{N}\text{-Ge}(\text{Pr}_2\text{bzam})(\text{HMDS})\}(\text{CO})_7]$ (**3**) has been easily prepared in good yield by treating the bis(*iso*-propyl) germylene $\text{Ge}(\text{Pr}_2\text{bzam})(\text{HMDS})$ (**1**) with $[\text{Ru}_3(\text{CO})_{12}]$ in toluene at 90 °C (Scheme 1).¹¹ However, an analogous reaction using the known¹³ and bulkier bis(*tert*-butyl) germylene $\text{Ge}(\text{tBu}_2\text{bzam})(\text{HMDS})$ (**4**; Scheme 2) only led to intractable decomposition products (no reaction was observed at room temperature). This intriguing



Scheme 1 Reported reactions of germylene **1** with $[\text{Co}_2(\text{CO})_8]$ and $[\text{Ru}_3(\text{CO})_{12}]$.

Departamento de Química Orgánica e Inorgánica-IUQOEM, Universidad de Oviedo-CSIC, 33071-Oviedo, Spain. E-mail: jac@uniovi.es; pga@uniovi.es

† Electronic supplementary information (ESI) available: Complete experimental, spectral and characterization data. CCDC 999866 and 1001195. For ESI and crystallographic data in CIF or other electronic format see DOI: 10.1039/c4ra05972g



Scheme 2 Reactions of germynes 4 and 5 with $[Ru_3(CO)_{12}]$ (toluene, 90 °C).

result prompted us to try a new gernylene, $Ge(Etbzam^tBu)$ - (HMDS) (5), which has only one *tert*-butyl group on the amidinate fragment (it was prepared in two steps from 1-*tert*-butyl-3-ethylcarbodiimide, LiPh and Li(HMDS); see ESI†). This reaction led to the coordinatively unsaturated ruthenium(0) derivative $[Ru_2\{\mu-\kappa^2 Ge, N-Ge(Etbzam^tBu)(HMDS)\}(CO)_6]$ (6), which was isolated in 64% yield (Scheme 2).

An X-ray diffraction (XRD) study (Fig. 1) showed that complex 6 is binuclear and contains a bridging gernylene in a similar $\kappa^2 Ge, N$ -coordination mode as that found previously in the bis(*iso*-propyl) complex 3 (Scheme 1).¹¹ The interesting feature of complex 6 is that, in contrast with complex 3, the Ru atom that is attached to the amidinate N atom is coordinatively unsaturated, its vacant coordination site being partially protected by an interaction with a hydrogen atom of the closest *tert*-butyl group ($Ru\cdots H$ distances in the two independent molecules 2.21(4) Å and 2.27(4) Å). This unsaturation can also be

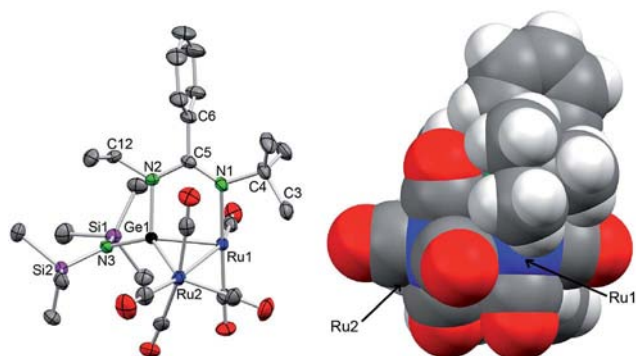


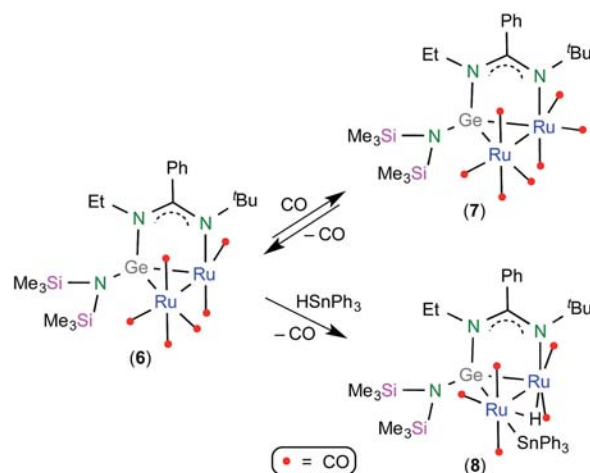
Fig. 1 ORTEP (40% thermal ellipsoids) and space-filling views of one of the two independent but very similar molecules found in the crystals of compound 6. H atoms have been omitted. Selected bond distances (Å): Ru1–Ru2 2.9450(2), Ru1–N1 2.118(2), Ru1–Ge1 2.3778(3), Ru2–Ge1 2.4940(3), Ge1–N2 1.928(2), Ge1–N3 1.853(2), N1–C4 1.501(3), N1–C5 1.313(3), N2–C5 1.355(3), N2–C12 1.472(3), N3–Si1 1.763(2), N3–Si2 1.749(2), C3–C4 1.527(4), C5–C6 1.497(3).

claimed as responsible for the fact that the crystals are constituted by “dimers” formed by two independent but very similar molecules. In each “dimer”, the unsaturated Ru atom of one molecule is close to a carbonyl O atom of the other molecule ($Ru\cdots O$ distances 4.253(2) Å and 3.599(2) Å). The ESI file contains a figure (Fig. SI-15†) that shows these $Ru\cdots H$ and $Ru\cdots O$ interactions.

The room temperature 1H and ^{13}C NMR spectra of 6 (ESI file†) indicate that, in solution, the *tert*-butyl group that interacts with the Ru atom rotates freely about the N–C bond (its methyl groups are observed as a singlet in both spectra). In contrast, these spectra also indicate that the rotations about the Ge1–N3, N2–C12 and C5–C6 axes are sterically impeded (two $SiMe_3$ groups, two methylene H atoms and six phenyl C atoms are observed in the corresponding spectra), confirming that the *N*-ethyl group is very close to the phenyl and HMDS groups. These data provide an explanation to why a bis(*tert*-butyl) analogue of complex 6 cannot be prepared and why, given the asymmetry of gernylene 5, its reaction with $[Ru_3(CO)_{12}]$ gives only the regioisomer that has the Ge atom attached to the N–Et group and not to the N-*t*Bu group (*i.e.*, complex 6): it seems that there is not enough room between the phenyl and HMDS groups to accommodate a very bulky *tert*-butyl group. However, the existence of complex 3 (Scheme 1) indicates that this small space should be able to accommodate an *iso*-propyl group.

The isolation of complex 6 is remarkable because coordinatively unsaturated diruthenium(0) complexes are extremely rare. In fact, as far as we are aware, only two compounds of this type have been hitherto reported, namely $[Ru_2\{\mu-\kappa^2 P, P'-(RO)_2-PN(Et)P(OR)_2\}_2(\mu-CO)_2(CO)_2]$ ($R = Me, iPr$).¹⁴

The unique features of complex 6 led us to investigate its derivative chemistry. Two preliminary results of this study are depicted in Scheme 3 (CO was chosen as a representative 2-electron-donor ligand and a triorganotin hydride as a reagent that easily adds to low-valent transition metal carbonyl complexes¹⁵).



Scheme 3 Reactions of complex 6 with CO and $HSnPh_3$ (toluene, 20 °C).

Complex **6** reacted easily with CO (the gas was bubbled for 15 min through a toluene solution of **6** at room temperature) to give the heptacarbonyl derivative, $[\text{Ru}_2\{\mu\text{-}\kappa^2\text{Ge}, N\text{-Ge}(\text{Etbzam}^t\text{Bu})\text{-}(\text{HMDS})\}_2(\text{CO})_7]$ (**7**), whose IR ν_{CO} absorption pattern is nearly identical to that of **3**.¹¹ However, complex **7** could not be isolated in pure form because its solutions were only stable under a CO atmosphere, reverting to complex **6** when they were left to stand under argon or when the solvent was removed under vacuum. These data clearly confirm that the steric hindrance applied by the *tert*-butyl group of **7** over the new CO ligand is so strong that the system prefers to release that CO despite this process leads to a coordinatively unsaturated product (**6**).

The reaction of complex **6** with HSnPh_3 also proceeded smoothly in toluene at room temperature, leading to the hydrido-stannyl derivative $[\text{Ru}_2\{\mu\text{-}\kappa^2\text{Ge}, N\text{-Ge}(\text{Etbzam}^t\text{Bu})\text{-}(\text{HMDS})\}_2(\mu\text{-H})(\text{SnPh}_3)(\text{CO})_5]$ (**8**) in quantitative yield (Scheme 3). An XRD study on the solvate $\mathbf{8} \cdot \text{C}_7\text{H}_8$ (Fig. 2) revealed that the complex maintains the vacant site of its predecessor, also having a *tert*-butyl H atom very close to Ru1 (2.26(4) Å). The original HSnPh_3 reagent has oxidatively substituted an equatorial CO ligand of Ru2 in such a way that the resulting hydride ligand spans the Ru1–Ru2 edge, being almost in the same plane as the Ge–Ru1–Ru2 triangle, while the stannyl ligand occupies an equatorial position on Ru2, being *cis* to the hydride and *trans* to the Ge atom. In the crystals of $\mathbf{8} \cdot \text{C}_7\text{H}_8$, the toluene solvent is packed in close proximity to the Ru1 atom (Ru–ring centroid distance 4.41(5) Å; see Fig. SI-16 of the ESI file.)[†] The ^1H NMR spectrum of **8** showed the hydride at –10.50 ppm, the remaining features of the ^1H and ^{13}C NMR spectra being as those commented above for complex **6**.

In conclusion, this work describes the synthesis of a rare coordinatively unsaturated diruthenium(0) complex (**6**) by treatment of $[\text{Ru}_3(\text{CO})_{12}]$ with the asymmetric amidinate germylene **5**. The reaction proceeds through an unusual ring-

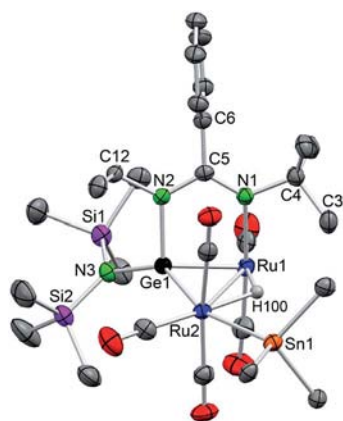


Fig. 2 ORTEP (40% thermal ellipsoids) view of compound **8**. H atoms (except the hydride ligand) have been omitted. For clarity, only the C_{ipso} atoms of the SnPh_3 phenyl rings are shown. Selected bond lengths (Å): Ru1–Ru2 3.0453(3), Ru1–N1 2.131(2), Ru1–Ge1 2.3713(4), Ru2–Ge1 2.4949(4), Ru1–H100 1.79(4), Ru2–H100 1.85(3), Ru2–Sn1 2.6906(3), Ge1–N2 1.926(2), Ge1–N3 1.852(2), N1–C4 1.497(4), N1–C5 1.318(4), N2–C5 1.348(4), N2–C12 1.478(3), N3–Si1 1.760(2), N3–Si2 1.752(3), C3–C4 1.532(5), C5–C6 1.497(4).

opening of the germylene that enables it to act as a bridging $\kappa^2\text{Ge}, N$ -ligand. This work also sheds light on the key role that the volume of the amidinate R groups play in the reactions of amidinate germylenes of the type $\text{Ge}(\text{R}^1\text{bzamR}^2)(\text{HMDS})$ with $[\text{Ru}_3(\text{CO})_{12}]$. The lability of the heptacarbonyl derivative **7** and the persistence of the vacant coordination site in the hydrido-stannyl derivative **8** are also remarkable. Further work on the reactivity and catalytic ability of complex **6** is underway.

Acknowledgements

This work has been supported by Spanish MINECO-FEDER grants (CTQ2010-14933, DELACIERVA-09-05 and RYC-2012-10491) and an EU Marie Curie reintegration grant (FP7-2010-RG-268329).

Notes and references

- V. Y. Lee and A. Sekiguchi, *Organometallic compounds of low coordinate Si, Ge, Sn and Pb: From phantom species to stable compounds*, Wiley, Chichester, UK, 2010.
- For recent reviews on the general chemistry of heavier tetrylenes, see: (a) S. K. Mandal and H. W. Roesky, *Acc. Chem. Res.*, 2012, **45**, 298; (b) M. Asay, C. Jones and M. Driess, *Chem. Rev.*, 2011, **111**, 354; (c) S. Yao, Y. Xiong and M. Driess, *Organometallics*, 2011, **30**, 1748; (d) M. Kira, *Chem. Commun.*, 2010, **46**, 2893; (e) Y. Mizuhata, T. Sasamori and N. Tokitoh, *Chem. Rev.*, 2009, **109**, 3479; (f) S. Nagendran and H. W. Roesky, *Organometallics*, 2008, **27**, 457.
- For relevant reviews on the coordination chemistry of heavier tetrylenes, see: (a) B. Blom, M. Stoelzel and M. Driess, *Chem.–Eur. J.*, 2013, **19**, 40; (b) A. V. Zabula and F. E. Hahn, *Eur. J. Inorg. Chem.*, 2008, 5165; (c) W.-P. Leung, K.-W. Kan and K.-H. Chong, *Coord. Chem. Rev.*, 2007, **251**, 2253; (d) R. Waterman, P. G. Hayes and T. D. Tilley, *Acc. Chem. Res.*, 2007, **40**, 712; (e) O. Kühl, *Coord. Chem. Rev.*, 2004, **248**, 411; (f) M. Okazaki, H. Tobita and H. Ogino, *Dalton Trans.*, 2003, 493; (g) B. Gehrhuis and M. F. Lappert, *J. Organomet. Chem.*, 2001, **617–618**, 209; (h) M. F. Lappert and R. S. Rowe, *Coord. Chem. Rev.*, 1990, **100**, 267; (i) W. Petz, *Chem. Rev.*, 1986, **86**, 1019.
- For a recent review on *N*-heterocyclic silylene complexes in catalysis, see: B. Blom, D. Gallego and M. Driess, *Inorg. Chem. Front.*, 2014, **1**, 134.
- D. Gallego, A. Brück, E. Irran, F. Meier, M. Kaupp, M. Driess and J. F. Hartwig, *J. Am. Chem. Soc.*, 2013, **135**, 15617.
- B. Blom, S. Enthaler, S. Inoue, E. Irran and M. Driess, *J. Am. Chem. Soc.*, 2013, **135**, 6703.
- W. Wang, S. Inoue, S. Enthaler and M. Driess, *Angew. Chem., Int. Ed.*, 2012, **51**, 6167.
- A. Brück, D. Gallego, W. Wang, E. Irran, M. Driess and J. F. Hartwig, *Angew. Chem., Int. Ed.*, 2012, **51**, 11478.
- N. C. Breit, T. Szilvási, T. Suzuki, D. Gallego and S. Inoue, *J. Am. Chem. Soc.*, 2013, **135**, 17958.
- (a) L. Álvarez-Rodríguez, J. A. Cabeza, P. García-Álvarez and D. Polo, *Organometallics*, 2013, **32**, 3557; (b) J. A. Cabeza, J. M. Fernández-Colinas, P. García-Álvarez and D. Polo, *Inorg.*

- Chem.*, 2012, **51**, 3896; (c) J. A. Cabeza, P. García-Álvarez and D. Polo, *Inorg. Chem.*, 2012, **51**, 2569; (d) J. A. Cabeza, P. García-Álvarez and D. Polo, *Inorg. Chem.*, 2011, **50**, 6195.
- 11 J. A. Cabeza, P. García-Álvarez and D. Polo, *Dalton Trans.*, 2013, 1329.
- 12 J. A. Cabeza, P. García-Álvarez, E. Pérez-Carreño and D. Polo, *Chem.–Eur. J.*, 2014, **20**, 8654.
- 13 P. P. Samuel, A. P. Singh, S. P. Sarish, J. Matussek, I. Objartel, H. W. Roesky and D. Stalke, *Inorg. Chem.*, 2013, **52**, 1544.
- 14 (a) J. S. Field, R. J. Haines, J. Sundermeyer and S. F. Woollam, *J. Chem. Soc., Chem. Commun.*, 1991, 1382; (b) J. S. Field, R. J. Haines, M. W. Stewart, J. Sundermeyer and S. F. Woollam, *J. Chem. Soc., Dalton Trans.*, 1991, 947.
- 15 (a) J. A. Cabeza, A. Llamazares, V. Riera, S. Triki and L. Ouahab, *Organometallics*, 1992, **11**, 3334; (b) J. A. Cabeza, S. García-Granda, A. Llamazares, V. Riera and J. F. van der Maelen, *Organometallics*, 1993, **12**, 157.

ELECTRONIC SUPPLEMENTARY INFORMATION

Influence of the volume of the NR groups of amidinate germylenes in their reactivity with ruthenium carbonyl: Isolation of a coordinatively unsaturated diruthenium(0) derivative

Javier A. Cabeza,* José M. Fernández-Colinas, Pablo García-Álvarez,* and Diego Polo

Departamento de Química Orgánica e Inorgánica-IUQOEM, Universidad de Oviedo-CSIC, E-33071 Oviedo, Spain

General procedures. All manipulations were performed under argon using standard glove-box and Schlenk-vacuum line techniques. Solvents were dried over sodium diphenyl ketyl and distilled under nitrogen before use. The reactions were routinely monitored by solution IR spectroscopy (carbonyl stretching region). The reagents PhLi (1.8 M solution in dibutyl ether), 1,3-bis(*tert*-butyl)carbodiimide, 1-*tert*-butyl-3-ethylcarbodiimide, Li(HMDS) (1.0 M solution in hexanes) and [Ru₃(CO)₁₂] were purchased from Sigma-Aldrich; GeCl₂·dioxane was purchased from Gelest. Ge(^tBu₂zam)(HMDS) (**4**)¹ was prepared following a previously reported procedure.¹ All reaction products were vacuum-dried for several hours prior to being weighted and analyzed. IR spectra were recorded in solution on a Perkin-Elmer Paragon 1000 FT spectrophotometer. NMR spectra were run in C₆D₆ on a Bruker DPX-300 instrument; the residual protic solvent resonance [δ (C₆HD₅) 7.16 ppm] was used as reference for ¹H, while the solvent resonance [δ (C₆D₆) 128.1 ppm] was used as reference for ¹³C. Microanalyses were obtained from the University of Oviedo Microanalytical Service. Positive FAB mass spectra were obtained from the University of A Coruña Mass Spectrometric Service (30 kV Cs⁺ gun, 3-nitrobenzyl alcohol as matrix); the given MS data refer to the most abundant molecular ion isotopomer.

Ge(Etbzam^tBu)Cl: LiPh (5.4 mL of a 1.8 M solution in dibutyl ether, 9.7 mmol) was added to a cold solution (−78 °C) of 1-*tert*-butyl-3-ethylcarbodiimide (1.5 mL, 9.7 mmol) in diethyl ether (100 mL). The solution was allowed to warm up to room temperature and was then stirred for 4 h. The resulting pale orange solution was cooled down again to −78° C and then transferred dropwise with a cannula to a stirred suspension of GeCl₂·dioxane (2.23 g, 9.7 mmol) in diethyl ether (20 mL) kept at −78° C. The reaction mixture was allowed to warm up to room temperature and was then stirred for 18 h. The solvents were removed under reduced pressure and the residue was extracted with hexane (2 x 30 mL). The filtrate was evaporated to dryness under vacuum to yield

Ge(Etbzam^tBu)Cl as a pale yellow oil (2.83 g, 94 %). Anal. Calcd. for C₁₃H₁₉ClGeN₂ (MW = 311.37 amu): C, 50.15; H, 6.15; N, 9.00. Found: C, 50.25; H, 6.28; N, 8.87. ¹H NMR (C₆D₆, 300.1 MHz, 293 K): δ = 7.08–6.87(m, 5 H; 5 CH of Ph), 2.76–2.68 (m, 2 H; CH₂ of Et), 1.04 (s, 9 H; Me₃ of ^tBu), 0.91 (t, *J* = 7.2 Hz, 3 H; Me of Et) ppm. ¹³C{¹H} NMR (C₆D₆, 75.5 MHz, 293 K): δ = 174.1 (NCN), 132.5 (C_{ipso} of Ph), 129.9 (2 CH of Ph), 128.6 (2 CH of Ph), 127.5 (CH of Ph), 53.7 (C of ^tBu), 39.6 (CH₂ of Et), 31.8 (Me₃ of ^tBu), 16.4 (Me of Et) ppm.

Ge(Etbzam^tBu)(HMDS) (5): Li(HMDS) (8.2 mL of a 1.0 M solution in hexanes, 8.2 mmol) was added to a cold (−78 °C) solution of Ge(Etbzam^tBu)Cl (2.56 g, 8.2 mmol) in diethyl ether (30 mL). The resulting suspension was allowed to warm up to room temperature and was then stirred for 12 h. The solvents were removed under reduced pressure and the residue was extracted into hexane (2 x 30 mL). The filtered extract was evaporated to dryness under vacuum to give **5** as a yellowish oily solid (3.24 g, 91 %). Anal. Calcd. for C₁₉H₃₇GeN₃Si₂ (MW = 436.30 amu): C, 52.30; H, 8.55; N, 9.63. Found: C, 52.52; H, 8.70; N, 9.59. ¹H NMR (C₆D₆, 300.1 MHz, 293 K): δ = 7.12–6.84(m, 5 H; 5 CH of Ph), 3.05–2.81 (m, 2 H; CH₂ of Et), 1.15 (s, 9 H; Me₃ of ^tBu), 1.05 ppm (t, *J* = 7.2 Hz, 3 H; Me of Et), 0.49 (s, 18 H; Me₆ of HMDS) ppm. ¹³C{¹H} NMR (C₆D₆, 75.5 MHz, 293 K): δ = 165.3 (NCN), 134.2 (C_{ipso} of Ph), 129.1 (2 CH of Ph), 128.5 (CH of Ph), 128.4 (CH of Ph), 127.4 (CH of Ph), 53.7 (C of ^tBu), 40.3 (CH₂ of Et), 32.4 (Me₃ of ^tBu), 17.3 (Me of Et), 5.8 (Me₆ of HMDS) ppm.

Reaction of Ge(^tBu₂zcam)(HMDS) (4) with [Ru₃(CO)₁₂]: Germylene **4** (0.25 mL of a 0.32 M solution in toluene, 0.080 mmol) was added to a suspension of [Ru₃(CO)₁₂] (50 mg, 0.080 mmol) in toluene (10 mL) and the mixture was stirred at room temperature for 60 min. As no reaction occurred (IR analysis), the temperature was progressively raised to 90 °C. After 60 min, a complex mixture was formed (¹H NMR analysis) that could not be separated. The use of different Ru₃/Ge ratios led in all cases to complex mixtures of products that could not be identified.

[Ru₂{μ-κ²Ge,N-Ge(Etbzam^tBu)(HMDS)}(CO)₆] (6): Germylene **5** (3.2 mL of a 0.38 M solution in toluene, 1.20 mmol) was added to a suspension of [Ru₃(CO)₁₂] (0.5 g, 0.8 mmol) in toluene (20 mL) and the mixture was heated at 90 °C for 2 h. The initial orange color changed to dark red. Purification by flash chromatography (2 x 5 cm silica gel column packed in hexane) with hexane as eluant furnished compound **6** as a dark orange solid (620 mg, 64 %). Leaving to stand a concentrated solution of **6** in hexane at −20 °C afforded suitable crystals for X-ray crystallographic analysis. Anal. Calcd. for C₂₅H₃₇GeN₃O₆Ru₂Si₂ (MW = 806.50 amu): C, 37.23; H, 4.62; N, 5.21. Found: C, 37.53; H, 4.50; N, 4.89. (+)-FAB MS: *m/z* = 751 [*M* − 2CO]⁺. IR (toluene): ν_{CO} = 2073 (m), 2000 (vs), 1985 (s), 1977 (m), 1992 (m), 1924 (m) cm^{−1}. ¹H NMR (C₆D₆, 300.1 MHz, 293 K):

$\delta = 7.14\text{--}6.78$ (m, 5 H; 5 CH of Ph), 3.39 (m, 1 H; CH of Et), 2.42 (m, 1 H; CH of Et), 0.86 (s, 9 H; Me_3 of t Bu), 0.84 (t, $J = 7.2$ Hz, 3 H; Me of Et), 0.45 (s, 9 H; Me_3 of HMDS) 0.43 (s, 9 H; Me_3 of HMDS) ppm. $^{13}\text{C}\{^1\text{H}\}$ NMR (C_6D_6 , 75.5 MHz, 293 K): $\delta = 203.6$ (COs), 203.0 (CO), 197.7 (CO), 164.4 (NCN), 135.8 (C_{ipso} of Ph), 128.9 (2 CH of Ph), 128.7 (CH of Ph), 128.1 (CH of Ph), 127.5 (CH of Ph), 63.6 (C of t Bu), 40.0 (CH_2 of Et), 27.1 (Me_3 of t Bu), 17.9 (Me of Et), 6.4 (Me_3 of HMDS), 4.8 (Me_3 of HMDS) ppm.

$\text{Ru}_2\{\mu\text{-}\kappa^2\text{Ge}, N\text{-Ge}(\text{Etbzam}'\text{Bu})(\text{HMDS})\}(\text{CO})_7$ (7): Carbon monoxide was gently bubbled for 15 min through a solution of complex **6** (56 mg, 0.069 mmol) in toluene (8 mL) at room temperature. The initial dark red-orange color changed to red. An IR spectrum of this solution confirmed the quantitative formation of complex **7**. This product was only characterized in solution because it loses CO rapidly, regenerating complex **6** upon removal of the CO atmosphere. IR (toluene): $\nu_{\text{CO}} = 2085$ (m), 2033 (s), 2014 (m), 2004 (s), 1994 (m), 1977 (w), 1956 (w) cm^{-1} . ^1H NMR (C_6D_6 , 300.1 MHz, 293 K, CO atmosphere): $\delta = 7.13\text{--}6.84$ (m, 5 H; 5 CH of Ph), 3.47 (m, 1 H, CH of Et), 2.43 (m, 1 H, CH of Et), 1.11 (s, 9 H, Me_3 of t Bu), 0.81 (t, $J = 7.1$ Hz, 3 H; Me of Et), 0.47 (s, 9 H; Me_3 of HMDS) 0.42 (s, 9 H, Me_3 of HMDS) ppm.

$[\text{Ru}_2\{\mu\text{-}\kappa^2\text{Ge}, N\text{-Ge}(\text{Etbzam}'\text{Bu})(\text{HMDS})\}(\mu\text{-H})(\text{SnPh}_3)(\text{CO})_5]$ (8): Solid HSnPh_3 (33 mg, 0.094 mmol) was added to a solution of complex **6** (30 mg, 0.037 mmol) in toluene (10 mL) and the resulting solution was stirred at room temperature for 1 h. The initial orange color changed to dark orange. The solvent was removed under reduced pressure and the crude reaction mixture was separated by column chromatography on silica-gel (2 x 5 cm). Compound **8** was eluted with hexane/ CH_2Cl_2 (1:1) and was isolated as an orange solid (38 mg, 91 %). Anal. Calcd. for $\text{C}_{42}\text{H}_{53}\text{GeN}_3\text{O}_5\text{Ru}_2\text{Si}_2\text{Sn}$ (MW = 1129.52 amu): C, 44.66; H, 4.73; N, 3.72; found: C, 4.69; H, 4.84; N, 3.66. (+)-FAB MS: $m/z = 1129$ [M] $^+$. IR (toluene): $\nu_{\text{CO}} = 2071$ (w), 2013 (vs), 1995 (m), 1944 (m) cm^{-1} . ^1H NMR (C_6D_6 , 300.1 MHz, 293 K): $\delta = 8.05\text{--}7.92$ (m sat, 6 H; CH_{ortho} of Ph), 7.30 (t, $J = 7.1$ Hz, 6 H; CH_{meta} of Ph), 7.11–6.90 (m, 8 H; CH of Ph), 3.46 (m, 1 H; CH of Et), 2.40 (m, 1 H, CH of Et), 0.97 (t, $J = 7.0$ Hz, 3 H; Me of Et), 0.68 (s, 9 H; Me_3 of t Bu), 0.47 (s, 9 H; Me_3 of HMDS) 0.40 (s, 9 H; Me_3 of HMDS), -10.50 (s sat, 1 H; $\text{RuH}\text{--}\text{Ru}$) ppm. $^{13}\text{C}\{^1\text{H}\}$ NMR (C_6D_6 , 75.5 MHz, 293 K): $\delta = 202.7$ (CO), 200.5 (CO), 198.2 (CO), 197.3 (CO), 195.7 (CO), 164.7 (NCN), 144.7 (C_{ipso} of Ph), 137.9–125.7 (Ph groups of germylene and SnPh_3 ligands), 63.6 (C of t Bu), 41.1 (CH_2 of Et), 27.9 (Me_3 of t Bu), 17.7 (Me of Et), 6.0 (Me_3 of HMDS), 5.4 (Me_3 of HMDS) ppm.

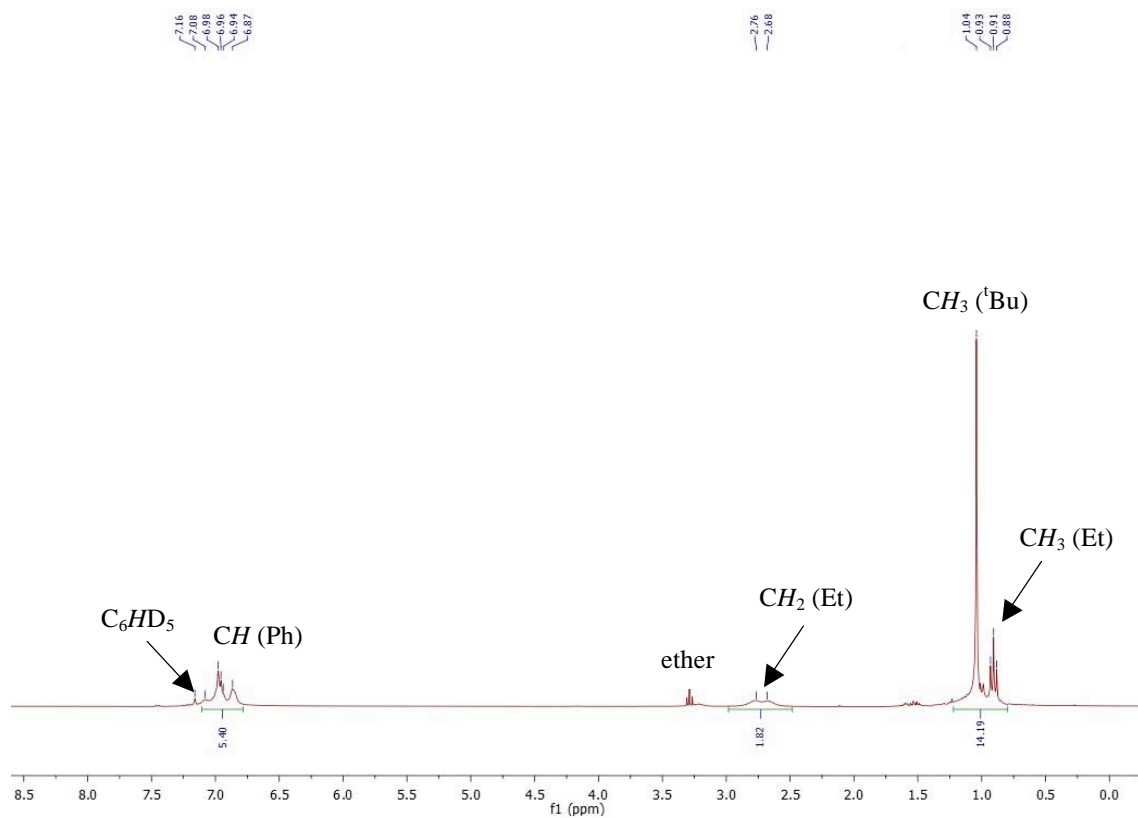


Fig SI-1 ^1H NMR spectrum of $\text{Ge}(\text{Etbzam}'\text{Bu})\text{Cl}$ (C_6D_6 , 25 $^\circ\text{C}$, 300.1 MHz).

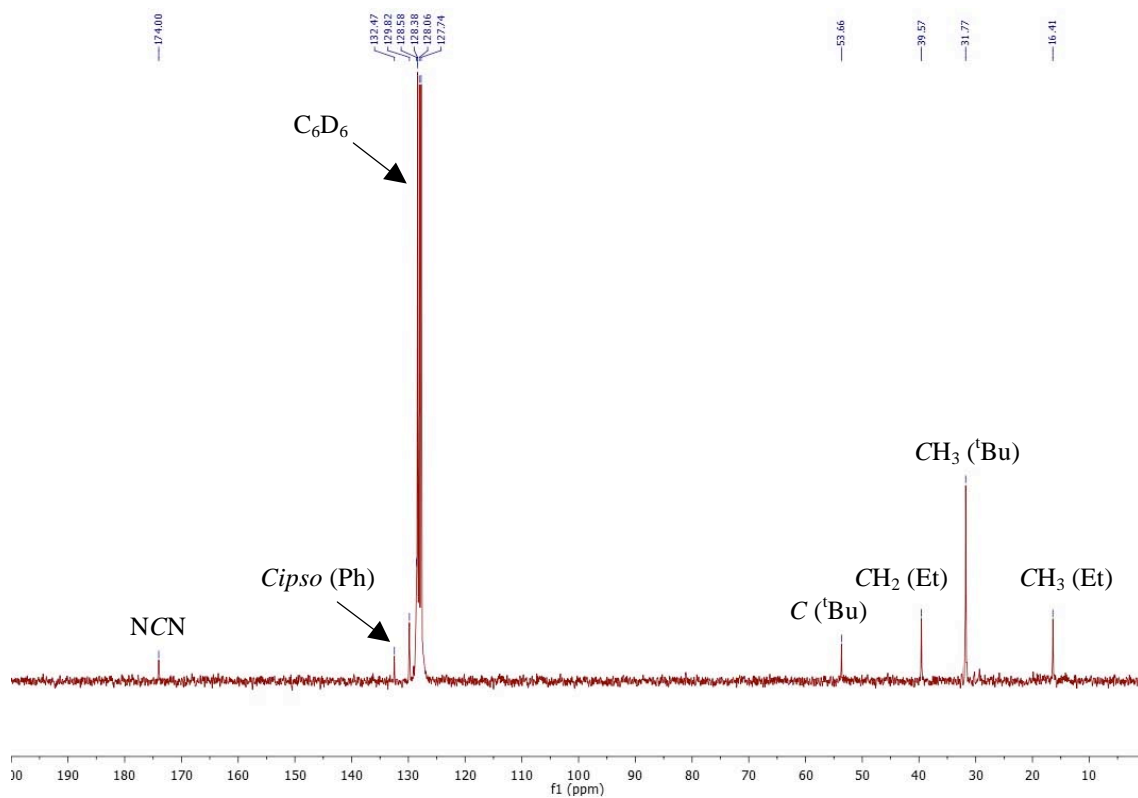


Fig SI-2 $^{13}\text{C}\{^1\text{H}\}$ NMR spectrum of $\text{Ge}(\text{Etbzam}'\text{Bu})\text{Cl}$ (C_6D_6 , 25 $^\circ\text{C}$, 75.5 MHz).

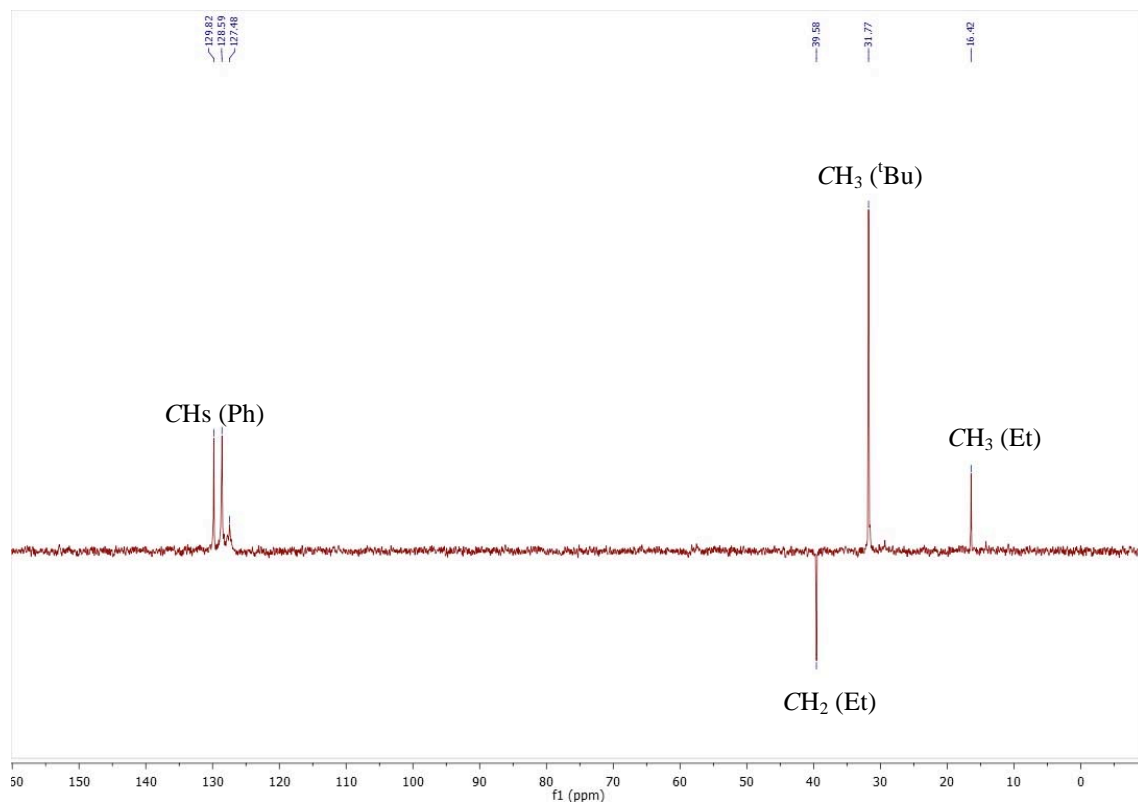


Fig SI-3 ¹³C DEPT-135 NMR spectrum of Ge(Etbzam^tBu)Cl (C₆D₆, 25 °C, 75.5 MHz).

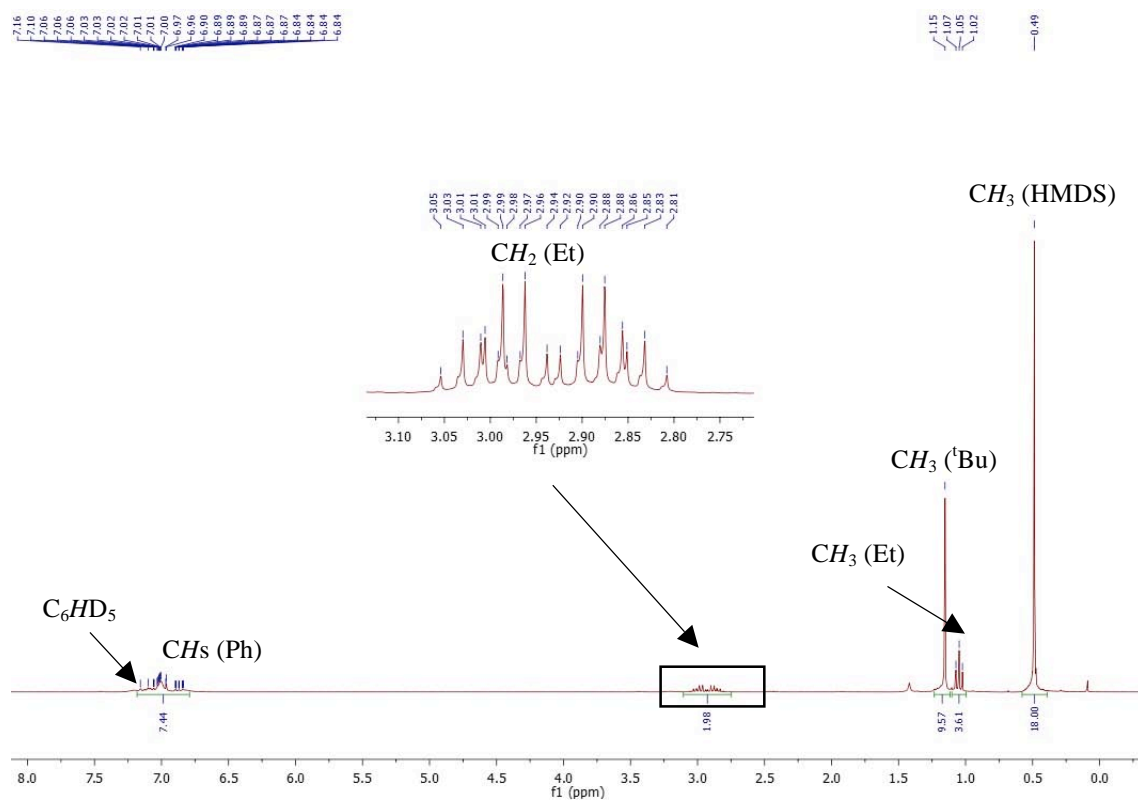


Fig SI-4 ¹H NMR spectrum of germylene **5** (C₆D₆, 25 °C, 300.1 MHz).

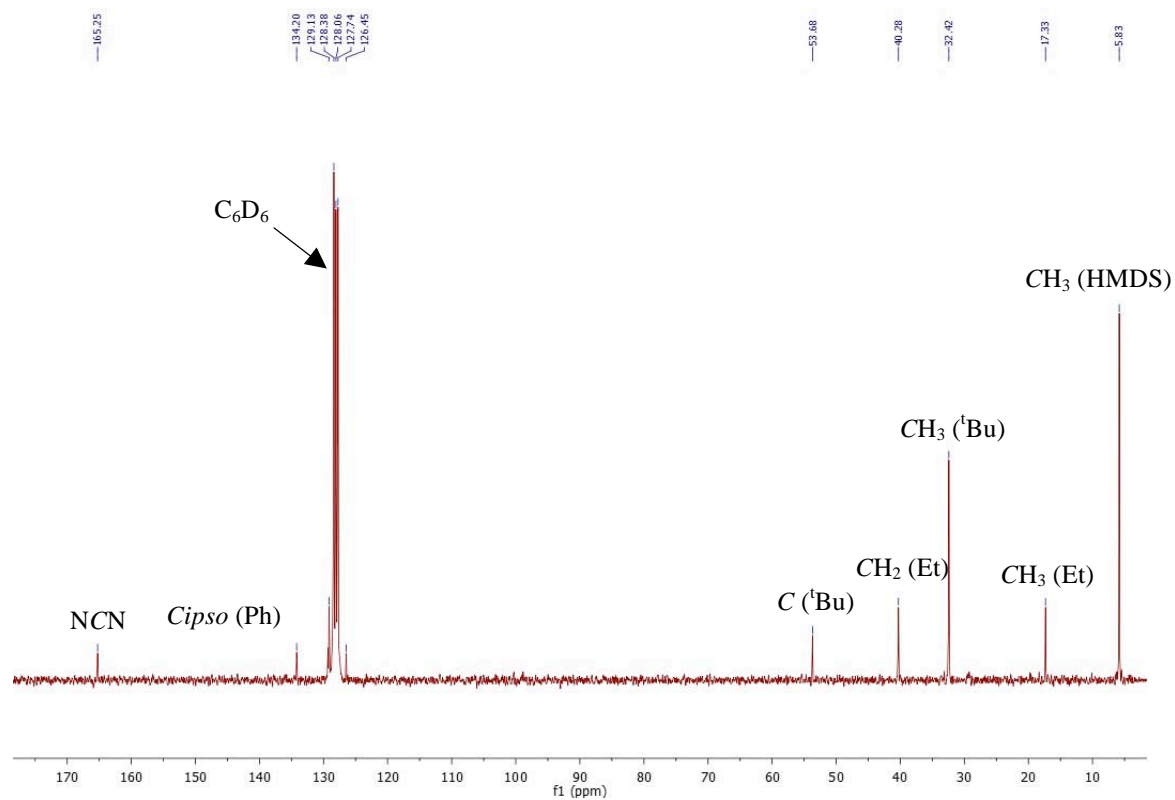


Fig SI-5 $^{13}\text{C}\{^1\text{H}\}$ NMR spectrum of germylene **5** (C_6D_6 , 25 °C, 75.5 MHz).

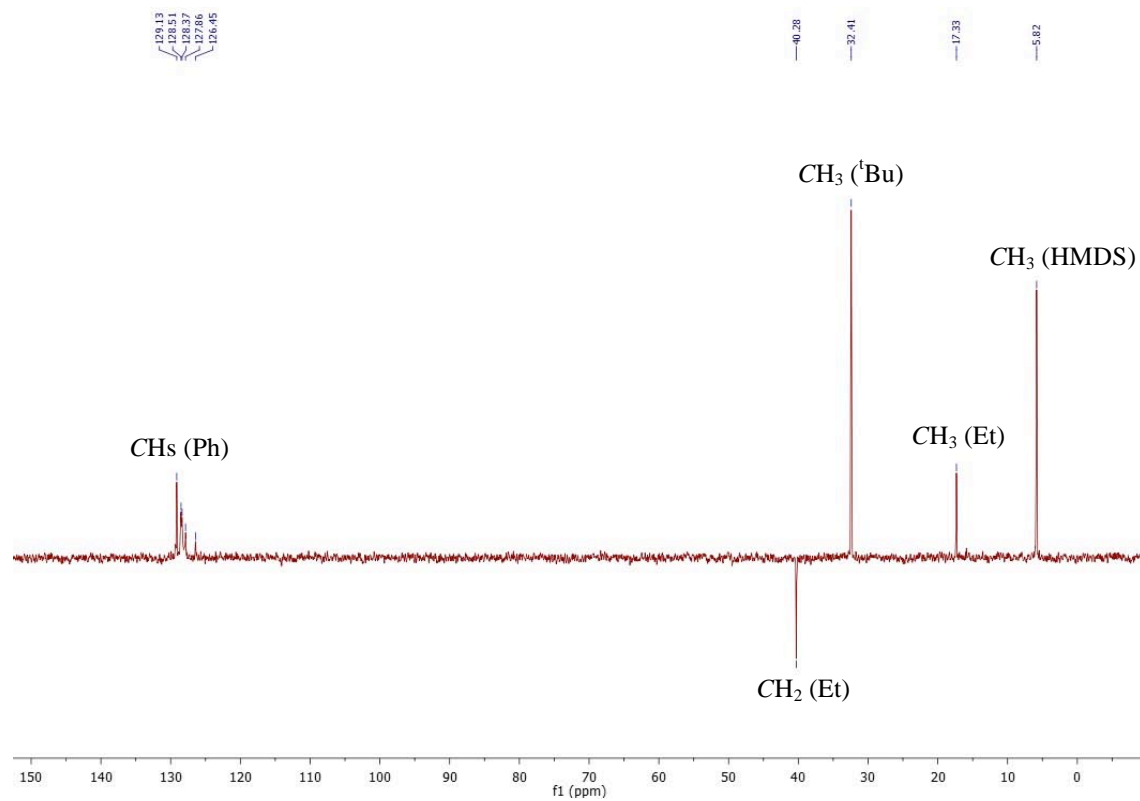


Fig SI-6 ^{13}C DEPT-135 NMR spectrum germylene **5** (C_6D_6 , 25 °C, 75.5 MHz).

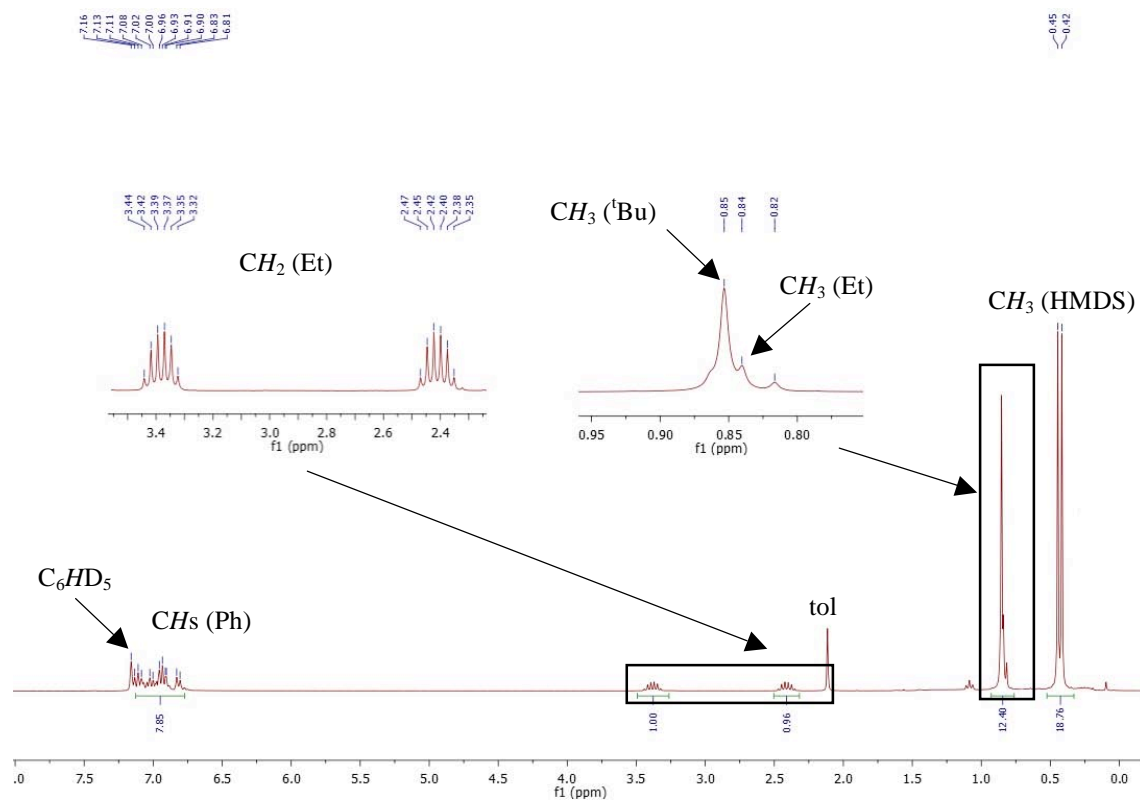


Fig SI-7 ^1H NMR spectrum of complex **6** (C_6D_6 , 25 $^\circ\text{C}$, 300.1 MHz).

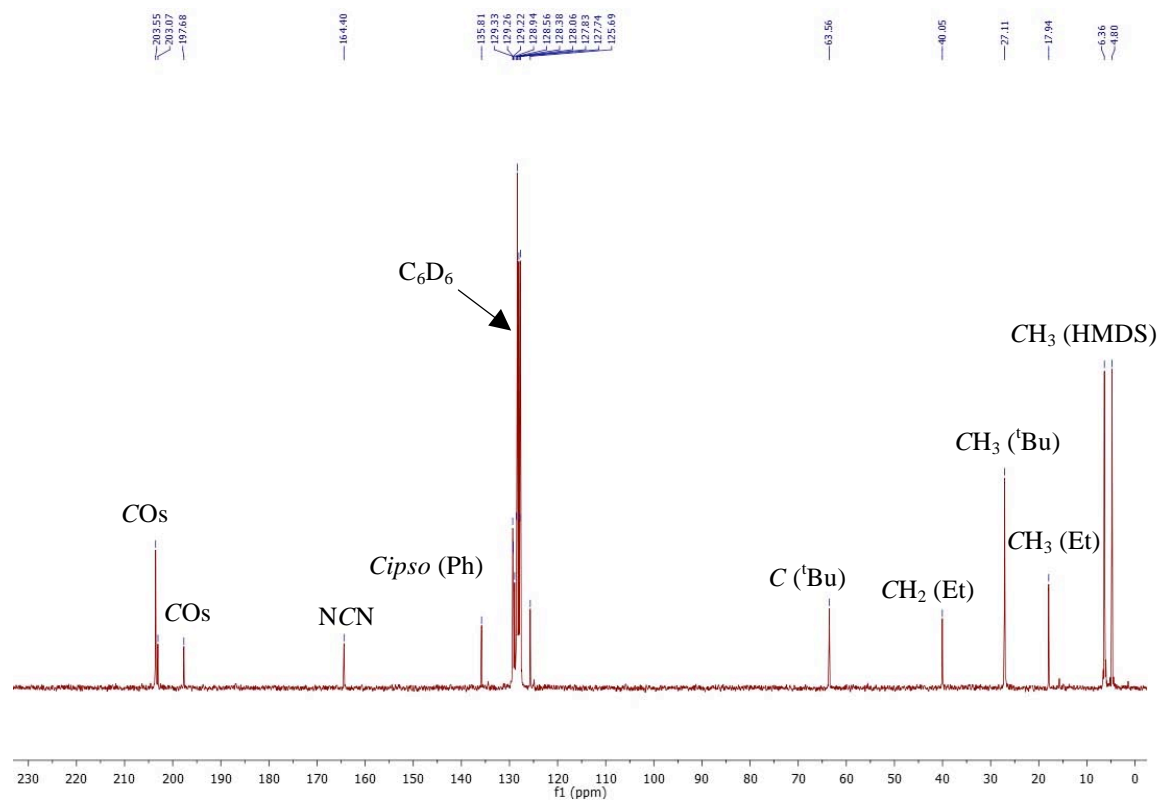


Fig SI-8 $^{13}\text{C}\{^1\text{H}\}$ NMR spectrum of complex **6** (C_6D_6 , 25 $^\circ\text{C}$, 75.5 MHz).

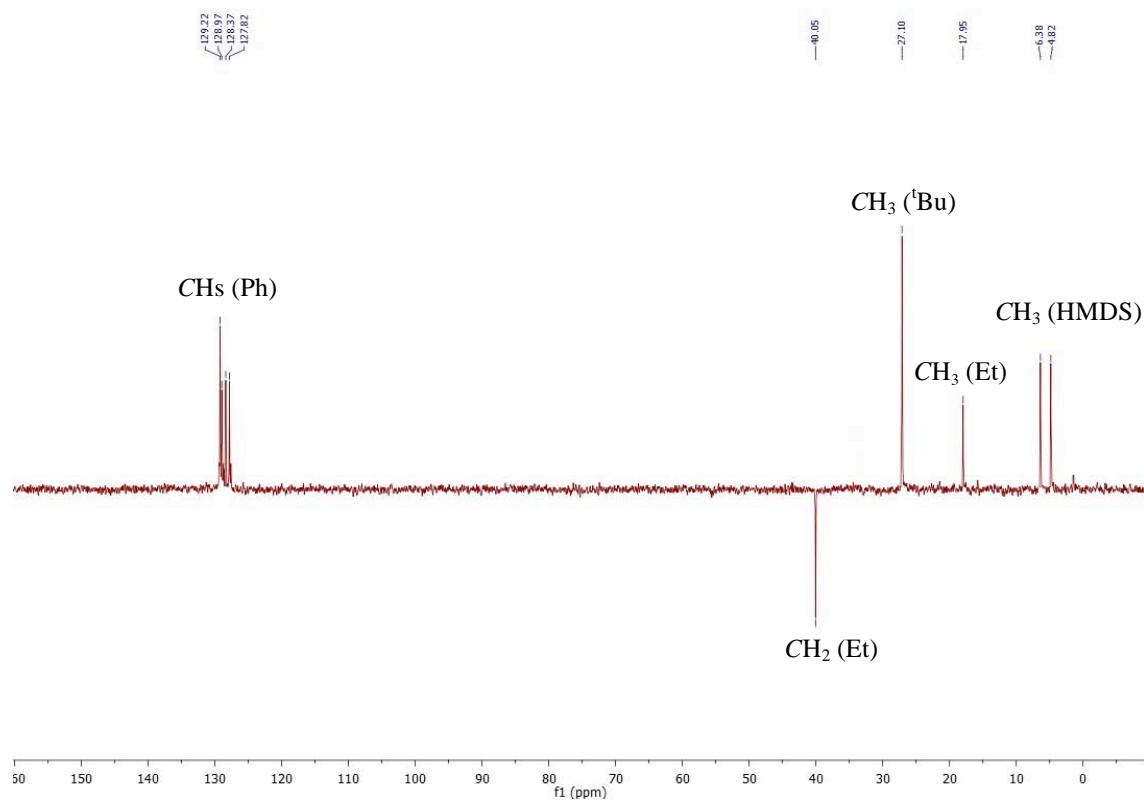


Fig SI-9 ¹³C DEPT-135 NMR spectrum complex **6** (C₆D₆, 25 °C, 75.5 MHz).

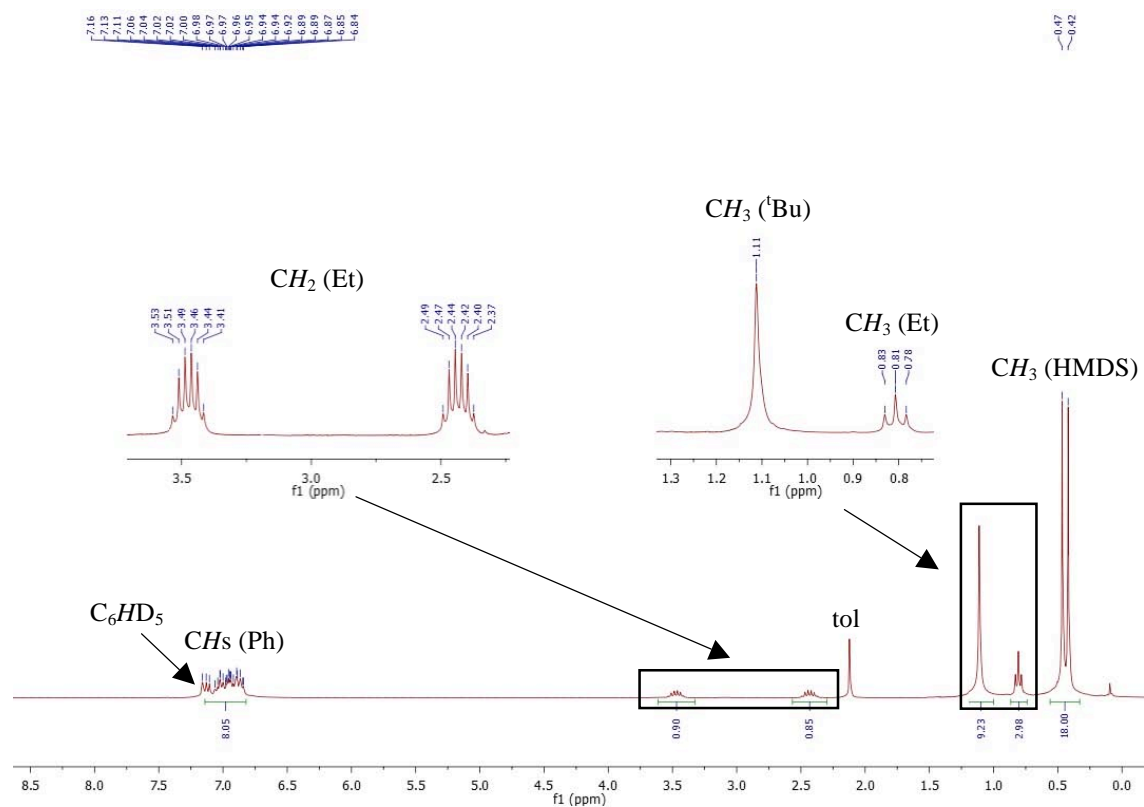


Fig SI-10 ¹H NMR spectrum of complex **7** (C₆D₆, 25 °C, 300.1 MHz, CO atmosphere).

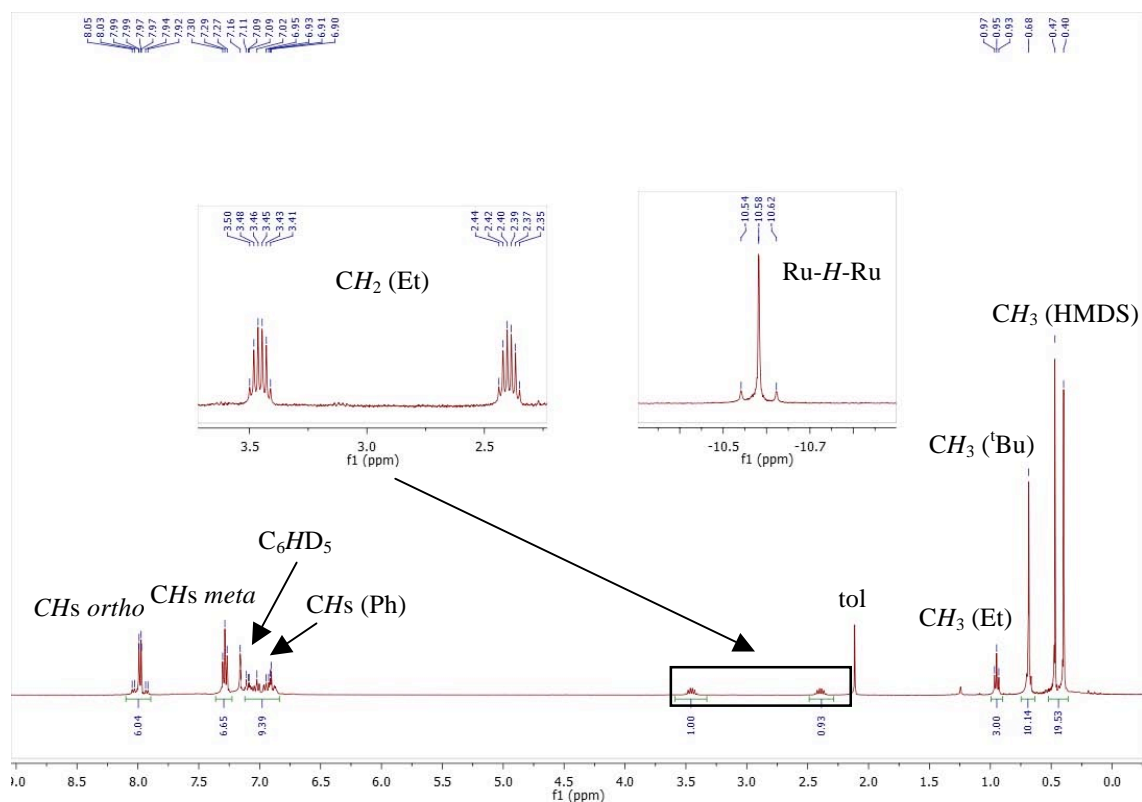


Fig SI-11 ^1H NMR spectrum of complex **8** (C_6D_6 , 25 $^\circ\text{C}$, 300.1 MHz).

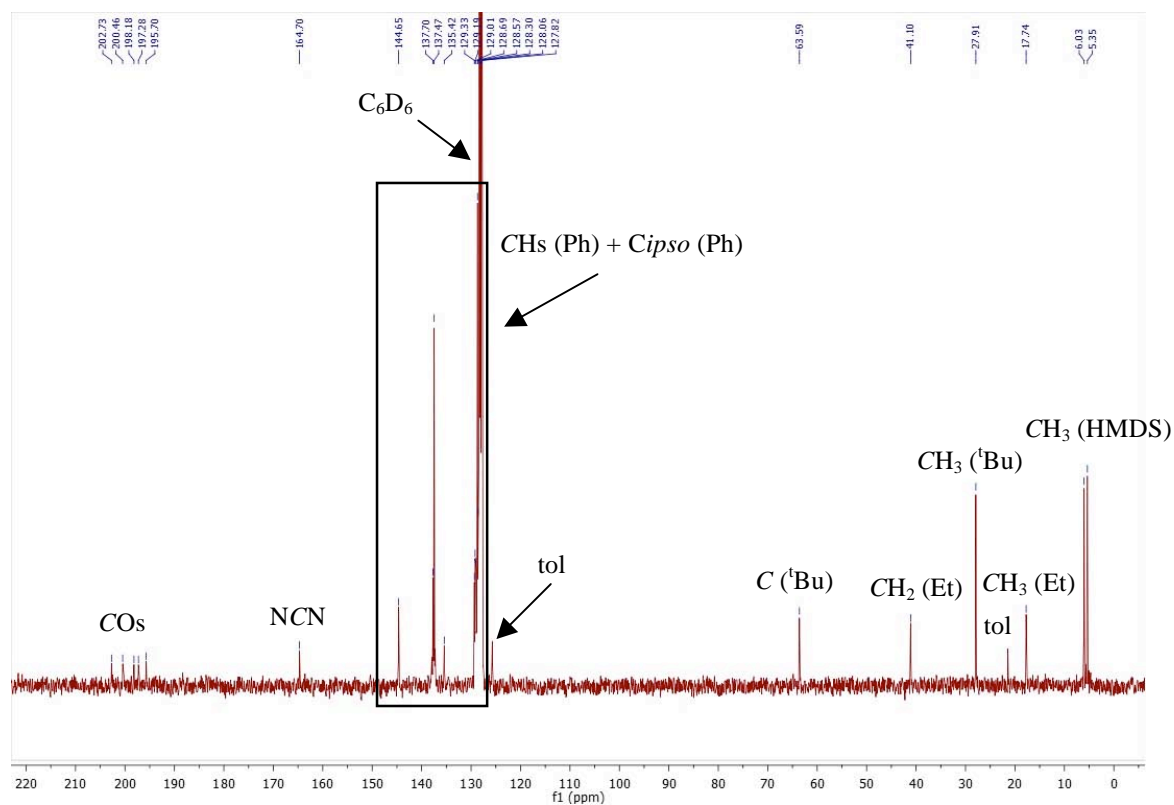


Fig SI-12 $^{13}\text{C}\{^1\text{H}\}$ NMR spectrum of complex **8** (C_6D_6 , 25 $^\circ\text{C}$, 75.5 MHz).

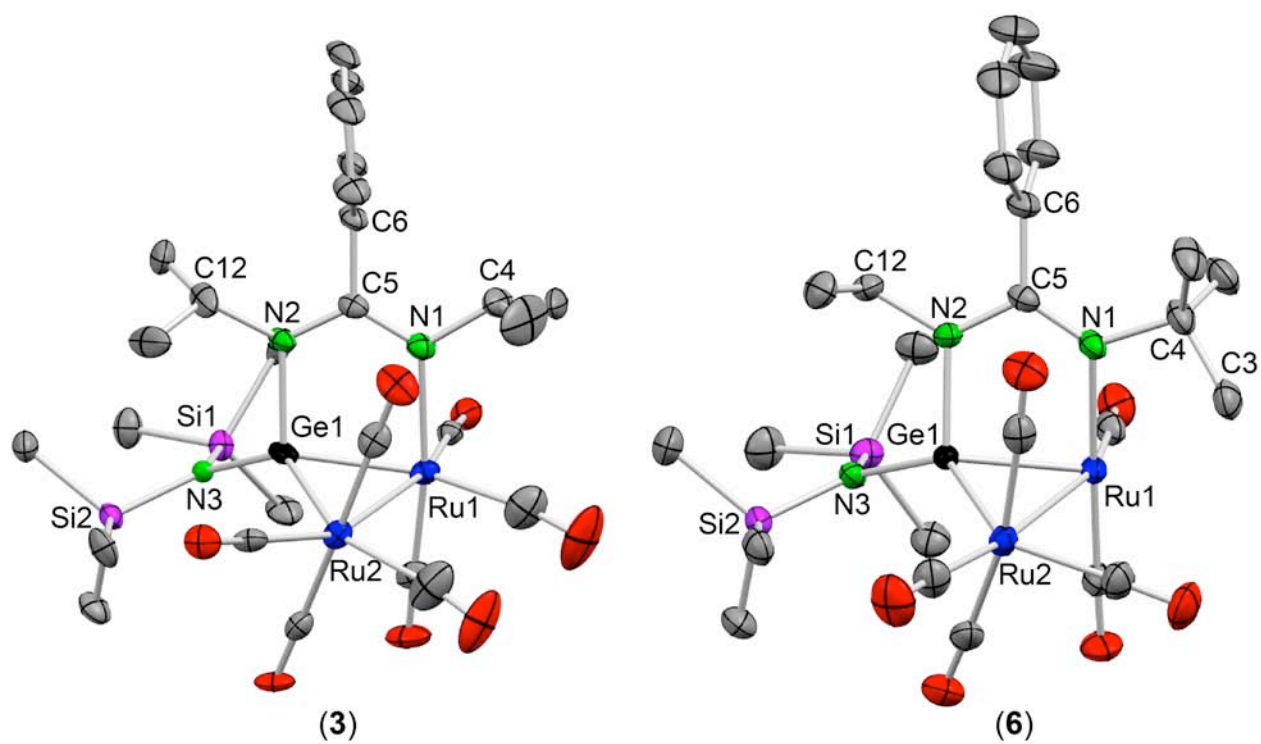


Fig SI-13 Comparative ORTEP views of the molecular structures of complexes **3** and **6**.

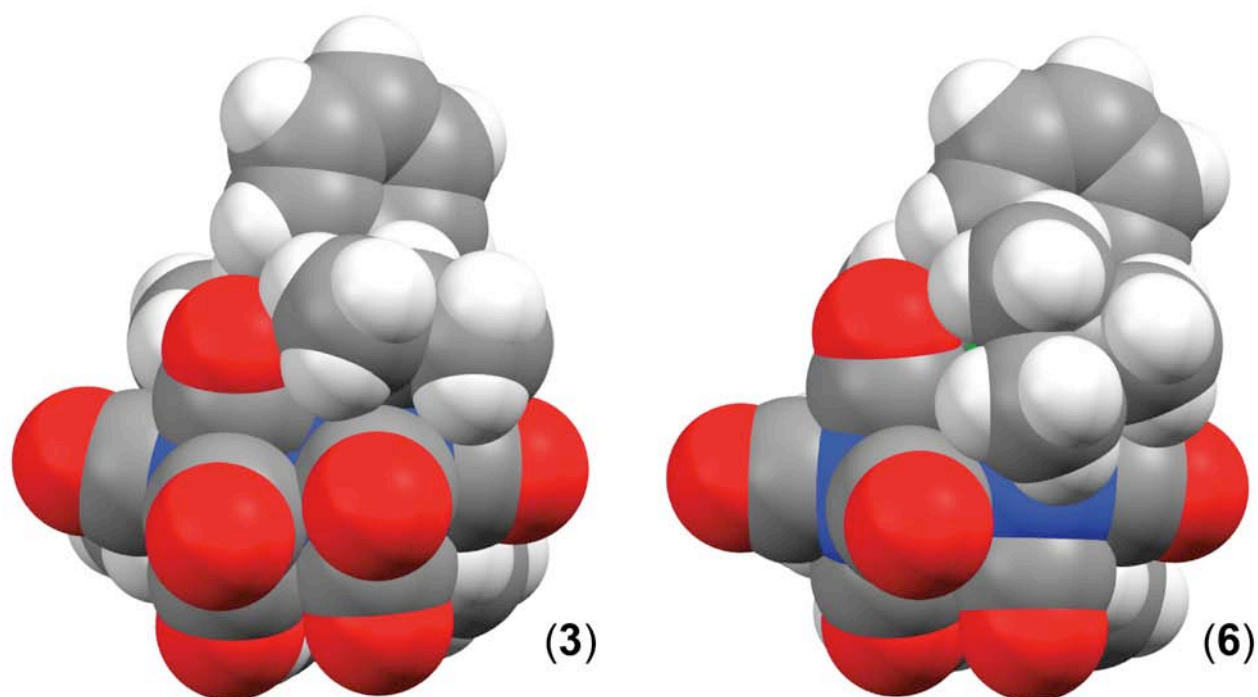


Fig SI-14 Comparative space-filling views of the molecular structures of complexes **3** and **6**, showing that atom Ru1 of **6** is only partially protected by a *tert*-butyl methyl group.

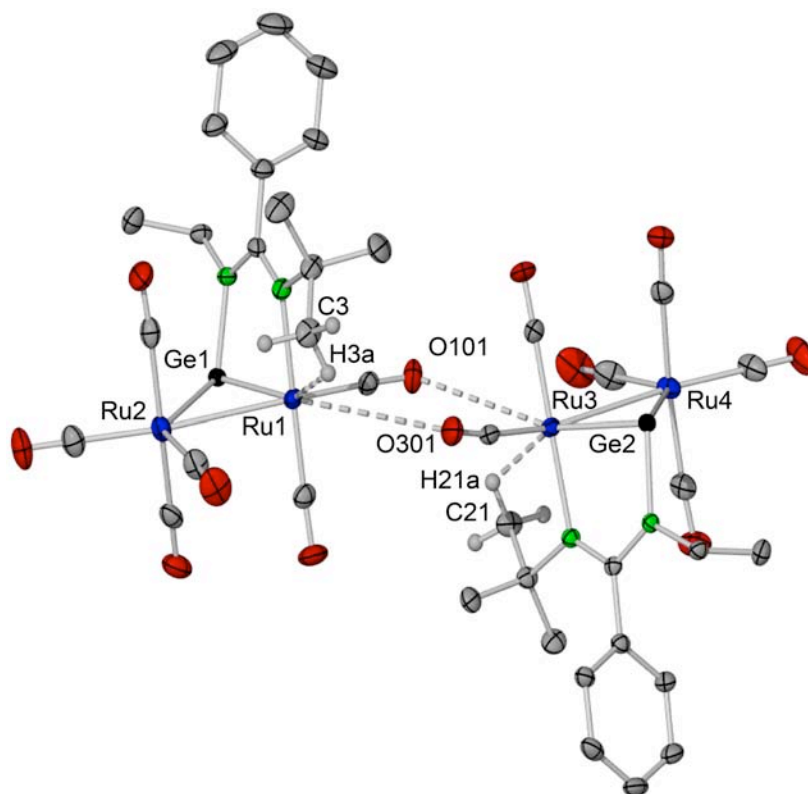


Fig SI-15 The molecular pair found in the crystals of complex **6**. All H atoms (except those attached to C3 and C21) have been omitted for clarity. The Ru1–O301 and Ru3–O101 distances are 4.252(2) Å and 3.599(2) Å, respectively. The Ru1–H3a and Ru3–H21a distances are 2.21(4) Å and 2.27(4) Å, respectively.

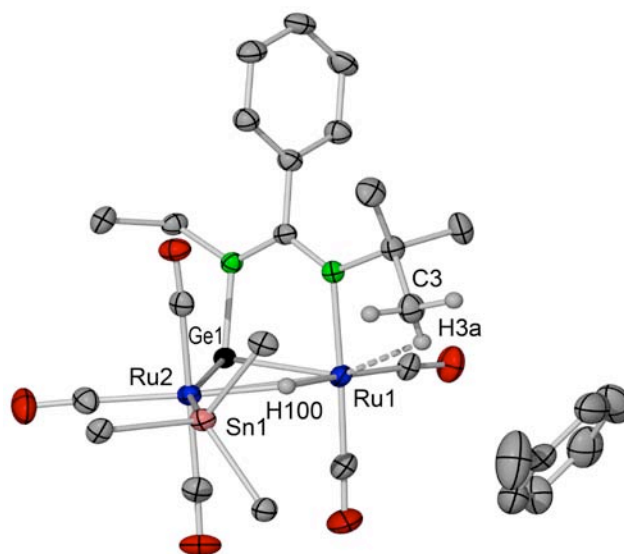


Fig SI-16 Structure **8**·C₇H₈. The HMDS fragment, the SnPh₃ phenyl groups (except the C_{ipso} atoms) and all H atoms (except the hydride and those attached to C3) have been omitted for clarity. Only one of the two positions in which the toluene molecule was found to be disordered is depicted. The Ru1–H3a distance is 2.26(4) Å.

Artículo VIII

***“Amidinatogermylene Derivatives of Ruthenium
Carbonyl: New Insights into the Reactivity of
[Ru₃(CO)₁₂] with 2-Electron-Donor Reagents of High
Basicity”***

Amidinatogermylene Derivatives of Ruthenium Carbonyl: New Insights into the Reactivity of $[\text{Ru}_3(\text{CO})_{12}]$ with Two-Electron-Donor Reagents of High Basicity

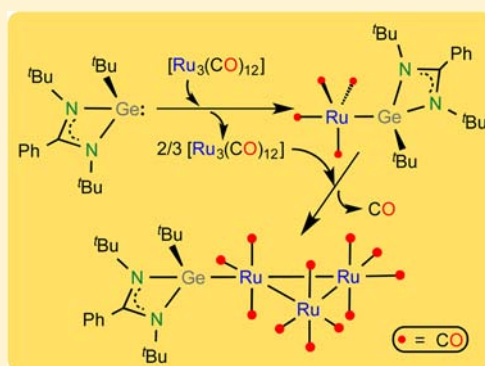
Lucía Álvarez-Rodríguez,[†] Javier A. Cabeza,^{*,†} Pablo García-Álvarez,^{*,†} Enrique Pérez-Carreño,[‡] and Diego Polo[†]

[†]Departamento de Química Orgánica e Inorgánica-IUQOEM, Universidad de Oviedo-CSIC, E-33071 Oviedo, Spain

[‡]Departamento de Química Física y Analítica, Universidad de Oviedo, E-33071 Oviedo, Spain

Supporting Information

ABSTRACT: The reactivity of ruthenium carbonyl with amidinatogermynes of the type $\text{Ge}(\text{R}_2\text{bzam})^t\text{Bu}$ ($\text{R}_2\text{bzam} = \text{N,N}'\text{-disubstituted benzamidinate}$) was studied for $\text{R} = {}^t\text{Bu}$ ($\text{I}_{t\text{Bu}}$) and ${}^i\text{Pr}$ ($\text{I}_{i\text{Pr}}$). The mono-, bi-, and/or trinuclear derivatives $[\text{Ru}(\text{I}_{\text{R}})(\text{CO})_4]$, $[\text{Ru}(\text{I}_{\text{R}})_2(\text{CO})_3]$, $[\text{Ru}_2(\text{I}_{i\text{Pr}})(\text{CO})_7]$, $[\text{Ru}_3(\text{I}_{t\text{Bu}})(\text{CO})_{11}]$, $[\text{Ru}_3(\text{I}_{t\text{Bu}})_2(\text{CO})_{10}]$, and $[\text{Ru}_3(\text{I}_{\text{R}})_3(\text{CO})_9]$ ($\text{R} = {}^t\text{Bu}, {}^i\text{Pr}$) were isolated in yields that depend upon the reactant ratio and the reaction temperature. The experimental data are consistent with the proposal that, at room temperature, the trinuclear complexes $[\text{Ru}_3(\text{CO})_{12}]$, $[\text{Ru}_3(\text{I}_{\text{R}})(\text{CO})_{11}]$, and $[\text{Ru}_3(\text{I}_{\text{R}})_2(\text{CO})_{10}]$ form an adduct with the germylene I_{R} that may evolve through two different reaction pathways, (a) releasing a CO ligand (thus leading to the corresponding trinuclear CO-substituted product) and/or (b) cleaving the cluster framework (thus leading to mononuclear germylene-containing products). At 90 °C, additional processes are also possible, such as the reactions of I_{R} with $[\text{Ru}(\text{I}_{\text{R}})(\text{CO})_4]$ or $[\text{Ru}_3(\text{I}_{\text{R}})_3(\text{CO})_9]$, which both give $[\text{Ru}(\text{I}_{\text{R}})_2(\text{CO})_3]$, or the reactions of $[\text{Ru}(\text{I}_{t\text{Bu}})(\text{CO})_4]$ and $[\text{Ru}(\text{I}_{i\text{Pr}})(\text{CO})_4]$ with $[\text{Ru}_3(\text{CO})_{12}]$, which give $[\text{Ru}_3(\text{I}_{t\text{Bu}})(\text{CO})_{11}]$ and $[\text{Ru}_2(\text{I}_{i\text{Pr}})(\text{CO})_7]$, respectively. This wide reaction panorama helps rationalize previously reported outcomes of reactions of $[\text{Ru}_3(\text{CO})_{12}]$ with other reagents of high basicity, such as trialkylphosphines or N-heterocyclic carbenes, including results for which no satisfactory explanation has been hitherto provided.

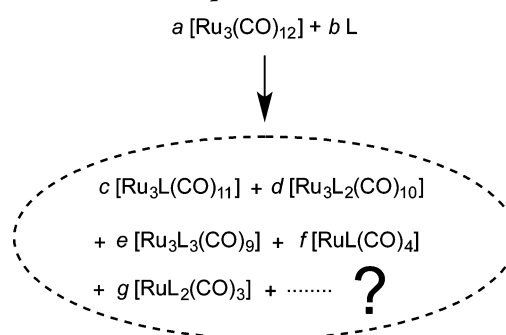


INTRODUCTION

The most common ruthenium carbonyl, $[\text{Ru}_3(\text{CO})_{12}]$, is a fundamental reagent of key importance for the synthesis of a great variety of carbonyl ruthenium complexes. Its reactions involve, in many cases, CO-substitution processes. In this context, it is well-known that common two-electron-donor reagents (L), such as monodentate phosphines¹ (PR_3) or N-heterocyclic carbenes (NHCs),² may give one or various mono- and/or trinuclear ruthenium carbonyl derivatives (Scheme 1).

Many reactivity and kinetics studies involving PR_3 ligands (those with NHCs are much more scarce) have also shown that these reactions proceed through mechanisms that can be dissociative, associative, or a mixture of both and that the type of mechanism and the nature and ratio of the reaction products depend upon the ratio of the reactants, the reaction conditions (concentration and temperature), and the nature of the nucleophilic reagent.¹ In the case of reagents of high σ -basicity and/or weak π -acidity, such as trialkylphosphines³ and NHCs,⁴ the reactions are generally fast (occurring at room temperature), preferably associative, and lead to extensive cluster fragmentation at low $[\text{Ru}_3(\text{CO})_{12}]$ -to-reagent ratios. However, a general “how-and-why” explanation of these experimental results has not been hitherto provided. Therefore, given the

Scheme 1. Possible Products of a Reaction of $[\text{Ru}_3(\text{CO})_{12}]$ with a Two-Electron-Donor Reagent ($\text{L} = \text{PR}_3, \text{NHC}$) at Room or Moderate Temperature



current importance that $[\text{Ru}_3(\text{CO})_{12}]$ has as a primary reagent, not only in inorganic synthesis but also in catalysis,⁵ any new insight that could shed more light into the reaction pathways

Received: January 12, 2015

Published: February 25, 2015

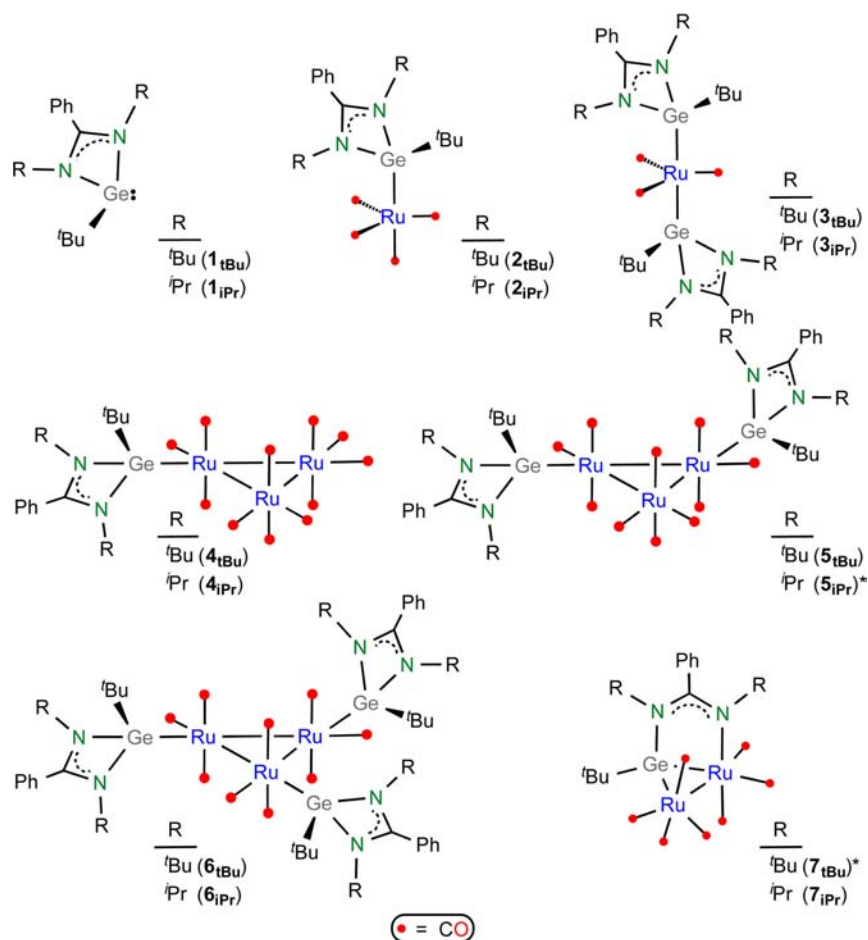


Figure 1. Schematic structures and abbreviated names of the germylenes used in this work and their reaction products. Those marked with an asterisk were not isolated or detected in the reaction mixtures.

pertinent to its reactions with two-electron-donor reagents would be greatly appreciated.

The past few years have witnessed an exponential growth of the chemistry of heavier tetrylenes (HTs).^{6–10} Among the currently known HTs, those stabilized by an amidinate group have played a role of utmost importance in the development of the coordination chemistry of these two-electron-donor ligands,^{8,9} since almost all of the elements of the transition metal (TM) series are nowadays known to form amidinato-HT–TM derivatives.⁹ Some of these complexes have already been successfully tested as catalyst precursors for useful reactions in organic synthesis.^{9a–e,10}

Continuing with our investigations on the coordination chemistry of HTs^{11–14} and, in particular, on the reactivity of amidinatogermylenes with TM carbonyls,^{11a,12–14} we now report that a study of the reactions of $[\text{Ru}_3(\text{CO})_{12}]$ with benzamidinatogermylenes of the type $\text{Ge}(\text{R}_2\text{bzam})^t\text{Bu}$ ($\text{R}_2\text{bzam} = N,N'$ -disubstituted benzamidinate) under different reaction conditions has allowed us to observe more reaction intermediates, products, and connections between them than those previously described for reactions of $[\text{Ru}_3(\text{CO})_{12}]$ with other two-electron-donor ligands. We also demonstrate herein that this wide reaction panorama can be used as a general tool that helps rationalize the outcomes of reactions of $[\text{Ru}_3(\text{CO})_{12}]$ with other reagents of high basicity, such as trialkylphosphines or NHCs, including results for which no satisfactory explanation has been hitherto provided.

RESULTS

The schematic structures of the two amidinatogermylenes used in this work, namely, $\text{Ge}(^t\text{Bu}_2\text{bzam})^t\text{Bu}$ ($1_{t\text{Bu}}$) and $\text{Ge}(^i\text{Pr}_2\text{bzam})^i\text{Pr}$ ($1_{i\text{Pr}}$), and all of their (possible) ruthenium carbonyl derivatives (not all of these products were detected and/or isolated for both amidinatogermylenes) are depicted in Figure 1. Table 1 collects a summary of the reactions reported in this work, including the reaction conditions and the molar ratio of the reaction products containing germylene ligands (in some cases, the presence of $[\text{Ru}_3(\text{CO})_{12}]$ among the reaction products was verified by IR spectroscopy, but its amount was not quantified).

Reactions Involving $\text{Ge}(^t\text{Bu}_2\text{bzam})^t\text{Bu}$ ($1_{t\text{Bu}}$). Ruthenium carbonyl reacted readily with 1 equiv of $1_{t\text{Bu}}$ at room temperature (Table 1, entry 1) to give a mixture of mononuclear ($2_{t\text{Bu}}$ and $3_{t\text{Bu}}$) and trinuclear derivatives ($4_{t\text{Bu}}$, $5_{t\text{Bu}}$ and $6_{t\text{Bu}}$) in which $2_{t\text{Bu}}$ was the major product. While all of $1_{t\text{Bu}}$ had reacted, some $[\text{Ru}_3(\text{CO})_{12}]$ remained among the reaction products. Increasing the initial amount of $1_{t\text{Bu}}$ to 4 equiv (Table 1, entry 2) favored the formation of mononuclear $2_{t\text{Bu}}$ and $3_{t\text{Bu}}$ but decreased the amounts of trinuclear $4_{t\text{Bu}}$ and $5_{t\text{Bu}}$ down to undetectable levels, while the amount of $6_{t\text{Bu}}$ (relative to that of $2_{t\text{Bu}}$) did not change. A small amount of $[\text{Ru}_3(\text{CO})_{12}]$ accompanied the reaction products.

As stated above, formation of mono- and/or trinuclear complexes of the types $[\text{Ru}_n(\text{CO})_{5-n}]$ ($n = 1, 2$) and/or $[\text{Ru}_3\text{L}_n(\text{CO})_{12-n}]$ ($n = 1–3$) have been previously observed in

Table 1. A Selection of the Reactions Discussed in This Work^a

No.	reactants	T, °C	t, h	[Ru(1_R)(CO) ₄] (2_R) ^b	[Ru(1_R) ₂ (CO) ₃] (3_R) ^b	[Ru ₃ (1_R) (CO) ₁₁] (4_R) ^b	[Ru ₃ (1_R) ₂ (CO) ₁₀] (5_R) ^b	[Ru ₃ (1_R) ₃ (CO) ₉] (6_R) ^b	[Ru ₂ (1_R) ₂ (CO) ₇] (7_R) ^b	
Reactions Involving 1_{tBu}										
1	[Ru ₃ (CO) ₁₂] + 1_{tBu}	20	1	100 ^c	10	7	10	4	0	
2	[Ru ₃ (CO) ₁₂] + 4 1_{tBu}	20	1	100 ^c	20	0	0	3	0	
3	[Ru ₃ (CO) ₁₂] + 1_{tBu} + CO ^d	20	1	100 ^c	0	0	0	0	0	
4	4_{tBu} + CO ^d	20	2	0	0	100 ^c	0	0	0	
5	4_{tBu} + 1_{tBu}	20	1	100 ^c	35	0	16	2	0	
6	4_{tBu} + 3 1_{tBu}	20	1	100	44	0	0	10	0	
7	5_{tBu} + 4 1_{tBu}	20	1	0	0	0	0	100	0	
8	[Ru ₃ (CO) ₁₂] + 1_{tBu}	90	2	0	0	100 ^c	15	0	0	
9	2/3 [Ru ₃ (CO) ₁₂] + 2_{tBu}	90	2	0	0	100	0	0	0	
10	[Ru ₃ (CO) ₁₂] + 8 1_{tBu}	100	3	0	100	0	0	0	0	
11	2_{tBu} + 2 1_{tBu}	100	3	0	100	0	0	0	0	
12	6_{tBu} + 4 1_{tBu}	100	3	0	100	0	0	0	0	
13	2_{tBu}	110	3	0 ^e	0	0	0	0	0	
Reactions Involving 1_{iPr}										
14	[Ru ₃ (CO) ₁₂] + 1_{iPr}	20	1	100 ^c	x ^f	x ^f	x ^f	x ^f	0	
15	[Ru ₃ (CO) ₁₂] + 4 1_{iPr}	20	1	100 ^c	x ^f	0	0	x ^f	0	
16	[Ru ₃ (CO) ₁₂] + 1_{iPr}	90	2	0	0	0	0	0	100 ^c	
17	1/3 [Ru ₃ (CO) ₁₂] + 2_{iPr}	90	2	0	0	0	0	0	100	
18	[Ru ₃ (CO) ₁₂] + 8 1_{iPr}	100	3	0	100	0	0	0	0	
19	7_{iPr} + 4 1_{iPr}	100	1	0 ^e	0	0	0	0	0	
20	2_{iPr}	110	3	0 ^e	0	0	0	0	0	

^aAll reactions were performed in toluene under argon (except entries 3 and 4) and were monitored by IR spectroscopy (ν_{CO} stretching region).

^bRelative molar amounts were estimated by ¹H NMR integration of the crude reaction mixture, assigning a value of 100 to the major reaction product. ^cThe presence of [Ru₃(CO)₁₂] in the product mixture was detected by IR spectroscopy. ^dCO bubbled (1 atm). ^eDecomposition to an unidentified material was observed. ^fThe relative amount of this product could not be estimated by ¹H NMR due to severe overlapping of signals of different products, but its presence in the crude reaction mixture was confirmed by IR spectroscopy.

reactions of [Ru₃(CO)₁₂] with monodentate P-donor ligands¹ and NHCs² under thermal conditions, but the nuclearity and ratio of the reaction products and their relationship with the type and ratio of the reactants have never been satisfactorily explained.

With the aim of gaining insight into the pathways followed by the above-described reactions, additional experiments were performed. Surprisingly and very importantly, the reaction of [Ru₃(CO)₁₂] with 1 equiv of **1_{tBu}** was not inhibited by the presence of CO (the gas was bubbled through the solution; Table 1, entry 3), but gave the mononuclear monogermylene **2_{tBu}** as the only reaction product. After 1 h, all **1_{tBu}** was consumed, while some [Ru₃(CO)₁₂] remained unreacted. Therefore, [Ru₃(CO)₁₂] may undergo cluster fission through an associative pathway that is independent of CO.

The fact that the trinuclear monogermylene complex **4_{tBu}** was a minor product of the reaction of entry 1 and that it was not observed in the product mixtures of the reactions of entries 2 and 3 of Table 1 led us to investigate its reactivity with CO and **1_{tBu}**. We found that **4_{tBu}** is stable under CO (1 atm) at room temperature (a trace amount of [Ru₃(CO)₁₂] was the only reaction product after 2 h, Table 1, entry 4), but it reacted readily with 1 equiv of **1_{tBu}** (Table 1, entry 5) to give the mononuclear complexes **2_{tBu}** and **3_{tBu}** as major reaction products (in ca. 3/1 mol ratio) accompanied by a considerable amount of the trinuclear digermylene complex **5_{tBu}** and some trinuclear trigermylene **6_{tBu}**. An increase of the amount of reagent **1_{tBu}** (Table 1, entry 6) resulted in an increase of **3_{tBu}** and **6_{tBu}** and the complete disappearance of **5_{tBu}** while the

mononuclear monogermylene **2_{tBu}** was maintained as the major reaction product. Thus, **4_{tBu}** is a precursor to **2_{tBu}**, **3_{tBu}**, **5_{tBu}** and **6_{tBu}** but in the reaction of [Ru₃(CO)₁₂] with **1_{tBu}** some (or much) of **2_{tBu}** can also be formed directly without the intermediacy of **4_{tBu}**.

The trinuclear digermylene complex **5_{tBu}** was quantitatively converted at room temperature into the trinuclear trigermylene derivative **6_{tBu}** by treating the former with an excess of **1_{tBu}** (Table 1, entry 7). This experiment also confirmed that **5_{tBu}** and **6_{tBu}** are not precursors to the mononuclear complexes **2_{tBu}** and **3_{tBu}** at room temperature, even in the presence of **1_{tBu}**.

Interestingly, the above-described scenario changed completely when the reactions were performed at higher temperature (90–100 °C). Thus, the treatment of [Ru₃(CO)₁₂] with 1 equiv of **1_{tBu}** at 90 °C (Table 1, entry 8) led only to two trinuclear products, namely, the monogermylene derivative **4_{tBu}** (major product) and the digermylene derivative **5_{tBu}** (some [Ru₃(CO)₁₂] remained unreacted). Therefore, as the mononuclear germylene complex **2_{tBu}** should be the first product formed in this reaction (it is formed at room temperature, see above), it should react with [Ru₃(CO)₁₂] at 90 °C to give the triruthenium monogermylene derivative **4_{tBu}**. This proposal was subsequently verified by treating **2_{tBu}** with 2/3 equiv of [Ru₃(CO)₁₂] at 90 °C (Table 1, entry 9), since this reaction quantitatively led to compound **4_{tBu}**.

At room temperature, the reaction of [Ru₃(CO)₁₂] with a large excess (8 equiv) of **1_{tBu}** led to a ca. 2:1 mixture of the mononuclear complexes **2_{tBu}** and **3_{tBu}** as well as a small amount of **6_{tBu}** leaving intact ca. 4 equiv of **1_{tBu}** in the reaction solution.

When this solution was heated at 100 °C, 3_{tBu} was observed as the only final product (Table 1, entry 10). This fact implied that both 2_{tBu} and 6_{tBu} should also react with 1_{tBu} at high temperature to give 3_{tBu} . This was subsequently confirmed by treating 2_{tBu} and 6_{tBu} with 1_{tBu} at 100 °C (Table 1, entries 11 and 12).

Finally, we heated a toluene solution of the mononuclear monogermylene complex 2_{tBu} to reflux temperature to check whether this complex could also be a precursor to the trinuclear trigermylene derivative 6_{tBu} upon thermal decarbonylation and subsequent trimerization (Table 1, entry 13). However, the thermolysis of 2_{tBu} slowly led to a very dark brown suspension that did not contain any previously identified complex.

Reactions Involving $\text{Ge}(\text{Pr}_2\text{bzam})\text{tBu}$ (1_{IPr}). The IR spectra in the ν_{CO} region of the solutions obtained by treating $[\text{Ru}_3(\text{CO})_{12}]$ with 1 and 4 equiv of 1_{IPr} in toluene at room temperature (Table 1, entries 14 and 15) were comparable to those described above using 1_{tBu} instead of 1_{IPr} (Table 1, entries 1 and 2). This fact confirmed that both germynes 1_{tBu} and 1_{IPr} gave analogous reaction mixtures in their reactions with $[\text{Ru}_3(\text{CO})_{12}]$ at room temperature, but, in the case of 1_{IPr} , we were unable to unambiguously quantify the relative amounts of each complex in the reaction mixtures because the ^1H NMR signals of the isopropyl and tertbutyl groups of the trinuclear complexes (minor products) were overlapped with those of the mononuclear complexes (major products), hampering a reliable integration of the signals of each product in the mixture. This fact prevented us from repeating all the reactions with 1_{IPr} that we performed with 1_{tBu} .

Interestingly, when the reaction of $[\text{Ru}_3(\text{CO})_{12}]$ with 1 equiv of 1_{IPr} was performed at 90 °C (Table 1, entry 16), the binuclear monogermylene 7_{IPr} was the only reaction product after 1 h. While some $[\text{Ru}_3(\text{CO})_{12}]$ was observed at the end of this reaction, the trinuclear monogermylene 4_{IPr} was detected by IR as a transient intermediate. We also prepared 7_{IPr} in quantitative yield by reacting 2_{IPr} with 1/3 equiv of $[\text{Ru}_3(\text{CO})_{12}]$ in toluene at 90 °C (Table 1, entry 17), and again, the trinuclear monogermylene 4_{IPr} was detected by IR as a transient intermediate. However, as occurred with 1_{tBu} , the treatment of $[\text{Ru}_3(\text{CO})_{12}]$ with a large excess of 1_{IPr} (8 equiv) in toluene at 100 °C (Table 1, entry 18) led to the corresponding mononuclear digermylene (3_{IPr}) as the only reaction product. In this case, 2_{IPr} was the only observed reaction intermediate (4_{IPr} and 7_{IPr} were not detected at any stage of the reaction). We subsequently corroborated that 7_{IPr} is not a precursor to the mononuclear species 2_{IPr} and 3_{IPr} , since the treatment of 7_{IPr} with an excess of 1_{IPr} (4 equiv) in toluene at 100 °C (Table 1, entry 19) gave a complex mixture of unidentified products.

Finally, as in the case of the mononuclear monogermylene 2_{tBu} , the thermolysis of 2_{IPr} in toluene at reflux temperature slowly led to extensive decomposition (Table 1, entry 20), probably due to the low thermal stability of the germylene ligand.

A discussion of all these reactivity results in the context of the hitherto reported reactivity of $[\text{Ru}_3(\text{CO})_{12}]$ with other two-electron-donor ligands, such as trialkylphosphines and NHCs, is provided in the following pages.

Structural Analysis of the Reaction Products. All isolated products were characterized by elemental analysis, mass spectrometry, IR and NMR spectroscopies, and in some cases (3_{IPr} , 4_{tBu} , 6_{IPr} , and 7_{IPr}) by single-crystal X-ray diffraction. Complete analytical data are given in the Experimental Section

of this paper (graphical NMR spectra are given as Supporting Information). As the types of compounds described in this paper are structurally unexceptional (complexes of these types having other two-electron-donor ligands have already been reported), the following paragraphs are only devoted to the particular X-ray diffraction and spectroscopic features that are directly associated with the presence of the amidinatogermylene ligands in these complexes.

The molecular structures of 3_{IPr} , 4_{tBu} , 6_{IPr} , and 7_{IPr} , determined by single-crystal X-ray diffraction, are shown in Figures 2–5. Selected bond distances are given in the figure

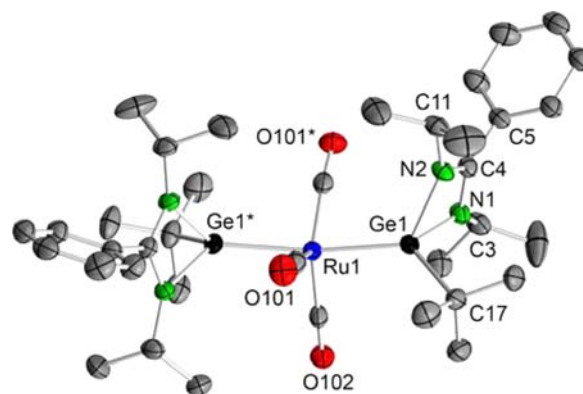


Figure 2. X-ray diffraction molecular structure of 3_{IPr} . Thermal ellipsoids set at 40% probability. H atoms were omitted for clarity. Selected bond lengths (Å) and angles (deg): Ru1–Ge1 2.3988(4), Ge1–C17 1.9998(3), Ge1–N1 1.988(3), Ge1–N2 1.999(3), N1–C3 1.463(5), N1–C4 1.335(4), N2–C4 1.317(4), N2–C11 1.466(4), C4–C5 1.484(5); Ru1–Ge1–N1 119.22(9), Ru1–Ge1–N2 119.87(9), C17–Ge1–Ru1 126.9(1), C17–Ge1–N1 104.3(2), C17–Ge1–N2 104.2(1), N1–Ge1–N2 66.1(1), Ge1–N1–C4 91.7(2), Ge1–N2–C4 91.8(2), N1–C4–N2 110.1(3), Ge1–Ru1–Ge1* 170.51(2).

captions. They all confirm the structures proposed for these complexes in Figure 1. In the crystal, compound 3_{IPr} displays C_2 symmetry (Figure 2). To minimize steric interactions between the germynes and the CO ligands, the Ru–Ge1 and Ru–Ge1* bonds are not colinear, the Ge1–Ru–Ge1* bond angle being 170.51(2)°. A similar situation was found in $[\text{Ru}\{\text{Ge}(\text{HMDS})_2\}_2(\text{CO})_3]$ (HMDS = $\text{N}(\text{SiMe}_3)_2$), which is the only ruthenium carbonyl complex having a terminal germylene ligand whose structure has been previously determined by X-ray diffraction crystallography.^{11c} In complexes 4_{tBu} (Figure 3) and 6_{IPr} (Figure 4), the germylene ligands are similarly located on equatorial coordination sites of their corresponding triruthenium cluster. The molecule of 6_{IPr} displays a non-crystallographic C_3 symmetry, having the three benzamidinate groups positioned at the same side of the Ru_3 plane.

The molecular structure of 7_{IPr} (Figure 5) is entirely analogous to that of $[\text{Ru}_2\{\mu\text{-}\kappa^2\text{-Ge-N-Ge}(\text{Pr}_2\text{bzam})\}(\text{HMDS})\text{-(CO)}_7]$,¹² but the former has a *tert*-butyl group (instead of an HMDS group) attached to the Ge atom. Both isopropyl groups of 7_{IPr} have their central CH hydrogen atoms close to the benzamidinate phenyl ring, which is perpendicular to the N1–C4–N2 and Ru1–Ru2–Ge1 planes. This situation minimizes steric interactions not only between the phenyl and isopropyl groups but also between the *tert*-butyl methyl groups and its closest isopropyl methyl groups. These binuclear complexes, in which the amidinatogermynes act as 4-electron-donor κ^2 -

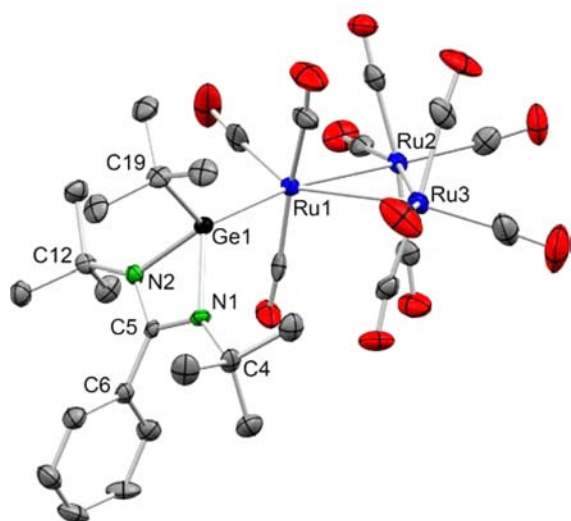


Figure 3. X-ray diffraction molecular structure of 4_{tBu} . Thermal ellipsoids set at 60% probability. H atoms were omitted for clarity. Selected bond lengths (Å) and angles (deg): Ru1–Ru2 2.8504(6), Ru1–Ru3 2.8834(6), Ru2–Ru3 2.8418(6), Ru1–Ge1 2.4363(7), Ge1–C19 2.007(5), Ge1–N1 1.984(4), Ge1–N2 1.993(4), N1–C4 1.493(6), N1–C5 1.338(6), N2–C5 1.331(6), N2–C12 1.475(7), C5–C6 1.486(7); Ru1–Ge1–N1 120.2(1), Ru1–Ge1–N2 116.3(1), C19–Ge1–Ru1 126.2(1), C19–Ge1–N1 106.8(2), C19–Ge1–N2 104.9(2), N1–Ge1–N2 66.6(2), Ge1–N1–C5 91.9(3), Ge1–N2–C5 91.8(3), N1–C5–N2 109.7(4).

N,Ge -ligands,^{12–14} are rare exceptions to the general two-electron-donor behavior of amidinato-HT ligands.^{9,15}

A notable feature of the IR spectra of the complexes involved in this work is that they present their ν_{CO} absorptions at very low frequencies. For comparison purposes, Table 2 contains IR ν_{CO} data of four groups of ruthenium carbonyl complexes that contain two-electron-donor ligands and that are structurally analogous to 2_{R} , 3_{R} , 4_{R} , and 6_{R} .^{3d,4,16–20} These data demonstrate that the amidinatogermynes used in this work (1_{tBu} and 1_{iPr}) are ligands of remarkable basicity, their electron-donating character being even higher than those of trialkylphosphines and comparable in some cases with those of N -heterocyclic carbenes (NHCs). Table 2 also indicates that 1_{tBu} is a slightly stronger electron-donor than 1_{iPr} .

While the room-temperature ^1H and $^{13}\text{C}\{^1\text{H}\}$ NMR spectra of compounds $2_{\text{R}}–6_{\text{R}}$ display the resonances of a symmetric (mirror symmetry) amidinatogermylene ligand in which the two benzamidinate $N–R$ groups of each ligand are equivalent, the corresponding spectra of compound 7_{iPr} clearly indicate that its two isopropyl groups are nonequivalent, reflecting the asymmetry of this complex.

Density Functional Theory Calculation of Thermodynamic Parameters. Table 3 contains the density functional theory (DFT)-calculated Gibbs energies at two temperatures, 298.15 and 363.15 K, computed at the wB97XD/LanL2DZ/6-31G(d,p) level and corrected for solvation effects (CPCM model, toluene), for selected reactions relevant to the present work.

Without exceptions, all reactions involving the free germynes 1_{R} as reactants (Table 3 entries 1–7, 10, and 12) are thermodynamically favored at both 298.15 and 363.15 K. Therefore, those that are not experimentally observed at room temperature (entries 6, 7) should be kinetically disfavored at this temperature (high energy barrier).

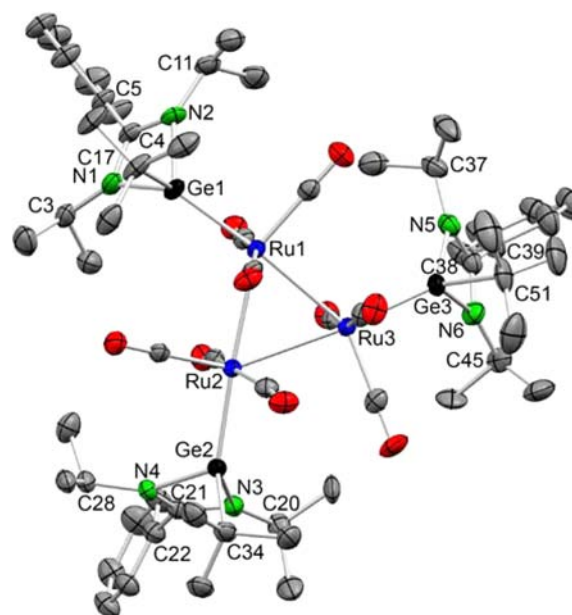


Figure 4. X-ray diffraction molecular structure of 6_{iPr} . Thermal ellipsoids set at 40% probability. H atoms were omitted for clarity, and only one of the two positions in which the two disordered isopropyl groups (C20 and C45 are their methine carbon atoms) were found is shown. Selected bond lengths (Å) and angles (deg): Ru1–Ru2 2.8756(6), Ru1–Ru3 2.8706(5), Ru2–Ru3 2.8781(6), Ru1–Ge1 2.3984(7), Ru2–Ge2 2.4052(7), Ru3–Ge3 2.3955(8), Ge1–C17 2.015(6), Ge1–N1 1.999(5), Ge1–N2 2.002(5), N1–C3 1.473(9), N1–C4 1.322(8), N2–C4 1.324(8), N2–C11 1.464(9), C4–C5 1.493(8), Ge2–C34 2.019(6), Ge2–N3 2.014(5), Ge2–N4 1.989(5), N3–C21 1.329(8), N4–C21 1.314(8), N4–C28 1.464(8), C21–C22 1.493(9), Ge3–C51 2.003(7), Ge3–N5 1.988(5), Ge3–N6 2.012(6), N5–C37 1.448(9), N5–C38 1.326(8), N6–C38 1.317(9), C38–C39 1.49(1) (the N3–C20 and N6–C45 bond distances are not given because C20 and C45 atoms are involved in positional disorder); Ru1–Ge1–N1 123.2(2), Ru1–Ge1–N2 116.7(2), C17–Ge1–Ru1 127.0(2), C17–Ge1–N1 104.5(3), C17–Ge1–N2 102.3(2), N1–Ge1–N2 65.9(2), Ge1–N1–C4 91.7(4), Ge1–N2–C4 91.5(4), N1–C4–N2 110.7(5), Ru2–Ge2–N3 123.4(2), Ru2–Ge2–N4 117.6(2), C34–Ge2–Ru2 126.9(2), C34–Ge2–N3 103.3(2), C34–Ge2–N4 102.9(2), N3–Ge2–N4 65.6(2), Ge2–N3–C21 91.2(4), Ge2–N4–C21 92.8(4), N3–C21–N4 110.3(5), Ru3–Ge3–N5 126.4(2), Ru3–Ge3–N6 116.8(2), C51–Ge3–Ru3 125.9(3), C51–Ge3–N5 102.8(3), C51–Ge3–N6 101.6(3), N5–Ge3–N6 65.9(2), Ge3–N5–C38 92.0(4), Ge3–N6–C38 91.2(4), N5–C38–N6 110.9(6).

Of particular interest are the reactions of entries 8 ($2_{\text{tBu}} + 2/3[\text{Ru}_3(\text{CO})_{12}] \rightarrow 4_{\text{tBu}} + \text{CO}$) and 11 ($2_{\text{iPr}} + 1/3[\text{Ru}_3(\text{CO})_{12}] \rightarrow 7_{\text{iPr}} + \text{CO}$) of Table 3 because they imply processes never studied before for other mononuclear $[\text{RuL}(\text{CO})_4]$ complexes. In these cases, the Gibbs energies are positive at both temperatures, but their absolute values are very small. As these reactions do proceed experimentally, although only at high temperature (Table 1, entries 9 and 17), their driving force should be their irreversible release of CO (the reactions were not performed in sealed vessels), which drives their corresponding reaction equilibrium toward the right. Entry 9 of Table 3 indicates that the transformation of 4_{iPr} into 7_{iPr} and $1/3[\text{Ru}_3(\text{CO})_{12}]$ should not be possible at room temperature but may occur at higher temperatures, as in fact it does (Table 1, entry 14 vs entry 16).

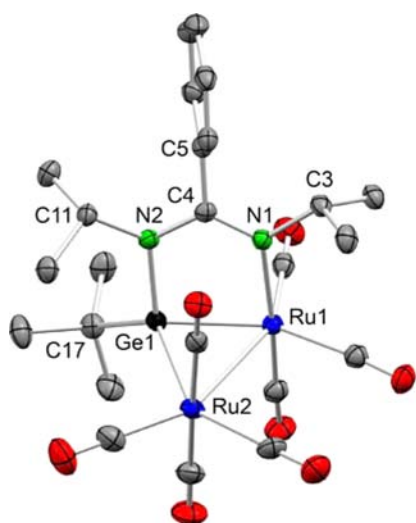


Figure 5. X-ray diffraction molecular structure of 7_{IPr} . Thermal ellipsoids set at 40% probability. H atoms were omitted for clarity. Selected bond lengths (Å) and angles (deg): Ru1–Ru2 2.9773(4), Ru1–N1 2.174(3), Ru1–Ge1 2.4073(5), Ru2–Ge1 2.5127(4), Ge1–C17 2.001(4), Ge1–N2 1.943(3), N1–C3 1.503(5), N1–C4 1.322(4), N2–C4 1.354(5), N2–C11 1.504(4), C4–C5 1.507(5); Ru1–Ge1–N2 98.44(9), Ru2–Ge1–N2 109.73(8), C17–Ge1–Ru1 126.8(1), C17–Ge1–Ru2 128.4(1), C17–Ge1–N2 111.5(1), Ru1–Ge1–Ru2 74.44(1), Ru1–Ru2–Ge1 51.16(1), Ge1–Ru1–Ru2 54.40(1), Ge1–N2–C4 115.3(2), Ru1–N1–C4 123.2(2), N1–C4–N2 122.0(3).

Table 2. Comparative IR ν_{CO} Data

complex	L	solvent	ν_{CO} absorptions/ cm^{-1}	reference	
[RuL(CO) ₄]	PPh ₃	<i>n</i> -heptane	2062 (s), 1988 (m), 1953 (vs)	16	
	PBu ₃	<i>n</i> -heptane	2059 (s), 1983 (m), 1944 (vs)	16	
	PCy ₃	<i>n</i> -heptane	2056 (s), 1978 (m), 1943 (vs), 1936 (vs)	16	
	IMes	nujol	2044 (s), 2007 (m), 1955 (s), 1921 (s)	4a	
	1_{tBu}	toluene	2042 (s), 1965 (m), 1933 (vs), 1924 (vs)	this work	
	1_{iPr}	toluene	2043 (s), 1966 (m), 1927 (vs)	this work	
[RuL ₂ (CO) ₃]	PPh ₃	<i>n</i> -heptane	1910 (s)	16	
	PBu ₃	<i>n</i> -heptane	1890 (s)	16	
	PCy ₃	<i>n</i> -heptane	1882 (s), 1867 (s)	16	
	IMes	KBr	1950, 1879, 1830 ^a	17	
	ICy	C ₆ D ₆	2009, 1930, 1870, 1839 ^a	18	
	IEt ₂ Me ₂	C ₆ D ₆	1931 (w), 1833 (vs)	4b	
	IME ₄	nujol	1840 (vs)	19	
	1_{tBu}	toluene	1937 (w), 1868 (vs), 1852 (vs)	this work	
[Ru ₃ L(CO) ₁₁]	PPh ₃	<i>c</i> -hexane	2097 (m), 2047 (m), 2031 (sh), 2026 (sh), 2017 (s), 2001 (w), 1986 (w)	3d	
	PCy ₃	<i>c</i> -hexane	2082 (m), 2047 (s), 2026 (s), 2016 (vs), 1996 (s), 1985 (s), 1970 (m), 1945 (m)	21	
	PMe ₃	<i>c</i> -hexane	2086 (m), 2066 (sh), 2056 (m), 2040 (s), 2023 (s), 2011 (vs), 1990 (sh), 1978 (sh), 1943 (m)	21	
	<i>a</i> -IAd	nujol	2094, 2068, 2036, 2019, 2000, 1988, 1982, 1967, 1960, 1927 ^a	4c	
	<i>a</i> -ItBu	KBr	2085 (m), 2034 (s), 2013 (s), 1996 (s), 1984 (s), 1977 (sh), 1962 (m), 1943 (m)	4d	
	IMes	CH ₂ Cl ₂	2090 (m), 2035 (s), 2020 (s), 2008 (s), 1971 (w)	4e	
	IMe	CH ₂ Cl ₂	2093 (m), 2038 (s), 2019 (s), 2005 (vs), 1975 (w), 1949 (w)	4e	
	1_{tBu}	toluene	2091 (m), 2040 (s), 2017 (s), 2007 (vs), 1980 (m), 1934 (w), 1921 (w)	this work	
	[Ru ₃ L ₃ (CO) ₉]	PPh ₃	<i>c</i> -hexane	2044 (m), 1978 (sh), 1967 (vs),	20
		PMe ₃	<i>c</i> -hexane	2044 (w), 2015 (sh), 1997 (sh), 1975 (sh), 1943 (vs)	20
1_{tBu}		toluene	2020 (w), 1954 (vs), 1946 (vs), 1921 (vs)	this work	
1_{iPr}		toluene	2025 (w), 1962 (vs), 1955 (vs), 1925 (vs)	this work	

^aNo information on band intensity available.

Table 3. Density Functional Theory-Computed Gibbs Energies for Selected Reactions^a

No.	reaction	$\Delta G_{298.15}$	$\Delta G_{363.15}$
1	1_{tBu} + 1/3[Ru ₃ (CO) ₁₂] → 2_{tBu}	−24.5	−23.5
2	1_{tBu} + [Ru ₃ (CO) ₁₂] + → 4_{tBu} + CO	−22.0	−20.9
3	1_{tBu} + 4_{tBu} → 5_{tBu} + CO	−18.1	−16.6
4	1_{tBu} + 5_{tBu} → 6_{tBu} + CO	−21.2	−20.5
5	1_{tBu} + 1/3 4_{tBu} → 2/3 2_{tBu} + 1/3 3_{tBu}	−23.7	−22.9
6	1_{tBu} + 2_{tBu} → 3_{tBu} + CO	−19.5	−19.0
7	1_{tBu} + 1/3 6_{tBu} → 3_{tBu}	−23.5	−23.2
8	2_{tBu} + 2/3[Ru ₃ (CO) ₁₂] → 4_{tBu} + CO	2.5	2.6
9	4_{iPr} → 7_{iPr} + 1/3[Ru ₃ (CO) ₁₂]	0.4	−0.4
10	1_{iPr} + 2/3[Ru ₃ (CO) ₁₂] → 7_{iPr} + CO	−22.4	−22.2
11	2_{iPr} + 1/3[Ru ₃ (CO) ₁₂] → 7_{iPr} + CO	1.5	0.7
12	1_{iPr} + 1/3[Ru ₃ (CO) ₁₂] → 2_{iPr}	−23.9	−22.9

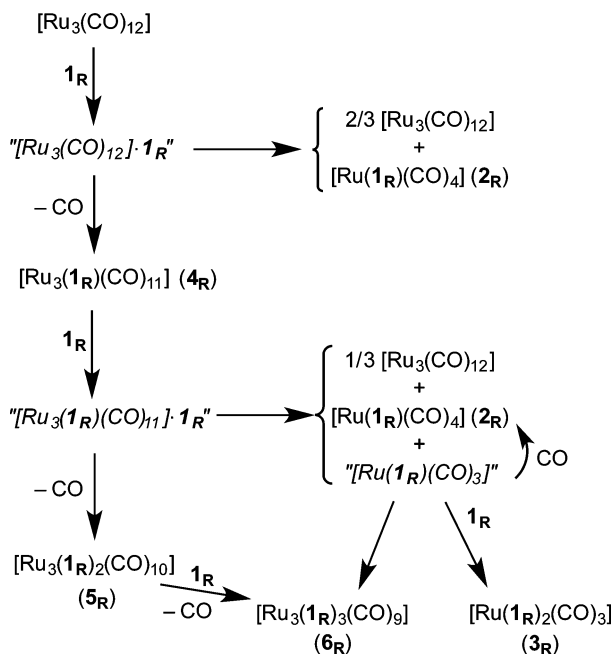
^aData (in kcal mol^{−1}) calculated at the wB97XD/LanL2DZ/6-31G(d,p) level (toluene solvent, CPCM model).

DISCUSSION

Room Temperature Reactions. A mechanistic proposal that accounts for the experimental outcomes of reactions of [Ru₃(CO)₁₂] with different amounts of the amidinatogermynes **1_{tBu}** and **1_{iPr}** at room temperature is depicted in Scheme 2.

We propose that the first step of the reactions of [Ru₃(CO)₁₂] with germynes **1_R** is the formation of a transient adduct between these two molecules, “[Ru₃(CO)₁₂]**·1_R**”, that may evolve by either releasing CO to give [Ru₃(**1_R**)(CO)₁₁] (**4_R**) or by breaking Ru–Ru bonds to give [Ru(**1_R**)(CO)₄] (**2_R**)

Scheme 2. Relationships between Products Arising from Reactions of $[\text{Ru}_3(\text{CO})_{12}]$ with Amidinatogermynes $\mathbf{1}_R$ ($R = i\text{Pr}, t\text{Bu}$) at Room Temperature^a



^aFormulas in *italic* typeface represent transient unstable species.

and $2/3[\text{Ru}_3(\text{CO})_{12}]$ (the latter should rapidly be formed by recombination of unsaturated $[\text{Ru}_2(\text{CO})_8]$ and/or $[\text{Ru}(\text{CO})_4]$ species). Similarly, we propose that the reaction of $\mathbf{4}_R$ with $\mathbf{1}_R$ also proceeds through a transient adduct, $[\text{Ru}_3(\mathbf{1}_R)(\text{CO})_{11}]\cdot\mathbf{1}_R$ that may also evolve by either releasing CO to give $[\text{Ru}_3(\mathbf{1}_R)_2(\text{CO})_{10}]$ ($\mathbf{5}_R$) or by breaking Ru–Ru bonds to give $1/3[\text{Ru}_3(\text{CO})_{12}]$, more $[\text{Ru}(\mathbf{1}_R)(\text{CO})_4]$ ($\mathbf{2}_R$), and the unsaturated species $[\text{Ru}(\mathbf{1}_R)(\text{CO})_3]$. The latter should be very unstable and should react rapidly with either CO (some may be available because it was released to the solution during the formation of $\mathbf{4}_R$), to give more $\mathbf{2}_R$, or with $\mathbf{1}_R$ (if available) to give the mononuclear digermylene complex $[\text{Ru}(\mathbf{1}_R)_2(\text{CO})_3]$ ($\mathbf{3}_R$). In the absence of CO and $\mathbf{1}_R$, $[\text{Ru}(\mathbf{1}_R)(\text{CO})_3]$ should undergo trimerization to give $[\text{Ru}_3(\mathbf{1}_R)_3(\text{CO})_9]$ ($\mathbf{6}_R$). The reaction of the trinuclear digermylene complex $\mathbf{5}_R$ with $\mathbf{1}_R$ (if available) may also provide more $\mathbf{6}_R$ (this may also take place through an intermediate adduct of the type $[\text{Ru}_3(\mathbf{1}_R)_2(\text{CO})_{10}]\cdot\mathbf{1}_R$, not depicted in Scheme 2). If all reactions displayed in Scheme 2 are possible at room temperature, the ratio of the final reaction products should depend on the rate of each particular reaction step and on the ratio of the reactants.

The key features of this reaction pathway (Scheme 2) are the participation of the intermediate adducts $[\text{Ru}_3(\text{CO})_{12}]\cdot\mathbf{1}_R$ and $[\text{Ru}_3(\mathbf{1}_R)(\text{CO})_{11}]\cdot\mathbf{1}_R$ and the proposal that, in addition to releasing CO to give the corresponding CO-substituted trinuclear derivatives, these adducts can spontaneously undergo cluster fission liberating mononuclear germylene species.

Regarding the nature of the intermediate trinuclear adducts, the attack of anionic nucleophiles (Nu^- , such as hydride, alkoxides, or amides) to $[\text{Ru}_3(\text{CO})_{12}]$ and $[\text{Os}_3(\text{CO})_{12}]$ at the C atom of a CO ligand (to form a transient anionic trinuclear derivative containing an acyl $\kappa^1\text{-C}(\text{O})\text{Nu}$ ligand) was proposed by Kesz and co-workers as a key step in Nu^- -promoted CO-substitution reactions on these clusters;²¹ however, the

corresponding anionic clusters $[\text{M}_3\{\text{C}(\text{O})\text{Nu}\}(\text{CO})_{11}]^-$ ($M = \text{Ru}, \text{Os}$) have never been isolated. In the case of neutral nucleophiles, the formation of a weak acid–base adduct between the nucleophile (Nu) and the C atom of a CO ligand was proposed by Morris and Basolo as a key step of Nu-promoted CO-substitution reactions on $[\text{Fe}(\text{CO})_2(\text{NO})_2]$;²² however, it has not been until very recently that Huynh, Leong, and co-workers have succeeded in isolating and fully characterizing by X-ray diffraction the first adducts between neutral two-electron-donor nucleophiles and carbonyl ligands.²³ Studying the reactivity of $[\text{Os}_3(\text{CO})_{12}]$ with bulky NHCs at room temperature, they were able to isolate various “acyl” trinuclear adducts of the type $[\text{Os}_3\{\text{C}(\text{O})\text{NHC}\}(\text{CO})_{11}]$ and to prove that these adducts slowly liberate CO to give $[\text{Os}_3(\text{NHC})(\text{CO})_{11}]$ derivatives. No mononuclear derivatives were formed in this case, probably because Os–Os bonds are quite strong, and hence cluster fission does not occur at mild temperatures.²⁴

50-Electron reaction intermediates of general formula $[\text{Ru}_3\text{L}(\text{CO})_{12}]$, which would result from the opening of an edge of the $[\text{Ru}_3(\text{CO})_{12}]$ metal triangle upon an associative attack of the incoming nucleophile (L) to a metal atom, have also been proposed to explain CO-substitution reactions in this cluster,²⁵ but intermediates of this type have never been experimentally verified.

Although we were unable to isolate or even detect the adducts formulated as $[\text{Ru}_3(\text{CO})_{12}]\cdot\mathbf{1}_R$ and $[\text{Ru}_3(\mathbf{1}_R)(\text{CO})_{11}]\cdot\mathbf{1}_R$ in Scheme 2, the participation of these species in the reactions studied in this contribution is clear because the processes that involve cluster fission are substrate-promoted. Given the similar characteristics (high basicity, large volume) of NHCs and the gerylenes used in this work, we believe that the “acyl” structures depicted in Figure 6 may well represent

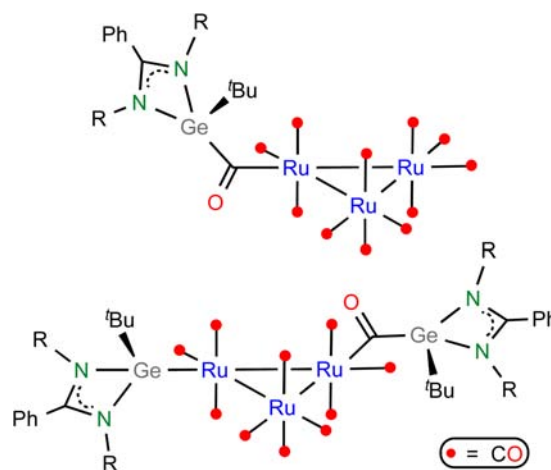


Figure 6. Proposed structures for the adducts labeled $[\text{Ru}_3(\text{CO})_{12}]\cdot\mathbf{1}_R$ (upper) and $[\text{Ru}_3(\mathbf{1}_R)(\text{CO})_{11}]\cdot\mathbf{1}_R$ (lower) in Scheme 2 ($R = t\text{Bu}, i\text{Pr}$).

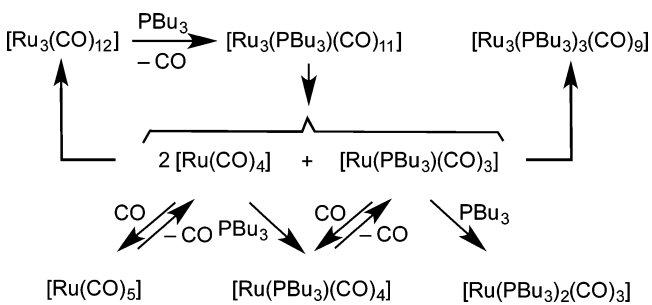
the structures of the adducts $[\text{Ru}_3(\text{CO})_{12}]\cdot\mathbf{1}_R$ and $[\text{Ru}_3(\mathbf{1}_R)(\text{CO})_{11}]\cdot\mathbf{1}_R$. These neutral zwitterionic species should have a negative charge at the metallic core and a positive charge at the acyl gerylene fragment.²³

Our proposal (Scheme 2) helps justify (a) why the mononuclear monogermylene complexes $[\text{Ru}(\mathbf{1}_R)(\text{CO})_4]$ ($\mathbf{2}_R$) were always the major products of the reactions of $[\text{Ru}_3(\text{CO})_{12}]$ with $\mathbf{1}_R$ at room temperature, regardless of the ratio of the reactants (Table 1, entries 1, 2, 14, and 15); (b) the

additional formation of smaller amounts of 3_R-6_R in the reactions of $[\text{Ru}_3(\text{CO})_{12}]$ with only 1 equiv of 1_R (Table 1, entries 1 and 14); (c) the fact that 2_{tBu} was the only product of the reaction of $[\text{Ru}_3(\text{CO})_{12}]$ with 1_{tBu} under CO (Table 1, entry 3); (d) the fact that 4_{tBu} was stable under CO (Table 1, entry 4) but reacted with 1_{tBu} to give 2_{tBu} and 3_{tBu} (Table 1, entries 5 and 6); (e) the fact that 4_{tBu} reacted with 1_{tBu} (Table 1, entries 5 and 6) to give higher yields of 3_{tBu} (compared with those of 2_{tBu}) than the reactions of $[\text{Ru}_3(\text{CO})_{12}]$ with 1_{tBu} (Table 1, entries 1 and 2).

Studying reactions of $[\text{Ru}_3(\text{CO})_{12}]$ with PBu_3 ($\text{Bu} = n$ -butyl), Poë and Twigg obtained $[\text{Ru}(\text{PBu}_3)(\text{CO})_4]$, $[\text{Ru}(\text{PBu}_3)_2(\text{CO})_3]$, and $[\text{Ru}_3(\text{PBu}_3)_3(\text{CO})_9]$ as reaction products in ratios that depended on the initial ratio of the reagents; high $[\text{Ru}_3(\text{CO})_{12}]$ -to- PBu_3 ratios led to more trinuclear product, while low ratios led to more mononuclear products.^{3f} When mainly mononuclear products were formed, a ca. 1:2 ratio of $[\text{Ru}(\text{PBu}_3)_2(\text{CO})_3]$ to $[\text{Ru}(\text{PBu}_3)(\text{CO})_4]$ was obtained, and this was justified by proposing that the cluster fission should occur in $[\text{Ru}_3(\text{PBu}_3)(\text{CO})_{11}]$ (this trinuclear complex was proposed as the first intermediate product, but it was not observed) to give “ $[\text{Ru}(\text{PBu}_3)(\text{CO})_3]$ ” and two “ $[\text{Ru}(\text{CO})_4]$ ” fragments that subsequently would react with PBu_3 to finally give $[\text{Ru}(\text{PBu}_3)_2(\text{CO})_3]$ and $[\text{Ru}(\text{PBu}_3)(\text{CO})_4]$ in a 1:2 ratio, whereas at high initial $[\text{Ru}_3(\text{CO})_{12}]$ to PBu_3 ratios the unsaturated “ $[\text{Ru}(\text{PBu}_3)(\text{CO})_3]$ ” and “ $[\text{Ru}(\text{CO})_4]$ ” species would have a strong tendency to trimerize rather than to add an additional ligand, preferably giving $[\text{Ru}_3(\text{PBu}_3)_3(\text{CO})_9]$ and $[\text{Ru}_3(\text{CO})_{12}]$ (Scheme 3).^{3f} However, Poë and Twigg’s

Scheme 3. Poë and Twigg’s Proposal to Explain the Reactivity of $[\text{Ru}_3(\text{CO})_{12}]$ with PBu_3



proposal (a) does not justify the cases in which the $[\text{Ru}_2(\text{CO})_3]$ to $[\text{RuL}(\text{CO})_4]$ ratios differ from 1:2 (as are the reactions described in this paper); (b) is also unable to rationalize why $[\text{Ru}_3\text{L}(\text{CO})_{11}]$ is stable under CO (Table 1, entry 4), since it predicts the formation of $[\text{RuL}(\text{CO})_4]$ and $[\text{Ru}_3(\text{CO})_{12}]$; and (c) does not explain why $[\text{Ru}_3(\text{CO})_{12}]$ does react with L in the presence of CO to give $[\text{RuL}(\text{CO})_4]$ (Table 1, entry 3), since $[\text{Ru}_3\text{L}(\text{CO})_{11}]$ should not be formed from $[\text{Ru}_3(\text{CO})_{12}]$ and L under CO.

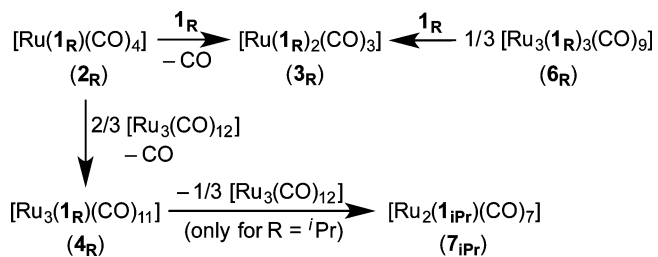
Subsequently, studying the reactions of the individual clusters $[\text{Ru}_3(\text{PBu}_3)_x(\text{CO})_{12-x}]$ ($x = 1-3$) with PBu_3 , Brodie and Poë demonstrated that all these clusters may undergo both formal CO-substitution (to give trinuclear derivatives) and associative cluster-scission (to give mononuclear derivatives) depending on the reaction conditions.^{3f}

Our proposal (Scheme 2) is not only compatible with the experimental results on the reactivity of $[\text{Ru}_3(\text{CO})_{12}]$ with PBu_3 but is also valid to explain the outcomes of reactions of $[\text{Ru}_3(\text{CO})_{12}]$ with other phosphines of high basicity (such as

PEt_2Ph ,^{3b} PEt_3 ,^{3b} PMePh_2 ,^{3d} and PCy_3 ,^{3d}), in which the formation of mononuclear products seems to be favored at room temperature (in each case, the product ratio should depend upon the ratio of the reactants and upon the rates of each particular reaction step, which, in turn, should depend upon the basicity and volume of the ligands). Less basic P-donor ligands, such as PPh_3 , $\text{P}(\text{O}i\text{Pr})_3$, or $\text{P}(\text{OCH}_2)_3\text{C}i\text{Pr}$ do not give mononuclear products at mild temperatures.^{3c} A kinetic analysis of the reaction of $[\text{Ru}_3(\text{CO})_{12}]$ with PPh_3 indicated that it follows a dissociative pathway.²⁶ Probably, PPh_3 may not be able to attack a coordinated CO and thus form the key adduct responsible for the fission of the trinuclear cluster under thermal conditions. However, upon UV irradiation, which favors metal–metal bond cleavage, the products of these reactions are $[\text{Ru}(\text{PR}_3)(\text{CO})_4]$ and $[\text{Ru}(\text{PR}_3)_2(\text{CO})_3]$.²⁷

Concerning room-temperature reactions of $[\text{Ru}_3(\text{CO})_{12}]$ with NHCs, some compounds of the types $[\text{Ru}(\text{NHC})_2(\text{CO})_3]$,^{4b} $[\text{Ru}(\text{NHC})(\text{CO})_4]$,^{4a} and $[\text{Ru}_3(\text{NHC})(\text{CO})_{11}]$ ^{4c-f} have been isolated using 1:6, 1:3, and 1:1, reactant ratios, respectively, but inseparable mixtures of products have been reported to be formed when other reactant ratios were used. These results can be explained if all the initial reaction adduct “ $[\text{Ru}_3(\text{CO})_{12}]\cdot\text{NHC}$ ” evolves toward $[\text{Ru}(\text{NHC})(\text{CO})_4]$ and $2/3[\text{Ru}_3(\text{CO})_{12}]$ (Scheme 2) and if $[\text{Ru}(\text{NHC})(\text{CO})_4]$ is able to react with more NHC to give $[\text{Ru}(\text{NHC})_2(\text{CO})_3]$. If there is no more NHC available, $[\text{Ru}(\text{NHC})(\text{CO})_4]$ may react with $[\text{Ru}_3(\text{CO})_{12}]$ to give $[\text{Ru}_3(\text{NHC})(\text{CO})_{11}]$. In our case, we observed similar reactions, albeit at a higher temperature, between 2_{tBu} and 1_{tBu} to give 3_{tBu} (Table 1, entry 11; Scheme 4), and between 2_{tBu} and $[\text{Ru}_3(\text{CO})_{12}]$, to give 4_{tBu} (Table 1,

Scheme 4. Reactions Involving Germylene-Containing Ruthenium Carbonyl Complexes That Do Not Occur at Room Temperature but Take Place at 90–100 °C



entry 9; Scheme 4). The higher basicity of NHCs may allow these reactions to occur at room temperature. This proposal also explains why no trinuclear $[\text{Ru}_3(\text{NHC})(\text{CO})_{11}]$ complexes were formed when 1:3 and 1:6 ratios of $[\text{Ru}_3(\text{CO})_{12}]$ to NHC were used. Above room temperature, the reactions of $[\text{Ru}_3(\text{CO})_{12}]$ with NHCs are known to give cyclometalated derivatives that arise from intramolecular C–H and C–N bond-activation processes.^{4c,d,f,28}

High-Temperature Reactions. At higher temperatures, additional processes having higher activation barriers are also possible. In fact, the outcomes of reactions of $[\text{Ru}_3(\text{CO})_{12}]$ with different amounts of 1_R at 90–100 °C (Table 1, entries 8–12 and 16–18) were very different from those obtained at room temperature. Scheme 4 clearly indicates that the mononuclear digermylene 3_R is the thermodynamically controlled product when an excess of 1_R is available, no matter whether the ruthenium starting material is $[\text{Ru}_3(\text{CO})_{12}]$ or 2_R-6_R , because both 2_R and 6_R were transformed at 90–100 °C

into 3_R in the presence of 1_R . In the absence of free germylene, 2_R reacted with $[\text{Ru}_3(\text{CO})_{12}]$ at 100 °C to give 4_R (Table 1, entry 9), while 4_{tBu} was stable at the working temperature, 4_{iPr} spontaneously decomposed to give the binuclear derivative 7_{iPr} and $1/3[\text{Ru}_3(\text{CO})_{12}]$ (Table 1, entry 17). Therefore, the thermodynamically controlled products at high $[\text{Ru}_3(\text{CO})_{12}]$ -to- 1_{tBu} or -1_{iPr} ratios (≥ 1) are 4_{tBu} or 7_{iPr} , respectively.

The discovery that trinuclear complexes of the type $[\text{Ru}_3\text{L}(\text{CO})_{11}]$ may in many cases arise from the condensation of mononuclear $[\text{RuL}(\text{CO})_4]$ complexes with $2/3[\text{Ru}_3(\text{CO})_{12}]$ and not from a direct CO-substitution reaction on $[\text{Ru}_3(\text{CO})_{12}]$ is a very important result because, despite the great amount of work already done on reactions of $[\text{Ru}_3(\text{CO})_{12}]$ with two-electron-donor reagents, such a process has never been observed or even proposed before, although it rationalizes hitherto unexplained experimental results. As commented above, the selective formation of trinuclear $[\text{Ru}_3(\text{NHC})(\text{CO})_{11}]$ complexes upon treatment of $[\text{Ru}_3(\text{CO})_{12}]$ with various NHCs in 1:1 mol ratio^{4c} can be explained if the initially formed mononuclear $[\text{Ru}(\text{NHC})(\text{CO})_4]$ species are able to react with $2/3[\text{Ru}_3(\text{CO})_{12}]$ to give $[\text{Ru}_3(\text{NHC})(\text{CO})_{11}]$. This type of reaction also explains why the room-temperature treatment of $[\text{Ru}_3(\text{CO})_{12}]$ with PBU_3 at a high reactant ratio (≥ 1) leads predominantly to mononuclear products but to trinuclear products at higher temperatures.^{3f}

In previous works, using the HMDS-substituted germynes $\text{Ge}(\text{R}_2\text{bzam})(\text{HMDS})$ as starting reagents, we have demonstrated that steric factors are responsible for the instability of binuclear germylene-bridged derivatives similar to 7_{iPr} when both R groups of the R_2bzam fragment are *tert*-butyl groups (the amidinate N–R groups are very close to the amidinate phenyl ring).^{13,14} The same steric factors are valid to explain why the *tert*-butyl analogue of 7_{iPr} (7_{tBu}) cannot be not prepared.

CONCLUSIONS

The study of the reactivity of $[\text{Ru}_3(\text{CO})_{12}]$ with the amidinatogermynes 1_R ($R = \text{tBu}$ and iPr), in addition to extending the coordination chemistry of amidinatogermynes to mononuclear (2_R and 3_R) and trinuclear (4_R , 5_R , and 6_R) ruthenium carbonyl derivatives, has allowed the observation of a wide reaction panorama that includes the relationships between all the possible reaction products at room (Scheme 2) and at higher (Scheme 4) temperatures.

At room temperature, the mononuclear derivatives 2_R and 3_R are formed by associative cluster-fission from $[\text{Ru}_3(\text{CO})_{12}]$ (2_R) and 4_R (2_R and 3_R), while 4_R and 5_R are formed by direct (presumably associative) CO-substitution reactions from $[\text{Ru}_3(\text{CO})_{12}]$ and 4_R , respectively. The trinuclear trigermylene derivative 6_R can be formed from 5_R (by direct CO-substitution) or from 4_R (by associative cluster scission and trimerization of the resulting unsaturated mononuclear “[$\text{Ru}(\text{I}_R)\text{CO}_3$]” species). Of particular interest is the reaction of $[\text{Ru}_3(\text{CO})_{12}]$ with 1_{tBu} under CO at room temperature, which, giving 2_{tBu} , has demonstrated that this mononuclear species can be formed directly from $[\text{Ru}_3(\text{CO})_{12}]$ by an associative cluster-fission process.

At higher temperatures (90–100 °C), both 2_R and 6_R lead to 3_R in the presence of excess of 1_R . These reactions are valid in explaining why the mononuclear digermynes 3_R are the final products of high-temperature reactions using low $[\text{Ru}_3(\text{CO})_{12}]$ -to- 1_R ratios ($\leq 1/6$). However, the final products of reactions performed at 90 °C using high $[\text{Ru}_3(\text{CO})_{12}]$ -to- 1_R ratios (≥ 1)

are the trinuclear monogermylene derivative 4_{tBu} or the binuclear monogermylene derivative 7_{iPr} , depending on the nature of 1_R ($R = \text{tBu}$ or iPr). Of particular interest are the reactions of 2_R with $[\text{Ru}_3(\text{CO})_{12}]$ at 90 °C, which give 4_R (while 4_{tBu} is stable, 4_{iPr} subsequently leads to 7_{iPr}) because the reaction of a mononuclear complex of the type $[\text{RuL}(\text{CO})_4]$ with $[\text{Ru}_3(\text{CO})_{12}]$ has never been observed before for other two-electron-donor reagents, although it explains why trinuclear derivatives of the type $[\text{Ru}_3\text{L}(\text{CO})_{11}]$ ($L = \text{triarylphosphine, NHC}$) are the thermodynamically controlled products of reactions involving $[\text{Ru}_3(\text{CO})_{12}]$ to L in ratios ≥ 1 .

Finally, Schemes 2 and 4, in addition to summarizing and explaining the results reported in this paper, can also be used as a general tool to rationalize previously reported reactions of $[\text{Ru}_3(\text{CO})_{12}]$ with different amounts of other two-electron-donor reagents of high basicity (L), such as trialkylphosphines and NHCs.

EXPERIMENTAL SECTION

General Procedures. Solvents were dried over appropriate desiccating reagents and were distilled and kept under argon before use. All reactions were performed under argon, using drybox and/or Schlenk vacuum line techniques and were routinely monitored by solution IR spectroscopy. The germynes $\text{Ge}(\text{tPr}_2\text{bzam})\text{tBu}$ (1_{iPr})^{11a} and $\text{Ge}(\text{tBu}_2\text{bzam})\text{Cl}$ ²⁹ were prepared following published procedures. All remaining reagents were purchased from commercial sources. A selection of the reactions discussed in this work is collected in Table 1. Selected synthetic procedures are given below. All reaction products were vacuum-dried for several hours prior to being weighted and analyzed. NMR spectra were run on a Bruker DPX-300 instrument; a residual protic solvent resonance was used as reference for ^1H [$\delta(\text{C}_6\text{H}_5\text{D}_5) = 7.16$ ppm; $\delta(\text{C}_6\text{D}_5\text{CHD}_2) = 2.08$ ppm], whereas a solvent resonance was used as reference for ^{13}C [$\delta(\text{C}_6\text{D}_6) = 128.1$ ppm; $\delta(\text{C}_6\text{D}_5\text{CD}_3) = 20.4$ ppm]. Microanalyses were obtained from a PerkinElmer 2400 microanalyzer. Mass spectra (MS) were run on a VG Autospec double-focusing mass spectrometer operating in the fast-atom bombardment (FAB+) mode; ions were produced with a standard Cs^+ gun at ~ 30 kV; 3-nitrobenzyl alcohol was used as matrix; data given correspond to the most abundant isotopomer of the molecular ion or of the greatest mass fragment.

$\text{Ge}(\text{tBu}_2\text{bzam})\text{tBu}$ (1_{tBu}). A dibutyl ether solution of Li^+tBu (6.0 mL, 1.7 M, 10.2 mmol) was added to a cold (-78 °C) solution of $\text{Ge}(\text{tBu}_2\text{bzam})\text{Cl}$ (3.43 g, 10.1 mmol) in diethyl ether (30 mL). The resulting suspension was allowed to warm to room temperature, and then it was stirred for 6 h. The solvents were removed under reduced pressure, and the residue was extracted into hexane (3×30 mL). The filtrate was evaporated to dryness under vacuum to give 1_{tBu} as a yellowish powder (3.07 g, 84%). Anal. Calcd for $\text{C}_{19}\text{H}_{32}\text{GeN}_2$ ($M_w = 361.08$): C, 63.20; H, 8.93; N, 7.76. Found: C, 63.22; H, 8.95; N, 7.1%. ^1H NMR (C_6D_6 , 300.1 MHz, 293 K): δ 7.14–6.95 (m, 5 H, 5 CH of Ph), 1.40 (s, 9 H, 3 Me of tBu), 1.03 (s, 18 H, 6 Me of 2 tBu). $^{13}\text{C}\{^1\text{H}\}$ NMR (C_6D_6 , 75.5 MHz, 293 K): δ 165.4 (s, NCN), 136.9 (C_{ipso} of Ph), 130.1 (s, CH of Ph), 129.3 (CH of Ph), 129.1 (CH of Ph), 127.7 (CH of Ph), 127.4 (CH of Ph), 52.7 (2 C of 2 tBu), 32.5 (6 Me of 2 tBu), 31.3 (C of tBu), 28.7 (3 Me of tBu).

$[\text{Ru}(\text{tBu})_4(\text{CO})_4]$ (2_{tBu}) and $[\text{Ru}(\text{tBu})_2(\text{CO})_3]$ (3_{tBu}). A toluene solution of 1_{tBu} (1.10 mL, 0.30 M, 0.330 mmol) was added to a toluene (8 mL) suspension of $[\text{Ru}_3(\text{CO})_{12}]$ (50 mg, 0.080 mmol), and the mixture was stirred at room temperature for 1 h. The initial orange color changed to red. The crude reaction solution was concentrated to ca. 2 mL and was placed at -20 °C. Some crystals appeared after 1 d, which were filtered, washed with hexane (2×5 mL), and dried in vacuum to give 3_{tBu} as a white solid (58 mg, 27%). The filtered solution was evaporated to dryness under reduced pressure to give a solid residue that was washed with hexane (2×5 mL) to give 2_{tBu} as a red solid (84 mg, 61%). A greater yield of 3_{tBu} was obtained by heating a mixture of $[\text{Ru}_3(\text{CO})_{12}]$ (25 mg, 0.040 mmol) and 1_{tBu} (1.10 mL of

a 0.30 M solution in toluene, 0.330 mmol) in toluene (8 mL) at 100 °C for 3 h. The initial orange color changed to light red. The solvents were removed under reduced pressure, and the residue was washed with hexane (2 × 5 mL) and dried in vacuum (95 mg, 88%). *Data for 2_{tBu}*: Anal. Calcd for C₂₃H₃₂GeN₂O₄Ru (*M_w* = 574.20): C, 48.11; H, 5.62; N, 4.88. Found: C, 48.15; H, 5.65; N, 4.84%. (+)-FAB MS: *m/z* 574 [*M*]⁺. IR (toluene, cm⁻¹): ν_{CO} 2042 (s), 1965 (m), 1933 (vs), 1924 (br, vs). ¹H NMR (C₆D₆, 300.1 MHz, 293 K): δ 7.38 (m, 1 CH of Ph), 7.04–6.87 (m, 4 H, 4 CH of Ph), 1.33 (s, 9 H, 3 Me of ^tBu), 1.01 (s, 18 H, 6 Me of 2 ^tBu). ¹³C{¹H} NMR (C₆D₆, 75.5 MHz, 293 K): δ 207.8 (COs), 169.8 (NCN), 133.3 (C_{ipso} of Ph), 130.1–127.7 (5 CH of Ph), 54.6 (2 C of 2 ^tBu), 37.0 (C of ^tBu), 32.0 (6 Me of 2 ^tBu), 27.8 (3 Me of ^tBu). *Data for 3_{tBu}*: Anal. Calcd for C₄₁H₆₄Ge₂N₄O₃Ru (*M_w* = 907.26): C, 54.28; H, 7.11; N, 6.18. Found: C, 54.32; H, 7.17; N, 6.09%. (+)-FAB MS: *m/z* 908 [*M*]⁺. IR (toluene, cm⁻¹): ν_{CO} 1937 (w), 1868 (vs), 1852 (vs). ¹H NMR (C₆D₆, 300.1 MHz, 293 K): δ 7.73 (m, H, CH of Ph), 7.09–6.89 (m, 4 H, 4 CH of Ph), 1.60 (s, 9 H, 3 Me of ^tBu), 1.27 (s, 18 H, 6 Me of 2 ^tBu). ¹³C{¹H} NMR (C₆D₆, 75.5 MHz, 293 K): δ 213.6 (COs), 168.1 (NCN), 134.8 (C_{ipso} of Ph), 130.3–127.6 (5 CH of Ph), 54.2 (2 C of 2 ^tBu), 36.9 (C of ^tBu), 32.3 (6 Me of 2 ^tBu), 28.2 (3 Me of ^tBu) ppm.

[Ru(1_{iPr})(CO)₄] (2_{iPr}) and [Ru(1_{iPr})₂(CO)₃] (3_{iPr}). A toluene solution of 1_{iPr} (1.30 mL, 0.25 M, 0.325 mmol) was added to a toluene (8 mL) suspension of [Ru₃(CO)₁₂] (50 mg, 0.080 mmol), and the mixture was stirred at room temperature for 1 h. The initial orange color changed to dark orange. The crude reaction solution was concentrated to ca. 2 mL and placed at –20 °C for 3 d. A crystalline solid precipitated, which was filtered, washed with hexane (2 × 5 mL), and dried in vacuum to give 3_{iPr} as an off-white solid (65 mg, 32%). The filtered solution was evaporated to dryness to give a solid residue that was washed with hexane (2 × 5 mL) and dried in vacuum to give 2_{iPr} as a dark orange solid (81 mg, 62%). A greater yield of 3_{iPr} was obtained by heating a mixture of [Ru₃(CO)₁₂] (25 mg, 0.040 mmol) and 1_{iPr} (1.30 mL of a 0.25 M solution in toluene, 0.330 mmol) in toluene (8 mL) at 100 °C for 3 h. The initial orange color remained unchanged. The solvents were removed under reduced pressure, and the residue was washed with hexane (2 × 5 mL) and dried in vacuum (97 mg, 95%). *Data for 2_{iPr}*: Anal. Calcd for C₂₁H₂₈GeN₂O₄Ru (*M_w* = 546.14): C, 46.18; H, 5.17; N, 5.13. Found: C, 46.23; H, 5.21; N, 5.09%. (+)-FAB MS: *m/z* 546 [*M*]⁺. IR (toluene, cm⁻¹): ν_{CO} 2043 (s), 1966 (m), 1927 (vs). ¹H NMR (C₇D₈, 300.1 MHz, 293 K): δ 7.08–6.97 (m, 5 H, 5 CH of Ph), 3.36 (m, 2 H, 2 CH of 2 ⁱPr), 1.29 (s, 9 H, 3 Me of ^tBu), 1.14 (d, *J* = 6.5 Hz, 6 H, 2 Me of ⁱPr), 0.85 (d, *J* = 6.5 Hz, 6 H, 2 Me of ⁱPr). ¹³C{¹H} NMR (C₇D₈, 75.5 MHz, 293 K): δ 207.4 (COs), 169.8 (NCN), 129.3–127.3 (C_{ipso} + 5 CH of Ph), 47.9 (2 CH of 2 ⁱPr), 36.8 (s, C of ^tBu), 26.7 (3 Me of ^tBu), 26.7 (2 Me of ⁱPr), 26.5 (2 Me of ⁱPr). *Data for 3_{iPr}*: Anal. Calcd (%) for C₃₇H₅₆Ge₂N₄O₃Ru (*M_w* = 851.16): C, 52.21; H, 6.63; N, 6.58. Found: C, 52.26; H, 6.68; N, 6.56. (+)-FAB MS: *m/z* 852 [*M*]⁺. IR (toluene, cm⁻¹): ν_{CO} 1939 (w), 1867 (vs), 1853 (vs). ¹H NMR (C₆D₆, 300.1 MHz, 293 K): δ 7.13–7.07 (m, 5 H, 5 CH of Ph), 3.54 (m, 2 H, 2 CH of 2 ⁱPr), 1.53 (s, 9 H, 3 Me of ^tBu), 1.43 (d, *J* = 6.5 Hz, 6 H, 2 Me of ⁱPr), 1.04 (d, *J* = 6.5 Hz, 6 H, 2 Me of ⁱPr). ¹³C{¹H} NMR (C₆D₆, 75.5 MHz, 293 K): δ 212.9 (COs), 168.1 (NCN), 130.4–127.7 (C_{ipso} + 5 CH of Ph), 47.8 (2 CH of 2 ⁱPr), 36.6 (C of ^tBu), 26.9 (3 Me of ^tBu), 25.0 (2 Me of ⁱPr), 24.7 (2 Me of ⁱPr).

[Ru₃(1_{tBu})(CO)₁₁] (4_{tBu}) and [Ru₃(1_{tBu})₂(CO)₁₀] (5_{tBu}). A toluene solution of 1_{tBu} (0.3 mL of a 0.30 M, 0.090 mmol) was added to a toluene (8 mL) suspension of [Ru₃(CO)₁₂] (50 mg, 0.080 mmol), and the mixture was heated at 90 °C for 2 h. The initial orange color changed to dark red. Purification by flash chromatography (2 × 5 cm silica gel column packed in hexane) eluting with hexane (20 mL) and hexane/CH₂Cl₂ (3:1) (20 mL) afforded 4_{tBu} which was isolated as a light red solid (55 mg, 71%). Subsequent elution of the column with hexane/CH₂Cl₂ (2:1) (20 mL) and hexane/CH₂Cl₂ (1:1) (20 mL) separated 5_{tBu} which was isolated as a dark red solid (15 mg, 14%). *Data for 4_{tBu}*: Anal. Calcd for C₃₀H₃₂GeN₂O₁₁Ru₃ (*M_w* = 972.40): C, 37.05; H, 3.32; N, 2.88. Found: C, 37.21; H, 3.41; N, 2.84%. (+)-FAB MS: *m/z* 974 [*M*]⁺. IR (toluene, cm⁻¹): ν_{CO} 2091 (m), 2040 (s), 2017 (s), 2007 (vs), 1980 (m), 1934 (w), 1921 (w). ¹H NMR (C₆D₆, 300.1

MHz, 293 K): δ 7.25 (m, 1 H, 1 CH of Ph), 6.98–6.88 (m, 4 CH of Ph), 1.31 (s, 9 H, 3 Me of ^tBu), 0.96 (s, 18 H, 6 Me of 2 ^tBu). ¹³C{¹H} NMR (C₆D₆, 75.5 MHz, 293 K): δ 205.0 (COs), 170.9 (NCN), 133.0 (C_{ipso} of Ph), 130.2–127.6 (5 CH of Ph), 54.3 (2 C of 2 ^tBu), 38.0 (C of ^tBu), 32.1 (6 Me of 2 ^tBu), 27.8 (3 Me of ^tBu) ppm. *Data for 5_{tBu}*: Anal. Calcd for C₄₈H₆₄Ge₂N₄O₁₀Ru₃ (*M_w* = 1305.47): C, 44.16; H, 4.94; N, 4.29. Found: C, 44.20; H, 4.98; N, 4.14%. (+)-FAB MS: *m/z* 1305 [*M*]⁺. IR (toluene, cm⁻¹): ν_{CO} 2061 (m), 2002 (s), 1981 (vs, br), 1938 (m, br). ¹H NMR (C₆D₆, 300.1 MHz, 293 K): δ 7.38 (m, 1 H, 1 CH of Ph), 7.00–6.86 (m, 4 H, 4 CH of Ph), 1.47 (s, 9 H, 3 Me of ^tBu), 1.10 (s, 18 H, 6 Me of 4 ^tBu). ¹³C{¹H} NMR (C₆D₆, 75.5 MHz, 293 K): δ 210.6 (COs), 170.0 (NCN), 133.8 (C_{ipso} of Ph), 130.4–127.4 (5 CH of Ph), 54.1 (2 C of 2 ^tBu), 37.9 (C of ^tBu), 32.3 (6 Me of 2 ^tBu), 28.1 (3 Me of ^tBu).

[Ru₃(1_{tBu})₃(CO)₉] (6_{tBu}). A toluene solution of 1_{tBu} (0.55 mL of a 0.30 M, 0.165 mmol) was added to a solution of [Ru₃(1_{tBu})₂(CO)₁₀] (5_{tBu}) (50 mg, 0.038 mmol) in toluene (8 mL), and the mixture was stirred at room temperature for 1 h. The initial red color remained unchanged. Purification by flash chromatography (2 × 5 cm silica gel column packed in hexane) eluting with hexane/CH₂Cl₂ (2:1) (20 mL) and hexane/CH₂Cl₂ (1:1) (30 mL) furnished 6_{tBu} as a dark red solid (49 mg, 79%). Anal. Calcd (%) for C₆₆H₉₆Ge₃N₆O₉Ru₃ (*M_w* = 1638.54): C, 48.38; H, 5.91; N, 5.13. Found: C, 48.50; H, 6.00; N, 5.09. (+)-FAB MS: *m/z* 1639 [*M*]⁺. IR (toluene, cm⁻¹): ν_{CO} 2020 (w), 1954 (vs), 1946 (vs), 1921 (vs). ¹H NMR (C₇D₈, 300.1 MHz, 293 K): δ 7.55 (m, 1 H, 1 CH of Ph), 7.11–6.86 (m, 4 H, 4 CH of Ph), 1.59 (s, 9 H, 3 Me of ^tBu), 1.21 (s, 18 H, 6 Me of 3 ^tBu). ¹³C{¹H} NMR (C₇D₈, 75.5 MHz, 293 K): δ 215.9 (COs), 169.2 (NCN), 134.5 (C_{ipso} of Ph), 130.9–127.3 (5 CH of Ph), 53.9 (2 C of 2 ^tBu), 38.1 (C of ^tBu), 32.5 (6 Me of 2 ^tBu), 28.6 (3 Me of ^tBu).

[Ru₃(1_{iPr})₃(CO)₉] (6_{iPr}). A toluene solution of 1_{iPr} (1.40 mL, 0.24 M, 0.336 mmol) was added to a solution of [Ru₃(CO)₁₂] (50 mg, 0.080 mmol) in 8 mL of toluene, and the mixture was stirred at room temperature for 1 h. The initial orange color turned to dark orange. Purification by flash chromatography (2 × 3 cm silica gel column packed in hexane) eluting with CH₂Cl₂ (20 mL) furnished 6_{iPr} as an orange solid (8 mg, 6%). Anal. Calcd for C₆₀H₈₄Ge₃N₆O₉Ru₃ (*M_w* = 1554.38): C, 46.36; H, 5.45; N, 5.41. Found: C, 46.56; H, 5.66; N, 5.40%. (+)-FAB MS: *m/z* 1554 [*M*]⁺. IR (toluene, cm⁻¹): ν_{CO} 2025 (w), 1962 (vs), 1955 (vs), 1925 (vs). ¹H NMR (C₆D₆, 300.1 MHz, 293 K): δ 6.99 (m, 5 H, 5 CH of Ph), 3.49 (m, 2 H, 2 CH of 2 ⁱPr), 1.58 (s, 9 H, 3 Me of ^tBu), 1.31 (d, *J* = 6.6 Hz, 6 H, 2 Me of ⁱPr), (d, *J* = 6.6 Hz, 6 H, 2 Me of ⁱPr). The ¹³C{¹H} NMR spectrum of this compound could not be obtained due to insufficient amount of sample.

[Ru₂(μ-κ²-Ge,N-1_{iPr})(CO)₇] (7_{iPr}). A toluene solution of 1_{iPr} (0.3 mL, 0.35 M, 0.105 mmol) was added to a toluene (8 mL) suspension of [Ru₃(CO)₁₂] (50 mg, 0.080 mmol), and the mixture was stirred at 90 °C for 2 h. The initial orange color changed to dark red. Purification by flash chromatography (2 × 5 cm silica gel column packed in hexane) eluting with hexane (20 mL) and hexane/CH₂Cl₂ (1:1) (20 mL) afforded 7_{iPr} which was isolated as a light red solid (52 mg, 59%). Anal. Calcd for C₂₄H₂₈GeN₂O₇Ru₂ (*M_w* = 731.24): C, 39.42; H, 3.86; N, 3.83. Found: C, 39.47; H, 3.89; N, 3.80%. (+)-FAB MS: *m/z* = 676 [*M* – 2CO]⁺. IR (toluene, cm⁻¹): ν_{CO} 2081 (m), 2028 (vs), 2005 (s), 1999 (s), 1981 (m), 1950 (m). ¹H NMR (C₆D₆, 300.1 MHz, 293 K): δ = 6.91–6.85 (m, 4 H, 4 CH of Ph), 6.60 (m, 1 H, 1 CH of Ph), 3.71 (m, 1 H, CH of ⁱPr), 3.34 (m, 1 H, CH of ⁱPr), 1.46 (s, 9 H, 3 Me of ^tBu), 1.15 (d, *J* = 6.6 Hz, 3 H, Me of ⁱPr), 0.93 (d, *J* = 6.9 Hz, 3 H, Me of ⁱPr), 0.80 (d, *J* = 6.5 Hz, 3 H, Me of ⁱPr), 0.65 (d, *J* = 7.0 Hz, 3 H, Me of ⁱPr). ¹³C{¹H} NMR (C₆D₆, 75.5 MHz, 293 K): δ 202.7 (COs), 202.6 (COs), 202.4 (COs), 201.3 (COs), 169.8 (NCN), 137.1 (C_{ipso} of Ph), 128.6–126.5 (5 CH of Ph), 55.0 (CH of ⁱPr), 51.9 (CH of ⁱPr), 40.6 (C of ^tBu), 30.6 (3 Me of ^tBu), 26.1 (Me of ⁱPr), 24.1 (Me of ⁱPr), 22.9 (Me of ⁱPr), 22.2 (Me of ⁱPr).

X-ray Diffraction Analyses. Diffraction data were collected on Oxford Diffraction Xcalibur Onyx Nova (3_{iPr}, 6_{iPr}-C₇H₈, and 7_{iPr}; Cu Kα radiation) and Xcalibur Ruby Gemini (4_{tBu}; Mo Kα radiation) single-crystal diffractometers. Empirical absorption corrections were applied using the SCALE3 ABSPACK algorithm as implemented in

CrysAlisPro RED.³⁰ The structures were solved using SIR-97.³¹ Isotropic and full matrix anisotropic least-squares refinements were performed using SHELXL.³² All non-H atoms were refined anisotropically. The toluene solvent molecule and two of the isopropyl groups (C20 and C45 are their methyne carbon atoms) of $6_{\text{IPr}}\text{-C}_7\text{H}_8$ were found disordered over two positions in 66:34, 57:43, and 53:47 ratios, respectively. Restraints were applied on the thermal and geometrical parameters of the atoms involved in this positional disorder. All H atoms were set in calculated positions and refined riding on their parent atoms. The WINGX program system³³ was used throughout the structure determinations. A selection of crystal, measurement, and refinement data is given in Table S1 of the Supporting Information. CCDC deposition numbers: 1032651 (3_{IPr}), 1032652 (4_{IBu}), 1032653 ($6_{\text{IPr}}\text{-C}_7\text{H}_8$), and 1032654 (7_{IPr}).

Computational Details. DFT calculations were performed using the wB97XD functional,³⁴ which includes the second generation of Grimme's dispersion interaction correction³⁵ as well as long-range interactions effects. This functional was chosen because it provided the best overall performance in a study that compared its efficiency in reproducing the X-ray diffraction molecular structures of 3_{IPr} , 4_{IBu} , 6_{IPr} , and 7_{IPr} with those of the two popular density functionals B3LYP³⁶ and M06.³⁷ The wB97XD functional reproduces the local coordination geometry of transition metal compounds very well, and it also corrects the systematic overestimation of nonbonded distances seen for all the density functionals that do not include estimates of dispersion.³⁸ The LanL2DZ basis set,³⁹ with relativistic effective core potentials, was used for the Ru and Ge atoms. The basis set used for the remaining atoms was the 6-31G(d,p).⁴⁰ All stationary points were fully optimized in gas phase and confirmed as energy minima by analytical calculation of frequencies (all positive eigenvalues). The electronic energies of the optimized structures were used to calculate the zero-point corrected energies and the enthalpic and entropic contributions via vibrational frequency calculations. Solvation free energies were obtained from the gas-phase calculations using the self-consistent reaction field approximation to the standard continuum solvation model (CPCM).^{41,42} Free energies of reactions (Table 3) were obtained using the Born–Haber thermodynamic cycle. All calculations were performed with the Gaussian09 package.⁴³ DFT-calculated atomic coordinates of all the DFT-optimized structures are given in the Supporting Information file (Tables S2–S12).

■ ASSOCIATED CONTENT

■ Supporting Information

Figures containing ^1H and ^{13}C NMR spectra, crystallographic data (including CIF files), and atomic coordinates of all the DFT-optimized structures. This material is available free of charge via the Internet at <http://pubs.acs.org>.

■ AUTHOR INFORMATION

■ Corresponding Authors

*E-mail: jac@uniovi.es. (J.A.C.)

*E-mail: pga@uniovi.es. (P.G.-A.)

■ Notes

The authors declare no competing financial interest.

■ ACKNOWLEDGMENTS

This work was supported by a European Union Marie Curie reintegration grant (No. FP7-2010-RG-268329) and by Spanish MINECO-FEDER research grants (Nos. CTQ2010-14933, MAT2013-40950-R, CTQ2013-40619-P, and RYC-2012-10491).

■ REFERENCES

(1) For a review on the reactivity of $[\text{Ru}_3(\text{CO})_{12}]$ with triorganophosphines, see: Bruce, M. I. In *Comprehensive Organometallic Chemistry*; Wilkinson, G., Stone, F. G. A., Abel, E. W., Bruce, M. I., Eds.; Pergamon: Oxford, U.K., 1982; Vol. 4, pp 843–888.

(2) For a review on the reactivity of $[\text{Ru}_3(\text{CO})_{12}]$ with NHCs, see: Cabeza, J. A.; García-Álvarez, P. *Chem. Soc. Rev.* **2011**, *40*, 5389–5405.

(3) (a) Piacenti, F.; Bianchi, M.; Benedetti, E.; Sbrana, G. *J. Inorg. Nucl. Chem.* **1967**, *29*, 1389–1391. (b) Candlin, J. P.; Shortland, A. C. *J. Organomet. Chem.* **1969**, *16*, 289–299. (c) Bennett, R. L.; Bruce, M. I.; Stone, F. G. A. *J. Organomet. Chem.* **1972**, *38*, 325–334. (d) Bruce, M. I.; Shaw, G.; Stone, F. G. A. *J. Chem. Soc., Dalton Trans.* **1972**, 2094–2099. (e) Poë, A. J.; Twigg, M. V. *J. Chem. Soc., Dalton Trans.* **1974**, 1860–1866. (f) Poë, A. J.; Twigg, M. V. *Inorg. Chem.* **1974**, *13*, 2982–2985. (g) Brodie, N. M. J.; Poë, A. J. *Inorg. Chem.* **1988**, *27*, 3156–3159.

(4) (a) Bruce, M. I.; Cole, M. L.; Fung, R. S. C.; Forsyth, C. M.; Hilder, M.; Junk, P. C.; Konstas, K. *Dalton Trans.* **2008**, 4118–4128. (b) Ellul, C. E.; Saker, O.; Mahon, M. F.; Apperley, D. C.; Whittlesey, M. K. *Organometallics* **2008**, *27*, 100–108. (c) Crittall, M. R.; Ellul, C. E.; Mahon, M. F.; Saker, O.; Whittlesey, M. K. *Dalton Trans.* **2008**, 4209–4211. (d) Ellul, C. E.; Mahon, M. F.; Saker, O.; Whittlesey, M. K. *Angew. Chem., Int. Ed.* **2007**, *46*, 6343–6345. (e) Cabeza, J. A.; del Río, I.; Miguel, D.; Pérez-Carreño, E.; Sánchez-Vega, M. G. *Organometallics* **2008**, *27*, 211–217. (f) Zhang, C.; Li, B.; Song, H.; Xu, S.; Wang, B. *Organometallics* **2011**, *30*, 3029–3036.

(5) See, for example: (a) Alper, H.; Amaratunga, S. *Tetrahedron Lett.* **1980**, *21*, 2603–2604. (b) Blum, Y.; Reshef, D.; Shvo, Y. *Tetrahedron Lett.* **1980**, *22*, 1541–1544. (c) Cenini, S.; Crotti, C.; Pizzotti, M.; Porta, F. *J. Org. Chem.* **1988**, *53*, 1243–1250. (d) Ragaini, F.; Cenini, S.; Tollari, S.; Tummolillo, G.; Beltrami, R. *Organometallics* **1999**, *18*, 928–942. (e) Ragaini, F.; Cenini, S. *Organometallics* **1999**, *18*, 4925–4933. (f) Tobisu, M.; Chatani, N.; Asaumi, T.; Amako, K.; Fukumoto, Y.; Ie, Y.; Murai, S. *J. Am. Chem. Soc.* **2000**, *122*, 12663–12674. (g) Pinggen, D.; Müller, C.; Vogt, D. *Angew. Chem., Int. Ed.* **2010**, *49*, 8130–8133. (h) Wu, L.; Fleischer, I.; Jackstell, R.; Profir, I.; Franke, R.; Beller, M. *J. Am. Chem. Soc.* **2013**, *135*, 14306–14312.

(6) Lee, V. Y.; Sekiguchi, A. *Organometallic Compounds of Low Coordinate Si, Ge, Sn and Pb: From Phantom Species to Stable Compounds*; Wiley-VCH: Chichester, U.K., 2010.

(7) For recent reviews on the synthesis and general chemistry of HTs, see: (a) Izod, K. *Coord. Chem. Rev.* **2013**, *257*, 924–945. (b) Xiong, Y.; Yao, S.; Driess, M. *Angew. Chem., Int. Ed.* **2013**, *52*, 4302–4311. (c) Mandal, S. K.; Roesky, H. W. *Acc. Chem. Res.* **2012**, *45*, 298–307. (d) Yao, S.; Xiong, Y.; Driess, M. *Organometallics* **2011**, *30*, 1748–1767. (e) Mizuhata, Y.; Sasamori, T.; Tokitoh, N. *Chem. Rev.* **2009**, *109*, 3479–3511.

(8) For recent reviews on the derivative chemistry of HTs, including TM complexes, see: (a) Blom, B.; Stoelzel, M.; Driess, M. *Chem.—Eur. J.* **2013**, *19*, 40–62. (b) Ghadwal, R. S.; Azhakar, R.; Roesky, H. W. *Acc. Chem. Res.* **2013**, *46*, 444–456. (c) Roesky, H. W. *J. Organomet. Chem.* **2013**, *730*, 57–62. (d) Asay, M.; Jones, C.; Driess, M. *Chem. Rev.* **2011**, *111*, 354–396. (e) Mandal, S. K.; Roesky, H. W. *Chem. Commun.* **2010**, *46*, 6016–6041. (f) Kira, M. *Chem. Commun.* **2010**, *46*, 2893–2903. (g) Nagendran, S.; Roesky, H. W. *Organometallics* **2008**, *27*, 457–492. (h) Zabula, A. V.; Hahn, F. E. *Eur. J. Inorg. Chem.* **2008**, 5165–5179. (i) Leung, W.-P.; Kan, K.-W.; Chung, K.-H. *Coord. Chem. Rev.* **2007**, *251*, 2253–2265. (j) Waterman, R.; Hayes, P. G.; Tilley, T. D. *Acc. Chem. Res.* **2007**, *40*, 712–719.

(9) For TM complexes containing amidinate-tetrylene ligands, see: (a) Gallego, D.; Brück, A.; Irran, E.; Meier, F.; Kaupp, M.; Driess, M.; Hartwig, J. F. *J. Am. Chem. Soc.* **2013**, *135*, 15617–15626. (b) Blom, B.; Enthaler, S.; Inoue, S.; Irran, E.; Driess, M. *J. Am. Chem. Soc.* **2013**, *135*, 6703–6713. (c) Someya, C. I.; Haberberger, M.; Wang, W.; Enthaler, S.; Inoue, S. *Chem. Lett.* **2013**, *42*, 286–288. (d) Wang, W.; Inoue, S.; Enthaler, S.; Driess, M. *Angew. Chem., Int. Ed.* **2012**, *51*, 6167–6171. (e) Brück, A.; Gallego, D.; Wang, W.; Irran, E.; Driess, M.; Hartwig, J. F. *Angew. Chem., Int. Ed.* **2012**, *51*, 11478–11482. (f) Blom, B.; Driess, M.; Gallego, D.; Inoue, S. *Chem.—Eur. J.* **2012**, *18*, 13355–13360. (g) Azhakar, R.; Ghadwal, R. S.; Roesky, H. W.; Hey, J.; Stalke, D. *Chem. Asian. J.* **2012**, *7*, 528–533. (h) Azhakar, R.; Ghadwal, R. S.; Roesky, H. W.; Wolf, H.; Stalke, D. *J. Am. Chem. Soc.* **2012**, *134*, 2423–2428. (i) Junold, K.; Baus, J. A.; Burschka, C.; Tacke, R. *Angew. Chem., Int. Ed.* **2012**, *51*, 7020–7023. (j) Azhakar, R.;

- Roesky, H. W.; Holstein, J. J.; Dittrich, B. *Dalton Trans.* **2012**, *41*, 12096–12100. (k) Wang, W.; Inoue, S.; Irran, E.; Driess, M. *Angew. Chem., Int. Ed.* **2012**, *51*, 3691–3694. (l) Azhakar, R.; Sarish, S. P.; Roesky, H. W.; Hey, J.; Stalke, D. *Inorg. Chem.* **2011**, *50*, 5039–5043. (m) Tavčar, G.; Sen, S. S.; Azhakar, R.; Thorn, A.; Roesky, H. W. *Inorg. Chem.* **2010**, *49*, 10199–10202. (n) Wang, W.; Inoue, S.; Yao, S.; Driess, M. *J. Am. Chem. Soc.* **2010**, *132*, 15890–1589. (o) Matioszek, D.; Katir, N.; Saffon, N.; Castel, A. *Organometallics* **2010**, *29*, 3039–3046. (p) Sen, S. S.; Kritzler-Kosch, M. P.; Nagendran, S.; Roesky, H. W.; Beck, T.; Pal, A.; Herbst-Irmer, R. *Eur. J. Inorg. Chem.* **2010**, 5304–5311. (q) Yang, W.; Fu, H.; Wang, H.; Chen, M.; Ding, Y.; Roesky, H. W.; Jana, A. *Inorg. Chem.* **2009**, *48*, 5058–5060. (r) Jones, C.; Rose, R. P.; Stasch, A. *Dalton Trans.* **2008**, 2871–2878. (s) Junold, K.; Baus, J. A.; Burschka, C.; Vent-Schmidt, T.; Riedel, S.; Tacke, R. *Inorg. Chem.* **2013**, *52*, 11593–11599. (t) Azhakar, R.; Ghadwal, R. S.; Roesky, H. W.; Hey, J.; Krause, L.; Stalke, D. *Dalton Trans.* **2013**, *42*, 10277–10281. (u) Tan, G.; Blom, B.; Gallego, G.; Driess, M. *Organometallics* **2014**, *33*, 363–369. (v) Sen, S. S.; Kratzer, D.; Stern, D.; Roesky, H. W.; Stalke, D. *Inorg. Chem.* **2010**, *49*, 5786–5788. (w) Breit, N. C.; Szilvási, T.; Suzuki, T.; Gallego, D.; Inoue, S. *J. Am. Chem. Soc.* **2013**, *135*, 17958–17968.
- (10) For a recent review on N-heterocyclic silylene complexes in catalysis, see: Blom, B.; Gallego, D.; Driess, M. *Inorg. Chem. Front.* **2014**, *1*, 134–148.
- (11) (a) Cabeza, J. A.; García-Álvarez, P.; Pérez-Carreño, E.; Polo, D. *Inorg. Chem.* **2014**, *53*, 8735–8741. (b) Álvarez-Rodríguez, L.; Cabeza, J. A.; García-Álvarez, P.; Polo, D. *Organometallics* **2013**, *32*, 3557–3561. (c) Cabeza, J. A.; Fernández-Colinas, J. M.; García-Álvarez, P.; Polo, D. *Inorg. Chem.* **2012**, *51*, 3896–3903. (d) Cabeza, J. A.; García-Álvarez, P.; Polo, D. *Inorg. Chem.* **2012**, *51*, 2569–2576. (e) Cabeza, J. A.; García-Álvarez, P.; Polo, D. *Inorg. Chem.* **2011**, *50*, 6195–6199.
- (12) Cabeza, J. A.; García-Álvarez, P.; Polo, D. *Dalton Trans.* **2013**, *42*, 1329–1332.
- (13) Cabeza, J. A.; Fernández-Colinas, J. M.; García-Álvarez, P.; Polo, D. *RSC Adv.* **2014**, *4*, 31503–31506.
- (14) Cabeza, J. A.; García-Álvarez, P.; Pérez-Carreño, E.; Polo, D. *Chem.—Eur. J.* **2014**, *20*, 8654–8663.
- (15) A related chelating $\kappa^2\text{-N,Si}$ -imine-silylene behavior has been recently observed in carbonyl group-6 TM complexes for guanidinate-silylene ligands containing isopropyl groups on the coordinated N atoms: Mück, F. M.; Kloss, D.; Baus, J. A.; Burschka, C.; Tacke, R. *Chem.—Eur. J.* **2014**, *20*, 9620–9626.
- (16) Chen, L.; Poë, A. J. *Inorg. Chem.* **1989**, *28*, 3641–3647.
- (17) Jazzar, R. F. R.; Bhatia, P. H.; Mahon, M. F.; Whittlesey, M. K. *Organometallics* **2003**, *22*, 670–683.
- (18) Burling, S.; Kociok-Köhn, G.; Mahon, M. F.; Whittlesey, M. K.; Williams, J. M. J. *Organometallics* **2005**, *24*, 5868–5878.
- (19) Davies, C. J. E.; Lowe, J. P.; Mahon, M. F.; Poulten, R. C.; Whittlesey, M. K. *Organometallics* **2013**, *32*, 4927–4937.
- (20) Bruce, M. I.; Matison, J. G.; Nicholson, B. K. *J. Organomet. Chem.* **1983**, *247*, 321–343.
- (21) (a) Mayr, A.; Lin, Y. C.; Boag, N. M.; Kaesz, H. D. *Inorg. Chem.* **1982**, *21*, 1704–1706. (b) Jensen, C. M.; Lynch, T. J.; Knobler, C. B.; Kaesz, H. D. *J. Am. Chem. Soc.* **1982**, *104*, 4679–4680. (c) Lavigne, G.; Kaesz, H. D. *J. Am. Chem. Soc.* **1984**, *106*, 4647–4648.
- (22) (a) Morris, D. E.; Basolo, F. J. *J. Am. Chem. Soc.* **1968**, *90*, 2531–2535. (b) Basolo, F. *Inorg. Chim. Acta* **1981**, *50*, 65–70.
- (23) Liu, Y.; Ganguly, R.; Huynh, H. V.; Leong, W. K. *Angew. Chem., Int. Ed.* **2013**, *52*, 12110–12113.
- (24) Connor, J. A. *Top. Curr. Chem.* **1977**, *71*, 71–110.
- (25) Dyson, P. J.; McIndoe, J. S. *Transition Metal Carbonyl Cluster Chemistry*; Gordon and Breach Science Publishers: Amsterdam, 2000; p 94.
- (26) Malik, S. K.; Poë, A. J. *Inorg. Chem.* **1978**, *17*, 1484–1488.
- (27) (a) Johnson, B. F. G.; Lewis, J.; Twigg, M. V. *J. Organomet. Chem.* **1974**, *67*, C75–C76. (b) Forebs, E. J.; Goodhand, N.; Jones, D. L.; Hamor, T. A. *J. Organomet. Chem.* **1979**, *182*, 143–154.
- (28) See, for example: (a) Cabeza, J. A.; del Río, I.; Miguel, D.; Pérez-Carreño, E.; Sánchez-Vega, M. G. *Dalton Trans.* **2008**, 1937–1942. (b) Cabeza, J. A.; Pérez-Carreño, E. *Organometallics* **2008**, *27*, 4697–4702. (c) Cabeza, J. A.; del Río, I.; Miguel, D.; Sánchez-Vega, M. G. *Angew. Chem., Int. Ed.* **2008**, *47*, 1920–1922. (d) Cabeza, J. A.; del Río, I.; Pérez-Carreño, E.; Sánchez-Vega, M. G.; Vázquez-García, D. *Angew. Chem., Int. Ed.* **2009**, *48*, 555–558.
- (29) Nagendran, S.; Sen, S. S.; Roesky, H. W.; Koley, D.; Brubmüller, H.; Pal, A.; Herbst-Irmer, R. *Organometallics* **2008**, *27*, 5459–5463.
- (30) *CrysAlisPro RED*, version 1.171.34.36; Oxford Diffraction Ltd.: Oxford, U.K., 2010.
- (31) Altomare, A.; Burla, M. C.; Camalli, M.; Cascarano, G. L.; Giacovazzo, C.; Guagliardi, A.; Moliterni, A. G. C.; Polidori, G.; Spagna, R. *J. Appl. Crystallogr.* **1999**, *32*, 115–119.
- (32) Sheldrick, G. M. *Acta Crystallogr.* **2008**, *A64*, 112–122.
- (33) Farrugia, L. J. *J. Appl. Crystallogr.* **1999**, *32*, 837–838.
- (34) Chai, J.-D.; Head-Gordon, M. *Phys. Chem. Chem. Phys.* **2008**, *10*, 6615–6620.
- (35) (a) Ehrlich, S.; Moellmann, J.; Grimme, S. *Acc. Chem. Res.* **2013**, *46*, 916–926. (b) Grimme, S. *Comp. Mol. Sci.* **2011**, *1*, 211–228. (c) Schwabe, T.; Grimme, S. *Acc. Chem. Res.* **2008**, *41*, 569–579.
- (36) (a) Becke, A. D. *J. Chem. Phys.* **1993**, *98*, 5648–5652. (b) Lee, C.; Yang, W.; Parr, R. G. *Phys. Rev. B* **1988**, *37*, 785–789.
- (37) Zhao, Y.; Truhlar, D. G. *Theor. Chem. Acc.* **2008**, *120*, 215–241.
- (38) Minenkov, Y.; Singstad, Å.; Occhipinti, G.; Jensen, V. R. *Dalton Trans.* **2012**, *41*, 5526–5541.
- (39) Hay, P. J.; Wadt, W. R. *J. Chem. Phys.* **1985**, *82*, 299–310.
- (40) Hariharan, P. C.; Pople, J. A. *Theor. Chim. Acta* **1973**, *28*, 213–222.
- (41) Barone, V.; Cossi, M. *J. Phys. Chem. A* **1998**, *102*, 1995–2001.
- (42) Cossi, M.; Rega, N.; Scalmani, G.; Barone, V. *J. Comput. Chem.* **2003**, *24*, 669–681.
- (43) Frisch, M. J.; Trucks, G. W.; Schlegel, H. B.; Scuseria, G. E.; Robb, M. A.; Cheeseman, J. R.; Scalmani, G.; Barone, V.; Mennucci, B.; Petersson, G. A.; Nakatsuji, H.; Caricato, M.; Li, X.; Hratchian, H. P.; Izmaylov, A. F.; Bloino, J.; Zheng, G.; Sonnenberg, J. L.; Hada, M.; Ehara, M.; Toyota, K.; Fukuda, R.; Hasegawa, J.; Ishida, M.; Nakajima, T.; Honda, Y.; Kitao, O.; Nakai, H.; Vreven, T.; Montgomery, J. A., Jr.; Peralta, J. E.; Ogliaro, F.; Bearpark, M.; Heyd, J. J.; Brothers, E.; Kudin, K. N.; Staroverov, V. N.; Keith, T.; Kobayashi, R.; Normand, J.; Raghavachari, K.; Rendell, A.; Burant, J. C.; Iyengar, S. S.; Tomasi, J.; Cossi, M.; Rega, N.; Millam, N. J.; Klene, M.; Knox, J. E.; Cross, J. B.; Bakken, V.; Adamo, C.; Jaramillo, J.; Gomperts, R.; Stratmann, R. E.; Yazyev, O.; Austin, A. J.; Cammi, R.; Pomelli, C.; Ochterski, J. W.; Martin, R. L.; Morokuma, K.; Zakrzewski, V. G.; Voth, G. A.; Salvador, P.; Dannenberg, J. J.; Dapprich, S.; Daniels, A. D.; Farkas, Ö.; Foresman, J. B.; Ortiz, J. V.; Cioslowski, J.; Fox, D. J. *Gaussian 09*, revision B.01; Gaussian, Inc.: Wallingford, CT, 2010.

SUPPORTING INFORMATION

Amidinatogermylene Derivatives of Ruthenium Carbonyl: New Insights into the Reactivity of [Ru₃(CO)₁₂] with 2-Electron-Donor Reagents of High Basicity

Lucía Álvarez-Rodríguez,[†] Javier A. Cabeza,^{†*} Pablo García-Álvarez,^{†*} Enrique Pérez-Carreño,[‡] and Diego Polo[†]

[†]*Departamento de Química Orgánica e Inorgánica-IUQOEM, Universidad de Oviedo-CSIC, E-33071 Oviedo, Spain*

[‡]*Departamento de Química Física y Analítica, Universidad de Oviedo, E-33071 Oviedo, Spain*

CONTENTS

Pages

¹ H and ¹³ C{ ¹ H} NMR Spectra	2–11
---	------

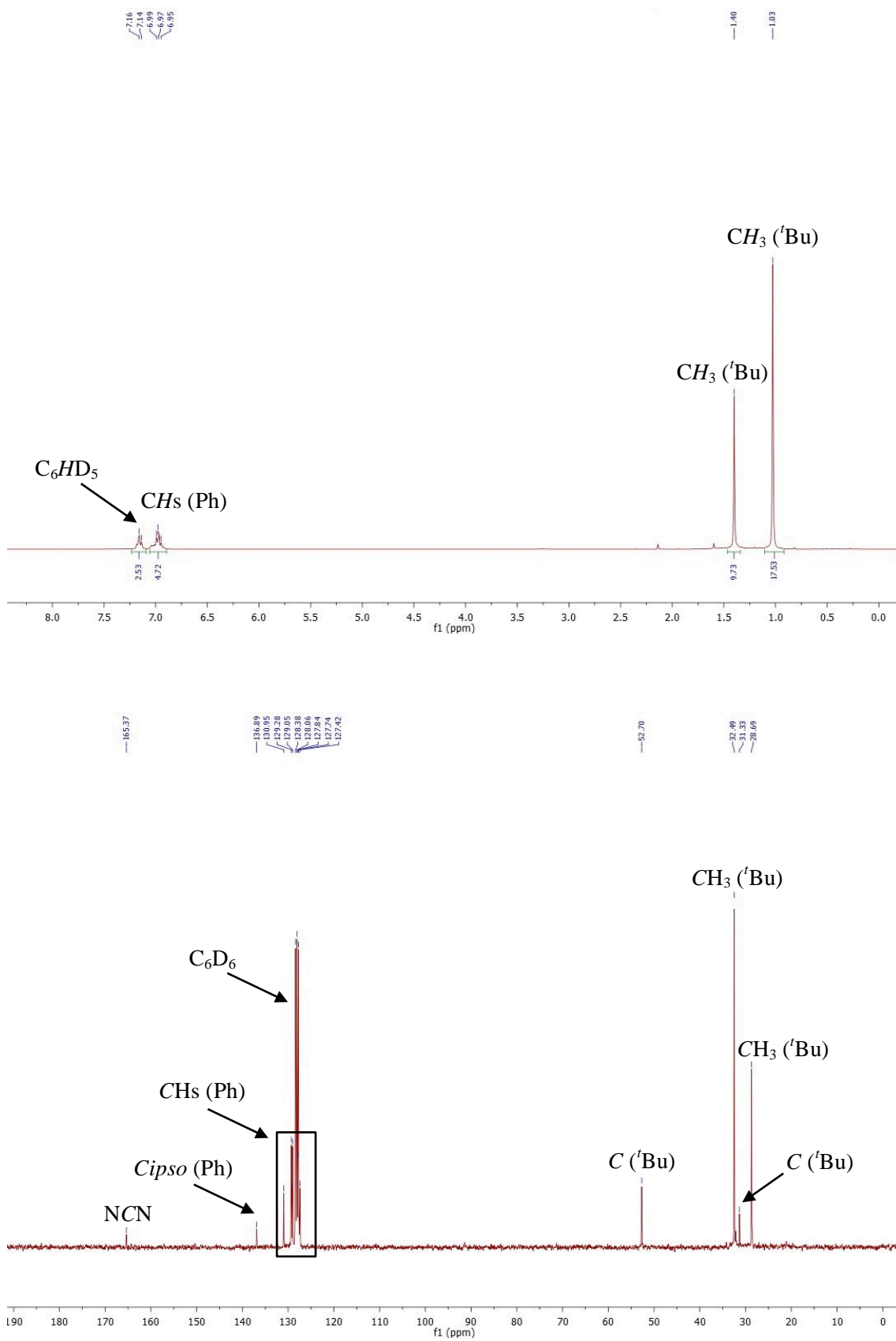


Figure S1. ^1H (top) and $^{13}\text{C}\{^1\text{H}\}$ (bottom) NMR spectra of $\text{Ge}(\text{tBu}_2\text{bzam})\text{tBu}$ ($\mathbf{1}_{\text{tBu}}$) in C_6D_6 (20°C).

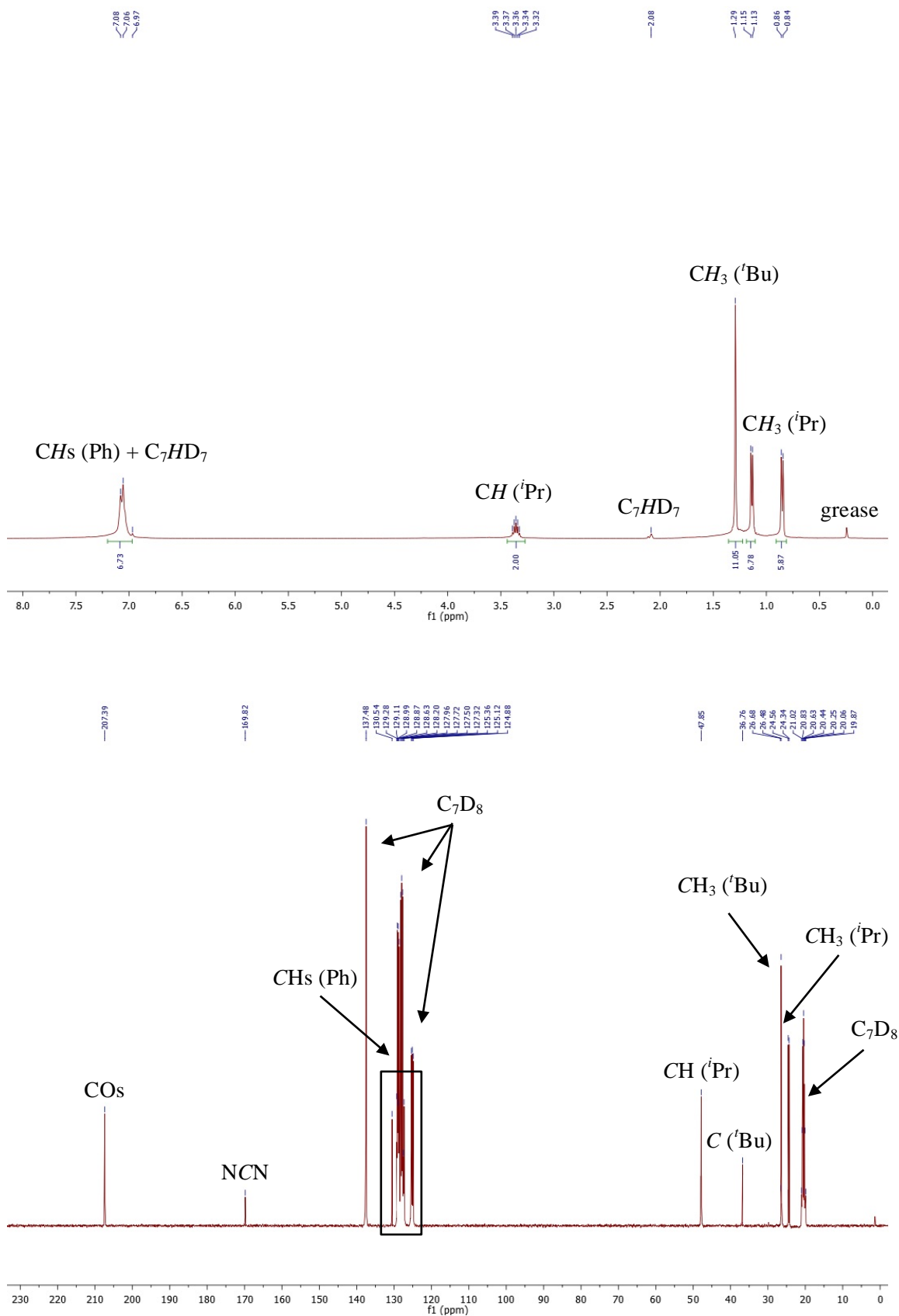


Figure S2. ^1H (top) and $^{13}\text{C}\{^1\text{H}\}$ (bottom) NMR spectra of $[\text{Ru}(\mathbf{1}_{\text{iPr}})\text{CO}]_4$ ($\mathbf{2}_{\text{iPr}}$) in C_7D_8 (20°C).

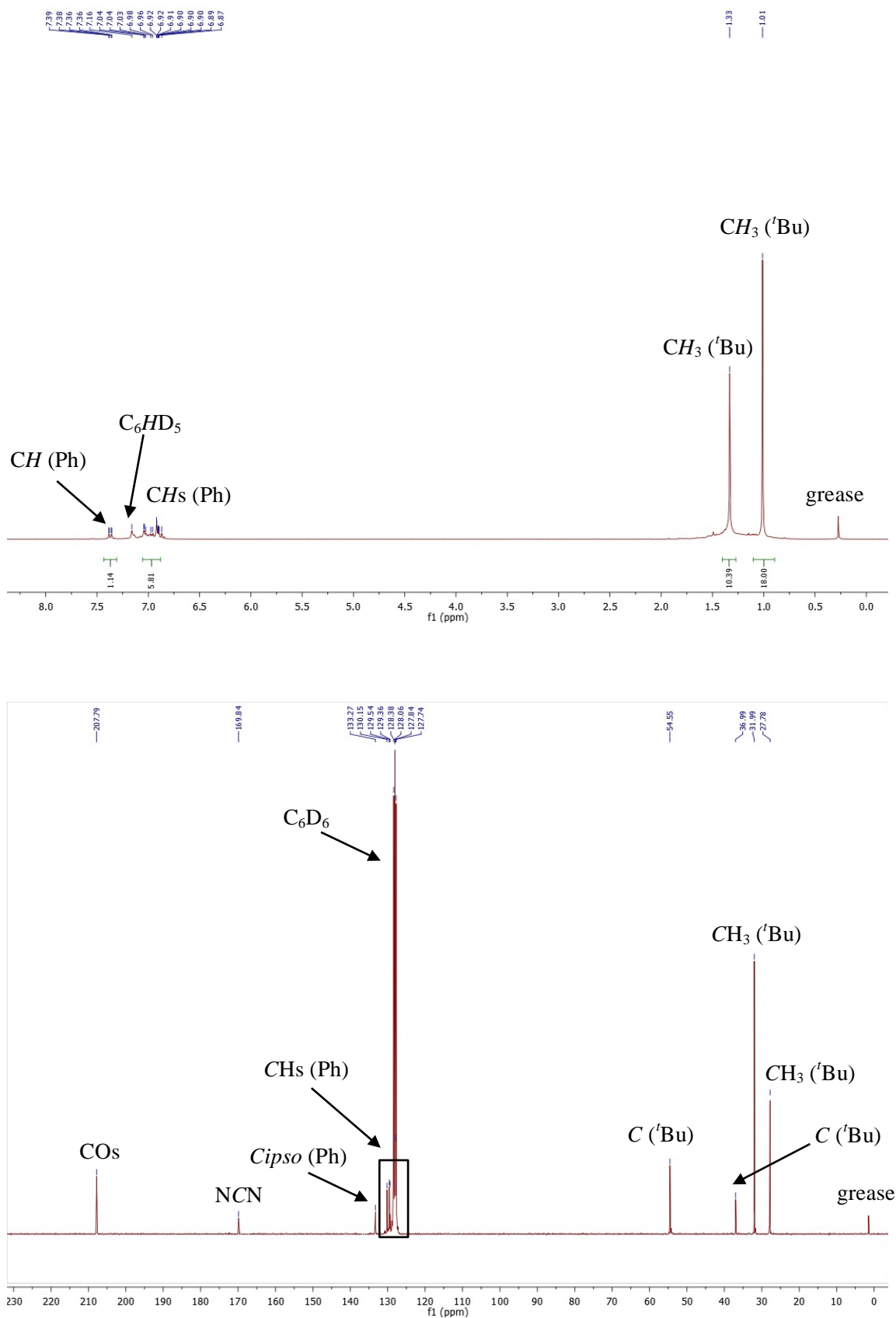


Figure S3. ^1H (top) and $^{13}\text{C}\{^1\text{H}\}$ (bottom) NMR spectra of $[\text{Ru}(\mathbf{1}_{\text{tBu}})\text{CO}]_4$ ($\mathbf{2}_{\text{tBu}}$) in C_6D_6 (20°C).

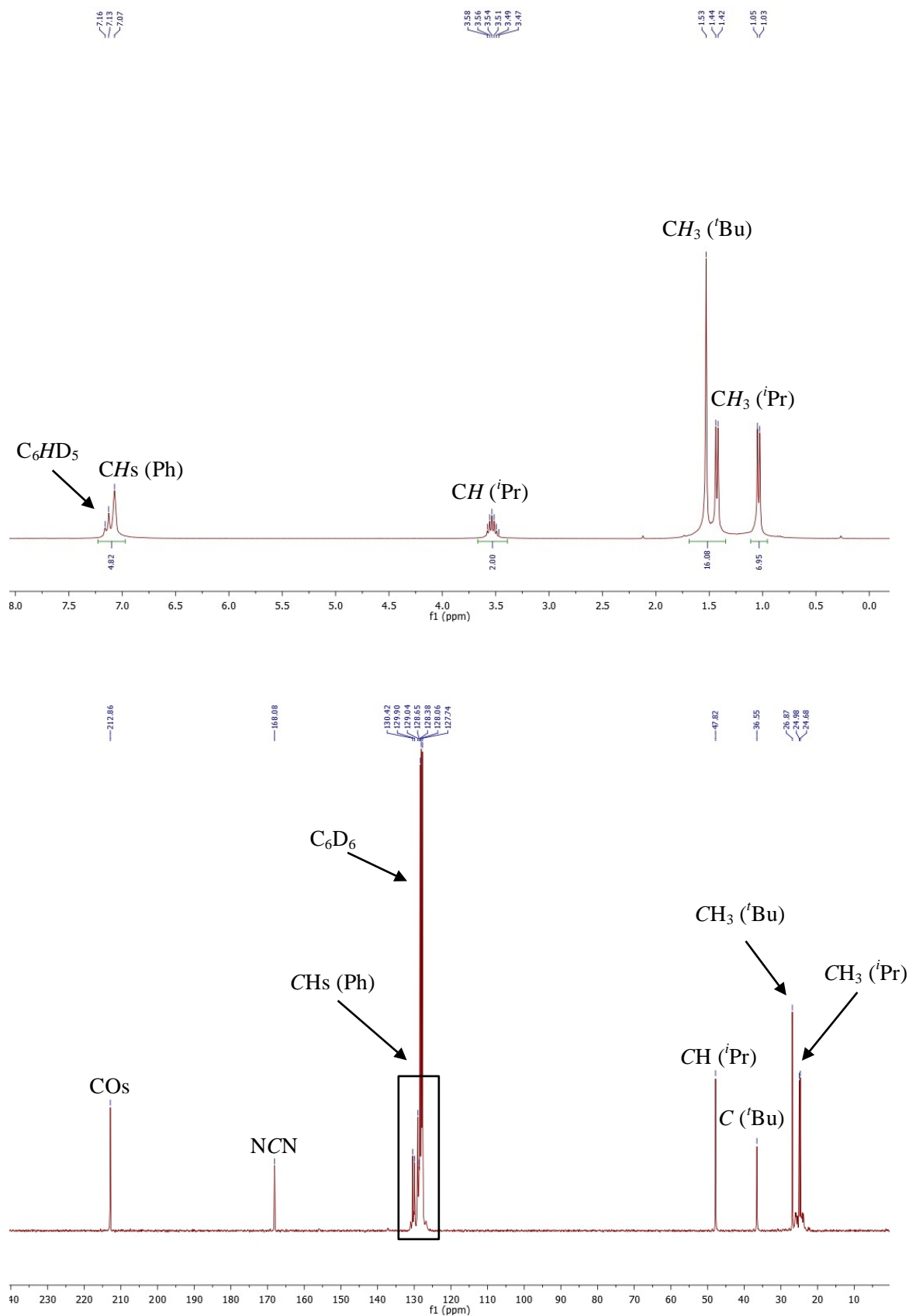


Figure S4. ^1H (top) and $^{13}\text{C}\{^1\text{H}\}$ (bottom) NMR spectra of $[\text{Ru}(\mathbf{1}_{\text{IPr}})_2(\text{CO})_3]$ ($\mathbf{3}_{\text{IPr}}$) in C_6D_6 (20°C).

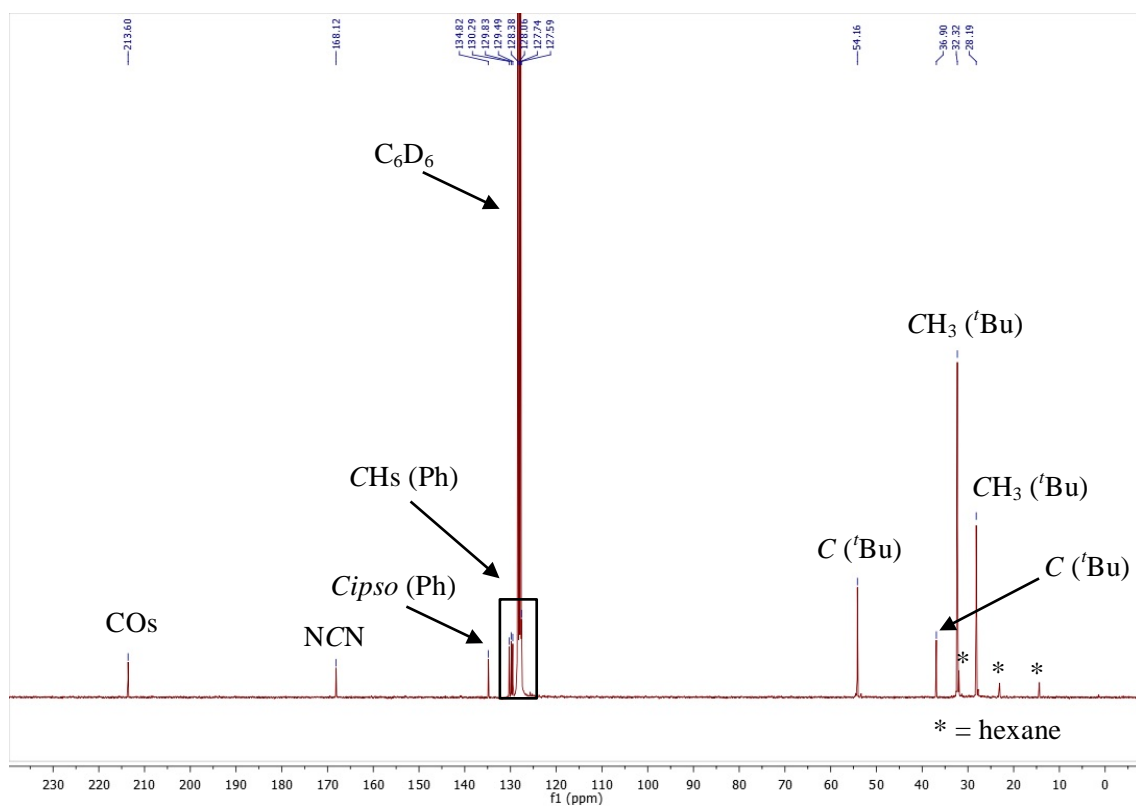
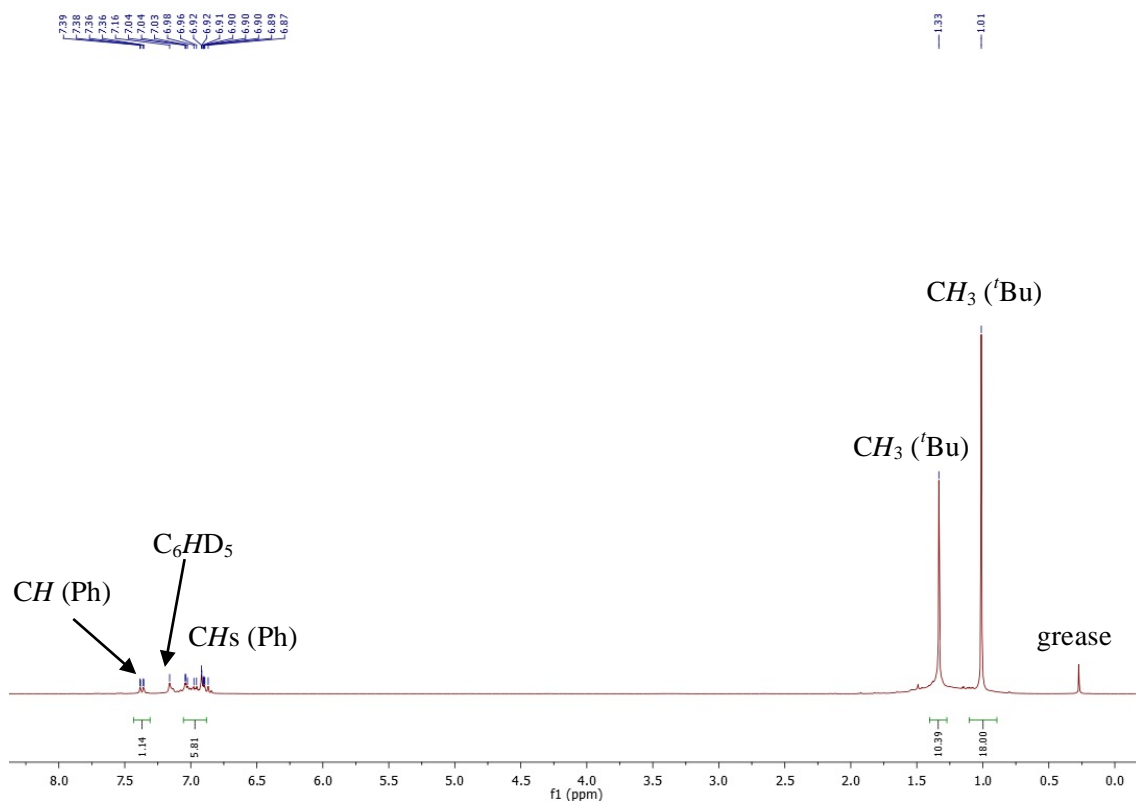


Figure S5. ¹H (top) and ¹³C{¹H} (bottom) NMR spectra of [Ru(**1**_{tBu})₂(CO)₃] (**3**_{tBu}) in C₆D₆ (20 °C).

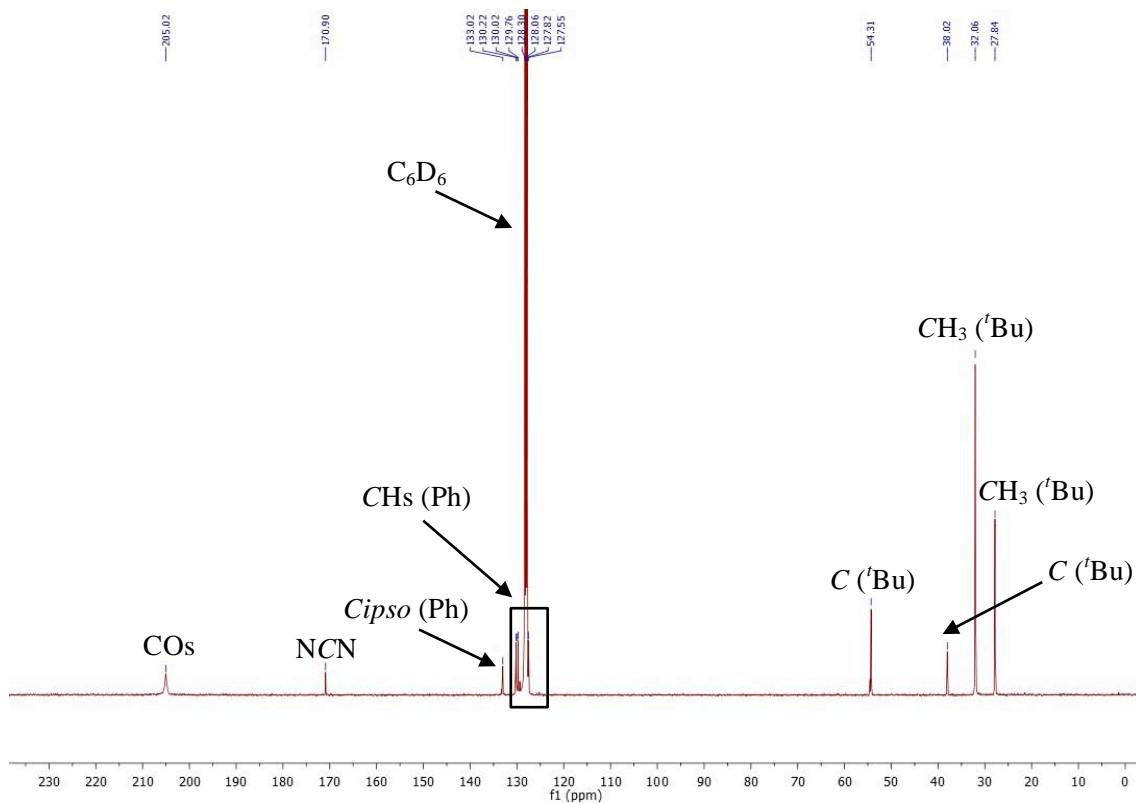
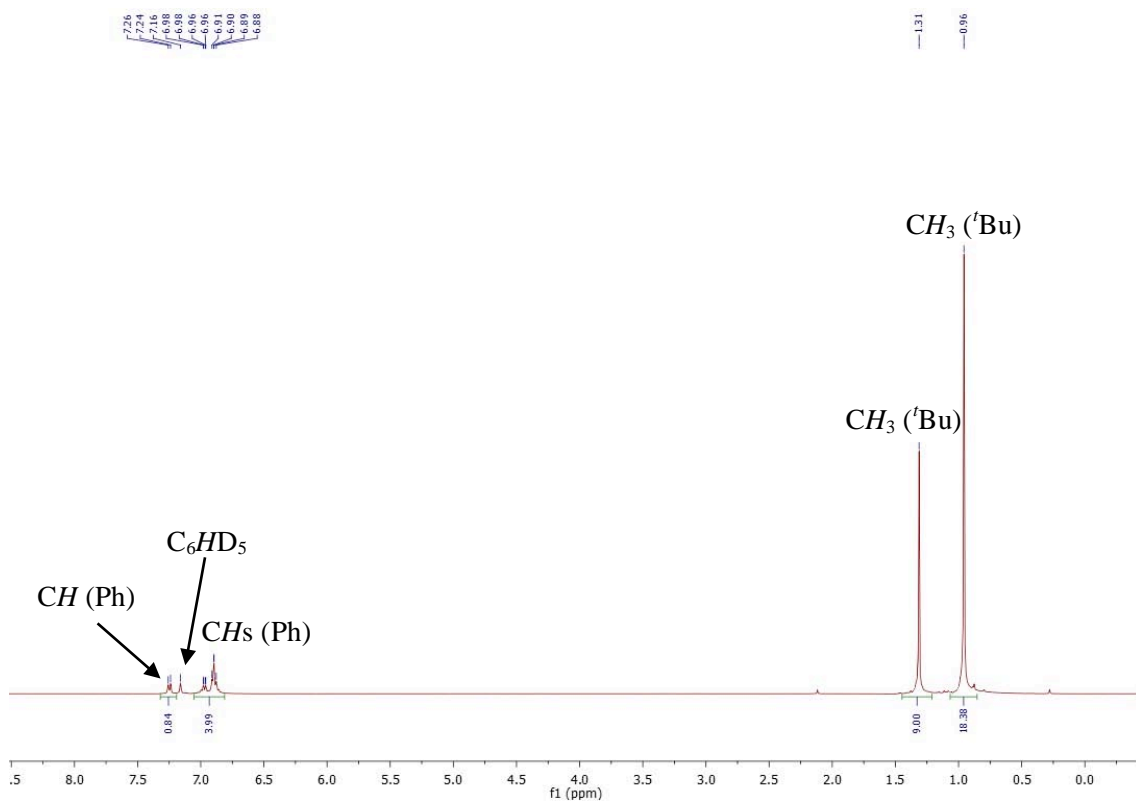


Figure S6. ^1H (top) and $^{13}\text{C}\{^1\text{H}\}$ (bottom) NMR spectra of $[\text{Ru}_3(\mathbf{1}_{\text{tBu}})(\text{CO})_{11}] (\mathbf{4}_{\text{tBu}})$ in C_6D_6 (20 °C).

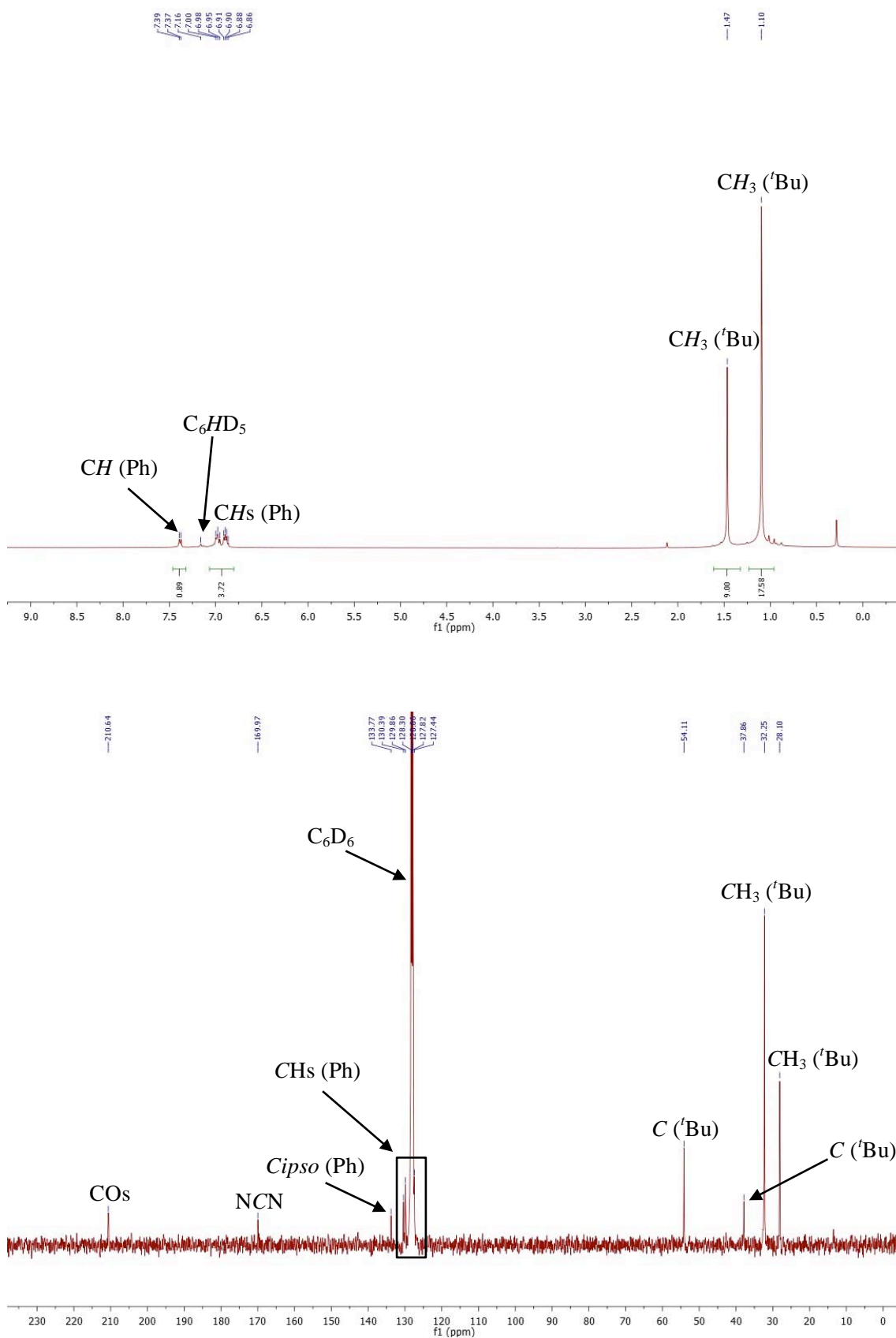


Figure S7. ^1H (top) and $^{13}\text{C}\{^1\text{H}\}$ (bottom) NMR spectra of $[\text{Ru}_3(\mathbf{1}_{\text{tBu}})_2(\text{CO})_{10}]$ ($\mathbf{5}_{\text{tBu}}$) in C_6D_6 (20°C).

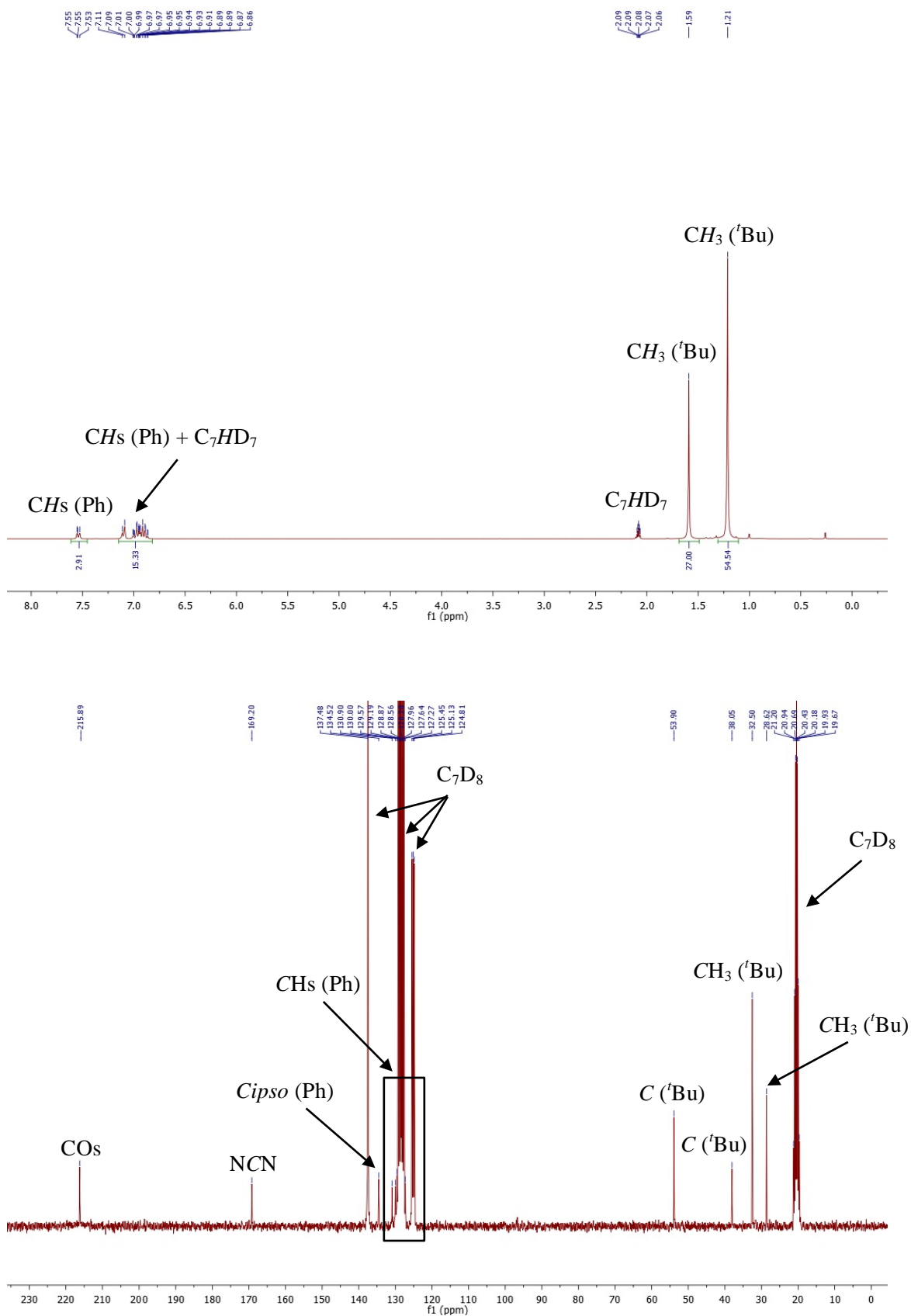


Figure S8. ^1H (top) and $^{13}\text{C}\{^1\text{H}\}$ (bottom) NMR spectra of $[\text{Ru}_3(\mathbf{1}_{\text{tBu}})_3(\text{CO})_9]$ ($\mathbf{6}_{\text{tBu}}$) in C_7D_8 (20°C).

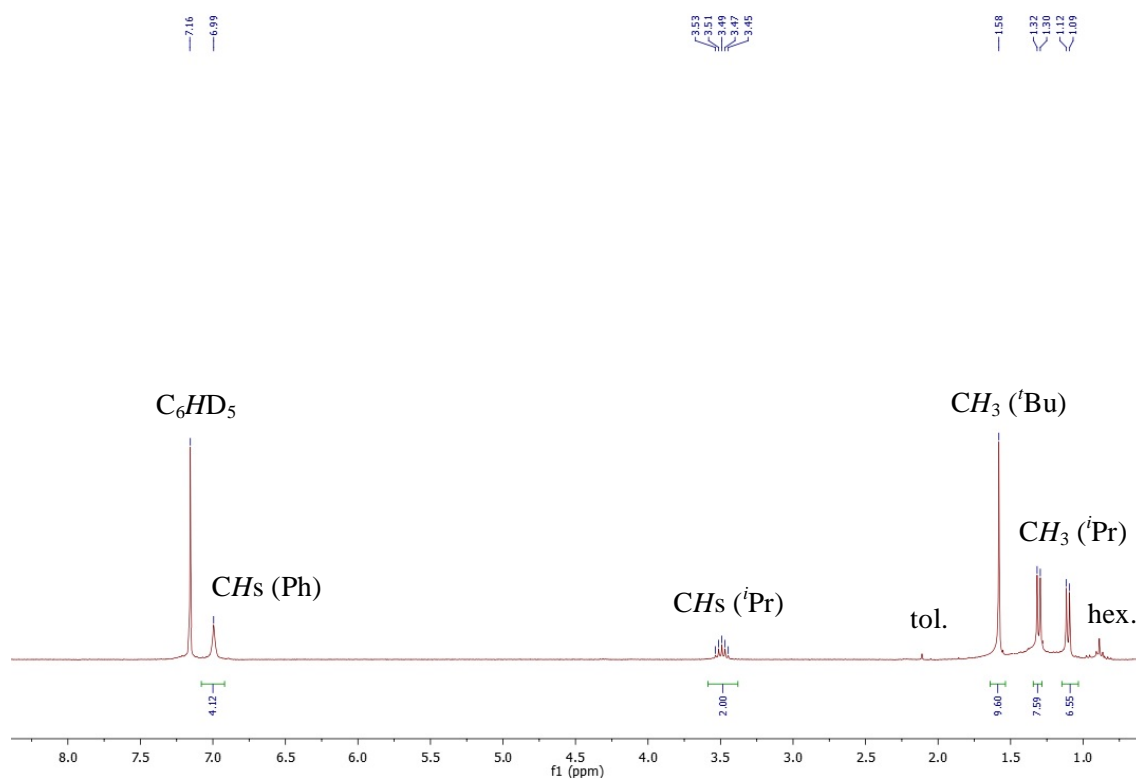


Figure S9. ^1H NMR spectra of $[\text{Ru}_3(\mathbf{1}_{\text{iPr}})_3(\text{CO})_9]$ ($\mathbf{6}_{\text{iPr}}$) in C_6D_6 (20 °C).

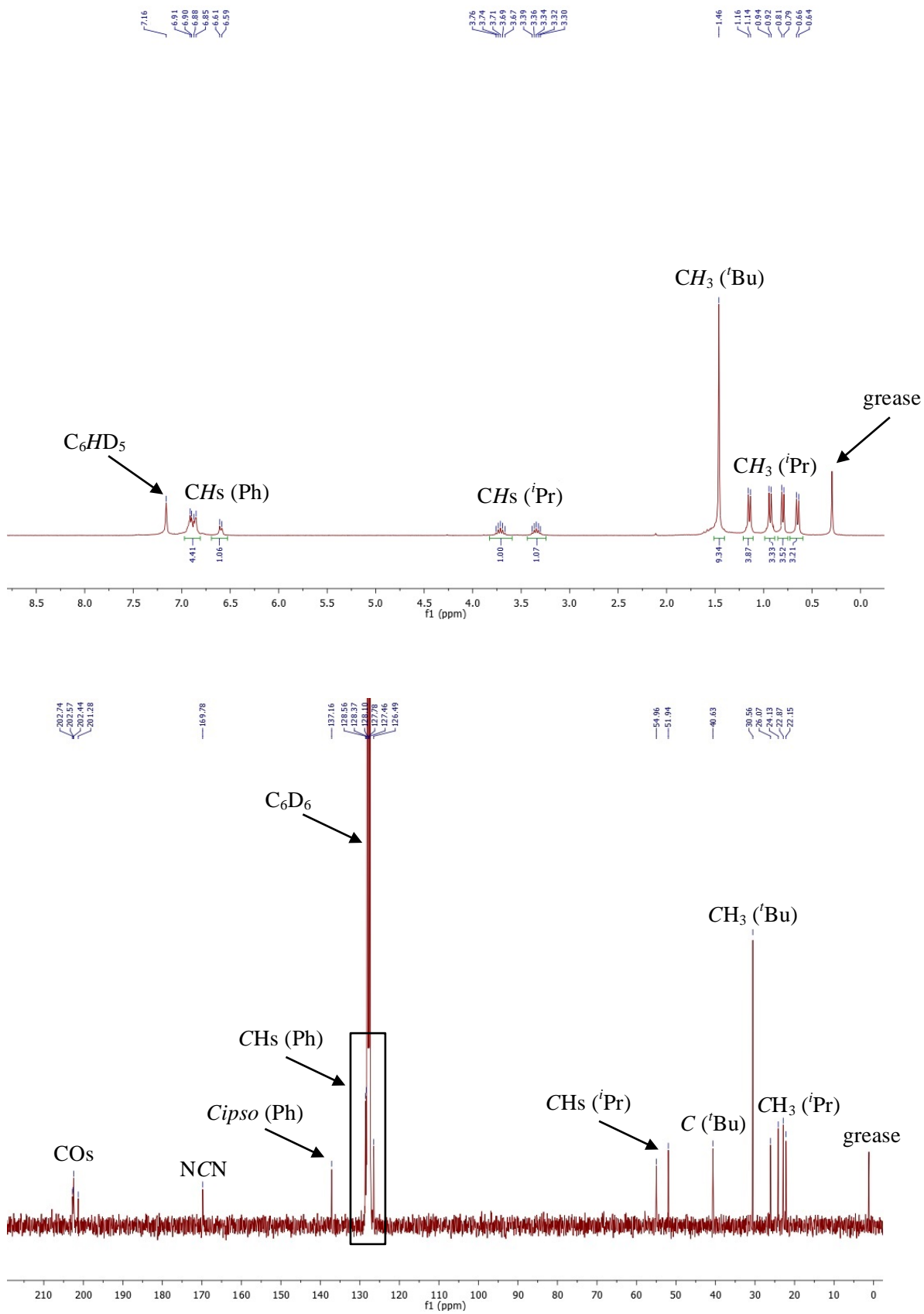


Figure S10. ^1H (top) and $^{13}\text{C}\{^1\text{H}\}$ (bottom) NMR spectra of $[\text{Ru}_2\{\mu\text{-}\kappa^2\text{Ge,N-1iPr}\}(\text{CO})_7]$ (7_{iPr}) in C_6D_6 (20°C).

Artículo IX

***“Conversion of a Monodentate Amidinate-Germylene
Ligand into Chelating Imine-Germanate Ligands (on
Mononuclear Manganese Complexes)”***

Conversion of a Monodentate Amidinate–Germylene Ligand into Chelating Imine–Germanate Ligands (on Mononuclear Manganese Complexes)

Javier A. Cabeza,^{*,†} Pablo García-Álvarez,^{*,†} Enrique Pérez-Carreño,[‡] and Diego Polo[†]

[†]Departamento de Química Orgánica e Inorgánica—IUQOEM, Universidad de Oviedo—CSIC, E-33071 Oviedo, Spain

[‡]Departamento de Química Física y Analítica, Universidad de Oviedo, E-33071 Oviedo, Spain

Supporting Information

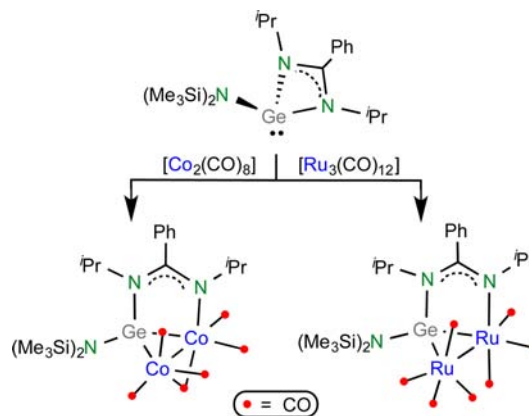
ABSTRACT: The unprecedented transformation of a terminal two-electron-donor amidinate–germylene ligand into a chelating three-electron-donor κ^2 -*N*,*Ge*-imine–germanate ligand has been achieved by treating the manganese amidinate–germylene complex $[\text{MnBr}\{\text{Ge}(\text{}^i\text{Pr}_2\text{bzam})\text{}^t\text{Bu}\}(\text{CO})_4]$ (**1**; $\text{}^i\text{Pr}_2\text{bzam} = N,N'$ -bis(isopropyl)-benzamidinate) with LiMe or $\text{Ag}[\text{BF}_4]$. In these reactions, which afford $[\text{Mn}\{\kappa^2\text{Ge}_2N\text{-GeMe}(\text{}^i\text{Pr}_2\text{bzam})\text{}^t\text{Bu}\}(\text{CO})_4]$ (**2**) and $[\text{Mn}\{\kappa^2\text{Ge}_2N\text{-GeF}(\text{}^i\text{Pr}_2\text{bzam})\text{}^t\text{Bu}\}(\text{CO})_4]$ (**3**), respectively, the anionic nucleophile, Me^- or F^- , ends on the Ge atom while an arm of the amidinate fragment migrates from the Ge atom to the Mn atom. In contrast, the reaction of **1** with AgOTf ($\text{OTf} = \text{triflate}$) leads to $[\text{Mn}(\text{OTf})\{\text{Ge}(\text{}^i\text{Pr}_2\text{bzam})\text{}^t\text{Bu}\}(\text{CO})_4]$ (**4**), which maintains intact the amidinate–germylene ligand. Complex **4** is very moisture-sensitive, leading to $[\text{Mn}_2\{\mu\text{-}\kappa^4\text{Ge}_2\text{O}_2\text{-Ge}_2\text{}^t\text{Bu}_2(\text{OH})_2\text{O}\}(\text{CO})_8]$ (**5**) and $[\text{}^i\text{Pr}_2\text{bzamH}_2]\text{OTf}$ (**6**) in wet solvents. In **5**, a novel digermanate(II) ligand, $[\text{}^t\text{Bu}(\text{OH})\text{GeOGe}(\text{OH})\text{}^t\text{Bu}]^{2-}$, doubly bridges two $\text{Mn}(\text{CO})_4$ units. The structures of **1**–**6** have been characterized by spectroscopic (IR, NMR) and single-crystal X-ray diffraction methods.

INTRODUCTION

The coordination chemistry of heavier carbene analogues (also known as heavier tetrylenes, HTs) stabilized by amidinate groups has experienced an exponential growth in the past few years.^{1–8} They form stable complexes with almost all of the elements of the transition metal (TM) series and, importantly, some of their TM complexes have already been successfully tested as catalyst precursors for useful reactions,^{1a} such as Sonogashira cross-couplings,^{3a} ketone hydrosilylations,^{3b} cross-coupling reactions of aryl halides with organometallic zinc and Grignard reagents,^{3f} $[2 + 2 + 2]$ cycloadditions,^{4a} and arene C–H borylations.^{4b}

The vast majority of the hitherto reported amidinate–HT–TM complexes have their amidinate–HTs behaving as terminal ligands attached to the TM atom through the corresponding group-14 donor atom, and this situation is maintained in the products of their reactions. We have recently discovered a remarkable exception to this spectator behavior of amidinate–HT ligands, since the germylene $\text{Ge}(\text{}^i\text{Pr}_2\text{bzam})(\text{HMDS})$ [$\text{}^i\text{Pr}_2\text{bzam} = N,N'$ -bis(isopropyl)benzamidinate; $\text{HMDS} = \text{N}(\text{SiMe}_3)_2$], which is equipped with just one lone pair of electrons on the Ge atom, can be transformed into a bridging four-electron-donor κ^2 -*N*,*Ge*-imine–germylene ligand when treated with $[\text{Co}_2(\text{CO})_8]$ ^{2b} and $[\text{Ru}_3(\text{CO})_{12}]$ ^{2c,3g} (Scheme 1). Until then, such a bidentate coordination mode, which implies the opening of the germylene GeN_2C ring and the subsequent coordination of one of the arms of the amidinate fragment to the TM, was unknown for amidinate–HT ligands. In a related work, Tacke et al. have described the opposite ligand behavior,

Scheme 1. Reported Reactivity of $\text{Ge}(\text{}^i\text{Pr}_2\text{bzam})(\text{HMDS})$ with Cobalt and Ruthenium Carbonyls



since the bis(amidinate)–silylene $\text{Si}(\text{}^i\text{Pr}_2\text{bzam})_2$, which contains one chelating and one terminal amidinate, closes its pendant imine arm toward the silicon atom upon coordination of the latter to a tungsten center.^{4f}

In this contribution, we report (a) the first amidinate–germylene derivatives of manganese (the only amidinate–HT–Mn complexes hitherto known are silylene derivatives^{4g,5}), (b) the unprecedented observation that a terminal two-electron-donor amidinate–germylene ligand can be converted into

Received: June 16, 2014

Published: August 1, 2014

chelating three-electron-donor κ^2N,Ge -imine–germanate ligands, and (c) a hydrolysis reaction that leads to a neutral dimanganese(I) derivative that contains the novel digermanate(II) $[^tBu(OH)GeOGe(OH)^tBu]^{2-}$ as a bridging $\kappa^2Ge_2O_2$ -ligand.

RESULTS AND DISCUSSION

The manganese(I) amidinate-germylene complex $[MnBr\{Ge(^iPr_2bzam)^tBu\}(CO)_4]$ (**1**) was easily prepared by treating $[MnBr(CO)_5]$ with 1 equiv of the germylene $Ge(^iPr_2bzam)^tBu$ at room temperature (toluene, 10 min). An X-ray diffraction (XRD) study (Figure 1) confirmed the cis arrangement of its

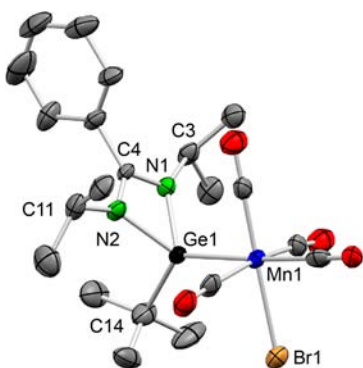
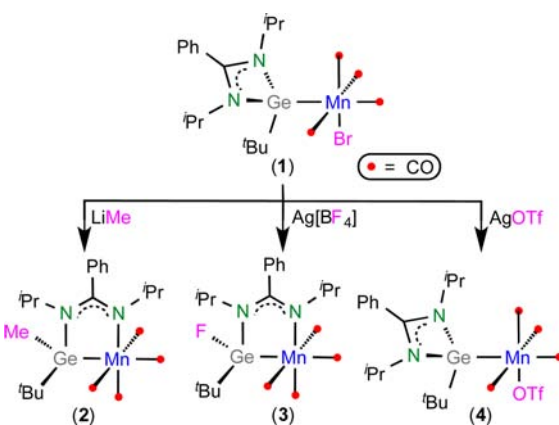


Figure 1. XRD molecular structure of **1** (40% displacement ellipsoids; H atoms omitted for clarity; only one of the four symmetry-independent but analogous molecules found in the asymmetric unit is shown). Selected interatomic distances (Å): Mn1–Ge1 2.398(1), Ge1–C14 1.994(9), Ge1–N1 1.988(6), Ge1–N2 1.998(7), N1–C3 1.46(1), N1–C4 1.30(1), N2–C4 1.34(1), N2–C11 1.46(1). The Mn–Br distance is not given because the Br atom and one CO ligand are involved in exchange positional disorder.

Br and $Ge(^iPr_2bzam)^tBu$ ligands. Its IR (four ν_{CO} absorptions) and NMR spectra (equivalent isopropyl groups) are compatible with a molecule having an average C_s symmetry, confirming that, in solution at room temperature, there is free rotation about the Ge–Mn bond.

In a recent paper, Driess, Inoue, and co-workers have reported the opening of a palladium-bound amidinate–silylene SiNCN ring induced by a hydride shift from Pd to Si; however, in that case, the amidinate open arm remained uncoordinated.^{4h} That paper prompted us to introduce a hydride into our system, looking for a similar $GeNCN$ ring opening, but, unfortunately, all attempted reactions of complex **1** with hydride donors, such as $Na[BH_4]$, $K[BH^tBu_3]$, or $Li[BHET_3]$, led to dark suspensions, the 1H NMR spectra of which contained many broad peaks, including various hydride resonances. Due to the air- and moisture-sensitivity of these mixtures, they could not be separated by chromatographic methods, and they were not further investigated. Additionally, trying to induce a Mn-to-Ge shift of the Br atom of **1**, we heated this complex in toluene at 90 °C, but an inseparable mixture was again obtained. These results led us to attempt a replacement of a methyl group for the bromine atom of **1**, reasoning that a Mn-to-Ge shift of a methyl group could be easier than that of the bromide. The room temperature treatment of a toluene solution of complex **1** with an ethereal solution of $LiMe$ led to a product that was subsequently identified as $[Mn\{\kappa^2Ge,N-GeMe(^iPr_2bzam)^tBu\}(CO)_4]$ (**2**; Scheme 2).

Scheme 2. Reactions of Complex 1 with $LiMe$, $Ag[BF_4]$, and $AgOTf$



The 1H and $^{13}C\{^1H\}$ NMR spectra of **2** confirmed the incorporation of the methyl group (singlets at δ_H 0.96 ppm and δ_C 24.6 ppm, respectively, in C_6D_6), but, surprisingly, they also indicated the absence of any symmetry in the molecule. The XRD structure of **2** (Figure 2) determined that the molecule is

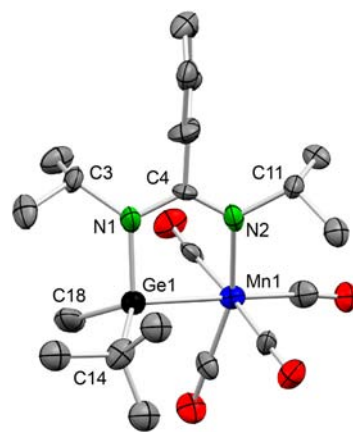


Figure 2. XRD molecular structure of **2** (25% displacement ellipsoids; H atoms omitted for clarity). Selected interatomic distances (Å): Mn1–Ge1 2.428(5), Mn1–N2 2.12(2), Ge1–C14 1.97(3), Ge1–C18 1.88(3), Ge1–N1 1.91(2), N1–C3 1.55(3), N1–C4 1.37(3), N2–C4 1.30(3), N2–C11 1.54(3).

a tetracarbonyl manganese derivative containing a chelating κ^2N,Ge -imine–germanate ligand that formally results from the addition of a Me^- group to the Ge atom of **1**, the opening of a Ge–N bond of the $GeNCN$ ring of the original germylene ligand, and the displacement of the bromide group from the Mn atom by the resulting imine arm of the open amidinate fragment.

We also treated $[MnMe(CO)_5]$ with $Ge(^iPr_2bzam)^tBu$, but no reaction occurred in toluene at 20 °C and extensive decomposition was observed when the solution was heated at 90 °C.

Complex **2** contains an anionic chelating three-electron-donor κ^2N,Ge -imine–germanate ligand, a coordination mode previously unknown for amidinate–HT ligands. Interestingly, a few days prior to the submission of the revised version of this paper, Tacke and co-workers reported the synthesis of group-6 metal carbonyl complexes containing a chelating four-electron-donor imine–silylene ligand by treating the corresponding

metal carbonyl with a bis(guanidinate)–silylene that contains one chelating and one terminal guanidinate.⁹ However, in this case, the reaction products do not arise from an insertion of the corresponding group-6 metal atom into an Si–N bond, but from the coordination to the group-6 metal atom of both the Si atom and the free N atom of the pendant (not chelating) guanidinate group of the starting silylene.

Pursuing our objective of preparing a mononuclear complex containing a chelating four-electron-donor imine–germylene ligand, we reasoned that the simple insertion of the Mn atom of **1** into a Ge–N bond of its amidinate–germylene ligand (without adding a nucleophile to the Ge atom) could be facilitated by removing the bromide ligand of **1** with a silver salt of a noncoordinating anion. However, (and interestingly), the room temperature reaction of complex **1** with 1 equivalent of Ag[BF₄] led to a product, [Mn{κ²Ge,N-GeF(^tPr₂bzam)^tBu}(CO)₄]**3** (Scheme 1), whose molecular structure, determined by analytical, spectroscopic (Supporting Information), and XRD methods (Figure 3), is entirely analogous to that of

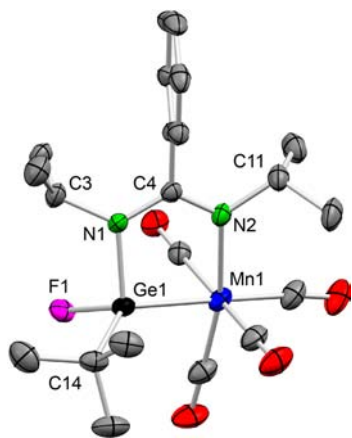


Figure 3. XRD molecular structure of **3** (30% displacement ellipsoids; H atoms omitted for clarity). Selected interatomic distances (Å): Mn1–Ge1 2.3647(9), Mn1–N2 2.126(4), Ge1–C14 1.986(5), Ge1–F1 1.776(2), Ge1–N1 1.901(3), N1–C3 1.494(6), N1–C4 1.352(5), N2–C4 1.314(6), N2–C11 1.490(6).

complex **2** but having a fluoride instead of a methyl group on the Ge atom. Therefore, [BF₄][−] anion has in this occasion behaved as a source of F[−] anion, a role that is unusual but not unknown.¹⁰

With the aim of getting a mechanistic insight into the processes that lead to compounds **2** and **3**, low-temperature reactions were monitored by IR spectroscopy (ν_{CO} region). In both cases, the reagents were initially mixed in toluene at −80 °C, but, as no reaction was observed, the temperature was slowly raised. In the reaction of **1** with LiMe, the ν_{CO} absorptions of the starting material were replaced by those of compound **2** at ca. 0 °C (no transient species were detected). However, in the reaction of **1** with Ag[BF₄], the ν_{CO} absorptions of complex **1** disappeared at ca. −30 °C, being replaced by those of an intermediate complex having a ν_{CO} pattern very similar to that of **1** but with the bands shifted to higher frequencies [2091 (m), 2026 (m), 2002 (vs), 1946 (m) cm^{−1}], as expected for [Mn(BF₄){Ge(^tPr₂bzam)^tBu}(CO)₄]. Above ca. 0 °C, the absorptions of this intermediate species were finally transformed into those of complex **3**. Therefore, the synthesis of compound **3** (and probably also that of **2**) begins with the replacement of the Br[−] anion of **1** by the

corresponding nucleophile. This is in complete agreement with the results of a DFT molecular orbital study (Figure 4), which

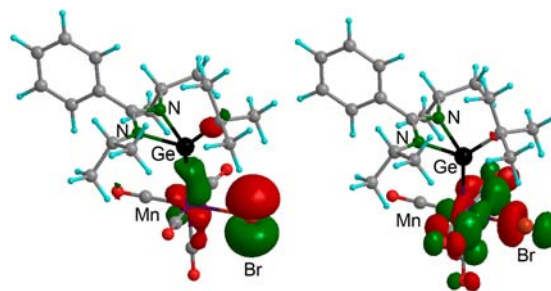


Figure 4. HOMO (left) and LUMO (right) of complex **1**, shown at an isosurface value of ±0.05.

has shown that both HOMO and LUMO of compound **1** are separated by a very large energy gap (103.1 kcal mol^{−1}), have a large contribution from the Br atom, and that, as the LUMO contains a σ -antibonding overlap between Mn and Br with negligible contribution from the atoms of the germylene ligand, complex **1** is prone to break the Mn–Br bond upon treatment with Lewis bases.

Pursuing the synthesis of an elusive mononuclear complex containing a chelating four-electron-donor imine–germylene ligand, we decided to use AgOTf (OTf = triflate) as bromide abstractor because the triflate anion is a weakly coordinating ligand and, in contrast to Ag[BF₄], it has never been reported as a source of fluoride anions. In this case, a comparison of the analytical and spectroscopic data of the product obtained by treating complex **1** with AgOTf with those of complexes **1**–**3** (and a subsequent XRD study, see below) determined that the triflate complex is [Mn(OTf){Ge(^tPr₂bzam)^tBu}(CO)₄]**4** (Scheme 1) and, therefore, that it arises from the simple substitution of the triflate for the bromide anion in **1**. Additionally, trying to induce a Mn-to-Ge shift of the OTf group of **4**, we heated this complex in toluene at 90 °C, but an inseparable mixture was again obtained.

Therefore, the results described above do not yet provide satisfactory answers to questions such as why and how do the reactions of **1** with LiMe or Ag[BF₄] lead to compounds **2** and **3** or why imine–germanate derivatives analogous to **2** and **3** are not obtained from the reaction of **1** with AgOTf or from the thermolyses of **1** and **4**. To shed more light on these questions, we are currently studying reactions of complex **1** with other inorganic and organic nucleophiles and performing mechanistic DFT calculations.

With the aim of completely determining the structure of triflate **4**, a crystal obtained from a hexane solution of this complex was analyzed by XRD. It resulted to contain a 1:1 mixture of triflate **4** and a dimanganese(I) complex of formula [Mn_{2}{μ-κ⁴Ge₂O₂-Ge₂(^tBu)₂(OH)₂O}(CO)₈]**5**. While the molecular structure of **4** (Figure 5) was as it was expected, that of complex **5** was very surprising (Figure 6), since it consists of two Mn(CO)₄ fragments doubly bridged in cis coordination sites by an unprecedented digermanate(II) ligand, [^tBu(OH)GeOGe(OH)^tBu]^{2−}, which comprises an HOGeO-GeOH chain in which each Ge atom is also attached to a *tert*-butyl group. In the complex, each Mn atom is attached to a Ge atom and to the O atom of an OH group in such a way that the molecule has C₂ symmetry (noncrystallographic), with the twofold axis passing through the midpoint of the Mn–Mn}

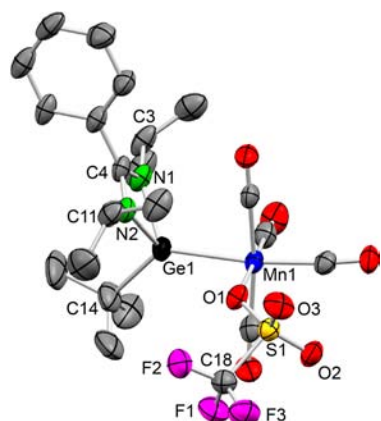


Figure 5. XRD molecular structure of **4** in **4·5** (35% displacement ellipsoids; H atoms omitted for clarity). Selected interatomic distances (Å): Mn1–Ge1 2.4232(7), Mn1–O1 2.088(3), Ge1–C14 1.989(5), Ge1–N1 1.971(3), Ge1–N2 1.971(3), N1–C3 1.471(6), N1–C4 1.315(5), N2–C4 1.324(5), S1–O1 1.461(3), S1–O2 1.423(3), S1–O3 0.421(3). The N2–C11 distance is not given because the C11 atom is involved in positional disorder.

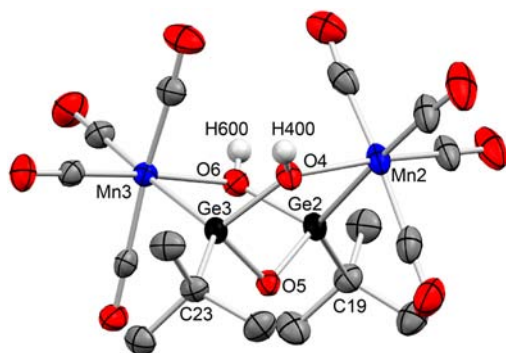


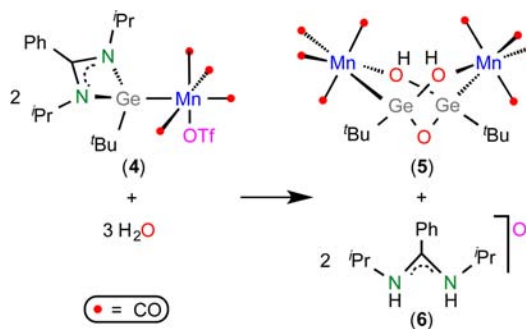
Figure 6. XRD molecular structure of **5** in **4·5** (35% displacement ellipsoids; H atoms, except those of the OH groups, omitted for clarity). Selected interatomic distances (Å): Mn2–Ge2 2.4384(6), Mn3–Ge3 2.4200(7), Mn2–O4 2.096(2), Mn3–O6 2.108(2), Ge2–O5 1.801(2), Ge2–O6 1.874(2), Ge3–O4 1.874(2), Ge3–O5 1.796(2), Ge2–C19 1.981(3), Ge3–C23 1.978(4), Ge2...Ge3 2.902(2), Mn2...Mn3 4.6995(1).

segment and through the O atom that connects the two Ge atoms. In the crystals of **4·5**, both complexes are packed in chains in which each OH group is hydrogen-bonded to one of the two uncoordinated O atoms of the triflate ligand (Supporting Information, Figure SI-8).

As complex **5** in the crystal of **4·5** clearly resulted from an adventitious hydrolysis of complex **4**, we subsequently treated a toluene solution of the triflate complex **4** with water. This reaction immediately led to a 1:2 mixture of **5** and the amidinium salt [ⁱPr₂bzamH₂]⁺OTf⁻ (**6**) (Scheme 3), which were easily separated and isolated in high yields.

As expected from its symmetry, the ¹H and ¹³C{¹H} NMR spectra of compound **5** are very simple, their most relevant feature being the low chemical shift of the OH proton resonance, δ_H –0.91 ppm. The solid-state structure of the amidinium salt **6** was determined by XRD. In the crystal, cations and anions are connected to each other by hydrogen bonds that involve an amidinium NH group and a triflate O atom (Supporting Information, Figure SI-9).

Scheme 3. Hydrolysis of Complex 4



Most of the hitherto known TM complexes equipped with oxo-, hydroxo-, or alkoxo-germanate ligands result from oxidation, hydrolysis, or alcoholysis processes on TM complexes having Ge-donor ligands.^{4i,11–13} As far as we are aware, only one hydrolysis of an amidinate–germylene TM complex has been hitherto reported, namely, that of the rhodium(I) complex [RhCl(cod){κ¹Ge–Ge–(Me₃SibzamSiMe₃)₂}] (cod = 1,5-cyclooctadiene; Me₃SibzamSiMe₃ = *N,N'*-bis(trimethylsilyl)benzamidinate), which leads to the oxo-bridged-digermylene dirhodium(I) derivative [Rh₂Cl₂(cod)₂{μ–κ²Ge, Ge'–Ge₂O–(Me₃SibzamSiMe₃)₂}], reported by Castel and co-workers.⁴ⁱ

CONCLUSIONS

In summary, this contribution, in addition to reporting the first amidinate–germylene derivatives of manganese (**1** and **4**), also describes the unprecedented transformation of a terminal two-electron-donor amidinate–germylene ligand (that of **1**) into chelating three-electron-donor κ²-*N,Ge*-imine–germanate ligands (those of **2** and **3**). The instability of these amidinate–germylene derivatives of manganese toward water has been established by isolating and characterizing compound **5**, which contains a novel oxo-dihydroxo-digermanate(II) ligand bridging two manganese atoms.

On the other hand, the herein reported results provide additional data supporting that the coordination of one of the N atoms of amidinate–HTs to a TM is only a favorable process if the final product does not contain a three-coordinate HT donor atom. In fact, besides this work (complexes **2** and **3**), such a ligand behavior has only been observed in (a) binuclear TM complexes where the HT donor atom is finally attached to four atoms (two TM atoms, an amidinate N atom, and an additional anionic group)^{2b,c,3g} and (b) bis(guanidinate)–silylenes in group-6 metal complexes, where the Si atom is surrounded by one metal atom and three amidinate N atoms.⁹

Given the strong interest that is currently being devoted to the coordination chemistry of HTs, it is expected that these results will have implications in future stoichiometric and catalytic reactions involving amidinate–HTs and TM complexes.

EXPERIMENTAL SECTION

General Procedures. Solvents were dried over appropriate desiccating reagents and were distilled under argon before use. All reactions were carried out under argon, using drybox and/or Schlenk-vacuum line techniques and were routinely monitored by solution IR spectroscopy. All reaction products were vacuum-dried for several hours prior to being weighed and analyzed. The germylene Ge(ⁱPr₂bzam)Cl was prepared following a published procedure.^{3g} All remaining reagents were purchased from commercial sources. NMR

spectra were run on a Bruker DPX-300 instrument, using as standards a residual protic solvent resonance for ^1H [$\delta(\text{C}_6\text{HD}_6) = 7.16$ ppm; [$\delta(\text{CHCl}_3) = 7.26$ ppm], a solvent resonance for ^{13}C [$\delta(\text{C}_6\text{D}_6) = 128.1$ ppm; [$\delta(\text{CHCl}_3) = 77.16$ ppm], and an external solution of trifluoroacetic acid in CDCl_3 for ^{19}F [$\delta(\text{CF}_3\text{CO}_2\text{H}) = -76.55$ ppm]. Elemental analyses were obtained from a PerkinElmer 2400 microanalyzer. Mass spectra (MS) were run on a VG Autospec double-focusing mass spectrometer operating in the FAB+ mode; ions were produced with a standard Cs^+ gun at about 30 kV; 3-nitrobenzyl alcohol was used as matrix; data given correspond to the most abundant isotopomer of the molecular ion or of the greatest mass fragment.

$\text{Ge}(\text{Pr}_2\text{bzam})\text{Bu}$. Li^tBu (5.8 mL, 1.7 M in pentane, 9.9 mmol) was added to a solution of $\text{Ge}(\text{Pr}_2\text{bzam})\text{Cl}$ (3.04 g, 9.8 mmol) in diethyl ether (30 mL) at -78°C . The resulting suspension was allowed to warm up to room temperature and then stirred for 6 h. The solvent was removed under reduced pressure, the residue was extracted into hexane (2×30 mL), and the filtrate was evaporated to dryness under vacuum to give $\text{Ge}(\text{Pr}_2\text{bzam})\text{Bu}$ as an orange oily material (2.78 g, 85%). ^1H NMR (C_6D_6 , 300.1 MHz, 293 K): δ 7.12–7.04 (m, 5 H, 5 CH of Ph), 3.39 (sept, 2 H, $J = 6.4$ Hz, 2 CH of 2 ^iPr), 1.35 (s, 9 H, 3 Me of ^tBu), 1.09 (d, $J = 6.4$ Hz, 6 H, 2 Me of ^iPr), 0.95 (d, $J = 6.4$ Hz, 6 H, 2 Me of ^iPr) ppm. $^{13}\text{C}\{^1\text{H}\}$ NMR (C_6D_6 , 75.5 MHz, 293 K): δ 165.7 (NCN), 131.9 (C_{ipso} of Ph), 129.6 (2 CH of Ph), 129.1 (2 CH of Ph), 128.9 (s, CH of Ph), 47.1 (2 CH of 2 ^iPr), 31.1 (C of ^tBu), 27.6 (3 Me of ^tBu), 27.0 (2 Me of ^iPr), 25.3 (2 Me of ^iPr).

$[\text{MnBr}(\text{Ge}(\text{Pr}_2\text{bzam})\text{Bu})(\text{CO})_4]$ (1). A toluene solution of $\text{Ge}(\text{Pr}_2\text{bzam})\text{Bu}$ (0.20 mL, 0.37 M, 0.074 mmol) was added to a solution of $[\text{MnBr}(\text{CO})_5]$ (20 mg, 0.073 mmol) in toluene (10 mL). The initial yellow color changed to light orange. After stirring at room temperature for 10 min, the solvent was removed under reduced pressure and the crude reaction mixture was separated by column chromatography on silica gel (2×3 cm). Hexane–dichloromethane (1:2) eluted compound 1, which was isolated as a yellow solid (35 mg, 82%). Anal. (%) Calcd for $\text{C}_{21}\text{H}_{28}\text{BrGeMnN}_2\text{O}_4$ (MW = 579.91 amu): C, 43.49; H, 4.87; N, 4.83; found: 43.51; H, 4.89; N, 4.82. (+)-FAB MS: m/z 580 $[\text{M}]^+$. IR (toluene): ν_{CO} 2068 (m), 2001 (m), 1981 (vs), 1935 (m) cm^{-1} . ^1H NMR (C_6D_6 , 300.1 MHz, 293 K): δ 7.22 (m, 1 H, CH of Ph), 7.03–6.89 (m, 4 H, 4 CH of Ph), 3.35 (sept, $J = 6.6$ Hz, 2 H, 2 CH of 2 ^iPr), 1.39 (s, 9 H, ^tBu), 1.09 (d, $J = 6.6$ Hz, 6 H, 2 Me of ^iPr), 1.01 (d, $J = 6.6$ Hz, 6 H, 2 Me of ^iPr) ppm. $^{13}\text{C}\{^1\text{H}\}$ NMR (C_6D_6 , 75.5 MHz, 293 K): δ 219.7 (CO), 215.7 (2 CO), 213.1 (CO), 171.8 (NCN), 130.5–127.3 (5 CHs + 1 C_{ipso} of Ph), 48.1 (2 CH of 2 ^iPr), 39.0 (C of ^tBu), 27.0 (3 Me of ^tBu), 24.9 (2 Me of ^iPr), 23.7 (2 Me of ^iPr) ppm.

$[\text{Mn}(\kappa^2\text{Ge}_2\text{N-GeMe}(\text{Pr}_2\text{bzam})\text{Bu})(\text{CO})_4]$ (2). A toluene solution of $\text{Ge}(\text{Pr}_2\text{bzam})\text{Bu}$ (0.20 mL, 0.37 M, 0.074 mmol) was added to a solution of $[\text{MnBr}(\text{CO})_5]$ (20 mg, 0.073 mmol) in toluene (10 mL). The initial yellow color changed to light orange. After stirring at room temperature for 10 min, LiMe (45 μL , 1.6 M in diethyl ether, 0.072 mmol) was added and the mixture was stirred at room temperature for 30 min. The initial yellow color changed to orange. The solvent was removed under reduced pressure, and the crude reaction mixture was separated by column chromatography on silica gel (2×3 cm). Dichloromethane eluted compound 2, which was isolated as a light yellow solid (20 mg, 53%). Anal. (%) Calcd for $\text{C}_{22}\text{H}_{31}\text{GeMnN}_2\text{O}_4$ (MW = 515.04 amu): C, 51.30; H, 6.07; N, 5.44; found: C, 51.42; H, 6.12; N, 5.83. (+)-FAB MS: m/z 516 $[\text{M}]^+$. IR (toluene): ν_{CO} 2063 (w), 1984 (vs), 1965 (m), 1940 (m) cm^{-1} . ^1H NMR (C_6D_6 , 300.1 MHz, 293 K): δ 6.94–6.89 (m, 3 H, 3 CH of Ph), 6.76–6.66 (m, 2 H, 2 CH of Ph), 3.40–3.25 (m, 2 H, 2 CH of 2 ^iPr), 1.30 (s, 9 H, ^tBu), 1.01 (d, $J = 6.5$ Hz, 3 H, Me of ^iPr), 0.96 (s, 3 H, Ge–Me) 0.90–0.86 (m, 6 H, 2 Me of ^iPr), 0.57 (d, $J = 6.5$ Hz, 3 H, Me of ^iPr) ppm. $^{13}\text{C}\{^1\text{H}\}$ NMR (C_6D_6 , 75.5 MHz, 293 K): δ 173.7 (NCN), 138.5 (C_{ipso} of Ph), 128.7–127.0 (5 CHs of Ph), 54.4 (CH of ^iPr), 51.3 (CH of ^iPr), 31.4 (C of ^tBu), 28.3 (3 Me of ^tBu), 24.6 (Me of Ge–Me and 2 Me of ^iPr), 24.4 (Me of ^iPr), 22.2 (Me of ^iPr) ppm.

$[\text{Mn}(\kappa^2\text{Ge}_2\text{N-GeF}(\text{Pr}_2\text{bzam})\text{Bu})(\text{CO})_4]$ (3). A toluene solution of $\text{Ge}(\text{Pr}_2\text{bzam})\text{Bu}$ (0.20 mL, 0.37 M, 0.074 mmol) was added to a

solution of $[\text{MnBr}(\text{CO})_5]$ (20 mg, 0.073 mmol) in toluene (10 mL). The initial yellow color changed to light orange. After stirring at room temperature for 10 min, solid $\text{Ag}[\text{BF}_4]$ (15 mg, 0.074 mmol) was added and the mixture was stirred at room temperature for 2 h. The initial yellow solution changed to dark brown suspension. The solvent was removed under reduced pressure, and the crude reaction mixture was separated by column chromatography on silica gel (2×3 cm). THF eluted compound 3, which was isolated as a light yellow solid (31 mg, 82%). Anal. (%) Calcd for $\text{C}_{21}\text{H}_{28}\text{FGeMnN}_2\text{O}_4$ (MW = 519.00 amu): C, 48.60; H, 5.44; N, 5.40; found: C, 48.65; H, 5.47; N, 5.38. (+)-FAB MS: m/z 408 $[\text{M} - 3 \text{CO}]^+$. IR (toluene): ν_{CO} 2063 (w), 1984 (vs), 1965 (m), 1940 (m) cm^{-1} . ^1H NMR (C_6D_6 , 300.1 MHz, 293 K): δ 6.93 (m, 3 H, 3 CH of Ph), 6.68–6.60 (m, 2 H, 2 CH of Ph), 3.65–3.57 (m, 1 H, CH of ^iPr), 3.36–3.27 (m, 1 H, CH of ^iPr), 1.43 (s, 9 H, ^tBu), 1.06 (d, $J = 6.6$ Hz, 3 H, Me of ^iPr), 0.90–0.87 (m, 9 H, 3 Me of ^iPr) ppm. $^{13}\text{C}\{^1\text{H}\}$ NMR (C_6D_6 , 75.5 MHz, 293 K): δ 174.6 (NCN), 137.63 (C_{ipso} of Ph), 129.0–126.9 (5 CHs of Ph), 55.0 (CH of ^iPr), 50.9 (CH of ^iPr), 37.9 (d, $J = 12.5$ Hz, C of ^tBu), 27.7 (3 Me of ^tBu), 24.5 (Me of ^iPr), 24.3 (Me of ^iPr), 24.2 (Me of ^iPr), 22.1 (Me of ^iPr) ppm. $^{19}\text{F}\{^1\text{H}\}$ NMR (C_6D_6 , 282.4 MHz, 293 K): δ –168.4 (s) ppm.

$[\text{Mn}(\text{OTf})(\text{Ge}(\text{Pr}_2\text{bzam})\text{Bu})(\text{CO})_4]$ (4). A toluene solution of $\text{Ge}(\text{Pr}_2\text{bzam})\text{Bu}$ (0.20 mL, 0.37 M, 0.074 mmol) was added to a solution of $[\text{MnBr}(\text{CO})_5]$ (20 mg, 0.073 mmol) in toluene (10 mL). After stirring at room temperature for 10 min, solid AgOTf (40 mg, 0.156 mmol) was added and the mixture was stirred at room temperature for 20 min. The initial yellow solution changed to dark brown suspension. The solvent was removed under reduced pressure, and the crude reaction mixture was extracted into hexane (2×5 mL). The filtered extract was evaporated to dryness under vacuum to give 4 as a yellow solid (36 mg, 76%). Anal. (%) Calcd for $\text{C}_{22}\text{H}_{28}\text{F}_3\text{GeMnN}_2\text{O}_7\text{S}$ (MW = 649.08 amu): C, 40.71; H, 4.34; N, 4.32; found: C, 40.76; H, 4.37; N, 4.30. IR (toluene): ν_{CO} 2087 (m), 2022 (m), 1998 (vs), 1947 (m). ^1H NMR (C_6D_6 , 300.1 MHz, 293 K): δ 7.34 (m, 1 H, CH of Ph), 7.11–6.90 (m, 4 H, 4 CH of Ph), 3.29 (sept, $J = 6.5$ Hz, 2 H, 2 CH of 2 ^iPr), 1.30 (s, 9 H, ^tBu), 0.98 (d, $J = 6.5$ Hz, 6 H, 2 Me of ^iPr), 0.87 (d, $J = 6.6$ Hz, 6 H, 2 Me of ^iPr) ppm. $^{19}\text{F}\{^1\text{H}\}$ NMR (C_6D_6 , 282.4 MHz, 293 K): δ –76.1 (s) ppm. $^{13}\text{C}\{^1\text{H}\}$ NMR (C_6D_6 , 75.5 MHz, 293 K): δ 218.1 (CO), 214.6 (2 CO), 210.0 (CO), 173.0 (NCN), 131.0–127.7 (C + 5 CHs of Ph), 120.3 (q, $J = 319$ Hz, CF_3), 47.9 (2 CH of 2 ^iPr), 39.3 (C of ^tBu), 26.2 (3 Me of ^tBu), 24.7 (2 Me of ^iPr), 23.8 (2 Me of ^iPr).

$[\text{Mn}_2\{\mu-\kappa^4\text{Ge}_2\text{O}_2\text{-Ge}_2\text{Bu}_2(\text{OH})_2\text{O}\}(\text{CO})_4]$ (5) and $[\text{Pr}_2\text{bzamH}_2]\text{OTf}$ (6). Water (5 μL , 0.277 mmol) was added to a toluene (8 mL) solution of 4 (45 mg, 0.070 mmol), and the mixture was stirred at room temperature for 60 min. The initial yellow color changed to light orange. The solvent was removed under reduced pressure, and the crude reaction mixture was extracted into hexane (2×5 mL). The hexane solution was separated from a white solid by filtration. The filtrate was evaporated to dryness under vacuum to give compound 5 as a yellow solid (19 mg, 84%). The white solid was identified as $[\text{Pr}_2\text{bzamH}_2]\text{OTf}$ (6) (22 mg, 88%). Data for 5: Anal. Calcd for $\text{C}_{16}\text{H}_{20}\text{Ge}_2\text{Mn}_2\text{O}_{11}$ (MW = 643.42 amu): C, 29.87; H, 3.13; found: C, 30.01; H, 3.19. (+)-FAB MS: $m/z = 644$ $[\text{M}]^+$. IR (toluene): ν_{CO} 2064 (m), 1991 (vs), 1969 (m), 1933 (m) cm^{-1} . ^1H NMR (C_6D_6 , 300.1 MHz, 293 K): δ 1.10 (s, 18 H, 2 ^tBu), –0.91 (s, 2 H, 2 OH) ppm. $^{13}\text{C}\{^1\text{H}\}$ NMR (C_6D_6 , 75.5 MHz, 293 K): δ 219.9 (COs), 37.8 (C of ^tBu), 25.9 (6 Me of ^tBu) ppm. Data for 6: Anal. (%) Calcd for $\text{C}_{14}\text{H}_{21}\text{F}_3\text{N}_2\text{O}_3\text{S}$ (MW = 354.39 amu): C, 47.45; H, 5.97; N, 7.91; found: C, 47.51; H, 7.94; N, 7.87. (+)-FAB MS: $m/z = 205.2$ $[\text{Pr}_2\text{bzamH}_2]^+$. ^1H NMR (CDCl_3 , 300.1 MHz, 293 K): δ 8.90 (s, br, 2 H, 2 NH), 7.66–7.35 (m, 5 H, 5 CH of Ph), 3.25 (m, 2 H, 2 CH of ^iPr), 1.18 (s, br, 12 H, 4 Me of ^iPr) ppm. $^{19}\text{F}\{^1\text{H}\}$ NMR (C_6D_6 , 282.4 MHz, 293 K): $\delta = -78.4$ (s) ppm. $^{13}\text{C}\{^1\text{H}\}$ NMR (CDCl_3 , 75.5 MHz, 293 K): δ 164.4 (NCN), 132.4 (CH of Ph), 130.2 (2 CH of Ph), 126.6 (2 CH of Ph), 126.0 (C_{ipso} of Ph), 48.3 (2 CH of ^iPr), 22.9 (4 Me of ^iPr) ppm.

X-ray Diffraction Analyses. Diffraction data were collected on an Oxford Diffraction Xcalibur Onyx Nova (1, 3, 4-5, and 6) and an

Xcalibur Ruby Gemini (2) single-crystal diffractometers. Empirical absorption corrections were applied using the SCALE3 ABSPACK algorithm as implemented in CrysAlisPro RED¹⁴ (for 1, 3, 4-5, and 6) and XABS2¹⁵ (for 2). The structures were solved using SIR-97.¹⁶ Isotropic and full matrix anisotropic least-squares refinements were carried out using SHELXL.¹⁷ The hydrogen atoms of the OH (H400, H600 in 5) and NH (H100, H200 in 6) groups were located in their corresponding Fourier maps. The remaining hydrogen atoms of all the compounds were set in calculated positions and refined riding on their parent atoms. The crystals of 1 and 2 were racemic twins and were refined using the TWIN order. The crystal of 1 was found to contain four symmetry-independent but analogous molecules in the asymmetric unit, each molecule exhibiting some positional disorder involving the Br atom and an adjacent CO ligand cis to the germylene ligand. This two ligands exchange their positions with occupancy ratios of 96:4, 83:17, 78:22, and 81:19, respectively, for molecules 1, 2, 3, and 4, the greater occupancy corresponding to a situation in which the Br atom is aligned syn to the ^tBu group. Restraints on the thermal and geometrical parameters of the atoms involved in this positional disorder were applied. For 2, restraints on the thermal parameters of the methyl carbon atoms of the *tert*-butyl group were required due to their tendency to give nonpositive definite ellipsoids. In the crystal of 4-5, the isopropyl group attached to the N2 atom of 4 was found disordered over two positions with an occupancy ratio of 74:26; restraints were applied on the thermal and geometrical parameters of the atoms involved. The WINGX program system¹⁸ was used throughout the structure determinations. The molecular plots were made with MERCURY.¹⁹ A selection of measurement and refinement data is given in Table SI-1 of the Supporting Information. CCDC deposition numbers: 1008617 (1), 1008618 (2), 1008619 (3), 1012976 (4-5), and 1012977 (6).

Computational Details. DFT calculations were carried out using the Becke's three-parameter hybrid exchange-correlation functional²⁰ and the hybrid B3LYP nonlocal gradient correction.²¹ The LanL2DZ basis set,²² with relativistic effective core potentials, was used for the Mn atom. The basis set used for the remaining atoms was the 6-31G(d,p).²³ The optimized structure of complex 1 was confirmed as an energy minimum by analytical calculation of frequencies (all positive eigenvalues). The corresponding Cartesian coordinates are given in the Supporting Information (Table SI-2). Molecular orbital data were obtained from the natural bond order (NBO) analysis of the data.²⁴ All calculations were carried out without symmetry constraints employing the Gaussian09 package.²⁵

■ ASSOCIATED CONTENT

■ Supporting Information

Crystal, acquisition, and refinement XRD data, DFT-calculated atomic coordinates, ¹H and ¹³C{¹H} NMR spectra, and X-ray crystallographic data in CIF format. This material is available free of charge via the Internet at <http://pubs.acs.org>.

■ AUTHOR INFORMATION

Corresponding Authors

*E-mail: jac@uniovi.es.

*E-mail: pga@uniovi.es.

Author Contributions

The manuscript was written through contributions of all authors. All authors have given approval to the final version of the manuscript.

Notes

The authors declare no competing financial interest.

■ ACKNOWLEDGMENTS

This work has been supported by a European Union Marie Curie reintegration grant (FP7-2010-RG-268329) and by Spanish MINECO-FEDER research grants (CTQ2010-14933,

MAT2010-15094, DELACIERVA-09-05, and RYC-2012-10491).

■ REFERENCES

- (1) For recent reviews on chemistry and/or catalysis of amidinate–HT–TM complexes, see: (a) Blom, B.; Gallego, D.; Driess, M. *Inorg. Chem. Front.* **2014**, *1*, 134. (b) Blom, B.; Stoelzel, M.; Driess, M. *Chem.—Eur. J.* **2013**, *19*, 40. (c) Asay, M.; Jones, C.; Driess, M. *Chem. Rev.* **2011**, *111*, 354.
- (2) (a) Tan, G.; Blom, B.; Gallego, G.; Driess, M. *Organometallics* **2014**, *33*, 363. (b) Cabeza, J. A.; García-Álvarez, P.; Pérez-Carreño, E.; Polo, D. *Chem.—Eur. J.* **2014**, *20*, 8654. (c) Cabeza, J. A.; Fernández-Colinas, J. M.; García-Álvarez, P.; Polo, D. *RSC Adv.* **2014**, *4*, 31503.
- (3) (a) Gallego, D.; Brück, A.; Irran, E.; Meier, F.; Kaupp, M.; Driess, M.; Hartwig, J. F. *J. Am. Chem. Soc.* **2013**, *135*, 15617. (b) Blom, B.; Enthaler, S.; Inoue, S.; Irran, E.; Driess, M. *J. Am. Chem. Soc.* **2013**, *135*, 6703. (c) Breit, N. C.; Szilvási, T.; Suzuki, T.; Gallego, D.; Inoue, S. *J. Am. Chem. Soc.* **2013**, *135*, 17958. (d) Junold, K.; Baus, J. A.; Burschka, C.; Vent-Schmidt, T.; Riedel, S.; Tacke, R. *Inorg. Chem.* **2013**, *52*, 11593. (e) Azhakar, R.; Ghadwal, R. S.; Roesky, H. W.; Hey, J.; Krause, L.; Stalke, D. *Dalton. Trans.* **2013**, *42*, 10277. (f) Someya, C. I.; Haberberger, M.; Wang, W.; Enthaler, S.; Inoue, S. *Chem. Lett.* **2013**, *42*, 286. (g) Cabeza, J. A.; García-Álvarez, P.; Polo, D. *Dalton. Trans.* **2013**, *42*, 1329.
- (4) (a) Wang, W.; Inoue, S.; Enthaler, S.; Driess, M. *Angew. Chem., Int. Ed.* **2012**, *51*, 6167. (b) Brück, A.; Gallego, D.; Wang, W.; Irran, E.; Driess, M.; Hartwig, J. F. *Angew. Chem., Int. Ed.* **2012**, *51*, 11478. (c) Blom, B.; Driess, M.; Gallego, D.; Inoue, S. *Chem.—Eur. J.* **2012**, *18*, 13355. (d) Azhakar, R.; Ghadwal, R. S.; Roesky, H. W.; Hey, J.; Stalke, D. *Chem.—Asian J.* **2012**, *7*, 528. (e) Azhakar, R.; Ghadwal, R. S.; Roesky, H. W.; Wolf, H.; Stalke, D. *J. Am. Chem. Soc.* **2012**, *134*, 2423. (f) Junold, K.; Baus, J. A.; Burschka, C.; Tacke, R. *Angew. Chem., Int. Ed.* **2012**, *51*, 7020. (g) Azhakar, R.; Roesky, H. W.; Holstein, J. J.; Dittrich, B. *Dalton. Trans.* **2012**, *41*, 12096. (h) Wang, W.; Inoue, S.; Irran, E.; Driess, M. *Angew. Chem., Int. Ed.* **2012**, *51*, 3691. (i) Matioszek, D.; Saffon, N.; Sotiropoulos, J.-M.; Miqueu, K.; Castel, A.; Escudí, J. *Inorg. Chem.* **2012**, *51*, 11716.
- (5) Azhakar, R.; Sarish, S. P.; Roesky, H. W.; Hey, J.; Stalke, D. *Inorg. Chem.* **2011**, *50*, 5039.
- (6) (a) Tavčar, G.; Sen, S. S.; Azhakar, R.; Thorn, A.; Roesky, H. W. *Inorg. Chem.* **2010**, *49*, 10199. (b) Wang, W.; Inoue, S.; Yao, S.; Driess, M. *J. Am. Chem. Soc.* **2010**, *132*, 15890. (c) Matioszek, D.; Katir, N.; Saffon, N.; Castel, A. *Organometallics* **2010**, *29*, 3039. (d) Sen, S. S.; Kritzler-Kosch, M. P.; Nagendran, S.; Roesky, H. W.; Beck, T.; Pal, A.; Herbst-Irmer, R. *Eur. J. Inorg. Chem.* **2010**, 5304. (e) Sen, S. S.; Kratzer, D.; Stern, D.; Roesky, H. W.; Stalke, D. *Inorg. Chem.* **2010**, *49*, 5786.
- (7) Yang, W.; Fu, H.; Wang, H.; Chen, M.; Ding, Y.; Roesky, H. W.; Jana, A. *Inorg. Chem.* **2009**, *48*, 5058.
- (8) Jones, C.; Rose, R. P.; Stasch, A. *Dalton Trans.* **2008**, 2871.
- (9) Mück, F. M.; Kloss, D.; Baus, J. A.; Burschka, C.; Tacke, R. *Chem.—Eur. J.* **2014**, DOI: 10.1002/chem.201402889.
- (10) See, for example: (a) Reger, D. L.; Watson, R. P.; Gardinier, J. R.; Smith, M. D.; Pellechia, P. J. *Inorg. Chem.* **2006**, *45*, 10088 and references therein. (b) Coleman, K. S.; Fawcett, J.; Harding, D. A. J.; Hope, E. J.; Singh, K.; Solan, G. A. *Eur. J. Inorg. Chem.* **2010**, 4310 and references therein.
- (11) (a) Huang, M.; Kireenko, M. M.; Djekavov, P. B.; Zaitsev, K. V.; Oprunenko, Y. F.; Churakov, A. V.; Tyurin, D. A.; Karlov, S. S.; Zaitseva, G. S. *J. Organomet. Chem.* **2013**, *735*, 15. (b) Greene, J.; Curtis, M. D. *Inorg. Chem.* **1978**, *17*, 2324.
- (12) (a) Adams, R. D.; Trufan, E. *Organometallics* **2010**, *29*, 4346. (b) Adams, R. D.; Captain, B.; Hollandsworth, C. B.; Johansson, M.; Smith, J. L., Jr. *Organometallics* **2006**, *25*, 3848. (c) Renner, G.; Huttner, G.; Rutsch, P. *Z. Naturforsch., B: J. Chem. Sci.* **2001**, *56*, 1328. (d) Filippou, A. C.; Steck, R.; Kociok-Kohn, G. *J. Chem. Soc., Dalton Trans.* **1999**, 2267. (e) Adams, R. D.; Cotton, F. A.; Frenz, B. A. *J. Organomet. Chem.* **1974**, *73*, 93.
- (13) Knoth, W. H. *J. Am. Chem. Soc.* **1979**, *101*, 2211.

- (14) *CrysAlisPro RED*, version 1.171.34.36; Oxford Diffraction Ltd.: Oxford, U.K., 2010.
- (15) Parkin, S.; Moezzi, B.; Hope, H. *J. Appl. Crystallogr.* **1995**, *28*, 53.
- (16) Altomare, A.; Burla, M. C.; Camalli, M.; Cascarano, G. L.; Giacovazzo, C.; Guagliardi, A.; Moliterni, A. G. C.; Polidori, G.; Spagna, R. *J. Appl. Crystallogr.* **1999**, *32*, 115.
- (17) *SHELXL*: Sheldrick, G. M. *Acta Crystallogr.* **2008**, *A64*, 112.
- (18) *WINGX*, version 1.80.05 (2009): Farrugia, L. J. *J. Appl. Crystallogr.* **1999**, *32*, 837.
- (19) *MERCURY*, CSD 3.1 (build RCS); Cambridge Crystallographic Data Centre: Cambridge, U.K., 2013.
- (20) Becke, A. D. *J. Chem. Phys.* **1993**, *98*, 5648.
- (21) Lee, C.; Yang, W.; Parr, R. G. *Phys. Rev. B* **1988**, *37*, 785.
- (22) Hay, P. J.; Wadt, W. R. *J. Chem. Phys.* **1985**, *82*, 299.
- (23) Hariharan, P. C.; Pople, J. A. *Theor. Chim. Acta* **1973**, *28*, 213.
- (24) (a) Reed, A. E.; Weinstock, R. B.; Weinhold, F. *J. Chem. Phys.* **1985**, *83*, 735. (b) Reed, A. E.; Curtis, L. A.; Weinhold, F. *Chem. Rev.* **1988**, *88*, 899.
- (25) Frisch, M. J.; Trucks, G. W.; Schlegel, H. B.; Scuseria, G. E.; Robb, M. A.; Cheeseman, J. R.; Scalmani, G.; Barone, V.; Mennucci, B.; Petersson, G. A.; Nakatsuji, H.; Caricato, M.; Li, X.; Hratchian, H. P.; Izmaylov, A. F.; Bloino, J.; Zheng, G.; Sonnenberg, J. L.; Hada, M.; Ehara, M.; Toyota, K.; Fukuda, R.; Hasegawa, J.; Ishida, M.; Nakajima, T.; Honda, Y.; Kitao, O.; Nakai, H.; Vreven, T.; Montgomery, J. A., Jr.; Peralta, J. E.; Ogliaro, F.; Bearpark, M.; Heyd, J. J.; Brothers, E.; Kudin, K. N.; Staroverov, V. N.; Kobayashi, R.; Normand, J.; Raghavachari, K.; Rendell, A.; Burant, J. C.; Iyengar, S. S.; Tomasi, J.; Cossi, M.; Rega, N.; Millam, N. J.; Klene, M.; Knox, J. E.; Cross, J. B.; Bakken, V.; Adamo, C.; Jaramillo, J.; Gomperts, R.; Stratmann, R. E.; Yazyev, O.; Austin, A. J.; Cammi, R.; Pomelli, C.; Ochterski, J. W.; Martin, R. L.; Morokuma, K.; Zakrzewski, V. G.; Voth, G. A.; Salvador, P.; Dannenberg, J. J.; Dapprich, S.; Daniels, A. D.; Farkas, Ö.; Foresman, J. B.; Ortiz, J. V.; Cioslowski, J.; Fox, D. J. *Gaussian 09*, revision A.01; Gaussian, Inc.: Wallingford, CT, 2009.

SUPPORTING INFORMATION (*Inorg. Chem.*, Ms. ID: ic-2014-01418p)

Conversion of a Monodentate Amidinate-Germylene Ligand into Chelating Imine-Germanate Ligands (on Mononuclear Manganese Complexes)

Javier A. Cabeza,^{*,†} Pablo García-Álvarez,^{*,†} Enrique Pérez-Carreño,[‡] and Diego Polo[†]

[†]*Departamento de Química Orgánica e Inorgánica-IUQOEM, Universidad de Oviedo-CSIC, E-33071 Oviedo, Spain*

[‡]*Departamento de Química Física y Analítica, Universidad de Oviedo, E-33071 Oviedo, Spain*

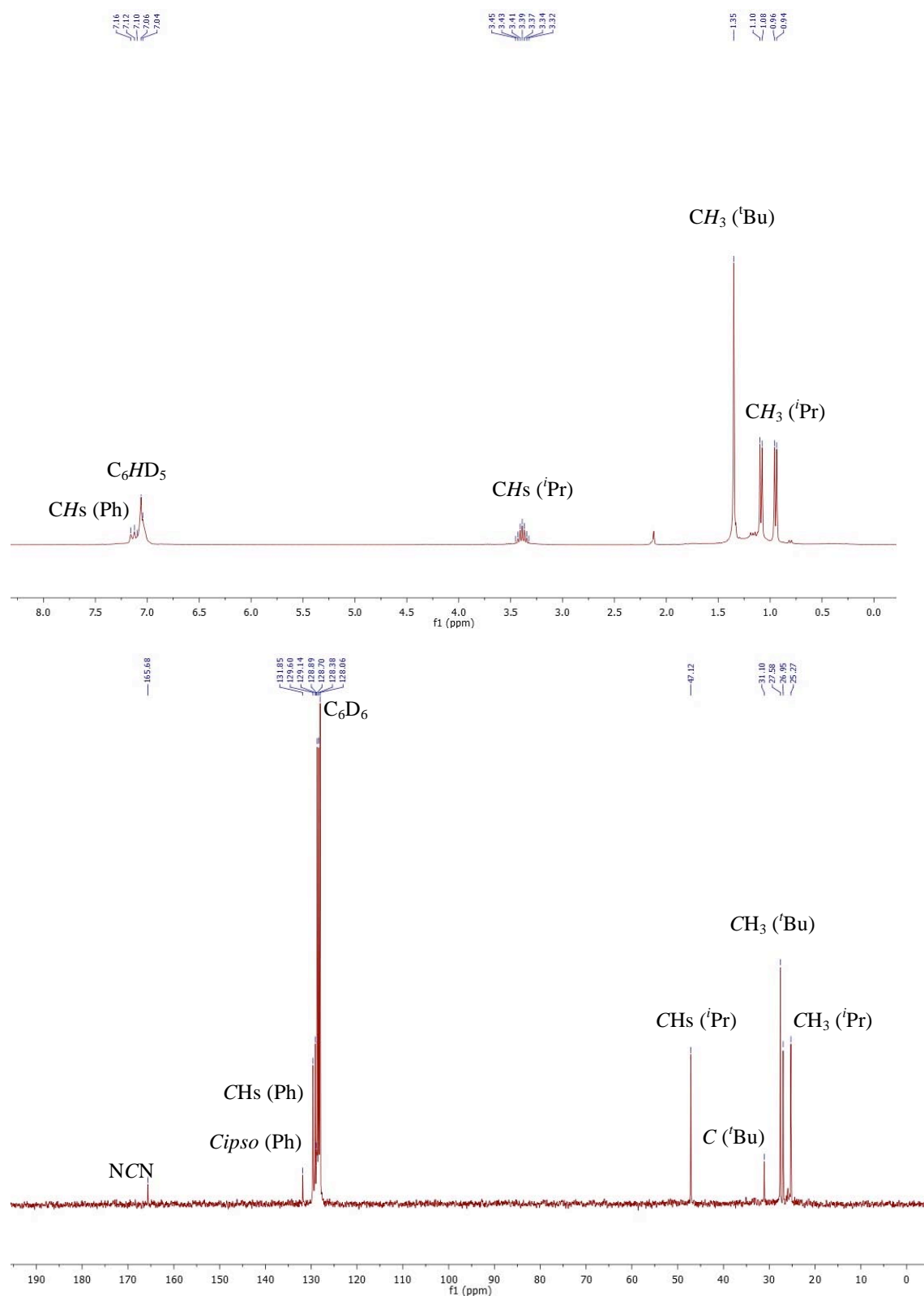


Figure SI-1. ^1H (top; 300.1 MHz) and $^{13}\text{C}\{^1\text{H}\}$ (bottom; 75.5 MHz) NMR spectra of $\text{Ge}(i\text{Pr}_2\text{bam})\text{Bu}$ (in C_6D_6 at 25°C).

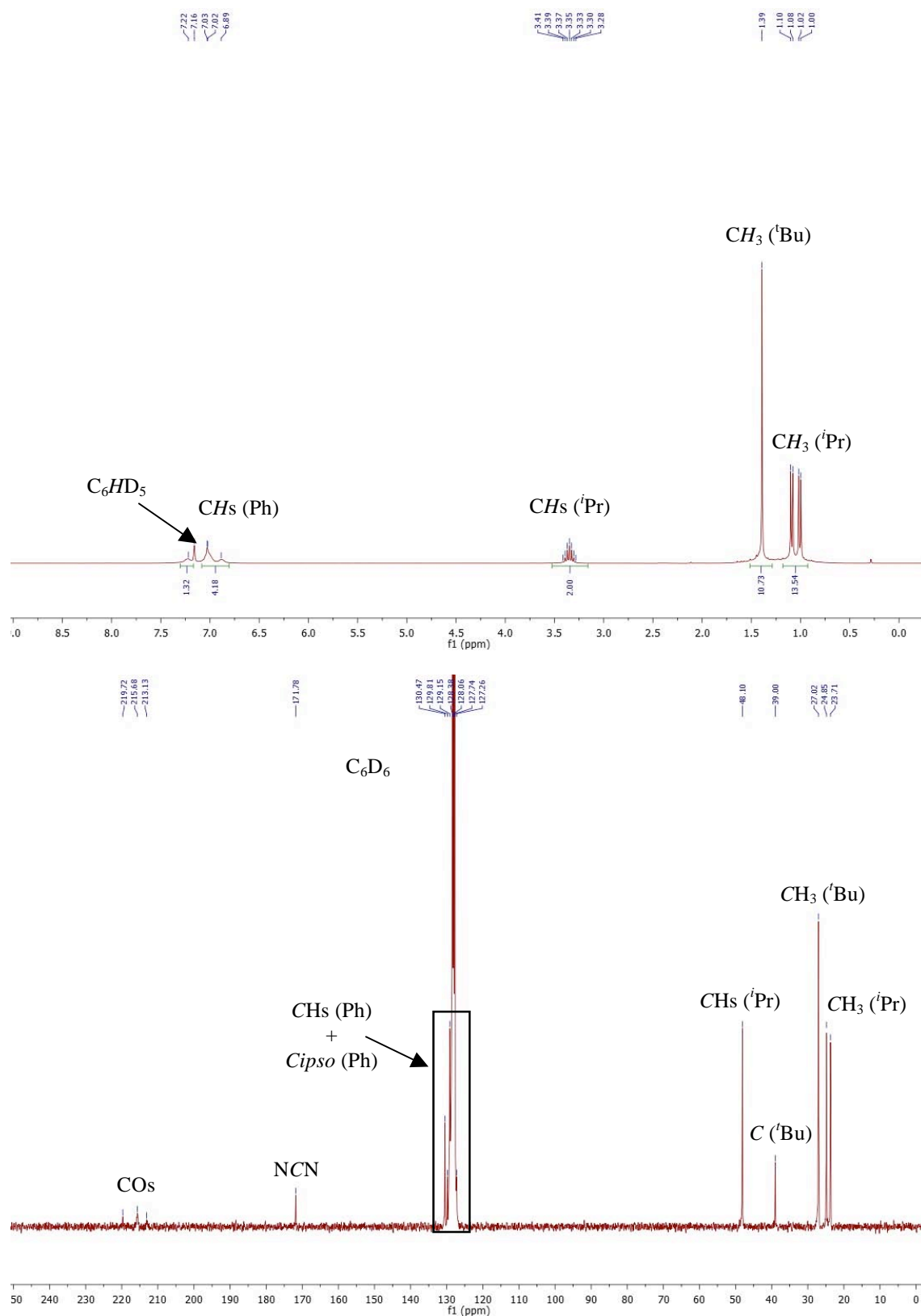


Figure SI-2. ^1H (top; 300.1 MHz) and $^{13}\text{C}\{^1\text{H}\}$ (bottom; 75.5 MHz) NMR spectra of $[\text{MnBr}\{\text{Ge}(\text{iPr}_2\text{bzam})\text{Bu}\}(\text{CO})_4]$ (1) in C_6D_6 at 25 °C.

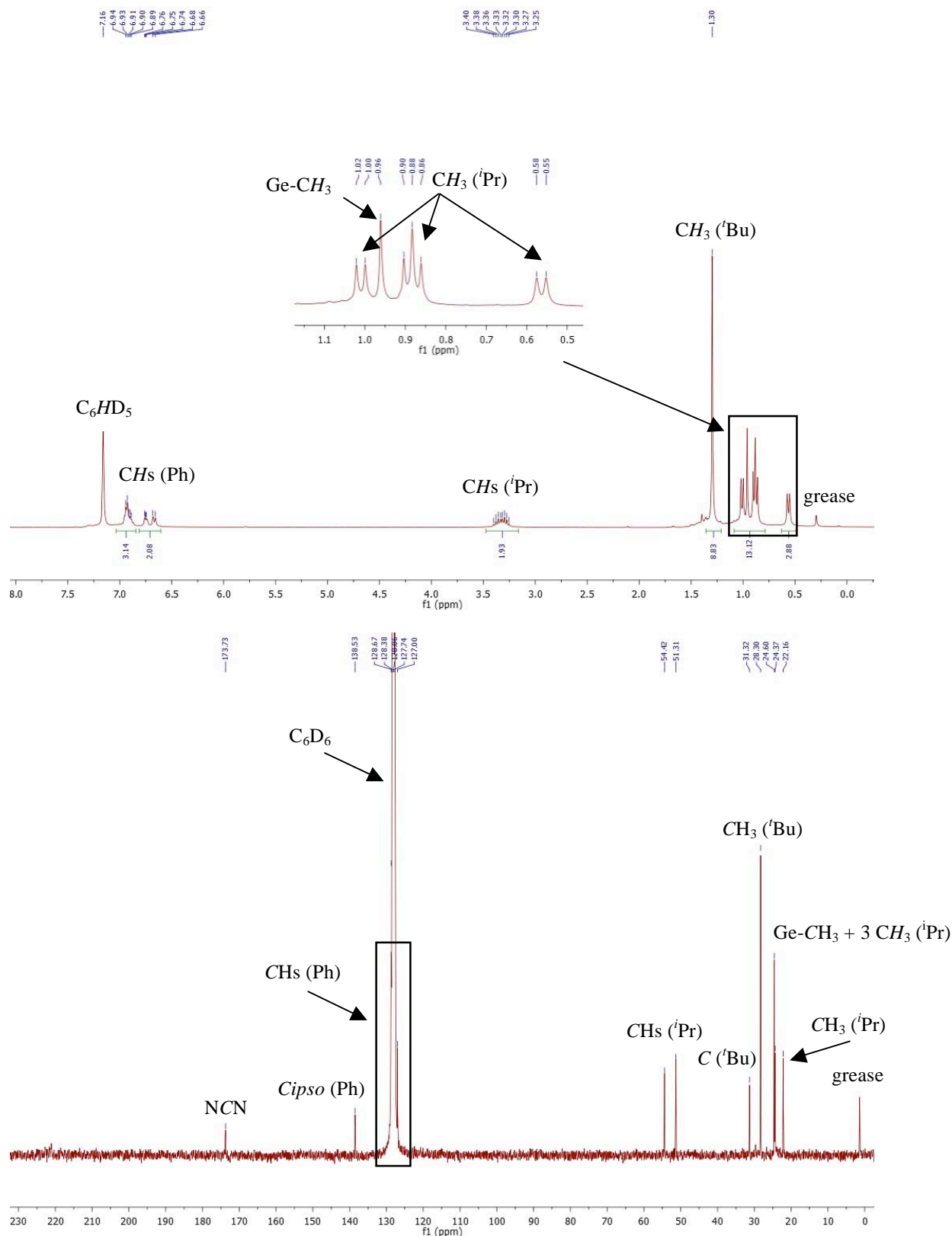


Figure SI-3. ^1H (top; 300.1 MHz) and $^{13}\text{C}\{^1\text{H}\}$ (bottom; 75.5 MHz) NMR spectra of $[\text{Mn}\{\kappa^2\text{Ge}, N\text{-GeMe}(\text{iPr}_2\text{bzam})\text{tBu}\}(\text{CO})_4]$ (2) in C_6D_6 at 25°C .

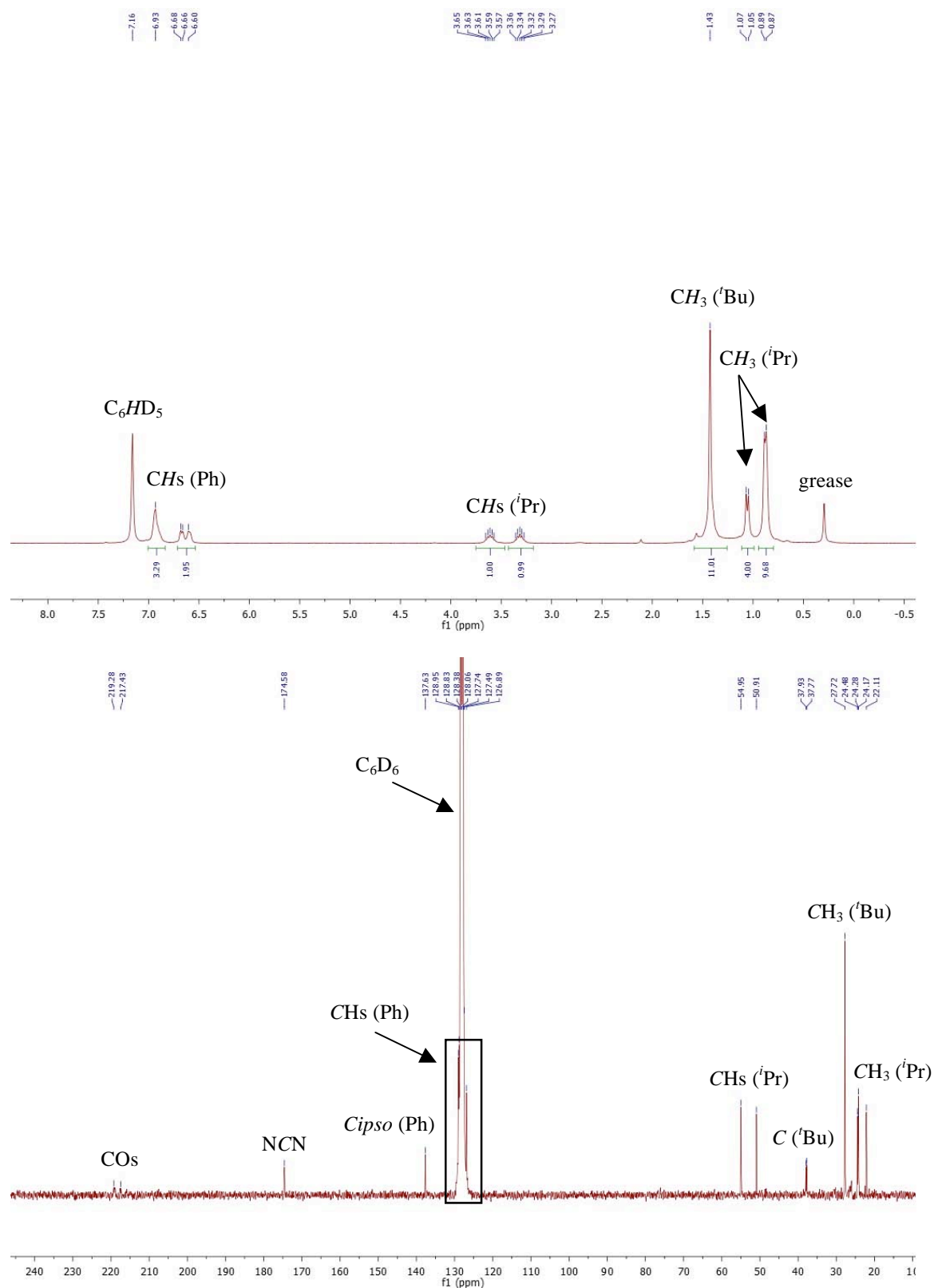


Figure SI-4. ^1H (top; 300.1 MHz) and $^{13}\text{C}\{^1\text{H}\}$ (bottom; 75.5 MHz) NMR spectra of $[\text{Mn}\{\kappa^2\text{Ge,N-GeF}(\text{iPr}_2\text{bzam})\text{tBu}\}(\text{CO})_4]$ (**3**) in C_6D_6 at 25 °C.

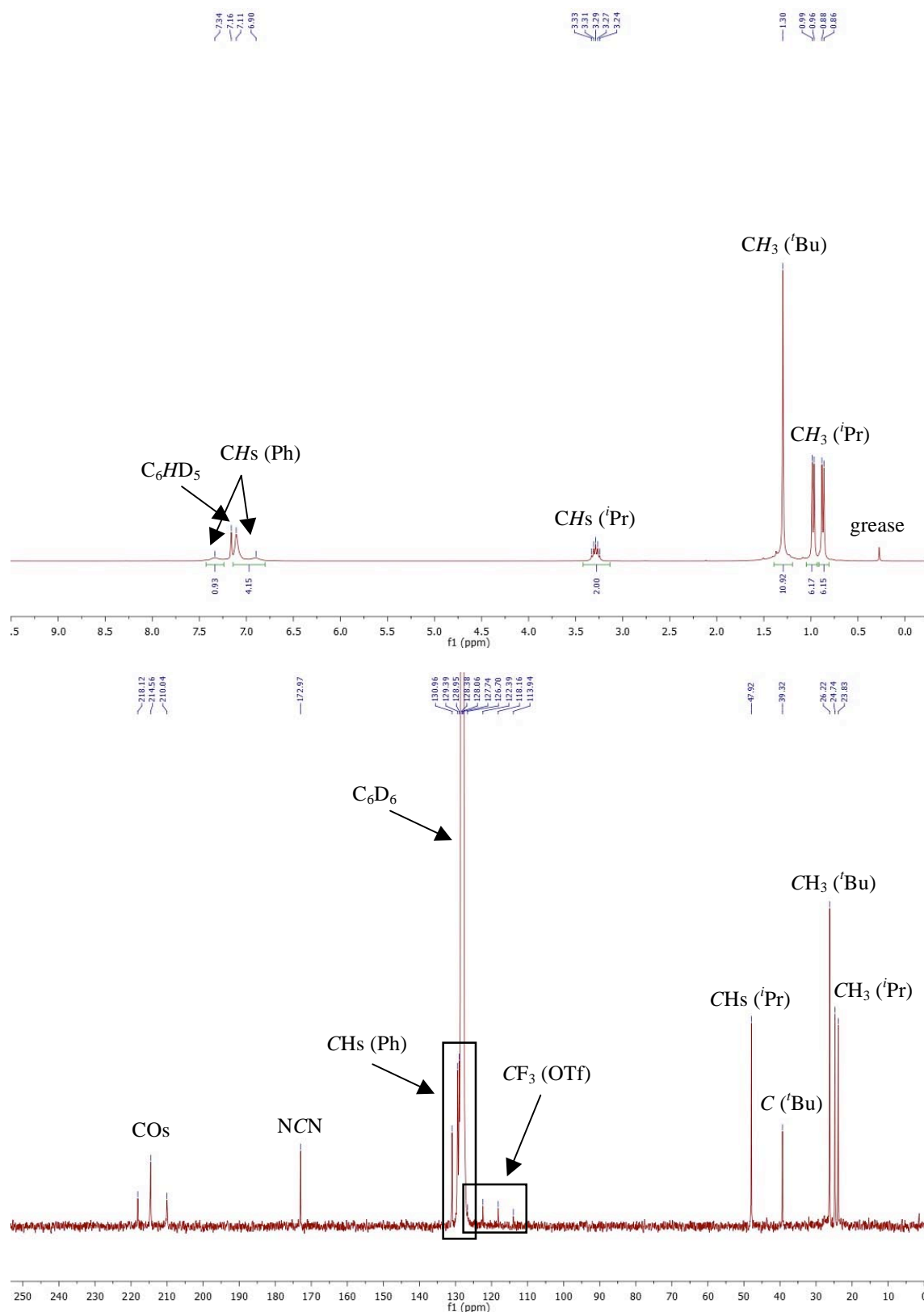


Figure SI-5. ^1H (top; 300.1 MHz) and $^{13}\text{C}\{^1\text{H}\}$ (bottom; 75.5 MHz) NMR spectra of $[\text{Mn}(\text{OTf})\{\text{Ge}(\text{Pr}_2\text{bzam})^i\text{Bu}\}(\text{CO})_4]$ (**4**) in C_6D_6 at 25°C .

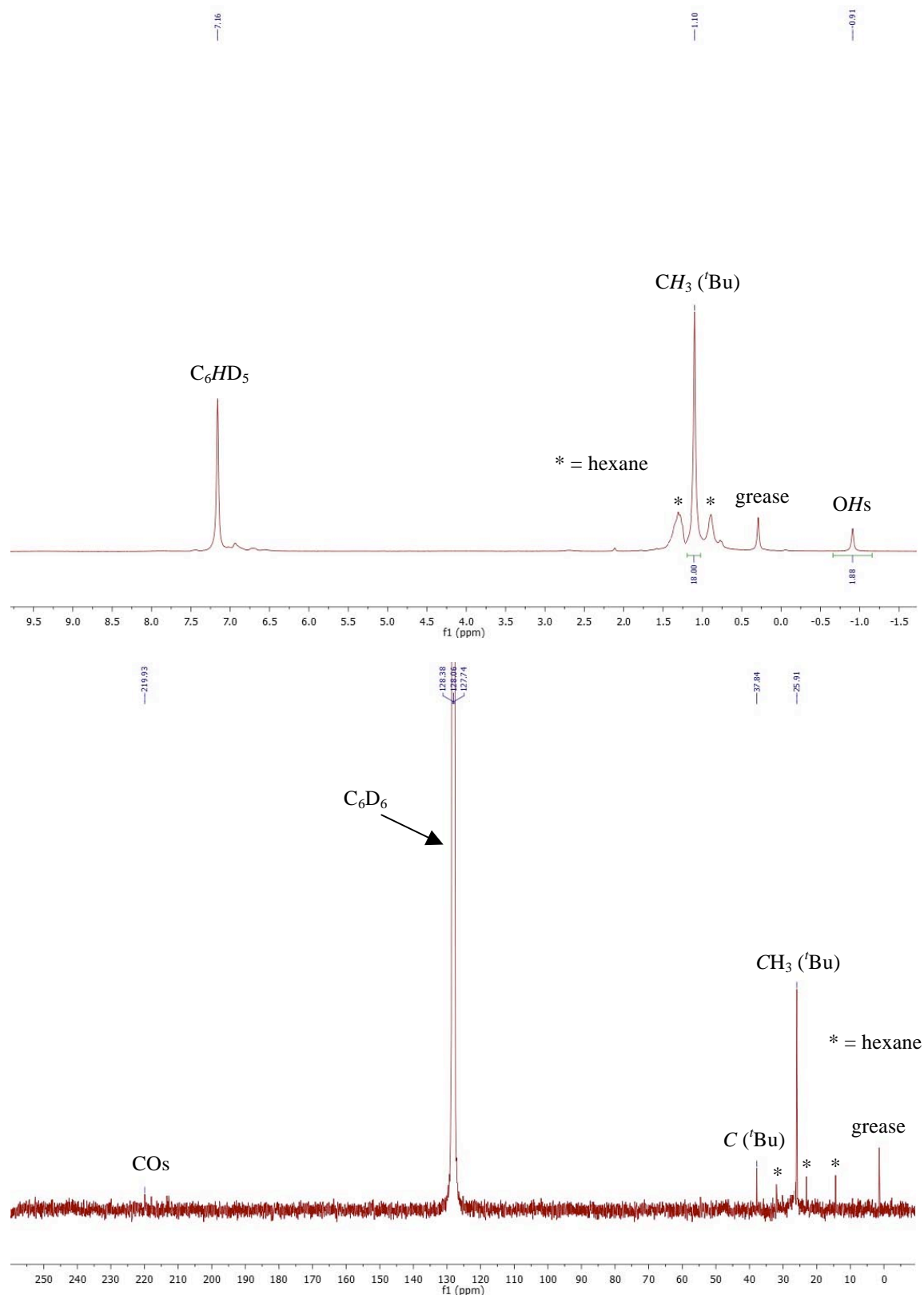


Figure SI-6. ^1H (top; 300.1 MHz) and $^{13}\text{C}\{^1\text{H}\}$ (bottom; 75.5 MHz) NMR spectra of $[\text{Mn}_2\{\mu\text{-}\kappa^4\text{Ge}_2\text{O}_2\text{-Ge}_2\text{tBu}_2(\text{OH})_2\text{O}\}(\text{CO})_8]$ (**5**) in C_6D_6 at 25°C .

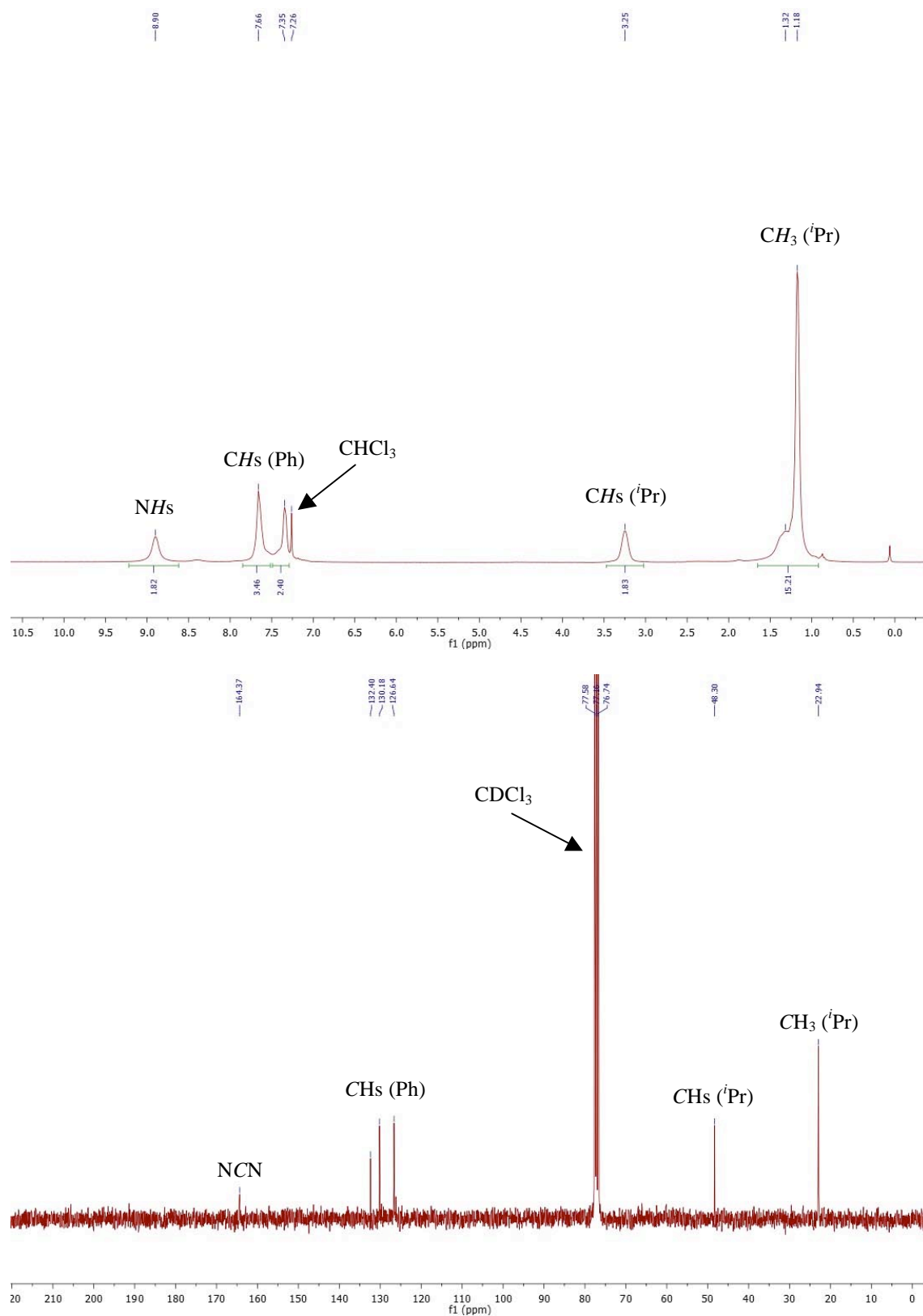


Figure SI-7. ^1H (top; 300.1 MHz) and $^{13}\text{C}\{^1\text{H}\}$ (bottom; 75.5 MHz) NMR spectra of $[\text{Pr}_2\text{bzamH}_2]\text{OTf}$ (**6**) (in CDCl_3 at 25 °C).

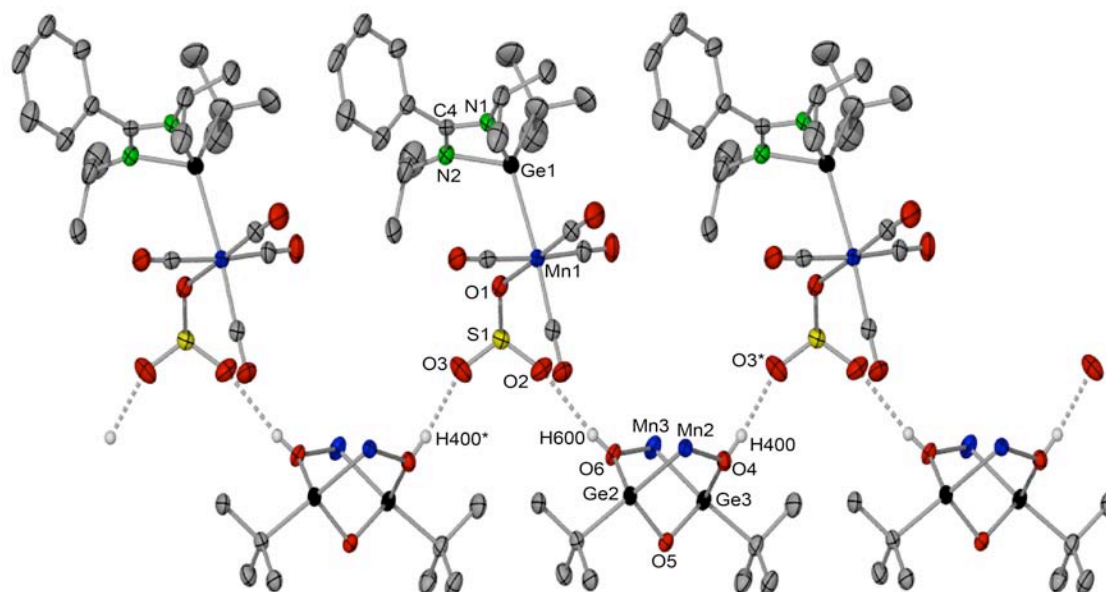


Figure SI-8. Chain arrangement found in the crystal of **4·5** (35% displacement ellipsoids). The carbonyl ligands of **5**, the hydrogen atoms (except those involved in hydrogen bonding), and the triflate CF_3 moieties have been omitted for clarity. Selected interatomic distances (\AA): O2–H600 2.218(1), O3–H400* 1.931(1).

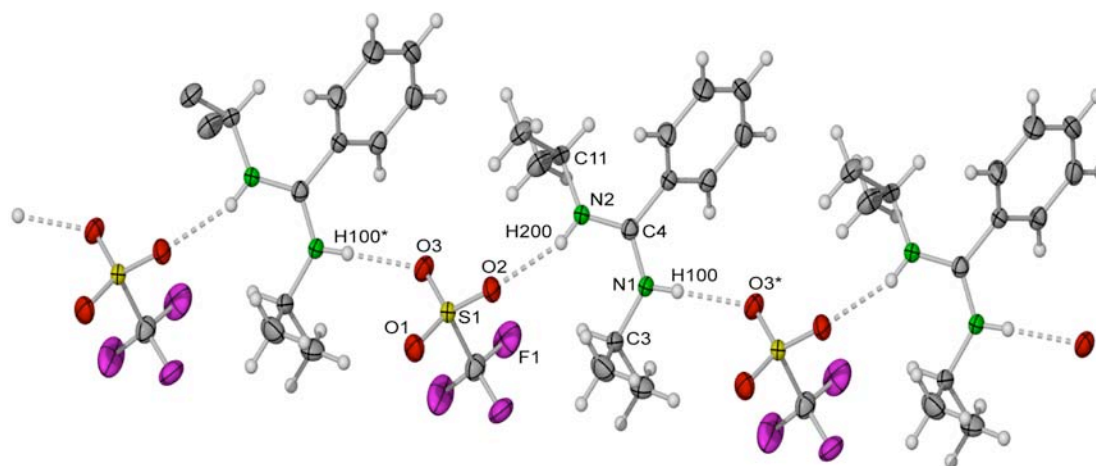


Figure SI-9. Chain arrangement found in the crystal of **6** (50% displacement ellipsoids). Selected interatomic distances (\AA): N1–C3 1.472(2), N1–C4 1.371(2), N2–C4 1.325(2), N2–C11 1.479(2), S1–O1 1.428(1), S1–O2 1.442(1), S1–O3 1.437(1), O2–H200 2.131(1), O3–H100* 2.060(1).

Artículo X

***“The Transition-Metal Chemistry of
Amidinosilylenes, -germylenes and -stannylenes”***



Review

The transition-metal chemistry of amidinatosilylenes, -germylenes and -stannylenes



Lucía Álvarez-Rodríguez, Javier A. Cabeza*, Pablo García-Álvarez*, Diego Polo

Departamento de Química Orgánica e Inorgánica-IUQOEM, Universidad de Oviedo-CSIC, E-33071 Oviedo, Spain

Contents

1. Introduction	2
2. Amidinato-HT ligands	3
3. Amidinato-HT metal complexes	4
3.1. Group 4 metal complexes	4
3.2. Group 5 metal complexes	4
3.3. Group 6 metal complexes	6
3.4. Group 7 metal complexes	8
3.5. Group 8 metal complexes	10
3.6. Group 9 metal complexes	15
3.7. Group 10 metal complexes	19
3.8. Group 11 metal complexes	23
3.9. Group 12 metal complexes	24
3.10. Latest additions	25
4. Conclusions	25
Acknowledgements	25
References	26

ARTICLE INFO

Article history:

Received 27 March 2015

Accepted 27 April 2015

Available online 6 May 2015

Keywords:

Transition-metal complexes

Heavier tetrylenes as ligands

Silylene ligands

Germylene ligands

Stannylenes ligands

Amidines

ABSTRACT

The transition-metal (TM) chemistry of heavier tetrylenes (HTs), also known as heavier carbene analogs, group 14 metalenes or group 14 metalylenes (compounds containing Si, Ge, Sn or Pb in +2 oxidation state), has experienced an exponential growth in the last few years because new families of HTs have emerged to the main-group chemistry arena. One of these families is characterized by the presence of an amidinato group attached to the group 14 element. Although the first report dealing with amidinato-HT-TM complexes appeared only seven years ago, nearly one hundred TM complexes containing amidinato-HT ligands are currently known and, remarkably, some of them have already been recognized as catalyst precursors for useful transformations of organic substrates (Sonogashira, Kumada and Negishi cross-couplings, ketone hydrosilylations, cycloadditions, arene C–H borylations, etc.). Thus, amidinato-HTs have emerged as promising alternatives to widely used classical ligands, such as phosphines or *N*-heterocyclic carbenes. This review comprehensively surveys the TM chemistry of

Abbreviations: Å, angstrom; Ad, adamantyl; Ar, aryl; br, broad; ^tBu, *tert*-butyl; ^tBuAdbzam, 1-*tert*-butyl-3-adamantylbenzamidinate; ^tBu₂bzam, 1,3-di-(*tert*-butyl)benzamidinate; ^tBuDiipbzam, 1-*tert*-butyl-3-(2,5-di-(*iso*-propyl)phenyl)benzamidinate; ^tBuDiipdmaam, 1-*tert*-butyl-3-(2,5-di-(*iso*-propyl)phenyl)-2-dimethylaminoamidinate; °C, degree Celsius; cm, centimeter; Cp, cyclopentadienyl; cod, 1,5-cyclooctadiene; coe, cyclooctene; d, doublet or distance; dd, doublet of doublets; DFT, density functional theory; Diip, 2,6-di-(*iso*-propyl)phenyl; Diip₂dmaam, 1,3-bis(2,6-di-(*iso*-propyl)phenyl)-2-dimethylaminoamidinate; Diip₂tbam, 1,3-bis(2,6-di-(*iso*-propyl)phenyl)-2-*tert*-butylamidinate; dma, dimethylamino; DMAP, 4-dimethylaminopyridine; dme, dimethoxyethane; dmpe, 1,2-bis(dimethylphosphino)ethane; dt, doublet of triplets; e.g., for example; Et, ethyl; Et^tBubzam, 1-ethyl-3-*tert*-butylbenzamidinate; Fc, 1,1'-ferrocenediyl; {¹H}, proton decoupled; HMDS, hexamethyl-disilazane; HOMO, highest occupied molecular orbital; MS, mass spectrum; HT, heavier tetrylene; Hz, Hertz; *I*, nuclear spin; IR, infrared; L, generic ligand; LUMO, lowest unoccupied molecular orbital; M, heavier group 14 element; m, multiplet or medium; Me, methyl; Me₂acam, N,N'-dimethylacetamidinate; nbd, norbornadiene; NBO, natural bond orbital; NHC, *N*-heterocyclic carbene; NMR, nuclear magnetic resonance; OTf, triflate; Ph, phenyl; pin, pinacolate; ppm, part per million; ¹Pr, *iso*-propyl; ¹Pr₂bzam, 1,3-di-(*iso*-propyl)benzamidinate; ¹Pr₂Diaam, 1,3-di-(*iso*-propyl)-2-di-(*iso*-propyl)aminoamidinate; PSQP, pseudo square pyramidal; py, pyridine; quint, quintuplet; R₂BrH₂, 4,6-di-(*tert*-butyl)-2-bromoresorcinol; R₂H₃, 4,6-di-(*tert*-butyl)resorcinol; ref., reference; RT, room temperature; s, singlet or strong; sh, shoulder; t, triplet; TBP, trigonal bipyramidal; THF, tetrahydrofuran; TM, transition metal; tmeda, N,N,N',N'-tetramethylethylenediamine; TMS, trimethylsilyl; TMS₂bzam, 1,3-bis(trimethylsilyl)benzamidinate; tol, toluene; vs, very strong; vw, very weak; w, weak.

* Corresponding authors. fax: +34 985103446.

E-mail addresses: jac@uniovi.es (J.A. Cabeza), pga@uniovi.es (P. García-Álvarez).

amidinato-HTs published up to the end of 2014, examining not only the synthesis and characterization of these complexes, but paying special attention to reactivity studies, theoretical investigations and catalytic applications.

© 2015 Elsevier B.V. All rights reserved.

1. Introduction

“Tetrylene” is a chemical term that refers to a compound having a group 14 element in the +2 oxidation state. Heavier tetrylenes (HTs), also known as heavier carbene analogs, group 14 metaleens or group 14 metalylenes, are compounds of fundamental interest in main-group chemistry [1]. The simplest members of this family are species of general formula MX_2 ($M = Si, Ge, Sn, Pb$; $X = \text{anionic group}$). Due to (i) their marked dual Lewis acid–base character (in their fundamental state they possess both a lone-pair of electrons and a vacant p orbital on the M atom; Fig. 1), (ii) the high polarity of their M–X bonds, and (iii) their great versatility (four M atoms are available and X can virtually be any anionic group), they display a unique and very rich reactivity [2,3]. For example, they are able to activate small molecules, insert into organic and inorganic σ -bonds, add to unsaturated substrates, promote cycloadditions, participate in redox processes, form donor–acceptor Lewis adducts and act as σ -donor– π -acceptor ligands in TM complexes (Fig. 1).

The coordination chemistry of HTs [3,4], although covering a wide range of TMs, is still far from the maturity achieved by that of their carbene analogs and, particularly, that of *N*-heterocyclic carbenes (NHCs) [5], because systematic reactivity studies (stoichiometric or catalytic) involving HT–TM complexes are still comparatively scarce. This underdevelopment can be mainly ascribed to some synthetic problems and to the general lower stability of HTs and also of their TM complexes toward air, moisture, and/or substitution processes. In contrast to NHCs, coordinated HTs are generally weakly bonded to TMs (the M–TM bond strength decreases on going down group 14 column of the Periodic Table [6]) and are prone to undergo oxidation and/or hydrolysis processes [7]. Additionally, the syntheses of most of the HT–TM complexes reported to date are generally tackled using free HT reagents, which are very air-sensitive. However, the use of pure NHCs is often unnecessary for the preparation of NHC–TM complexes (for example, imidazol-2-ylidenes can be generated *in situ* from readily available imidazolium salts). Silylene–TM complexes are specially difficult to prepare because silicon(II) precursors are not commercially available and a reduction of silicon(IV) reagents is required. Other methods that do not require the use of pure HT reagents to form HT–TM complexes have been developed mainly for the synthesis of silylene derivatives [4c]. For example, the double salt metathesis of MR_2X_2 ($X = \text{halide}$) species with appropriate metallic precursors (e.g., $K_2[Fe(CO)_4]$) [8], the abstraction of anionic X groups from XR_2M –TM ($X = Cl, OTf$) complexes using electrophilic reagents (e.g., $Na[BPh_4]$) [9], the 1,2-migration of a substituent (generally H) of an MHR_2 ligand, mediated by the generation of

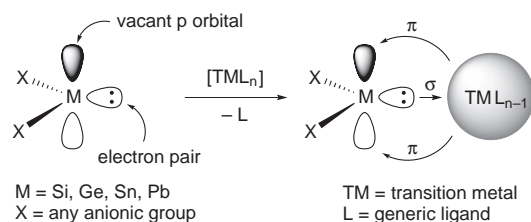


Fig. 1. Representation of a simple heavier tetrylene in its fundamental state (left) and its capacity to bind a transition metal complex (right).

a vacant coordination site on the TM [10], the capture of photochemically generated transient MR_2 fragments by an appropriate metal center [11], the metathesis of dianionic $[MR_2]^{2-}$ species with metallic dihalide precursors (e.g., $[TiCp_2Cl_2]$) [12], etc. However, despite the synthetic and stability issues mentioned above, the last 40 years have witnessed an incessant research activity devoted to prepare and study the chemistry of novel HT–TM complexes. These investigations have been associated with the emergence of new kinds of HT molecules in the main-group chemistry arena.

A very general classification of HT ligands is summarized in Fig. 2. They can be simple (S) or donor-stabilized (DS). Simple HTs can be acyclic (equipped with two terminal anionic groups; S_a) or cyclic (in which the M atom is chelated by a dianionic fragment, S_c). Donor-stabilized HTs formally result from an intramolecular (DS_{intra}) or intermolecular (DS_{inter}) interaction of a two-electron-donor group (D) with the M atom of simple HTs.

Fig. 3 collects the most representative examples of HTs that have been most used as ligands in TM complexes. As of the early stages of the HT–TM chemistry, the readily accessible dichlorides $GeCl_2 \cdot \text{dioxane}$, $SnCl_2$ and $PbCl_2$ (I in Fig. 3) and their TM complexes have been used to prepare more sophisticated HTs and HT–TM derivatives *via* transmetalation procedures [2e,4f]. The synthesis of some $SiCl_2$ derivatives of TMs [3a,b] has followed the recent discovery (Roesky, 2009) that the elusive $SiCl_2$ molecule can be stabilized with bulky NHCs (II) [13]. Since their discovery by Lappert 40 years ago, the diamido- or dialkyl-HTs $M(HMDS)_2$ or $M\{CH(TMS)_2\}_2$ ($M = Ge, Sn, Pb$; III), or related HTs also equipped with bulky anionic groups, have been incorporated in a large number of TM complexes [4e,f,g]. The cyclic heavier tetrylenes reported by Veith et al., particularly $M\{(N^tBu)_2SiMe_2\}$ ($M = Ge, Sn$; IV) [2h] have been integrated in several metal complexes since the 80s [14]. Note that the silylene versions of both Lappert’s and Veith’s HTs, namely, $Si(HMDS)_2$ [15] and $Si\{(N^tBu)_2SiMe_2\}$ [16], are known but they are stable only at low temperatures. A major breakthrough in the coordination chemistry of HTs was the synthesis by Denk et al. in 1994 of the first stable *N*-heterocyclic silylene, namely, $Si\{(N^tBu)_2C_2H_2\}$ (V) [17], which is a silicon analog of Arduengo’s type NHCs [5]. Its coordination chemistry (or that of related systems equipped with different NR groups, saturated backbones, benzoannulated rings, etc.) was then extensively investigated [3j,k], giving also rise to a few catalytic applications [18]. Related *N*-heterocyclic stannylenes [19] and

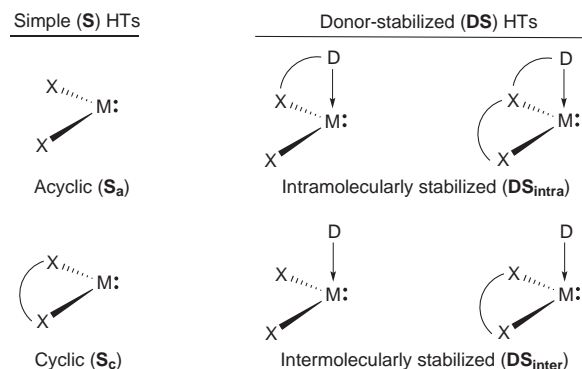


Fig. 2. Simple and donor-stabilized HTs.

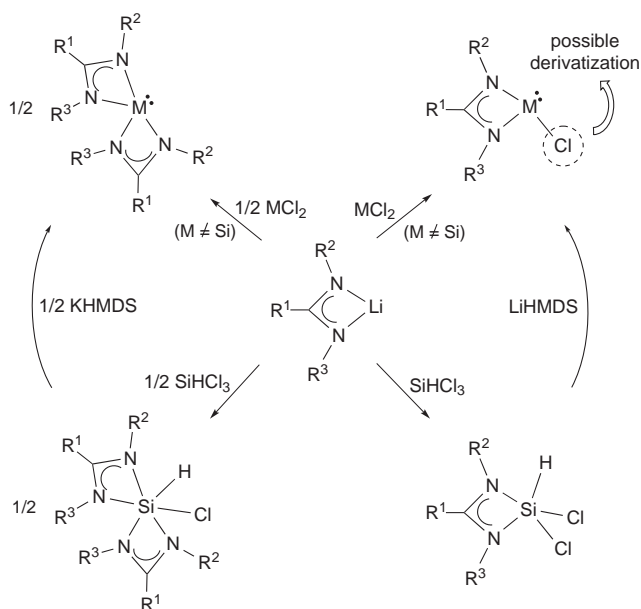


Fig. 4. Common methods for the synthesis of amidinato-HTs.

are generally better ligands than their heavier group 14 analogs [6], the discovery of an efficient route to amidinatosilylenes was a major breakthrough in the coordination chemistry of amidinato-HTs. It is important to remark that the derivatization of (amidinato)chloro-HTs *via* chlorine replacement (by metathesis with an anionic group) is a very useful and versatile method that has allowed the synthesis of a great variety of amidinato-HT ligands that, maintaining the original amidinato fragment, may differ in their electronic and steric properties.

Table 1 contains a list of the amidinato-HTs that have been used as reagents to prepare amidinato-HT-TM complexes. In this table, the ligands are organized in order of appearance in the following sections of this review. Amidinato-HT ligands of complexes that have been prepared by derivatization of preformed amidinato-HT-TM complexes (e.g., by chlorine replacement on (amidinato)chloro-HT-TM complexes) are not included in Table 1, although they are discussed with their corresponding complexes in the following sections of this review.

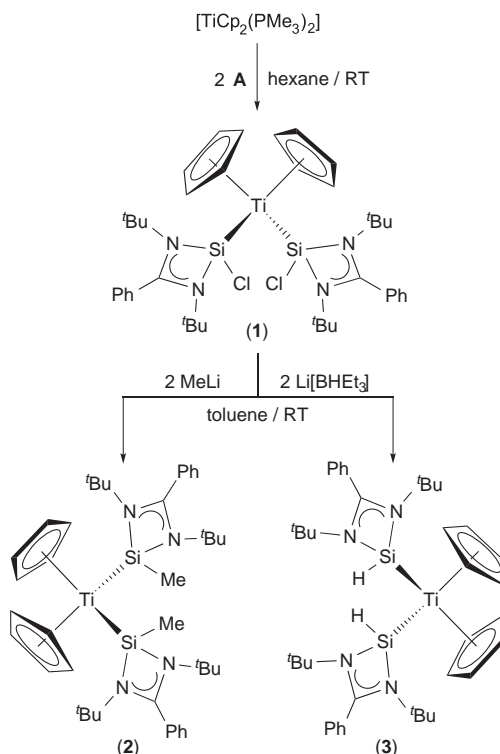
3. Amidinato-HT metal complexes

For clarity, the TM complexes whose chemistry is surveyed in this review are classified according to the column (group) of the Periodic Table to which the TM atom belongs. Within each group, the reactions are roughly in chronological order, *i.e.*, those that were reported earlier are discussed before those that were reported later. Relevant data for the known amidinato-HT-TM complexes of the metals of each TM group of the Periodic Table (including group 12), such as yield, color, ^{29}Si or ^{119}Sn NMR chemical shifts, IR $\nu(\text{CO})$ absorptions, M–TM bond distances and reported reactivity/catalytic studies, are given in tabular form.

No amidinato-HT complexes of group 3 metals have been hitherto reported.

3.1. Group 4 metal complexes

The only members of this group are the bis(silylene) titanium(II) complexes $[\text{TiCp}_2\{\text{Si}(\text{tBu}_2\text{bzam})\text{X}\}_2]$ ($\text{X} = \text{Cl}$ (**1**), Me (**2**), H (**3**)) (Scheme 1, Table 2), reported by Driess, Inoue and co-workers in 2012 [30]. Complex **1** was prepared by reacting $[\text{TiCp}_2(\text{PMe}_3)_2]$ with two equivalents of $\text{Si}(\text{tBu}_2\text{bzam})\text{Cl}$ (**A**) [64]. Transmetalation

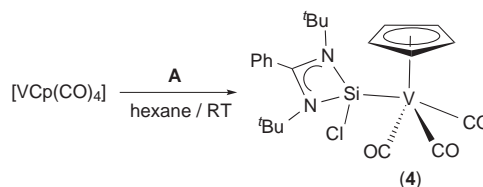


Scheme 1. Synthesis of complexes 1–3.

of **1** with MeLi and Li[BHET₃] resulted in the derivatives **2** and **3**, respectively. The reaction of $[\text{TiCp}_2(\text{PMe}_3)_2]$ with two equivalents of the germylene $\text{Ge}(\text{tBu}_2\text{bzam})\text{Cl}$ led to the titanium(III) derivative $[\text{TiClCp}_2(\text{PMe}_3)]$ along with other unidentified reaction products. DFT calculations, including NBO analyses, showed that: (i) the Ti–Si bond in **1–3** is heavily polarized, following the order $\mathbf{1} > \mathbf{3} > \mathbf{2}$, (ii) there is some multiple bonding between Ti and Si, and (iii) two σ and one π -type molecular orbitals are delocalized over the Si–Ti–Si framework, as it has been found for other related bis(silylene) group 4 metal complexes [6b]. The $^{29}\text{Si}\{^1\text{H}\}$ NMR spectrum of **1–3** (Table 2) showed one resonance at lower field than that of the free ligand **A** ($\delta = 14.6$ ppm in C_6D_6 [64]). Interestingly, the ^{29}Si chemical shifts of these compounds are inversely proportional to the Hammett constant of their R^4 substituent ($\sigma_p = 0.23$ (Cl), -0.17 (Me), 0 (H)) [66], indicating that both inductive and resonance effects of the substituent contribute to the ^{29}Si chemical shift.

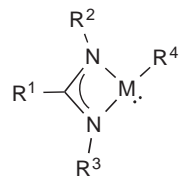
3.2. Group 5 metal complexes

Group V is just represented by the silylene vanadium(I) derivative $[\text{VCp}(\text{CO})_3\{\text{Si}(\text{tBu}_2\text{bzam})\text{Cl}\}]$ (**4**) (Table 2), synthesized in good yield by Roesky and Stalke by simple CO displacement on $[\text{VCp}(\text{CO})_4]$ (Scheme 2) [31]. The $^{29}\text{Si}\{^1\text{H}\}$ NMR signal of **4** ($\delta = 116.1$ ppm), again downfield-shifted compared with that of the uncoordinated ligand **A** [64], was very broad due to the quadrupolar moment of ^{51}V ($I = 7/2$). The downfield shift of the ^{29}Si NMR



Scheme 2. Synthesis of complex 4.

Table 1
Amidinato-HTs that have been used as reagents to prepare amidinato-HT-TM complexes.



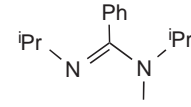
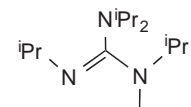
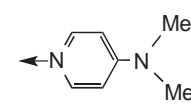
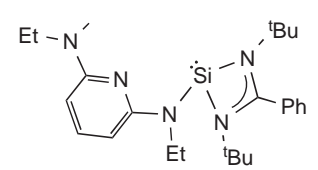
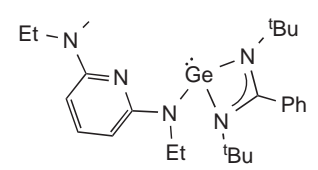
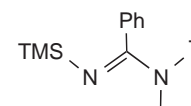
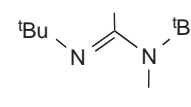
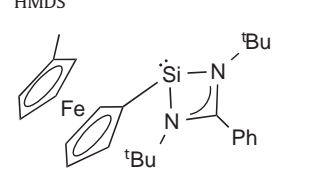
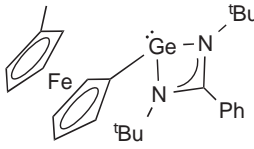
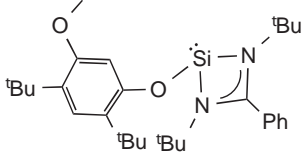
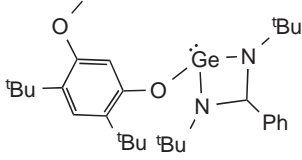
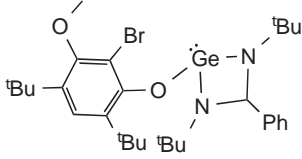
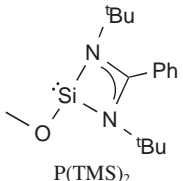
HT	M	R ¹	R ²	R ³	R ⁴
A	Si	Ph	^t Bu	^t Bu	Cl
B	Ge	^t Bu	Diip	Diip	Cl
C	Ge	Ph	TMS	TMS	Cl
D	Si	Ph	<i>i</i> Pr	<i>i</i> Pr	
E	Si	N ^{<i>i</i>} Pr ₂	<i>i</i> Pr	<i>i</i> Pr	
F[OTf]	Si	Ph	^t Bu	^t Bu	
G	Si	Ph	^t Bu	^t Bu	NPh ₂
H	Ge	Ph	<i>i</i> Pr	<i>i</i> Pr	^t Bu
I	Si	Ph	^t Bu	^t Bu	O ^{<i>t</i>} Bu
J	Sn	Ph	^t Bu	^t Bu	Cl
K	Ge	Ph	^t Bu	^t Bu	HMDS
L	Ge	Ph	<i>i</i> Pr	<i>i</i> Pr	HMDS
M	Ge	Ph	^t Bu	Et	HMDS
N	Si	Ph	^t Bu	^t Bu	
O	Ge	Ph	^t Bu	^t Bu	
P	Ge	Ph	TMS	TMS	
Q	Ge	Ph	^t Bu	^t Bu	
R	Si	Ph	^t Bu	^t Bu	HMDS
S	Si	Ph	^t Bu	^t Bu	

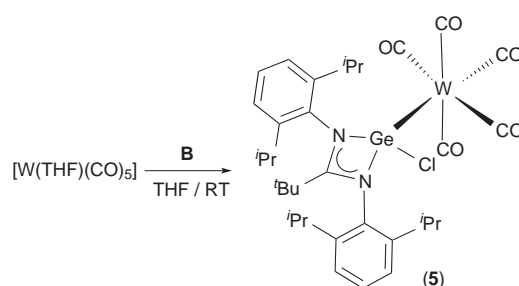
Table 1 (Continued)

HT	M	R ¹	R ²	R ³	R ⁴
T	Ge	Ph	^t Bu	^t Bu	
U	Si	Ph	^t Bu	^t Bu	
V	Ge	Ph	^t Bu	^t Bu	
W	Ge	Ph	^t Bu	^t Bu	
X	Si	Ph	^t Bu	^t Bu	
Y	Si	Ph	^t Bu	^t Bu	P(TMS) ₂
Z	Si	Ph	^t Bu	^t Bu	NMe ₂

signal of coordinated silylenes (with respect to the ²⁹Si NMR signal of the corresponding free silylene) is a common feature for the majority of the complexes discussed in this review. Consequently, this observation only will be pointed out again in the sections that follow when it provides different or additional information.

3.3. Group 6 metal complexes

Jones and co-workers, as part of a reactivity study with amidinato- and guanidinogermynes, reported the synthesis of the germylene tungsten complex [W(CO)₅{Ge(Diip₂tbam)Cl}] (**5**) in 2008 [32]. This compound was prepared by reacting Ge(Diip₂tbam)Cl (**B**) [63c] with [W(THF)(CO)₅] (Scheme 3, Table 3).



Scheme 3. Synthesis of complex 5.

Table 2
Relevant data of group 4 and group 5 metal complexes containing amidinato-HT ligands.

Complex	Yield (%), color	M{ ¹ H} NMR, δ (ppm)	IR ν(CO) (cm ⁻¹)	d(M-TM) (Å)	Reactivity	Ref.
[TiCp ₂ {Si(^t Bu ₂ bzam)Cl}] ₂ (1)	67, red-brown	²⁹ Si, 120.6 (s) ^a		2.486(1)	Replacement of Cl	[30]
[TiCp ₂ {Si(^t Bu ₂ bzam)Me}] ₂ (2)	57, purple	²⁹ Si, 189.2 (s) ^a		2.515(1)		[30]
[TiCp ₂ {Si(^t Bu ₂ bzam)H}] ₂ (3)	40, purple	²⁹ Si, 153.2 (s) ^a				[30]
[VCp(CO) ₃ {Si(^t Bu ₂ bzam)Cl}] (4)	71, yellow	²⁹ Si, 116.1 (s, br) ^a	2027 (s), 1951 (vw), 1930 (s), 1905 (vw) ^b	2.3866(5)		[31]

^a In C₆D₆.

^b In Nujol.

Table 3
Relevant data of group 6 metal complexes containing amidinato-HT ligands.

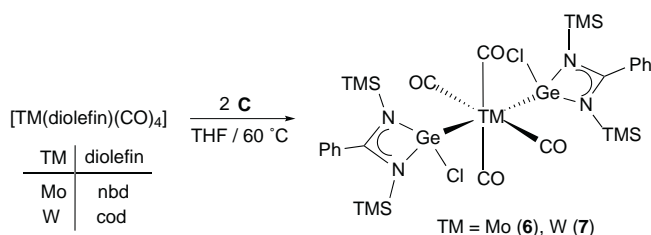
Complex	Yield (%), color	M{ ¹ H} NMR, δ (ppm)	IR ν(CO) (cm ⁻¹)	d(M–TM) (Å)	Reactivity	Ref.
[W(CO) ₅ {Ge(Diip ₂ tbam)Cl}] (5)	56, colorless		2073 (s), 1978 (s), 1948 (s) ^a	2.5564(6)		[32]
[Mo(CO) ₄ {Ge(TMS ₂ bzam)Cl}] (6)	24, pale yellow		1903 (s) ^b	2.4990(2)		[33]
[W(CO) ₄ {Ge(TMS ₂ bzam)Cl}] (7)	22, yellow		1941 (sh), 1894 (s) ^b	2.4984(3)		[33]
[Cr(CO) ₅ {Si(^t Bu ₂ bzam)Cl}] (8)	91, not given	²⁹ Si, 92.3 (s) ^c	Not given	2.3458(7)	Replacement of Cl	[34]
[Mo(CO) ₅ {Si(^t Bu ₂ bzam)Cl}] (9)	84, not given	²⁹ Si, 72.8 (s) ^c	Not given	2.455(1)	Replacement of Cl	[34]
[W(CO) ₅ {Si(^t Bu ₂ bzam)Cl}] (10)	85, not given	²⁹ Si, 53.0 (s) ^c	Not given	2.509(1)	Replacement of Cl	[34]
[Cr(CO) ₅ {Si(^t Bu ₂ bzam)F}] (11)	83, not given	²⁹ Si, 74.0 (d) ^c	Not given	2.3398(4)		[34]
[Mo(CO) ₅ {Si(^t Bu ₂ bzam)F}] (12)	77, not given	²⁹ Si, 56.7 (d) ^c	Not given			[34]
[W(CO) ₅ {Si(^t Bu ₂ bzam)F}] (13)	88, not given	²⁹ Si, 41.8 (d) ^c	Not given	2.4990(8)		[34]
[Cr(CO) ₅ {Si(^t Pr ₂ bzam) ₂ }] (14)	76, colorless	²⁹ Si, –22.3 (s) ^d	Not given	2.4181(7)		[36]
[Mo(CO) ₅ {Si(^t Pr ₂ bzam) ₂ }] (15)	89, colorless	²⁹ Si, 6.9 (s) ^d	Not given	2.5784(6)		[36]
[W(CO) ₅ {Si(^t Pr ₂ bzam) ₂ }] (16)	92, colorless	²⁹ Si, –13.3 (s) ^d	Not given	2.5803(9)		[35,36]
[Cr(CO) ₄ {κ ² Si,N-Si(^t Pr ₂ Diaam) ₂ }] (17)	65, yellow	²⁹ Si, 81.6 (s) ^d	Not given	2.3400(8)		[37]
[Mo(CO) ₄ {κ ² Si,N-Si(^t Pr ₂ Diaam) ₂ }] (18)	73, yellow	²⁹ Si, 68.9 (s) ^d	Not given	2.4877(7)		[37]
[W(CO) ₄ {κ ² Si,N-Si(^t Pr ₂ Diaam) ₂ }] (19)	72, yellow	²⁹ Si, 66.5 (s) ^d	Not given	2.4899(8)		[37]
[W(CO) ₅ {Si(^t Bu ₂ bzam)(DMAP)}][OTf] (20)	67, pale yellow	²⁹ Si, 51.6 (s) ^c	2070 (s), 1991 (s), 1921 (s) ^a	2.497(1)		[38]

^a In Nujol.

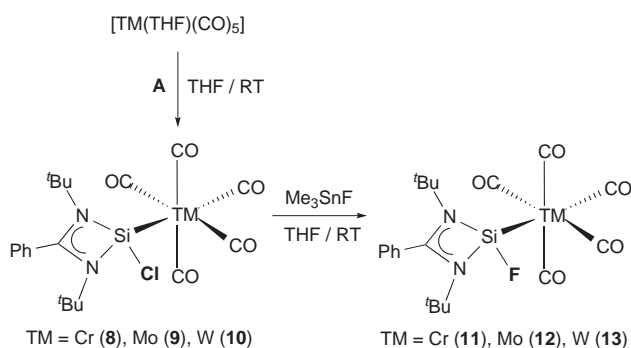
^b In KBr.

^c In C₆D₆.

^d In THF-*d*₈.



Scheme 4. Synthesis of complexes **6** and **7**.

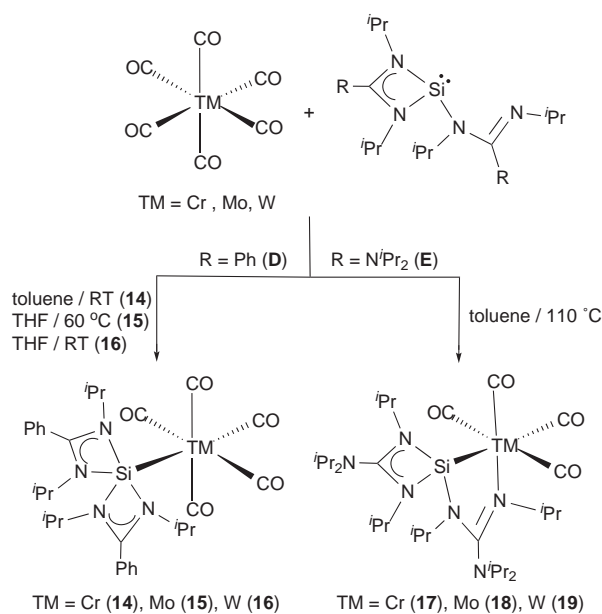


Scheme 5. Synthesis of complexes **8–13**.

As mentioned above, **5** and an iron derivative (**31**) were the first amidinato-HT-TM complexes ever described [32].

The group of Castel prepared the *trans*-bis(germylene) derivatives [TM(CO)₄{Ge(TMS₂bzam)Cl}]₂ (TM = Mo (**6**), W (**7**)) (Table 3) in low yields by treating [Mo(nbd)(CO)₄] and [W(cod)(CO)₄] with Ge(TMS₂bzam)Cl (**C**) at 60 °C (Scheme 4) [33]. The Ge–W bond distance in **7** (both germylene ligands are crystallographically equivalent) is *ca.* 0.06 Å shorter than that of the monogermylene tungsten complex **5**, evidencing the greater steric hindrance exerted by the Diip groups of **B** in **5**.

Roesky, Stalke, Ghadwal et al. accomplished in 2012 the syntheses of the first structurally characterized fluorosilylene TM complexes [TM(CO)₅{Si(^tBu₂bzam)F}] (TM = Cr (**11**), Mo (**12**), W (**13**)) (Scheme 5, Table 3) by treating [TM(CO)₅{Si(^tBu₂bzam)Cl}] (TM = Cr (**8**), Mo (**9**), W (**10**)), easily prepared from [TM(THF)(CO)₅] and **A**, with Me₃SnF [34]. The ²⁹Si chemical shifts of **8–10** in C₆D₆ are shifted to lower field than those of the fluorinated derivatives **11–13** in the same solvent (Table 3). This indicates that, as



Scheme 6. Synthesis of complexes **14–19**.

previously seen for the bis(silylene) titanium compounds **1–3**, inductive effects are not the only factors affecting the ²⁹Si chemical shifts. Comparing **8** vs **11** and **10** vs **13**, it can be observed that the replacement of fluoride by chloride in **8** and **10** does not induce significant differences in the Si–TM bond distances (Table 3).

Tacke et al. reported in 2012–2014 a remarkable reactivity of bis(amidinato/guanidinato)silylenes with group 6 metal hexacarbonyls. While the reactions of [TM(CO)₆] (TM = Cr, Mo, W) with the bis(amidinato)silylene Si(^tPr₂bzam)₂ (**D**) [35] led to the monosubstituted complexes [TM(CO)₅{Si(^tPr₂bzam)₂}] (TM = Cr (**14**), Mo (**15**), W (**16**)) [35,36], in which both amidinato groups chelate the Si atom, the bis(guanidinato)silylene Si(^tPr₂diaam)₂ (**E**) [65a] reacted at 110 °C to afford the tetracarbonyl derivatives [TM(CO)₄{κ²Si,N-Si(^tPr₂Diaam)₂}] (TM = Cr (**17**), Mo (**18**), W (**19**)), in which a guanidinato group bridges the Si and TM atoms (Scheme 6, Table 3) [37]. Note that **14–16** did not evolve toward complexes similar to **17–19** even after prolonged reaction times at 110 °C. The tungsten complex **16** was the first five-coordinate silicon(II) species ever reported. The formation of **14–16** implies that **D**, equipped

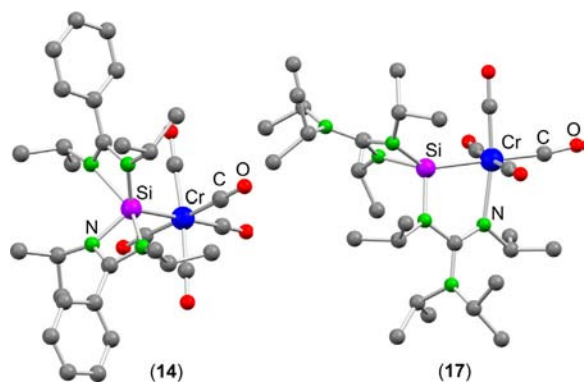
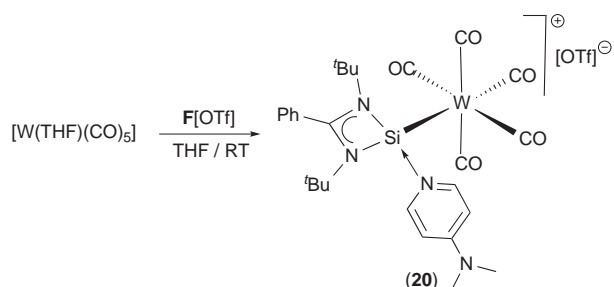


Fig. 5. Crystal structures of compounds **14** and **17**.

Adapted from Refs. [36,37].

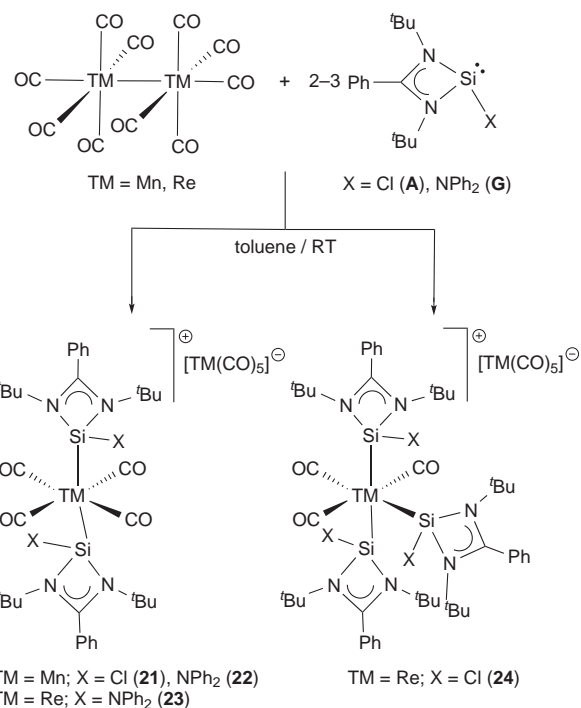


Scheme 7. Synthesis of complex salt **20**.

with both bidentate and monodentate amidinato fragments as a free molecule [35], closes its pendant imino arm toward the silicon atom upon coordination to the TM, possibly because the Si–TM interaction increases the Lewis acidity of the Si atom. The κ^2M,N -bidentate coordination of an amidinato-HT, as in **17–19**, was first described by our research group in 2013, working with amidinatogermynes and ruthenium or cobalt carbonyls (*vide supra*) [44]. The Si–TM bond distances of **14–16** are ca. 0.1 Å longer than those of the corresponding guanidinato derivatives **17–19** (Table 3). This fact is attributed to the higher coordination number of silicon in the amidinato complexes (Fig. 5). DFT calculations performed with **14–16** indicated that the Si–TM bonds of these complexes are best described as single bonds. The $^{29}\text{Si}\{^1\text{H}\}$ NMR signals of **14–16** (Table 3) are in all cases at lower field than that of the free ligand **D** ($\delta = -31.4$ ppm in C_6D_6) [35]. In the case of **17–19**, this shift to lower field is even greater (the ^{29}Si chemical shift of the free ligand **E** in C_6D_6 is -25.6 ppm [65a]) because, upon coordination to the TM, the increase of the Lewis acidity of the Si atom is not compensated by a coordination of the pendant imino arm of **E** to the silicon atom, as occurs in **14–16**.

The group of Tacke also reported that the reactions of silylene **D** with $[\text{TMCPH}(\text{CO})_3]$ (TM = Mo, W) led to the silicon(IV) salts $[\text{SiH}(\text{}^i\text{Pr}_2\text{bzam})_2][\text{TMCP}(\text{CO})_3]$ [67]. These acid-base/redox reactions will not be further discussed here because they do not lead to amidinato-HT–TM complexes.

The cationic complex $[\text{W}(\text{CO})_5\{\text{Si}(\text{}^t\text{Bu}_2\text{bzam})(\text{DMAP})\}][\text{OTf}]$ (**20**) (DMAP = 4-dimethylaminopyridine) was prepared by So and co-workers in 2014 treating the cationic silylene $[\text{Si}(\text{}^t\text{Bu}_2\text{bzam})(\text{DMAP})][\text{OTf}]$ (**F[OTf]**) with $[\text{W}(\text{THF})(\text{CO})_5]$ (Scheme 7, Table 3) [38]. The cationic silylene **F[OTf]** was synthesized by reaction of the amidinato-silicon(I) dimer $[\text{Si}_2(\text{}^t\text{Bu}_2\text{bzam})_2]$ (previously prepared by reduction of $\text{Si}(\text{}^t\text{Bu}_2\text{bzam})\text{Cl}_3$ with an excess of K_2C_8 [68]) with one equivalent of N-trimethylsilyl-4-dimethylaminopyridinium triflate in the presence of two equivalents of DMAP [69].



Scheme 8. Synthesis of complex salts **21–24**.

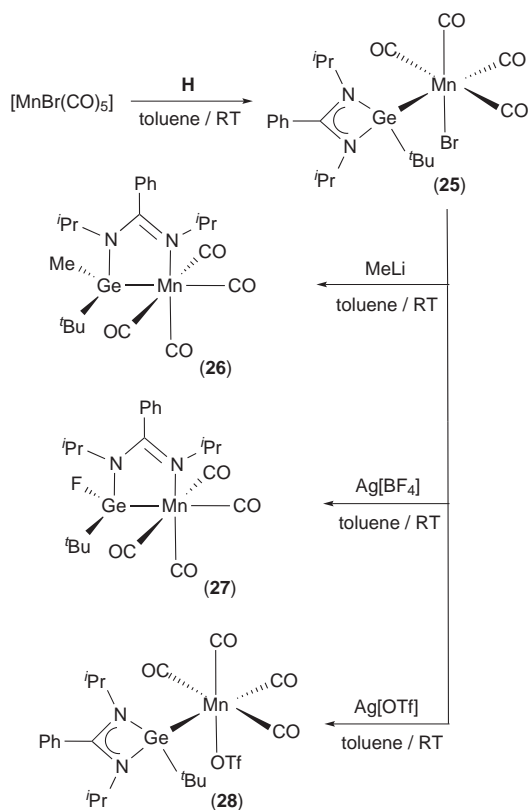
3.4. Group 7 metal complexes

In 2011 and 2012, the groups of Roesky and Stalke studied the reactivity of the silylenes $\text{Si}(\text{}^t\text{Bu}_2\text{bzam})\text{X}$ (X = Cl (**A**), NPh_2 (**G**)) with $[\text{Mn}_2(\text{CO})_{10}]$ and $[\text{Re}_2(\text{CO})_{10}]$ [39,40]. The salts $[\text{TM}(\text{CO})_4\{\text{Si}(\text{}^t\text{Bu}_2\text{bzam})\text{X}\}_2][\text{TM}(\text{CO})_5]$ (TM = Mn, X = Cl (**21**), NPh_2 (**22**); TM = Re, X = NPh_2 (**23**)) and $[\text{Re}(\text{CO})_3\{\text{Si}(\text{}^t\text{Bu}_2\text{bzam})\text{Cl}\}_3][\text{Re}(\text{CO})_5]$ (**24**) were obtained in good yields when two or more equivalents of the silylene reagents were used (Scheme 8, Table 4). Silylene **G** was prepared by chlorine replacement on **A** [70]. The formation of these complex salts implies disproportionation processes. The grade of substitution in the cationic fragment depends on the size of the TM atom and the volume of the silylene reagent. Thus, the trisubstituted cation is only formed for Re and the smaller silylene **A**. The different volume of silylenes **A** and **G** also affects the Si–TM bond distances of their complexes, since those corresponding to the bulkier silylene **G** (**22**, **23**) are ca. 0.06 Å longer than those of **21** and **24** (Table 4). Note that in **24**, which features two different Si–Re bond distances, only the mutually *trans* Si–Re bonds have been considered in the previous comparison.

In 2014, our research group described the transformation of a two electron-donor $\kappa^1\text{Ge}$ -amidinatogermylene into a chelating anionic three-electron-donor $\kappa^2\text{N,Ge}$ -iminegermanato(II) ligand [41], a process never reported before for amidinato-HTs, that was accomplished by treating the manganese complex $[\text{MnBr}(\text{CO})_4\{\text{Ge}(\text{}^i\text{Pr}_2\text{bzam})\text{}^t\text{Bu}\}]$ (**25**) (easily prepared from $[\text{MnBr}(\text{CO})_5]$ and $\text{Ge}(\text{}^i\text{Pr}_2\text{bzam})\text{}^t\text{Bu}$ (**H**)) with MeLi or $\text{Ag}[\text{BF}_4]$ (Scheme 9, Table 4). Germylene **H** was made by reacting $\text{Ge}(\text{}^i\text{Pr}_2\text{bzam})\text{Cl}$ with $\text{}^t\text{BuLi}$ [41]. In these reactions, which afforded the structurally analogous complexes $[\text{Mn}(\text{CO})_4\{\kappa^2\text{Ge,N-GeMe}(\text{}^i\text{Pr}_2\text{bzam})\text{}^t\text{Bu}\}]$ (**26**) and $[\text{Mn}(\text{CO})_4\{\kappa^2\text{Ge,N-GeF}(\text{}^i\text{Pr}_2\text{bzam})\text{}^t\text{Bu}\}]$ (**27**), the anionic nucleophile, Me^- or F^- , ends on the Ge atom while an arm of the amidinato fragment migrates from the Ge atom to the Mn atom (Scheme 9, Fig. 6). Note that the source of F^- is the $[\text{BF}_4]^-$ anion, which is unusual but not unknown [71]. The planar five-membered MnGeN_2C ring observed

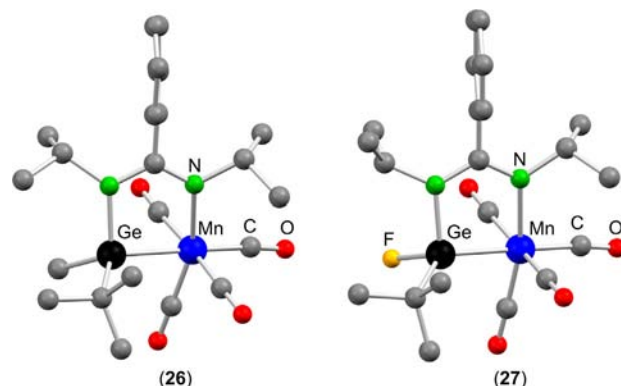
Table 4
Relevant data of group 7 metal complexes containing amidinato-HT ligands.

Complex	Yield (%), color	M{ ¹ H} NMR, δ(ppm)	IR ν(CO) (cm ⁻¹)	d(M–TM) (Å)	Reactivity	Ref.
[Mn(CO) ₄ {Si(^t Bu ₂ bzam)Cl ₂ }] [Mn(CO) ₅] (21)	72, pale yellow	²⁹ Si, 92.5 (s) ^a	2080 (s), 2045 (s), 2012 (s), 1982(s), 1921 (br) ^b	2.2816(8), 2.2789(8)		[39]
[Mn(CO) ₄ {Si(^t Bu ₂ bzam)NPh ₂ }] [Mn(CO) ₅] (22)	87, pale yellow	²⁹ Si, 61.1 (s) ^c	2023 (s), 1999 (s), 1955 (sh), 1955 (sh), 1925 (br) ^b	2.3521(7), 2.3571(7)		[40]
[Re(CO) ₄ {Si(^t Bu ₂ bzam)NPh ₂ }] [Re(CO) ₅] (23)	79, yellow	²⁹ Si, 22.2 (s) ^c	2075 (s), 2022 (s), 2008 (s), 1992 (s), 1957 (br), 1902 (br) ^b	2.482(2), 2.485(2)		[40]
[Re(CO) ₃ {Si(^t Bu ₂ bzam)Cl ₃ }] [Re(CO) ₅] (24)	71, yellow	²⁹ Si, 40.3 (s), 47.4(s) ^a	2101 (s), 2070 (s), 2033 (s), 2013(s), 1992 (s), 1959 (sh), 1941 (s), 1901 (m) ^b	2.438(2), 2.435(2), 2.493(2)		[39]
[MnBr(CO) ₄ {Ge(ⁱ Pr ₂ bzam) ^t Bu}] (25)	82, yellow		2068 (m), 2001 (m), 1981 (vs), 1935 (m) ^d	2.398(1)	Replacement of Br	[41]
[Mn(CO) ₄ {κ ² Ge,N-GeMe(ⁱ Pr ₂ bzam) ^t Bu}] (26)	53, pale yellow		2063 (w), 1984 (vs), 1965 (m), 1940 (m) ^d	2.428(5)		[41]
[Mn(CO) ₄ {κ ² Ge,N-GeF(ⁱ Pr ₂ bzam) ^t Bu}] (27)	82, pale yellow		2063 (w), 1984 (vs), 1965 (m), 1940 (m) ^d	2.3647(9)		[41]
[Mn(OTf)(CO) ₄ {Ge(ⁱ Pr ₂ bzam) ^t Bu}] (28)	76, yellow		2087 (m), 2022 (m), 1998 (vs), 1947 (m) ^d	2.4232(7)	Hydrolysis	[41]

^a In C₆D₆.^b In Nujol.^c In THF-*d*₈.^d In toluene.**Scheme 9.** Synthesis of complexes 25–28.

in complexes **26** and **27** is similar to that of Tacke's complexes **17–19** (Scheme 6, Fig. 5), which display a TMSiN_2C ring (TM = Cr, Mo, W), but the ligand in Tacke's complexes is a chelating neutral four-electron-donor $\kappa^2\text{N,Si-iminesilylene}$ [37].

Regarding the mechanism of the processes that lead to **26** and **27**, two plausible pathways can be considered: (i) the replacement of the Br^- anion of **25** by the anionic nucleophile and its subsequent transfer to the Ge atom while an arm of the amidinato fragment migrates to the Mn atom, or (ii) a direct attack of

**Fig. 6.** Crystal structures of complexes **26** and **27**. Adapted from Ref. [41].

the nucleophile to the Ge atom while the coordination of one arm of the amidinato fragment to Mn forces the release of Br^- anion. In this respect, the reactions of **25** with MeLi and $\text{Ag}[\text{BF}_4]$ were monitored by IR spectroscopy (ν_{CO} region). In the case of $\text{Ag}[\text{BF}_4]$, a transient species, which above ca. 0°C evolved quantitatively to **27**, was detected at lower temperatures. The ν_{CO} absorption pattern of this species is very similar to that of **25**, as expected for $[\text{MnX}(\text{CO})_4\{\text{Ge}(\textit{iPr}_2\text{bzam})\textit{tBu}\}]$ ($\text{X} = [\text{BF}_4]^-$ or F^-). Therefore, the synthesis of compound **27** (and probably also that of **26**) begins with the replacement of the Br^- anion of **25** by the corresponding anionic nucleophile. This is in complete agreement with the results of a DFT molecular orbital study, which indicated that both HOMO and LUMO of compound **25** have a large contribution from the Br atom (Fig. 7), and that, as the LUMO contains a σ -antibonding overlap between Mn and Br (with negligible contribution from the atoms of the germylene ligand), complex **25** is prone to break the Mn–Br bond upon treatment with nucleophiles [41]. Complex **25** was also treated with $\text{Ag}[\text{OTf}]$, leading to $[\text{Mn}(\text{OTf})(\text{CO})_4\{\text{Ge}(\textit{iPr}_2\text{bzam})\textit{tBu}\}]$ (**28**), which is structurally analogous to **25** (Scheme 9, Table 4). This result is also in agreement with the mechanism proposed for the reaction of **25** with nucleophiles; however, in this case, the $[\text{OTf}]^-$ anion did not end on the Ge atom. Complex **28** is very moisture sensitive, forming the germanato(II) derivative $[\text{Mn}_2(\text{CO})_8\{\mu-\kappa^4\text{Ge}_2\text{O}_2-\text{Ge}_2\textit{tBu}_2(\text{OH})_2\text{O}\}]$ and $[\textit{iPr}_2\text{bzamH}_2][\text{OTf}]$

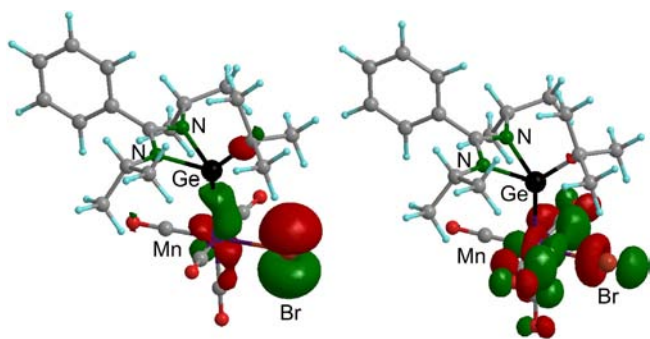
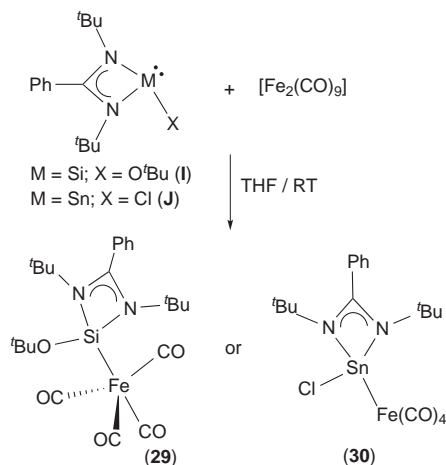


Fig. 7. HOMO (left) and LUMO (right) of complex **25**.

Adapted from Ref. [41].



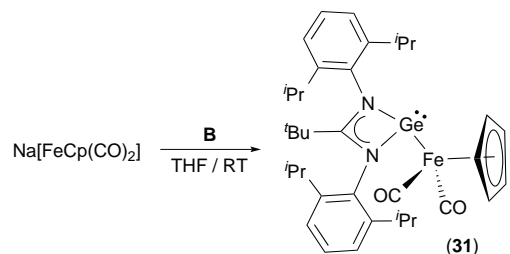
Scheme 10. Synthesis of complexes **29** and **30**.

in wet solvents [41]. The factors controlling the different reactivity observed when replacing the Br[−] anion of **25** with different nucleophiles or even why the Br[−] anion of **25** does not end on the germanium atom are still unknown.

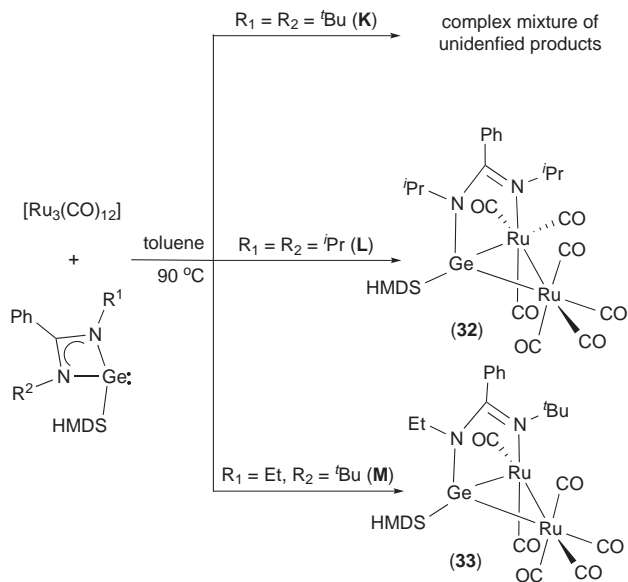
3.5. Group 8 metal complexes

The iron complexes [Fe(CO)₄{M(^tBu₂bzam)X}] (M = Si, X = O^tBu (**29**); M = Sn; X = Cl (**30**)) (Scheme 10, Table 5) were prepared in 2009 and 2010 by Roesky and co-workers from [Fe₂(CO)₉] and Si(^tBu₂bzam)O^tBu (**I**) and Sn(^tBu₂bzam)Cl (**J**) [42,43]. Silylene **I** was prepared by chlorine replacement on chlorosilylene **A** [70]. The ligand arrangement around the iron atom of complex **29** is distorted trigonal bipyramidal, with the silylene ligand occupying an apical position. In the case of **30**, the position of the stannylene is unknown, since no IR [72] or crystallographic data are available for it. It is noteworthy that **30** is the only amidinatostannylene TM complex hitherto reported. As expected, the ¹¹⁹Sn{¹H} NMR signal of **30** (Table 5) is observed at lower field than that of the free ligand **J** (δ = 29.6 ppm (THF-*d*₈) [43]).

Jones and co-workers reported in 2008 the synthesis of the ferrylgermylene [FeCp{Ge(Diip₂tbam)}(CO)₂] (**31**), which was prepared reacting Na[FeCp(CO)₂] with Ge(Diip₂tbam)Cl (**B**) (Scheme 11, Table 5) [32]. In this complex, the Ge(Diip₂tbam) group behaves as a one-electron-donor ligand. The presence of a lone pair of electrons on the germanium atom, which is singly bonded to the iron atom, is confirmed by its pyramidal coordination geometry. This feature has also been reported for other metalylyl-HTs [73].



Scheme 11. Synthesis of complex **31**.



Scheme 12. Synthesis of complexes **32** and **33**.

Working with [Ru₃(CO)₁₂] as TM precursor, our group reported in 2013 and 2014 the first reactivity studies of amidinato-HTs with TM clusters [44,45]. The germylenes Ge(R¹R²bzam)(HMDS) (R¹ = R² = ^tBu (**K**); R¹ = R² = ⁱPr (**L**); R¹ = Et, R² = ^tBu (**M**)), equipped with a very bulky HMDS group and different R groups on their N atoms were reacted with [Ru₃(CO)₁₂]. Interestingly, while the reaction with **K** led to a complex mixture of unidentified products, the binuclear heptacarbonyl [Ru₂(CO)₇{μ-κ²Ge,N-Ge(ⁱPr₂bzam)(HMDS)}] (**32**) and the unsaturated binuclear hexacarbonyl [Ru₂(CO)₆{μ-κ²Ge,N-Ge(Et^tBubzam)(HMDS)}] (**33**) were isolated using germylenes **L** and **M**, respectively (Scheme 12, Table 5). Germylenes **K** [74], **L** [44] and **M** [45] were prepared by chlorine replacement on the chloro derivatives Ge(^tBu₂bzam)Cl [75], Ge(ⁱPr₂bzam)Cl [44] and Ge(Et^tBubzam)Cl [45], respectively. Fig. 8 shows the molecular structures of **32** and **33**. Both contain a GeRu₂ triangle with a Ge–Ru edge bridged by the amidinato group. Therefore, their formation implied the unprecedented transformation of the amidinatogermylenes **L** and **M** (equipped with just one accessible lone pair of electrons on the Ge atom), into bidentate four-electron-donor μ-κ²Ge,N-ligands. A remarkable structural feature of **33** is that the Ru atom bonded to the amidinato N atom (Ru1 in Fig. 8) is coordinatively unsaturated. Fig. 8 also displays comparative space-filling views of **32** and **33**, showing that the vacant coordination site of **33** is occupied by a CO ligand in **32**. The vacant site in **33** is partially protected by an interaction of the Ru1 with a hydrogen atom of the closest ^tBu group (Ru1...H distance 2.24 Å [45]). Coordinatively unsaturated diruthenium(0) complexes are extremely rare [76]. These results indicate that, in the reactions of [Ru₃(CO)₁₂] with amidinatogermylenes of the type Ge(R¹R²bzam)(HMDS), the formation of μ-κ²Ge,N-ligands (like in

Table 5
Relevant data of group 8 metal complexes containing amidinato-HT ligands.

Complex	Yield (%), color	M{ ¹ H} NMR, δ (ppm)	IR ν (CO) (cm ⁻¹)	d(M-TM) (Å)	Reactivity	Ref.
[Fe(CO) ₄ {Si(^t Bu ₂ bzam)(O ^t Bu)}] (29)	72, brown-red	²⁹ Si, 40.3 (s) ^a	2026 (m), 1949 (s), 1899 (s) ^b	2.237(7)		[42]
[Fe(CO) ₄ {Sn(^t Bu ₂ bzam)Cl}] (30)	61, red-brown	¹¹⁹ Sn, 255.0 (s) ^c	Not given			[43]
[FeCp{Ge(Diip ₂ tbam)}(CO) ₂] (31)	56, red		1964 (s), 1921 (s) ^d	2.442(1)		[32]
[Ru ₂ (CO) ₇ { μ - κ^2 Ge, <i>N</i> -Ge(^t Pr ₂ bzam)(HMDS)}] (32)	62, light orange		2085 (m), 2034 (vs), 2013 (m), 2002 (s), 1992 (m), 1973(w), 1959 (w) ^e	2.3957(7)		[44]
[Ru ₂ (CO) ₆ { μ - κ^2 Ge, <i>N</i> -Ge(Et ^t Bubzam)(HMDS)}] (33)	64, dark orange		2073 (m), 2000 (vs), 1985 (s), 1992 (m), 1977 (m), 1994 (m), 1924 (m) ^e	2.3778(3), 2.4940(3)	Reactions with CO and HSnPh ₃	[45]
[Ru ₂ (CO) ₇ { μ - κ^2 Ge, <i>N</i> -Ge(Et ^t Bubzam)(HMDS)}] (34)	Not isolated, orange		2085 (m), 2033 (s), 2014 (m), 2004 (s), 1994 (m), 1977(w), 1956(w) ^e			[45]
[Ru ₂ (μ -H)(SnPh ₃)(CO) ₅ { μ - κ^2 Ge, <i>N</i> -Ge(Et ^t Bubzam)(HMDS)}] (35)	91, orange		2071 (w), 2013 (vs), 1995 (m), 1944 (m) ^e	2.3713(4), 2.4949(4)		[45]
[Fe(CO) ₄ {Si(^t Pr ₂ bzam) ₂ }] (36)	65, green	²⁹ Si, -12.7 (s) ^c	Not given	2.3175(6)		[36]
[Fe(CO) ₄ {Si(^t Pr ₂ Diiaam) ₂ }] (37)	80, yellow	²⁹ Si, -41.3 (s) ^f	Not given	2.3630(8), 2.3390(8) ^g		[37]
[Fe(dmpe) ₂ {Si(^t Bu ₂ bzam)Cl}] (38)	81, orange	²⁹ Si, 43.1 (quint) ^f		2.1634(9)	Replacement of Cl	[46]
[Fe(dmpe) ₂ {Si(^t Bu ₂ bzam)Me}] (39)	67, red	²⁹ Si, 102.5 (quint) ^f		2.200(2)		[46]
[Fe(dmpe) ₂ {Si(^t Bu ₂ bzam)H}] (40)	89, red brown	²⁹ Si, 63.6 (quint) ^f		2.184(2)	Catalytic hydrosilylation of ketones	[46]
[Fe(CO) ₄ {Si(^t BuDiipbzam)H}] (41)	20, brown	²⁹ Si, 99.6 (s) ^f	2013 (s), 1984 (s), 1887 (s) ^b			[47]
[Fe(CO) ₄ {Si(^t BuAdbzam)H}] (42)	92, brown	²⁹ Si, 86.5 (s) ^f	Not given			[47]
[Fe(CO) ₄ {Si(^t BuDiipdmaam)H}] (43)	57, brown	²⁹ Si, 83.6 (s) ^f	2022 (s), 1944 (s), 1909 (s) ^b	2.234(1)		[47]
[FeCl ₂ { κ^2 Si, <i>Si</i> -(Si(^t Bu ₂ bzam)NEt) ₂ py}] (44)	73, yellow	Not given		2.5256(7), 2.5110(7)	Reactions with KC ₈ and PMe ₃	[48]
[FeCl ₂ { κ^2 Ge, <i>Ge</i> -(Ge(^t Bu ₂ bzam)NEt) ₂ py}] (45)	83, yellow			2.5670(4), 2.5509(4)	Reactions with KC ₈ and PMe ₃	[48]
[Fe(PMe ₃) ₂ { κ^3 Si, <i>N</i> , <i>Si</i> -(Si(^t Bu ₂ bzam)NEt) ₂ py}] (46)	77, purple	²⁹ Si, 68.3 (dd) ^h		2.164(2), 2.170(1)	Reaction with CO and catalytic hydrosilylation of ketones	[48]
[Fe(PMe ₃) ₂ { κ^3 Ge, <i>N</i> , <i>Ge</i> -(Ge(^t Bu ₂ bzam)NEt) ₂ py}] (47)	90, dark red				Reaction with CO	[48]
[Fe(CO) ₂ { κ^3 Si, <i>N</i> , <i>Si</i> -(Si(^t Bu ₂ bzam)NEt) ₂ py}] (48)	85, orange	²⁹ Si, 98.3 (s) ^f	1830 (s), 1778 (s) ^b	2.158(2), 2.166(2)		[48]
[Fe(CO) ₂ { κ^3 Ge, <i>N</i> , <i>Ge</i> -(Ge(^t Bu ₂ bzam)NEt) ₂ py}] (49)	39, not given		1855 (s) 1805 (s) ^b	2.2086(9), 2.2092(9)		[48]
[Fe(CO) ₃ { κ^2 Si, <i>Si</i> -(Si(^t Bu ₂ bzam)NEt) ₂ py}] (50)	No data provided	Not given	Not given	2.196(1), 2.295(1)		[48]
[Fe(CO) ₃ { κ^2 Ge, <i>Ge</i> -(Ge(^t Bu ₂ bzam)NEt) ₂ py}] (51)	30, not given		1956 (s), 1883 (s), 1869 (s) ^b			[48]
[Fe(CO) ₂ (PMe ₃) ₃ { κ^2 Ge, <i>Ge</i> -(Ge(^t Bu ₂ bzam)NEt) ₂ py}] (52)	No data provided		Not given	2.2767(9), 2.2956(9)		[48]

^a In CDCl₃.

^b In KBr.

^c In THF-*d*₈.

^d In Nujol.

^e In toluene.

^f In C₆D₆.

^g Two molecules in the asymmetric unit.

^h In toluene-*d*₈.

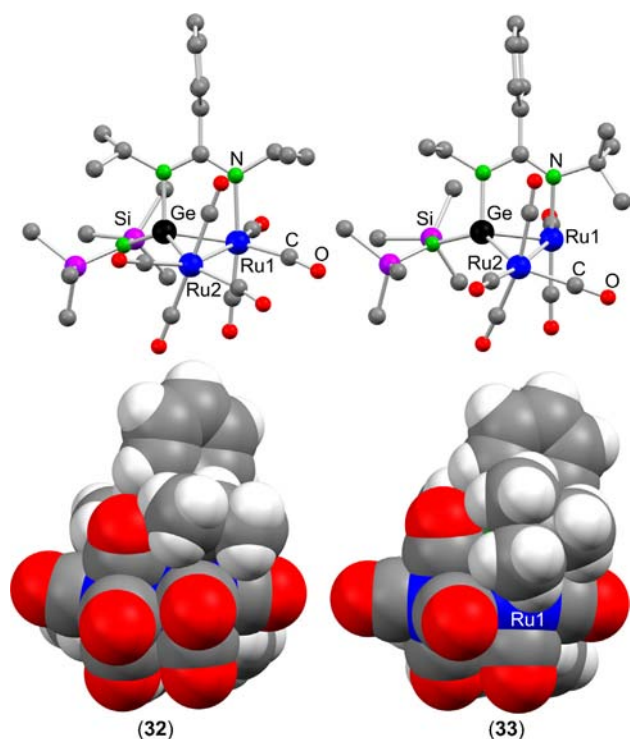


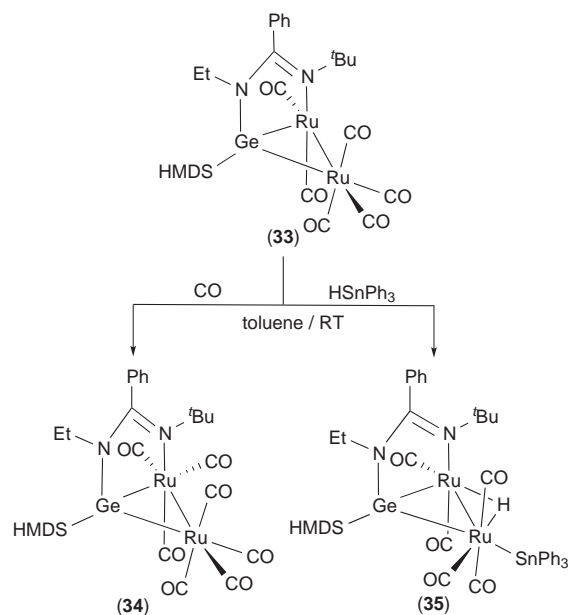
Fig. 8. Ball and stick (top) and space-filling views (bottom) of **32** and **33**. Hydrogen atoms on the ball and stick view have been omitted for clarity.

Adapted from Ref. [45].

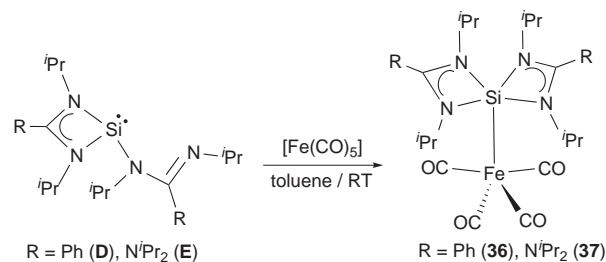
32 and **33** is only possible when one of the amidinato NR groups is less bulky than a ^tBu group (note that the reaction of [Ru₃(CO)₁₂] with the asymmetric ligand **M** gives only the regioisomer that has the Ge atom attached to the N^{Et} group and not to the N^{^tBu} group). NMR data of **32** and **33** [44,45] indicated that the NR group attached to the Ge atom is very close to the Ph and HMDS groups. This observation suggests that the space between these two groups can accommodate an ⁱPr (like in **32**) or an Et (like in **33**), but is not large enough for a ^tBu moiety.

The unsaturated complex **33** reacted easily with CO to give the saturated species [Ru₂(CO)₇{μ-κ²Ge,N-Ge(Et^tBubzam)(HMDS)}] (**34**) (Scheme 13, Table 5) [45]. The IR νCO absorption pattern of **34** and that of the heptacarbonyl **32** are nearly identical (Table 5), indicating that the extra CO ligand in **34** must formally occupy the vacant coordination site of **33**. Pure **34** could not be isolated because its solutions were only stable under a CO atmosphere, reverting to **33** when they were left under argon or when the solvent was removed under vacuum. These facts indicate that the steric hindrance exerted by the ^tBu group of **34** over the new CO ligand is so strong that the system prefers to release that CO despite this process leads to a coordinatively unsaturated product (**33**). Complex **32**, equipped with a smaller ⁱPr group on that position, is stable. The reaction of **33** with HSnPh₃ led to the unsaturated hydridostannyl derivative [Ru₂(μ-H)(SnPh₃)(CO)₅{μ-κ²Ge,N-Ge(Et^tBubzam)(HMDS)}] (**35**), which maintains the vacant site of its precursor (Scheme 13, Table 5) [45].

The aforementioned bis(amidinato/guanidinato)silylenes **D** [35] and **E** [65a] were also used by Tacke et al. to prepare the iron complexes [Fe(CO)₄{Si(ⁱPr₂bzam)₂}] (**36**) [36] and [Fe(CO)₄{Si(ⁱPr₂Diaam)₂}] (**37**) [37], respectively (Scheme 14, Table 5). The ligand arrangement around the iron atom is distorted trigonal bipyramidal in both compounds, with the silylene occupying an equatorial position. Both **36** and **37** contain five-coordinate silicon(II) ligands. As observed for the related group 6 derivatives **14–16** (Scheme 6), the formation of **36** and **37** implies that **D** and



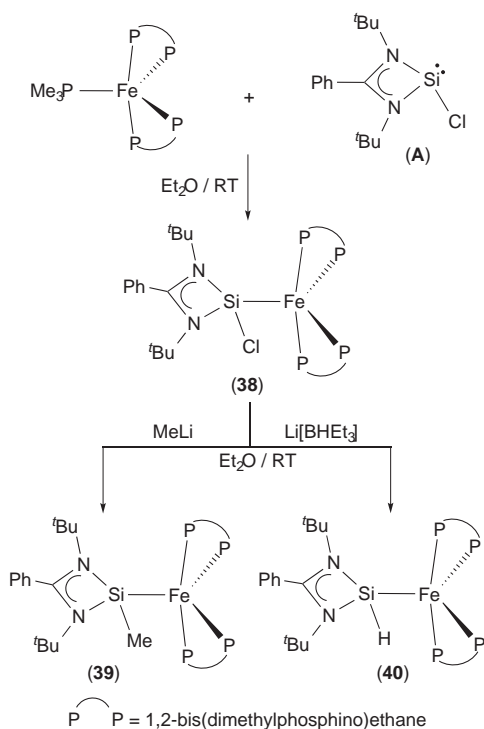
Scheme 13. Synthesis of complexes **34** and **35**.



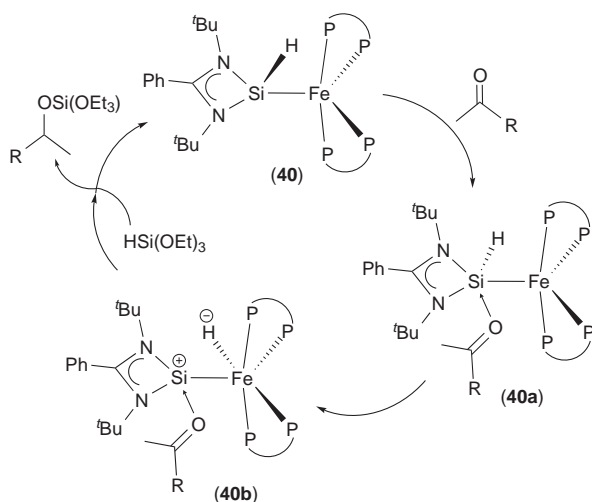
Scheme 14. Synthesis of complexes **36** and **37**.

E close their pendant imino arm toward the silicon when it coordinates to the metal center. The bidentate κ²N,Si-coordination of the guanidinato ligand **E** in the group 6 carbonyls **17–19** was not observed in this case. Noteworthy, while the ²⁹Si NMR chemical shift of **36** is at lower field (Table 5) than that of the free ligand **D** (δ = −31.4 ppm in C₆D₆ [35]), that of **37** is high-field shifted with respect to that of **E** (δ = −25.6 ppm in C₆D₆ [65a]). This fact reveals the different electronic nature of the amidinato and guanidinato fragments. DFT calculations indicated that the Si–Fe bond of **36** is best described as a single bond [36].

Driess and coworkers prepared the very electron-rich iron complex [Fe(dmpe)₂{Si(^tBu₂bzam)Cl}] (**38**) by reacting [Fe(dmpe)₂(PMe₃)] with silylene **A**. Complex **38** was subsequently treated with MeLi and Li[BHET₃] to yield the derivatives [Fe(dmpe)₂{Si(^tBu₂bzam)X}] (X = Me (**39**), H (**40**), respectively) (Scheme 15, Table 5) [46]. In these compounds, the ligand arrangement around the iron center is distorted trigonal bipyramidal, with the silylene occupying an equatorial position, which generally is the preferred position for π-accepting ligands in a trigonal-bipyramidal geometry, suggesting the π-acceptor character of the Si(^tBu₂bzam)X ligands. This situation, which differs from the structural arrangement observed in the iron complexes **29** [42] and **41–43** [47] (*vide supra*), in which the amidinatosilylene occupies an apical position, has to be related to the presence in **38–40** of the very basic dmpe ligand, which makes the iron atom very electron-rich. The Fe–Si bond distances in **38–40** (Table 5) are ca. 0.06 Å shorter than those of the carbonylic **29** and **43** (Table 5), reflecting a greater π-backbonding component in the Fe–Si bonds



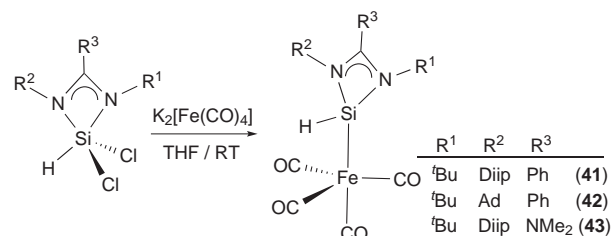
Scheme 15. Synthesis of complexes 38–40.



Scheme 16. Proposed catalytic cycle for the hydrosilylation of ketones promoted by complex 40.

of 38–40. This multiple bonding character was also confirmed by DFT calculations (Fe–Si Wiberg bond index >1 for all compounds). The $^{29}\text{Si}\{^1\text{H}\}$ NMR signals of 38–40 ($\delta = 43.1$, 102.5 and 63.6 ppm, respectively) are, as observed for the bis(silylene) titanium complexes 1–3 [30], inversely proportional to the Hammett constant of the Cl, Me or H substituent of their silicon atom.

The hydrido(amidinato)silylene iron complex 40 was used as a precatalyst for the hydrosilylation of various ketones (having different steric and electronic properties) with $\text{HSi}(\text{OEt})_3$. The catalytic activity of 40 was comparable to that of other iron-based benchmark systems [77], giving excellent conversions to the corresponding alcohols, even at room temperature [46]. A catalytic cycle was proposed (Scheme 16) that implies the coordination of the ketone to the silicon(II) center of 40 to give intermediate 40a, which, through a 1,2-hydride migration from silicon to iron, leads to



Scheme 17. Synthesis of complexes 41–43.

the betaine-like silyliumylideneiron(0) hydrido intermediate 40b. A subsequent reaction with $\text{HSi}(\text{OEt})_3$ affords the desired silylated product, regenerating the catalyst 40. Evidence for this mechanism was found analyzing by ^1H NMR the stoichiometric reaction of 40 with 2-acetonaphthone in the absence of $\text{HSi}(\text{OEt})_3$, which showed the formation of a new iron hydrido species ($\delta = -13.94$ ppm). Additionally, complex 40 proved to be stable in the absence of ketone even after prolonged heating. This observation supports that the hydride transfer process is induced by the ketone and, therefore, confirms the initial formation of the ketone adduct 40a. A simplified model of the proposed intermediate 40b was modeled by DFT calculations, which showed a substantial increase in the NBO charge of the silicon atom of 40b compared with that of 40 and an elongation of the C=O bond of the coordinated ketone. These results are a good evidence of the potential of HTs as non-innocent ligands for substrate activation.

Driess and coworkers have very recently reported the synthesis of hydrido(amidinato)silylene iron complexes derived from asymmetric amidinates [47]. These researchers prepared a series of asymmetric carodiimides (reducing N,N' -disubstituted thioureas with LiHMDS), which were subsequently used as precursors to asymmetric amidinatosilanes, such as $\text{Si}(^t\text{BuDiipbzam})\text{HCl}_2$, $\text{Si}(R^1R^2\text{bzam})\text{HCl}_2$ ($R^1 = ^t\text{Bu}$, $R^2 = \text{Diip}$; $R^1 = ^t\text{Bu}$, $R^2 = \text{Ad}$) and $\text{Si}(^t\text{BuDiipdmaam})\text{HCl}_2$. The reduction of these dichlorosilanes using traditional methods [64] did not lead to the expected silylenes. However, reacting these dichlorohydrosilanes with $\text{K}_2[\text{Fe}(\text{CO})_4]$ led to the isostructural complexes $[\text{Fe}(\text{CO})_4\{\text{Si}(R^1R^2\text{bzam})\text{H}\}]$ ($R^1 = ^t\text{Bu}$, $R^2 = \text{Diip}$ (41); $R^1 = ^t\text{Bu}$, $R^2 = \text{Ad}$ (42)) and $[\text{Fe}(\text{CO})_4\{\text{Si}(^t\text{BuDiipdmaam})\text{H}\}]$ (43) (Scheme 17, Table 5) [47]. Since the traditional synthesis of hydrido(amidinato)silylene TM complexes generally follows the three-step methodology (a) preparation of the chloro(amidinato)silylene, (b) coordination to the TM center and (c) chlorine replacement using a hydride salt [25b,30,46], the novel approach used to prepare 41–43 represents an important alternative to the synthesis of this kind of complexes. The IR spectra of these complexes [72] and the crystal structure of 43 helped establish that the silylene ligand occupies an apical position of a distorted trigonal bipyramidal ligand arrangement. These asymmetric complexes (41–43) were tested as catalyst precursors for hydrosilylation of pro-chiral ketones, but they proved to be inactive. This observation contrasts with the catalytic activity observed for the same reaction using the more electron-rich complex 40 [46].

Driess and co-workers also described the synthesis, structures and catalytic activity of the first TM complexes equipped with MNM pincer-type bis(silylene)- and bis(germylene)pyridine ligands [48]. The ligands, namely, $\{\text{M}(^t\text{Bu}_2\text{bzam})\text{NET}\}_2\text{py}$ ($\text{M} = \text{Si}$ (N), Ge (O)); $(\text{HNET})_2\text{py} = 2,6\text{-bis}(\text{ethylamino})\text{pyridine}$) were synthesized by transmetalation of the dilithiated diamino pyridine with two equivalents of A [64] or Ge($^t\text{Bu}_2\text{bzam}$)Cl [75], respectively. The reactions of FeCl_2 with N and O at room temperature led to the iron(II) complexes $[\text{FeCl}_2\{\kappa^2\text{M},\text{M}-(\text{M}(^t\text{Bu}_2\text{bzam})\text{NET})_2\text{py}\}]$ ($\text{M} = \text{Si}$ (44), Ge (45)) (Scheme 18, Table 5). In contrast with other iron(II) complexes having related PNP, NNN, CNC and NNP pyridine-based

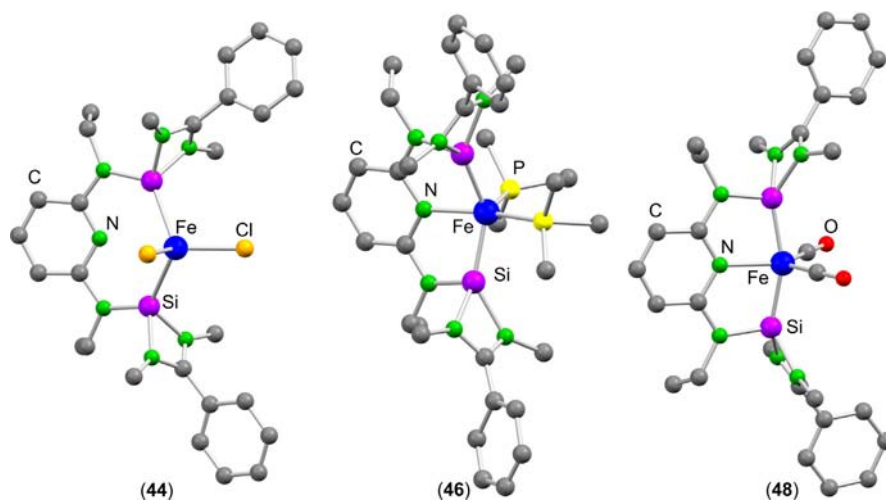
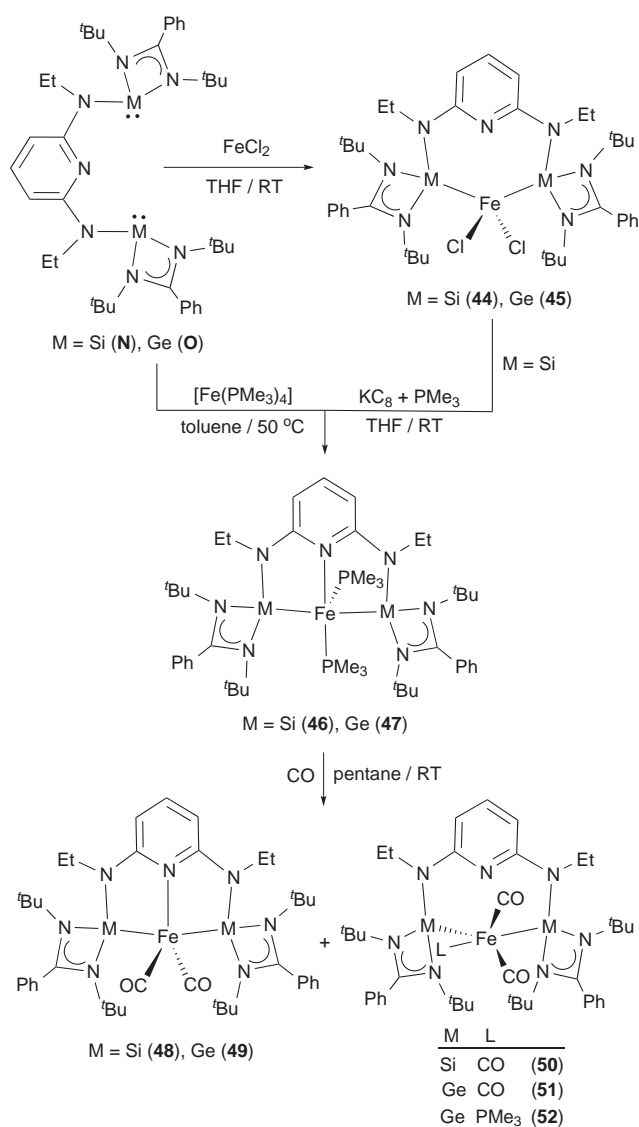


Fig. 9. Crystal structures of complexes **44**, **46** and **48**.

Adapted from Ref. [48].

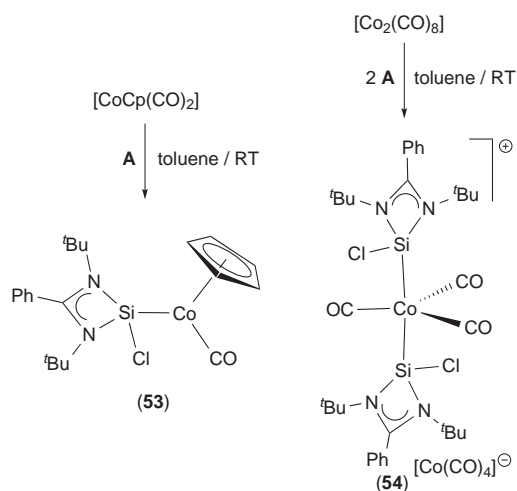


Scheme 18. Synthesis of complexes **44**–**52**.

pincer ligands, in which the iron center is pentacoordinated [78], the iron atom of **44** (Fig. 9) and **45** is in a distorted tetrahedral coordination environment with no clear interaction with the pyridine N atom (the N–Fe distance is 3.304 Å in **44** and 3.543 Å in **45**). The authors, who prior to this work had demonstrated the very strong σ -donor character of related amidinato-HT ligands (*vide supra* [53,58]), suggest that, among other factors, the high basicity of the ligands makes the iron(II) center too electron-rich to achieve pentacoordination. Magnetic measurements and ⁵⁷Fe Mössbauer spectroscopy confirmed that compounds **44** and **45** are distorted tetrahedral high-spin iron(II) complexes [48].

The reactions of the iron(0) complex [Fe(PMe₃)₄] with **N** and **O** led to the pincer-type derivatives [Fe(PMe₃)₂{ κ^3 M,N,M-(M(^tBu₂bzam)NET)₂py}}] (M = Si (**46**), Ge (**47**)). Alternatively, **46** was also prepared by reduction of the iron(II) derivative **44** with KC₈ in the presence of PMe₃ (Scheme 18, Table 5) [48]. The crystal structure of **46** (Fig. 9) revealed that the ligand environment of the iron(0) atom is pseudo-square pyramidal (PSQP), with a PMe₃ ligand occupying the apical position. The Fe–Si bond distances are ca. 0.35 Å shorter than those of the tetrahedral κ^2 Si₂ complex **44**. The NMR spectra of **46** and **47** are very similar, suggesting analogous structures. NMR spectroscopy revealed that the PSQP coordination of **46** and **47** (C_s symmetry), which is very unusual for Fe(0) low-spin complexes, was maintained at 70 °C. ⁵⁷Fe Mössbauer spectroscopy confirmed that both complexes feature Fe(0) centers equipped with redox innocent ligands. DFT calculations conducted on **46** showed heavily polarized Fe–Si bonds, which is also indicative of zero-valent iron. The Fe–Si Wiberg bond indices of **46**, which are >1, indicate some multiple bond character, in agreement with the short experimental Fe–Si bond distances, 2.164(2) and 2.170(1) Å. Good catalytic activities were observed when **46** was used a catalyst precursor for the hydrosilylation of several acetophenones at 70 °C [48].

In order to establish the donating abilities of the pincer ligands **N** and **O**, compounds **46** and **47** were reacted with CO at atmospheric pressure, leading, in both cases, to a mixture of two major products, [Fe(CO)₂{ κ^3 M,N,M-(M(^tBu₂bzam)NET)₂py}}] (M = Si (**48**) or Ge (**49**)) and [Fe(CO)₃{ κ^2 M,M-(M(^tBu₂bzam)NET)₂py}}] (M = Si (**50**) or Ge (**51**)). When using germylene **47**, another product, [Fe(CO)₂(PMe₃){ κ^2 Ge,Ge-(Ge(^tBu₂bzam)NET)₂py}}] (**52**), featuring one phosphine and two CO ligands was also isolated (Scheme 18, Table 5) [48]. A comparison of the IR ν (CO) absorptions of **48** and **49** (1830, 1778 cm⁻¹ and 1855, 1805 cm⁻¹, respectively) with those of the related complexes [Fe(CO)₂(κ^3 L,N,L-L₂py)] complexes [79–84]

Scheme 19. Synthesis of complexes **53** and **54**.

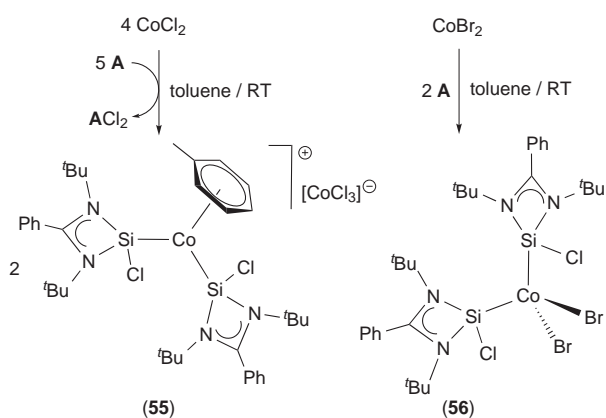
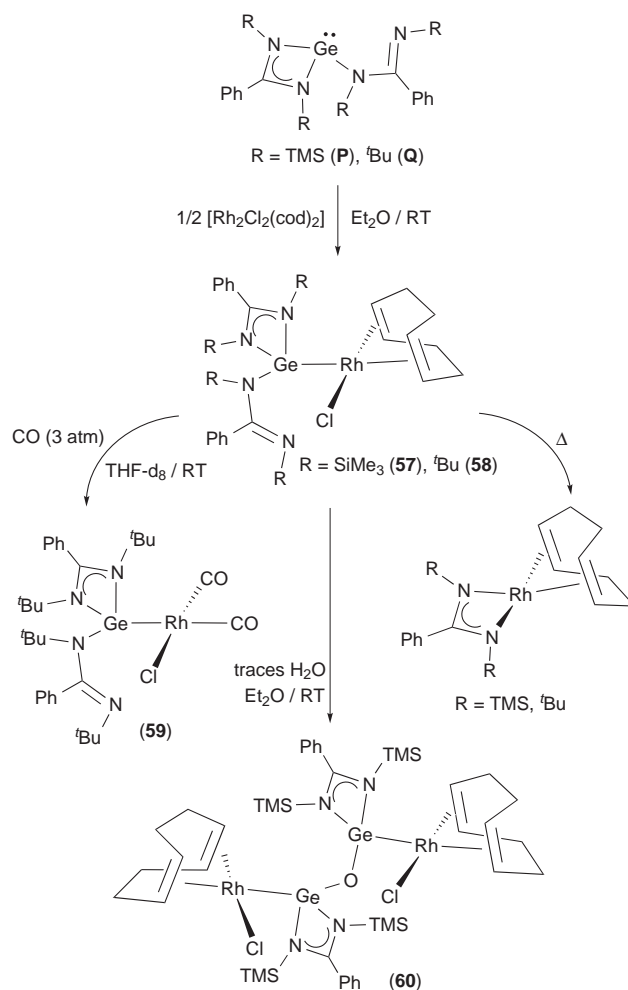
indicated that the bis(silylene)pyridine **N** is a stronger electron donor than the bis(germylene)pyridine **O** and that both ligands are stronger donors than related L_2py pincers with $L =$ phosphines [79,84], pyridines [79], imines [80,83,84] or NHCs [81,82]. Interestingly, while the phosphine complexes **46** and **47** feature a PSQP structure in solution and in the solid state, the dicarbonyl derivatives **48** and **49** exhibit a TBP environment around the iron center in the solid (X-ray diffraction; M atoms in apical positions, Fig. 9) and in solution (NMR, C_{2v} symmetry). However, the crystal structures of **50** and **52** established that the M atoms occupy one apical and one equatorial position of a TBP coordination environment around the metal atom. The $^{29}Si\{^1H\}$ NMR spectrum of **46** shows one resonance signal at 68.3 ppm, whereas that of its dicarbonyl derivative **48** appears at 98.3 ppm. This is possibly due to the higher electron density of the iron atom in **46**, which is equipped with more basic PMe_3 ligands.

3.6. Group 9 metal complexes

The neutral cobalt(I) complex $[CoCp(CO)\{Si(tBu)_2bzam\}Cl]$ (**53**) and the disproportionation salt $[Co(CO)_3\{Si(tBu)_2bzam\}Cl]_2[Co(CO)_4]$ (**54**) were prepared by Roesky et al. reacting chlorosilylene **A** with $[CoCp(CO)_2]$ and $[Co_2(CO)_8]$, respectively (Scheme 19, Table 6) [31]. The cobalt atom of the cation of **54** is in a slightly distorted TBP geometry with both silylenes in the apical positions. It has been reported that the formation of these disproportionation salts from $[Co_2(CO)_8]$ and neutral ligands, instead of simple CO substitution, is favored for highly basic ligands, such as alkyl phosphines [85] or NHCs [86]. Thus, the formation of **54** confirms the high basicity of **A**.

Roesky, Stalke and co-workers reported in 2013 the first carbonyl-free mixed-valence cobalt(I)/cobalt(II) derivative, the complex salt $[Co(\eta^6-tol)\{Si(tBu)_2bzam\}Cl]_2[CoCl_3]$ (**55**), which was prepared reacting $CoCl_2$ with silylene **A** in toluene, with concomitant release of $Si(tBu)_2bzam\}Cl_3$ (Scheme 20, Table 6) [49]. The related cobalt(I)/cobalt(II) complex $[Co(CO)_3\{SiCl_2L\}_2][CoCl_3(THF)]$ ($L = 1,3$ -bis(2,6-diisopropylphenyl)imidazol-2-ylidene), prepared reacting $[Co_2(CO)_8]$ with $SiCl_2L$, was also reported by the same authors [87]. In the synthesis of **55**, silylene **A** behaves as a reducing agent as well as a neutral two-electron-donor ligand. In contrast, an analogous reaction with $CoBr_2$ (instead of $CoCl_2$) led exclusively to the adduct $[CoBr_2\{Si(tBu)_2bzam\}Cl]_2$ (**56**) (Scheme 20, Table 6) [49].

Working with $[Rh_2Cl_2(cod)_2]$ as TM precursor and the bis(amidinato)germylenes $Ge(R_2bzam)_2$ ($R = TMS$ (**P**), tBu (**Q**),

Scheme 20. Synthesis of complexes **55** and **56**.Scheme 21. Synthesis of complexes **57–60**.

the group of Castel reported that the NR group on the amidinato fragment strongly affects the stability of the reaction products [50]. Thus, the monomeric germylene rhodium(I) complexes $[RhCl(cod)\{Ge(R_2bzam)_2\}]$ ($R = TMS$ (**57**), tBu (**58**)) (Scheme 21, Table 6), prepared from the parent bis(amidinato)germylenes and $[Rh_2Cl_2(cod)_2]$, decomposed in solution to the amidinato rhodium derivatives $[Rh(R_2bzam)(cod)]$ ($R = TMS, tBu$). However, this decomposition was so fast for **57** that this complex could not be isolated. Additionally, **57** quickly reacted with traces of

Table 6
Relevant data of group 9 metal complexes containing amidinato-HT ligands.

Complex	Yield (%), color	M{ ¹ H} NMR, δ (ppm)	IR ν(CO) (cm ⁻¹)	d(M–TM) (Å)	Reactivity	Ref.
[CoCp(CO){Si(^t Bu ₂ bzam)Cl}] (53)	90, red	²⁹ Si, 54.3 (s, br) ^a	1968 (s) ^b	2.1143(4)		[31]
[Co(CO) ₃ {Si(^t Bu ₂ bzam)Cl}] ₂ [Co(CO) ₄] (54)	78, greenish-blue	²⁹ Si, 68.3 (s) ^a	2057 (vw), 2004 (sh), 1976 (s) ^b	2.2060(6), 2.2017(6)		[31]
[Co(η ⁶ -tol){Si(^t Bu ₂ bzam)Cl}] ₂][CoCl ₃] (55)	68, green	²⁹ Si, 48.3 (s), 49.5(s) ^c		2.1553(9), 2.150(1)		[49]
[CoBr ₂ {Si(^t Bu ₂ bzam)Cl}] (56)	85, violet	Not observed		2.1940(5), 2.1793(5)		[49]
[RhCl(cod){Ge(TMS ₂ bzam) ₂ }] (57)	Not isolated					[50]
[RhCl(cod){Ge(^t Bu ₂ bzam) ₂ }] (58)	49, yellow			2.445(1)	Reaction with CO	[50]
[RhCl(CO) ₂ {Ge(^t Bu ₂ bzam) ₂ }] (59)	Not isolated		1971 (s), 2058 (s) ^d			[50]
[Rh ₂ Cl ₂ (cod) ₂ {μ-κ ² Ge,Ge-(Ge(TMS ₂ bzam)) ₂ O}] (60)	Not isolated			2.351(1)		[50]
[Co ₂ (CO) ₇ {Ge(^t Pr ₂ bzam)(HMDS)}] (61)	75, light orange		2073 (m), 2016 (m), 1989 (vs), 1944 (m) ^e		Thermolysis	[51]
[Co ₂ (CO) ₇ {Si(^t Bu ₂ bzam)(HMDS)}] (62)	33, orange	Not given	2066 (m), 2005 (m), 1973 (vs), 1932 (m) ^e		Thermolysis	[51]
[Co ₂ (CO) ₇ {Ge(^t Bu ₂ bzam)(HMDS)}] (63)	78, light orange		2072 (m), 2013 (m), 1983 (vs), 1940 (m) ^e	2.2938(8)	Thermolysis	[51]
[Co ₂ (μ-CO)(CO) ₅ {μ-κ ² Ge,N-Ge(^t Pr ₂ bzam)(HMDS)}] (64)	71, light orange		2058 (m), 2017 (vs), 1996 (m), 1974 (m, br), 1814(w, br) ^e	2.2983(4), 2.3633(4)		[44,51]
[Co ₂ (CO) ₆ {Ge(^t Pr ₂ bzam)(HMDS)} ₂] (65)	Not isolated		1960 (m), 1937 (vs) ^e			[51]
[Co ₂ (CO) ₆ {Si(^t Bu ₂ bzam)(HMDS)} ₂] (66)	37, dark orange	Not given	1936 (m), 1920 (vs), 1900 (w) ^e			[51]
[Co ₂ (CO) ₆ {Ge(^t Bu ₂ bzam)(HMDS)} ₂] (67)	90, dark orange		1958 (m), 1937 (vs), 1912 (w) ^e	2.2959(6)		[51]
[CoCp{κ ² Si,Si-(Si(^t Bu ₂ bzam)) ₂ Fc}] (68)	30, deep red	²⁹ Si, 82.0 (s) ^a		2.120(1), 2.125(1)	Catalytic [2 + 2 + 2] cycloadditions	[52]
[CoCp{κ ² Ge,Ge-(Ge(^t Bu ₂ bzam)) ₂ Fc}] (69)	61, deep red			2.1967(6), 2.1979(6)	Catalytic [2 + 2 + 2] cycloadditions	[52]
[Co ₂ Cp ₂ (CO) ₄ {μ-κ ² Si,Si-(Si(^t Bu ₂ bzam)) ₂ Fc}] (70)	87, brown	²⁹ Si, 85.7 (s) ^a	1888 (s) ^f			[52]
[IrHCl(coe){κ ³ Si,C,Si-(Si(^t Bu ₂ bzam)) ₂ Rc}] (71)	92, off-white	²⁹ Si, 54.9 (s) ^g		2.301(1), 2.305(1)	Catalytic borylation of benzene	[53]
[IrHCl(coe){κ ³ Ge,C,Ge-(Ge(^t Bu ₂ bzam)) ₂ Rc}] (72)	91, off-white				Catalytic borylation of benzene	[53]
[IrH ₂ (CO){κ ³ Si,C,Si-(Si(^t Bu ₂ bzam)) ₂ Rc}] (73)	88, colorless	²⁹ Si, 35.9 (s) ^g	1958 (s) ^f			[53]
[RhHCl(PPh ₃) ₃ {κ ³ Si,C,Si-(Si(^t Bu ₂ bzam)) ₂ Rc}] (74)	84, colorless	²⁹ Si, 66.4 (dd) ^g				[53]
[Rh ₂ (μ-Cl) ₂ (cod){Si(^t Bu ₂ bzam)(DMAP)} ₂][OTf] ₂ (75)	20, yellow	²⁹ Si, 40.5 (d) ^a				[38]

^a In C₆D₆.

^b In Nujol.

^c In THF-*d*₈.

^d In THF.

^e In toluene.

^f In KBr.

^g In CDCl₃.

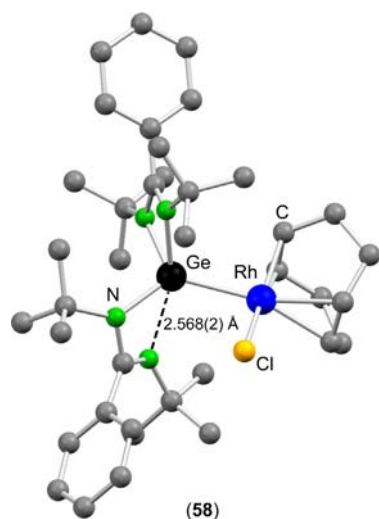


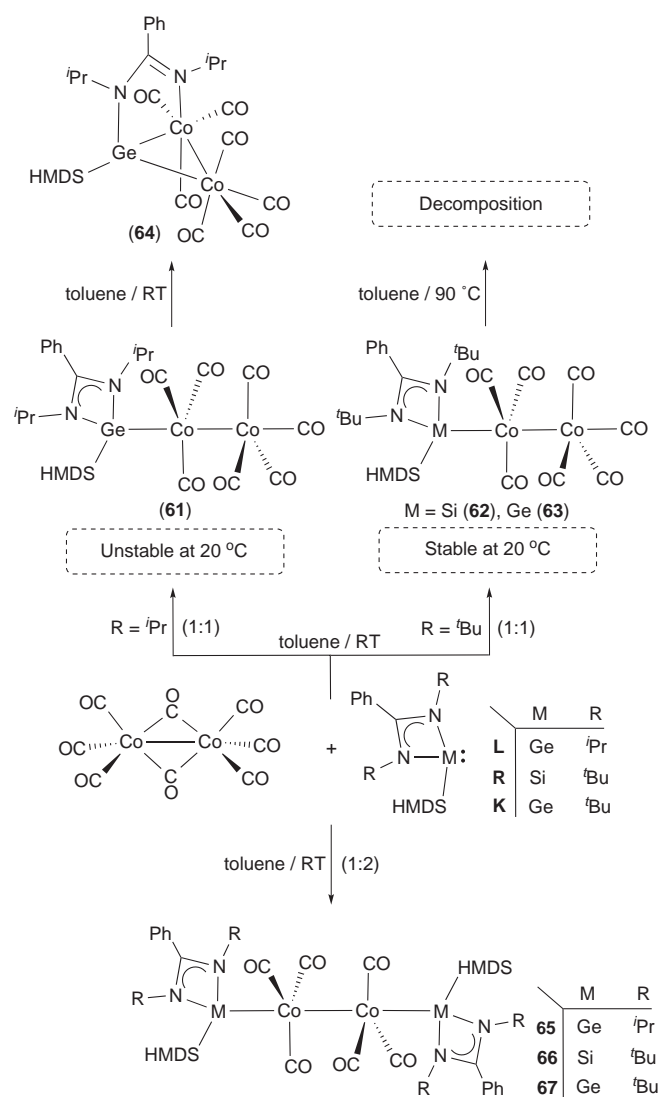
Fig. 10. Crystal structure of complex **58**.

Adapted from Ref. [50].

moisture to form the oxide derivative $[\text{Rh}_2\text{Cl}_2(\text{cod})_2\{\mu\text{-}\kappa^2\text{Ge, Ge}-(\text{Ge}(\text{TMS}_2\text{bzam}))_2\text{O}\}]$ (**60**) (Scheme 21, Table 6). Germynes **P** and **Q** were prepared from the corresponding lithium amidinato salts and GeCl_2 -dioxane [33]. The crystal structure of **58** (Fig. 10) confirmed that the bidentate and monodentate attachments of the amidinato groups observed in the solid state for **Q** [33] are maintained in complex **58**, in which the Ge–N bond distances are 1.991(2), 2.043(2), 1.898(2) and 2.568(2) Å. Complex **58** was converted into the dicarbonyl derivative $[\text{RhCl}(\text{CO})_2\{\text{Ge}(\text{tBu}_2\text{bzam})_2\}]$ (**59**) upon treatment with carbon monoxide. A comparison of its IR $\nu(\text{CO})$ absorptions with those of related $[\text{RhCl}(\text{CO})_2\text{L}]$ complexes (L = two-electron-donor ligand) indicated that the donor character of **Q** is comparable with that of the strongest electron-donating NHCs. Additionally, DFT calculations on **58** and **59** confirmed the existence in both complexes of strong donor–acceptor interactions and polarized covalent Ge–Rh bonds [50].

Our group has recently described the reactivity of $\text{M}(\text{R}_2\text{bzam})(\text{HMDS})$ ($\text{R}=\text{iPr}$, $\text{M}=\text{Ge}$ (**L**); $\text{R}=\text{tBu}$, $\text{M}=\text{Si}$ (**R**); $\text{R}=\text{tBu}$, $\text{M}=\text{Ge}$ (**K**)) with $[\text{Co}_2(\text{CO})_8]$ and has also studied the thermal stability of the resulting products [44,51]. The ligands **L** [44], **R** [70] and **K** [74] were prepared by chlorine replacement on the parent chloro(amidinato)-HTs. The room temperature reactions of $[\text{Co}_2(\text{CO})_8]$ with one equivalent of **L**, **R** and **K** led to the mono-substituted complexes $[\text{Co}_2(\text{CO})_7\{\text{M}(\text{iPr}_2\text{bzam})(\text{HMDS})\}]$ ($\text{M}=\text{Ge}$, $\text{R}=\text{iPr}$ (**61**), $\text{M}=\text{Si}$, $\text{R}=\text{tBu}$ (**62**), $\text{M}=\text{Ge}$, $\text{R}=\text{tBu}$ (**63**)) (Scheme 22, Table 6) [51]. When using silylene **R**, the disproportionation salt $[\text{Co}(\text{CO})_3\{\text{Si}(\text{tBu}_2\text{bzam})(\text{HMDS})\}_2][\text{Co}(\text{CO})_4]$ was also formed, reflecting the higher basicity of silylenes in comparison with that of germynes [85,86]. Interestingly, while the Co_2Si and Co_2Ge *tert*-butyl derivatives **62** and **63** are stable at room temperature, the Co_2Ge *iso*-propyl derivative **61** evolved quantitatively at 20 °C to the ligand-bridged derivative $[\text{Co}_2(\mu\text{-CO})(\text{CO})_5\{\mu\text{-}\kappa^2\text{Ge, N-Ge}(\text{iPr}_2\text{bzam})(\text{HMDS})\}]$ (**64**) (Scheme 22, Table 6). The formation of **64**, which features a Co_2Ge triangle that has a Co–Ge edge bridged by the amidinato fragment, implied the transformation of the amidinatogermylene **L** into a bidentate four-electron-donor $\mu\text{-}\kappa^2\text{Ge, N}$ -ligand. This coordination behavior has also been observed when reacting **L** or the asymmetric amidinatogermylene $\text{Ge}(\text{Et}^t\text{Bubzam})(\text{HMDS})$ (**M**) with $[\text{Ru}_3(\text{CO})_{12}]$ (formation of **32** and **33**, respectively) [44,45].

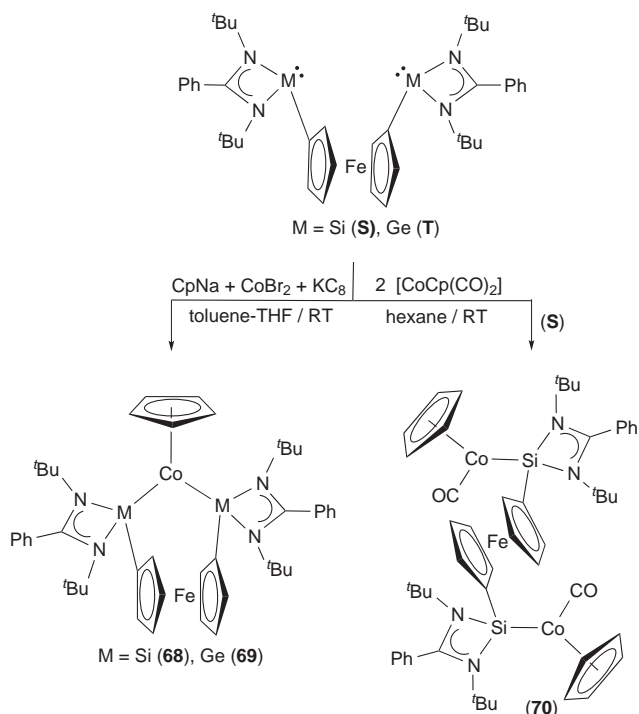
The disubstituted derivatives $[\text{Co}_2(\text{CO})_6\{\text{M}(\text{R}_2\text{bzam})(\text{HMDS})\}_2]$ ($\text{M}=\text{Ge}$, $\text{R}=\text{iPr}$ (**65**); $\text{M}=\text{Si}$, $\text{R}=\text{tBu}$ (**66**); $\text{M}=\text{Ge}$, $\text{R}=\text{tBu}$ (**67**)) have been synthesized by treating $[\text{Co}_2(\text{CO})_8]$ with two equivalents of



Scheme 22. Synthesis of complexes **61–67**.

the corresponding amidinato-HT at room temperature (Scheme 22, Table 6) [51]. According to the IR spectra of these complexes in the $\nu(\text{CO})$ region, the electron-donating character of germynes **L** and **K** is comparable to that of trialkylphosphines and 1,3-diarylimidazol-2-ylidenes, while that of silylene **R** is even stronger.

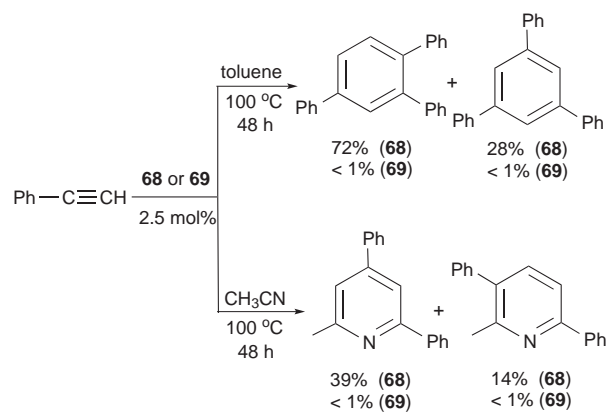
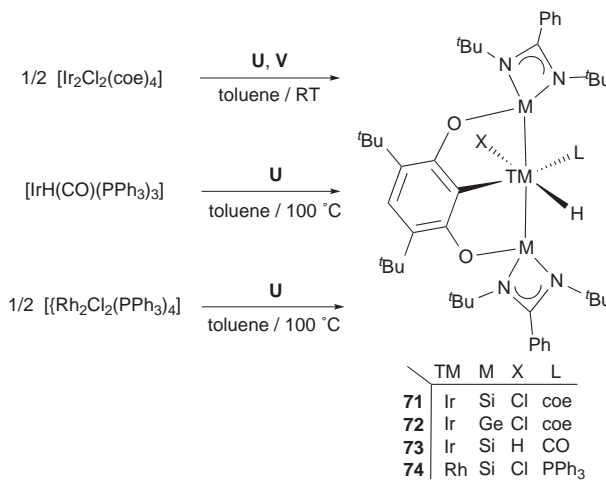
The bridging behavior displayed by ligands **L** and **M** in the diruthenium complexes **32** (using **L**) and **33** (using **M**) and the dicobalt derivative **64** (using **L**) is remarkable because the increase in Lewis acidity of the M atom generated by its coordination to the TM should also reinforce its interaction with the amidinato group [35,36]. However, in this case, a factor that may facilitate the $\kappa^2\text{Ge, N}$ coordination of ligands **L** and **M** is the poly-metallic character of the TM reagents employed, $[\text{Co}_2(\text{CO})_8]$ and $[\text{Ru}_3(\text{CO})_{12}]$, since the release of an amidinato arm from the Ge atom, which will leave a divalent germylene bonded only to the HMDS group and to a pendant amidinato fragment, can be compensated by the formation of a germanium bridge between two metal atoms. Bridging $\mu\text{-}\kappa^1\text{M}$ -coordination is very common for divalent HTs [88]. Another additional factor to consider is the volume of the ligands, both equipped with sterically encumbered HMDS groups. In fact, the reactions of binuclear $[\text{Fe}_2(\text{CO})_9]$, $[\text{Co}_2(\text{CO})_8]$, $[\text{Mn}_2(\text{CO})_{10}]$ and $[\text{Re}_2(\text{CO})_{10}]$ with related amidinato-HTs having anionic groups smaller than HMDS do not afford derivatives containing bridging ligands, but products having monodentate

Scheme 23. Synthesis of complexes **68–70**.

κ^1M -HTs (*vide supra*). In addition, the κ^1Ge to μ - κ^2Ge,N ligand transformation that occurs when **61** ends in **64** reduces the steric interactions between the HMDS group and the nearby CO ligands [51]. Therefore, the presence of a very bulky group on the M atom seems necessary to achieve the μ - κ^2Ge,N coordination observed in **32**, **33** and **64**. The mechanism of the transformation of the model compounds $[Co_2(CO)_7\{M(Me_2acam)(NMe_2)\}]$ (M = Si, Ge; $Me_2acam = N,N'$ -dimethylacetamidinato) into $[Co_2(\mu-CO)(CO)_5\{\mu-\kappa^2M,N-M(Me_2acam)(NMe_2)\}]$ (M = Si, Ge) + CO has been studied by DFT calculations [51], which have also shown that the κ^1M to μ - κ^2M,N ligand rearrangement in these dicobalt complexes is negligibly influenced by the nature of the group 14 donor atom (M = Si or Ge) but is strongly dependent on the size of the amidinato N–R groups, since the process is thermodynamically favorable for R = ^tPr but not for R = ^tBu.

Driess et al. reported the synthesis of bis(silylenyl)- and bis(germylenyl)-substituted ferrocenes $\{M(^tBu_2bzam)\}_2Fc$ (M = Si (**S**), Ge (**T**)) reacting 1,1'-dilithioferrocene with $Si(^tBu_2bzam)Cl$ (**A**) [64] and $Ge(^tBu_2bzam)Cl$ [75]. The reaction of **S** and **T** with an *in situ* generated "CpCo" fragment led to the complexes $[CoCp\{\kappa^2M,M-(M(Si(^tBu_2bzam)))_2Fc\}]$ (M = Si (**68**), Ge (**69**)), respectively, in which the bidentate ligands are chelating the cobalt center (Scheme 23, Table 6) [52]. Additionally, the bis(silylene)-bridged dicobalt complex $[Co_2Cp_2(CO)_4\{\mu-\kappa^2Si,Si-(Si(^tBu_2bzam))_2Fc\}]$ (**70**) was prepared when $[CoCp(CO)_2]$ and **S** were reacted in a 2:1 ratio [52]. The Co–Ge bond lengths of **60**, 2.1967(6) and 2.1979(6) Å, are the shortest known to date. The IR spectrum of **70** shows a strong $\nu(CO)$ absorption at 1888 cm^{-1} , which is at much lower frequency than that of the chlorosilylene complex **53**, 1968 cm^{-1} [31], indicating that each silylene unit of **S** is a much stronger σ -donor than chlorosilylene **A**.

Compounds **68** and **69** were tested as catalyst precursors for the trimerization of phenylacetylene and for the [2 + 2 + 2] cycloaddition of phenylacetylene and acetonitrile (Scheme 24). High conversions were achieved for both reactions using the bis(silylene) **68** as catalyst, but the bis(germylene) **69** proved to be inactive. The authors attributed this inactivity to a stronger coordination of the

Scheme 24. Catalytic [2 + 2 + 2] cycloaddition reactions promoted by complexes **68** and **69**.Scheme 25. Synthesis of complexes **71–74**.

Ge(II) donor centers to the cobalt atom, which impedes the creation of the necessary active sites. However, this explanation contrasts with the general believe that, for HTs equipped with the same substituents (such as **S** and **T**), the M–TM bond strength decreases on going down along group 14 of the Periodic Table [4a,6].

Hartwig, Driess, et al. described in 2012 the first iridium and rhodium complexes equipped with MCM (M = Si, Ge) pincer-type ligands, namely, $[IrHCl(coe)\{\kappa^3M,C,M-(M(^tBu_2bzam))_2Rc\}]$ (M = Si (**71**), Ge (**72**)), $[IrH_2(CO)\{\kappa^3Si,C,Si-(Si(^tBu_2bzam))_2Rc\}]$ (**73**) and $[RhHCl(PPh_3)\{\kappa^3Si,C,Si-(Si(^tBu_2bzam))_2Rc\}]$ (**74**) (Scheme 25, Table 6) and reported the use of **71** and **72** as catalyst precursors for C–H borylation of arenes [53]. These isostructural complexes were prepared reacting common group 9 TM precursors, such as $[Ir_2Cl_2(coe)_4]$, $[IrH(CO)(PPh_3)_3]$ or $[Rh_2Cl_2(PPh_3)_4]$, with the bis(HT)s $\{M(^tBu_2bzam)\}_2RcH$ (M = Si (**U**), Ge (**V**)). The ligands **U** and **V** were synthesized by transmetalation of the dilithiated Rch fragment with two equivalents of the chloro-HTs **A** [64] and $Ge(^tBu_2bzam)Cl$ [75], respectively [53,57]. The formation of **71** and **72** implied, among other processes, a C–H oxidative addition of the C²–H bond of the Rc ring. The octahedral iridium(III) complexes thus formed contain the hydride and chloride ligands *trans* to each other and *cis* to the M atoms of the pincer. The remaining coordination site is occupied by the coe (Fig. 11). The capability of the ligands to promote the observed oxidative addition and consequently achieve the MCM pincer-type coordination was evaluated using several TM precursors. Vaska's complex, $[IrCl(CO)(PPh_3)_2]$, led to a mixture of unknown products when it

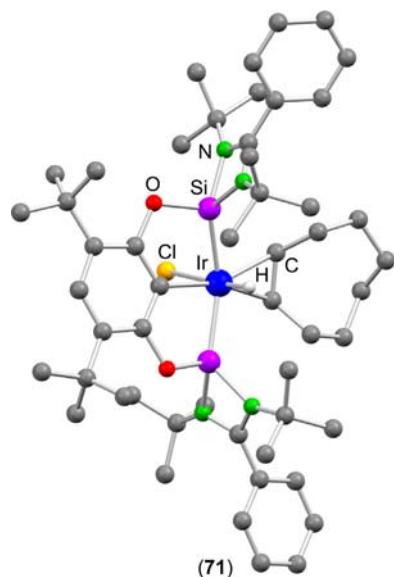
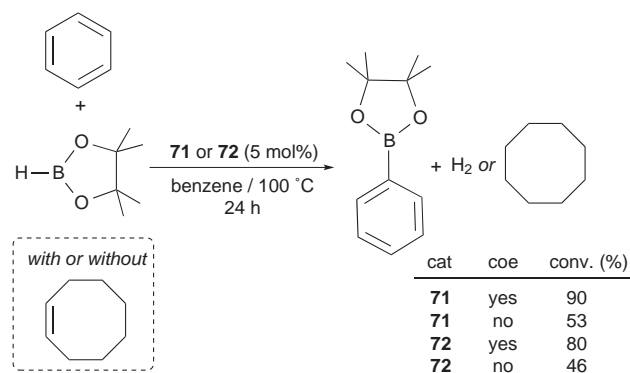


Fig. 11. Crystal structure of complex **71**.

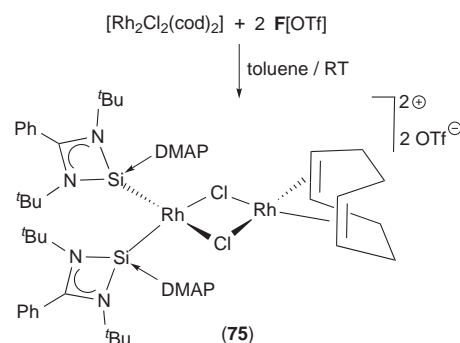
Adapted from Ref. [53].

reacted with **U** and **V**, but $[\text{IrH}(\text{CO})(\text{PPh}_3)_3]$ reacted cleanly with **U** at 100°C to give the dihydrido derivative **73**; however, under the same reaction conditions, the bis(germylene) **V** only led to decomposition products with no sign of the formation of new hydrido species. The rhodium precursors $[\text{Rh}_2\text{Cl}_2(\text{coe})_4]$, $[\text{Rh}_2\text{Cl}_2(\text{CO})_4]$ and $[\text{Rh}_2\text{Cl}_2(\text{PPh}_3)_4]$ only led to successful MCM coordination in the reaction of Wilkinson's dimer with **U**, which gave complex **74**. The lower electron-donating capacity of the bis(germylene) compared with that of the bis(silylene) can explain its lower success at forming MCM–pincer complexes, since the C–H oxidative addition step will be easier for the bis(silylene) **U**. For the iridium derivatives **71** and **72**, which feature a coordinated coe ligand, the authors used the NMR chemical shifts of the olefinic groups and the C–C double bond distances as probes to establish the electronic richness of the metal. Taking into account that, in metal–olefin complexes, a more electron-rich metal center lengthens the C–C double bond distance and shifts the olefinic ^1H and ^{13}C NMR resonances to higher-field due to stronger π -backbonding to the olefin (Chatt–Dewar–Duncanson bonding model) [89], a comparison between the structural and NMR data of **71**, **72** and other isostructural iridium complexes equipped with PCP pincer ligands (P stands for phosphine donor) indicated that **U** is a stronger donor than **V** and that both are much more electron-donating than the PCP systems.

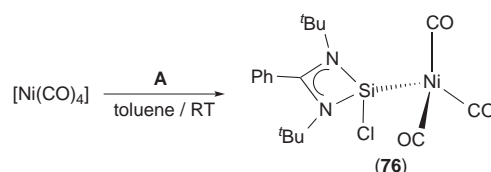
Compounds **71** and **72** were recognized as efficient precatalysts for the catalytic borylation of benzene with pinacolborane (HBpin) at 100°C [53]. Both systems were similarly active, showing higher yields in the presence of additional coe, which facilitates the release of H_2 (Scheme 26). Toluene could also be borylated (ArBpin yield: 91%, meta/para = 1.6:1 for **71**; 39%, meta/para = 1.5:1 for **72**), but more substituted arenes, such as *ortho*- and *meta*-xylenes, led only to 3–15% of ArBpin, the main products resulting from coe hydroboration and vinylic C–H borylation. No conversion was observed using mesitylene. This catalytic activity, although higher than that of related iridium PCP complexes [53], is significantly lower than that of benchmark systems equipped with smaller bidentate nitrogen ligands [89]. Although the metal atoms of **71** and **72** are very electron-rich and this facilitates the B–H and C–H oxidative additions involved in arene borylation reactions, their **U** and **V** ligands are very bulky and this aspect may be negative for certain processes.



Scheme 26. C–H borylation of benzene with HBpin and the precatalysts **71** or **72**.



Scheme 27. Synthesis of complex **75**.



Scheme 28. Synthesis of complex **76**.

So and co-workers have very recently isolated the complex salt $[\text{Rh}_2(\mu\text{-Cl})_2(\text{cod})\{\text{Si}(\text{tBu}_2\text{bzam})(\text{DMAP})_2\}][\text{OTf}]_2$ (**75**) in low yield from a reaction of the cationic silylene **F**[OTf] [69] with $[\text{Rh}_2\text{Cl}_2(\text{cod})_2]$ (Scheme 27, Table 6) [38]. Remarkably, the chlorobridged nature of the rhodium precursor is maintained in **75**.

3.7. Group 10 metal complexes

The first group 10 metal complex containing an amidinato-HT was reported in 2010 by Roesky et al., who prepared the nickel(0) complex $[\text{Ni}(\text{CO})_3\{\text{Si}(\text{tBu}_2\text{bzam})\text{Cl}\}]$ (**76**) by reacting $[\text{Ni}(\text{CO})_4]$ with one equivalent of silylene **A** (Scheme 28, Table 7) [54]. Its Ni–Si bond distance $2.2111(8)\text{Å}$ is similar to those of other silylene nickel complexes [90].

Driess et al. reported the remarkable synthesis of the first oxygen-bridged bis(silylene) $\{\text{Si}(\text{tBu}_2\text{bzam})\}_2\text{O}$ (**X**) by dehydrochlorination of the corresponding disiloxane, $\{\text{SiHCl}(\text{tBu}_2\text{bzam})\}_2\text{O}$ with LiHMDS [55]. This disiloxane was prepared by reacting 1,1,3,3-tetrachlorodisiloxane with two equivalents of the lithiated amidinate. The reaction of **X** with $[\text{Ni}(\text{cod})_2]$ led to $[\text{Ni}(\text{cod})\{\kappa^2\text{Si}_2\text{Si}(\text{tBu}_2\text{bzam})_2\text{O}\}]$ (**77**) (Scheme 29, Table 7) [55]. Castel and co-workers have also reported other complex containing an oxygen-bridged bis(amidinato-HT) ligand, the rhodium derivative $[\text{Rh}_2\text{Cl}_2(\text{cod})_2\{\mu\text{-}\kappa^2\text{Ge}_2\text{Ge}(\text{Ge}(\text{TMS}_2\text{bzam})_2\text{O})\}]$ (**60**) (Scheme 21).

Table 7
Relevant data of group 10 metal complexes containing amidinato-HT ligands.

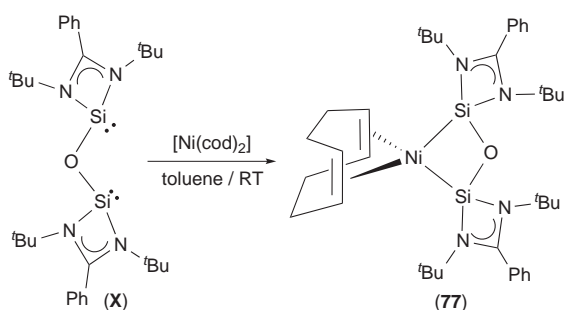
Complex	Yield (%), color	M(¹ H) NMR, δ (ppm)	IR ν (CO) (cm ⁻¹)	d(M–TM) (Å)	Reactivity	Ref.
[Ni(CO) ₃ {Si(^t Bu ₂ bzam)Cl}] (76)	55, colorless	²⁹ Si, 62.7 (s) ^a	1984 (s), 1969 (s) ^b	2.2111(8)	Catalytic Negishi and Kumada C–C coupling	[54]
[Ni(cod){ κ^2 Si,Si-(Si(^t Bu ₂ bzam)) ₂ O}] (77)	91, deep red	²⁹ Si, 32.8 (s) ^c		2.1969(7), 2.1908(7)		[55]
[Pd{ κ^3 Si,C,Si-Si(^t Bu ₂ bzam)RcSi(^t Bu ₂ bzam)H}{ κ^1 Si-(Si(^t Bu ₂ bzam)) ₂ Rc}] (78)	81, colorless	²⁹ Si, –8.7 (s), 39.7 (s), 62.3 (s), 65.8 (s) ^a		2.356(1), 2.327(7), 2.304(1)		[57]
[NiBr{ κ^3 Si,C,Si-(Si(^t Bu ₂ bzam)) ₂ Rc}] (79)	70, yellow	²⁹ Si, 20.2 (s) ^a		2.1737(7), 2.1716(7)	Catalytic Sonogashira C–C coupling	[58]
[NiBr{ κ^3 Ge,C,Ge-(Ge(^t Bu ₂ bzam)) ₂ Rc}] (80)	80, dark red			2.2113(6), 2.2190(6)	Catalytic Sonogashira C–C coupling	[58]
[Ni(CCPPh){ κ^3 Si,C,Si-(Si(^t Bu ₂ bzam)) ₂ Rc}].[CuBr] (81)	No data provided	²⁹ Si, 44.7 (s) ^a		2.296(1), 2.137(1)		[58]
[Ni{CC-(2,6-Ph ₂ C ₆ H ₃)}{ κ^3 Ge,C,Ge-(Ge(^t Bu ₂ bzam)) ₂ Rc}].[CuBr] (82)	No data provided			2.3254(6), 2.1786(6)		[58]
[Ni{ κ^3 Si,C,Si-(Si(^t Bu ₂ bzam)) ₂ Rc}] (83)	66, orange	²⁹ Si, 30.7 (s) ^a		2.2113(6), 2.2190(6)	Catalytic Sonogashira C–C coupling	[58]
[Pt ₂ { μ -P(TMS) ₂ }(PPh ₃) ₂ { μ - κ^1 Si-Si(^t Bu ₂ bzam)}]} (84)	52, red-brown	²⁹ Si, 234.5 (dt) ^a		2.274(2), 2.285(2)		[59]
[Pd ₂ { μ -P(TMS) ₂ }(PPh ₃) ₂ { μ - κ^1 Si-Si(^t Bu ₂ bzam)}]} (85)	Not isolated	²⁹ Si, 187.8 (dt) ^d				[59]
[Ni(cod){ κ^2 Si,Si-(Si(^t Bu ₂ bzam)) ₂ P(TMS)}]} (86)	73, red	²⁹ Si, 51.5 (d) ^a		2.201(2), 2.202(1)		[59]

^a In C₆D₆.

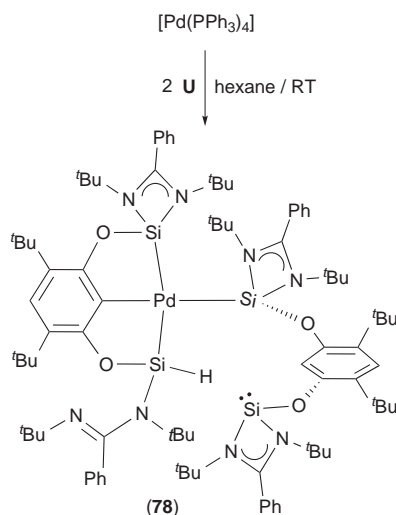
^b In Nujol.

^c In CDCl₃.

^d In THF-*d*₈.



Scheme 29. Synthesis of complex 77.



Scheme 30. Synthesis of complex 78.

However, **60** resulted from a reaction of the monogermylene complex $[\text{RhCl}(\text{cod})\{\text{Ge}(\text{TMS}_2\text{bzam})_2\}]$ (**57**) with moisture [50].

Compound **77** was tested by the groups of Enthaler and Inoue as a precatalyst in cross-coupling reactions of aryl halides with organometallic zinc and Grignard reagents [56]. Good to excellent performances, in terms of yield and selectivity (particularly for the Negishi cross-coupling), were observed for various substrates working in mild conditions (70 °C).

Driess and Inoue's group reported in 2012 the formation of an unexpected mixed Si(II)–C–Si(IV) pincer-type palladium(II) complex, namely, $[\text{Pd}\{\kappa^3\text{Si},\text{C},\text{Si}-\text{Si}(\text{tBu}_2\text{bzam})\text{RcSi}(\text{tBu}_2\text{bzam})\text{H}\}\{\kappa^1\text{Si}(\text{Si}(\text{tBu}_2\text{bzam})_2\text{Rc})\}]$ (**78**), reacting the bis(silylene) $\{\text{Si}(\text{tBu}_2\text{bzam})\}_2\text{RcH}$ (**U**) with $[\text{Pd}(\text{PPh}_3)_4]$ (Scheme 30, Table 7, Fig. 12) [57]. The two Si(II)–Pd bond distances, (2.327(1) and 2.304(1) Å, are similar to those found in other silylene palladium complexes [91], but are shorter than that involving the Si(IV) atom, 2.356(1) Å), indicating some multiple bond character in the Si(II)–Pd interactions. A theoretical mechanistic DFT study has shed light on the steps that lead to complex **78**. A 1,2-hydride shift from palladium to silicon gives rise to the Si–H group, additionally promoting the cleavage of one Si–N bond to give the pendant amidinato group. The origin of the hydrido ligand is an oxidative addition of the resorcinol ring C²–H bond to the Pd atom [57]. The $^{29}\text{Si}\{^1\text{H}\}$ NMR spectra in CDCl_3 of **78** showed four singlets at –8.7, 39.7, 62.3 and 65.8 ppm, which reflect the different coordination environments of the silicon atoms and are, even in the case of the signal corresponding to the uncoordinated silicon, at lower fields than that of the free ligand **U** ($\delta = -24.0$ ppm in C_6D_6) [57].

Disilylene **U**, its germanium counterpart **V** and $\{\text{Ge}(\text{tBu}_2\text{bzam})\}_2\text{RcBr}$ (**W**) (Scheme 31) were used by Hartwig,

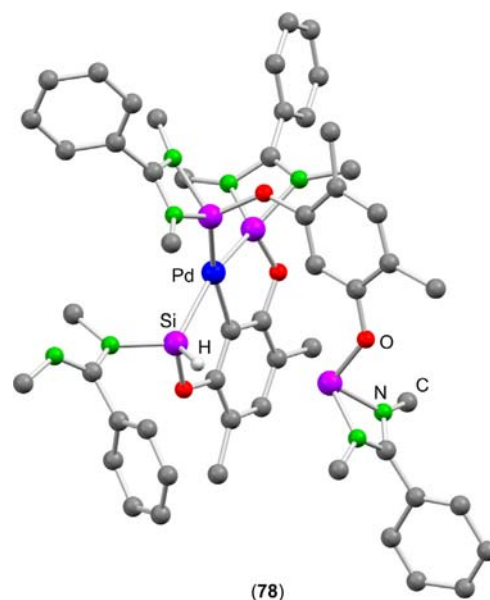
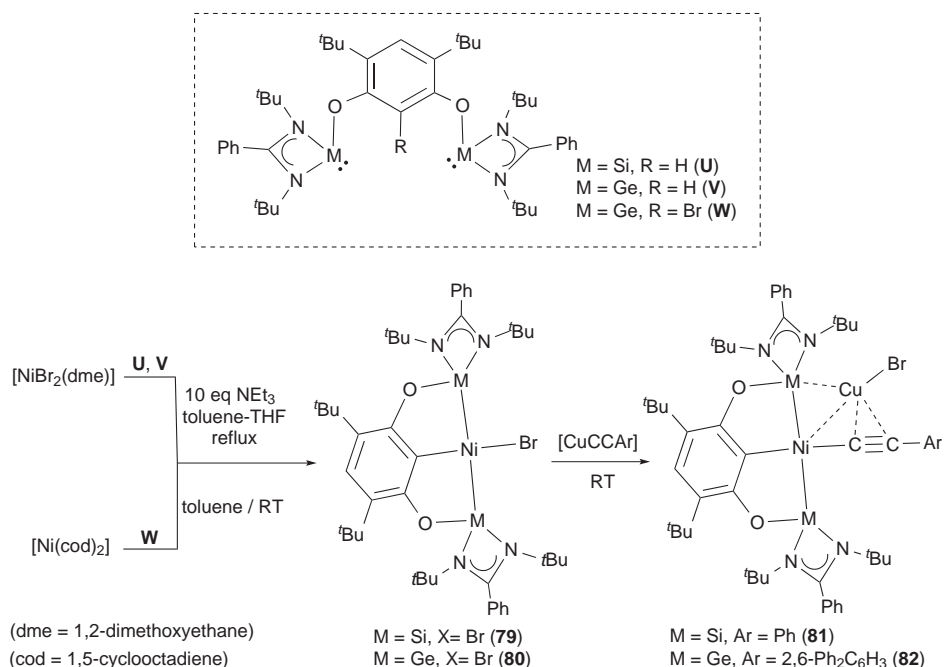


Fig. 12. Crystal structure of complex **78**. The methyl C atoms of the N^tBu groups have been omitted for clarity.

Adapted from Ref. [57].

Driess, et al. to prepare the first nickel complexes equipped with MCM pincer-type ligands ($\text{M}=\text{Si}, \text{Ge}$) [58]. Germylene **W** was prepared by transmetalation of the dilithiated RcBr fragment with two equivalents of $\text{Ge}(\text{tBu}_2\text{bzam})\text{Cl}$ [58]. Attempts to synthesize the silicon analog of **W** were unsuccessful. The reactions of $[\text{NiBr}_2(\text{dme})]$ with **U** and **V** in the presence of an excess of NEt_3 allowed the isolation of the isostructural complexes $[\text{NiBr}\{\kappa^3\text{M},\text{C},\text{M}-(\text{M}(\text{tBu}_2\text{bzam})_2\text{Rc})\}]$ ($\text{M}=\text{Si}$ (**79**), Ge (**80**)) (Scheme 31, Table 7, Fig. 13). As occurred with complexes **71–74** and **78**, the formation of these $\kappa^3\text{M},\text{C},\text{M}$ -pincer nickel(II) derivatives implies the coordination of the ligand M atoms, the oxidative addition of the C²–H bond of the Rc ring of the original ligand, and, for **79** and **80**, the elimination of the resulting hydride as $[\text{HNEt}_3]\text{Br}$. Complex **80** was alternatively prepared in better yield (80% vs 57% using $[\text{NiBr}_2(\text{dme})]$ and **V**) by reaction of $[\text{Ni}(\text{cod})_2]$ with **W**, via C–Br oxidative addition to the nickel(0) precursor (Scheme 31).

The very electron-rich complexes **79** and **80** were tested as precatalysts for Sonogashira cross-coupling reactions (coupling of phenylacetylene with (*E*)-1-iodo-1-octene; 5 mol% of **79** or **80**; 5 mol% CuI , 2 equiv. of Cs_2CO_3 in dioxane at 100 °C) [58]. Although they gave modest conversions (40–50% of coupled product), stoichiometric reactions of **79** or **80** with different copper(I) acetylides (formed *in situ* from the terminal alkyne, Cs_2CO_3 and CuI) were studied with the aim of shedding some light on the mechanism of the catalytic reactions. Analyses of the reaction crudes by atmospheric pressure chemical ionization mass spectrometry (APCI-MS) showed, besides signals corresponding to **79** or **80** and to the expected transmetalation product $[\{\text{MCM}\}\text{NiCCR}]$, a signal assignable to $[\{\text{MCM}\}\text{NiCCR}]\cdot[\text{CuBr}]$, which proved to be the major reaction product for sterically hindered acetylides. The crystal structures of two of these adducts, namely, $[\text{Ni}(\text{CCPh})\{\kappa^3\text{Si},\text{C},\text{Si}-(\text{Si}(\text{tBu}_2\text{bzam})_2\text{Rc})\}]\cdot[\text{CuBr}]$ (**81**) and $[\text{Ni}(\text{CC}-(2,6\text{-Ph}_2\text{C}_6\text{H}_3))\{\kappa^3\text{Ge},\text{C},\text{Ge}-(\text{Ge}(\text{tBu}_2\text{bzam})_2\text{Rc})\}]\cdot[\text{CuBr}]$ (**82**), could be obtained (Scheme 31, Table 7, Fig. 13). Both compounds are isostructural and contain a Cu–Br unit in close proximity to the C≡C bond and to one of the M atoms. DFT calculations revealed that the bonding within the CC–Ni–M–Cu moiety implies an unusual M–Cu–Ni three-center-two-electron bonding with additional interactions between the Cu atom and the acetylide ligand.



Scheme 31. Synthesis of complexes **79–82**.

A subsequent reaction of **81** with 3 equivalents of (*E*)-1-iodo-1-octene led to $[\text{Ni}\{\kappa^3\text{Si},\text{C},\text{Si}(\text{Si}(\text{tBu}_2\text{bzam}))_2\text{Rc}\}]$ (**83**) (Table 7) and to the corresponding C–C coupled products in high yields (80–90%). Compound **83**, which is similar to its bromide analog **79**, was independently synthesized reacting $[\text{Ni}_2(\text{dme})]$ with **U**. Therefore, the reaction sequence of the Sonogashira coupling is transmetalation, oxidative addition and reductive elimination. Although the catalytic activity of complexes **79** and **80** in Sonogashira cross-coupling reactions is moderate, the non-spectator behavior of their HT ligands allowed the isolation of an elusive reaction intermediate, providing valuable information on the elementary steps of this catalytic process.

The most recent group 10 amidinato-HT–TM complexes were prepared in 2013 by Inoue and co-workers from the silicon(IV) ylide-like phosphasilene $(\text{TMS})\text{P}=\text{Si}(\text{tBu}_2\text{bzam})(\text{TMS})$, which reacted with $[\text{Pt}(\text{C}_2\text{H}_4)(\text{PPh}_3)_2]$ and $[\text{Pd}(\text{PPh}_3)_4]$ to give the

isostructural binuclear derivatives $[\text{TM}_2\{\mu\text{-P}(\text{TMS})_2\}(\text{PPh}_3)_2\{\mu\text{-}\kappa^1\text{Si}\text{-Si}(\text{tBu}_2\text{bzam})\}]$ (TM = Pt (**84**), Pd (**85**)) (Scheme 32, Table 7) [59]. The formation of both complexes, featuring a silyliumylidene moiety and a phosphido group bridging the two TM atoms, implied the formal breakage of the Si=P and Si–TMS bonds of the starting phosphasilene. The crystal structure of **84** (Fig. 14) revealed the existence of a Pt–Pt bond (the Pt–Pt distance, 2.6466(5) Å, is similar to those of Pt–Pt bonded molecules [92]), which was also confirmed by DFT calculations. The silyliumylidene character of the Si-donor ligand of **84** was confirmed by the NBO charges calculated for the Si (+0.974) and P (–0.715) atoms. Stable silyliumylidene cations are rare [93], but some DMAP-stabilized ones and their TM complexes (compounds **20** and **75**) have been previously discussed in this review [38]. The phosphasilene $(\text{TMS})\text{P}=\text{Si}(\text{tBu}_2\text{bzam})(\text{TMS})$ reacted with $[\text{Pt}(\text{C}_2\text{H}_4)(\text{PPh}_3)_2]$ at -30°C to give $[\text{Pt}(\text{TMS})(\text{PPh}_3)\{(\text{TMS})\text{P}=\text{Si}(\text{tBu}_2\text{bzam})\}]$, which

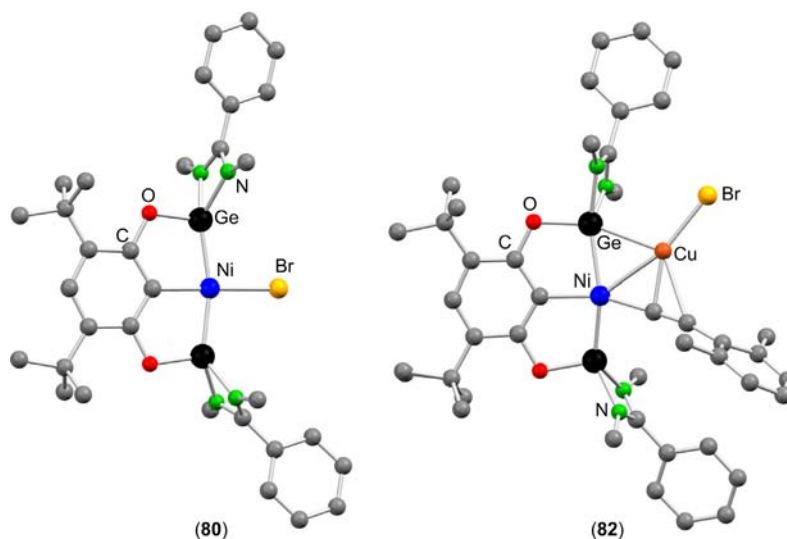
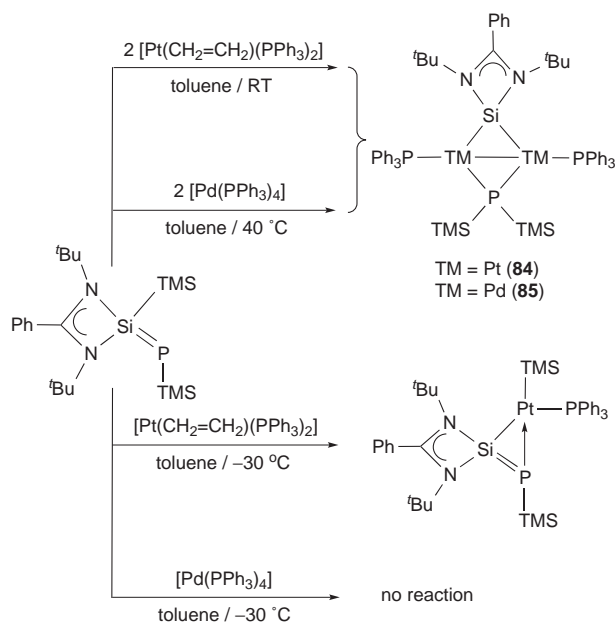


Fig. 13. Crystal structures of complexes **80** and **82**. The methyl C atoms of the N^tBu groups have been omitted for clarity.



Scheme 32. Synthesis of complexes **84**, **85** and $[\text{Pt}(\text{TMS})(\text{PPh}_3)\{\text{(TMS)P}=\text{Si}(\text{tBu}_2\text{bzam})\}]$.

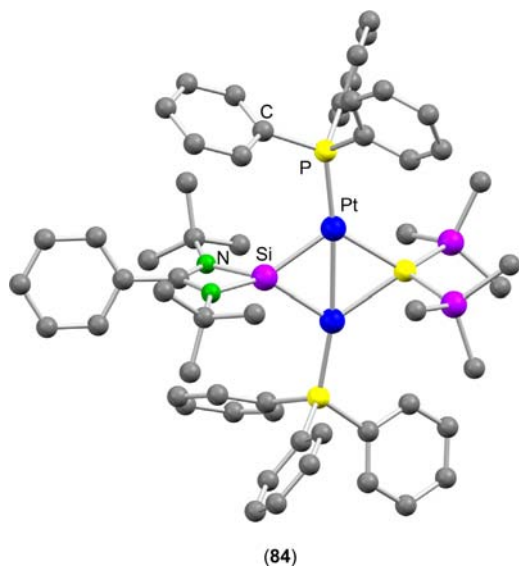
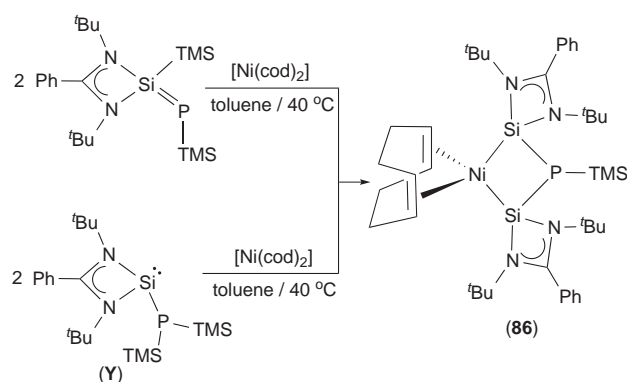


Fig. 14. Crystal structure of complex **84**.

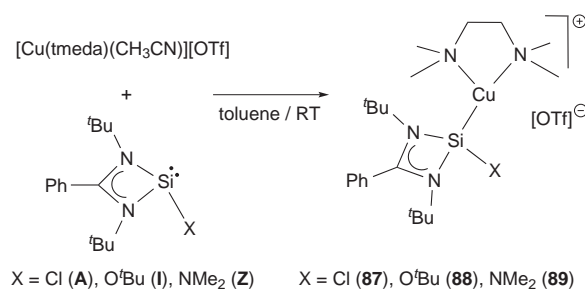
Adapted from Ref. [59].

results from the migration of the Si-bonded TMS group to the platinum atom (Scheme 32). This species, which was characterized by NMR, HR-MS and DFT calculations, could not be isolated because at room temperature it was transformed into complex **84** and the starting phosphasilene.

Inoue and co-workers also reacted phosphasilene $(\text{TMS})\text{P}=\text{Si}(\text{tBu}_2\text{bzam})(\text{TMS})$ with $[\text{Ni}(\text{cod})_2]$ [59]. This reaction led to the mononuclear derivative $[\text{Ni}(\text{cod})\{\kappa^2\text{Si}_2\text{Si}(\text{tBu}_2\text{bzam})_2\text{P}(\text{TMS})\}]$ (**86**) (Scheme 33, Table 7), which is very different from **84** or **85**. This complex contains a novel phosphinidene-bridged bis(silylene) whose formation implies the formal coupling of two phosphasilene units with concomitant release of $\text{P}(\text{TMS})_3$. Remarkably, the reaction of $\text{Si}(\text{tBu}_2\text{bzam})\text{P}(\text{TMS})_2$ (**Y**) with $[\text{Ni}(\text{cod})_2]$ also led to **86** as the main



Scheme 33. Syntheses of complex **86**.



Scheme 34. Synthesis of complexes **87–89**.

product. Complex **86** is structurally analogous to $[\text{Ni}(\text{cod})\{\kappa^2\text{Si}_2\text{Si}(\text{tBu}_2\text{bzam})_2\text{O}\}]$ (**77**), which is equipped with a related oxo-bridged bis(silylene) ligand [55].

DFT calculations were carried out to rationalize the different reactivity observed when $(\text{TMS})\text{P}=\text{Si}(\text{tBu}_2\text{bzam})(\text{TMS})$ was treated with platinum, palladium, and nickel sources [59]. The mechanisms involved in the formation of **84–86** were modeled. The cleavage of the Si–TMS bond of the starting phosphasilene is a favored process in all cases. In the case of nickel, the isomerization of the phosphasilene to silylene **Y** occurred prior to its coordination to the metal center, whereas platinum and palladium metals quickly insert into the Si–Si bond to form an unstable intermediate that leads to the final product. The different outcome of the reactions, dinuclear metal complexes (**84** and **85**) vs a bis(silylene) metal complex (**86**), can be in part explained attending to the different auxiliary ligands of each metallic precursor (cod for Ni, PPh_3 for Pt and Pd), which affect the thermodynamic stability of the final products. Note that this ligand influence could not be experimentally verified for nickel, since $[\text{Ni}(\text{PPh}_3)_4]$ did not react with the phosphasilene, even at high temperature.

The $^{29}\text{Si}\{^1\text{H}\}$ NMR signal of the silylene Si atom of **84–86** was observed at 234.5, 187.8 and 51.5 ppm, respectively. These data clearly reflect the different environment of the silylene fragment in each complex (bridging cationic for **84** and **85** vs terminal neutral for **86**) [59].

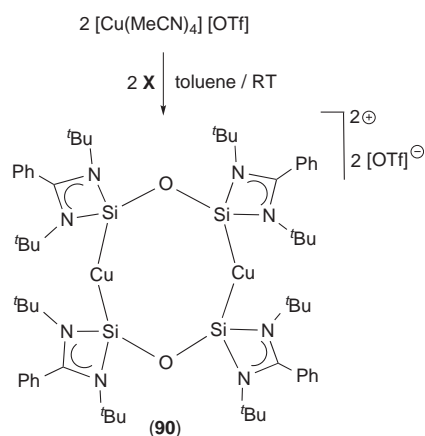
3.8. Group 11 metal complexes

Driess and co-workers reported the first representatives of this group very recently, in 2014 [60]. The silylenes $\text{Si}(\text{tBu}_2\text{bzam})\text{X}$ ($\text{X}=\text{Cl}$ (**A**), O^tBu (**I**), NMe_2 (**Z**)) were reacted with $[\text{Cu}(\text{tmeda})(\text{MeCN})][\text{OTf}]$ to give the analogous complex salts $[\text{Cu}(\text{tmeda})\{\text{Si}(\text{tBu}_2\text{bzam})\}\text{X}][\text{OTf}]$ ($\text{X}=\text{Cl}$ (**87**), O^tBu (**88**), NMe_2 (**89**)) (Scheme 34, Table 8). Silylenes **I** and **Z** were prepared by chlorine replacement on chlorosilylene **A** [70]. The different

Table 8
Relevant data of group 11 metal complexes containing amidinato-HT ligands.

Complex	Yield (%), color	M{ ¹ H} NMR, δ (ppm)	d(M–TM) (Å)	Ref.
[Cu(tmeda){Si(^t Bu ₂ bzam)Cl}][OTf] (87)	80, colorless	²⁹ Si, 32.9 (s) ^a	2.172(1)	[60]
[Cu(tmeda){Si(^t Bu ₂ bzam)(O ^t Bu)}][OTf] (88)	72, colorless	²⁹ Si, 5.4 (s) ^a	2.2003(6)	[60]
[Cu(tmeda){Si(^t Bu ₂ bzam)(NMe ₂)}][OTf] (89)	66, colorless	²⁹ Si, 18.3 (s) ^a	2.198(1)	[60]
[Cu{κ ² Si ₂ Si-(Si(^t Bu ₂ bzam)) ₂ O}][OTf] ₂ (90)	52, colorless	²⁹ Si, 3.3 (s), 7.7 (br) ^a	2.272(1), 2.285(1)	[60]

^a In CD₂Cl₂.



Scheme 35. Synthesis complex **90**.

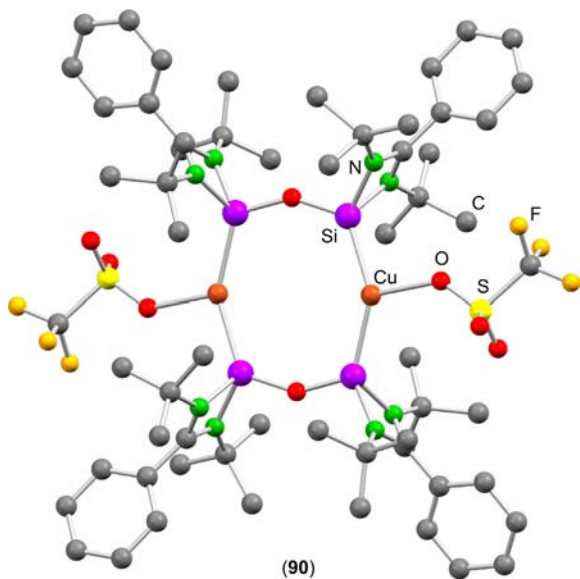
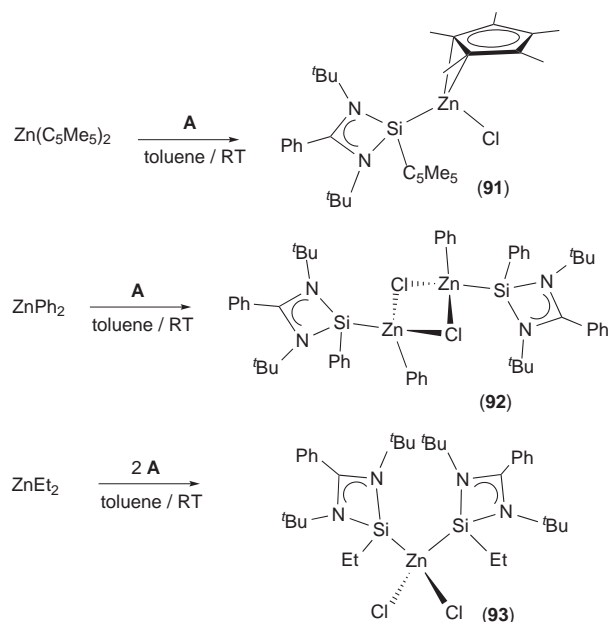


Fig. 15. Crystal structure of complex **90**.

Adapted from Ref. [60].

substituents on the silicon atom only affected the packing of the complexes in the solid state and the interaction of the triflate anion with the X group. The ²⁹Si{¹H} NMR spectra in CD₂Cl₂ of **87–89** showed one singlet resonance 32.9, 5.4 and 18.3 ppm, respectively. In this case, no negative correlation was found between the ²⁹Si chemical shift and the Hammett constant [66] of the X group.

The binuclear salt [Cu{κ²Si₂Si-(Si(^tBu₂bzam))₂O}][OTf]₂ (**90**) has been recently prepared (2014) by reaction of the bis(silylene) {Si(^tBu₂bzam)}₂O (**X**) [55] with [Cu(MeCN)₄][OTf] (Scheme 35, Table 8) [60]. In the solid state (Fig. 15), the cation features an interesting 8-membered ring exhibiting very strong interactions between the copper centers and the triflate anions (Cu...O=2.141 Å). The ²⁹Si{¹H} NMR spectrum in CD₂Cl₂ of **90** showed two resonances at 3.3 ppm (sharp singlet) and



Scheme 36. Synthesis of complexes **91–93**.

7.7 ppm (broad signal), indicating that some sort of coordination/decoordination of the OTf anions occurs in solution. The fact that these signals are shifted downfield from that of the free ligand **X** (δ = –16.1 ppm in C₆D₆) [55] rules out silylene decoordination in solution.

3.9. Group 12 metal complexes

The group of P. Roesky communicated the first amidinato-HT derivatives of group 12 metals a few months ago [61]. Reactions of silylene **A** with Zn(C₅Me₅)₂, ZnPh₂ and ZnEt₂ allowed the isolation of the derivatives [ZnCl(η²-C₅Me₅){Si(^tBu₂bzam)(C₅Me₅)}] (**91**), [Zn₂(μ-Cl)₂Ph₂{Si(^tBu₂bzam)Ph}2] (**92**) and [ZnCl₂{Si(^tBu₂bzam)Et}2] (**93**), respectively (Scheme 36, Table 9). In these cases, the coordination of the silylene to the zinc center is accompanied by an exchange between the chlorine atom of **A** and an organic group of the original ZnR₂ reagent. While **91**, equipped with C₅Me₅ groups, is monomeric, **92** is dimeric with chlorine bridges due to the smaller volume of the phenyl groups. In the case of **93**, the even smaller ethyl group allows the incorporation of two silylene units to the zinc coordination shell. The Zn–Si bond length of **91** (2.3750(9) Å) is significantly shorter than those of **92** (2.4171(7) Å) and **93** (2.416(2) and 2.418(2) Å). In solution, the complexes proved to be unstable, decomposing partially to Zn(C₅Me₅)₂ in the case of **91** and to zinc metal in the cases of **92** and **93**. Regarding complex **91**, IR, Raman and theoretical DFT data indicated that it contains a strong Zn–Si bond and a weak Zn–Cl bond, suggesting that the complex is better explained as an ion pair consisting of a silyl cation with a non-classical donor–acceptor Zn–Si single bond.

Table 9
Relevant data of group 12 metal complexes containing amidinato-HT ligands.

Complex	Yield (%), color	M{ ¹ H} NMR, δ (ppm)	d(M–TM) (Å)	Ref.
[ZnCl(η^2 -C ₅ Me ₅){Si(^t Bu ₂ bzam)(C ₅ Me ₅)}] (91)	33, colorless	²⁹ Si, 60.5 (s) ^a	2.3750(9)	[61]
[Zn ₂ (μ -Cl) ₂ Ph ₂ {Si(^t Bu ₂ bzam)Ph ₂ } ₂] (92)	65, colorless	²⁹ Si, 34.4 (s) ^a	2.4171(7)	[61]
[ZnCl ₂ {Si(^t Bu ₂ bzam)Et ₂ }] (93)	34, colorless	²⁹ Si, 55.4 (s) ^a	2.416(2), 2.418(2)	[61]

^a In C₆D₆.

3.10. Latest additions

The first months of 2015 (until the submission of the final version of this manuscript) have witnessed some additional reports dealing with the TM chemistry of amidinato-HTs. Madec et al. have described the synthesis and characterization of several amidinatogermynes bound to iron carbonyl fragments [94]. Our group, studying the reactivity of [Ru₃(CO)₁₂] with amidinatogermynes, have provided new mechanistic insights into the reactivity of this cluster with two-electron-donor ligands of high basicity [95] and has also published a thorough reactivity study on the diruthenium complex [Ru₂(CO)₇{ μ - κ^2 Ge,*N*-Ge(^tPr₂bzam)(HMDS)}] (**32**), which has revealed the reactive sites of this complex in CO substitution reactions and its ability to activate inorganic H–E bonds (E = Si, Sn, H) under mild conditions [96]. Additionally, although not specifically dealing with TM complexes, two relevant works by the groups of Driess and Blom have described the first amidinatossilene derivatives of s-block (calcium) [97] and f-block (samarium) [98] metal complexes.

4. Conclusions

Amidinato-HTs have recently boosted the coordination chemistry of HTs. In fact, nearly one hundred amidinato-HT–TM complexes, with examples belonging to almost all the TM groups of the Periodic Table (group 3 is the only exception), have been prepared after first members of this family were reported in 2008 by Jones et al. (compounds **5** and **31**) [32].

The current high interest in the use of amidinato-HTs as ligands in coordination chemistry can be attributed to a combination of the following factors: (i) as they are intramolecularly-stabilized HTs, they are electronically and sterically more stable and easier to handle than classical simple HTs (the interaction of the donor group with the M atom reduces the electrophilicity of the latter, which is also kinetically more protected because it is at least tricoordinated); (ii) their steric and electronic features can be more easily tuned than those of other intramolecularly-stabilized HTs because amidinato-HTs contain four groups (R¹, R², R³ and R⁴; Table 1) that can be easily changed; in particular, when R⁴ = halide, the transmetalation of the R⁴ group is essential for the synthesis of many of the polydentate ligands discussed in this review (ligands **N**, **O**, **S–X**; Table 1); (iii) the discovery of an easy route to prepare amidinatossilenes, by dehydrochlorinating the corresponding (amidinato)dichlorosilane with LiHMDS [64b], has boosted the development of their coordination chemistry (silylenes are generally better ligands than their heavier analogs); and (iv) they have proven to be strong electron-donating ligands, in many cases more basic than NHCs [48,51–53,57,58], and this factor is very important when electron-rich metal complexes are required to promote substrate activation processes.

The majority of the amidinato-HTs complexes reported to date are silylene and germylene derivatives. Although quite a few amidinatostannylenes and -plumbylenes have already been prepared [43,63d,e,f], amidinatoplumbylene TM complexes are still unknown and only one TM complex is known to contain an amidinatostannylene ligand (compound **30**) [43], probably because the stability of HT–TM complexes decreases on going down along group 14 column of the Periodic Table [4g,63f].

Additionally, environmental and health issues also account for the small progress of the coordination chemistry of plumbylenes.

Most amidinato-HTs behave as monodentate M-donor ligands. However, some amidinato-HTs are also capable to act as bidentate κ^2 M,*N*-ligands. Thus, four-electron-donor μ - κ^2 Ge,*N*- (**32–35**, **64** [44,45,51]) and κ^2 Si,*N*-ligands (**17–19** [37]) and three-electron-donor κ^2 Ge,*N*-anionic ligands (**26**, **27** [41]) have been described. The results obtained so far suggest that the coordination of an imino arm of an amidinato-HT to the TM can occur only if the M atom is tetracoordinated in the final product. Additionally, steric and electronic factors should also be taken into account because (i) the bis(benzamidinato)silylene **D** coordinates in a κ^1 Si manner to group 6 metal carbonyls, but the bis(guanidinato)silylene **E** gives rise to κ^2 Si,*N* ligands [37] in analogous reactions, and (ii) it has been proven in binuclear ruthenium and cobalt complexes that a μ - κ^2 M,*N*-coordination of benzamidinatogermynes and -silylenes can only be possible if the steric bulk of at least one of the NR groups of the benzamidinato fragment is smaller than that of the N^tBu group [44,45,51].

Noteworthy, contrasting with the few catalytic applications that have been found in the last 40 years for other stable HT–TM complexes [18,62], some amidinato-HT–TM have already been recognized as active precatalysts of important catalytic processes, such as ketone hydrosilylations [46,48], [2 + 2] cycloadditions [52], arene C–H borylations [53] and Kumada [56], Negishi [56] and Sonogashira [58] cross-couplings. Most catalytically active complexes contain their amidinato-HTs integrated into polydentate ligands (**46** [48]; **68**, **69** [52]; **71**, **72** [53]; **77** [55,56]; **79**, **80** [58]), complex **40** being the only exception [46]. The polydentate character of these ligands possibly enhances the stability of their complexes, helping the catalysts to perform without decomposition. Remarkably, a non-spectator behavior has been observed for HT ligands in some catalytic processes [46,58].

Finally, the results herein reviewed help envision many possibilities for the future development of the coordination chemistry of amidinato-HTs. For example: (i) the use of other TM precursors, since, currently, no examples of metals of group 3 are known and only a few complexes of metals of groups 4, 5, 11 and 12 have been described; (ii) the development of the stoichiometric and/or catalytic reactivity of already known amidinato-HT–TM complexes, for which, in most cases, very few studies of this kind have already been performed; (iii) the development of novel polydentate ligands taking advantage of the capacity that the imino arm of amidinato-HTs has to enter into the coordination sphere of metal complexes; and (iv) the use amidinatostannylenes as part of polydentate ligands to reduce the lower stability of the Sn–TM bond (for example, it would be very interesting to prepare complexes containing the tin versions of the polydentate ligands **N**, **O**, **S–X**; Table 1), which, according to the higher acidity of tin, may promote reactions different from those observed using their lighter counterparts.

Acknowledgements

This work has been supported by a European Union Marie Curie action (FP7-2010-RG-268329), by Spanish MINECO-FEDER research projects (CTQ2010-14933, RYC2012-10491 and

CTQ2013-40619-P), and by a research grant from the Government of Asturias (GRUPIN14-009).

References

- V.Y. Lee, A. Sekiguchi, *Organometallic Compounds of Low Coordinate Si, Ge, Sn and Pb: From Phantom Species to Stable Compounds*, Wiley, Chichester, UK, 2010.
 - For reviews on the synthesis and general chemistry of HTs, see:
 - K. Izod, *Coord. Chem. Rev.* 257 (2013) 924;
 - Y. Xiong, S. Yao, M. Driess, *Angew. Chem. Int. Ed.* 52 (2013) 4302;
 - S.K. Mandal, H.W. Roesky, *Acc. Chem. Res.* 45 (2012) 298;
 - S. Yao, Y. Xiong, M. Driess, *Organometallics* 30 (2011) 1748;
 - Y. Mizuhata, T. Sasamori, N. Tokitoh, *Chem. Rev.* 109 (2009) 3479;
 - J. Barrau, G. Rima, *Coord. Chem. Rev.* 178–180 (1998) 593;
 - W.P. Neumann, *Chem. Rev.* 91 (1991) 311;
 - M. Veith, *Angew. Chem. Int. Ed.* 26 (1987) 1.
 - For reviews on the synthesis and general chemistry of HTs, including TM coordination chemistry, see:
 - R.S. Ghadwal, R. Azhakar, H.W. Roesky, *Acc. Chem. Res.* 46 (2013) 444;
 - H.W. Roesky, *J. Organomet. Chem.* 730 (2013) 57;
 - M. Asay, C. Jones, M. Driess, *Chem. Rev.* 111 (2011) 354;
 - S.K. Mandal, H.W. Roesky, *Chem. Commun.* 46 (2010) 6016;
 - M. Kira, *Chem. Commun.* 46 (2010) 2893;
 - S. Nagendran, H.W. Roesky, *Organometallics* 27 (2008) 457;
 - A.V. Zabula, F.E. Hahn, *Eur. J. Inorg. Chem.* (2008) 5165;
 - W.-P. Leung, K.-W. Kan, K.-H. Chong, *Coord. Chem. Rev.* 251 (2007) 2253;
 - O. Köhl, *Coord. Chem. Rev.* 248 (2004) 411;
 - B. Gehrhus, M.F. Lappert, *J. Organomet. Chem.* 617–618 (2001) 209;
 - M. Haaf, T.A. Schmedake, R. West, *Acc. Chem. Res.* 33 (2000) 704;
 - N. Tokitoh, R. Okazaki, *Coord. Chem. Rev.* 210 (2000) 251.
 - For reviews focused on the TM coordination chemistry of HTs, see:
 - B. Blom, D. Gallego, M. Driess, *Inorg. Chem. Front.* 1 (2014) 134;
 - B. Blom, M. Stoelzel, M. Driess, *Chem. Eur. J.* 19 (2013) 40;
 - R. Waterman, P.G. Hayes, T.D. Tilley, *Acc. Chem. Res.* 40 (2007) 712;
 - M. Okazaki, H. Tobita, H. Ogino, *Dalton Trans.* (2003) 493;
 - M.F. Lappert, R.S. Rowe, *Coord. Chem. Rev.* 100 (1990) 267;
 - W. Petz, *Chem. Rev.* 86 (1986) 1019;
 - M.F. Lappert, P.P. Power, *J. Chem. Soc. Dalton Trans.* (1985) 51.
 - See, for example:
 - D. Martin, M. Melaimi, M. Soleilhavoup, G. Bertrand, *Organometallics* 30 (2011) 5304;
 - J.A. Cabeza, P. García-Álvarez, *Chem. Soc. Rev.* 40 (2011) 5389;
 - M. Melaimi, M. Soleilhavoup, G. Bertrand, *Angew. Chem. Int. Ed.* 49 (2010) 8810;
 - S. Díez-González, N. Marion, S.P. Nolan, *Chem. Rev.* 109 (2009) 3612;
 - O. Schuster, L. Yang, H.G. Raubenheimer, M. Albrecht, *Chem. Rev.* 109 (2009) 3445;
 - M. Poyatos, J.A. Mata, E. Peris, *Chem. Rev.* 109 (2009) 3677;
 - F.E. Hahn, M.C. Jahnke, *Angew. Chem. Int. Ed.* 47 (2008) 3122.
 - For some studies showing the weaker nature of M–TM bonds of HT–TM complexes compared with that of C–TM bonds of NHC–TM complexes, see:
 - T.A.N. Nguyen, G. Frenking, *Chem. Eur. J.* 18 (2012) 12733;
 - H. Arp, J. Baumgartner, C. Marschner, P. Zark, T. Müller, *J. Am. Chem. Soc.* 134 (2012) 10864;
 - C. Boehme, G. Frenking, *Organometallics* 17 (1998) 5801;
 - W.J. Evans, J.M. Perotti, J.W. Ziller, D.F. Moser, R. West, *Organometallics* 22 (2003) 1160;
 - W.A. Herrmann, P. Harter, C.W.K. Gstottmayr, F. Bielert, N. Seeboth, P. Sirsch, *J. Organomet. Chem.* 649 (2002) 141;
 - J.T. York, V.G. Young Jr., W.B. Tolman, *Inorg. Chem.* 45 (2006) 4191;
 - H. Yoo, P.J. Carroll, D.H. Berry, *J. Am. Chem. Soc.* 128 (2006) 6038.
 - For examples of oxidation and/or hydrolysis processes on coordinated HTs, see:
 - D. Matioszek, N. Saffon, J.-M. Sotiropoulos, K. Miqueu, A. Castel, J. Escudie, *Inorg. Chem.* 51 (2012) 11716;
 - M. Zhanga, X. Liua, C. Shia, C. Rena, Y. Dinga, H.W. Roesky, *Z. Anorg. Allg. Chem.* 634 (2008) 1755;
 - C. D. Amoroso, M. Haaf, G.P.A. Yap, R. West, D.E. Fogg, *Organometallics* 21 (2002) 534;
 - S.H.A. Petri, D. Eikenberg, B. Neumann, H.-G. Stammer, P.P. Jutzi, *Organometallics* 18 (1999) 2615.
 - For some examples, see:
 - B. Blom, M. Pohl, G. Tan, D. Gallego, M. Driess, *Organometallics* 33 (2014) 5272;
 - H. Handwerker, C. Leis, R. Probst, P. Bissinger, A. Grohmann, P. Kiprof, E. Herdtweck, J. Blumel, N. Auner, C. Zybilla, *Organometallics* 12 (1993) 2162;
 - C. Zybilla, G. Müller, *Angew. Chem. Int. Ed.* 26 (1987) 669;
 - T.J. Marks, *J. Am. Chem. Soc.* 93 (1971) 7090.
 - For some examples, see:
 - M.E. Fasulo, P.B. Glaser, T.D. Tilley, *Organometallics* 30 (2013) 5524;
 - P.B. Glaser, P.W. Wanandi, T.D. Tilley, *Organometallics* 23 (2004) 693;
 - S.K. Grumbine, G.P. Mitchell, D.A. Straus, T.D. Tilley, A.L. Rheingold, *Organometallics* 17 (1998) 5607;
 - S.K. Grumbine, T.D. Tilley, F.P. Arnold, A.L. Rheingold, *J. Am. Chem. Soc.* 116 (1994) 5495;
 - S.D. Grumbine, T.D. Tilley, F.P. Arnold, A.L. Rheingold, *J. Am. Chem. Soc.* 115 (1993) 7884;
 - D.A. Straus, S.D. Grumbine, T.D. Tilley, *J. Am. Chem. Soc.* 112 (1990) 7801;
 - D.A. Straus, T.D. Tilley, A.L. Rheingold, S.J. Geib, *J. Am. Chem. Soc.* 109 (1987) 5872;
 - M.E. Fasulo, T.D. Tilley, *Chem. Commun.* 48 (2012) 7690.
 - For some examples, see:
 - H.-J. Liu, C. Raynaud, O. Eisenstein, T.D. Tilley, *J. Am. Chem. Soc.* 136 (2014) 11473;
 - H.-J. Liu, J. Guihaumé, T. Davin, C. Raynaud, O. Eisenstein, T.D. Tilley, *J. Am. Chem. Soc.* 136 (2014) 13991;
 - E. Suzuki, T. Komuro, M. Okazaki, H. Tobita, *Organometallics* 28 (2009) 1791;
 - P.G. Hayes, C. Beddie, M.B. Hall, R. Waterman, T.D. Tilley, *J. Am. Chem. Soc.* 128 (2006) 428;
 - B.V. Mork, T.D. Tilley, *J. Am. Chem. Soc.* 126 (2004) 4375;
 - B.V. Mork, T.D. Tilley, A.J. Schultz, J.A. Cowan, *J. Am. Chem. Soc.* 126 (2004) 10428;
 - B.V. Mork, T.D. Tilley, *Angew. Chem. Int. Ed.* 42 (2003) 357;
 - J.D. Feldman, J.C. Peters, T.D. Tilley, *Organometallics* 21 (2002) 4065;
 - G.P. Mitchell, T.D. Tilley, *Angew. Chem. Int. Ed.* 37 (1998) 2524;
 - J.C. Peters, J.D. Feldman, T.D. Tilley, *J. Am. Chem. Soc.* 121 (1999) 9871.
 - For some examples, see:
 - J.D. Feldman, G.P. Mitchell, J.-O. Nolte, T.D. Tilley, *J. Am. Chem. Soc.* 120 (1998) 11184;
 - J.D. Feldman, G.P. Mitchell, J.-O. Nolte, T.D. Tilley, *Can. J. Chem.* 81 (2003) 1127.
 - For some examples, see:
 - V.Y. Lee, S. Aoki, T. Yokoyama, S. Horiguchi, A. Sekiguchi, H. Gornitzka, J.-D. Guo, S. Nagase, *J. Am. Chem. Soc.* 135 (2013) 2987;
 - N. Nakata, T. Fujita, A. Sekiguchi, *J. Am. Chem. Soc.* 128 (2006) 16024.
 - R.S. Ghadwal, H.W. Roesky, S. Merkel, J. Henn, D. Stalke, *Angew. Chem. Int. Ed.* 48 (2009) 5683.
 - See, for example:
 - J.K. West, G.L. Fondong, B.C. Noll, L. Stahl, *Dalton Trans.* 42 (2013) 3835;
 - P. Braunstein, M. Veith, J. Blin, V. Huch, *Organometallics* 20 (2001) 627;
 - M. Knorr, E. Hallauer, V. Huch, M. Veith, P. Braunstein, *Organometallics* 15 (1996) 3868;
 - M. Veith, A. Mueller, L. Stahl, M. Noetzel, M. Jarczyk, V. Huch, *Inorg. Chem.* 35 (1996) 3848;
 - M. Veith, L. Stahl, V. Huch, *Organometallics* 12 (1993) 1914;
 - M. Veith, L. Stahl, *Angew. Chem. Int. Ed.* 32 (1993) 106;
 - M. Veith, L. Stahl, V. Huch, *J. Chem. Soc. Chem. Commun.* (1990) 359;
 - M. Veith, L. Stahl, V. Huch, *Inorg. Chem.* 28 (1989) 3278;
 - M. Veith, H. Lange, K. Braeuer, R. Bachmann, *J. Organomet. Chem.* 216 (1981) 377.
 - G.-H. Lee, R. West, T. Müller, *J. Am. Chem. Soc.* 125 (2003) 8114.
 - M. Veith, E. Werle, R. Lisowsky, R. Löppe, H. Schnöckel, *Chem. Ber.* 125 (1992) 1375.
 - M. Denk, R. Lennon, R. Hayashi, R. West, A.V. Belyakov, H.P. Verne, A. Haaland, M. Wagner, N. Metzler, *J. Am. Chem. Soc.* 116 (1994) 2691.
 - (a) M. Zhang, X. Liu, C. Shi, C. Ren, Y. Ding, H.W. Roesky, *Z. Anorg. Allg. Chem.* 634 (2008) 1755;
 - (b) A. Fürstner, H. Krause, C.W. Lehmann, *Chem. Commun.* (2001) 2372.
- C.D. Schueffler Jr., J.J. Zuckerman, *J. Am. Chem. Soc.* 96 (1974) 7160.
- J. Pfeiffer, W. Maringgele, M. Noltmeyer, A. Meller, *Chem. Ber.* 122 (1989) 245.
- See, for example:
 - A. D. Heitmann, T. Pape, A. Hepp, C. Mück-Lichtenfeld, S. Grimme, F.E. Hahn, *J. Am. Chem. Soc.* 133 (2011) 11118;
 - S.M. Mansell, R.H. Herber, I. Nowik, D.H. Ross, C.A. Russell, D.F. Wass, *Inorg. Chem.* 50 (2011) 2252;
 - F. Ullah, O. Köhl, G. Bajor, T. Veszpremi, P.G. Jones, J. Heinicke, *Eur. J. Inorg. Chem.* (2009) 221;
 - O. Köhl, P. Lönnecke, J. Heinicke, *Inorg. Chem.* 42 (2003) 2836;
 - W.A. Herrmann, M. Denk, J. Behm, W. Scherer, F.R. Klingan, H. Bock, B. Solouki, M. Wagner, *Angew. Chem. Int. Ed.* 31 (1992) 1485.
- See, for example:
 - A.V. Zabula, T. Pape, A. Hepp, F.E. Hahn, *Dalton Trans.* (2008) 5886;
 - F.E. Hahn, A.V. Zabula, T. Pape, A. Hepp, R. Tonner, R. Haunschild, G. Frenking, *Chem. Eur. J.* 14 (2008) 10716;
 - F.E. Hahn, A.V. Zabula, T. Pape, A. Hepp, *Z. Anorg. Allg. Chem.* 634 (2008) 2397;
 - A.V. Zabula, T. Pape, A. Hepp, F.E. Hahn, *Organometallics* 27 (2008) 2756;
 - A.V. Zabula, F.E. Hahn, T. Pape, A. Hepp, *Organometallics* 26 (2007) 1972.
- M. Kira, S. Ishida, T. Iwamoto, C. Kabuto, *J. Am. Chem. Soc.* 121 (1999) 9722.
- See, for example:
 - Y. Inagawa, S. Ishida, T. Iwamoto, *Chem. Lett.* 43 (2014) 1665;
 - C. Watanabe, Y. Inagawa, T. Iwamoto, M. Kira, *Dalton Trans.* 39 (2010) 9414;
 - C. Watanabe, T. Iwamoto, C. Kabuto, M. Kira, *Angew. Chem. Int. Ed.* 47 (2008) 5386;
 - C. Watanabe, T. Iwamoto, C. Kabuto, M. Kira, *Chem. Lett.* 36 (2007) 284.
- See, for example:
 - M. Driess, S. Yao, M. Brym, C. van Wüllen, D. Lentz, *J. Am. Chem. Soc.* 128 (2006) 9628;
 - M. Stoelzel, C. Präsang, S. Inoue, S. Enthaler, M. Driess, *Angew. Chem. Int. Ed.* 51 (2012) 399;
 - A. Meltzer, S. Inoue, C. Präsang, M. Driess, *J. Am. Chem. Soc.* 132 (2010)

- 3038;
 (d) A. Meltzer, C. Prasang, C. Milsman, M. Driess, *Angew. Chem. Int. Ed.* 48 (2009) 3170;
 (e) A. Meltzer, C. Präsang, M. Driess, *J. Am. Chem. Soc.* 131 (2009) 7232.
- [26] See, for example:
 (a) N. Zhao, J. Zhang, Y. Yang, G. Chen, H. Zhu, H.W. Roesky, *Organometallics* 32 (2013) 762;
 (b) N. Zhao, J. Zhang, Y. Yang, H. Zhu, Y. Li, G. Fu, *Inorg. Chem.* 51 (2012) 8710;
 (c) L. Ferro, P.B. Hitchcock, M.P. Coles, J.R. Fulton, *Inorg. Chem.* 51 (2012) 1544;
 (d) A. Jana, P.P. Samuel, H.W. Roesky, C. Schulzke, *J. Fluorine Chem.* 131 (2010) 1096;
 (e) H. Arii, F. Nakadate, K. Mochida, *Organometallics* 28 (2009) 4909;
 (f) A. Jana, R. Azhakar, H.W. Roesky, I. Objartel, D. Stalke, *Z. Anorg. Allg. Chem.* 637 (2011) 1795;
 (g) A. Jana, H.W. Roesky, C. Schulzke, P.P. Samuel, *Inorg. Chem.* 49 (2010) 3461;
 (h) A. Jana, S.P. Sarish, H.W. Roesky, C. Schulzke, P.P. Samuel, *Chem. Commun.* 46 (2010) 707;
 (i) L.W. Pineda, V. Jancik, J.F. Colunga-Valladares, H.W. Roesky, A. Hofmeister, *J. Magull, Organometallics* 25 (2006) 2381;
 (j) I. Saur, S. Garcia Alonso, H. Gornitzka, V. Lemierre, A. Chrostowska, J. Barrau, *Organometallics* 24 (2005) 2988;
 (k) I. Saur, G. Rima, K. Miqueu, H. Gornitzka, J. Barrau, *J. Organomet. Chem.* 672 (2003) 77;
 (l) A. Akkari, J.J. Byrne, I. Saur, G. Rima, H. Gornitzka, J. Barrau, *J. Organomet. Chem.* 622 (2001) 190.
- [27] See, for example:
 (a) V.V. Bashilov, V.I. Sokolov, Y.L. Slovokhotov, Y.T. Struchkov, *J. Organomet. Chem.* 327 (1987) 285;
 (b) G.W. Bushnell, D.T. Eadie, A. Pidcock, A.R. Sam, R.D. Holmes-Smith, S.R. Stobart, E.T. Brennan, T.S. Cameron, *J. Am. Chem. Soc.* 104 (1982) 5837;
 (c) P.F.R. Ewings, P.G. Harrison, *Inorg. Chim. Acta* 28 (1978) L167;
 (d) A.B. Cornwell, P.G. Harrison, *J. Chem. Soc. Dalton Trans.* (1976) 1054;
 (e) A.B. Cornwell, P.G. Harrison, *J. Chem. Soc. Dalton Trans.* (1976) 1608;
 (f) A.B. Cornwell, P.G. Harrison, *J. Chem. Soc. Dalton Trans.* (1975) 1486;
 (g) A.B. Cornwell, P.G. Harrison, J.A. Richards, *J. Organomet. Chem.* 76 (1974) C26.
- [28] See, for example:
 (a) H.V.R. Dias, X. Wang, H.V.K. Diyabalanage, *Inorg. Chem.* 44 (2005) 7322;
 (b) A.E. Ayers, H.V.R. Dias, *Inorg. Chem.* 41 (2002) 3259;
 (c) H.V.R. Dias, Z. Wang, *Inorg. Chem.* 39 (2000) 3890;
 (d) H.V.R. Dias, Z. Wang, *J. Am. Chem. Soc.* 119 (1997) 4650.
- [29] See, for example:
 (a) S. Krabbe, M. Wagner, C. Löw, C. Dietz, M. Schürmann, A. Hoffmann, S. Herres-Pawlis, M. Lutter, K. Jurkschat, *Organometallics* 33 (2014) 4433;
 (b) M. Wagner, V. Deáky, C. Dietz, J. Martinová, B. Mahieu, R. Jambor, S. Herres-Pawlis, K. Jurkschat, *Chem. Eur. J.* 19 (2013) 6695;
 (c) M. Wagner, M. Henn, C. Dietz, M. Schürmann, M.H. Prosenc, K. Jurkschat, *Organometallics* 32 (2013) 2406;
 (d) R. Jambor, S. Herres-Pawlis, M. Schürmann, K. Jurkschat, *Eur. J. Inorg. Chem.* (2012) 344;
 (e) M. Henn, V. Deáky, S. Krabbe, M. Schürmann, M. Prosenc, S. Herres-Pawlis, B. Mahieu, K. Jurkschat, *Z. Anorg. Allg. Chem.* 637 (2011) 211;
 (f) J. Martinová, R. Dostálová, L. Dostál, A. Růžička, R. Jambor, *Organometallics* 28 (2009) 4823;
 (g) J. Martinová, R. Jambor, M. Schürmann, K. Jurkschat, J. Honzický, F.A. Almeida-Paz, *Organometallics* 28 (2009) 4778;
 (h) M. Henn, M. Schürmann, B. Mahieu, P. Zanelló, A. Cinquantini, K. Jurkschat, *J. Organomet. Chem.* 691 (2006) 1560;
 (i) J. Martinová, L. Dostál, A. Růžička, J. Taraba, R. Jambor, *Organometallics* 26 (2007) 4102;
 (j) M. Mehring, C. Löw, M. Schürmann, F. Uhlig, K. Jurkschat, M. Mahieu, *Organometallics* 19 (2000) 4613.
- [30] B. Blom, M. Driess, D. Gallego, S. Inoue, *Chem. Eur. J.* 18 (2012) 13355.
- [31] R. Azhakar, R.S. Ghadwal, H.W. Roesky, J. Hey, D. Stalke, *Chem. Asian J.* 7 (2012) 528.
- [32] C. Jones, R.P. Rose, A. Stasch, *Dalton Trans.* (2008) 2871.
- [33] D. Matioszek, N. Katir, N. Saffon, A. Castel, *Organometallics* 29 (2010) 3039.
- [34] R. Azhakar, R.S. Ghadwal, H.W. Roesky, H. Wolf, D. Stalke, *J. Am. Chem. Soc.* 134 (2012) 2423.
- [35] K. Junold, J.A. Baus, C. Burschka, R. Tacke, *Angew. Chem. Int. Ed.* 51 (2012) 7020.
- [36] K. Junold, J.A. Baus, C. Burschka, T. Vent-Schmidt, S. Riedel, R. Tacke, *Inorg. Chem.* 52 (2013) 11593.
- [37] F.M. Mück, D. Kloß, J.A. Baus, C. Burschka, R. Tacke, *Chem. Eur. J.* 20 (2014) 9620.
- [38] H.-X. Yeong, Y. Li, C.-W. So, *Organometallics* 33 (2014) 3646.
- [39] R. Azhakar, S.P. Sarish, H.W. Roesky, J. Hey, D. Stalke, *Inorg. Chem.* 50 (2011) 5039.
- [40] R. Azhakar, H.W. Roesky, J.J. Holstein, B. Dittrich, *Dalton Trans.* 41 (2012) 12096.
- [41] J.A. Cabeza, P. García-Álvarez, E. Pérez-Carreño, D. Polo, *Inorg. Chem.* 53 (2014) 8735.
- [42] W. Yang, H. Fu, H. Wang, M. Chen, Y. Ding, H.W. Roesky, A. Jana, *Inorg. Chem.* 48 (2009) 5058.
- [43] S.S. Sen, M.P. Kritzler-Kosch, S. Nagendran, H.W. Roesky, T. Beck, A. Pal, R. Herbst-Irmer, *Eur. J. Inorg. Chem.* 5304 (2010).
- [44] J.A. Cabeza, P. García-Álvarez, D. Polo, *Dalton Trans.* 42 (2013) 1329.
- [45] J.A. Cabeza, J.M. Fernández-Colinas, P. García-Álvarez, D. Polo, *RSC Adv.* 4 (2014) 31503.
- [46] B. Blom, S. Enthaler, S. Inoue, E. Irran, M. Driess, *J. Am. Chem. Soc.* 135 (2013) 6703.
- [47] B. Blom, M. Pohl, G. Tan, D. Gallego, M. Driess, *Organometallics* 33 (2014) 5272.
- [48] D. Gallego, S. Inoue, B. Blom, M. Driess, *Organometallics* 33 (2014) 6685.
- [49] R. Azhakar, R.S. Ghadwal, H.W. Roesky, J. Hey, L. Krause, D. Stalke, *Dalton Trans.* 42 (2013) 10277.
- [50] D. Matioszek, N. Saffon, J.-M. Sotiropoulos, K. Miqueu, A. Castel, J. Escudié, *Inorg. Chem.* 51 (2012) 11716.
- [51] J.A. Cabeza, P. García-Álvarez, E. Pérez-Carreño, D. Polo, *Chem. Eur. J.* 20 (2014) 8654.
- [52] W. Wang, S. Inoue, S. Enthaler, M. Driess, *Angew. Chem. Int. Ed.* 51 (2012) 6167.
- [53] A. Brück, D. Gallego, W. Wang, E. Irran, M. Driess, J.F. Hartwig, *Angew. Chem. Int. Ed.* 51 (2012) 11478.
- [54] G. Tavčar, S.S. Sen, R. Azhakar, A. Thorn, H.W. Roesky, *Inorg. Chem.* 49 (2010) 10199.
- [55] W. Wang, S. Inoue, S. Yao, M. Driess, *J. Am. Chem. Soc.* 132 (2010) 15890.
- [56] C.I. Someya, M. Haberberger, W. Wang, S. Enthaler, S. Inoue, *Chem. Lett.* 42 (2013) 286.
- [57] W. Wang, S. Inoue, E. Irran, M. Driess, *Angew. Chem. Int. Ed.* 51 (2012) 3691.
- [58] D. Gallego, A. Brück, E. Irran, F. Meier, M. Kaupp, M. Driess, *J. Am. Chem. Soc.* 135 (2013) 15617.
- [59] N.C. Breit, T. Szilvási, T. Suzuki, D. Gallego, S. Inoue, M. Driess, *J. Am. Chem. Soc.* 135 (2013) 17958.
- [60] G. Tan, B. Blom, D. Gallego, M. Driess, *Organometallics* 33 (2014) 363.
- [61] S. Schäfer, R. Köppe, M.T. Gamer, P.W. Roesky, *Chem. Commun.* 50 (2014) 11401.
- [62] (a) M.E. Fasulo, M.C. Lipke, T.D. Tilley, *Chem. Sci.* 10 (2013) 3882;
 (b) M.M. Kirilenko, K.V. Zaitsev, Y.F. Oprunenko, A.V. Churakov, V.A. Tafeenko, S.S. Karlov, G.S. Zaitseva, *Dalton Trans.* 42 (2013) 7901.
- [63] See, for example:
 (a) Refs. [33,42];
 (b) S.P. Green, C. Jones, P.C. Junk, K.-A. Lippert, A. Stasch, *Chem. Commun.* (2006) 3978;
 (c) S.R. Foley, C. Bensimon, D.S. Richeson, *J. Am. Chem. Soc.* 119 (1997) 10359;
 (d) Y. Zhou, D.S. Richeson, *J. Am. Chem. Soc.* 118 (1996) 10850;
 (e) C. Jones, S.J. Bonyhayd, N. Holzmann, G. Frenking, A. Stasch, *Inorg. Chem.* 50 (2011) 12315;
 (f) A. Stasch, C.M. Forsyth, C. Jones, P.C. Junk, *New J. Chem.* 32 (2008) 829.
- [64] (a) C.-W. So, H.W. Roesky, J. Magull, R.B. Oswald, W. Wang, S. Inoue, E. Irran, M. Driess, *Angew. Chem. Int. Ed.* 45 (2006) 3948;
 (b) S.S. Sen, H.W. Roesky, D. Stern, J. Henn, D. Stalke, *J. Am. Chem. Soc.* 132 (2010) 1123.
- [65] See, for example:
 (a) F.M. Mück, K. Junold, J.A. Baus, C. Burschka, R. Tacke, *Eur. J. Inorg. Chem.* (2013) 5821;
 (b) Ref. [35].
- [66] C. Hansch, A. Leo, R.W. Taft, *Chem. Rev.* 91 (1991) 165.
- [67] K. Junold, K. Sinner, J.A. Baus, C. Burschka, C. Fonseca Gerra, M. Bickelhaupt, R. Tacke, *Chem. Eur. J.* 20 (2014) 16462.
- [68] S.S. Sen, A. Jana, H.W. Roesky, C. Schulzke, *Angew. Chem. Int. Ed.* 48 (2009) 8536.
- [69] H.-X. Yeong, H.-W. Xi, Y. Li, K.H. Lim, C.-W. So, *Chem. Eur. J.* 19 (2013) 11786.
- [70] R. Azhakar, R.S. Ghadwal, H.W. Roesky, H. Wolf, D. Stalke, *Organometallics* 31 (2012) 4588.
- [71] See, for example:
 (a) D.L. Reger, R.P. Watson, J.R. Gardinier, M.D. Smith, P.J. Pellechia, *Inorg. Chem.* 45 (2006) 10088, and references therein;
 (b) K.S. Coleman, J. Fawcett, D.A.J. Harding, E.J. Hope, K. Singh, G.A. Solan, *Eur. J. Inorg. Chem.* (2010) 4310, and references therein.
- [72] C. Elschenbroich, *Organometallics*, 3rd ed., B.G. Teubner Verlag, Wiesbaden, 2006 (Chapter 14).
- [73] See, for example:
 (a) K.K. Pandey, C. Jones, *Organometallics* 32 (2013) 3395;
 (b) H. Lei, J.-D. Guo, J.C. Fettinger, S. Nagase, P.P. Power, *Organometallics* 30 (2011) 6316;
 (c) S. Inoue, M. Driess, *Organometallics* 28 (2009) 5032.
- [74] P.P. Samuel, A.P. Singh, S. Sarish, J. Matussek, I. Objartel, H.W. Roesky, D. Stalke, *Inorg. Chem.* 52 (2013) 1544.
- [75] S. Nagendran, S.S. Sen, H.W. Roesky, D. Koley, H. Grubmüller, A. Pal, R. Herbst-Irmer, *Organometallics* 27 (2008) 5459.
- [76] (a) J.S. Field, R.J. Haines, J. Sundermeyer, S.F. Woollam, *J. Chem. Soc. Chem. Commun.* (1991) 1382;
 (b) J.S. Field, R.J. Haines, M.W. Stewart, J. Sundermeyer, S.F. Woollam, *J. Chem. Soc. Dalton Trans.* (1991) 947.
- [77] See, for example:
 (a) K. Junge, K. Schröder, M. Beller, *Chem. Commun.* 47 (2011) 4849, and references therein;
 (b) D. Bezier, J.-D. Sortais, C. Darcel, *Adv. Synth. Catal.* 355 (2013) 19, and references therein.
- [78] See, for example:
 (a) D. Peng, Y. Zhang, X. Du, L. Zhang, X. Leng, M.D. Walter, Z.J. Huang, *J. Am. Chem. Soc.* 135 (2013) 19154;
 (b) S. Zlatogorsky, C.A. Muryn, F. Tuna, D.J. Evans, M.J. Ingleson, *Organometallics* 30 (2011) 4974;
 (c) S. Meyer, C.M. Orben, S. Demeshko, S. Dechert, F. Meyer, *Organometallics* 30 (2011) 6692;

- (d) Y. Nakajima, Y. Nakao, S. Sakaki, Y. Tamada, T. Ono, F. Ozawa, *J. Am. Chem. Soc.* 132 (2010) 9934;
(e) J. Zhang, M. Gandelman, D. Herrman, G. Leitus, L.J. Shimon, Y. Ben-David, D. Milstein, *Inorg. Chim. Acta* 359 (2006) 1955;
(f) R.K. O'Reilly, V.C. Gibson, A.J. White, D.J. Williams, *Polyhedron* 23 (2004) 2921;
(g) A.A. Danopoulos, N. Tsoureas, J.A. Wright, M.E. Light, *Organometallics* 23 (2004) 166;
(h) B.L. Small, M. Brookhart, A.M.A. Bennett, *J. Am. Chem. Soc.* 120 (1998) 4049.
- [79] T. Zell, P. Milko, K.L. Fillman, Y. Diskin-Posner, T. Bendikov, M.A. Iron, G. Leitus, Y. Ben-David, M.L. Neidig, D. Milstein, *Chem. Eur. J.* 20 (2014) 4403.
- [80] S.C. Bart, K. Chłopek, E. Bill, M.W. Bouwkamp, E. Lobkovsky, F. Neese, K. Wieghardt, P.J. Chirik, *J. Am. Chem. Soc.* 128 (2006) 13901.
- [81] J.M. Darmon, R.P. Yu, S.P. Semproni, Z.R. Turner, C.E. Stieber, S. DeBeer, P.J. Chirik, *Organometallics* 33 (2014) 5423.
- [82] A.A. Danopoulos, J.A. Wright, W.B. Motherwell, *Chem. Commun.* (2005) 784.
- [83] S.C. Bart, E. Lobkovsky, P.J. Chirik, *J. Am. Chem. Soc.* 126 (2004) 13794.
- [84] R.J. Trovitch, E. Lobkovsky, P.J. Chirik, *Inorg. Chem.* 45 (2006) 7252.
- [85] P. Szabo, L. Fekete, G. Bor, Z. Nagy-Magos, L. Markó, *J. Organomet. Chem.* 12 (1968) 245.
- [86] H. van Rensburg, R.P. Tooze, D.F. Foster, S. Otto, *Inorg. Chem.* 46 (2007) 1963.
- [87] J. Li, S. Merkel, J. Henn, K. Meindl, A. Döring, H.W. Roesky, R.S. Ghadwal, D. Stalke, *Inorg. Chem.* 49 (2010) 775.
- [88] For examples of bi- and trinuclear TM complexes containing bridging heavier tetrylene ligands, see:
(a) Refs. [14c,14d,59,20b];
(b) J.A. Cabeza, P. García-Álvarez, D. Polo, *Inorg. Chem.* 51 (2012) 2569;
(c) J.A. Cabeza, P. García-Álvarez, D. Polo, *Inorg. Chem.* 50 (2011) 6195;
(d) R.D. Adams, E. Trufan, *Organometallics* 29 (2010) 4346;
(e) R.D. Adams, B. Captain, E. Trufan, *J. Organomet. Chem.* 693 (2008) 3593;
(f) C.J. Cardin, D.J. Cardin, M.A. Convery, Z. Dauter, D. Fenske, M.M. Devereux, M.B. Power, *J. Chem. Soc. Dalton Trans.* (1996) 1133.
- [89] J.F. Hartwig, *Organotransition Metal Chemistry: From Bonding to Catalysis*, University Science Books, Sausalito, 2010, pp. 47.
- [90] (a) A. Meltzer, S. Inoue, C. Präsang, M. Driess, *J. Am. Chem. Soc.* 132 (2010) 3038;
(b) M. Haaf, R. Hayashi, R. West, *J. Chem. Soc. Chem. Commun.* (1994) 33.
- [91] See, for example:
(a) Refs. [6e,18b,20b,24b,24c];
(b) M. Tanabe, A. Mawatari, K. Osakada, *Organometallics* 26 (2007) 2937;
(c) T. Yamada, A. Mawatari, M. Tanabe, K. Osakada, T. Tanase, *Angew. Chem. Int. Ed.* 48 (2009) 568;
(d) M. Tanabe, J. Jiang, H. Yamazawa, K. Osakada, T. Ohmura, M. Sugimoto, *Organometallics* 30 (2011) 3981;
(e) W. Chen, S. Shimada, M. Tanaka, *Science* 295 (2002) 308.
- [92] For examples of dinuclear complexes featuring a Pt–Pt bond, see:
(a) J. Braddock-Wilking, J.Y. Corey, L.M. French, E. Choi, V.J. Speedie, M.F. Rutherford, S. Yao, H. Xu, N.P. Rath, *Organometallics* 25 (2006) 3974;
(b) M. Tanabe, D. Ito, K. Osakada, *Organometallics* 27 (2008) 2258;
(c) M. Tanabe, D. Ito, K. Osakada, *Organometallics* 26 (2007) 459;
(d) V. Gallo, M. Latronico, P. Mastroianni, C.F. Nobile, G.P. Suranna, G. Ciccarella, U. Englert, *Eur. J. Inorg. Chem.* (2005) 4607;
(e) E. Alonso, J. Forníés, C. Fortuño, A. Martín, A.G. Orpen, *Organometallics* 20 (2001) 850.
- [93] For examples of stable silyliumylidene cations, see:
(a) P. Jutzi, A. Mix, B. Rummel, W.W. Schoeller, B. Neumann, H.-G. Stammler, *Science* 305 (2004) 849;
(b) M. Driess, S. Yao, M. Brym, C. van Wüllen, *Angew. Chem. Int. Ed.* 45 (2006) 6730;
(c) Y. Xiong, S. Yao, S. Inoue, E. Irran, M. Driess, *Angew. Chem. Int. Ed.* 51 (2012) 10074;
(d) Y. Xiong, S. Yao, S. Inoue, J.D. Epping, M. Driess, *Angew. Chem. Int. Ed.* 52 (2013) 7147;
(e) A.C. Filippou, Y.N. Lebedev, O. Chernov, M. Straßmann, G. Schnakenburg, *Angew. Chem. Int. Ed.* 52 (2013) 6974.
- [94] M. El Ezzi, T.-G. Kocsor, F. D'Accrisio, D. Madec, S. Mallet-Ladeira, A. Castel, *Organometallics* 34 (2015) 571.
- [95] L. Álvarez-Rodríguez, J.A. Cabeza, P. García-Álvarez, E. Pérez-Carreño, D. Polo, *Inorg. Chem.* 54 (2015) 2983.
- [96] J.A. Cabeza, J.M. Fernández-Colinas, P. García-Álvarez, E. Pérez-Carreño, D. Polo, *Inorg. Chem.* 54 (2015), <http://dx.doi.org/10.1021/acs.inorgchem.5b00412> (in press).
- [97] B. Blom, G. Klatt, D. Gallego, G. Tan, M. Driess, *Dalton Trans.* (2015) 639.
- [98] R. Zitz, H. Arp, J. Hlina, M. Walewska, C. Marschner, T. Szilvási, B. Blom, J. Baumgartner, *Inorg. Chem.* 54 (2015) 3306.

